GENETIC, EPIGENETIC AND FUNCTIONAL ANALYSIS OF TUMORIGENESIS IN NEUROFIBROMATOSIS TYPE 1 (NF1)

By

Laura E. Thomas

A thesis submitted in candidature for the degree of Doctor of Philosophy

Department of Medical Genetics
School of Medicine
Cardiff University

ProQuest LLC
789 East Eisenhower Parkway
P.O. Box 1346
Ann Arbor, MI 48106-1346

SUMMARY

Neurofibromatosis Type 1 (NF1) is an autosomal dominant disorder caused by constitutional inactivation of the *NF1* gene. NF1 is associated with extreme phenotypic variability and results in an increased risk of developing benign and malignant peripheral nerve sheath tumours (MPNSTs). The molecular mechanisms that underlie NF1 tumorigenesis are poorly understood although inactivation of additional loci in conjunction with *NF1* mutations is postulated to be involved. A combinative approach encompassing genetic, epigenetic and functional analysis was employed to dissect the molecular mechanisms responsible for tumorigenesis and progression to malignancy in NF1.

Genetic analysis of benign cutaneous neurofibromas from NF1 patients with a high tumour burden was undertaken involving PCR, sequencing, Loss of Heterozygosity (LOH) and Multiplex Ligation-dependent Probe Amplification (MLPA) at the *NF1* locus. In addition, Microsatellite Instability (MSI) analysis and molecular analysis of the *TP53*, *RB1*, *CDKN2A* and *MMR* genes was performed in a subset of these tumours. It was revealed that a small proportion of tumours from such patients harbour LOH of the *TP53* and *RB1* genes, a novel finding which indicates that additional modifying loci may underlie the development of multiple cutaneous neurofibromas in patients with a high tumour burden. Furthermore, Schwann cell culture and Laser Capture Microdissection were used to enhance the somatic mutation detection rate in the *NF1* gene.

Pyrosequencing methylation analysis was employed to determine whether *NF1* gene methylation was associated with NF1 tumorigenesis. Promoter methylation of potential modifying genes; *RASSF1A* and *MGMT* was also assessed. Results of this study demonstrate that methylation of the *NF1* and *MGMT* genes is unlikely to contribute to NF1 tumorigenesis. *RASSF1A* promoter methylation was significantly higher in tumour samples in comparison to controls. *RASSF1A* promoter methylation was correlated with a reduction in *RASSF1A* gene expression, as evidenced by 5aza2dc treatment.

Non-synonymous missense mutations account for 15% of lesions in the *NF1* germline and somatic mutational spectrum; although without a suitable functional test, their pathogenicity cannot be defined with certainty. Site directed mutagenesis, a Ras ELISA and bioinformatic analysis were utilised to develop a novel functional assay to assess the potential pathogenicity of *NF1* gap related domain (GRD) missense variants. Of the 16 mutations functionally analysed, 11 were found to be pathogenic.

A panel of 14 candidate genes were found to be aberrantly expressed in 14 tumours and 5 MPNST tumour-derived cell lines by relative quantification. A number of genes in the Rho-GTPase pathway including *RAC1* and *ROCK2* are over-expressed in these tumours, suggesting that these genes might be critical for survival of MPNST cells. ShRNA (short hairpin RNA) for *RAC1* and *ROCK2* were used in adhesion, migration, invasion and wound healing assays on control and MPNST derived cell lines. *RAC1* and *ROCK2* knockdown in MPNST cell lines resulted in a significant increase in cell adhesion and a reduction in wound healing, migratory and invasive activity. The *cMET* gene was also over-expressed in MPNSTs. Treatment of MPNST cell lines with *cMET* inhibitors also resulted in a reduction of cell growth and migration. This study has identified several novel therapeutic targets for NF1-associated malignancies.

DECLARATION

This work has not previously been accepted in substance for any degree and is not concurrently submitted in candidature for any degree.

Signed ..... (candidate) Date 26.09.11

STATEMENT 1

This thesis is being submitted in partial fulfillment of the requirements for the degree of PhD

Signed ..... (candidate) Date 26.09.11

STATEMENT 2

This thesis is the result of my own independent work/investigation, except where otherwise stated.
Other sources are acknowledged by explicit references.

Signed ..... (candidate) Date 26.09.11

STATEMENT 3

I hereby give consent for my thesis, if accepted, to be available for photocopying and for inter-library loan, and for the title and summary to be made available to outside organisations.

Signed ..... (candidate) Date 26.09.11

STATEMENT 4: PREVIOUSLY APPROVED BAR ON ACCESS

I hereby give consent for my thesis, if accepted, to be available for photocopying and for inter-library loans after expiry of a bar on access previously approved by the Graduate Development Committee.

Signed ..... (candidate) Date

ACKNOWLEDGEMENTS

Firstly, I would like to thank my supervisors Prof Meena Upadhyaya and Prof Julian Sampson for their constant support and encouragement throughout this project. Meena in particular, I would like to thank you for being such an inspirational supervisor and for helping me to realise my full potential. Without you my PhD would not have been possible!

To all the members of the NF1 lab (past and present), I would like to thank you for not only providing me with your technical support but most importantly for your friendship. Gill especially; you made the transition from graduate to PhD student as easy as possible with your endless knowledge and protocols! I hope you enjoy your well deserved retirement! Thank you to Rhian for all your wonderful advice and also to Hoi, I wish you well with your own PhD.

To Becky, Mark, Chris, Kayleigh, Lyndsey and Hannah, Cleo, Dunc and JP, I have loved working with you all and can't thank you enough for your support throughout my PhD. Thanks to Shelley for keeping me sane and for all your technical support and experience, Medical Genetics would fall apart without you! Thank you to Nick Thomas and Dave Millar for reading sections of this thesis and related manuscripts, to Andy Tee and Elaine for their protein and cell culture expertise and to James for his computer knowledge. A big thank you to all the members of the NHS staff who have helped me out over the last 4 years, allowing me to 'borrow' reagents whenever needed, and more importantly for your friendship!

To my amazing and ever expanding family: the Thomas-Corrigans, Hendersons, Kellys and Skinners, my mum, James and Luke in particular. Thank you for always believing in me and for your constant encouragement. Finally, to Tom, without you I would never have had the courage to undertake a PhD. Thank you for all your love, support and never-ending optimism. It is to you that I dedicate this thesis.

PUBLICATIONS RELEVANT TO THIS THESIS

Analysis of NF1 somatic mutations in cutaneous neurofibromas from patients with high tumor burden. Thomas, L. *et al.* Neurogenetics. 2010.11(4):391-400

Identification of five novel SPRED1 germline mutations in Legius Syndrome. Laycock-van Spyk, S., Ping Jim, H., Thomas, L. *et al.* Clinical Genetics. 2011

Exploring the somatic *NF1* mutational spectrum in NF1-associated cutaneous neurofibromas. Thomas, L. *et al* (In submission)

Molecular heterogeneity in malignant peripheral nerve sheath tumours. Thomas, L. *et al* (In submission)

An Affymetrix SNP6.0 microarray-based copy number analysis of NF1-associated malignant peripheral nerve sheath tumours (MPNSTs). Upadhyaya, M., Thomas, L. *et al* (In submission)

Pathogenicity of NF1 Gap Related Domain Missense Mutations. Thomas L *et al* (In submission)

CpG Methylation Analysis of NF1 associated tumours. Thomas, L. *et al* (In submission).

ABBREVIATIONS

µg	Microgram
µL	Microlitre
µm	Micrometre
µM	Micromolar
A	Adenine
AC	Adenylate cyclase
bp	Base pairs
BSA	Bovine serum albumin
C	Cytosine
cAMP	Cyclic adenosine monophosphate
CALs	Café au Lait Spots
cDNA	Complementary DNA
Cm	Centimorgans
CRE	Cyclic AMP response element
CSRD	Cysteine serine rich domain
CTD	C terminal domain
dATP	Deoxyadenosine triphosphate
dCTP	Deoxycytosine triphosphate
dGTP	Deoxyguanosine triphosphate
DMEM	Dulbeccos modified eagle medium
DMSO	Dimethylsulphoxide
DNA	Deoxyribonucleic acid
DNase	Deoxyribonuclease
DTT	Dithiothreitol
dTTP	Deoxythymidine triphosphate
E.coli	*Escherichia coli*
ECACC	European Collection of Animal Cell Cultures
EDTA	Ethylenediaminetetraacetic acid-disodium salt
EGFR	Epidermal growth factor
EGFR	Epidermal growth factor receptor

FBS	Fetal bovine serum
FGFR	Fibroblast growth factor receptor
FISH	Fluorescene *in situ* hybridisation
FSNF	Familial Spinal Neurofibromatosis
g	Gram
G	Guanine
GAP	GTPase activating protein
GEF	Guanine nucleotide exchange factor
GIST	Gastrointestinal Stromal Tumour
GRD	Gap Related Domain
HGF	Hepatocyte growth factor
k	Kilobase(s)
kb	Kilobase pairs
kDa	KiloDalton
L	Litre
LB	Luria Bertani
LOH	Loss of Heterozygosity
LCM	Laser Capture Microdissection
M	Molar
mg	Milligram
MIM	Mendelian inheritance in man
ml	Millilitre
mM	Millimolar
mRNA	Messenger RNA
MMR	Mismatch Repair
MSI	Microsatellite Instability
MLPA	Multiplex Ligation Dependent Probe Amplification
MPNST	Malignant Peripheral Nerve Sheath Tumour
MRI	Magnetic resonance imaging
NAHR	Non-allelic homologous recombination
ng	Nannogram

nm	Nanometre
nmol	Nanomole
NF1	Neurofibromatosis Type 1
NF2	Neurofibromatosis Type 2
NIH	National Institute of Health
PCR	Polymerase Chain Reaction
PBS	Phosphate buffered saline
PDGFR	Platelet-derived growth factor receptor
PKC	Protein kinase C
pmol	Picomole
PHEO	Phaeochromocytomas
RasMAPK	Ras mitogen activated protein kinase
RNA	Ribonucleic acid
RNase	Ribonuclease
rpm	Revolutions per minute
RFLP	Restriction fragment length polymorphism
RT	Reverse transcriptase
RT-PCR	Reverse transcription-PCR
SDS	Sodium dodecyl sulphate
SNF1	Segmental NF1 ()
SNP	Single Nucleotide Polymorphism
T	Thymine
TAE	Tris-Acetic acid-EDTA buffer
TE	Tris-EDTA buffer
T_m	Melting temperature
Tris-HCL	Tris(hydroxymethyl)aminomethane hydrochloride
U	Units
UTR	Untranslated region
UV	Ultraviolet
v/v	Volume:volume ratio
w/v	Weight:volume ratio

ADDRESSES OF SUPPLIERS

Abcam	Cambridge, UK
Applied Biosystems	Warrington, Cheshire, UK
ATCC	Teddington, Middlesex, UK
Becton Dickenson	Oxford, UK
Biogene	Cambs, UK
Biogenex	Longfield, Kent, UK
BioRad	Hemel Hemstead, Hertfordshire, UK
Bio-Whittaker	Wokingham, Berkshire, UK
Carl Zeiss	Welwyn Garden City, Hertfordhire, UK
Cambio	Dry Drayton, Cambridge, UK
Dako	Cambridgeshire, UK
Eppendorf	Histon, Cambridge, UK
Eurogentec	Fawley Southampton, Hampshire, UK
Fisher Scientific	Loughborough, Leicestershire, UK
Fujifilm	Bedfordshire, UK
Gallenkamp	Loughborough, Leicestershire, UK
GE Healthcare	Amersham, UK
G-Storm	Byfleet, Surrey, UK
Gene Codes	Ann Arbor, MI, USA
Hettich Zentrifugen	Newport Pagnell, Buckinghamshire, UK
Hoefer	Holliston, MA, UK
Invitrogen	Paisley, Glasgow, UK
Marienfield	Lauda-Königshofen, Germany
Melford Laboratories	Chelsworth, Suffolk, UK
Merck	Hoddesdon, Hertfordshire, UK
Millipore (UK) Ltd	Watford, Hertfordshire, UK
MRC Holland	MRC Holland, Amsterdam, The Netherlands.
MWG-Biotech	Wolverhampton, UK
Nalgene	Rochester, NY, USA

New England Biolabs	Ipswich, UK
Perkin Elmer	Boston, MA
Promega	Southampton, UK
Qiagen	Crawley, West Sussex, UK
Q-Biogene	Luton, Bedfordshire, UK
R&D Systems	Abingdon, UK
Roche	Burgess Hill, West Sussex, UK
Santa Cruz Bio	Santa Cruz, CA, USA
Sarstedt	Leicester, UK
Sigma Aldrich	Poole, Dorset, UK
Thermo-Scientific	Loughborough, Leicestershire, UK
Vector labs	Peterborough, UK
VWR	Lutterworth, Leicestershire, UK

LIST OF TABLES

Supplementary Tables (located in the appendix)

LIST OF FIGURES

CHAPTER 1: General introduction

The neurofibromatoses are inherited autosomal dominant disorders which predispose to tumour formation, particularly of the nerve sheath, resulting in a profound impact on the nervous system. There are currently three recognised types of neurofibromatoses: Neurofibromatosis type 1 (NF1) (MIM_162200), Neurofibromatosis type 2 (NF2) (MIM_101000) and Schwannomatosis. In addition to tumour formation, NF1 has a major pigmentary component whereas the clinical manifestations of NF2 are primarily linked with the nervous systems, including the most distinctive NF2 lesion, schwannomas which are also the cardinal feature of Schwannomatosis. This thesis will only be concerned with genetic, epigenetic and functional analysis of tumorigenesis in neurofibromatosis type 1. The work of an international network of clinicians and researchers has led to significant advancements in the development of diagnostic criteria, management strategies, mouse models and importantly clinical trials for NF1.

1.1 Neurofibromatosis Type 1 (NF1)

Neurofibromatosis type 1, (NF1) (MIM 162200) has been classified by molecular genetics studies as a complex, inherited, autosomal dominant disorder affecting multiple cell types and body systems. Descriptions of individuals with NF1 features have been recorded throughout history (table 1.1) although NF1 became synonymous with von Recklinghausen's disease after Friedrich Daniel Von Recklinghausen (1833-1911) gave a classic description of Neurofibromatosis in 1882 (Von Recklinghausen, 1882). The gene responsible for Neurofibromatosis Type 1, the *NF1* gene was eventually mapped to chromosome 17q11.2 and cloned in 1990 (Cawthon *et al*,1990; Wallace *et al*, 1990; Viskochil *et al*, 1990). The *NF1* gene has a high mutation rate resulting in approximately one mutation occurring per 10,000 gametes per generation. Nearly half of all mutations arising in the *NF1* gene occur as *de novo* events resulting in a birth incidence of approximately 1 in 3500 people and an overall prevalence in the worldwide population of about 1 in 5000 people (Huson *et al*, 1989; Evans *et al*, 2010).

Table 1.1 Timeline of important events in the research and diagnosis of NF1.

Date	Described By	Description	Reference
13th Century	Heinricius - Cistercian monk	Drawing of a man with skin nodules suggested to be that of an NF1 patient	Zanca & Zanca,1980; Morse, 1999
1592	Ulisse Aldrovandi - Italian Physician	Recorded a case that was later published posthumously in an atlas, *Monstrorum Historia*, in 1642	Zanca & Zanca,1980; Morse, 1999
1768	Mark Akenside (1721-1770) - British Physician	Published the first description of NF in English	Akenside, 1768; Ober, 1978
1793	Ludwig and W. G. Tilesius	Description of a patient with multiple fibrous tumours of the skin under the title "Case History of Extraordinarily Unsightly Skin." The patient was described as having countless growths on the skin, cafe´ au lait spots, macrocephaly, and scoliosis	Zanca & Zanca,1980; Morse, 1999
1863	Rudolf L. Virchow (1821-1902)	Describes clinical and neuropathological features of NF in a series of reports. Virchow's classification of neuromas and fibromas on a pathological basis laid the groundwork for von Recklinghausen's landmark presentation	Zanca & Zanca,1980; Morse, 1999
1807-1883	Robert William Smith	Presented 2 new cases and postulated, but was unable to prove that the tumours arose from fibrous connective tissue of small nerves	Smith, 1849
1882	Friedrich Daniel von Recklinghausen	Report "On Multiple Cutaneous Fibromas and Their Relationship to Multiple Neuromas, in which he reviewed the existing literature and added 2 cases, with extensive description of the pathological characteristics including the cutaneous and neurologic manifestations, demonstrating its nervous origin.	Von Recklinghausen, 1882
1978		National Neurofibromatosis Foundation is established; now known as the Children's Tumor Foundation	
1987		NIH establishes the nomenclature for NF1 as well as diagnostic criteria and treatment guidelines. Genetic markers for NF1 are identified on chromosome 17	NIH, 1988

Date	Described By	Description	Reference
1990		Identification of the *NF1* gene	Cawthon *et al*,1990; Wallace *et al*, 1990; Viskochil *et al*, 1990
1992		Description of the protein encoded by *NF1* gene: neurofibromin	Gutmann and Collins 1993; Viskochil et al, 1993
1994		Strains of *Nf1*-mutant mice generated	Jacks *et al*, 1994; Brannan *et al*, 1994
1995		Direct testing for NF1 is made available	
1997	Dr. Andre Bernards (Massachusetts General Hospital Cancer Center and Harvard Medical School	*Drosophila melanogaster* model of NF1 is developed	

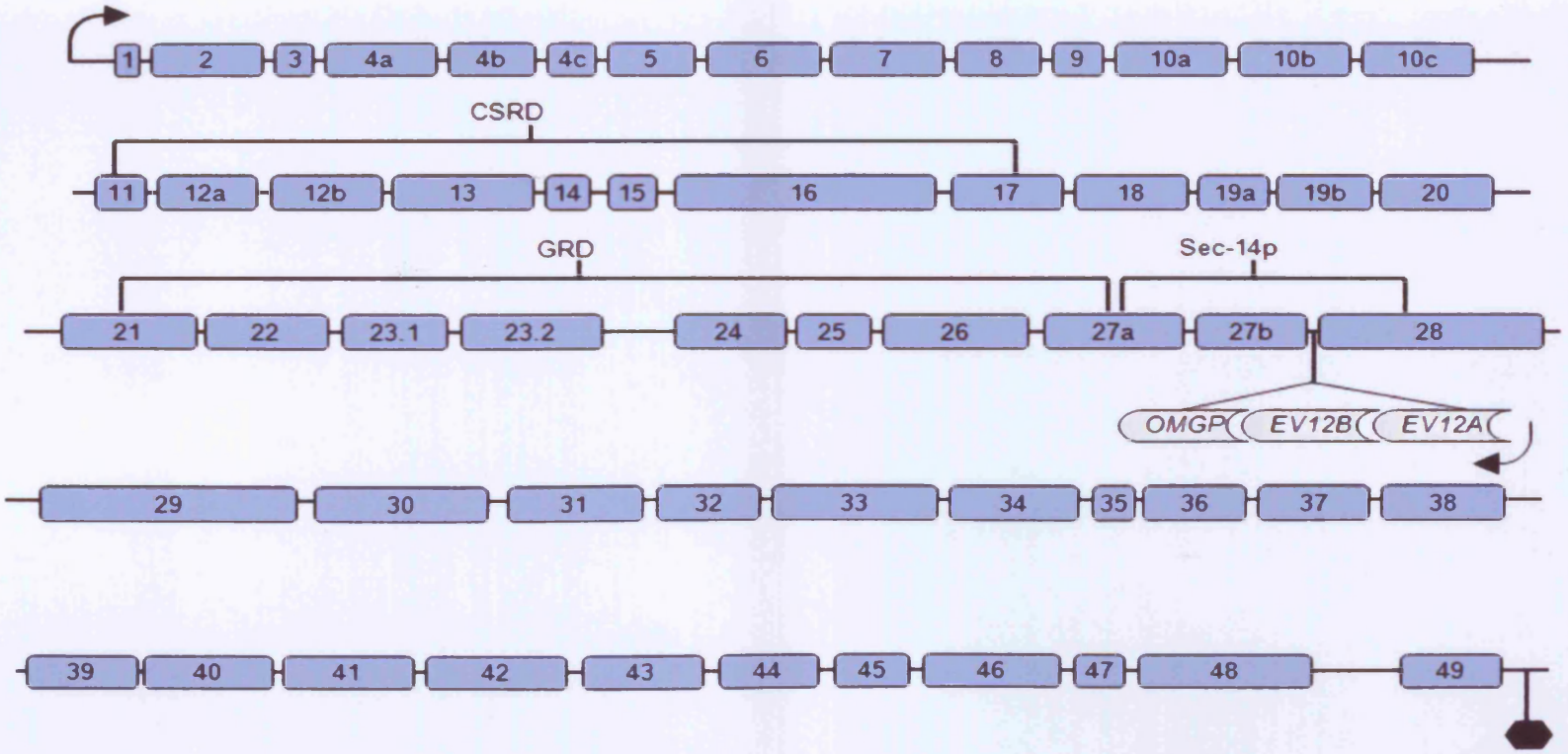

Figure 1.1 *NF1 gene organisation*. The *NF1* gene spans 283kb of genomic DNA, contains 61 exons; of which 4 are alternatively spliced (9a, 10a, 23a, 48a), although neither of these forms interrupt the correct reading of the frame (Reviewed by: Upadhyaya, 2008). The *NF1* gene is also transcribed into 12 kb mRNA, with an open reading frame of 8454 nucleotides (Viskochil, 1999) and also contains a well-defined isochore boundary (section 5.1). Three distinct genes: *EV12A*, *EV12b* and *OMgp* are situated within intron 27b (~61kb) and each consist of 2 exons which are transcribed in the reverse orientation from the complementary strand of the *NF1* gene (Viskochil *et al*, 1999). Additionally, an unprocessed pseudogene, Adenylate kinase 3 (*AK3*) has been identified in several loci throughout the genome including one located in intron 37 of the *NF1* gene which is transcribed in the same orientation as the *NF1* gene (Xu *et al*, 1992). The protein products of these genes do not appear to interact, and deletions of the *NF1* gene which also affect these embedded genes are not correlated with any specific phenotype (Viskochil *et al*, 1990). (Not drawn to scale). Arrows represent the direction of translation. Hexagon represents the stop codon.

1.2. Molecular genetics of NF1

1.2.1 Identification of the NF1 gene

In 1987 the *NF1* gene was assigned to chromosome 17 by gene linkage studies. More refined mapping located the gene to a region near to 17q11.2 by two independent groups (Barker *et al*, 1987; Seizinger *et al*, 1987). Subsequently, the gene was mapped to within 10-15 cM (Fain *et al*, 1987) and finally within 3cM of 17q11.2 corresponding to a region approximately 2-6x10^6 bp long (Barker *et al*, 1987; Seizinger *et al*, 1987; Goldgar *et al*, 1989). Two patients with a clinical diagnosis of NF1 both with balanced translocations, one involving chromosome 1 and 17 and the other 17 and 22 provided the key to a finer definition of the position of the *NF1* gene. It was determined that the breakpoint in both individuals was in 17q11.2, most likely on the proximal long arm (Schmidt *et al*, 1987; Leadbetter *et al*, 1989; Menon *et al*, 1989; Collins *et al*, 1989)

Pulsed-field gel electrophoresis encompassing probes close to the breakpoint (17L1 and IFIO), somatic cell hybrid technology and linking clones which were approximately 60kb apart were used to determine that a gene within the 17q11.2 locus was the gene altered by these rearrangements (Fountain *et al*, 1989; O'Connell *et al*, 1990). Further weight was given to 17q11.2 following a number of studies on patients harbouring centromere recombinants using a series of DNA markers (proximal HHH202 and distal EW206) to provide physical landmarks (Reviewed by: Goldgar *et al*, 1989. Skolnick *et al*, 1987; Pericak-Vance *et al,* 1987; Upadhyaya *et al,* 1987; Diehl *et al*, 1989; Kittur *et al*, 1989; Fain *et al*, 1989a and 1989b; Seizenger *et al*, 1989; Mathew *et al*, 1989; Stephens *et al*, 1989; Vance *et al*, 1989; vanTuinen *et al*, 1987).

A number of other candidate genes which all map to this region were also identified including; *EV12*, *NF1-c2* (NF1 candidate gene 2) the human oncogene homolog *ERBA1*, *ERBB2*, and *NGFR*, but neither were disrupted by the translocation or linked to the manifestations of NF1. This suggested that these genes are instead embedded within the *NF1* gene (Seizenger *et al*, 1987; O'Connell *et al*, 1990 Fountain *et al*, 1989;

Collins *et al*, 1989). The true *NF1* gene, initially termed *NF1LT* (Wallace *et al*, 1990) was subsequently identified by positional cloning experiments in 1990 located at 17q11.2 (Cawthon *et al*, 1990; Wallace *et al*, 1990; Viskochil *et al*, 1990) (figure 1.1).

1.2.2 NF1 promoter and 5'untranslated region

The 5' end of the *NF1* gene, in which the promoter is located, is highly conserved between humans and mice, consisting of several putative regulatory elements surrounding the transcription start site (TSS) (Hajra *et al*, 1994; Fishbein *et al*, 2005). The promoter is very GC rich and has no TATA or CCAAT boxes, a characteristic of promoters found in housekeeping genes (Hajra *et al*, 1994). The promoter also contains a 5' untranslated region (5'UTR) upstream of the translation initiation codon and the major transcriptional start site is approximately 484bp upstream of the initiation codon (Hajra *et al*, 1994). There are also minor transcription start sites 11 nucleotides upstream and 1 nucleotide downstream of the major transcription start sites (Hajra *et al*, 1994). Aberrant methylation at CpG sites in gene promoters has been implicated in a number of cancers (section 5.1). The presence of conserved transcription factor binding sites located in a -33 and +261bp region in addition to a large CpG island at the 5' end of the *NF1* gene which encompasses the *NF1* promoter, may provide possible targets for DNA methylation (Hajra *et al*, 1994).

There are a number of regulatory elements in the *NF1* promoter region, conserved in both humans and mice including; a cyclic adenosine 3',5'-monophosphate (cAMP) response element (CRE), -16bp from the translation initiation codon. Indeed, there is evidence that *NF1* expression in Schwann cells increases in response to high doses of cAMP (Gutmann *et al*, 1993b). Other elements include; SP1, +416 to +460bp upstream of the ATG codon, which may have an important role in regulating *NF1* transcription (Zou *et al*, 2004), several AP2 sites located at +72, +264, +306, +335 and +463, in addition to a serum response element (-14) (Hajra *et al*, 1994). Furthermore, a putative repressor region has been identified within the *NF1* promoter region that consists of CCCTC-rich sequences and is located between the transcription and translation start

sites and may be related to the AP2 sites (Zou *et al*, 2004). The evolutionary conservation of the *NF1* promoter region indicates that these sequence features are likely to be significant to the functional regulation of the *NF1* gene.

1.2.3 3'untranslated region

Polyadenylation motifs (AAUAAA) are important for cleavage and polyadenylation of mammalian pre-mRNAs (Bernards *et al*, 1993). In mammalian cells, the mRNA transcript is known to be cleaved within 30bp downstream of a polyadenylation signal and just upstream of a GU rich domain which has less sequence conservation (Jackson and Standart, 1990). The *NF1* 3'UTR is a large region of approximately 3.2kb in length, containing a stop codon located in exon 49 and a number of polyadenylation signals.

1.2.3.1 Role of the NF1 3'UTR

A definitive role for the 3'UTR has yet to be identified. Evidence derived from protein interactions indicates that the 3'UTR of various mRNAs may contain sequence motifs which have a role in mRNA stability, intracellular localisation and translation (Jackson and Standart, 1990; Bernards *et al*, 1993). At least five protein binding sites, termed NF1-protein binding regions 1–5 (NF1-PBR1- 5) have been identified in the *NF1* 3'UTR. The embryonic lethal abnormal visual (ELAV)-like protein HuR has been shown to interact with this region and is able to reduce the expression of a reporter gene (Haeussler *et al*, 2000). Additionally, the poly-A binding protein (PABP), common to most eukaryotes, is known to bind to 3'UTR's and is thought to enhance translation initiation in addition to modulation of the termination phase (Jackson and Standart, 1990; Hoshino *et al*, 1999). PABP interaction with the NF1 3' UTR has not, however, been studied. As with the 5'UTR, the 3'UTR also exhibits significant sequence conservation and homology to other species including mice, suggesting that it may be a target of inactivating mutations. In rare instances, this has proven to be the case as rare variants and polymorphisms have been identified in the 3'UTR, perhaps evidence of the functional significance of this region (Upadhyaya *et al*, 1995; Cowley *et al*, 1998).

1.2.4 Alternative splicing

Alternative splicing is an important mechanism by which diversity in the proteosome is generated. It is also important for regulating gene expression at different developmental stages and in different tissue types. Alternative splicing events are classified into five different splicing patterns: cassette exons, mutually exclusive cassette exons, alternative 5' splice site (SS), alternative 3'SS and retained introns. Deregulation of alternative splicing has been identified in tumorigenesis and alternative splicing has been investigated as a possible mechanism of genotype-phenotype correlations in NF1 patients (Eisenbarth *et al*, 1995). Switches in the ratio of transcripts have not, however, been linked with specific NF1-related manifestations (Eisenbarth *et al*, 1995). Alternatively used exons have been identified in the *NF1* gene sequence (Cawthon *et al*, 1990a; Gutmann *et al*, 1995).

1.2.4.1 Type 1 neurofibromin

Type 1 neurofibromin lacks both 23a and 48a exon protein sequences and is known to have superior affinity for Ras (Xu *et al*, 1990).

1.2.4.2 Type 2 neurofibromin

This protein transcript involves the insertion of 21 amino acids into exon 23a in the GAP (GTPase activating protein) related domain (GRD) of neurofibromin. This isoform has been detected in the majority of human and rodent tissues and is expressed in astrocytes but not central nervous system (CNS) neurons (Andersen *et al*, 1993; Gutmann *et al*, 1999). Induction of type 2 neurofibromin has also been demonstrated in neuroblasts and Schwann cells which have differentiated *in vitro,* potentially altering its functional properties (Nishi *et al*, 1991; Andersen *et al*, 1993; Gutmann *et al*, 1993c; Gutmann *et al*, 1995b,). This isoform is less efficient in Ras downregulation as the GAP function is disrupted (Andersen *et al*, 1993; Skuse *et al*, 1996).

1.2.4.3 Third neurofibromin isoform

This *NF1* transcript consists of an insertion of 18 amino acids into exon 48a in the carboxyl terminus. This transcript is expressed in the heart and skeletal muscle, correlating with cardiac and skeletal muscle abnormalities in $Nf1^{-/+}$ mice, although this is an usual finding due to the paucity of muscle related NF1 manifestations (Gutmann *et al*, 1995a).

1.2.4.4 Other neurofibromin isoforms

Other splice products of neurofibromin have been identified including an N-terminus isoform which contains both the 23a and 48a protein isoforms and a new exon, termed 10a-2 (Kauffman *et al*, 2002). The overall expression of the 10a-2 transcript is very low in comparison to the expression of the wild-type mRNA. Analysis of the amino acid sequence for this transcript revealed that this new splice product contains a transmembrane segment not found in wild-type neurofibromin. It is postulated that due to the overall expression of this isoform that it may have a housekeeping function on an intracellular membrane such as the endoplasmic reticulum (Kauffman *et al*, 2002).

The 9br transcript encodes 10 amino acids which are inserted into the amino terminal of neurofibromin after residue 1,260 (Danglot *et al*, 1995; Gutmann *et al*, 1999). The 9br isoform is exclusively expressed in the CNS with little or no expression in the cerebellum, brainstem, or spinal cord. It is suggested that as this isoform is identified in the neurons of the forebrain during the early stages of postnatal development it may have a conserved role in nervous system development and differentiation (Gutmann *et al*, 1999).

1.2.5 Embedded genes

Introns 1 and 27b are significantly larger than the rest of the introns in the *NF1* gene. Three distinct genes: *EV12A*, *EV12b* and *OMgp* are situated within intron 27b (~61kb) (figure 1.1)

1.2.5.1 *EV12A* and *EV12B*

EV12A and *EV12B* are human homologues of mouse genes: *Evi-2A* and *Evi-2B*. They have been implicated in retrovirus induced murine myeloid tumours suggesting that they may also act as oncogenes (O'Connell *et al*, 1990; Vourc'h and Andres, 2004). *EV12A* and *EV12B* encode transmembrane proteins for which the main functions are relatively unknown (Vourc'h and Andres, 2004). *EV12A* encodes a 232 amino acid polypeptide that is expressed in the brain, peripheral blood and bone marrow (Cawthon *et al*, 1990b). EVI2B is a protein consisting of 448 amino acids expressed in peripheral blood, bone marrow and fibroblasts (Cawthon *et al*, 1991).

1.2.5.2 *OMG*

OMG is a developmentally regulated gene primarily expressed in oligodendrocytes of the CNS (Viskochil *et al*, 1990b; Habib *et al*, 1998). *OMG* encodes oligodendrocyte myelin glycoprotein (OMgp) an extracellular adhesion protein (Mikol and Stephansson, 1988). The neuronal function of OMgp is not well known but murine models have demonstrated that OMgp can act as a tumour suppressor (Habib *et al*, 1998). Three alterations in *OMG* have also been identified in patients with non-syndromic mental retardation (Venturin *et al*, 2006; Vedrine *et al*, 2011) suggesting that *OMG* may also act as an inhibitor of neural stem cell proliferation and neurite outgrowth (Viskochil *et al*, 1991; Vourc'h and Andres, 2004). Furthermore, overexpression of *OMG* in NIH3T3 fibroblasts has growth suppressive effects and loss of *OMG* through deletions at the *NF1* locus could act as a possible mediator of the neurological defects associated with *NF1* microdeletions (Habib *et al*, 1998; Martina *et al*, 2009).

1.2.6 Pseudogene-like sequences

Pseudogenes are thought to arise by multiple duplications and intra-chromosomal transposition events (Luijten *et al*, 2001). They are non-functional sequences containing degenerative features such as premature stop codons and frameshift mutations which prevent expression of these sequences (Balakirev and Ayala, 2003). There are more than 30 known pseudogenes for the *NF1* gene with about 95% sequence homology, identified by analysis of the published sequence and through fluorescence *in situ* hybridisation (FISH) of *NF1* cDNA (Luijten *et al*, 2001). These occur on chromosomes 2q21.1, 14q11.1, 14q11.2, 15q11.2, 18p11.21, 21q11.2-q21.1, and 22q11.1 (NCBI Entrez Gene), (Marchuk *et al*, 1992; Legius *et al*, 1992; Suzuki *et al*, 1994; Purandare *et al*, 1995; Cummings *et al*, 1996; Hulsebos *et al*, 1996; Kehrer-Sawatzki *et al*, 1997; Régnier *et al*, 1997; Luijten *et al*, 2000b). Such pseudogenes are expressed in specific cell types further complicating the analysis of neurofibromin distribution (Section 1.2.6). Comparison of exon composition indicates that 24 exons of the *NF1* gene (7–9, 10b, 11–23-1 and 24–27b) have homologous counterparts in pseudogenes, which are generally disrupted by indels, the only exception being *NF1*-ch21 in which the reading frame was uninterrupted for the first two exons (Yu *et al*, 2005). Expression from *NF1* pseudogenes on chromosomes 2, 15 and 21 is thought to be possible, further complicating *NF1* molecular analysis (Yu *et al*, 2005). Very few characterised *NF1* mutations appear to have an equivalent on a pseudogene. Whether *NF1* pseudogenes represent junk sequences or have functional consequences is therefore still unclear. Indeed, even *NF1* pseudogenes which do not encode functional domains have been suggested to contribute to increased mutation rates, serving as a mutational reservoir (Marchuk *et al*, 1992; Balakirev and Ayala, 2003).

1.2.7 mRNA editing

mRNA editing is one of several mechanisms of posttranscriptional regulation by which the repertoire of sequence diversity can be increased, resulting in species and tissue specific modulation of gene expression (Maas and Rich, 2000). mRNA splicing

alterations occur in about 50% of NF1 patients indicating that mRNA processing may be an important consideration for assessing NF1 phenotypic variability (Park and Pivnick, 1998).

1.2.7.1 C>U editing of RNA

C>U editing of RNA has been postulated to be a possible mechanism for *NF1* inactivation, through a mechanism equivalent to biallelic *NF1* gene inactivation (Skuse *et al*, 1996; Skuse and Cappione 1997). A C>U variant can be generated at c.3916 which results in *NF1* gene inactivation, generating a UGA premature stop codon in the GRD of the edited version of the *NF1* mRNA resulting in truncation of the *NF1* mRNA (Skuse *et al*, 1996; Ashkenas 1997; Cappione *et al*, 1997; Skuse and Cappione 1997). Furthermore, there is a trend towards higher levels of C>U editing in malignant tumours with overall levels determined to be 4%-17% in comparison to non-tumour tissues (Skuse *et al*, 1996; Skuse and Cappione 1997). Such tumours have a number of distinguishing features including inclusion of the alternatively spliced exon 23a in the edited transcript and the presence of apobec-1 mRNA which mediates site specific deamination of single cytidine residues in apolipoprotein B (apoB) mRNA (Hadjiagapiou *et al*, 1994; Skuse *et al*, 1996; Mukhopadhyay *et al*, 2002). Inappropriate expression of such auxiliary editing factors may therefore contribute to variations in neurofibromin inactivation, potentially underlying the level of sporadic NF1 cases and supporting the role of modifying genes.

1.3 Neurofibromin

1.3.1 NF1 gene expression

1.3.1.1 cDNA sequence of the *NF1* gene

The *NF1* cDNA sequence was first described by Gutmann and Collins (1993), and Viskochil *et al* (1993). The NF1 protein product is neurofibromin, a large ~220-250kDa

(2818 amino acid) protein which is ubiquitously expressed correlating with the varied tissue distribution of NF1 clinical manifestations (DeClue *et al*, 1991; Gutmann *et al*, 1991; Daston *et al*, 1992).

1.3.1.2 Neurofibromin tissue distribution

NF1 mRNA can be identified at low concentrations in most adult tissues including; skin fibroblasts, spleen, lung, muscle and immortalised lymphoblastoid cell lines, with mRNA and protein levels varying between cell and tissue types (Wallace *et al*, 1990). The highest expression of neurofibromin is seen in neurons in the adult brain, CNS and peripheral nervous system (PNS), confirmed by GAP activity (Golubic *et al*, 1992), western blotting and immunostaining (DeClue *et al*, 1991; Daston *et al*, 1992; Norlund *et al*, 1993). Additionally, earlier studies demonstrated that neurofibromin levels are high during rat embryonic development with a role for neurofibromin in axonal path finding or target recognition, diminishing in non-neural tissues during postnatal development (Daston *et al*, 1992; Daston and Ratner, 1992). Importantly, neurofibromin is also expressed in non-myelinating but not myelin forming Schwann cells, concordant with evidence of *NF1* somatic mutations occurring in Schwann cells derived from neurofibromas (Daston *et al*, 1992; Maertens *et al*, 2006). The variation in neurofibromin tissue distribution in neural and non neural tissues is likely to underlie the differences in the function of neurofibromin, indicating that *NF1* mutations can generate a wide variety of pathologies based on the diverse expression of neurofibromin both within and outside of the CNS.

1.3.2 Intracellular distribution of neurofibromin

In cell signalling pathways such as the RasMAPK (Ras mitogen activated protein kinase) pathway, specific biological responses are generated dependent on the localisation of proteins in the cell. neurofibromin has been reported to localise to many subcellular compartments including the cytosol and within both the actin and tubulin

cytoskeleton structures (section 1.3.6) (Gregory *et al,* 1993; Li *et al,* 2001; Vandenbroucke *et al,* 2004; Leondartis *et al*, 2009).

1.3.2.1 Neurofibromin C-tail phosphorylation

Ser2808 is a primary target of PKC at the C-tail of neurofibromin and phosphorylation at this residue is correlated with the subcellular shuttling of the protein. Under basal conditions, nuclear neurofibromin is C-tail Ser2808 dephosphorylated whereas the cytosolic pool of the protein is substantially C-tail Ser2808 phosphorylated (Leondartis *et al*, 2009). Furthermore, activation of the RasMAPK pathway with a phorbol ester: tetradecanoyl phorbol acetate (TPA), a diacylglycerol analogue, resulted in C-tail phosphorylation and cytosolic localisation of neurofibromin, indicating that this may mediate or regulate nucleocytoplasmic shuttling of neurofibromin, a common feature to other tumour suppressor proteins (Fabbro and Henderson 2003; Leondartis *et al*, 2009). Furthermore, this phosphorylation event may involve the stabilisation and modulation of functional properties of the protein, through interactions with other cellular proteins and components including; Ras, cytosolic proteins such as microtubules (Gregory *et al,* 1993), the actin cytoskeleton (section 1.3.6) (Mangoura *et al,* 2006b), mitochondria (Roudebush *et al*, 1997) and even scaffold proteins such as 14-3-3. Indeed, cAMP dependent phosphorylation of serine and threonine residues in the C-terminal domain by PKA results in the interaction of neurofibromin with 14-3-3 which may result in modulation of biochemical and biological functions of neurofibromin (Feng *et al*, 2004). It is suggested therefore that prolonged C-tail phosphorylation is needed for regulation of the RasMAPK pathway through recruitment of neurofibromin from the nucleus to the cytosol, further evidence for potential non-GAP functions for neurofibromin within the nucleus which remain to be determined.

1.3.2.2 Protection against NF1 phenotypes

The localisation of neurofibromin has additionally thought to be associated with protection against some NF1 phenotypes, evidenced by the inability of an *NF1* mutant,

NF1-DE43 to undergo nuclear localisation (Vandenbroucke *et al,* 2002). Similarly, the microtubule-binding Ras effector, RASSF1c, is usually associated with the nucleus but following DNA damage experiments, RASSF1c becomes localised in the cytosol and is associated with components of microtubules where it is thought to activate the RasMAPK pathway and JNK 1 and 2 (Kitagawa *et al,* 2006).

1.3.3 Neurofibromin RasGAP function

There is very high conservation of the *NF1* gene between species, with ~98% homology between mouse and human and 60% between *Drosophila* and humans particularly in the GRD (Bernards *et al,* 1993; The *et al,* 1997). Neurofibromin has extensive sequence homology to two mammalian RAS-GTPases (Guanosine triphosphatase) including the first mammalian GAP to be identified: p120GAP (Trahey and McCormick *et al*, 1987), the *Drosophila* Gap1 protein and the IRA proteins (Ira1p/Ira2p), two inhibitory regulators of the Ras-cyclic AMP pathway found in the yeast *Saccharomyces cerevisiae* (Xu *et al*, 1990; Andersen *et al*, 1993; Weinberg, 2007). There are at least 160 genes which are now predicted to encode proteins that resemble GAPs (McTaggart *et al*, 2006). The catalytic domains of such proteins are crucial for binding to Ras proteins and stimulating the low intrinsic GTPase activity of Ras proteins to convert from the guanosine triphosphate (GTP) bound activated Ras to guanosine diphosphate (GDP) bound inactivated Ras (Ballester *et al*, 1990; Xu *et al*, 1990; DeClue *et al*, 1991) (figure 1.2).

Mutants of *IRA1/IRA2* demonstrate sensitivity to heat shock and nutrient starvation, phenotypes which are similar to those found in yeast cells expressing $RAS2^{val-19}$, a mutation equivalent to mammalian ras^{val-12} (Tanaka *et al*, 1989; Xu *et al*, 1990). Furthermore, neurofibromin demonstrates functional homology with the previously identified Ras-GTPases harbouring the ability to stimulate the intrinsic GTPase activity of both yeast *RAS2* and mammalian *HRAS*, although neurofibromin does have distinct physiological requirements for interactions (Xu *et al*, 1990). The main functional role of neurofibromin is therefore that of a highly conserved RAS-GAP with the gap related

domain encoded by exons 20 to 27a of neurofibromin. Under normal circumstances, neurofibromin is a major regulator of Ras signalling, accelerating the slow process of hydrolysis of GTP to GDP through its association with Ras (Ballester *et al*, 1990; Xu *et al*, 1990; McTaggart *et al*, 2006).

1.3.4 Neurofibromin Non-GAP function

Determining the *in vivo* interactions of neurofibromin is an important aspect of the design of therapeutic targets for the clinical manifestations of NF1, particularly NF1-associated benign and malignant tumour types (section 1.5.1). Studies on neurofibromin have largely focused on its RasGAP function and tumorigenesis although there is mounting evidence which indicates that neurofibromin has a number of other functional non-GAP roles. Indeed, mutations have been identified outside of the GRD; Ras inhibitors have only been found to rescue some phenotypes in *NF1* deficient cell lines and neurofibromin has also been found to co-localise and bind with other proteins. Furthermore, the GRD only accounts for about 10% of the protein as neurofibromin contains a number of other additional regions including: an N-terminus cysteine/serine-rich domain (CSRD) (section 1.3.4.1), a leucine-repeat domain upstream of the extreme carboxyl terminus domain (Martin *et al*, 1990), and a C-terminal helical domain containing a functional nuclear localization sequence (NLS-CTD) (Li *et al*, 2001; Vandenbroucke *et al*, 2004).

1.3.4.1 Neurofibromin cysteine serine rich domain (CSRD)

A region upstream of the GRD, located in exons 11-17 may represent a further functional domain (Izawa *et al*, 1996; Fahsold *et al*, 2000). This domain, termed the cysteine serine rich domain (CSRD) is located in the N-terminal of neurofibromin at amino acid residues 543–909 and contains three cysteine pairs (residues 622/632, 673/680, and 714/721). There are a number of potential functions for this domain based on its structural properties. The cysteine residues, for example, exhibit similarities to the ATP binding domain in the BCR protein (Maru and Witte, 1991) and there is additional

homology to MAP-2 and tau proteins, known to associate with microtubules (Gregory *et al*, 1993). Moreover, there are a number of cAMP dependent protein kinase A (PKA) recognition sites located at residues 583 and 815-834, potential evidence for neurofibromin mediation of cAMP signalling (Marchuk *et al*, 1991; Guo *et al*, 1997; The *et al*, 1997) (section1.3.4.2). Some of the most compelling evidence for the functional role of the CSRD in neurofibromin is the possible allosteric regulation of the GRD by the CSRD (Mangoura *et al*, 2006). Indeed, co-overexpression of CSRD+GRD results in a 30% downregulation of EGF stimulated Ras activation indicating that together the CSRD and GRD confer greater regulation on Ras (Mangoura *et al*, 2006). Moreover, chronic inhibition of PKC with TPA, results in a reduction in Ras-GAP activity of the CSRD-GRD and a significant increase in Ras activation following EGF stimulation, indicating that neurofibromin Ras-GAP activity may be regulated by PKC-dependent phosphorylation of the N-terminal CSRD (Mangoura *et al*, 2006; Griner and Kazanietz, 2007; Leondaritis *et al*, 2009).

1.3.4.2 Neurofibromin and cAMP signalling

The different domains of neurofibromin have been found to regulate immediate versus long term memory. The C terminal domain is thought to be responsible for learning and the regulation of immediate memory. Conversely, the GRD is thought to control long term memory formation and is additionally important for synaptic plasticity (Brambilla *et al*, 1997; Atkins *et al*, 1998). These two regions have, however, been found to contribute to different signal transduction pathways, underlying the association with distinct phases of memory (Ho *et al*, 2007). Whilst the GRD signals through the RasMAPK pathway (section 1.4.1), the C-terminal region is required for G-protein-dependent adenylyl cyclase activation, regulating intracellular cAMP (Guo *et al*, 1997, 2000; The *et al*, 1997; Tong *et al*, 2002; Dasgupta *et al*, 2003; Hannan *et al*, 2006).

Studies in both mice and drosophila have shown that cAMP regulation is stimulated by neurotransmitters such as serotonin and histamine (Hannan *et al*, 2006). In Drosophila *NF1* null mutants ($NF1^{P1}$ and $NF1^{P2}$), neurofibromin was essential for the cellular

response to neuropeptides, specifically: PACAP38 (pituitary adenylyl cyclase–activating polypeptide) at the neuromuscular junction (The *et al*, 1997). In conjunction with an effect on body size, this induced a 100-fold enhancement of potassium currents, activating the RasMAPK and cAMP pathways (The *et al*, 1997). This activity is eliminated in the mutants and rescued in a Ras independent manner, by exposure of cells to increased concentrations of cAMP (The *et al*, 1997). In *Drosophila*, neurofibromin consequently acts not only as a Ras-GAP but also as a regulator of the cAMP pathway that involves the *rutabaga* (*rut*)-encoded adenylyl cyclase (Guo *et al*, 1997; Guo *et al*, 2000).

Given the sequence homology between *Drosophila* and human neurofibromin, it is expected that similar mechanisms would be observed in humans indicating that signalling from both the GRD and C-terminal region may underlie the cognitive defects seen in individuals with NF1. Indeed, neurofibromin also regulates G-protein stimulated adenylyl cyclase activity in mammalian neurons (Tong *et al*, 2002) and *Nf1*-deficient astrocytes have impaired cAMP responses to PACAP, which is associated with decreased calcium influx, further evidence that mammalian neurofibromin functions at the level of adenylyl cyclase activation (Dasgupta *et al*, 2003).

1.3.4.3 Neurofibromin Sec14 PH domain

A novel bipartite element, distinct from the GRD has also been identified in neurofibromin. This region is located at the immediate C-terminus of the GRD and contains an N-terminal, lipid binding Sec14- homologous domain (Aravind *et al*, 1999) and a neighbouring C-terminal pleckstrin homology (PH)-like region (Bonneau *et al*, 2004; D'Angelo *et al*, 2006). Sec14-like domains have been previously identified in yeast where it acts as a phosphatidylinositol transfer protein (PITP) with a role in exchanging (3-sn-phosphatidyl)choline (PtdCho) and 1-(3-snphosphatidyl)-D-myo-inositol (PtdIns) between membrane compartments (Bonneau *et al*, 2004; Phillips *et al*, 2006). The PH domain is likely to regulate ligand binding in the Sec14 domain (D'Angelo *et al*, 2006; Welti *et al*, 2007).

A number of mutations have been identified in the Sec14-PH domain (Human Gene Mutation Database, HGMD). Mutations including p.K1750del and p.I1584V have also been created by site directed mutagenesis in the Sec14-PH domain and expressed in cultured cells of patients (Welti *et al*, 2011). No major change was observed in the composition of bound lipids in the non-truncating mutant proteins compared to the wild type and those carrying truncating mutations (p.K1750del) (Welti *et al*, 2011). PH domains are known to represent a family of typical protein interaction modules suggesting that this domain may control protein-protein interactions although the lipid binding activity of this domain may not represent the only functional role of the Sec14-PH domain (Blomberg *et al*, 1999). The natural ligand for this domain is yet to be identified but such ligand binding partners are thought to include phosphoproteins such as PtdInsPs or a similar species with strong local negative charge (D'Angelo *et al*, 2006; Welti *et al*, 2011). Two-hybrid screens or pull-down assays may reveal further interaction partners and insight into neurofibromin function.

1.3.5 Neurofibromin and ubiquitin mediated proteolysis

Ubiquitin-mediated proteolysis is involved in the regulation of a number of key cellular processes including cell cycle control, differentiation, and immune responses (Ciechanover *et al*, 2000). Ubiquitination via the ubiquitin-proteosome pathway involves the covalent attachment of ubiquitin molecules to lysine residues on the target protein, followed by its rapid degradation by the 26S proteosome (Ciechanover *et al*, 2000). It has been indicated in a number of cell lines including primary human lung embryonic fibroblasts (IMR90 cells) and a rat Schwannoma cell line that in response to serum stimulation, neurofibromin is degraded completely. This suggests that the duration and amplitude of Ras signalling may be regulated by the action of the ubiquitin-proteosome pathway on amino acids which lie upstream of the GRD in neurofibromin (Cichowski *et al*, 2003). The identification of this pathway as a crucial mediator of neurofibromin activity may have important implications in terms of therapeutic interventions which could be aimed at blocking *NF1* inactivation or by up-regulating the NF1 protein.

1.3.6 Neurofibromin-cytoskeleton association

Neurofibromin is localised in both the cytosol and is also associated with the membrane. No membrane spanning region has been identified in the sequence of neurofibromin, however, suggesting that it may not be an integral membrane protein (Marchuk *et al*, 1991; De Clue *et al*, 1991). Indeed, precipitation of neurofibromin with bovine brain Triton-insoluble fractions indicates that neurofibromin resides mainly in the particulate fraction and so may be associated with the cytoskeleton (Hattori *et al*, 1992). This indicates that cytoskeletal proteins may serve to regulate the activity and potentially the localisation of neurofibromin. Components of microtubule function which are important in cell division may therefore represent key therapeutic targets for chemotherapeutic agents such as colchicine (Myrdal and Auersperg, 1985; Bar-Sagi and Feramisco, 1986).

1.3.6.1 Tubulin and neurofibromin association

Neurofibromin isoform 1 (section 1.2.4.1) co-localises with cytoplasmic microtubules such as tubulin in fibroblasts and Schwann cells, suggesting that this complex could be important in the regulation of Ras activity (Gutmann and Collins, 1991; Bollag *et al*, 1993; Gregory *et al*, 1993; Gutmann *et al*, 1995a). The GAP activity of such tubulin-neurofibromin complexes is reduced, indicating that the GAP function of neurofibromin is partially inhibited by its association with tubulin and possibly other phospholipids. This interaction may therefore represent an important mechanism for rapidly generating high levels of activated Ras in the cell through downregulation of neurofibromin GAP function (Bollag *et al*, 1993; Gregory *et al*, 1993; Gutmann *et al*, 1995a). Furthermore, immunohistochemical and western blot analysis of neurofibromin has shown a potential interaction with mitochondria although the reason for this association is not clear and may relate to sequestration of neurofibromin so that it is unable to bind to Ras (Roudebush *et al*, 1997).

1.3.6.2 Embryonic development and cytoskeletal interaction

During embryonic development, interaction of neurofibromin with cytoskeletal components (intermediate filament cytoskeleton (cytokeratin 14), desmoplakin and β4 integrin) is a key event in the formation of desmosomes and hemidesmosomes (Koivunen *et al*, 2000). This suggests that during an early period of cellular development when *NF1* expression is high, neurofibromin is associated with bundles of intermediate filaments of the basal keratinocytes. This interaction may therefore be important for the polarisation of basal cells and the maturation of intercellular junctions (Malminen *et al*, 2002). Moreover, neurofibromin also localises with F-actin and the microtubule cytoskeleton during differentiation of telencephalic neurons (Li *et al*, 2001).

1.3.6.3 Syndecan association with neurofibromin

Syndecans are transmembrane proteoglycans which are involved in the organisation of cytoskeleton and/or actin microfilaments and can function as cell surface receptors during cell-cell and/or cell-matrix interactions. Syndecan association with neurofibromin has also been studied and it is indicated that they form a bipartite interaction with neurofibromin (Hsueh *et al*, 2001).

1.4 NF1 associated pathways

1.4.1 The RasMAPK pathway

1.4.1.1 G proteins

The role of the RasMAPK pathway is to integrate extracellular input from ligands including growth factors, and to transduce the signal to the intracellular environment (figure 1.2). Signal transduction through this pathway occurs with the use of an intricate system of membrane-bound as well as cellular molecules. GTP binding proteins (G proteins) are well characterised cytoplasmic proteins which belong to this pathway are involved in the regulation of many cellular processes including cell proliferation, differentiation and migration (Woods *et al*, 2002; Denayer *et al*, 2008). Aberrant G protein regulation consequently results in cellular transformation. The G protein family is divided into two distinct types: small guanosine nucleotide bound G proteins, including Rho, Rab, Ran and importantly Ras, which is disrupted in about 20% of all human cancers (Bos *et al*, 1989; Mitin *et al*, 2005), and heterotrimeric G proteins.

1.4.1.2 The Ras family

Ras exists as a multi-gene family consisting of *HRAS*, *KRAS* and *NRAS,* (Parada *et al*, 1982) all of which are activated by binding and stimulation of receptor tyrosine kinases (RTK) such as epidermal growth factor receptors (EGFR), G protein-coupled receptors, cytokine receptors and extracellular matrix receptors by growth factors (Tidyman and Rauen 2009). Ras functions as a biochemical switch mechanism, existing in two forms: the GTP-bound activated form and GDP-bound inactivated form, dependent upon the intracellular protein partner with which it is associated. These include GAPs (p120GAP and neurofibromin) or GEFs (guanine nucleotide exchange factors) including SOS, RasGRF and RasGRP (Mitin *et al*, 2005; McTaggart *et al*, 2006). The exchange of GDP and GTP and the state of Ras activity within a cell is therefore dependent on the levels of these proteins. As outlined in figure 1.2 and figure 1.3, upon activation of Ras through

GTP charging, there are a number of downstream intracellular targets for Ras which can be subsequently activated. In normal resting cells, upon growth factor binding the receptor interacts with the Src homology 2 domain (SH2) domain on the GRB2 adaptor protein (Mitin *et al*, 2005; Tidyman and Rauen, 2009). SOS is bound to GRB2 by the Src homology 3 domain (SH3) (Mitin, 2005). Upon receptor activation, GRB2 and consequently SOS are recruited to the plasma membrane where they are brought into direct proximity of Ras where the GEF activity of SOS increases the levels of activated Ras in the cell by catalysing the exchange of GDP for GTP (Tidyman and Rauen 2009). SHC acts as an anchor for GRB2 through tyrosine phosphorylation (figure 1.2 and 1.3).

1.4.2 Ras associated pathways

1.4.2.1 Ras-PI3K-PTEN-AKT-mTOR pathway

Ras can directly interact with the catalytic subunit of type 1 phosphatidylinositol 3-kinases (PI3Ks), which catalyses the formation of secondary messenger lipids: phosphatidylinositol 3,4,5triphosphate [$PI(3,4,5)P_3$] and phosphatidylinositol 3,4bisphosphate [$PI(3,4)P_2$] from phosphatidylinositol-4,5-bisphosphate ($PtdIns(4,5)P_2$) which bind to and augment the translocation of phosphoinositide-dependent protein kinases (PDK1) [3-phosphoinositide-dependent protein kinase-1] and AKT (PKB). (Rodriguez-Viciana *et al*, 1994; Pacold *et al*, 2000; Martelli *et al*, 2010) (figure 1.3).

1.4.2.1.1 PTEN

Negative regulation of the PI3K pathway is achieved through the tumour suppressor protein phosphatase and tensin homologue deleted on chromosome ten (PTEN). PtdIns(3,4,5)P3 is the main substrate for *PTEN* although other substrates include focal adhesion kinase (FAK), SHC exchange protein, transcriptional regulators ETS-2 and Sp1, and platelet-derived growth factor receptor (PDGFR) (Mahimainathan *et al*, 2004). PTEN point mutations, loss of heterozygosity and promoter methylation are often described in association with cancer. Moreover, *PTEN* is frequently mutated in NF1-associated malignant tumours (Gregorian, 2009; Mawrin *et al*, 2010).

1.4.2.2 PI3K and the cytoskeleton

Aspects of cytoskeletal regulation are also controlled by PI3K pathway activation, leading to stimulation of RAC, a RHO family protein involved in the regulation of both the actin cytoskeleton and a number of transcription-factor pathways including activating nuclear factor-κB (NF-κB) (section 6.1). A role for RAC in PI3K-dependent and independent mechanisms has also been defined in *RAS*-induced transformation (Lambert *et al*, 2002). Further evidence for Ras-independent NF1 involvement in cytoskeletal rearrangements is demonstrated by the ability of *NF1* overexpression to induce the expression of focal adhesion kinase (FAK) in addition to the modulation of MAPKs (Corral *et al*, 2003).

1.4.2.3 Ras-RALGDS pathway

Another family of effectors for Ras is the RAS-related (RAL) proteins involving three members: RAL guanine nucleotide dissociation stimulator (RALGDS), RALGDS-like gene (RGL/RSB2) and RGL2/RLF which are able to interact with Ras-GTP through their Ras association (RA) domains. (figure 1.3)

1.4.2.4 Ras-phospholipase Cε pathway

The connection between Ras and Phospholipase Cε as an effector has been reported only recently. Phospholipase Cε is known to have Ras association domains in addition to a Ras-GEF domain and a phospholipase C domain (figure 1.3).

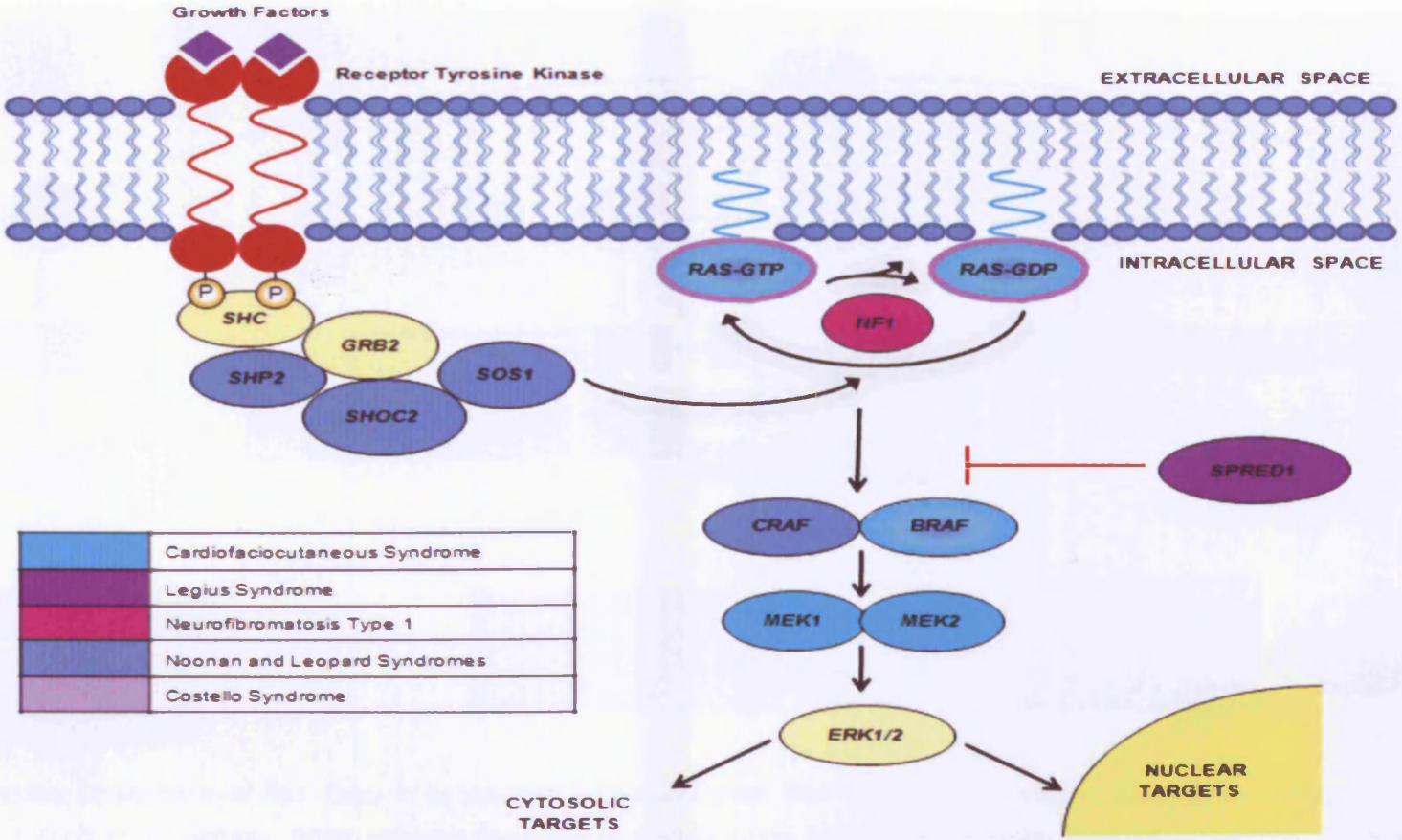

Figure 1.2. *RasMAPK signalling pathway and the 'Ras opathies'*. The tyrosine kinase Raf, is the primary Ras effector. Raf is activated by recruitment to the plasma membrane and phosphorylation by 'scaffold' proteins. The MAPK pathway consists of a highly conserved cascade of three structurally related protein kinases, each activating the next kinase in the pathway by phosphorylation. MEK1 and MEK2 (MKK – MAP kinase kinase), dual specificity kinases are activated by phosphorylation at either threonine or tyrosine residues. ERK1 and ERK2 (MK – Map kinase/ extracellular signal-regulated kinases 1 and 2) are the final kinases in the pathway and are activated following serine/threonine phosphorylation. Cytosolic and nuclear substrates for ERK include regulators of the expression of mediators of the cell cycle including FOS, c-JUN and D-cyclins which are involved in the G1 phase cell cycle progression. Adapted from Downward *et al* (2002)

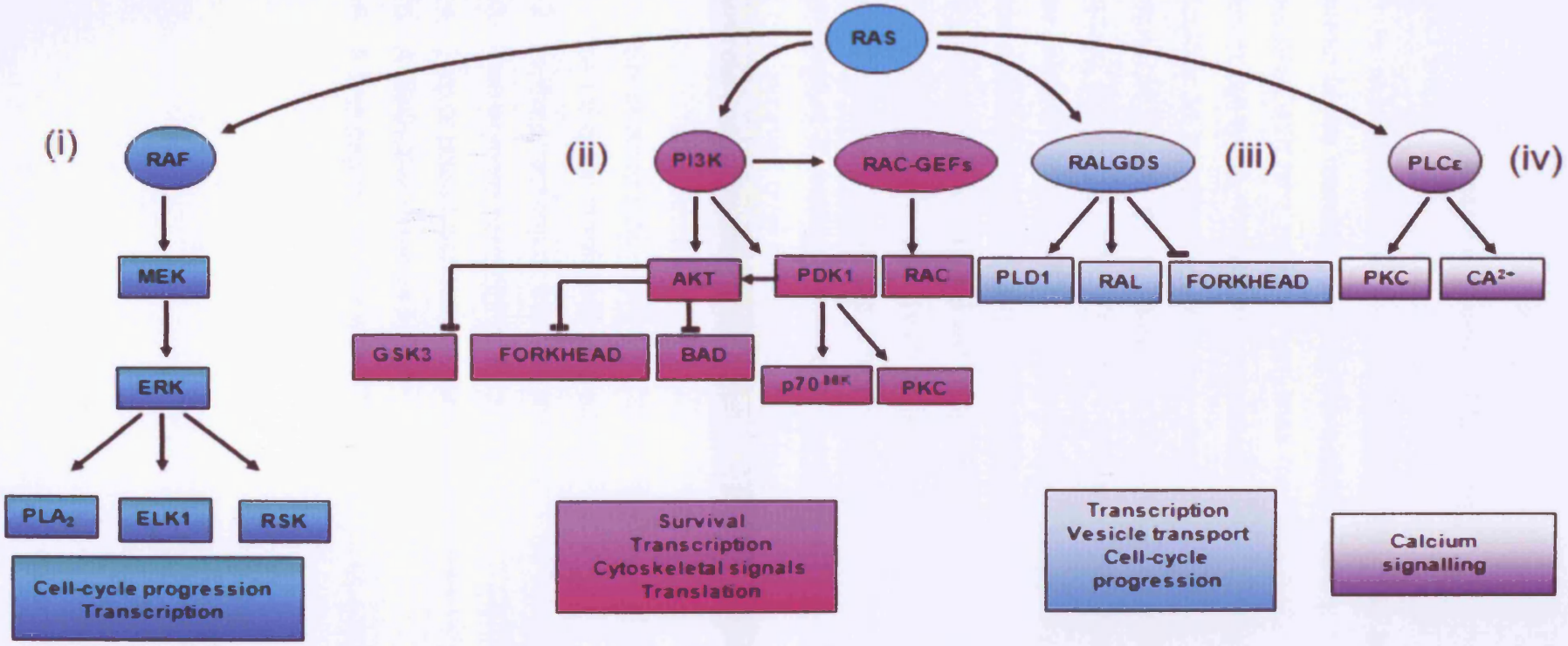

Figure 1.3. *Signalling Downstream of Ras.* Once in its activated GTP-bound state, Ras can activate numerous downstream effectors: (i) The RasMAPK pathway (figure 1.2) (ii) P13K pathway. PDK1 activates a number of kinases in the AGC family, including AKT, PKCs, p70S6K and RSK. Furthermore RacGEFs are activated by PI3K which able to activate RhoGTPases. (iii) Activation of the RAL GDS pathway results in stimulation of phospholipase D1 (PLD1) and activation of CDC42/RAC-GAP-RAL binding protein 1 (RALBP1) (Boettner *et al*, 2002; Feig *et al*, 2003). Downstream of the RALGDS pathway, these proteins, in concert with AKT are capable of inhibiting the FoxO family which are FORKHEAD transcription factors thought to be involved in induction of cyclin-dependent kinase inhibitor KIP1 (p27) which promotes arrest of the cell cycle through BIM and FAS LIGAND expression subsequently promoting apoptosis (De Ruiter *et al*, 2001). (iv) Phospholipase Cε is thought to function in the activation of PKC by Ras following the hydrolysis of PtdIns(4,5)P2 to diacylglycerol and inositol-1,4,5-trisphosphate (Ins(1,4,5)P3). Furthermore there is evidence that Ras could be linked to calcium mobilisation through this mechanism (Kelley *et al*, 2001) Adapted from Downward *et al* (2002).

1.5. NF1 diagnostic and clinical features

NF1 is characterised by highly variable symptoms and inconsistent severity, even between family members sharing the same mutation. The spectrum of clinical features associated with NF1 patients, indicates that *NF1* mutations must occur in a number of different cell types. The extreme variability of NF1 clinical manifestations has resulted in difficulties in establishing definitive clinical diagnostic criteria. In 1988, the National Institute of Health (NIH) issued a 'Consensus Statement' with the aim of defining standard diagnostic criteria for NF1 to help characterise NF1 and distinguish it from other related disorders (NIH, 1988). These features are highly specific in adults but in children with no family history of NF1, diagnosis can often be difficult as the majority of NF1 characteristics manifest with age. In children with a clear family history of NF1, the diagnosis is much simpler, with only one feature needed; usually the presence of a pigmentary anomaly such as Café au lait (CAL) macules. CAL macules normally occur in children of 2 years of age and frequently increase in numbers throughout childhood but can diminish over time. Two or more of the NIH diagnostic criteria (listed below) signify the presence of NF1.

1. Six or more CAL macules: (0.5 cm at largest diameter in pre-pubertal individuals or 1.5 cm in individuals past puberty)
2. Axillary freckling or freckling in inguinal regions due folding of the skin
3. Two or more neurofibromas of any type or 1 plexiform neurofibroma
4. Two or more Lisch nodules (iris hamartomas)
5. A distinctive osseous lesion
6. A first-degree relative with NF1 diagnosed by using the above-listed criteria

1.5.1 NF1-associated tumours

Patients with NF1 have an increased risk of developing a number of different benign and malignant tumour types as outlined below. The overall risk of cancer has been found to be 2.7 times higher in NF1 patients than in the general population, with a 20% cumulative risk of a malignancy by age 50 (Walker *et al*, 2006).

1.5.1.1 Cutaneous neurofibromas

Neurofibromas are benign tumours which originate from the peripheral nerve sheath. Cutaneous neurofibromas are confined to a single area and comprise of Schwann cells, fibroblasts, perineural cells, mast cells and axons (Kimura *et al*, 1974; Le and parade, 2007). Cutaneous neurofibromas are one of the hallmarks of NF1, occurring in the majority of patients during adolescence and the initial years of adulthood, increasing in size and number during both puberty and pregnancy (table 1.2). Despite no response to hormonal contraceptives, the timing of neurofibroma development indicates that there may be a role for hormonal factors in their formation (Mclaughlin *et al*, 2003). Neurofibromas have not been reported to undergo malignant transformation. There is currently no definitive treatment for neurofibromas as they are only removed for cosmetic reasons or if they are causing the patient pain or discomfort due to excessive size or location. Surgical excision is the standard treatment for cutaneous neurofibromas; however, this can involve the additional risk of producing thickened scarring and recurrence of neurofibromas post-surgery. More recently, laser treatment has also been found to be helpful for small lesions.

1.5.1.2 Subcutaneous neurofibromas

Subcutaneous neurofibromas are a cause of pain and neurological deficit. These tumours occur below the skin and are defined as superficially situated tumours in which the skin moves freely over the lesion (Tucker *et al*, 2005). Due to their subcutaneous location, these tumours can be mistaken for glomus tumours (section 1.5.1.9). As an

association of NF1 with breast cancer has been reported (section 1.6.3), it is important that women with subcutaneous breast lumps are referred to an NF1 specialist to distinguish neurofibromas from breast carcinomas (Sharif *et al*, 2007) (table 1.2).

1.5.1.3 Plexiform neurofibromas

Plexiform neurofibromas exhibit a similar composition to benign neurofibromas being comprised of an irregular mix of Schwann cells, local elements of supporting nerve fibres including perineural cells, neurons, fibroblasts, and blood vessels in addition to infiltrating mast cells (Ferner *et al*, 2007; Le *et al*, 2011). Plexiform neurofibromas are generally larger in size than cutaneous neurofibromas, implicate multiple nerve fascicles and are capable of infiltrating surrounding tissue and blood vessels (Reviewed by Upadhyaya, 2008a). Plexiform neurofibromas arise in ~60% of NF1 patients and are thought to be congenital due to their propensity for growth, usually growing during childhood and adolescence. Very large plexiform neurofibromas can cause extensive disfigurement and neurological deficit. Due to their infiltrative nature, they can be difficult to remove surgically and additionally, about 15% of plexiform neurofibromas undergo malignant transformation to become MPNSTs and so it is crucial the they are closely monitored (Ferner *et al*, 2007) (table 1.2). Plexiform neurofibromas are generally more problematic and equally as difficult to treat due to their size, location and involvement of multiple nerves. There have been a number of previous studies into the use of chemotherapeutic agents in the treatment of plexiform neurofibromas but the success of such studies has been relatively limited (supplementary table 1).

1.5.1.4 Malignant peripheral nerve sheath tumours (MPNSTs)

Individuals with NF1 have a 15 year decrease in life expectancy with mortality related to NF1-associated malignancies (Zoller *et al*, 1995; Rasmussen *et al*, 2001). MPNSTs are an extremely rare, aggressive malignancy, accounting for approximately 3-10% of soft tissue sarcomas (Grobmyer *et al*, 2008). These tumours can occur sporadically, later in life in the general population but up to 50% of MPNSTs are associated with NF1,

occurring in 10-15% of individuals (Evans *et al*, 2002). Commonly originating in the nerve roots, extremities and pelvis but also occurring at other sites, MPNSTs usually present as enlarged masses causing disability, pain and neurological deficit due to pressure on surrounding tissues. A pre-existing plexiform neurofibroma can undergo malignant transformation evident from a rapid change in size or development of pain. Indeed individuals with a subcutaneous neurofibroma are 20 times more likely to develop an MPNST indicating that close follow up of patients with such tumours is warranted to rapidly identify any malignant changes (Tucker *et al*, 2005) (table 1.2).

In terms of treatment options for MPNSTs, these are very limited and so consequently contribute to the low survival rates of such patients. The main treatment option for such patients is generally complete surgical resection with clear margins (Ferner and Gutmann, 2002). Chemotherapy has been used in numerous preclinical studies on MPNSTs and also in clinical trials for the treatment of MPNSTs but its efficacy is still debated (Supplementary table 1). Radiation therapy has also been employed in the adjuvant setting with some success (Ducatman *et al*, 1986) but is mostly avoided due to previous observations that radiotherapy is often associated with the occurrence of other malignant symptoms (Sharif *et al*, 2006).

The major focus of drug discovery for MPNSTs in addition to other NF1-associated malignancies such as optic gliomas (supplementary table 1) has involved targeting of specific aspects of Ras signalling. This includes Ras localisation and attachment to the inner membrane which mainly involves interference with post translational prenylation of Ras with the Statin family of drugs to inhibit Ras prenylation (FTI family (Farnesyl protein transferase inhibitor)). Geranylgeranyl transferase could also act as a secondary mechanism if prenylation is inhibited, indicating that a combinative approach of FTI and geranylgeranyl transferase inhibitors would be required. Other targets other than the RasMAPK pathway have been investigated in MPNSTs including mTOR, AKT, PI3K, EGFR, VEGF/VEGFR and PDGFR (supplementary table 1).

1.5.1.5 Spinal nerve root neurofibromas

Spinal nerve root neurofibromas occur in about 40% of individuals with NF1, but only about 2% are symptomatic, causing compressions of the spinal root or spinal cord, often appearing worse upon neuroimaging (MRI) than the resulting neurological deficit. (Thakkar *et al*, 1999; Ferner *et al*, 2007). Due to the pathology and risks associated with NF1 surgery, patients with such spinal tumours require strict observation (table 1.2).

1.5.1.6 Brain and optic pathway tumours

Gliomas have been detected in most parts of the CNS although they generally occur in the optic pathways, cerebellum and brainstem (Listernick *et al*, 2007). Astrocytomas are slow growing high grade gliomas representing 4-5% of all cancer related deaths each year (Woods *et al*, 2002). These tumours rarely metastasise but have an infiltrative and invasive nature, making surgical removal a major challenge. Pilocytic astrocytomas usually occur in adulthood but are occasionally diagnosed in children. Grade IV astrocytomas (glioblastoma multiforme) are the most malignant of all astrocytomas with a very aggressive nature and are typified by extensive vascularisation and areas of necrosis. Individuals with glioblastoma multiforme have an estimated 5 year survival of 2.7% with a mean survival time of less than a year (Sant *et al*, 2011). Approximately 15% of children with NF1 are found to have optic pathway gliomas which are rare in adults and are usually present by the age of 6. These gliomas are rarely symptomatic, but 5% result in visual impairment (Listernick *et al*, 2007). Diagnosis is difficult in children as they are unlikely to complain of defects in vision (table 1.2).

1.5.1.7 Phaeochromocytomas (PHEO)

Phaeochromocytomas (PHEO) are catecholamine-secreting tumours of the chromaffin cells of the adrenal medulla. Extra-adrenal tumours have also been identified and are known as paragangliomas (Mannelli *et al*, 2007). Germline mutations in *NF1*, *VHL*, *SDHD*, *SDHC* *SDHB* and *RET* are found in 25% of patients indicating an association

with several disorders including multiple endocrine neoplasia type 2 A or B, von Hippel-Lindau disease and NF1 (Mannelli *et al*, 2007). Recently, mutations in *TMEM127* were also identified in hereditary PHEO (Neumann *et al*, 2011). There are many reports of NF1 patients with PHEO in the literature and the incidence is estimated to be 5-10% although the underlying pathogenesis of PHEO and paragangliomas is unclear (Kramer *et al*, 2007; Erem *et al*, 2007; Mannelli *et al*, 2007; Babińska *et al*, 2008; Kobayashi *et al*, 2009). Urinary or plasma analysis of catecholamine or metanephrine in addition to MRI or CT scan of the abdomen or pelvis is required to determine the presence of PHEO. Correct diagnosis is important to prevent associated problems including cardiovascular complications (Babińska *et al*, 2008) (table 1.2).

1.5.1.8 Gastrointestinal stromal tumours (GIST)

Gastrointestinal stromal tumours (GIST) are rare mesenchymal soft tissue sarcomas which arise in the gastrointestinal tract and usually present with abdominal pain, bowel obstruction with and without perforation and gastrointestinal bleeding (Giuly *et al*, 2003). GISTs can occur sporadically or in a familial setting. In the latter case, GISTs are related to underlying mutations in the interstitial cells of Cajal (ICC) or their precursors (Yantiss *et al*, 2005). NF1 patients are known to be at an increased risk of developing GISTs with an estimated incidence of 3.9%-25% (Kramer *et al*, 2007; Hegyi *et al*, 2009). The occurrence of multiple GISTs in an NF1 patient may suggest that a subset of these patients have a germline *c-kit* mutation instead of *NF1* mutations (Yantiss *et al*, 2005). Indeed, germline mutations in *c-kit* results in a cutaneous hyperpigmented phenotype and *c-kit* somatic mutations are identified in GISTs (Yantiss *et al*, 2005). The underlying molecular mechanisms responsible for GIST development in the context of NF1 is yet to be fully established (table 1.2). Mutations in *c-kit* and *PDGFA* are rare and are likely to be late events in the development of these tumours indicating that NF1-associated GIST development is likely to be distinct from that of sporadic GISTs (Yantiss *et al*, 2005; Kang *et al*, 2007). An association of gastric carcinoid tumours with NF1 was also identified by Stewart *et al* (2007) in the absence of other predisposing factors such as pernicious anaemia.

1.5.1.9 Glomus tumours

Glomus tumours are rare benign tumours of the glomus body, a thermoregulatory shunt located in the digits which generate severe pain in response to alteration of temperature or pressure. The association of glomus tumours in the fingers and toes with NF1 has only recently been recognised (Ferner *et al*, 2007; Brems *et al*, 2009) (table 1.2).

1.5.1.10 Haematological malignancy

Juvenile myelomonocytic leukaemia (JMML) (MIM 607785) is a rare myeloproliferative disorder (MPD), clinically and cytogenetically distinct from adult chronic myeloid leukaemia with a highly variable disease course. 11% of individuals with JMML harbour germline *NF1* mutations indicating that NF1 patients have a 200-fold elevated risk of developing JMML (Stiller *et al*, 1994; Niemeyer and Locatelli, 2006) (table 1.2)

1.5.2 Nonverbal and verbal learning disabilities

Nonverbal and verbal learning disabilities have been identified in 30% to 65% of children with NF1. Deficits in IQ and motor function are well documented and suggest that abnormal expression of *NF1* or other genes commonly found to be deleted alongside the *NF1* gene may be implicated in non-syndromic mental retardation (North, *et al*, 1997; Rosser and Packer, 2003; Vedrine, 2011).

1.5.3 Non-nervous system NF1 symptoms

Other common manifestations of NF1 not associated with the nervous system defined by the consensus conference include osseous abnormalities including bone dysplasia such as sphenoid wing dysplasia and scoliosis in addition to short stature and macrocephaly (NIH, 1988).

Table 1.2 Somatic mutational events in NF1-associated benign and malignant tumours.

Tumour Type	Benign or Malignant	Underlying Somatic Mutations	Reference
Cutaneous neurofibromas	Benign	*NF1*	Chapter 3
Cutaneous neurofibromas from patients with high tumour burden	Benign	*NF1, TP53, RB1*	Chapter 3
Plexiform neurofibromas	Benign/Malignant Potential	*NF1, TP53, RB1, CDKN2A*	Chapter 3
Spinal neurofibromas	Benign	*NF1*	Upadhyaya *et al*, 2009
MPNSTs	Malignant	See chapter 6 for details	Chapter 6
Grade IV astrocytomas (glioblastoma multiforme)	Malignant- High Grade	50% *EGFR* activation	Yamazaki *et al*, 1988.
	Malignant- Low Grade	*PTEN*	
Paragangliomas and Phaeochromocytomas	Malignant	*NF1*	Mannelli *et al*, 2007; Neumann *et al*, 2011
		Tyrosine-kinases mutation	
		induction of hypoxia-inducible factor (HIF)	
		TMEM127	
Gastrointestinal Stromal Tumours	Malignant	*NF1* haploinsufficiency in ICC cells	Takazawa *et al*, 2005; Stewart *et al*, 2007
		5% *PDGFRA*	
		90-95% activating mutations in *c-kit*	
Glomus Tumours	Benign	*NF1*	Brems *et al*, 2009
Gastric Carcinoid Tumours	Malignant	*NF1, CTNNB1*	Stewart *et al*, 2007; Fujimori *et al*, 2001
JMML	Haematological Malignancy	See Table 1.5	Stiller et al, 1994; Niemeyer and Locatelli, 2006

1.6 NF1 associated syndromes

1.6.1 NF1 variant forms

There are two known NF1 variant forms including familial spinal neurofibromatosis (FSNF) (MIM 162210) and segmental NF1 (SNF1). Additionally, there are a number of syndromes with similar features to NF1 including Neurofibromatosis type 2 (NF2) (MIM 101000), familial Schwannomatosis (MIM 162091) and Watson syndrome (MIM 193520). These disorders are summarised in table 1.3.

1.6.2 The 'Ras-opathies'

The *NF1* gene is an integral part of the RasMAPK molecular signalling pathway, involved in cellular regulation and development. In addition to NF1, a number of seemingly unrelated developmental disorders have been characterised with underlying mutations in genes associated with the RasMAPK pathway (Denayer *et al*, 2008; Reviewed by Bennett *et al*, 2009) (table 1.3, table 1.4 and figure 1.2). General clinical features associated with these disorders suggest that the evolutionarily conserved RasMAPK pathway is not only important in oncogenesis but also has key roles in growth, development, cognition, the immune system and vascular development (Denayer *et al*, 2008). Diagnosis of these 'Ras-opathies' or Neuro-cardio-facio-cutaneous syndromes is complicated due to complex interactions between genes in the RasMAPK pathway which results in a high level of clinical overlap. Diagnosis cannot be based solely on clinical features and molecular characterisation is equally as difficult.

1.6.2.1 Noonan syndrome

Noonan syndrome (NS); (MIM 163950) is a clinically heterogeneous autosomal dominant disorder, although *de novo* mutations have been reported (Noonan *et al*, 1963). NS is characterised by pleomorphic features as outlined in table 1.3 and has an estimated prevalence of 1/1000-1/2500 (Noonan, 1968; Allanson, 1987). NS is often

difficult to distinguish from NF1, Leopard syndrome, cardio-facio-cutaneous syndrome and Costello syndrome. A distinctive facial phenotype as well as typical cardiac malformations is often a reliable clinical feature to aid in diagnosis, but can vary between family members and between patients with the same molecular aberration (Jorge, 2009). The underlying genetic causes of NS are outlined in table 1.3 Approximately 75% of individuals harbour mutations in *PTPN11*, *SOS1*, *KRAS*, *NRAS*, *RAF1*, *BRAF* or *MEK1*, indicating that this disorder is multifactorial with a very complex genetic basis and suggesting that additional genes responsible for this disorder remain to be identified. Additionally, mutations in *SHOC2* have recently been identified in Noonan-like syndrome with loose anagen hair (NS/LAH) (Cordeddu *et al*, 2009). The highest proportion of mutations are in the *PTPN11* gene (50%) (table 1.4), 90% of which are a small subset of missense mutations located in exons 3 and 8, which encode the N-SH2 and PTP domains. (Tartaglia *et al* 2001; Digilio, 2002; Legius, 2002). Furthermore, SHP-2 is expressed at high levels in hematopoietic cells and is required for correct haematological development, explaining the incidence of haematological abnormalities in NS including JMML, which has also been associated with NF1 (Choong *et al*, 1999; Loh *et al*, 2004; Qu *et al*, 1998).

1.6.2.2 LEOPARD syndrome

LEOPARD syndrome (LS) (MIM 151100) is a less prevalent autosomal dominant disorder labelled by Gorlin *et al* (1971) as an acronym of its principal features (table1.3). LS in children closely resembles NS and is especially difficult to diagnose as a hallmark feature; lentigines, do not appear until later in childhood. The underlying genetic basis of LS (table 1.3 and table 1.4) is similar to that of NS and the associated multiple giant cell lesion syndrome (MIM 163955) (Bertola *et al*, 2001) due to underlying *PTPN11* alterations, indicating that mutations in *PTPN11* give a broad spectrum of phenotypes. *PTPN11* mutations in LS are, however, associated with amino acids in the catalytic domain resulting in a reduction in SHP2 activity (Digilio *et al*, 2002; Legius *et al*, 2002; Kontaridis *et al*, 2006). Residual catalytic activity in the mutant SHP2 protein in LS may be sufficient to cause the overlapping clinical features of LS and NS (Oishi *et al*, 2009).

Table 1.3 NF1 variants, associated syndromes and disorders mapping to the RasMAPK pathway

Disorder	Phenotype	Causative Gene	Reference
Familial Spinal Neurofibromatosis (FSNF)	Few of the cardinal clinical features of NF1. Instead FSNF patients harbour multiple bilateral spinal tumours (section 1.5.1.5). Some patients have MPNSTs. Major spinal component of FSNF may be explained by differential impairment of neurofibromin in different progenitor cell types	Specific spectrum of *NF1* mutations: missense or splice site alterations	Kauffman *et al*, 2001; Wimmer *et al*, 2002; Kluwe *et al*, 2003; Messiaen *et al*, 2007; Fauth *et al*, 2009; Upadhyaya *et al*, 2009; Le *et al*, 2009
Segmental NF1 (SNF)	Estimated prevalence of ~0.0006% to 0.0018%, often presenting in one quarter or even half of the patients body.	Postzygotic *NF1* mutation occurring during embryogenesis, the timing of which triggers the resulting phenotype. *NF1* mutations are rarely identified in patients with SNF1; only five mutations reported to date, three of which encompassed atypical NF1 deletions (section 1.9.1.1.4).	Wolkenstein *et al*, 1995; Ingordo *et al*, 1995; Tinschert *et al*, 2000; Gottlieb *et al*, 2001; Youssoufian & Pyeritz, 2002; Redlick and Shaw, 2004; Consoli *et al*, 2005; Maertens *et al*, 2007; Kehrer-Sawatzki & Cooper, 2008; Erickson, 2010; Messiaen *et al*, 2011;
Neurofibromatosis Type 2 (NF2)	Affecting about 1 in 25,000. Hallmark feature of NF2 is Schwannomas, generally benign, encapsulated tumours which consist of Schwann cells alone and occur on or around the vestibular branches of both auditory nerves and even in the dermis	*NF2* gene (110 kb) which encodes Merlin (Schwannomin) tumour suppressor gene sporadic *NF2* mutations do occur	Trofatter *et al*, 1993; Rouleau *et al*, 1993; Huson and Hughes, 1994; Kluwe *et al*, 1996; Gutmann *et al*, 1997; Friedman *et al*, 1999; Korf & Rubenstein, 2005
Schwannomatosis	Difficult to distinguish from NF2. Incidence of approximately 1 in 30,000. Development of Schwannomas which do not occur on the vestibular nerve	Tumour suppressor gene *INI1/SMARCB1*, Somatic *NF2* have also been identified	MacCollin *et al*, 2003; Korf and Rubenstein, 2005; MacCollin *et al*, 2005; Hulsebos *et al*, 2007

Disorder	Phenotype	Causative Gene	Reference
Watson Syndrome	Clinical features reminiscent of both NF1 and Noonan syndrome. Lower frequency of CALs, Lisch nodules and neurofibromas, short stature, cognitive impairment and pulmonary stenosis with a distinct lack of other NF1 complications	Linkage between Watson syndrome and NF1 flanking markers and an 80-kb NF1 deletion have been reported	Watson, 1967; Allanson *et al*, 1991; Upadhyaya *et al*, 1992; Tassabehji et al, 1993; Ruggieri and Huson, 1999;
Noonan Syndrome	Congenital heart disease, facial dysmorphism, short stature, skeletal defects, cognitive deficits and haematological abnormalities.	*PTPN11, SOS1, RAF1, MEK1, KRAS, NRAS, BRAF*	Noonan, 1968; Allanson, 1987; Tartaglia *et al* 2001; Schubbert *et al*, 2006; Roberts *et al*, 2007; Razzaque *et al*, 2007; Pandit *et al*, 2007
Noonan-like syndrome (NS/LAH)	Loose anagen hair	*SHOC2*	Mazzanti *et al*, 2003; Cordeddu *et al*, 2009
LEOPARD Syndrome	Lentigines, electrocardiographic abnormalities, ocular hypertelorism, pulmonary valve stenosis, abnormal genitalia, retardation of growth and deafness.	*PTPN11, RAF1*	Digilio *et al*, 2002; Legius *et al*, 2002; Kontaridis *et al*, 2006
Legius Syndrome	NF1-Like Syndrome: café au lait macules, axillary freckling, mild neurocognitive impairment and macrocephaly	*SPRED1*	Brems *et al*, 2007, Pasmant *et al*, 2009, Spurlock *et al*, 2009
Costello Syndrome	Macrocephaly, cutis laxa, nasal and perioral papillomata, deep palmar and plantar creases, diffuse skin hyperpigmentation and nail dysmorphology. Increased risk of malignancy: rhabdomyosarcoma, transitional-cell carcinoma and neuroblastoma.	*HRAS* (c.34G>A; pG12S and p.G12A), *KRAS, BRAF, MEK1*	Costello, 1971; Costello, 1977; Gripp, 2005; Nava, 2007
Cardio-facio-cutaneous Syndrome	Craniofacial dysmorphology, ectodermal anomalies and cardiac defects. Coarse face, congenital heart defects, ectodermal anomalies (follicular and palmar hyperkeratosis), short stature, mental retardation (moderate to severe). Facial features reminiscent of NS and Costello syndrome.	*KRAS, BRAF, MEK1, MEK2, SOS1*	Rodriguez-Viciana *et al*, 2006; Schubbert, 2006; Schubbert *et al*, 2007; Niihori *et al*, 2006;

Table 1.4 Ras pathway related genes and their function

Gene	Gene Function	Location	Related Disorders
PTEN	**Acts as a dual specificity protein phosphatase** (Tumour suppressor) Negatively regulates AKT/PKB signalling pathway	10q23.3	Leopard Syndrome
PTPN11	**Protein Tyrosine Phosphatase.** encodes SHP-2, a Src homology-2 (SH2)-containing protein tyrosine phosphatase (PTP) Regulates cellular processes: cell growth, differentiation, mitotic cycle, and oncogenic transformation.	12q24	Noonan Syndrome, Acute Myeloid Leukaemia and Leopard Syndrome
SOS1	**Guanine nucleotide exchange factor for RAS (GEF)** Regulates Ras by facilitating the exchange of GTP for GDP.	2p22-p21	Gingivival fibromatosis type 1 and Noonan syndrome
BRAF	**Serine/threonine protein kinase.** Regulates MAP kinase/ERK signalling pathway: affects cell division, differentiation, secretion.	7q34	Cardio-facio-cutaneous syndrome and Costello Syndrome.
RAF1/CRAF	**MAP kinase kinase kinase (MAP3K)** functions downstream of the Ras family of membrane associated GTPases to which it binds directly Role in the control of gene expression, involved in cell division, apoptosis, cell differentiation and cell migration	3p25	Noonan Syndrome and Leopard Syndrome
HRAS	**Protein member of the GTPase superfamily.** Intrinsic GTPase activity. Functions in signal transduction pathways by binding to GTP and GDP.	11p15.5	Costello Syndrome

Gene	Gene Function	Location	Related Disorders
KRAS	**Protein member of the GTPase superfamily.** Intrinsic GTPase activity. Functions in signal transduction pathways by binding to GTP and GDP.	12p12.1	Leopard Syndrome, Noonan Syndrome, Cardio-facio-cutaneous Syndrome and Costello Syndrome
MAP2K1 / MEK1	**Dual specificity mitogen activated protein kinase.** Involved in cellular processes: proliferation, differentiation, transcription regulation and development.	15q22.1-q22.33	Cardio-facio-cutaneous syndrome, Noonan Syndrome and Costello Syndrome.
MAP2K2 / MEK2	**Dual specificity mitogen activated protein kinase 2** Critical role in mitogen growth factor signal transduction.	19p13.3	Cardio-facio-cutaneous syndrome
SMARCB1	**SWI/SNF related, matrix associated, actin dependent regulator of chromatin, subfamily b, member 1.** (tumour suppressor) Relieves repressive chromatin structures, allowing the transcriptional machinery to access its targets more effectively.	22q11	Malignant Rhabdoid Tumours
PI3Kγ	**pi3/pi4-kinase family of proteins.** Modulator of extracellular signals: elicited by E-cadherin-mediated cell-cell adhesion. Role in maintenance of the structural and functional integrity of epithelia and promoting assembly of adherens junctions.	7q22.3	Myeloid Leukaemia
SPRED1	**SPROUTY/SPRED family of proteins.** Tyrosine kinase substrates. Functions in the RasMAPK pathway between Ras and Raf, as a negative regulator of Ras	15q14	Legius Syndrome

1.6.2.3 Legius syndrome (Neurofibromatosis Type 1 like syndrome)

Patients with a clinical diagnosis of NF1 have been reported who exhibit a pigmentary phenotype and who do not develop any tumour related complications, usually clinically classified as 'autosomal dominant, café au lait spots only'. This phenotype is reminiscent of individuals harbouring c.2970–2972 delAAT p.990delM mutation in exon 17 of the *NF1* gene in which all patients exhibit the same pigmentary phenotype (Upadhyaya *et al*, 2007). Recently, however, mutations in the *SPRED1* gene have been identified in patients with this same phenotype and this disorder has been newly designated as Legius syndrome (MIM 611431) (figure 1.2 and table 1.3, table 1.4), an autosomal dominant disorder with many phenotypic characteristics in common with individuals with NF1 but no occurrence of Lisch nodules of the iris or tumours of the peripheral nervous system such as neurofibromas (Brems *et al*, 2007, Pasmant *et al*, 2009, Spurlock *et al*, 2009; Messiaen *et al*, 2009). Some individuals have even been described as having facial features reminiscent of individuals with NS demonstrating that especially in younger children, Legius syndrome is difficult to distinguish from NF1 and other disorders of the RasMAPK pathway (Brems *et al*, 2007). It is still currently unclear whether individuals with mutations in *SPRED1* are at an increased risk of developing cancer as is observed in patients with NF1.

1.6.2.4 Costello syndrome

The cardinal clinical features of Costello syndrome (MIM 218040) are outlined in Table 1.3. (Costello, 1971, 1977; Nava, 2007). Clinically overlapping phenotypic features in patients with Costello syndrome make it difficult to distinguish from that of NS and CFC, especially in new-borns. As the individual matures, the features become more pronounced and distinctive. Individuals with Costello syndrome are also at an increased risk of developing tumours (Gripp, 2005). 80% of identified mutations in Costello syndrome are heterogeneous *HRAS* germline mutations, which are not present in CFC syndrome (Estep *et al*, 2006; van Steensel *et al*, 2006; van der Burgt *et al*, 2007; Zampino *et al*, 2007; Gripp *et al*, 2008; Lo *et al*, 2008; Schulz *et al*, 2008) (table 1.4).

1.6.2.5 Cardio-facio-cutaneous syndrome (CFC)

Individuals with cardio-facio-cutaneous syndrome (CFC) (MIM 115150) Blumberg *et al* (1979) have many features which overlap with those of both NS and Costello syndromes, although a distinguishing feature of CFC is the occurrence of neurological abnormalities which are not present in individuals with NS (Yoon *et al*, 2007) (table 1.3). Unlike with NS and Costello syndromes, it is not clear whether individuals with CFC are at an increased risk of developing benign and malignant tumours. There have been instances recorded in the literature of individuals with CFC with *BRAF* and *MEK1* mutations and acute lymphoblastic leukaemia and a hepatoblastoma (Van den Burg *et al*, 1999; Gripp *et al*, 2005; Makita *et al*, 2007; Al-Rahawan *et al*, 2007). Mutations in at least four genes (*KRAS, BRAF, MEK1, MEK2*) have been characterised in CFC (table 1.4) (Upadhyaya *et al*, 2010). *M*ore recently *SOS1* has also been recognised as having a potential role in CFC (Bennett *et al*, 2009).

1.6.3 Association of NF1 with other syndromes

A number of syndromes have been identified which may have an association with NF1, although in many cases the co-occurrence may be purely coincidental and in other disorders there is a proven association. Furthermore there are a few disorders in which the underlying causes are in genes associated with the RasMAPK pathway. These disorders are detailed in table 1.5.

Table 1.5. Reported potential association between NF1 and other disorders

Disorder	Phenotype	Causative Gene	Reference
Tuberous Sclerosis	Hamartomas in multiple body systems, most commonly; the brain, kidneys, skin, heart and lungs. Neurological abnormalities, renal angiomyolipomas (AMLs) and pulmonary LAM (lymphangioleiomyomatosis).	*TSC1* MIM 191100, *TSC2* MIM 613254	Carsillo *et al*, 2000
MoyaMoya Disease (MIM 252350)	Chronic occlusive cerebrovascular disorder. Steno-occlusive changes in the circle of Willis. In children; transient ischaemic attacks and cerebral infarction. In adults; intracerebral, intraventricular or subarachnoid haemorrhages. Headaches and seizures occur in both adults and children.	17q25	Ohaegbulam, 2001; Tonsgard, 2006
HNPCC (Lynch Syndrome) (MIM 120435)	Early onset development of multiple tumours of the colon. Extra colonic cancer including endometrial, ovarian and urinary tract cancers.	*MLH1, MSH2, MSH6, PMS2.*	Lynch & de la Chapelle, 2003; Lynch et al, 2008; Boland *et al*, 2008
Juvenile myelomonocytic leukaemia JMML (MIM 607785)	Haematological Malignancy. Hypersensitivity to granulocyte–macrophage colony-stimulating factor (GM-CSF).	*NF1, NRAS, KRAS, PTPN11, BCR-ABL1* fusion gene (36%)	Kalra *et al*, 1994; Bader-Meunier *et al*, 1997; Niemeyer *et al*, 1997; Flotho *et al*, 1999; Flotho *et al*, 2007
Retinoblastoma (MIM 180200)	Unilateral/bilateral retinoblastomas	*RB1*	Friend *et al*, 1986; Nicholas *et al*, 2005; Broaddus *et al*, 2009

Disorder	Phenotype	Causative Gene	Reference
CMT	Weakness and atrophy of the distal muscle groups of the limbs, gait disturbance, impaired sensation in the hands and feet, decreased and/or absent deep tendon reflexes, and skeletal deformities including pes cavus and hammer toes.	CMT1A: *PMP-22;* CMT1B: myelin protein zero gene (MPZ) on chromosome 1.	Lupski *et al*, 1993; Pareyson *et al*, 1999; Berciano *et al*, 2003; Lancaster *et al*, 2010
Hereditary gingival fibromatosis (HGF) (MIM 135300)	Slow but progressive benign overgrowth of the keratinized gingiva.	*SOS1*	Hart *et al*, 1998; Hart *et al*, 2002
Capillary malformation–arteriovenous malformation (CM–AVM) (MIM 608354)	Arteriovenous malformations and fistulas. AVMs in skin, muscle, bone, heart and the brain.	*RASA1*	Eerola *et al*, 2003; Boon *et al*, 2005; Revencu *et al*, 2008
Autoimmune lymphoproliferative syndrome (ALPS) (MIM 601859)	Defective lymphocyte apoptosis, accumulation of non-malignant lymphocytes and increased risk of developing haematological malignancies.	CD95 pathway, *NRAS* (p.G13D), Loss of BCL-2-interacting mediator of cell death (*BIN*).	Oliveira *et al*, 2004; Bidere *et al*, 2006; Oliveira *et al*, 2007
Carney Complex (MIM 160980).	Neoplasias involving the heart, central nervous system and endocrine organs including schwannomas, cardiac myxomas, psammomatous melanotic schwannoma (PMS), acromegaly, large cell calcifying sertoli cell tumour (LCCSCT), thyroid carcinoma or nodule & breast adenoma. Cutaneous pigmentation abnormalities and mucosal lesions.	*PRKAR1α, p16*	Carney *et al*, 1986; Stratakis *et al*, 2001; Sandrini *et al*, 2003

1.7 NF1 tumour suppressor function

1.7.1 NF1 and tumour development

The idea of tumour suppressor genes was derived from both investigations of the familial incidence of retinoblastoma and cell-fusion experiments. Whilst many have contributed to the identification of mechanisms by which heritable tumours develop, the seminal two hit hypothesis for tumour suppressor genes (Knudson, 1971), eloquently explains the occurrence of the primary pathologies associated with NF1 tumours. Following loss of function of the *NF1* tumour suppressor gene, there is an associated increase in signalling through the RasMAPK pathway and its related signalling cascades (section 1.4). Individuals with NF1 are born with an *NF1* germline mutation resulting in loss of function of one *NF1* allele, leaving only one wild type copy of the *NF1* gene. The second hit hypothesis (Knudson, 1971), when applied to NF1 implies that NF1-associated pathologies arise as a result of a second mutational event causing somatic cell inactivation of the remaining wild type allele of the *NF1* gene and resulting in complete loss of *NF1* tumour suppressor function. Indeed, molecular analysis of tumour derived Schwann cells; the main cell constituent of neurofibromas demonstrates biallelic inactivation of the *NF1* gene resulting in tumorigenesis through aberrant Schwann cell proliferation (Serra *et al* 2001).

The nature of the cell type and the germ layers from which the cells are derived contribute to the different NF1 pathologies. Different benign and malignant NF1-associated tumours, for example, arise from cells of the neural crest including: *NF1* inactivation in Schwann cells which gives rise to the formation of neurofibromas, pheochromocytomas are a result of a second hit in chromaffin cells and pigmentary abnormalities including café-au-lait macules are caused by *NF1* loss in melanocytes (Zhu *et al*, 2002; Le and Parada, 2007). Furthermore the cells of the germ layer such as the skin-derived precursors (SKPs) (section 1.7.5) give rise to cutaneous neurofibromas, myelomonocytic leukaemia develops in myeloid cells and astrocytomas develop as a result of *NF1* inactivation in glial cells (Largaespada *et al*, 1996; Bajenaru

et al, 2003; Le and Parada, 2007; Yang *et al*, 2008; Le *et al*, 2009). Many questions remain unanswered, however, including the exact underlying mechanisms involved in the development of NF1 associated tumours, and whether other genetic modifiers are implicated in malignant progression.

1.7.2 Schwann cells and the peripheral nervous system (PNS)

The development of peripheral nerves requires co-operation from three distinct cell types; peripheral neurons, Schwann cells and fibroblasts. Schwann cells are the principle glial cells of the PNS, of which there are two well characterised types; myelinating and non-myelinating Schwann cells. A further class of non-myelinating Schwann cell, the terminal Schwann cell (TSC), also exists at the neuromuscular junction. Myelinating Schwann cells form part of the lipid rich myelin sheath which wraps around long segments of axons with a multilayered sheath of extended membrane. This forms a complex seal with the axon surface thereby defining the nodes of Ranvier at the junctions between adjacent Schwann cells. Myelination is important for a reduction in energy consumption and most importantly, an increase in the velocity of axonal conduction (Salzer, 1997). Non-myelinating Schwann cells (Remak cells), form Remak bundles by engulfing small-calibre C fibre axons which are involved in relaying pain signals and have the potential to myelinate, if given the appropriate signals (Griffin and Thompson, 2008). In normal nerves, these non-myelinating cells vastly outnumber the myelinating Schwann cells. The development of the Schwann cell lineage involves transition from migrating neural crest cells to Schwann cell precursors (SCPs) (glial restricted progenitor cells) and finally to the myelinating and non-myelinating mature Schwann cells (figure 1.4) (Jessen and Mirsky, 2005). Schwann cells, Remak cells and their respective precursors rely on neuregulin-1 type III, an axonal growth factor for their survival, proliferation and terminal differentiation (Nave and Salzer, 2006).

1.7.3 Schwann cells and NF1 tumorigenesis

The vast majority of tumours which arise in the PNS are derived from Schwann cells or their precursors (Urich and Tien, 1998). In the case of individuals with NF1, or the rarer disorders; NF2, Schwannomatosis or Carney Complex syndrome (section 1.6.3), such patients are at an increased risk of developing peripheral nerve sheath tumours in comparison to the general population. NF1-associated peripheral nerve sheath tumours are composed of a highly heterogeneous mixture of cellular subtypes (figure 1.5). These include: Schwann cell-like elements ("Schwann cells") which are p75 and S100b immunoreactive, mast cells, fibroblasts, vascular elements, perineurial-like cells which are characterised by long thin cytoplasmic processes, several pinocytotic vesicles, and a discontinuous basal lamina but lack the normal immunoreactivity of perineurial cells. Furthermore, there are also CD34-immunoreactive dendritic cells which were postulated to represent a novel nerve sheath cell type or may instead be macrophages (Weiss and Nickoloff, 1993; Cohen *et al*, 1993). It is now clear, however, that only Schwann cells harbour the *NF1* inactivating second hit in NF1-associated peripheral nerve sheath tumours (section 3.1).

1.7.4 NF1 Schwann cell culture

It is clear that the heterogeneity of cell types in neurofibromas extends to that of the Schwann cells as both $NF1^{+/-}$ and $NF1^{-/-}$ Schwann cells are present in neurofibromas. Recently a culture technique was developed which is capable of distinguishing between the two populations (section 2.1.3) (Serra *et al*, 2000; Rosenbaum *et al,* 2000; Maertens *et al*, 2006).

1.7.5 Skin-derived precursors (SKPs)

The precise cell type within the Schwann cell lineage that is responsible for neurofibroma formation has been a major subject of debate. Schwann cell precursors, immature Schwann cells, or mature Schwann cells have all been touted as the cell type

which may have the potential to give rise to neurofibromas. It is thought that there is a dual origin for the development of plexiform neurofibromas and cutaneous neurofibromas due to the way in which they are separated both temporally and spatially (Lu *et al*, 2009). Evidence for two distinct origins for such tumours comes from mouse models in which plexiform neurofibromas develop but the models fail to give rise to dermal tumours (Cichowski *et al*, 1999; Joseph *et al*, 2008; Vogel *et al*, 1999; Wu *et al*, 2008; Zheng *et al*, 2008; Zhu *et al*, 2002) (section 1.8). Following the identification of adult tissue stem cells, it was postulated that such cells may be the source of neurofibroma formation. Skin-derived precursors (SKPs) represented an attractive prospect for the origin of neurofibromas. SKPs are neural crest-like pluripotent stem cells, located in both the human and mouse dermis, which are capable of differentiating in both the neuronal and glial cell lines (Toma *et al*, 2001; Toma *et al*, 2005; Miller *et al*, 2005; Fernandes *et al*, 2006; McKenzie *et al*, 2006; Lu *et al*, 2009). The suggestion that somatic stem cells or their progenitors are the cells of origin of neurofibromas is important. This stem cell model of tumorigenesis has important implications for understanding early cellular events that dictate neurofibromagenesis, in addition to other tumour types. Furthermore, viewing NF1 as a disease of stem and progenitor cells has important implications for the development of NF1 associated therapy (Le *et al*, 2011).

1.7.7 NF1 haploinsufficiency and the tumour micro-environment

Whilst Schwann cells derived from peripheral nerve sheath tumours have been determined to harbour complete loss of *NF1*, the other constituents of these tumours such as the fibroblasts and mast cells retain one functional copy of the *NF1* gene. The consequence of this haploinsufficiency has been well studied in recent years and it has been concluded that tumour formation also requires *NF1* haploinsufficiency of the tumour microenvironment (Caroll and Ratner, 2008). Indeed, in the conditional knockout murine model of NF1, mice did not develop any neurofibromas and loss of *Nf1* in SKPs was demonstrated to be required but not sufficient to induce tumours (Zhu *et al*, 2001; Zhu *et al*, 2002) (section 1.8.4.2). This suggested that tumour formation was subject to

haploinsufficiency in the surrounding tumour microenvironment (Lu *et al*, 2009). Mast cells and other inflammatory cells are capable of infiltrating neurofibromas in large numbers indicating that inflammatory cells may be involved in the pathogenesis of NF1 tumours (Greggio, 1911). Schwann cells secrete high levels of stem cell factor (SCF), a ligand for the c-kit receptor tyrosine kinase on mast cells which is required to promote maturation, activation, survival and migration of mast cells (Demitsu *et al*, 1998; Hirota *et al*, 1993; Ryan *et al*, 1994).

Loss of neurofibromin enhances SCF secretion as $Nf1^{-/-}$ Schwann cells have been found to secrete up to 6-fold more SCF than both wild type and $Nf1^{-/+}$ Schwann cells (Yang *et al*, 2003). Activation of the c-KIT receptor is thought to result in the activation of the RasMAPK and downstream effector pathways including P13K, generating VEGF, TGFβ, NGF and MMPs which aid in propagation of mast cell proliferation, growth and survival (Hirota *et al*, 1993; Ingram *et al*, 2000, 2001; Yang *et al*, 2008). Furthermore, $Nf1^{+/-}$ mast cells which have been stimulated by SCF can alter the activity of $Nf1^{+/-}$ fibroblasts, another major cellular component of neurofibromas. Higher levels of TGF-β are secreted by the $Nf1^{+/-}$ mast cells and in response to this, fibroblasts are promoted to migrate, proliferate and synthesise collagen (Yang *et al*, 2006). This suggests that *NF1* haploinsufficiency modulates the fate of inflammatory cells such as mast cells in the tumour microenvironment and that haploinsufficiency, in conjunction with $NF1^{-/-}$ Schwann cells is required for the initial stages of NF1-associated neurofibroma formation. This hypothesis would, however, not apply to sporadic neurofibromas (Caroll and Ratner). Furthermore, a recent proposed model for development of cutaneous neurofibromas suggests that they are associated with hair and subcutaneous fat. Multipotent $NF1^{-/-}$ cells in these tissues may be a major source of neurofibroma-derived progenitors which can give rise to the different cell types found in cutaneous neurofibromas (Jouhilahti *et al*, 2011)

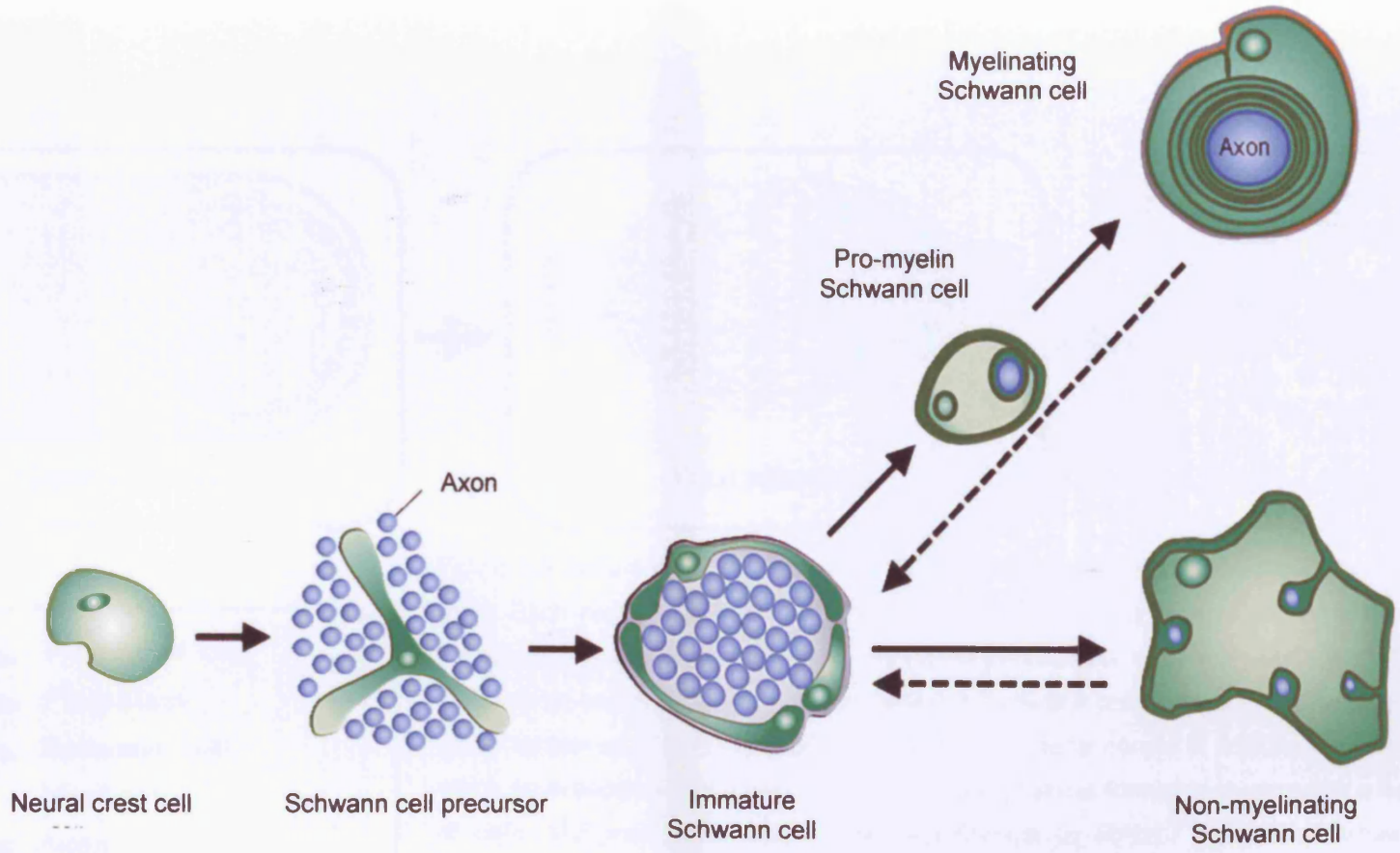

Figure 1.4. *Schematic illustration of the main cell types and developmental transitions involved in Schwann cell development* .The embryonic phase of Schwann cell development involves three transient cell populations. (i) Migrating neural crest cells, (ii) Schwann cell precursors (SCPs) which express differentiation markers that are not found in migrating neural crest cells (brain fatty acid-binding protein (BFABP), protein zero (P0) and desert hedgehog (DHH)) and (iii) immature Schwann cells. The fate of these immature Schwann cells is considered to be the same. Their developmental potential is therefore determined by the axons with which they associate. Adapted from Jessen and Mirsky (2005).

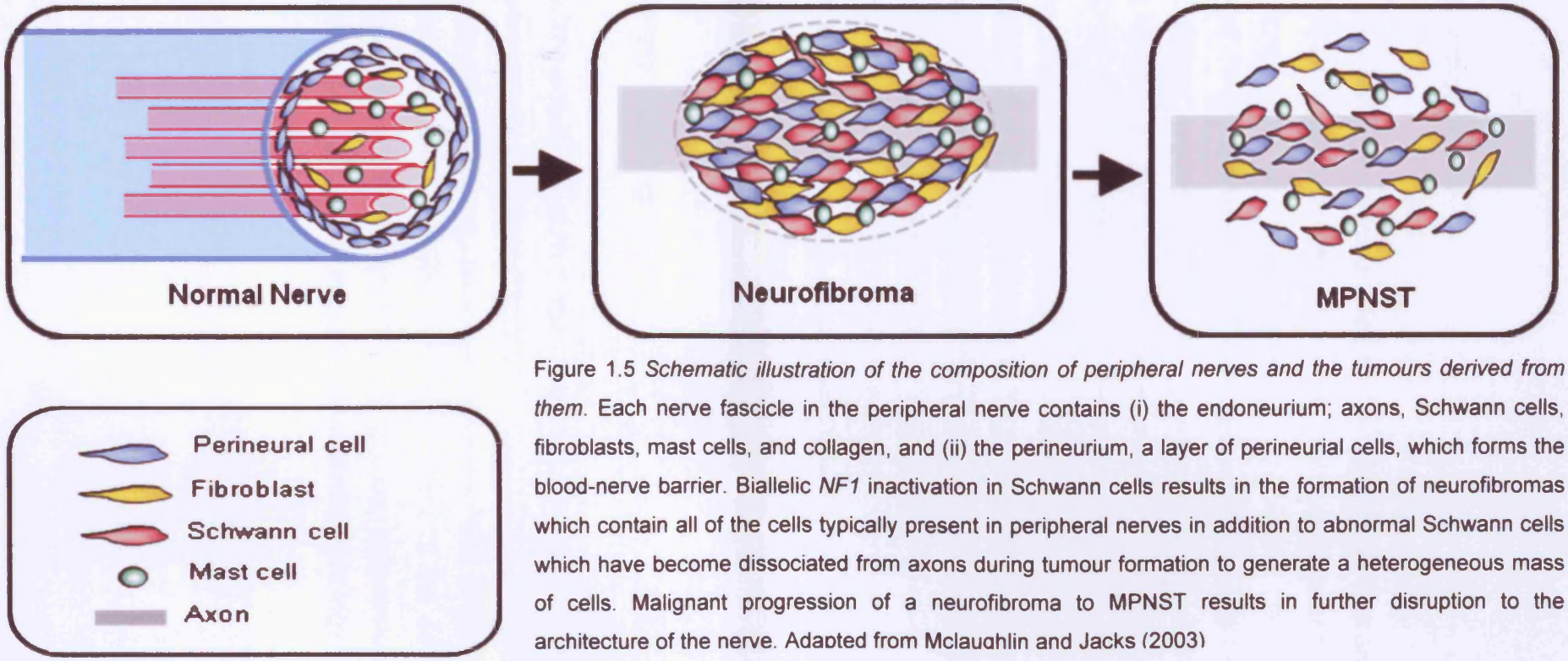

Figure 1.5 *Schematic illustration of the composition of peripheral nerves and the tumours derived from them.* Each nerve fascicle in the peripheral nerve contains (i) the endoneurium; axons, Schwann cells, fibroblasts, mast cells, and collagen, and (ii) the perineurium, a layer of perineurial cells, which forms the blood-nerve barrier. Biallelic *NF1* inactivation in Schwann cells results in the formation of neurofibromas which contain all of the cells typically present in peripheral nerves in addition to abnormal Schwann cells which have become dissociated from axons during tumour formation to generate a heterogeneous mass of cells. Malignant progression of a neurofibroma to MPNST results in further disruption to the architecture of the nerve. Adapted from Mclaughlin and Jacks (2003)

1.8 Mouse models

Animal models are of great importance to the study of genetic diseases such as NF1, providing the ability to study the natural history of a disease and the function of genes during embryogenesis and fetal development due to the relatively short lifespan of animals used. Animal models also generate new insight into the mechanisms of tumour formation, cellular regulation, and the relationship between mutations. Genotype-phenotype correlations and interacting pathways which underlie molecular mechanisms responsible for malignancy can also be studied. Importantly animal models provide a subject in which to study the *in vivo* effects of potential therapies for NF1 manifestations. There are, however, some disadvantages of animal models such as the size of smaller mammals which precludes the use of some surgical techniques and the cost, time and space needed to maintain the colonies of animals. These disadvantages are, however, far outweighed by the benefits and possibilities offered by animal models. In addition to *Drosophila* models of cognitive defects in NF1 and a number of naturally occurring NF1 animal tumour models, various different strategies have been developed to generate complex murine models of NF1:

1.8.1 Naturally occurring

Phenotypic characteristics of NF1 have been found to naturally occur in a wide variety of vertebrates including bicolour damselfish (*Pomacentrus partitus),* dogs, chickens and Holstein cattle (Goedegeburre, 1975; Schmale *et al*, 1983; Sartin *et al*, 1994 Reviewed by Riccardi *et al*, 1994). In such vertebrates, there is the development of isolated symptoms such as individual neurofibromas, gliomas, schwannomas and what appear to be Lisch nodules. All these features have similar histology to those observed in humans.

1.8.2 Chemically induced

Mutagenic and oncogenic agents have been successfully used to recapitulate tumour disorders in small mammals such as rats and mice. Using transplacental prenatal exposure to agents such as nitrosourea (ethyinitrosourea), neoplasms which are associated with NF1 can be generated (Cardesa *et al*, 1978; Nakamura *et al*, 1989). Prenatal exposure therefore may be capable of generating both germline and somatic mutations resulting in tumour formation (Riccardi *et al*, 1988). Genotoxic therapy induced tumours are a complication of cancer treatment in humans and this has also been investigated in mouse models of NF1. Mutagen exposed (radiation and cyclophosphamide) $Nf1^{+/-}$ mice develop secondary cancers that also occur in humans (Chao *et al*, 2005).

1.8.3 Targeted disruption

1.8.3.1 The *Nf1* heterozygote

The first *Nf1* knockout mouse was generated by Jacks *et al* (1994) and Brannan *et al* (1994). This mouse harboured a targeted disruption of exon 31 of the *Nf1* gene ($Nf1^{+/n31}$) which resulted in NF1 protein instability. Crucially, it was seen that compared to mice carrying the wild type *NF1* gene, heterozygous mice were predisposed to forming numerous cancers following their first year. This resulted in a shorter life expectancy and development of NF1-associated pathologies found in humans including pheochromocytomas and myeloid leukaemia which arose following LOH of the remaining wild type *Nf1* allele (Jacks *et al* 1994; Brannan *et al* 1994). The remaining hallmarks of NF1 identified in NF1 patients such as neurofibromas, Lisch nodules, or CAL macules, never arose in such mice. This suggested that the genetic background of these mice led to a decrease in the likelihood of a second-hit occurring especially as NF1 patients who only carry one functional copy of the *NF1* gene usually develop relatively ubiquitous symptoms. Although the $Nf1^{+/-}$ mouse model does not generate any additional information for those wishing to study neurofibroma development, the model

is not a complete failure as many studies have used it to investigate other pathologies associated with *Nf1*$^{+/-}$ cell lineages such as Schwann cells, fibroblasts, vascular cells, and hematopoietic cells.

Unfortunately, developing mice with a deletion of the *Nf1* gene resulting in mice which are homozygous for the *Nf1* gene (*Nf1*$^{-/-}$) is extremely difficult as such mice die at embryonic day 13.5, part way through the 19-20 day embryogenesis of a mouse. It has been found that these mice die as a result of defects in cardiac development resulting in the generation of a double outlet right ventricle due to the requirement for *Nf1* in the endothelial cells during the development of the endocardial cushion. This indicates that *Nf1* is required for normal embryonic development as has been found in the majority of other studied tumour suppressor genes (Brannan *et al*, 1994; Jacks *et al*, 1994).

1.8.3.2 The *Nf1* chimera

Cichowski *et al* (1999) developed a murine model to determine the tumour suppressor function of *Nf1* and to identify whether LOH precedes tumour formation. *Nf1*$^{-/-}$ chimeric mice were produced by injecting *Nf1*$^{-/-}$ embryonic stem (ES) cells into wild-type blastocysts. Only about 60% of the mice generated had the appropriate level of chimerism required to elicit survival and the desired phenotypic effect. The remaining mice developed myelodysplasia, neuromotor defects and importantly neurofibroma formation along multiple nerves with features reminiscent of the human tumours (Cichowski *et al*, 1999). It was indicated that tumour formation in these mice required *Nf1* nullizygosity based on the relatively uniform expression of a β-galactosidase transgene in these tumours (Cichowski *et al*, 1999). Advantages to this model included important evidence for *Nf1* tumour suppressor function and an indication that neurofibromas are derived from Schwann cells. It was still unclear; however what was the precise nature of the cell of origin for neurofibromas and what genetic and cellular conditions are required for tumour formation.

1.8.3.3 Genetic cooperativity

The close proximity of *NF1* and *p53* on both human and mouse chromosomes indicates that dual loss of two such tumour suppressor genes may cooperate to accelerate tumorigenesis. *Nf1* deficient mutant mice have therefore been generated which have been crossed with mice harbouring *p53* deficiencies in both the linked (*cis*) and unlinked (*trans*) configuration of mutant alleles (Cichowski *et al,* 1999; Vogel *et al*, 1999; Reilly *et al*, 2000). It was observed that the *cis* configuration in which both of the tumour suppressor mutations were in linkage with each other, resulted in a significantly more severe tumour phenotype. This included the development of aggressive MPNSTs and malignant astrocytomas between 6 and 12 months of age, most likely due to the loss of the majority of chromosome 11 which carries both *p53* and *Nf1*. Mice with the *cis* configuration had a more severe phenotype than mice harbouring mutations in *trans* or with only a single gene mutated (Cichowski *et al*, 1999; Vogel *et al*, 1999; Reilly *et al*, 2000). Interestingly, the genetic background of the mice affected the penetrance of NF1-associated pathologies indicating that variable expression of *NF1* is related to additional genetic modifications (Reilly *et al*, 2000, Reilly *et al*, 2004; Reilly *et al*, 2006).

1.8.3.4 Mouse models of myeloid malignancies associated with NF1.

Children with NF1 show a 200-500 fold increased likelihood of developing myeloid malignancies, namely JMML (section 1.6.3) (Bader-Meunier *et al*, 1999). A subset of children with NF1 who have undergone therapy involving alkylating agents in the treatment of anaplastic astrocytoma, glioblastoma, Wilms' tumour, or acute lymphoblastic leukaemia have developed AML (Maris *et al*, 1997). Mahgoub *et al* (1999) therefore tried to recapitulate this form of disease progression by treating $Nf1^{+/-}$ mice with alkylating agents. It was found that in the $Nf1^{+/-}$ mice, cyclophosphamide but not the topoisomerase II inhibitor etoposide is capable of inducing a myeloproliferative disorder (MPD) (Mahgoub *et al*, 1999). This mouse model could therefore help in further study of how alkylating agents induce leukaemia.

1.8.3.5 Mouse models of astrocytoma and optic glioma formation

Individuals with NF1 are at a higher risk of developing pilocytic astrocytomas, frequently associated with the optic nerve (section 1.5.1.6) and *Nf1*$^{+/-}$ mice have been found to have a 1.6-fold increase in astrocyte proliferation (Gutmann *et al*, 1999). *Nf1*$^{+/-}$ mice demonstrate that *Nf1*$^{+/-}$ astrocytes display a cell-autonomous increase in cellular proliferation and also demonstrate other genetic events including loss of *p53* and *RB1*. These mice are susceptible to cancer but don't develop gliomas. Mice with an *Nf1* conditional knockout in astrocytes were therefore developed using Cre/LoxP technology on embryonic day 14 (Bajenaru *et al*, 2002). These mice have increased numbers of astrocytes but still do not develop gliomas indicating that additional genetic inactivation or cellular components are required in the formation of these tumours. Therefore, *Nf1*$^{+/-}$ mice were generated which a conditional *Nf1* inactivation in astrocytes and these models successfully develop low-grade optic nerve and chiasm astrocytomas and so may represent a preclinical model (Bajenaru *et al*, 2003; Bajenaru *et al*, 2005).

1.8.3.6 Models of learning and memory deficits associated with NF1

Silva *et al* (1997) studied *Nf1*$^{+/-}$ mice (Jacks *et al*, 1994) using the Morris water maze which is specifically designed to test regions of the hippocampus in which *NF1* is highly expressed (Nordlund *et al*, 1995). *Nf1*$^{+/-}$ mice were found to exhibit defects in spatial learning and memory, traits which are also identified in NF1 patients (Silva *et al*, 1997). Repetition of trials improved mouse learning deficits indicating that this may be an important strategy for the treatment of learning abnormalities in NF1 patients (Silva *et al*, 1997). Furthermore, in *Nf1*$^{(+/-)}$ mice which were heterozygous for *Nmdar1* (*Nmdar1*$^{+/-}$) targeted disruption of *Nmdar1* had no affect by itself. In combination with heterozygous *Nf1*, it served to exacerbate the spatial learning and memory deficits of the *Nf1*$^{+/-}$ mice (Silva *et al*, 1997). In *Nf1*$^{+/-}$ mice crossed with mice heterozygous for a null mutation in the *K-ras* gene (*K-ras*$^{+/-}$,129T2/SvEmsJ), the *K-ras*$^{+/-}$ mutation can rescue learning deficits due to elevated levels of Ras. *Nf1*$^{+/-}$ mice can also be rescued with pharmacological intervention (Johnson *et al*, 1997 Costa *et al*, 2002).

1.8.4 Transgenic

1.8.4.1 Conditional *Nf1* knockout

Following earlier failed attempts to generate conditional $Nf1^{-/-}$ using homologous recombination, Cre-recombinase mediated gene deletion was utilised with *loxP* sites flanking exon 31 and 32 of *Nf1* (*Nf1flox/flox*) to create a conditional knockout murine model of NF1 (Zhu *et al*, 2001; Zhu *et al*, 2002). The *Nf1flox/flox* mice were then crossed with mice expressing Cre protein under control of the Krox20 promoter (Krox20cre) which specifically promotes transcription in 5-10% of Schwann cells removing the problem of embryonic lethality in an $Nf1^{-/-}$ mouse. The *Nf1flox/flox*; Krox20cre mouse, did not, however, develop any neurofibromas providing pivotal evidence for an important role for not only loss of *Nf1* in Schwann cells but additionally microenvironment haploinsufficiency (Zhu *et al*, 2001; Zhu *et al*, 2002).

To produce a haploinsufficient microenvironment with $Nf1^{-/-}$ Schwann cells, *Nf1flox/flox;* Krox20cre mice were intercrossed with an $Nf1^{+/-}$ mouse resulting in *Nf1flox/-;* Krox20cre mice (Zhu *et al*, 2002). In this mouse, normal development is seen until 10 to 12 months of age, when tumours with similarities to human plexiform neurofibromas develop which consist of Schwann cells, pervasive collagen bundles, fibroblasts and infiltrating mast cells. Such masses do not occur in *Nf1flox/flox;*Krox20cre mice which have $Nf1^{-/-}$ Schwann cells on a wild-type background (Zhu *et al*, 2002). This mouse therefore provides evidence for the hypothesis that haploinsufficiency of the microenvironment is required and provides a reliable model to study neurofibromagenesis.

1.8.4.2 $Nf1^{+/-}$ mast cells

Following studies by Zhu *et al* (2002), implicating the haploinsufficient microenvironment in the development of NF1-associated neurofibromas, Yang *et al* (2003) determined the role of mast cells in neurofibromagenesis using transplanted bone marrow from $Nf1^{+/-}$ mice which was introduced into lethally irradiated *Nf1flox/flox*; Krox20cre mice (Zhu *et*

al, 2002). To ensure that the donor engrafted haematopoietic cells had successfully reconstituted the hosts' bone marrow, a GFP reporter gene was carried by the donor cells (Yang *et al*, 2003). The resulting mice had *Nf1* haploinsufficient bone marrow cells, approximately 10% of Schwann cells were *Nf1* nullizygous and all other cells were functionally wild-type. These mice developed neuromotor defects, weight loss, dorsal root ganglia thickening, and an increased mortality rate within 6 months in comparison to the *Nf1flox/-*;Krox20cre mice (Zhu *et al*, 2002; Yang *et al*, 2003). Validation of these mice was completed by transplanting wild type bone marrow into the *Nf1flox/-*;Krox20cre mouse which consequently resulted in a lack of tumour development in this usually reliable tumorigenic model. These studies together suggested that haploinsufficiency in the bone marrow microenvironment is required for neurofibroma formation.

Additional experiments by Yang *et al* (2003) were undertaken with the focus of investigating whether mast cells which are stimulated by SCF are the primary effectors of the tumour microenvironment. $Nf1^{+/-}$ bone marrow cells carrying kinase inhibiting *c-kit* gene mutations were transplanted into *Nf1flox/flox*; Krox20cre mice. In these mice, there was no evidence for neuromotor defects, dorsal root ganglia enlargement, and mast cell infiltration indicating that this model of tumour development is dependent on loss of *Nf1* in Schwann cells in addition to c-kit-dependent *Nf1* haploinsufficiency in the bone marrow Yang *et al* (2003).

A model explaining the occurrence of sporadic plexiform neurofibromas has been generated in which Dhh-Cre $Nf1^{-/-}$ deletion in glial cells at a specific stage of murine development (E12.5) allows the development of neurofibromas which demonstrate loss of axon Schwann cell interaction, mast cell accumulation, and fibrosis. This indicates that these tumours are characteristic of plexiform neurofibromas which develop even on a wild type genetic background (Wu *et al*, 2008). The mTOR inhibitor analog RAD001 and Sorafenib, a multi-targeted kinase inhibitor have been tested on this model. It was found that RAD001 has no effect on neurofibroma growth where as Sorafenib may be of significant therapeutic benefit to neurofibromas based on this model.

1.9 The *NF1* gene mutational spectrum

The large size of the *NF1* gene, high mutation rate, lack of mutational hotspots, presence of pseudogenes and cellular heterogeneity within both benign and malignant NF1 associated tumours has hampered the search for both somatic and germline *NF1* mutations. Approximately 90% of germline *NF1* mutations are identified using the most current mutational detection methods in patients with a clinical diagnosis of NF1 (Messiaen *et al*, 2000; Ars *et al*, 2000). Somatic *NF1* mutation detection rates in NF1-associated tumours is, however, much lower with between 12% and 64% of somatic mutations identified in cutaneous neurofibromas (John *et al*, 2000; Serra *et al*, 2001b; Upadhyaya *et al* 2004; Spurlock *et al*, 2007), with an increase to 75% in cases in which DNA for mutational analysis is derived from Schwann cell cultures (Maertens *et al*, 2006). Only a few investigations have assessed the full spectrum of germline and somatic mutational events, across all tumour types, using a wide range of molecular techniques. Knowledge of the mutational type, nature and frequency of *NF1* somatic mutations in addition to the role of modifying loci are crucial to understanding possible genotype-phenotype relationships in NF1 and the underlying variability in clinical presentation seen in NF1 patients.

1.9.1 NF1 germline mutations

To date over 1273 *NF1* germline mutations have been identified through large whole gene studies (HGMD; Fahsold *et al*, 2000; Messiaen *et al*, 2000; Han *et al*, 2001; Ars *et al*, 2003) In general, the *NF1* germline mutational spectrum is highly varied. Truncating mutations represent about 80% of identified *NF1* germline mutations (Fahsold *et al*, 2000; Ars *et al*, 2003), which is similar to the mutational spectrum of other tumour-suppressor genes including *APC*, *TSC1*, *BRCA1*, *ATM* and *RB1* (Suzuki *et al,* 1998; Jones *et al,* 1999; Lohmann *et al,* 1996; 1997; Miki *et al,* 1994; Sandoval *et al,* 1999). The remaining 10-20% of *NF1* mutations; are either unidentified due to the above outlined features of the *NF1* gene or are characterised as missense variants of unknown pathogenicity (Ars *et al*, 2003).

1.9.1.1 Microdeletions

Deletions of the entire *NF1* gene locus and flanking regions occur in 5-10% of individuals with NF1 (Kluwe *et al*, 2004). These deletions are generally recurrent deletions which result from non allelic homologous recombination (NAHR) between the *NF1* proximal and distal low-copy repeats which flank the *NF1* gene (*NF1-REP-a* and –*c*) (Dorschner *et al*, 2000; Jenne *et al*, 2001; Lopez-Correa *et al*, 2001; De-Raedt *et al*, 2006; Kehrer-Sawatzki *et al*, 2008).

1.9.1.1.1 Type I microdeletion (1.4Mb)

This deletion is identified in 80% of patients with microdeletions, occurring between two recombination hotspots, termed paralogous recombination sites 1 and 2 (PRS1 and PRS2) (De-Raedt *et al*, 2006; Kehrer-Sawatzki *et al*, 2008; Pasmant *et al*, 2010; Messiaen *et al*, 2011).

1.9.1.1.2 Type 2 microdeletion (1.2 Mb)

This a smaller deletion with breakpoints located in the *SUZ12* gene (suppressor of zeste 12 homolog; NM_015355) and its pseudogene *SUZ12P.* These deletions are commonly mediated by NAHR (Kehrer-Sawatzki *et al*, 2004; Steinmann *et al*, 2007; Roehl *et al*, 2010).

1.9.1.1.3 Type 3 microdeletion (1.0Mb)

These recently identified recurrent deletions are also mediated by NAHR and encompass breakpoints in *NF1* REP B and *NF1* REP C (Bengesser *et al*, 2010; Pasmant *et al*, 2010).

1.9.1.1.4 'Atypical' micodeletions

'Atypical' deletions encompass breakpoints which are not recurrent and not homology mediated (Venturin *et al*, 2004). These deletions therefore vary widely in the number and types of genes which are deleted (Pasmant *et al*, 2008, 2010).

1.9.1.1.5 Non Allelic Homologous Recombination (NAHR)

The mechanisms underlying (NAHR) are not fully understood but are thought to be similar to those of allelic homologous recombination (AHR) but with the use of a nonallelic template to repair the initiating double strand break (Roehl *et al*, 2010). The occurrence of low copy repeats (LCRs) close to the breakpoints suggests that the unusual DNA structure surrounding the LCRs may confuse the DNA replication machinery resulting in breakpoints caused by replication errors (Roehl *et al*, 2010).

1.9.1.1.6 Mosaicism and microdeletions

Importantly, a number of patients who exhibit mosaicism possess large germline deletions of the *NF1* gene (section 1.9.1.1). Mosaicism in NF1 can cause both a mild phenotype, generalised across all limbs and body segments or alternatively regionally limited distribution of NF1 manifestations, (segmental mosaicism), associated with segmental NF1 (SNF1) (section 1.6.1) (Ruggieri and Huson, 2001). The excess of identified microdeletions in patients with mosaicism may be attributed to the ease in which large mosaic deletions can be identified at the single cell level by FISH analysis in comparison to nucleotide substitutions (Maertens *et al*, 2007).

The majority of deletions identified in mosaic patients so far have been type 2 or atypical deletions, with only one type 1 deletion identified to date which was only confirmed by MLPA and so the true breakpoints are unknown and it may be larger than 1.4Mb (De Luca *et al*, 2007; reviewed in Kehrer-Sawatzki and Cooper, 2008). A more recent study confirmed the presence of two mosaic type 1 deletions with breakpoint scanning PCR and SNP analysis. This indicates that at least 2% of type 1 deletions may exhibit mosaicism suggesting that *de novo* NAHR is not confined to the germline and maternal meiosis and may also occur postzygotically by mitosis (Messiaen *et al*, 2011). Interestingly, previous studies have also reported that there is a prevalence of females in mosaic founder patients and sporadic patients with type-2 *NF1* deletions (Steinmann *et al*, 2007; Messiaen *et al*, 2011). It has been suggested that FISH analysis should be used as an additional analysis technique on other cell types (e.g. buccal smears) in cases of potential mosaicism (Messiaen *et al*, 2011).

1.9.1.2 Gross rearrangements

In addition to *NF1* microdeletions, deletions of several hundred kb of the *NF1* gene as well as deletion of individual and multiple exons have also been reported and these mutations encompass ~7% of the current *NF1* mutational spectrum (Fang *et al*, 2001; Wimmer *et al*, 2006; De Luca *et al*, 2007; Upadhyaya *et al*, 2006; Bausch *et al*, 2007). Similarly, gross insertions of between 350bp and 10kb have been reported (Wallace *et al*, 1991; Upadhyaya *et al*, 1992; Fahsold *et al*, 2000; Wimmer *et al*, 2007) and duplications of single and multiple exons have also been detected, although these are a rare occurrence, with only 6 reported gross duplications and 4 gross insertions in the literature to date (HGMD) (De Luca *et al*, 2004; Tassabehji *et al*, 1993; Bausch *et al*, 2007; Wimmer *et al*, 2006)

1.9.1.3 Small insertions and deletions

Micro-Insertions and deletions in the *NF1* gene are commonly found to cause frameshifts where the correct reading of the frame is disrupted by insertion or deletion of bases. This disrupts single or multiple codons and results in a premature stop codon. In frame deletions are, however, also found to occur (Shen *et al*, 1993; Serra *et al*, 2001; Mattocks *et al*, 2004) and include the 3bp deletion in exon 17 which is associated with a milder phenotype (Upadhyaya *et al*, 2007) (section 1.10.5). Micro-insertions and deletions account for approximately 40% of all identified *NF1* mutations. Micro-deletions (27%) are more common than Micro-insertions (13%) (HGMD). Micro-insertions commonly involve between 1 and 2bp (Ars *et al*, 2003) although a few larger insertions of between 7bp and 11bp have been identified (Maynard *et al*, 1997; Ars *et al*, 2000; Bahuau *et al*, 2000; Serra *et al*, 2001). Four larger insertions have also been reported (350bp) (Wimmer *et al*, 2007; Upadhyaya *et al*, 1992; Fahsold *et al*, 2000) in addition to insertion of the *Alu* repetitive sequence into an intron resulting in the deletion of a downstream exon during splicing (Wallace *et al*, 1991). Micro deletions between 1bp and 4bps are common although microdeletions of 13-20bps have been reported (Ars *et al*, 2000; Kluwe *et al*, 2003; Baralle *et al*, 2005; Lee *et al*, 2006) and even deletions of

105bp (Heim *et al*, 1995). Whilst small insertions and deletions are individually relatively common in the *NF1* gene, a combination of both mutations occurring coincidentally is a relatively uncommon mutational mechanism, representing less than 2% of all published *NF1* germline mutations (HGMD).

1.9.1.4 Base-pair substitutions

These lesions include missense variants where one amino acid is substituted for that of another, nonsense mutations in which a premature stop codon is introduced and additionally splice site alterations. Altogether, these base substitutions account for nearly 50% of all identified mutations, approximately 20% of which constitute splice site alterations and about 30% are nonsense and missense mutations. Of this 30%, 57% represent nonsense mutations with the remainder representing missense mutations (HGMD). The pathogenicity of many missense mutations is uncertain and would require familial, biochemical and functional analysis to determine whether they are neutral or disease causing (chapter 4).

1.9.1.4.1 Transitions and transversions

Transitions which involve the substitution of two-ring purines (A>G) or one-ring pyrimidines (C>T) are generally more frequent than transversions which involve changes of purine for pyrimidine bases (e.g. A>C). 60% of *NF1* point mutations are found to be associated with transitions whilst the remaining 40% representing transversions (HGMD).

1.9.1.4.2 CpG dinucleotides

Methylation of CpG dinucleotides is a common transition in mammalian DNA and involves the deamination of methylated cytosine in CpG dinucleotides, most commonly resulting in a C>T transition (Cooper and Krawczak, 1993). Methylation and CpG dinucleotides are further discussed in section 5.1.

1.9.1.4.3 Splicing alterations

Splice site alterations account for a large proportion of *NF1* mutations (Ars *et al*, 2000; Messiaen *et al*, 2000) and evaluating the effect of splice site (SS) alterations could be an important tool for determining novel regulatory mechanisms. Splicing is a complex process by which introns are removed from pre-mRNA and successive exons are joined to produce a mature mRNA molecule. Canonical splice sites (SSs) are present at the 5' and 3' ends of exons in addition to the polypyrimidine tract and the branch point which are present upstream of the 3'SS (Hastings and Krainer, 2003). These sequence–specific SS's are recognized by the 'spliceosome', sequence specific splicing machinery which consists of a complex of small nuclear ribonucleoproteins (snRNPs) and associated proteins which assemble on the pre-mRNA (Mardon *et al*, 1987). U1 snRNP interaction with the 5'SS is considered to be one of the most important stages in the definition of SS's through an RNA-RNA interaction, although there are contradictory views for this idea (Seraphin *et al*, 1987; Eperon *et al*, 1993). Furthermore, non-splice site *cis*-acting sequence elements; enhancer and silencer elements are capable of enhancing the fidelity of a splicing reaction by increasing or decreasing exon and intron recognition. These include exon splicing enhancers (ESEs) and exon splicing silencers (ESS) in addition to intron splicing enhancers (ISEs) and intron splicing silencers (ISS). These additional elements are important for determination of correct splice sites from numerous cryptic splice sites which are also present (Kralovicova and Vorechovsky, 2007).

Disruptions affecting U1 snRNA binding and ESE's have been reported (Baralle *et al*, 2003; Hutter *et al*, 2004; Raponi *et al*, 2009). Furthermore, other factors including the genomic context including polypyrimidine tracts (Raponi *et al*, 2009) and external environmental stimuli *in vitro* such as pH, temperature and cellular stress can affect exon inclusion and induce splicing defects (Blaustein *et al*, 2007). Splicing mutations can generate several outcomes on the mature mRNA. These include: exon skipping from classical splice site mutations and single nucleotide substitutions within introns which create *de novo* splice sites resulting in cryptic exon inclusion. Single-nucleotide substitutions within exons can also cause the creation of *de novo* splice sites which

results in the loss of sections of an exon if these *de novo* SS's are used. Additionally mutations which disrupt the use of SS's can cause activation of cryptic intronic/exonic SS's and finally sequence aberrations in the exon can also cause exon skipping (Wimmer *et al*, 2007). The later consequence has been previously shown in the *NF1* gene to primarily disrupt ESE's which compromises exon recognition (Zatkova *et al*, 2004).

Recent evidence also suggests that nucleotide substitutions which occur in deeper intronic sequences can also affect splicing and have been demonstrated to be pathogenic (Pagani *et al*, 2000; Raponi *et al*, 2006). Analysis of *NF1* splicing mutations at exon 29 has demonstrated that positions +4 and +5 of the SS are less tolerant of base changes which differ from the wild type sequence (Raponi *et al*, 2009). Additionally, analysis of the same +5G>C splicing mutation at IVS3, IVS1 and IVS7 SS's, the mutation was only pathogenic at the IVS3 SS where it had an adverse impact on exon inclusion levels (Raponi *et al*, 2009). Such findings are important from a clinical point of view and indicate that splicing disruption is a key NF1pathogenic mechanism.

1.9.1.5 Chromosomal rearrangements

Rearrangements involving chromosome 17 such as t(1;17) (Schmidt *et al*, 1987) and t(17;22) (Ledbetter *et al*, 1989), importantly provided the key to the identification of the *NF1* gene and its associated locus. Deletions of chromosome 17 have therefore been previously reported as germline mutations (Andersen *et al*, 1990; Upadhyaya *et al*, 1996; Riva *et al*, 1996) in addition to inversions and transversions involving chromosome 17 (Schmidt *et al*, 1987; Ledbetter *et al*, 1989; Asamoah *et al*, 1995; Fahsold *et al*, 1995; Kehrer-Sawatzki *et al*, 1997). There are additionally a number of reports of complex rearrangements involving the deletion, insertion and rearrangements of multiple non-consecutive *NF1* exons (Wimmer *et al*, 2006; Mantripragada *et al*, 2006). Moreover, gross chromosomal alterations are a key feature of malignant NF1-associated tumours, likely contributing to the process of malignant transformation of such tumours (section 6.1).

1.9.2 Recurrent mutations

Approximately 50% of *NF1* germline and somatic mutations represent novel alterations indicating that about 50% are recurrent mutations as seen in recent large germline and somatic mutational studies (Fahsold *et al*, 2000; Ars *et al*, 2003; Mattocks *et al*, 2004; De Luca *et al*, 2004). Recurrent *NF1* mutations are found in both the germline and soma. A few studies have determined the recurrent nature of a large panel of germline mutations (Ars *et al*, 2003; Fahsold *et al*, 2000). Of the 1,273 germline mutations which have been described so far (HGMD), there are a number of commonly identified mutations (table 1.6). Approximately 215 somatic point mutations have been characterised so far to date, of these mutations, there are a number of recurrent point mutations which have been found in numerous NF1-associated benign and malignant tumour types including: c.2446T>C; p.R816X in both plexiform neurofibromas and MPNSTs (John *et al*, 2000; Bottillo *et al*, 2009) (table 1.7). Similarly, some recurrent mutations have been identified multiple times in both the germline and soma, including one of the most common germline mutations; c.910C>T p.R304X (table 1.7).

Additionally, there are no known mutational hotspots in the *NF1* gene as mutations appear to be relatively evenly distributed along the coding sequence (DeLuca *et al*, 2004). There are, however, some potential 'warm spots' in which *NF1* gene mutations occur more frequently than in the rest of the gene although they are not associated with any of the known functional domains of NF1. These include exons 4b and 37, which have a mutation rate 4- to 5-fold higher than average (Messiaen *et al*, 2000; Fahsold *et al*, 2000; Ars *et al*, 2003; DeLuca *et al*, 2004). Exon 7 also demonstrates a higher frequency of mutations than the rest of the gene which may be due to its propensity to undergo splicing errors due to weakly defined exon-intron boundaries (Fahsold *et al*, 2000; Ars *et al*, 2003; Bottillo *et al*, 2007). Analysis of the distribution of *NF1* mutations could be skewed due to previous bias in the exons which were analysed. Most analysis has, however, been weighted to account for this possibility (Fahsold *et al*, 2000). Of interest is the observation that there is no major clustering of mutations in any of the known NF1 functional domains including the GRD, CSRD (section 1.3) and there is also

a significant lack of mutations identified towards the 3' end of the gene in exons 48 and 49 (HGMD) (Fahsold *et al*, 2000; Ars *et al*, 2003; DeLuca *et al*, 2004). Analysis of the type and distribution of *NF1* mutations is clearly of importance for determining not only gene regions most likely to harbour mutations to increase the efficiency of mutation screening but also for determining potential genotype phenotype correlations.

1.9.3 NF1 somatic mutations

Thus far, neurofibromas whether from the same or different patients appear to exhibit distinct somatic mutations demonstrating that each neurofibroma is the consequence of discrete mutational incidents. Investigation of somatic mutations in a variety of benign and malignant NF1 related tumours may aid in the establishment of genotype-phenotype correlations and determination of inter-individual neurofibroma number and mutation rates. The somatic mutational spectrum is very similar to that of the germline with about 80% representing truncating mutations and 10-20% are missense mutations (Thomas *et al*, 2010). Additionally loss of heterozygosity (LOH) is an additional somatic mutational mechanism found in both benign and malignant tumours.

Table 1.6 Recurrent germline *NF1* mutations and the number of citations for each mutation.

Mutation	Affect on protein Function	Number of Citations	References
c. 6792C>A p.Y2264X	Exon 37 skipping	16	Robinson *et al*, 1995 (2); Messiaen *et al*, 1997 (1); Hoffmeyer *et al*, 1998 (2); Fahsold *et al*, 2000 (2); Ars *et al*, 2003 (6); Mattocks *et al*, 2004 (2); De Luca *et al*, 2004 (1)
c.5839C>T p.R1947X	Occurs at a CpG dinucleotide	16	Estivill *et al*, 1991 (1); Ainsworth *et al*, 1993 (1); Horiuchi *et al*, 1994 (2); Valero *et al*, 1994 (1); Lazaro *et al*, 1995 (2); Fahsold *et al*, 2000 (2); Messiaen *et al*, 2000 (1); Ars *et al*, 2003 (4); DeLuca *et al*, 2004 (2);
c.910C>T p.R304X	Exon 7 skipping	13	Hoffmeyer *et al*, 1998 (1); Fahsold *et al*, 2000 (1); Messiaen *et al*, 2000 (1); Ars *et al*, 2003 (7); Colapietro *et al*, 2003 (1); DeLuca *et al*, 2004 (1); Bottillo *et al*, 2007 (1);
c.4537C>T p.R1513X	Nonsense	12	Fahsold *et al*, 2000 (7); Messiaen *et al*, 2000 (1); Ars *et al*, 2003 (1); Mattocks *et al*, 2004 (2); DeLuca *et al*, 2004 (1)
c.499delTGTT		10	Fahsold *et al*, 2000 (6); Ars *et al*, 2003 (3); Mattocks *et al*, 2004 (1)
c.1885G>A p.G629R	Inactivation of the 3' consensus splice site and use of cryptic 3' splice site. Deletion of 41 nucleotides of exon 12b	9	Gasparini *et al*, 1996 (1); Ars *et al*, 2003 (5); Mattocks *et al*, 2004 (2); DeLuca *et al*, 2004 (1)
6789delTTAC		9	Robinson *et al*, 1995 (1); Hoffmeyer *et al*, 1998 (2); Fahsold *et al*, 2000 (5); Deluca *et al*, 2004 (1)
c.5546G>A p.R1849Q	Inactivation of the 5' splice site. Exon 29 skipping	8	Fahsold *et al*, 2000 (2); Messiaen *et al*, 2000 (1); Ars *et al*, 2003 (5)
c.1318C>T p.R440X		6	Fahsold *et al*, 2000 (3); Mattocks *et al*, 2004 (3)

Table 1.7 Recurrent somatic *NF1* mutations and the tumours in which they have been identified

Recurrent Mutation	Germline or Somatic	Tumour Type	References
c.4084C>T; p.R1362X	Somatic	Cutaneous neurofibroma JMML	Eisenbarth *et al*, 2000; Thomas *et al*, 2010; Steinemann *et al*, 2009
c.1260+1G>A	Somatic Germline	Cutaneous neurofibroma	Serra *et al*, 2001
c.910C>T; p.R304X	Somatic Germline	Cutaneous neurofibroma Plexiform neurofibroma	Upadhyaya *et al*, 2004; Upadhyaya *et al*, 2008; Upadhyaya *et al*, 2008
c.2088delG; p.W696X	Somatic	Cutaneous neurofibroma	Upadhyaya *et al*, 2004; Thomas *et al*, 2010
c.4083insT; p.L1361fsX13	Somatic	Cutaneous neurofibroma Plexiform neurofibroma	Upadhyaya *et al*, 2004; Upadhyaya *et al*, 2008
c.4537C>T; p.R1513X	Somatic	Cutaneous neurofibroma	Maertens *et al*, 2006; Spurlock *et al*, 2007
c.2041C>T; p.R681X	Somatic Germline	Cutaneous neurofibroma	Thomas *et al*, 2010; Serra *et al*, 2001
c.2446T>C; p.R816X	Somatic Germline	Plexiform neurofibroma MPNST	John *et al*, 2000; Bottillo *et al*, 2009; Bottillo *et al*, 2009
c.1246C>T; p.R315X	Somatic Germline	Plexiform neurofibroma	Upadhyaya *et al*, 2008; Maertens *et al*, 2006
c.5242C>T; p.R1748X	Somatic Germline	GIST	Maertens *et al*, 2006; Steinemann *et al*, 2009

1.9.3.1 Loss of Heterozygosity (LOH)

LOH (Loss of Heterozygosity) of the *NF1* gene is a relatively common somatic event in NF1 associated benign and malignant tumours. LOH results in the loss of the remaining wild type copy of the *NF1* gene and is known to occur through a variety of mechanisms including: mitotic recombination (copy neutral LOH), deletion, chromosomal loss due to non-disjunction and chromosomal loss followed by reduplication (Serra *et al*, 2001). Distinguishing between these mechanisms is not possible with LOH analysis alone, but it is possible to rule out the latter two mechanisms with additional analysis techniques including MLPA or FISH. In cases where no deletion is found in samples which harbour LOH, it is likely that mitotic recombination is the cause of LOH. LOH is found in both benign and malignant tumour but occurs at different rates. LOH occurs in approximately 25% of neurofibromas (Upadhyaya *et al*, 2004; Serra *et al*, 2007; De Raedt *et al*, 2006) and at significantly higher levels of up to 50-85% in plexiform neurofibromas and MPNSTs (Upadhyaya *et al*, 2008, 2009; Laycock-VanSpyk *et al*, 2011).

1.9.3.2 Aberrant methylation of the *NF1* gene

Loss of function of tumour suppressor genes is classically associated with DNA mutations including base substitutions, splicing alterations and gene deletions. DNA methylation is, however, becoming increasingly recognised as an important mechanism of gene inactivation especially in relation to tumour suppressor genes due to the inverse relationship between the level of gene methylation and transcriptional activity (Rodenhiser *et al*, 1993). The low level of *NF1* somatic mutational detection, the spontaneity of new mutations and the proportion of mutations involving CpG dinucleotides (~20%) suggests that methylation of the *NF1* gene and perhaps other genetic loci such as *MGMT, p16 (CDKN2A), TP53, RB1, MLH1, MSH2* and *RASSF1A* (table 1.8) may be involved in NF1 tumorigenesis. Analysis of aberrant methylation of the *NF1* gene and additional genetic loci is discussed in more detail in section 5.1.

Table 1.8 Frequently methylated genes and the cancers with which they are commonly associated. Adapted from Cheung *et al* (2009) with data from www.mit.lifescience. ntu.edu.tw

Gene	Function	Cancer Association	References To Date	Reference
p16 (CDKN2A)	Protein product (ARF) functions as a stabilizer of the tumour suppressor protein p53 as it can interact with, and sequester, MDM1, a protein responsible for the degradation of p53	Lung Cancer Colorectal cancer Breast Cancer Hepatocellular Carcinoma	>450	Nakata *et al*, 2006; Nosho *et al*, 2007; Oue *et al*, 2003
Ras association domain family 1 isoform (*RASSF1A*)	RASSF1A is thought to interact with KRAS through a Ras association domain and is known to have several key cellular effects including promotion of apoptosis, cell cycle arrest, and maintenance of genomic stability Inhibits proliferation through negatively regulating cell cycle progression at G1/S phase transition by inhibiting accumulation of cyclin D1	Lung cancer Colorectal Carcinomas Breast Cancer Prostate Cancer Ovarian cancer Liver Cancer Renal Cancer Cervical Hepatocellular Carcinoma	>270	Hesson *et al*, 2004; Kim *et al*, 2003; Teodoridis *et al*, 2005
O-6-methylguanine-DNA methyltransferase (*MGMT*)	Cellular defence against the biological effects of O6-methylguanine in DNA; involved in DNA repair and drug resistance. *MGMT* expression protects against G:C to A:T DNA transitions	Colorectal Cancer Glioblastoma Glioma Lung Cancer Brain Cancer Lymphoma Small Cell Lung cancer Melanoma	>210	Hanabata *et al*, 2004; Ogino *et al*, 2007; Yu *et al*, 2004

Gene	Function	Cancer Association	References To Date	Reference
MLH1	Responsible for DNA mismatch repair; also implicated in DNA damage signalling	Colorectal Cancer Endometrial Cancer Ovarian cancer	>140	Nan *et al*, 2005; Ogino *et al*, 2007; To *et al*, 2002
APC	Tumour suppressor which acts as an antagonist of the Wnt signalling pathway; also involved in cell migration and adhesion, transcriptional activation, and apoptosis	Colorectal Lung Cancer Gastric Prostate Cancer Breast Cancer	>130	Arnold *et al*, 2004; Sarbia *et al*, 2004; Suzuki *et al*, 2006
RARB	Receptor for retinoic acid; limits growth of many cell types by regulating gene expression	Lung Cancer Prostate Cancer Kidney Cancer	>100	Dulaimi *et al*, 2004; Florl *et al*, 2004; Maruyama *et al*, 2004

1.9.5 Modifying loci

There are numerous modifying loci including biallelic defects in mismatch repair genes (*MMR*) and *TP53*, *CDKN2A* and *RB1* alterations which are thought to modulate NF1 phenotypic expression and NF1-associated tumour development. These are discussed in detail in section 3.1.

1.10 Mutation detection techniques

Our current knowledge of the molecular mechanisms that underlie NF1 tumorigenesis is still relatively limited. The characterisation of germline and somatic mutations present in a large series of tumours from unrelated patients will provide data on the mutational type, nature and frequency of *NF1* somatic mutations. This is a crucial step towards understanding the complex genotype-phenotype relationships in NF1 and in the identification of relevant biological pathways affected in NF1 associated tumours. The following is an overview of the most commonly used analysis methods for *NF1* somatic and germline mutational analysis in addition to new techniques with important future applications.

1.10.1 Identification of microlesions and gross chromosomal rearrangements

1.10.1.1 Fluorescence *In Situ* Hybridisation (FISH)

The detection and characterisation of microdeletions has been historically very difficult and laborious. Whilst not available in all labs, FISH has been widely used in conjunction with other approaches encompassing YAC (yeast artificial chromosome) clones of an *NF1* gene region followed by locus specific cloned PCR product clones as part of a high resolution FISH technique. FISH is a reliable technique for determining how many copies of a specific chromosome are present without having to produce a full karyotype. FISH is also a rapid technique as cells for analysis by FISH do not have to be cultured. However FISH is, unable to give as much information as a full karyotype including

changes at other chromosomes or details on the structure of chromosomes which are identified through this analysis. Furthermore, the patient to be analysed has to present with fairly typical clinical symptoms for use of the correct probes for a specific disorder.

Fluorescent dye probes which are specific to the chromosome of interest including RP5-1002G3 (detected by red fluorescent signals) which is located in the telomeric region of the *NF1* gene and RP5-926B9 (green) which covers the centromeric part of the *NF1* gene have been used to label samples through hybridisation for *NF1* analysis (de Raedt *et al*, 2004). Slides with hybridised probes and chromosomes are subsequently analysed using fluorescence microscopes and the number of signals seen from these probes determines the number of chromosomes present. Using this method it has been possible to not only identify *NF1* gene deletions but also to distinguish between type 1 and type 2 microdeletions (Wimmer *et al*, 2006; Griffiths *et al*, 2007; Messiaen *et al*, 2011.) Furthermore, FISH analysis has been successfully used for NF1 pre-implantation genetic diagnosis (PGD) on single blastomeres (Vanneste *et al*, 2009).

1.10.1.2 Multiplex Ligation-dependent Probe Amplification (MLPA)

MLPA is an important molecular tool which allows the identification and characterisation of aberrant copy number changes in many genomic DNA sequences through the use of one simple PCR based reaction. MLPA is an alternative method of detection of single and multiple exonic deletions and duplications. MLPA assays for the *NF1* gene have been developed (MRC, Holland) including the SALSA P081/082 and SALSA P122 assays. The SALSA P081/082 *NF1* MLPA assay (v. 04) consists of 81 probes but only tests 51 of the 60 *NF1* exons. The SALSA P122 (v.01) has 5 probes in the *NF1* gene and 7 probes in the regions flanking the *NF1* gene. These kits are able to define both germline and somatic single and multiple exon deletions (De Luca *et al*, 2007; Upadhyaya *et al*, 2008b) but are also able to distinguish between different types of microdeletions with the use of only two probes (Wimmer *et al*, 2006; Messiaen *et al*, 2011; Valero *et al*, 2011).

The basic MLPA technique as outlined by MRC Holland, has 5 main stages: denaturation, hybridisation of the probes to the target sequences, ligation of the probes through a thermostable ligase, amplification using a universal primer pair to amplify all ligated probes and quantification, which for the purposes of this study involved the use of a 3100 Genetic Analyser (ABI Biosystems). Each peak seen when the data is generated represents the amplification product of a specific probe. Samples tested are compared to one positive and five negative controls allowing a difference in relative peak height to be observed. These differences indicate copy number variation of the target sequence of a particular probe.

There are several key advantages of MLPA. These include the ability to perform the technique using small quantities of DNA (20ng) which can even be partially degraded such as from paraffin, formalin treated tissues and free fetal DNA from maternal plasma. Variability in temperature also has very little effect on the efficiency and effectiveness of this technique and it is able to discriminate between sequences which differ in only a single nucleotide. Furthermore, MLPA is a rapid and relatively inexpensive initial method of screening for *NF1* microdeletions which is complementary to a high-resolution technique such as array CGH and can be used in conjunction with LOH analysis to help determine the mechanism of LOH. Additionally, it is also possible to apply this technique to look at epigenetics including hypermethylation of p53 in tumours and imprinting defects in Prader-Willi or Angelman syndromes.

There are also a number of disadvantages to the use of MLPA for detection of microdeletions and the reciprocal duplications. It has been reported that MLPA occasionally produces false positive results which can occur due to the presence of SNPs and point mutations either within or close to the sites at which the MLPA probes ligate to the DNA (Pasmant *et al*, 2010). MLPA is also unable to determine the breakpoints of atypical deletions, a substantial concern given that atypical deletions are present in ~10% of patients with large *NF1* deletions (Pasmant *et al*, 2010; Messiaen *et al*, 2011). It is thought that larger atypical deletions may in fact consist of deletions of genes such as *GOSR1, TBC1D29, RHOT1, RHBDL3* and *C17orf75* in addition to the 14

genes present within the type-1 deletions. It is hoped that our current knowledge of atypical deletions should allow improvements in the positioning of probes in future MLPA kits. Furthermore, there have been reports of false positives due to underlying levels of mosaicism, indicating that it is important to use other methods such as FISH to confirm the analysis (Messiaen *et al*, 2010)

1.10.1.3 CGH arrays

Microarrays have been recently developed specifically for detection of deletions and duplications of the *NF1* gene which are both cost effective and efficient, thereby overcoming previous issues of lack of FISH facilities in some labs and the problem of heterogeneity in MLPA analysis. Previous studies have employed two types of microarray for CGH analysis of the *NF1* gene derived from pooled PCR products of the *NF1* locus. Firstly, Mantripragada *et al* (2006) developed an array containing 183 probes covering a 2.24 Mb of region 17q11.2, with an average resolution of 12 kb. Shen *et al* (2007) developed a second array with an average resolution of 4.5 kb and 493 pooled probes measuring 200 to 998 bp. Neither of these two array CGH platforms were capable of producing exon level resolution, could not differentiate between type 1 and type 2 microdeletions or determine some atypical breakpoints and did not cover all the exons of the *NF1* gene. However, they were able to identify molecular rearrangements within the *NF1* gene sequence. More recently, a higher resolution oligonucleotide array CGH was developed by Pasmant *et al* (2009). This array was able to detect large *NF1* rearrangements, distinguish between type 1 and type 2 microdeletions, covers a higher density of the *NF1* gene and provides enough information to allow for sequencing of the breakpoint regions. Moreover, this technique was found to be accurate for *NF1* microdeletion characterisation, rapid (analysing 8 patients simultaneously on 15K slides), efficient (€100 per patient) and sensitive.

Arrays have also been recently employed to screen for genes which are upregulated or downregulated in MPNSTs by comparing the molecular profiles of malignant NF1 tumours with those of normal tissue or benign tumours. This has allowed genes which

are involved in MPNST development to be determined. Identification of aberrations in numerous genes affecting multiple pathways in MPNSTs demonstrates that MPNST development is a complicated, multistep process requiring the inactivation of many genes. These genes clearly provide new targets for future therapy of MPNSTs (section 6.1).

Major advantages of CGH array analysis over other methods include the ability to analyse the equivalent of hundreds of FISH or MLPA analyses on all 46 chromosomes in only one test. Array CGH also has more sensitivity and resolution than karyotyping, FISH or MLPA to detect chromosomal abnormalities. The ability of array CGH to detect and evaluate low-level mosaicism is unclear. It is suggested that array CGH will not detect mosaicism below 20% although it has been reported in some array CGH analyses of routine diagnostic samples (Ballif *et al*, 2006). Furthermore array CGH can be performed on very small amounts of starting material and there is no requirement for dividing cells so it can be performed on frozen stored samples and post-mortem samples. Array CGH is also amenable to automation suggesting that costs can be reduced due to less input from technical staff. There are, however, a few disadvantages of CGH analysis including the inability to detect balanced inversions and translocations, especially rare ones, and currently costs are higher than with G banded karyotyping.

1.10.1.4 LOH analysis

The analysis of LOH in the *NF1* gene is typically carried out by performing a comparison between normal cells and tumour cells or blood, utilising a panel of molecular markers distributed throughout the length of the gene. The disadvantage of LOH studies is that they are complicated in NF1 patients due to the large gene size and the problem of mixed populations of cells. Despite this, however, microsatellite markers as well as RFLP's can be utilised in LOH detection to identify not only the presence of LOH but also to characterise it in terms of the size of deletion and the position of specific areas of LOH within the *NF1* gene. For example, neurofibromas which are positive for LOH at all markers used including flanking 3' and 5' regions and intragenic markers, suggests that

there is LOH throughout the whole gene. In this way therefore, this technique is useful for not only detecting the form of *NF1* somatic inactivation but also for complete characterisation of the 17p and 17q gene regions. The results produced from LOH are analysed with simple formulas to calculate the ratio of peak heights of each allele. Calculation of LOH in tumour uses the formula (Tb/Ta)/(Bb/Ba), where T is the tumour peak ratio between alleles a and b and B is the blood peak ratio between alleles a and b (Neves *et al*, 2002). The percentage difference between the peak heights of the two alleles is scored and LOH noted in alleles with less than the cut off point of around 50%. Allelic loss is therefore scored if the area under one allelic peak in the tumour was reduced by 50% or more relative to the other allele, after correcting for the relative peak areas by using normal DNA (Dasgupta *et al*, 2003).

1.10.2 Identification of point mutations

1.10.2.1 Direct sequencing

The advent of sequencing technology and consequent improvements to such methods has been critical to the identification of microlesions (Maxam and Gilbert, 1977; Sanger *et al*, 1977). Sanger and Coulson (1975) first introduced the plus minus method for DNA sequencing which was based on a comparison of the "plus" and "minus" DNA sequences but used polyacrylamide gels to separate the products and was only able to determine the sequence of single stranded DNA (ssDNA). The Maxam and Gilbert (1977) method was very similar to that of Sanger and Coulson (1975) in that it was based on resolving fragments in a polyacrylamide gel but these bands were based on termination of a double-stranded DNA restriction fragment which was radio-labelled with 32P. The bands on the gel represented cleavage of the fragment by base specific chemical reactions resulting in the production of a band for every sequence position which was not possible with the plus minus method.

The 'dideoxy' method introduced by Sanger (1977) is widely regarded as a superior method for DNA sequencing, which solved the problems of the plus minus method. It is

based on the use of chain-terminating nucleotide analogues which were used instead of the four natural dNTPs to induce termination at specific bases during four reactions, each consisting of one analogue. When the analogues are incorporated into the growing strand, the *E. coli Pol I* enzyme is unable to extend the DNA strand any further initiating chain termination. Refinements of these sequencing methods have allowed the use of both DNA and cDNA to not only identify but also characterise a wide variety of point mutations such as nonsense, missense and splice site mutations as well as small insertions, deletions and SNPs. Sequencing has been widely used in *NF1* analysis to identify germline and somatic mutations with mutation detection rates with sequencing alone up to 79% using DNA from purified Schwann cell cultures (Maertens *et al*, 2006b).

The main advantages to sequencing are the ability to automate many of the processes involved allowing determination of the complete genetic information in an individual or organism with minimal input from technical staff. Additionally, genome organisation and evolution can be studied using sequencing. Most importantly, sequencing has opened up avenues for functional genomics and a better understanding of molecular interactions and the basis of disease manifestation. Furthermore, genetic components such as SNPs have become more prominent and the underlying mechanisms for individual responses to drugs can be determined (pharmacogenetics). Conversely, disadvantages of sequencing include the relatively short read length produced, reliance on PCR to generate the products for sequencing, both especially problematic in large genes such as *NF1*. Furthermore, there is the occasional occurrence of artefacts due to contamination, indicating that whilst sequencing is mostly accurate and reliable, repetition of the reaction and subsequent confirmation is required.

1.10.2.2 Single Stranded Conformation Polymorphism (SSCP)

SSCP is a simple and inexpensive technique for the detection of point mutations. It is based on the electrophoretic separation of single-stranded DNA (SS DNA) due to changes in the sequence, often as subtle as a single base pair change (Orita *et al*, 1989). The major disadvantage of SSCP is that the tertiary structure of SS DNA

changes under changing physiological conditions including temperature and the ionic environment, indicating that these variables may affect the outcome of the analysis if not kept constant. Under optimal conditions SSCP is capable of detecting a high proportion of base changes and has been successfully used in *NF1* mutational analysis (Origone *et al*, 2002; Pros *et al*, 2006).

1.10.2.3 Heteroduplex analysis

Heteroduplexes are formed following mixing of wild type and mutant DNA which is subsequently denatured by heating and re-annealed upon cooling. Heteroduplex analysis is based on the distinct electrophoretic mobility of homoduplexes and heteroduplexes in non-denaturing polyacrylamide gels. Heteroduplex DNA contains mismatched DNA which generates molecules with an unusual structure which can be easily distinguished from homoduplex DNA by gel analysis (Keen *et al*, 1991). Heteroduplex analysis is a precursor to DHPLC and is a simple method which is capable of producing a high mutation detection rate. It can be applied to large numbers of samples, particularly PCR products with no need to manipulate the PCR product and with the added capability of detection of allele specific mutations. Additionally, there are a number of other methods for detecting heteroduplex DNA formation including: chemical cleavage of mismatch (CCM) (Cotton *et al*, 1988), enzymatic cleavage analysis (Shenk *et al*, 1975; Myers *et al*, 1985; Lu and Hsu, 1992; Youil *et al*, 1995).

1.10.2.4 Denaturing High Performance Liquid Chromatography (DHPLC)

DHPLC (Oefner and Underhill, 1995; Underhill *et al*, 1997) is a sensitive method for detection of heteroduplex DNA, capable of detecting single base substitutions. It is based on the analysis of heteroduplexes generated by DNA mismatches through denaturation and reverse-phase chromatography. Advantages of DHPLC include its relatively low cost, the ability to semi-automate the process allowing a reduction of personal interaction and its sensitivity and specificity, especially as there is no requirement for DNA pre-treatment or for primers containing modifications or labels.

DHPLC has been widely used in *NF1* mutation analysis (Upadhyaya *et al*, 2004) and can detect up to 73% of mutations (De Luca *et al*, 2003; DeLuca *et al*, 2004), although in a recent study, DHPLC was used in a sensitive strategy involving MLPA which detected germline mutations in 95% of individuals (Valero *et al*, 2011).

1.10.2.5 Comparative Sequence Analysis (CSA)

CSA is a low cost, simple and rapid sequence analysis method for identifying and characterising point mutations (Mattocks *et al*, 2000). CSA is completed on raw sequence data and is the comparative analysis of normalised peak heights in a sample trace compared to a reference trace. CSA has been used to analyse the *NF1* gene and has produced high mutation detection rates (89%) (Mattocks *et al*, 2004). Furthermore, Baralle *et al*, (2003b), identified *NF1* mutations in patients with Neurofibromatosis–Noonan Syndrome (NFNS) using this technique.

1.10.2.6 Protein Truncation Test (PTT)

Approximately 80% of *NF1* germline and somatic mutations have been found to result in protein truncation (Shen *et al*, 1996, Ars *et al*, 2000; Fahsold *et al*, 2000; Ars *et al*, 2003). PTT was first described by (Roest *et al*, 1993) and has been routinely used in previous analysis of the *NF1* gene as an alternative to SSCP and heteroduplex analysis (Klose *et al*, 1999; Osborn and Upadhyaya, 1999; Ars *et al*, 2000; Origone *et al*, 2002; Upadhyaya *et al*, 2003; DeLuca *et al*, 2004). This method can screen large fragments up to 2kb in size which is a clear advantage when analysing a gene as large as the *NF1* gene. The mutation detection rate is, however, fairly low (39%-53%) (Osborn and Upadhyaya, 1999; DeLuca *et al*, 2004) which may reflect the inability to detect mutations which are not truncating and which account for approximately 10-20% of mutations in the *NF1* gene.

1.10.3 Splice site alterations and the hybrid minigene splicing assay

As with other point mutations, detection of splice site mutations is usually through direct sequencing. Whilst splice site mutations can be detected in DNA, cDNA sequencing uncovers splicing defects which may not be detectable in genomic DNA. There are many underlying reasons for this including the possibility that the mutation lies outside of the sequence which is analysed such as deep intronic mutations. These mutations can result in the inclusion of a cryptic exon as these mutations may create novel splice sites (Perrin *et al*, 1996). Furthermore, the mutation may be detected in genomic DNA but based on this sequence it cannot be classified as a pathogenic alteration. cDNA analysis can give further insight into the disruption of splicing caused by the mutation (Messiaen and Wimmer, 2005).

To unequivocally determine the effect of splice site mutations, functional assays such as the minigene assay (Raponi *et al*, 2006; Bottillo *et al*, 2007; Raponi *et al*, 2009) and bioinformatic analysis tools have been employed. The hybrid minigene assay is based on the generation of constructs of human genomic DNA which is amplified from normal and mutated exons to produce DNA fragments which contain the exon, in addition to flanking intronic regions (Raponi *et al*, 2006; Raponi *et al*, 2009). Oligonucleotides for specific exons harbour a restriction site for the enzyme *Nde1* at the 5' end. These are used to clone the product into the alpha-globin-fibronectin EDB minigene which has been modified to remove the alternatively-spliced EDB exon generating a site for the insertion of the exons of interest (Pagani *et al*, 2000; Raponi *et al*, 2006; Raponi *et al*, 2009). Transfection of wild type *NF1* constructs and the minigene intronic mutation constructs into HeLa cells followed by RT–PCR analysis determines the percentage of transcripts which are analogous to those identified in the normal control samples. Aberrant transcripts can be sequenced to determine the pathogenic effect of the mutation on the *NF1* gene (Raponi *et al*, 2006; Raponi *et al*, 2009.

1.10.4 Next generation technologies

With the advent and increasing application of array and more importantly next generation technology, it may be possible to identify the whole spectrum of somatic and germline mutations and much more, using one standardised platform. Such technology is still very much in its infancy but is rapidly evolving to allow for more cost effective solutions with very little technical input due to the increasing application of robotics. Whole genome sequencing has seen a huge advancement in technology since the first whole genomes were sequenced (Venter *et al*, 2001; Lander *et al*, 2001).
Refinements to the basic 'dideoxy' sequencing method (Sanger, 1977) have now made it possible, through the use of 2nd generation sequencing technologies including Roche 454; based on pyrosequencing technology, the Illumina Genome Analyser (GAI) and ABI Supported Oligonucleotide Ligation and Detection system (SOLID) to sequence an entire genome in only 2 weeks, producing 30-fold coverage for only £2000-3000. 3rd Generation Technologies are also becoming available (Pacific Biosciences) although they currently represent a major leap in technology from that of capillary sequencing.

The actual methods used in the sequencing phase does differ substantially between the sequencers. All of these technologies are 'massively parallel' meaning that the number of sequence reads is far greater than with the original 96 which can be obtained with capillary sequencing. It is clear that next generation sequencing technologies offer an advantage over existing technologies including arrays and capillary sequencing. There are, however, numerous technical challenges associated with such technology, the most prevalent of which is the handling, storage and analysis of such large quantities of data. Additionally, the alignment of Indels, determination of important changes from the sheer number of SNPs which are generated in addition to the presence of gross chromosomal rearrangements are also significant challenges.

2nd and 3rd Generation technologies do not represent a replacement of capillary sequencing but instead offer a number of new and far reaching applications. These include: re-sequencing such as genome-wide exome sequencing in which the

identification of non-synonymous SNPs is possible, transcriptome sequencing, gene expression analysis (SAGE) mutation analysis, methylation detection and miRNA discovery. *De Novo* sequencing is another important application of next generation sequencing technologies which is especially important in metagenomics and the technology can also be applied to CHiPseq. Importantly, it would also be possible to apply such technologies to the analysis of degraded tissue such as paraffin embedded tissue.

Next generation sequencing technologies have been utilised in numerous recent studies for the identification of variants involved in several cancers (Reviewed by: Meyerson *et al*, 2010). Additionally, Chou *et al* (2010) recently used *NF1* as a model for next generation sequence analysis to evaluate a microarray-based sample-enrichment process and the efficiency of the Roche/454 GS FLX system for re-sequencing purposes. It is clear that this technology could provide important insight into the underlying molecular mechanisms responsible for tumorigenesis and malignancy in NF1 associated tumours and may represent the future of *NF1* somatic analysis.

1.10.5 Genotype-phenotype correlations

NF1 is characterised by highly variable clinical features and a distinct lack of general genotype-phenotype correlations. There are, however, two recognised genotype-phenotype correlations which occur in a small percentage of patients. The 'microdeletion syndrome' occurs in about 10% of individuals (section 1.9.1.1) and generally results in a more severe phenotype. Microdeletion patients exhibit larger numbers of neurofibromas and an earlier age of onset of benign neurofibromas, developmental delay and learning disabilities, dysmorphic features and importantly, a possible higher incidence of MPNSTs (Upadhyaya *et al*, 1998; Riva *et al*, 2000; De Raedt *et al*, 2003; Venturin *et al*, 2004; Pasmant *et al*, 2010). This is a likely genotype-phenotype correlation but should be treated with caution based on the phenotypic variability which still exists within such patients, the lack of microdeletions which have been extensively studied (~150), imprecise definition of boundaries and lack of

appropriate controls (Pasmant *et al*, 2010). Patients with the delAAT mutation in exon 17 have a much milder phenotype with patients only exhibiting minor pigmentary abnormalities with no known reports of neurofibromas or malignancies (Upadhyaya *et al*, 2007). This lack of genotype phenotype correlations means that predicting the clinical course of patients without either of these two mutations is not possible. Larger studies of germline and somatic data are clearly warranted to aid in the detection of genotype-phenotype correlations.

1.10.6 Evolution to malignancy

The development of cutaneous neurofibromas is the hallmark feature of NF1, and these benign growths, when located on the face, neck and arms of patients, often present distressful cosmetic problems. These tumours are known to harbour a primary hit in one *NF1* allele and a secondary somatic hit in the wild type *NF1* allele resulting in a loss of neurofibromin function. Cutaneous neurofibromas are known to be benign and have not been exclusively shown to progress to malignancy. The loss of neurofibromin is therefore clearly necessary for tumour formation but is not sufficient for progression of the tumour to malignancy. A myriad of genetic changes have been identified in MPNSTs including gross chromosomal rearrangements, copy number changes and aberrant gene expression in multiple genes and genetic pathways including the commonly identified; *TP53, CDKN2A, RB1, EGFR* genes, (Mantripragada *et al*, 2008; Kourea *et al*, 1999a; Kourea *et al*, 1999b; Nielsen *et al*, 1999; Mawrin *et al*, 2002), in addition to less frequently associated changes in genes such as *CDK2, CDK4, HGF, MET, PDGFRA, ITGB4, MMP1 HMMR* (Mantripragada *et al*, 2008; Perrone *et al*, 2009) (section 6.1). Such changes and the genes and mechanisms by which they elicit malignant transformation are, however, not fully understood and a molecular profile which distinguishes sporadic MPNSTs from NF1-associated MPNSTs has not been determined (Watson *et al*, 2004). The underlying mechanisms of NF1-associated tumorigenesis and malignancy are discussed further in section 6.1.

1.11 Aims of thesis

NF1 is associated with extreme phenotypic variability and commonly results in an increased risk of developing benign and malignant peripheral nerve sheath tumours (MPNSTs). Identification of somatic mutations in NF1-associated tumours remains notoriously challenging and the molecular mechanisms that underlie NF1 tumorigenesis are still poorly understood. It is postulated that in addition to *NF1* germline and somatic mutations, somatic lesions in other genes may be involved in NF1 tumorigenesis. A combinative approach encompassing genetic, epigenetic and functional analysis is therefore required to dissect the molecular mechanisms responsible for tumorigenesis in NF1. The primary aims of this thesis are:

1. Identification of underlying molecular mechanisms responsible for development of different NF1 associated tumours
2. Development of a novel strategy for functionally characterising variants of unknown pathogenicity located in the GRD of neurofibromin.
3. Elucidating the role of aberrant methylation in NF1-associated tumour development.
4. To investigate potential therapeutic options for NF1-associated malignant peripheral nerve sheath tumours (MPNSTs).

CHAPTER 2: General methods and materials

2.1 Materials

2.1.1 General buffers, solutions, reagents and chemicals

Phosphate-Buffered Saline (PBS) (1X), liquid

10mM sodium phosphate, 138mM NaCl, 2.7mM KCl, pH7.4 (Invitrogen, cat no: 20012-019)

Tris-HCL

Stock solutions of 1M Tris-HCl were prepared at pH7.4 and pH8.0, (Sigma, cat no:T3253)

Ethylenediaminetetraacetic acid (EDTA)

0.5M EDTA adjusted to pH8.0 with NaOH pellets. (Sigma, cat no: ED2SS)

Boric Acid (Sigma, cat no: B7901)

Tris-Borate-EDTA (TBE) buffer (5X)

0.445M Tris-HCL, 0.445M boric acid, 0.01M EDTA

Diluted to 1X for use in gel electrophoresis with dH_2O: 0.089M Tris, 0.089M boric acid and 0.002M EDTA

Tris-EDTA (TE) Buffer (1x)

10mM Tris-HCL pH8.0, 1mM EDTA pH8.0

10x TBS-T pH 7.6

Tris 24.2g, NaCl 80g (Fisher Scientific, cat no: S/3160/60), 0.1% (w/v) Tween 20 (Sigma, cat no: 274348)

Bovine Serum Albumin (BSA) (Promega, cat no: R396E)

Ethanol (Fisher Scientific, cat no: E/0600/DF17)

Propan-2-ol (Isopropanol) (Fisher Scientific, cat no: P/7490/17)

Methanol (Fisher Scientific, cat no: M/3900/17)

Acetone (VWR, cat no: 20063.296)

Glycerol (Sigma, cat no: G5516)

Sodium Acetate (Sigma, cat no: S2889)

DNA extraction buffer
Tris 20mM, EDTA 25Mm and NaCl 0.1M

Sodium Dodecyl Sulfate (SDS) (Sigma, cat no: L4390)

DMSO (Sigma, cat no: D2650)

TRIzol (Invitrogen, cat no: 15596-026)

AquaPhenol (Q-BIOgene, cat no: AQUAPH01)

Chloroform:Isoamyl alcohol 24:1 (Sigma, cat no: C0549)

Ammonium Acetate (Sigma, cat no: A1542)

Powdered Milk (Merck, cat no: 1.15363.0500)

'Blenis' lysis buffer
10 mM K2PO4 (pH 7.4), 1 mM EDTA pH 7.05, 5 mM EGTA, 10 mM MgCl2, 50 mM β-glycerol phosphate, 1 mM Na3VO4 (Added fresh before use), 2 mM DTT (Added fresh before use.) Protease inhibitors: cOmplete, Mini Protease Inhibitor Cocktail tablets. (Roche, cat no: 04693124001). Each tablet is sufficient for a volume of 10 ml extraction solution.

1x running buffer for SDS PAGE

20ml of 20X NuPAGE® MES SDS Running Buffer (for Bis-Tris Gels only) (Invitrogen, cat no: NP0002) or 20X NuPAGE® Tris-Acetate SDS Running Buffer (Invitrogen, cat no: LA0041) in 400ml dH_2O

Western blot transfer buffer (500ml)

50ml 20X NUPAGE transfer buffer (Invitrogen, cat no: NP00061), 425ml of dH_2O, 25ml 100% methanol

ECL Prime western blotting detection reagent (GE Healthcare, cat no: RPN2232)

1M DTT (Invitrogen, cat no: P2325)

Hi-Di™ Formamide (Applied Biosystems, cat no: 4311320)

2.1.2 Bacterial culture

2.1.2.1 Bacterial strains

One Shot®OmniMAX 2T 1 ^{R} T1 phage resistant chemically competent cell line. For all cloning applications. (Invitrogen, cat no:C8540-03)

2.1.2.2 Bacterial culture reagents

Luria Bertani (LB) culture medium

10g Tryptone, 5g Yeast extract, (Becton, Dickinson cat no:211705 and 212750) 10g NaCl in 1L dH_2O

LB-Agar medium

15g Bacterial agar (Becton, Dickinson cat no:214010), 10g Tryptone, 5g Yeast extract, 5g NaCl in 1L dH_2O

SOC medium (Invitrogen, cat no:15544-034)

Formulation per 1 litre: 2% Tryptone, 0.5% Yeast extract, 10mM Sodium chloride, 2.5mM Potassium chloride, 10mM Magnesium chloride, 10mM Magnesium sulphate, 20mM Glucose

Ampicillin stock solution

50mg/ml ampicillin sodium salt (Melford Laboratories LTD, cat no: A0104) in dH_2O, filter sterilised and stored at -20°C. Final concentration of 100ug/ml.

Kanamycin stock Solution

50mg/ml kanamycin disulfate salt (Sigma, cat no: K1876) in dH_2O, filter sterilised and stored at -20°C. Final concentration of 100ug/ml.

Qiagen plasmid extraction kits

QIAprep miniprep plasmid kits (Qiagen, cat no: 27104) and QIAprep maxi kits (Qiagen, cat no: 12263).

2.1.3 Cell culture

2.1.3.1 Cell lines

Tumour derived cell lines were either directly cultured from primary tissue (neurofibroma derived Schwann cell lines) or obtained from our collaborators in the department of Maxillofacial Surgery, University Medical Centre Hamburg Eppendorf, Martinistrasse 52, 20246, Hamburg, Germany or the Brain Tumour Research Centre The Hospital for Sick Children RI, 101 College Street Toronto Medical Discovery Tower, East Tower, 11-401E Toronto, ON, Canada. The cell lines used were:

Patient derived MPNST cell lines: SNF96.2, SNF94.3, ST8814, T530 and T532
Kindly donated by Abhijit Guha (University of Toronto, Canada)

Patient derived MPNST cell lines: T566, T567 and T568
Kindly donated by Victor Mautner (University Medical Centre, Hamburg)

Neurofibroma derived Schwann cell lines: T534, T535A, T535B, T536A, T536B, T539, T541.1, T541.2, T541.3, T543.1, T543.2 and T543.3. Tissue kindly donated by our NF1 patients.

Patient derived fibroblast cell lines: Tissue kindly donated by our NF1 patients and relatives.

Human embryonic kidney cells (HEK293): ATCC, cat no: CRL-1573 (Kindly donated by Dr Andrew Tee, Cardiff University, Cardiff)

2.1.3.2 Cell culture reagents

Dulbecco's Modified Eagle Medium (DMEM)
L-glutamine, 4500 mg/L D-glucose, 110mg/L sodium pyruvate (Gibco, Invitrogen, cat no: 41966-029)

Fetal Bovine Serum (FBS) (Gibco, Invitrogen, cat no: 10106 169)

Penicillin/Streptomycin (Pen/Strep)
10 000 units of penicillin (base) and 10 000 units of streptomycin (base)/ml utilising penicillin G (sodium salt) and streptomycin sulphate in 0.85% saline (Invitrogen, cat no:15140-122)

Opti-MEM® I reduced serum medium 1x
Contains: HEPES buffer, 2,400mg/L sodium bicarbonate, hypoxanthine, thymidine, Sodium Pyruvate, L-glutamine, No phenol red. (Invitrogen, cat no:11058-021)

Trypsin-EDTA solution (Invitrogen, cat no: R-001-100)

Cell freezing medium
10% DMSO, DMEM, 10%FBS

Lipofectamine 2000 transfection reagent (Invitrogen, cat no: 11668-019).

3-Isobutyl-1-methylxanthine (IBMX)

Powder dissolved in 50% Ethanol and used at 0.5M (Sigma cat no: 15879)

Insulin

1mg/ml stock in PBS plus 5µl of 1M HCL (Sigma, cat no: 16634-50MG)

Forskolin

2µM stock in 96% ETOH. (Sigma, cat no: F-6886)

β-Heregulin (rhNRG-1-β1/HRG-β1)

0.2mM stock: 50µg in 31.25µl PBS and 1%BSA (R&D Systems, cat no: 396-HB)

Collagenase (278U/mg)

2780U/ml stock: 10mg/1ml in DMEM and 10% FBS (Sigma, cat no: C0130-100MG)

Dispase I (6U/mg)

30U/ml: 5mg/1ml in dH_2O (Roche, cat no: 04942086001)

N2 supplement (Gibco, cat no: 17502-018)

Poteinase K

1mg/ml stock in dH_2O (Sigma, cat no: P2308-500MG)

Poly-L-Lysine

0.1 mg/ml stock (Sigma, cat no: P4707)

Natural mouse laminin

1mg/ml Stock. 4µg/ml working concentration. (Invitrogen, cat no: 23017-015)

2.1.4 Molecular biology solutions and reagents

Ethidium bromide (Sigma, cat no: E1510)

DNA loading solution

0.03g Bromophenol Blue (Sigma, cat no: B8026), 0.03g Xylene Cyanol (Sigma, cat no:X4126), 7.5g Ficoll 400 (Sigma, cat no: F9378) and 0.558g EDTA in 50ml dH_2O

NuPAGE® LDS sample buffer (4X) (10 ml) (Invitrogen, cat no: NP0007)

Novex® Sharp pre-stained protein standard (Invitrogen, cat no:LC5800)

1Kb plus ladder (250µg)
Suitable for sizing linear double stranded DNA fragments from 100 to 12kb. The ladder consists of 12 bands ranging in size from 1000bp to 12000bp in exact 1000bp increments as well as 7 bands from 100bp to 850bp (Invitrogen cat no: 10787-018).

Primers
All primers for use in PCR and sequencing were unless otherwise stated designed using Primer3 V. 0.4.0 (Rozen and Skaletsky, 2000) and synthesised by Eurogentec using standard purification and 10nm synthesis scale. All primers containing a HEX, FAM or TET fluorescent label were synthesised on a 40nm scale. All primers were put through BLAT software (Kent, 2002) to ensure specificity.

Deoxynucleotide triphosphates (4x 25µm)
100mM stock. dNTP set consisting of dATP, dCTP, dGTP, dTTP for PCR and cDNA synthesis (Invitrogen, cat no: 10297-018)

Agarose (multipurpose) (Roche, cat no: 11388991001)

Bioresolve agarose, hi-strength, low melting point (Biogene, cat no: 300-750)

NuPAGE® polyacrylamide gel
NuPAGE® Novex 4-12% Bis-Tris Gel 1.0 mm (Invitrogen, cat no: NP0322)
NuPAGE® Novex 3-8% Tris-Acetate Gel 1.0 mm (Invitrogen, cat no: EA03752)

Whatmann chromatography paper (Sigma, Cat no: Z270903).

Immobilon- P membrane PVDF (Millipore, cat no: IPVH 000 10)

X-ray film (Fujifilm, cat no: 4741008389)

2.1.5 Molecular biology enzymes

AmpliTaq Gold® DNA polymerase with gold buffer and $MgCl_2$ solution (2U/µl) (Applied Biosystems, cat no: 4311818)

Big Dye terminator v1 cycle sequencing kit (Applied Biosystems, cat no: 4337450)

Power SYBR® Green PCR master mix (Applied Biosystems, cat no: 4367659)

SuperScript II reverse transcriptase (Invitrogen, cat no: 18064-014)

RNAsin ribonuclease inhibitor (Promega cat no: N2111)

Shrimp Alkaline Phosphatase (SAP) (GE Healthcare, cat no: E70092Z)

2.1.5.1 Restriction enzymes

Enzyme	Buffer	Company	Catalogue Number
Msp	10x Buffer	Cambio	REZ-MSP-2K
Rsa1	10x RE_{ACT} Buffer	Invitrogen	515424-013
*Hind*III	10x Buffer E	Promega	R604A and R005A
*EcoR*I	SuRE/Cut Buffer H	Roche	11175084001
DpnI	10x NE Buffer 4	New England Biolabs	R0176S and B7004S)
ExoI		New England Biolabs	M0293

2.1.6 Immunohistochemistry reagents

Citrate buffer (pH6)

2.1g Citric Acid Monohydrate (Sigma, Cat no: 33114), 1 Litre dH_2O

Hydrogen Peroxide

300ml dH_2O and 3ml H_2O_2 (Sigma: Cat no: H1009)

VECTASTAIN ABC kit (rabbit IgG) (Vector labs, cat no: PK-4001)

Block buffer: 500µl TBS and 7.5µl goat serum

Secondary antibody: 500µl TBS, 7.5µl goat serum, 2.5µl goat Biotinylated secondary antibody anti rabbit

ABC peroxidase: 10µl buffer A, 10µl buffer B, 500µl TBS

VECTASTAIN ABC kit (mouse IgG) (Vector labs, cat no: PK-4002)

Block buffer: 500µl TBS and 7.5µl horse serum

Secondary antibody: 500µl TBS, 7.5µl horse serum, 2.5µl goat Biotinylated secondary antibody anti mouse

ABC peroxidase: 10µl buffer A, 10µl buffer B, 500µl TBS

Peroxidase substrate kit DAB

2.5ml dH_2O, 1 drop buffer, 2 drops DAB, 1 drop H_2O_2 peroxidase (Vector Labs, Cat no: SK-4100)

DPX (VWR, cat no: 360294H)

Gills Haematoxylin (Sigma, cat no: GHS132-1L)

Poly-L-Lysine (Sigma, cat no: P8920)

Diluted 1:10 with dH_2O

2.1.7 Antibodies

2.1.7.1 Primary antibodies (TBS-T + 2% BSA)

- Mouse monoclonal Rac1: 1:500 (Abcam, ab33186)
- Mouse monoclonal ROCK2: 1:1000 (Abcam: ab56661)
- Mouse monoclonal V5 (1:5000) (Abcam: ab27671)

- Rabbit polyclonal IgG, c-Met HRP (1:10,000) (Santa Cruz Bio, Cat no:C-28)
- Mouse monoclonal p53 pre-diluted antibody (Biogenex, cat no: MU239-UC)
- Rabbit polyclonal anti-S100 (1:100) (Dako, cat no: Z0311)

2.1.7.2 Secondary antibodies

- Anti-mouse IgG, HRP-linked Antibody (1:1000) (NEB: 7076S): Rac1 and ROCK2:
- Rabbit polyclonal secondary antibody to mouse IgG HRP conjugated (1:10,000) (Abcam: ab6728): V5 and p-cMET:

2.1.8 Laser capture microdissection

LCM PALM 1.0 PEN membrane slides (Carl Zeiss, cat no: 415190-9041-001)

Leica RM 2235 microtome (Leica)

Axiovert S100 inverted phase contrast and fluorescence microscope (Zeiss)

2.1.9 Equipment and instruments

Thermocyclers for PCR reactions and incubations included a Primus 96+ (MWG-Biotech), GS1 (G-STORM) and Gene Amp PCR System 2700 (Applied Biosystems). Horizontal gel tank apparatus were supplied by Biorad. Centrifugations were performed in a bench-top microcentrifuge, Eppendorf 5415C (Eppendorf) as well as a Universal 320 (Hettich Zentrifugen). Purified sequencing reactions were analysed using an ABI Prism 3730 Genetic Analyser and all LOH, MSI and MLPA reactions were run on an ABI Prism 3100 (Applied Biosystems). Relative quantification was completed on an ABI 7500 (Applied Biosystems). The transfer system for SDS PAGE was from Hoefer and the Minigel Western blot electrophoresis module was from Novex, supplied by Invitrogen. Following nucleic acid extraction, the resulting concentration was determined using 2µl of the DNA or RNA on a Nannodrop 8000 spectrophotometer (Thermo Scientific).

2.2 Methods

2.2.1 Bacterial culture

2.2.1.1 General growth of bacteria

All bacterial culture was completed under sterile conditions. All solutions and glassware were autoclaved prior to use and sterile plastic ware was used. Universals were used for all small scale culture and large scale culture was contained in glassware.

2.2.1.2 Preparation of LB culture medium

All bacteria were cultured in LB medium. This was prepared as described in section 2.1.2.2 and adjusted to pH7. The lid was screwed loosely onto the bottle and held in place with a strip of autoclave tape and autoclaved using the liquid cycle.

2.2.1.3 Preparation of LB-agar plates

LB plates (section 2.1.2.2) were prepared in the same manner as the LB culture medium but with the addition of bacterial agar. Following autoclaving on the liquid cycle, the LB-agar was cooled to 55°C and the appropriate antibiotic at the appropriate concentration was added. A thin layer of agar (approx 20ml) was poured into each 80mm sterile petri dish and allowed to set. Plates were stored in a plastic bag at 4°C.

2.2.1.4 Transformation of bacterial cells

The E.coli strain one Shot®OmniMAX 2T1^R were chosen as they are a chemically competent cell line suitable for all cloning applications including gateway technology. One Shot®OmniMAX 2T1^R chemically competent bacteria were thawed on ice and 25µl of bacteria were transferred to a pre-chilled 1.5ml eppendorf tube. 2.5µl of the plasmid DNA was added to the bacterial cells, mixed gently and incubated on ice for 30 minutes. A control transformation was also carried out by adding 5µl of pUC19

high copy number control plasmid to a separate aliquot of 25µl of cells and incubated as above. Cells were heat shocked at 42°C for 30 seconds and incubated on ice for 2 minutes. 250µl of SOC media was added to the cells and the cells were then shaken horizontally for an hour at 37°C in an orbital shaker at 220rpm (Innova 4000, New Brunswick Scientific). During this growth period, selective antibiotics were omitted to allow the cells to express antibiotic resistance genes prior to exposure. At the same time agar plates containing the appropriate antibiotic were placed in the incubator (Prime series, Gallenkamp) at 37°C to warm up.

Following the hour incubation, the pUC19 control transformations were diluted 1:50 in LB medium and 100µl was spread onto LB-agar plates containing the appropriate antibiotic. Unless otherwise stated, experimental transformation reactions were centrifuged at 6500rpm using a microcentrifuge for 2 minutes to concentrate the cells. The resulting pellets were re-suspended in 150µl of LB medium and spread onto LB agar plates. The plates were allowed to dry for 10 minutes and incubated at 37°C for approximately 14-16 hours, after which colonies were counted and the transformation efficiency calculated according to the number of colonies on the control transformation plate. Plates were stored at 4°C.

2.2.1.5 Starter cultures

Sterile pipette tips were used to isolate single colonies from freshly streaked selective LB-agar plates and used to inoculate 5ml of LB medium containing the appropriate selective antibiotic. This was incubated for 14 hours at 37°C in an orbital shaker at 220rpm and the cells were either harvested by centrifugation for 2 minutes at 13,000 rpm in a microcentrifuge, added to glycerol for long term storage (section 2.2.1.6) or diluted 1/5 with LB and transferred to 250ml large scale cultures (section 2.2.1.8).

2.2.1.6 Long term storage of transformed bacteria

50% Glycerol was made by adding 250ml 100% glycerol to 250ml distilled water. The bottle was capped but not tightened and autoclaved on a liquid cycle. After cooling the lid was tightened and the 50% stock was stored at room temperature. For

long term storage, glycerol stocks were prepared by adding 500µl of overnight culture to 500µl of 50% glycerol in a 2ml screw top tube, vortexed to mix and stored at -80°C. Bacterial transformants were recovered from glycerol stocks by streaking a sterile transfer loop of the glycerol stock onto an LB-agar plate containing the appropriate antibiotic and incubating overnight at 37°C.

2.2.1.7 Small scale plasmid purification

Small scale purification of plasmid DNA was completed using a QIAprep spin miniprep kit for purification of 1-5ml of plasmid DNA using a microcentrifuge and using the manufacturers protocol (Qiagen). The protocol is based on the alkaline lysis method by Birnboim and Doly (1979). Briefly, bacterial cells were harvested by centrifugation (as above) then resuspended in 250µl of buffer P1, containing RNaseA (100µg/ml) and transferred to a microcentrifuge tube. 250µl of buffer P2 (lysis buffer) was added to the tube and inverted 4-6 times to mix and cause lysis of the bacterial cells. 350µl of buffer N3 (neutralisation buffer) was then added to the tube and again inverted 4-6 times to mix and neutralise the reaction. The reaction was then centrifuged for 10 minutes at 13,000rpm. A solid white pellet formed and the supernatant was transferred to a spin column and centrifuged for a further minute after which the flow through was discarded. The QIAprep spin column silica membrane was then washed by adding 750µl of buffer PE and centrifuged for 1 minute to remove salts. The flow through was discarded and the column centrifuged for an additional minute to remove residual wash buffer. Finally, the QIAprep column was put into a clean 1.5ml microcentrifuge tube and 50µl buffer EB (10mM TrisHCl, pH 8.5) or dH_2O was applied to the centre of each QIAprep column to elute the DNA. This was left to incubate at room temperature for 1 minute and then centrifuged for 1 minute at 13,000rpm.

2.2.1.8 Large scale plasmid purification

The HiSpeed Plasmid maxiprep kit (Qiagen) was used for purification of low copy plasmid DNA using the manufacturers' protocol. Briefly, bacterial cells were harvested by centrifugation at 6000 x *g* for 15 min at 4°C and then resuspended in 10ml of buffer P1. 10ml buffer P2 was added to the tube and inverted 4-6 times to

mix and cause lysis of bacterial cells; this was incubated for 5 minutes. 10ml pre-chilled buffer P3 was added to the mixture and this was immediately poured into the barrel of a QIAfilter Cartridge and incubated at room temperature for 10 minutes. During this incubation, a HiSpeed Maxi Tip was equilibrated by applying 10 ml Buffer QBT and this was allowed to flow through the column by gravity flow. The cap from the QIAfilter outlet nozzle was removed and the plunger was inserted into the QIAfilter Maxi Cartridge and the cell lysate filtered into the previously equilibrated HiSpeed Tip. The cleared lysate was allowed to enter the resin by gravity flow. The HiSpeed Maxi Tip was then washed with 60ml Buffer QC and the DNA was eluted with 15ml Buffer QF. The DNA was precipitated by adding 10.5ml (0.7 volumes) room temperature isopropanol and mixed and incubated at room temperature for 5 minutes. During the incubation the plunger was removed from a 30 ml syringe and attached to the QIAprecipitator Maxi Module outlet nozzle. The QIAprecipitator was placed over a waste bottle and the eluate/isopropanol mixture was transferred into the 30ml syringe, the plunger inserted, and the eluate/isopropanol mixture was filtered through the QIAprecipitator using constant pressure. 2ml 70% ethanol was then added to the syringe and the DNA was washed by inserting the plunger and pressing the ethanol through the QIAprecipitator using constant pressure. The membrane was dried twice by pressing air through the QIAprecipitator quickly and forcefully and the outlet nozzle of the QIAprecipitator was dried with absorbent paper to prevent ethanol carryover. Finally the DNA was eluted by holding the outlet of the QIAprecipitator over a 1.5ml collection tube and 1ml of Buffer TE was added to a 5ml syringe and filtered using constant pressure.

2.2.2 Cell culture

2.2.2.1 Growth and maintenance of cell lines

All patient derived MPNST cell lines (SNF 96.2, SNF94.3, ST8814, T530, T532, T566, T567, T568) and HEK293 cells were grown in T75 flasks (Helena Biosciences, cat no:90076) in 10ml of DMEM, 10% FCS and 1% pen/strep. Neurofibroma derived Schwann cell lines were grown as described in section 2.2.2.5 and passaged using the same method described below.

2.2.2.2 Splitting cells

All adherent cell lines were passaged using the same method. The cells were first washed with 5ml of PBS and then detached with 2ml of Trypsin-EDTA and incubated at 37°C for a few minutes (cells rounded up when inspected under a microscope). The trypsinised cells were then transferred into two separate falcon tubes and the medium was made up to 10ml with DMEM and 10% FBS. The tubes were centrifuged at 1200rpm for 7-10 minutes to produce a cell pellet at the bottom of the tube. The medium was removed from the falcon tube (leaving the pellet at the bottom) and the pellet was resuspended in the appropriate volume of medium. The cells were then mixed into this medium using a pipette to distribute the cells and the medium was divided evenly between the appropriate number of flasks (coated in the case of neurofibroma derived Schwann cells, section 2.2.2.5.3). Flasks were incubated at 37°C with CO_2 and either split, cryopreserved (section 2.2.2.4), or the medium was changed when appropriate.

2.2.2.3 Determination of cell density

Accurate numbers in a cell suspension were calculated by counting the cells in a Neubauer improved bright line haemocytometer (Marienfield, cat no: 0630030). Cells were trypsinised as previously described and resuspended in 1ml DMEM and 10% FBS. Cells were thoroughly dispersed and 30µl of the cell suspension was mixed with 30µl 0.1% w/v trypan blue in PBS solution (BioWhittaker, cat no: 17-942E); non-viable cells were stained blue. This was immediately mixed well and a sufficient volume to fill a side of the haemocytometer chamber was aspirated. Viable cells in each of the four corner squares bordered by triple lines were counted, omitting cells lying on these lines. The mean count of the total viable cells per four corner squares was calculated using the following formula:

$$C_1 = t \times tb \times 1/4 \times 10^4$$

t = total viable cell count of four corner squares

tb = correction for the trypan blue dilution (counting dilution was 1/tb)

1/4 = correction to give mean cells per corner square

10^4 = conversion factor for counting chamber

C_1 = initial cell concentration per ml

The working concentration was then obtained by mixing 1 volume of the original cell suspension with the appropriate volume of growth medium. Cells were dispensed in growth medium and seeded into the appropriate vessel and incubated as per the standard protocol as previously described. The dilution factor (d) was calculated to obtain the working cell concentration per ml (C_2) using the following formula:

$$d = C_2 \text{ (working cell concentration)} / C_1 \text{ (initial cell concentration)}$$

2.2.2.4 Cryopreservation

The medium was removed and cells were washed with 5ml PBS and 2ml of Trypsin as previously described. The entire contents of the flask was transferred into one falcon tube and centrifuged at 12000rpm for 7-10minutes to produce a pellet. Following centrifugation, the medium was removed and the cell pellet was resuspended in 0.5ml of the freeze mix: DMEM and 10% FBS and 10% DMSO. The mixture was transferred to a cryogenic vial and frozen to -80°C using a freezing container; Mr Frosty (Nalgene®) filled with isopropanol. This creates a temperature gradient, freezing the cells by 1°C per minute to prevent the formation of ice crystals within the cells which could rupture the membrane. Cells were transferred to liquid nitrogen for long term storage. Cells were defrosted rapidly at 37°C and quickly transferred to the appropriate flask containing the correct pre-warmed medium.

2.2.2.5 Schwann cell culture

Culture conditions for neurofibroma derived Schwann cells have been reported by Rosenbaum *et al*, (2000) and Serra *et al*, (2000) and are described in detail below. The presence of forskolin in the medium promotes the proliferation of Schwann cells. This occurs through elevation of intracellular cAMP and suppression of fibroblast growth. Replacement of proliferation medium by serum-free N2 medium (Bottenstein and Sato, 1979) followed by medium without forskolin, promotes schwann cell differentiation. N2 medium is a serum-free synthetic medium supplemented with insulin, transferrin, progesterone, selenium, and putrescine. Cells respond to the removal of serum through extensive process formation and retention of other differentiated properties. Growth of neuronal cells is stimulated with the N2 medium

and non-neuronal growth is suppressed. Cells were passaged when cultures were confluent and harvested not earlier than at passage eight.

2.2.2.5.1 Preincubation

3ml of preincubation medium (DMEM +10% FBS, 1% Pen/strep Forskolin [2μM]) filtered once through Millex syringe driven 0.22μM filters (Millipore, cat no:SLGS033SS) was added to each well on a 6 well plate (Nunclon, cat no: 140675). The tumours were dissected in DMEM + 10% FBS and a small piece from the centre of the tumour was dissected out and put into the pre-incubation medium in the 6 well plate. The tumour sections were then left to incubate for 10-14 days with the medium changed every 3 days without changing the plate or washing with PBS.

2.2.2.5.2 Incubation

Following the 10-14 day incubation in the preincubation medium, the tissue was transferred to a new 6 well plate and dissected into smaller pieces using a scalpel. Samples were then incubated for 24 hours in 3ml of DMEM + 10% FBS, 1% PenStrep, Collagenase [160U/ml] and Dispase I [0.8U/ml] filtered once with the Millex 0.22μM filter.

2.2.2.5.3 Coating flasks and plates

A T25 flask (Nunclon, cat no:136196) was coated with 1.2ml of sterile Poly-L-Lysine solution. This was left for 1 hour at room temperature and was then washed with sterile PBS. 1.2ml of 4μg/ml laminin was then filtered and added to each flask. This was incubated for 1 hour at 37°C, excess removed and then the flask was washed with PBS. The tissue in the 6 well plate was broken up using a pipette, transferred to a falcon tube and centrifuged for 10 minutes at 1200rpm. The supernatant was discarded and the pellet was resuspended in 5ml of DMEM + 10% FBS, 1% Pen/Strep, IBMX, [0.5mM], β-Heregulin [10nM], Forskolin [2μM] and Insulin [2.5μg/ml] and incubated for 24 hours. The medium was removed the following day and the N2 medium was prepared (10ml DMEM F12, 100μl/10ml N2 Supplement and 1% Pen/Strep) filtered as before, added to the 6 well plate and incubated for 24 hours. The following day the N2 medium was removed and replaced with 5ml of medium without Forskolin: DMEM +10% FBS, 1% Pen/Strep, IBMX [0.5mM], β-

Heregulin [10nM] and Insulin[2.5µg/ml] and incubated for 6 days under standard conditions, with the medium replaced after 3 days. After 6 days the cells were confluent and so were transferred to a larger T75 flask, coated with laminin and poly-l-lysine as previously described. The cultures were then harvested following the 8^{th}-12^{th} passage, the Schwann cell content of each culture being established by S100 immunohistochemistry (Serra *et al.*, 2000). S100 is a calcium binding protein specifically found in Schwann cells of the peripheral nerve (Mirsky and Jessen, 1996). Immunohistochemical analysis of Schwann cell lines used in all experiments was carried out to ensure that the population of cells that had been cultured was pure. Due to the method of fixation used for these cultures, while differential S100 staining could be identified, the morphology of the cells was often disrupted.

2.2.2.6 Plasmid DNA transfection

Transfection using lipofectamine (lipofection) was used to introduce plasmid DNA into cell lines. Synthetic cationic lipids including lipofectamine, interact spontaneously with DNA to form lipid-DNA complexes. These complexes can then fuse with the plasma membrane of cells in culture resulting in uptake of DNA and consequently expression of the DNA (Felgner et al, 1987). Lipofection is effective for both transient and stable expression of transfected DNA and can have greater transfection efficiency than calcium phosphate and electroporation.

2.2.2.6.1 Forward Transfection

One day prior to transfection, cells were seeded at the appropriate concentration ($6x10^5$ for HEK293) in 2ml of growth medium (DMEM and 10% FCS) in 6 well plates (Jencons, cat no: 734-0948) without antibiotics. Cells were seeded at a high density to ensure high transfection efficiency, high expression levels and to minimise cytotoxicity. For each transfection sample 3 complexes were prepared: (i) 4.0µg of plasmid DNA was diluted in 250µl of opti-MEM I reduced serum medium and gently mixed. (ii) Lipofectamine 2000 was gently mixed prior to use and then 10µl diluted in 250µl of opti-MEM I Reduced Serum Medium and incubated for 5 minutes at room temperature. (iii) After 5 minutes, complexes 1 and 2 were combined and gently mixed and incubated for 20 minutes at room temperature. The entire 500µl volume containing the two complexes was added to each well containing the cells and

medium. The plates were mixed by rocking the plate gently. Cells were incubated at 37°C with CO_2 for 48 hours. The medium was replaced after 6 hours.

2.2.2.6.2 Reverse Transfection for shRNA

On the day of transfection, 200ul of optimem and 2ml pen/strep free media per plate was pre-warmed to 37°C for an hour along with trypsin and enough pen/strep free media for resuspension of cells following trypsinisation. For each transfection sample the following complexes were prepared: (i) 2.5ug shRNA vector was added to an eppendorf along with 100ul of pre-warmed opti-MEM I Reduced serum medium and gently mixed. (ii) Lipofectamine 2000 was gently mixed prior to use and then 6.25µl diluted in 100µl of opti-MEM I Reduced Serum Medium (1:2.5 ratio of shRNA (ug):Lipofectamine 2000 (ul)) and incubated for 5 minutes at room temperature. (iii) After 5 minutes, complexes 1 and 2 were combined and gently mixed and incubated for 25 minutes at room temperature. After 25 minutes, the transfection mixture was added to a 35mm plate (Helena Biosciences, cat no: 93040). Cells were trypsinised as described above and during this period, 2ml pen/strep free media was added to the 35mm plate and mixed with the transfection mixture. Cells were seeded at the appropriate concentration, mixed and then incubated at 37°C with CO2 for 4-6 hours before changing the media to DMEM, 10% FCS and 1% Pen/strep. Cells were cultured for an additional 48 hours, and the media was changed if necessary.

2.2.2.6.3 Creating a stable knockdown

shRNA vectors used in this study contained a puromycin resistance cassette ensuring that cells successfully transfected with these vectors can survive even in the presence of the puromycin antibiotic. MPNST derived cell lines were treated with 2.5µg/ml puromycin every two days for 2 weeks (if significant cell death was seen, media was changed). After two weeks colonies formed which were individually trypsinised by pipetting 100µl of trypsin onto the colony, mixing in the pipette and then seeded separately in to new plates to continue growing.

2.2.3 Molecular biology

2.2.3.1 NF1 patient DNA and tissue samples

Tumours and DNA samples from patients fulfilling the NF1 NIH diagnostic criteria were provided by genetic centres in the UK (Cardiff, Institute of Medical Genetics, Cardiff University), Germany (Hamburg, Laboratory for Tumor Biology and Developmental Disorders, University Hospital Eppendorf.) and Canada (The Brain Tumour Research Centre The Hospital for Sick Children RI, 101 College Street Toronto Medical Discovery Tower, East Tower, 11-401E Toronto). Samples were obtained from patients with informed consent and all studies gained ethical approval from all the relevant institutional research boards. All tissue was kept at -80°C until required in order to ensure preservation of DNA and labile RNA.

2.2.3.1.1 DNA extraction from tissue samples

Once removed from the freezer, a scalpel was used to excise tumour tissue from surrounding tissue. Excised tissue for DNA extraction was finely chopped up using a scalpel and transferred to a 1.5ml microcentrifuge tube containing: 500µl extraction buffer, 50µl proteinase K and 12.5µl 20% SDS. The tube was incubated in a water bath at 65°C for 2 hours (alternatively 37°C overnight) and vortexed briefly every half hour. Once dissolved, 500µl Phenol was added to each tube and centrifuged at 13,000 rpm for 15 minutes using a microcentrifuge. The supernatant was subsequently transferred to a 15ml tube (Sarstedt) and 25µl of 7.5M Ammonium Acetate and 1.5ml of 100% Ethanol were added to the tube. The tube was slowly inverted until the DNA had spooled into a ball. The DNA was then transferred to a clean microcentrifuge tube containing 70% ethanol, inverted a few times and left for a minute to remove any salt in the solution which could interfere with PCR and digestions. The alcohol was then removed and the DNA pellet left to air dry for 10 minutes. 1x TE at a volume appropriate to the amount of DNA present (typically 200-400µl) was added and the tube put on a rotating wheel to dissolve overnight.

2.2.3.1.2 RNA extraction from tissue samples

All RNA work was carried out using sterile RNase-free plastic ware and reagents designed to reduce the risk of RNase contamination and RNA degradation. The frozen sample was removed from the freezer just prior to extraction when it was powdered by grinding with liquid Nitrogen with a pestle and motar. To prevent thawing in the mortar, it was previously chilled in a -80°C freezer for 10 minutes. By grinding the tissue in this manner, cellular disruption is more complete allowing for a high yield of RNA. The powdered tissue was transferred using a spatula to a universal tube containing 1ml TRIZOL. TRIzol contains guanidinium isothiocyanate, a powerful protein denaturant used to inactivate RNases. The tube was then incubated at 30°C for 10 minutes and 200μl of chloroform was added. Chloroform allows for the partitioning of RNA into aqueous supernatant for separation. Low pH is crucial since at neutral pH DNA not RNA partitions into the aqueous phase. The aqueous phase contains RNA; the interphase holds the DNA and the proteins and lipids are found in the organic phase.

The tube was vortexed for 15 seconds and incubated at 30°C for 3 minutes. The tube was then centrifuged at 14,000 rpm for 10 minutes at 4°C. The upper layer was transferred to a clean microfuge tube and 500μl of isopropyl alcohol was added and the tube was incubated on ice for 10 minutes. Isopropyl alcohol is better than alcohol precipitation for smaller amounts of RNA as there is less risk of losing very small nucleic acid pellets and it also reduces the risk of organic solvent contamination. After the incubation, the tube was centrifuged again under the same conditions as before. After centrifuging, the supernatant was removed without dislodging the RNA pellet, and 1ml of 75% ethanol was added and the tube centrifuged at 7,500 rpm for 5 minutes at 4°C. In the final stage, the ethanol was removed and the pellet was allowed to air dry for 10 minutes before 50μl RNA free water was added in addition to 0.5μl RNAsin. 2μl of RNA was run on a 1% LMT agarose (low melting temp) gel with 5μl of loading dye to ensure the RNA had not degraded.

2.2.3.1.3 Extraction of DNA from peripheral blood

All DNA extractions from peripheral blood were carried out by the NHS molecular genetics department, Cardiff, using the Gentra Nucleic Acid Purification System (Autopure)

2.2.3.1.4 DNA and RNA extraction from cultured cells

Cells were pelleted at 12,000rpm for 10 minutes in a centrifuge. Excess medium was removed and the pellets were washed with PBS to remove any inhibitory compounds. DNA and RNA was extracted using the protocols detailed in sections 2.2.3.1.1 and 2.2.3.1.2

2.2.3.1.5 Purification of DNA from agarose gels

The MinElute gel extraction kit protocol (Qiagen, cat no:28604) was used to purify PCR products from 1.5% agarose gels following the protocol supplied by the manufacturer. Briefly, DNA fragments were excised from the gel with a clean, sharp scalpel and extra agarose was removed. The gel slices were weighed and 3 volumes of Buffer QG was added to 1 volume of gel (100mg/100µl). The tube was incubated at 50°C for 10 minutes (or until the gel slice has dissolved). The tube was vortexed every 2-3 minutes to help the gel to dissolve. One volume of isopropanol was added to the sample and the content of the tube was mixed by inverting the tube several times. The entire sample was applied to the membrane of a MinElute column and centrifuged for 1 minute at 12,000rpm. The flow through was discarded and 500µl of Buffer QG was applied to the membrane and the column centrifuged again for 1 minute at 12,000rpm. The flow through was removed and 750µl of wash buffer PE was added to the column and centrifuged under the same conditions. Again the flow through was removed and the column was centrifuged to remove any residual ethanol containing buffer to ensure there is no interference with downstream applications. The tube was placed in a clean 1.5ml microcentrifuge tube and 10µl of elution buffer/dH_2O was applied to the membrane and left to stand for 1 minute. Finally the tube was centrifuged at 12,000rpm for 1 minute to elute the DNA.

2.2.3.1.6 DNA extraction from FFPE tissues

DNA extraction was completed using the QIAamp DNA micro kit (Qiagen, cat no: 56304) following the manufacturers protocol. Briefly, this involved the addition of 15µl of Buffer ATL to the laser-microdissected sample. 10µl of proteinase K was then also added and this was mixed by pulse-vortexing for 15 seconds. The sample was placed in a thermomixer and incubated at 56°C for 3hours with occasional agitation. Following this incubation, 25µl of buffer ATL was added in addition to 50µl of buffer AL and this was again mixed by pulse-vortexing for 15 seconds. 50µl 100% ethanol was also added and this was again mixed thoroughly by pulse-vortexing for 15 seconds and incubated for 5 min at room temperature (15–25°C) followed by brief centrifugation to remove drops from inside the lid. The entire lysate was transferred to the QIAamp MinElute column (in a 2 ml collection tube) and this was centrifuged at 8000rpm for 1 minute. The QIAamp MinElute column was placed in a clean 2 ml collection tube, and the previous collection tube containing the flow-through was discarded. 500µl buffer AW1 was added to the column and centrifuged 8000rpm for 1 min. Again the collection tube was changed and 500µl buffer AW2 was added to the column and centrifuged at 8000rpm for 1 min. The collection tube was changed again and the column was centrifuged at 14,000 rpm for 3 min to dry the membrane completely. Finally, the QIAamp MinElute column was placed into a clean 1.5ml microcentrifuge tube and 50µl buffer AE was added to the centre of the membrane and incubated at room temperature for 1 minute. The column was then centrifuged at 14,000rpm for 1 minute to elute the DNA. Extracted DNA was stored at -80°C until used for *NF1* gene analysis (section 3.3.3).

2.2.3.2 Polymerase chain reaction (PCR)

Direct sequencing allows the myriad of changes such as deletions, insertions and single base pair substitutions to be detected. For optimal product purification and recovery of small PCR products (<300bp) of the *NF1* gene, a 25µl PCR reaction was set up using DNA at a concentration of 6ng/µl and carried out on a thermal cycler at an annealing temperature of 60°C using the primers in supplementary table 2 and the following reagents and conditions:

Reagent Volume	25µl	Cycle Conditions	x35 Cycles
DNA [6ng/µl]	5µl		
Buffer	2.5µl	95°C	10 Minutes
Mg [50mM]	1µl		
dNTP's [10µM]	2µl	94°C	1 Minute
Sense Primer [1pm/µl]	1µl	60°C	1 Minute
Antisense Primer [1pm/µl]	1µl	72°C	1 Minute
Taq	0.1µl		
H_2O	12.4µl	72°C	10 Minute

2.2.3.2.1 Agarose gel electrophoresis

1.5% agarose gels were made by combining 1.5g multipurpose agarose with 100ml of 1X TBE and heated in a microwave for 2 minutes to melt the agarose. 100ml of 1.5% agarose gel was stained with 4µl of Ethidium Bromide, poured into the gel moulds and left to set prior to loading of PCR product. Unless otherwise stated, 4µl of PCR product was combined with 5µl of DNA loading dye and loaded onto the 1.5% multipurpose agarose gels. Gel tank equipment (Biorad) was set to 100Volts (0.4Amps) and run for 30 minutes. After running the gel, bands were visualised under UV with a GelDoc Imaging Station and Quantity One Software (Biorad)

2.2.3.3 DNA sequencing

2.2.3.3.1 ExoSAP PCR purification

This method of purification involves the enzymatic removal of excess nucleotides and primers from the PCR reactions. 1µl of SAP and *ExoI* was added to the PCR product to be purified in a 2:1 ratio. The PCR product was then incubated for 1 hour at 37°C to activate the *ExoI* and then 80°C for 15minutes to deactivate the *ExoI.*

2.2.3.3.2 Big Dye terminator reaction

The BigDye terminator mix was prepared using the following reagents and cycle conditions:

Reagent Volume	10µl	Cycle Conditions	x30 Cycles
DNA (PCR product)	1.5µl	96°C	5 minutes
BigDye	0.25µl		
Buffer	2µl	96°C	30seconds
Primer[10µM]	0.16µl	50°C	15 seconds
H_2O	6.09µl		
		60°C	4 minutes

2.2.3.3.3 Isopropanol sequencing purification

This method removes unincorporated dyes by isopropanol precipitation. 40µl of 75% isopropanol was added to each well and mixed gently. The reaction was incubated at room temperature for 30 minutes followed by centrifugation at 4000rpm for 45 minutes. After centrifugation, the plate was inverted on to absorbent paper to remove the isopropanol and then placed inverted into the rotor bucket and centrifuged at 500rpm for 30 seconds. The plate was left to air dry in a dark box for 10 minutes and DNA was finally resuspended in 10µl of Hi-Di™ Formamide and analysed on an ABI 3730 analyser (Applied Biosystems).

2.2.3.4 RNA analysis

2.2.3.4.1 RNA first strand synthesis and reverse transcription

Following RNA extraction, first strand synthesis was carried out in a 12µl reaction volume with random primers (200ng/µl), dNTP mix (10mM) and RNA (2.5ng/µl). The reaction mixture was heated to 65°C for 5 minutes to disrupt any template secondary structures and then was briefly chilled on ice to prevent re-formation of secondary structures. 1µl of SuperScript II Reverse Transcriptase (200U/µl) was added to each reaction and heated for 2 minutes at 25°C. 4µl 5x First Strand buffer, 2µl 0.1 M DTT and 1µl RNAsin was then added to each reaction and reactions were heated at 25°C for 10 minutes, 42°C for 50 minutes and finally 70°C for 15 minutes.

2.2.3.4.2 cDNA PCR

A 25µl cDNA PCR was set up using the following reagents, cycle conditions, and the primers in supplementary table 3 at an annealing temperature of 58°C. Gel analysis, PCR purification, sequencing and sequence purification were also completed as previously described

Reaction Volume	25µl	Cycle Conditions	x35 Cycles
cDNA	1µl		
Buffer	2.5µl	94°C	1 Minute
Mg [50mM]	0.27µl	56°C	1 Minute
dNTP's [10µM]	0.5µl	72°C	1 Minute
Sense Primer [10pm/µl]	0.5µl		
Antisense Primer [10pm/µl]	0.5µl	72°C	10 Minutes
Taq	0.2µl		
H_2O	19.05µl		

2.2.3.5 Characterisation of Sequence Alterations

All sequence alterations were fully characterized by direct sequencing using an ABI 3730 analyser (Applied Biosystems). The resulting sequence was analysed using Sequencher software (Gene Codes, USA)

2.2.4 Immunohistochemistry (IHC)

2.2.4.1 *Preparation of slides for IHC*

For all IHC except laser capture microdissection, Superfrost microscopy slides (VWR, cat no: 8037/1) were pre-treated with UV for 30 minutes, immersed in poly-l-lysine for 5 minutes and then incubated at 40°C in an incubator overnight to dry. 5µm thick sections were cut from pre-chilled formalin fixed paraffin embedded (FFPE) blocks using a microtome and mounted onto the slides using a water bath at 40°C. The slides were then incubated at 40°C in an incubator overnight.

2.2.4.2 Preparation of LCM PALM membrane slides

LCM PALM membrane 1.0 PEN slides were pre-treated with UV light for 30 minutes and then with Poly-L-Lysine for 5 minutes. The slides were then incubated at 40°C overnight to dry. Blocks of paraffin embedded tissues were cut into 10µm thick sections using a Microtome. Dependent on the size of the tumour, up to 3 sections were cut for H&E staining and mounted onto the central membrane area of the LCM slides using a water bath at 40°C. An adjacent section was also cut for S100 staining and mounted onto normal pre-treated microscopy slides. The LCM slides were then incubated at 60°C overnight (40°C for S100 slides) to melt the wax and fix the samples to the slides.

2.2.4.3 IHC on FFPE tissues

Deparaffinisation was completed using sequencial wash steps. Two xylene washes for 5 minutes each, two 100% ethanol washes (5 minutes each), a 70% ethanol wash (5 minutes), 50% ethanol wash (5 minutes) and finally a dH_2O wash for 2 minutes. Slides were then put into Citrate Buffer to aid in antigen recovery and heated on high power in a microwave to start the buffer boiling and then for 10 minutes on medium power to maintain boiling of the buffer. The slides were rinsed in running tap water for 5 minutes and put into 3% H_2O_2 to block endogenous peroxide for 20 minutes. After another 5 minute wash in running tap water and then a 5 minute TBS wash, slides were put into a tray and the sample was circled with a wax pen. The block buffer was prepared (section 2.1.6) and 100µl added to each slide and incubated at room temperature for 20 minutes.

Following the incubation, the buffer was tapped off and the primary antibody was prepared at the recommended dilution (section 2.1.7.1) and 100µl was added per slide and incubated at 4°C overnight. Following this incubation, the slides were washed twice with TBS for 5 minutes each. During these wash steps, the ABC peroxidase and secondary antibodies were prepared (section 2.1.7.2). The slides were then incubated with 100µl of secondary antibody at room temperature for 30 minutes. The slides were washed twice more with TBS for 5 minutes each and then

each slide was incubated with 100µl ABC peroxidase at room temperature for 30 minutes. The slides were washed twice more with TBS for 5 minutes each and during the second incubation; the DAB was prepared (section 2.1.6). 200µl DAB was added to each slide and the colour was allowed to develop and then immediately the DAB was tapped off and slides were washed in TBS for 2 minutes and dH_2O for 2 minutes. If a counterstain was required (e.g. Gills Haematoxylin), slides were immersed in the counterstain for 1 minute and then rinsed in running water for 5 minutes. The slides were finally dehydrated using sequencial washes: 50% ethanol (5 minutes), 70% ethanol (5 minutes), two 100% ethanol washes for 5 minutes each and two xylene washes for 5 minutes each. Slides were finally mounted using DPX.

2.2.4.4 Modified Haematoxylin and Eosin staining for FFPE tissues for LCM

A modified H&E stain was applied to each of the slides using an automated Varistain Gemini (Thermo Scientific). Slides were initially dewaxed and hydrated using sequencial washes of xylene (5 minutes) followed by a fresh xylene wash (2 minutes), 100% ethanol wash (1 minute), 95% ethanol (1minute), 70% ethanol (1 minute) and a running water wash (1 minute). The sections were then stained with Harris Haematoxylin (2 minutes) followed by two running water washes for 1 minute each. Slides were immersed in bluing reagent for 1 minute and Eosin for 10 seconds followed by two running water washes for 1 minute each. Finally slides were dehydrated with 70% ethanol (1 minute), 95% ethanol (1 minute) and 100% ethanol for 1 minute. Following staining, H&E stained slides were stored at -80°C until used in LCM.

2.2.4.5 mmunocytochemistry (ICC)

Cells were grown as previously described. Once confluent, cells were split and $2x10^5$ cells were resuspended in DMEM, 10% FBS and 1% Pen/strep and plated onto small 22x26mm coverslips placed into each well on a six well plate. Cells were left to adhere to the coverslip for 4 hours before the wells were filled with 2ml of the same medium and incubated at 37°C overnight. Leaving the cells for longer than this led to detachment from the plate due to the cells becoming over confluent.

The following day, the medium was removed and the wells were washed twice with PBS for 1 minute. 1ml of methanol and acetone in a 1:1 ratio was added to each well

and incubated at -20°C for 20 minutes to fix the cells. The methanol and acetone was then removed and 1ml of PBS was added to the wells to wash the cells. The cells on the coverslips were stained as described in section 2.2.4.5 with the omission of the deparaffinisation, antigen recovery and hydrogen peroxide steps which were not required.

2.2.5 Relative quantification (qPCR)

Relative quantification PCR (qPCR) is a method by which changes in expression of a nucleic acid sequence (the target) in a test sample can be determined relative to the same sequence in a calibrator sample such as an untreated control or a sample at time point zero in a time course study (Livak and Schmittgen, 2001). Without needing to determine the exact copy number of the template, relative quantification can give an accurate comparison between the initial levels of template in each sample. Relative quantification was used to determine a relative increase or decrease in expression of the genes of interest as determined by the delta delta ct method [ΔΔct] (comparative ct) given by the equation: t=0=2-ΔΔct. The ct values of the samples of interest are compared with that of a control (calibrator sample - RNA from normal tissue). The ct values of both the calibrator and the samples of interest are then normalized to an appropriate endogenous housekeeping gene (B2M) (Ponchel et al, 2003). Relative quantification was completed with the use of real-time PCR in which it is possible to observe the progress of a PCR reaction as it takes place with data collected throughout the reaction not just at the end point. The reaction is typified by the point during the cycle at which the target to be amplified is first detected instead of the amount of target which is accumulated by the end of the reaction. Primers for use in real time PCR were designed using Primer Express (Applied Biosystems). Relative quantification was carried out using the following reagents and cycle conditions:

Reagent Volume	12.5µl	SYBR® Green	6.5µl
DNA (5ng/µl)	1µl	Sense Primer [2µM]	1µl

Antisense Primer [2μM]	1μl	95°C	10 minutes
H_2O	3μl		
		95°C	15seconds
Cycle Conditions	x40 Cycles	60°C	1minute
50°C	2minutes		

Three replicates were used per experiment and Beta-2-Macroglobulin (B2M) served as an endogenous control. Control reactions were used to eliminate the presence of contaminants in the DNA samples and specificity of PCRs were determined by gel analysis and the addition of a dissociation step, producing a single peak upon analysis representing a specific reaction. All data was analysed with the ABI 7500 SDS System software (Applied Biosystems). All reactions were assessed for PCR efficiency by producing standard curves. The ct values were plotted against the log concentration of the template and a linear trend line was applied. The qPCR standard curve slope to efficiency calculator (Stratagene) was used to assess the efficiency based on the equation: Efficiency = -1+10(-1/slope). A slope of −3.32 represents optimal efficiency (100%), assays with amplification efficiencies of between 90 and 100% considered acceptable with an r^2 close to 1 and a Y-intercept similar for all assays. All qPCR assays in this study were >97% efficient.

2.2.6 Immunoprecipitation (IP)

Immunoprecipitation uses the antigen-antibody reaction principle to identify a specific protein of interest. A protein can therefore be purified from a mixture of proteins to assess its quantity or physical characteristics. Cells were lysed in 1ml of lysis buffer (see above). Samples were put through several freeze thaw cycles to aid in cell lysis and finally sonicated in a 2ml tube surrounded by ice for 10 seconds or homogenised for 20seconds per sample to break up cells (the homogeniser was washed with dH_2O in between each sample). The cells were then centrifuged at 13,000rpm for 8 minutes at 4°C to pellet cell debris and remove air bubbles. A 1.5ml eppendorf tube corresponding to each sample was pre-chilled on ice and the *cMET* rabbit polyclonal antibody was added to the tube at a concentration of 1μg/ml (5μl). 600μl of cell lysate was added to each tube containing the antibody and incubated at 4°C overnight with agitation. The 20% ethanol in which G-coupled Sepharose beads are stored was removed by inverting and briefly centrifuging at 3000rpm for 2 minutes at

4°C. G-coupled Sepharose beads were resuspended in 1ml lysis buffer containing protease inhibitors and the beads were washed by centrifuging them at 3000rpm for 3 minutes, followed by removal of the lysis buffer and addition of an equal volume of fresh lysis buffer to the volume of compacted beads. Pipette tips with 5mm cut from the end were used to prevent damage to the beads. This was repeated twice more. The final bead slurry was mixed well to ensure a homogenous suspension of beads before 30µl of beads was added to the 600µl of each cell lysate and antibody. The lysate-bead mixture was incubated at 4°C under rotary agitation for 30 minutes. Following incubation, the tubes were centrifuged at 3000rpm for 3 minutes to remove the supernatant. 500ul of fresh lysis buffer was added to each tube and the process was repeated 3 more times for a total of 4 washes. Following the final wash step, all of the supernatant was removed and 30µl of each cell lysate (~50µg) was added to 8µl of NuPAGE loading dye and 2µl of DTT. The samples were then either frozen at -80°C or run on SDS-PAGE.

2.2.7 Western blot

Prior to completion of downstream assays, gene expression was determined by western blot. Cells were washed twice with ice cold PBS and then lysed in 200µl of the appropriate buffer. 'Blenis' lysis buffer was used for all cell lysis except for cells used in the Ras ELISA assay (Section 4.3.6) in which the buffer provided with the kit was used. Cells were scraped from the plate and incubated on ice in a microcentrifuge tube for 15 minutes. Total proteins in the cell lysates were then vortexed or sonicated for 10 seconds and centrifuged at 14,000rpm for 10 minutes at 4°C. The supernatant was then either run with SDS-PAGE or stored at -80°C. DTT and 4x NUPAGE loading dye were combined in a 1:4 ratio and 10µl of this mix was added to 30µl of cell lysate for each sample (~50µg). The tube was gently flicked to mix and incubated at 70°C for 10minutes on a heat block. The samples were briefly centrifuged to collect the sample and 20µl of each sample was loaded into each well of the gel followed by 4µl of pre-stained ladder. Sample extracts were resolved on NuPAGE Novex 4-12% Bis-Tris gel or NuPAGE Novex 3-8% Tris-Acetate gels depending on the size of the protein. The combs were removed; the gels were rinsed

with dH_2O to remove any un-polymerised gel and slotted into the gel apparatus. The tank was filled with 1x running buffer and the gel was then run at 150v for an hour.

The membrane was briefly pre-treated with 100% methanol and then washed off in 1x transfer buffer for 5 minutes. Following SDS-PAGE, the total proteins were transferred to Immobilon PVDF membrane (Millipore) and the transfer apparatus was constructed (Hoefer) with sponges and a piece of whatmann paper below the membrane and the same above. All components were pre-rinsed in 1x transfer buffer to prevent the membrane from drying out. Bubbles were removed by rolling a stripette over the surface of the whatmann paper. The blotting apparatus was then run at 25v for 2 hours.

The membrane was blocked with 5% (w/v) powdered milk in TBS-T. The membrane was washed briefly with H_2O to remove methanol before the membrane was incubated for 30minutes with the milk with gentle agitation. The milk was washed once with dH_2O and then incubated in 10ml of primary antibody overnight at 4°C on an orbital shaker. Following the overnight incubation, the antibody was removed and kept for future use. The membrane was then washed once in 1x TBS-T. 10ml of the appropriate secondary antibody was added to the membrane and it was incubated at room temperature on an orbital shaker for 30 minutes. The membrane was then washed 3-4 times with TBS-T.

1ml of the ECL mix in a 1:1 ratio was put on a pre-cleaned glass plate. The membrane was blotted on to a piece of paper towel and then put in the ECL mix. The mix was washed over the surface and incubated for 2 minutes. The membrane was removed from the mix and placed face down on to a piece of Clingfilm. The excess Clingfilm and creases were removed and then the membrane in the Clingfilm was taped into a cassette and developed by exposing it on x-ray film.

CHAPTER 3: Analysis of somatic mutations in cutaneous neurofibromas

3.1 Introduction

This chapter focuses on two main aspects of *NF1* somatic mutation detection; firstly the validation of methods of somatic mutation enrichment in heterogeneous tumours and secondly implementation of such methods for somatic *NF1* mutation detection in benign cutaneous neurofibromas derived from patients with high tumour burden. These patients represent the extreme end of the spectrum of NF1 manifestations. In this study they are defined as patients with >500 benign cutaneous neurofibromas, harbouring more tumours than patients of a comparable age.

Cutaneous neurofibromas are considered to be the hallmark feature of NF1. Within these neurofibromas, Schwann cells which harbour the somatic *NF1* mutations are the predominant cell type, although they only comprise between 40% and 80% of cells (Peltonen *et al*, 1988; Wallace *et al*, 2000). A number of heterozygous fibroblasts, mast cells and perineural cells make up the remainder of the total cell content. (Kimura *et al*, 1974; Le and parade, 2007). There are several lines of evidence responsible for the conclusion that Schwann cells bear somatic *NF1* mutations. Although wild-type and neurofibroma derived $NF1^{-/-}$ Schwann cells have the same proliferative activities (anchorage dependent growth and normal axon interaction), they have distinct invasive and angiogenic capabilities (Sheela *et al*, 1990; Muir, 1995). Additionally, LOH of the *NF1* gene can only be identified in Schwann cells but not fibroblasts which were both isolated from within the same tumour (Kluwe *et al*, 1999; Rutkowski *et al*, 2000). Furthermore, in a pivotal study by Zhu *et al* (2002), mice with a deletion of the *NF1* gene in the Schwann cell lineage were found to develop neurofibromas (section 1.8). Although the cell of origin of neurofibromas has been a major subject of debate, recent studies have confirmed that skin-derived precursor cells are the cell type from which neurofibromas are derived (Le *et al*, 2009; Le *et al*, 2011). Biallelic inactivation of *NF1* in Schwann cells is, however, not sufficient to promote tumorigenesis and thus a role for the tumour microenvironment has been postulated and indeed demonstrated in mouse models (Zhu *et al*, 2002;Yang *et al*, 2003; Le *et al*, 2009) (section 1.9.4.1).

Cutaneous neurofibromas therefore represent heterogeneous entities with high biological heterogeneity relating to the cellular composition of these tumours and also genetic heterogeneity due to the presence of both *NF1* hemizygous and homozygous cell populations. The somatic mutation detection rate in DNA derived from whole cutaneous neurofibromas in previous studies varies between 12% and 64% (John *et al*, 2000; Serra *et al*, 2001b; Upadhyaya *et al* 2004; Spurlock *et al*, 2007). This paucity of identified mutations is partly related to the size and complexity of the *NF1* gene but is more likely a problem of the cellular and molecular heterogeneity of these tumours. It is clear that to be able to accurately and efficiently assess the mechanisms of tumorigenesis in neurofibromas, improvements to somatic mutation detection methods need to be sought.

Mutation detection methods are continually evolving to ensure that mutation detection is both efficient and cost effective. The type of mutation detection methods employed in genotyping studies are dependent on the types of mutation which are most commonly associated with the gene of interest. The application of a set of complementary techniques that allow the detection of the different mutation types is therefore important. However, this in itself is a challenge as the use of multiple methods results in increased costs, labour and analysis time. The most common methods of mutation detection employed to identify and characterise the range of *NF1* germline and somatic mutations detected in NF1 patients are outlined in section 1.10. These techniques include; FISH, MLPA, LOH analysis and the use of microarrays for identification of microdeletions and microinsertions. Point mutations are detected through direct sequencing of DNA or cDNA, SSCP, heteroduplex analysis and the protein truncation test (PTT). There is, however, no standardised, routine platform for the analysis of the whole spectrum of *NF1* mutations and no consistently used method to resolve the issue of cellular heterogeneity in NF1-associated tumours.

Serra *et al* (2000) have established an improved culture technique for Schwann cells which is capable of purifying populations of *NF1* heterozygous ($NF1^{+/-}$) as well as homozygous ($NF1^{-/-}$) Schwann cells from primary peripheral nerve sheath tumours (Rosenbaum *et al*, 2000; Serra *et al*, 2000). This technique has been successfully used to enhance the mutation detection rate in small cohorts of neurofibromas, although the

challenges associated with this technique need to be addressed (Maertens *et al*, 2006). Furthermore, laser capture microdissection (LCM) has been utilised to isolate specific alterations in distinct cell types from a heterogeneous cellular background. LCM has been employed in the analysis of many tumour samples including breast carcinomas and is readily applicable to targeting Schwann cells from within heterogeneous NF1-associated tumours (Edward, 2007; Zanni and Chan, 2011). This method has not previously been applied to *NF1* somatic mutation detection; however, indicating that determination of the efficacy of LCM in routine *NF1* somatic mutation analysis is warranted.

There is considerable variation in the number and distribution of neurofibromas even between family members and individuals with the same *NF1* germline mutation. This indicates that other genetic loci including *TP53*, *CDKN2A*, *RB1* and mismatch repair (*MMR*) genes may be modifying the phenotypic expression of NF1, particularly in patients with a high tumour burden. In predisposition cancer syndromes, multiple genetic abnormalities frequently occur in pre-malignant lesions which are not present in the normal tissue. Malignant neoplasms usually arise due to the accumulation of genetic alterations typically involving loss of function of regulatory elements of the cell cycle machinery including *TP53, CDKN2A* and *RB1* which can mediate abnormal cell cycle arrest through DNA damage and aberrant apoptosis. Such genes are frequently found to be mutated in MPNSTs (Kourea *et al*, 1999; Nielsen *et al*, 1999; Mawrin *et al*, 2002; Mantripragada *et al*, 2008) although only two previous studies (Upadhyaya *et al*, 2008; Stewart *et al*, 2008) have identified *TP53* LOH in plexiform neurofibromas and there is no previous indication of the involvement of these genes in the development of benign cutaneous neurofibromas (Carroll and Ratner, 2008; Le *et al*, 2009; Parrinello and Lloyd, 2009; Upadhyaya *et al*, 2004).

TP53 is a prime candidate for loss of function in malignant tumours and has been widely investigated in the case of both sporadic and NF1-associated MPNSTs. *TP53* is a key tumour suppressor gene involved in regulation of the cell cycle, with a major role in cell survival. Loss of *TP53* function is seen in about half of all human cancers where p53 protein expression is frequently lost or apoptosis fails to be initiated due to accumulation

of non-functioning proteins in the nucleus (Menon *et al*, 1990; Legius *et al*, 1994; Kindblom *et al*, 1995; Schneider-Stock *et al*, 1997; Birindelli *et al*, 2001; Mawrin *et al*, 2002). Mice carrying cis-linked *Nf1* and *TP53* mutations develop MPNSTs, indicating that accumulation of mutations at various oncogenic loci is important in malignancy. (Cichowski *et al*, 1999; Vogel *et al*, 1999; Reilly *et al*, 2000). *TP53* and other cell cycle related genes; *CDKN2A* and *RB1* may therefore represent important modifying genes in neurofibroma development.

CDKN2A/p16^{INK4a} which encodes p16INK4A and p14ARF has also been investigated in NF1 malignancies due to its prominent role in the cell cycle and its involvement in the development of other tumour types. Several studies have described deletions in *CDKN2A*, in MPNSTs in addition to inactivation of the *CDKN1B* gene which encodes the cell cycle regulator p27 (KIP1) (Kourea *et al*, 1999a Kourea *et al*, 1999b; Nielsen *et al*, 1999; Perry *et al*, 2002; Holtkamp *et al*, 2008). Additionally, the *RB1* gene responsible for the development of retinoblastoma has been found to be mutated in a number of sarcomas including MPNSTs (Birindelli *et al*, 2001). *RB1* is a tumour suppressor gene, which regulates G1/S transition (Weinberg, 1995), causing cell cycle arrest in G1 through suppression of E2F transcription factors and by E2F independent mechanisms (Riley *et al*, 1994; Cobrinik, 2005). *RB1* therefore controls cellular differentiation during embryogenesis and in adult tissues, as well as regulation of apoptotic cell death, maintenance of permanent cell cycle arrest and preservation of chromosomal stability (Dannenberg *et al*, 2006). Loss of *RB1* consequently results in increased proliferation due to induction of cell-cycle regulators such as cyclin D1 and suppression of cell cycle inhibitors including KIP1. (Downward *et al*, 2002).

Bi-allelic defects in mismatch repair genes (*MMR*) can cause instability of microsatellite repeats and are known to be associated with an "NF1-like phenotype". Heterozygous mutations in *MLH1* (Wang *et al*, 1999), homozygous *MSH6* mutations (Menko *et al*, 2004), homozygous *PMS2* (Kruger *et al*, 2008) and most recently homozygous *MSH2* mutations (Toledano *et al*, 2009) have all been linked to this "NF1-like phenotype" including the presence of multiple café au lait macules. It is therefore indicated that *NF1* inactivation may be an important step in malignant progression in mismatch repair

deficient cells (Wimmer and Etzler, 2008; Wang *et al*, 2003). Indeed, bi-allelic defects in mismatch repair genes (MMR) are often associated with colonic and extra-colonic tumours, especially in HNPCC, an autosomal dominant disorder in which the underlying mutational mechanisms involve germline mutations in a mismatch repair gene (*MMR*) including: *MLH1*, *MSH2*, *MSH6* or *PMS2* (Lynch *et al*, 2008). The MMR proteins function in the process of detection and repair of DNA replication errors, specifically short insertions and deletions which form loops in addition to single basepair mismatches (Boland *et al*, 2008). Somatic mutation of one of these genes in the remaining wild type copy in patients with a constitutional mismatch repair deficiency therefore results in cells with defective MMR. This primarily affects repeat sequences which cause microsatellite instability (MSI) and consequently lead to tumour development suggesting that defective MMR may also act as a modifier for neurofibroma development.

Animal models which harbour deficiencies in one or all of the major *MMR* genes have also been developed which recapitulate to an extent, NF1 in humans (de Wind *et al*, 1995; Reitmair *et al*, 1995; Reitmair *et al*, 1996; Sohn *et al*, 2003; Gutmann *et al*, 2003; Chen *et al*, 2005; Feitsma *et al*, 2008). While zebrafish mutants develop MPNSTs and neurofibromas at low frequencies (Feitsma *et al*, 2008), some *MMR* knockout animal models including the mouse *MMR* models do not develop the full spectrum of NF1 features (Reitmair *et al*, 1996; Chen *et al*, 2005). It has, however, been found that in the *MLH1* knockout mouse model, *MLH1* deficiency exacerbates the consequences of an $NF1^{+/-}$ mutation, acting to accelerate myeloid leukaemia in such models (Gutmann *et al*, 2003). In previous studies, MSI has been detected in around 25% of neurofibromas (Ottini *et al*, 1995; DeRaedt *et al*, 2006; Thomas *et al*, 2010) and upwards of 50% in MPNSTs (Serra *et al*, 1997; Spurlock *et al*, 2007), further evidence for a possible association of MMR deficiencies with NF1 tumorigenesis.

Our understanding of the molecular mechanisms that underlie NF1 tumorigenesis is still relatively limited. Identification of the precise genetic pathways altered during neurofibroma formation and more importantly the factors responsible for malignant transformation are crucial for complete comprehension of NF1 tumorigenesis. It is

important to determine why some types of neurofibroma develop only during adolescence whilst others are present from birth in addition to the underlying initiating events in neurofibroma growth and the mechanism responsible for variability in the number and distribution of neurofibromas. To date, more than 1,273 different germline *NF1* mutations have been reported (HGMD) but only about 215 different characterised somatic *NF1* mutations have been reported in cutaneous neurofibromas. This demonstrates a clear need to expand the *NF1* somatic mutational database. Improvements to somatic mutational detection methods and enrichment strategies will facilitate the identification of common mutations and mechanisms for somatic *NF1* inactivation. Knowledge of the nature, type and frequency of somatic mutations in the *NF1* gene, in addition to the identification of other modifying loci are all key steps for elucidating the mechanisms controlling neurofibromagenesis.

This study was undertaken in two parts; (i) validation of Schwann cell culture and laser capture microdissection as a strategy for improving somatic mutation detection. (ii) Utilisation of such techniques in the analysis of 89 benign cutaneous neurofibromas derived from NF1 patients with very high tumour burden in which some neurofibromas studied were also present adjacent to each other. Such high burden of tumours may indicate that alterations of additional modifying loci are underlying the development of tumours in these severely affected patients. The three basic aims of this chapter are:

1) To develop and assess the efficacy of Schwann cell culture and LCM for improving *NF1* somatic mutation detection
2) Application of LCM to the analysis of cutaneous neurofibromas derived from NF1 patients with high tumour burden.
3) To determine whether somatic mutations in other 'modifying' genes, including the *TP53*, *CDKN2A*, *RB1* and *MMR* genes, are also involved in the growth of neurofibromas in patients with high burden of cutaneous neurofibromas.

3.2 Methods

3.2.1 Patients

3.2.1.1 Clinical presentation

Upon clinical examination, all 31 unrelated NF1 patients from whom neurofibromas were derived exhibited the NIH diagnostic criteria for NF1 (section 1.5). Additional complications for patients with multiple neurofibromas are summarised in table 3.1.

3.2.1.2 Tissue samples

Schwann cell culture and LCM were employed in an enrichment strategy with the aim of increasing the somatic mutational detection rate by enriching the Schwann cell population. All 13 fresh cutaneous neurofibroma samples for Schwann cell culture were surgically removed from 3 unrelated patients and stored at 4°C in McCoys medium until cultured as described in section 2.2.2.5. DNA and RNA from Schwann cell cultures was extracted as described in sections 2.2.3.1.1 and 2.2.3.1.2. Tumour DNA for LCM was derived from 35 formalin fixed paraffin embedded (FFPE) samples; 30 benign cutaneous neurofibromas, 4 plexiform neurofibromas and 1 MPNST derived from 25 individuals, in which DNA from all fresh tumour samples had been previously analysed but no somatic *NF1* mutations had been identified.

Following validation of the effectiveness of Schwann cell culture and LCM using the above samples, 89 neurofibromas derived from patients with multiple benign cutaneous neurofibromas were analysed for somatic *NF1* mutations. Three unrelated NF1 patients, 2 females, aged 44 and 46 (patients 1 and 2 respectively) and 1 male aged 60 (patient 3) all with a high burden of cutaneous neurofibromas (>550) were recruited for this study. DNA and RNA were extracted from paired blood and whole tumour tissue from all 3 patients (forty tumours from patient 1, forty tumours from patient 2 and nine from patient 3). The exact anatomical location from which the majority of these tumours were excised is unknown, 20 of these neurofibromas were located in close proximity to each

Table 3.1. Overview of results of the analysis of 89 tumours and paired blood DNA samples from three NF1 patients with a high tumour burden

Patient	Germline Mutation	Somatic Mutation		Somatic Mutation Detection Rate	MSI	Clinical Details
		LOH	Direct Sequencing			
1	E17: c.2875 C>T p.Q959X	7/40	19/40	65%	4/40	>6 CAL Spots
						>550 Cutaneous Neurofibromas
						>2 Lisch Nodules
						First Degree Relative with *NF1*
						Abnormal Learning and Development
						Osteopenia
2	E10b: c.1413-1414delAG p.KfsX4	15/40	9/40	60%	12/40	>6 CAL Spots
						>550 Cutaneous Neurofibromas
						>2 Lisch Nodules
						Sporadic
						Abnormal Learning and Development
						MPNST in Pelvis
3	E36: c.6756+2 T>G	0/9	7/9	78%	5/9	>6 CAL Spots
						>550 Cutaneous Neurofibromas
						>2 Lisch Nodules
						Sporadic
						Abnormal Learning and Development
						Facial Plexiform Neurofibroma
						Spinal Neurofibromas
						Chronic lymphocytic leukaemia (B-CLL)
Total		**22/89 (25%)**	**35/89 (40%)**	**57/89 (64%)**	**21/89 (24%)**	

other, i.e. adjacent tumours which were directly touching and sharing the underlying skin. These 20 tumours are shown by hatched shading in table 3.4. The remaining tumours are believed to be randomly distributed across the patients' bodies. DNA and RNA were extracted using the methods described in sections 2.2.3.1.1 and 2.2.3.1.2.

3.2.2 Laser Capture Microdissection (LCM)

Laser micromanipulation enables microscopic high-resolution control of sample composition by allowing selection (or rejection) of user defined areas of tissue sections. Slides were prepared from FFPE tissue as described in section 2.2.4.2. Following immunohistochemical staining with S100 and H&E as described in section 2.2.4.3 and 2.2.4.4, LCM was carried out using an Axiovert S100 (Zeiss) through which a pulsed ultra-violet PALM microlaser is interfaced and focused. LCM provides clear resected margins for the selected tissue without affecting the adjacent tissues. The user defined parameters for LCM were: cut Speed; 30, zoom; 5x, laser energy; 94 and laser focus; 85. The cap from a 0.75ml microcentrifuge tube was cut off and labelled to correspond to the slide being cut. The cap was filled with 1µl of mineral oil and tissue sections (totalling approximately $100_{\mu m}^2$) were outlined on the computer screen which was attached to the microscope for the laser to cut. Sections of paraffin embedded tissue which had been laser cut were catapulted into the lid of the tube which was positioned above the slide. The bottom of the tube was then placed onto the cap and these were stored at -80°C prior to DNA extraction as described in section 2.2.3.1.6.

3.2.3 NF1 gene analysis

Schwann cell culture and LCM were validated as a strategy for enrichment of the *NF1* somatic mutation harbouring Schwann cell population. DNA and RNA from 13 neurofibroma-derived Schwann cell lines and DNA samples derived from 35 LCM tumour samples were analysed by loss of heterozygosity (LOH) analysis, MSI analysis, multiplex ligation dependent probe amplification (MLPA) and direct sequencing of the *NF1* gene. Following validation of these techniques, LCM was applied to the analysis of

42 of the 89 tumour samples derived from three patients with high tumour burden in which somatic *NF1* mutations were not identified (15 samples from patient 1, 23 samples from patient 2 and 4 samples from patient 3) (figure 3.1). LCM of FFPE samples was used in this analysis as fresh whole tumour was not available for Schwann cell culture.

3.2.3.1 Loss of Heterozygosity (LOH) analysis at the NF1 locus

LOH analysis was completed on DNA from all neurofibromas and corresponding lymphocyte samples utilising a panel of fluorescently-tagged microsatellite markers and 4 polymorphic RFLP's (supplementary table 4 and supplementary table 5) that spanned the entire *NF1* gene and also the majority of chromosome 17 (17p13 to 17q25). All reactions for microsatellite markers were carried out at an annealing temperature of 56°C and RFLPs at an annealing temperature of 54°C. The following reagents and cycle conditions were used to amplify both microsatellite markers and RFLPs.

PCR Reaction	25µl	Cycle Conditions	x35 Cycles
DNA [6ng/µl]	5µl		
Buffer	2.5µl	94°C	10 Minutes
Mg [50mM]	3µl		
dNTP's [10µM]	2µl	94°C	1 Minute
Sense Primer [10pm/µl]	1µl	Tm	1 Minute
Antisense Primer [10pm/µl]	1µl	72°C	1 Minute
Taq	0.05µl		
H_2O	10.45µl	72°C	10 Minutes

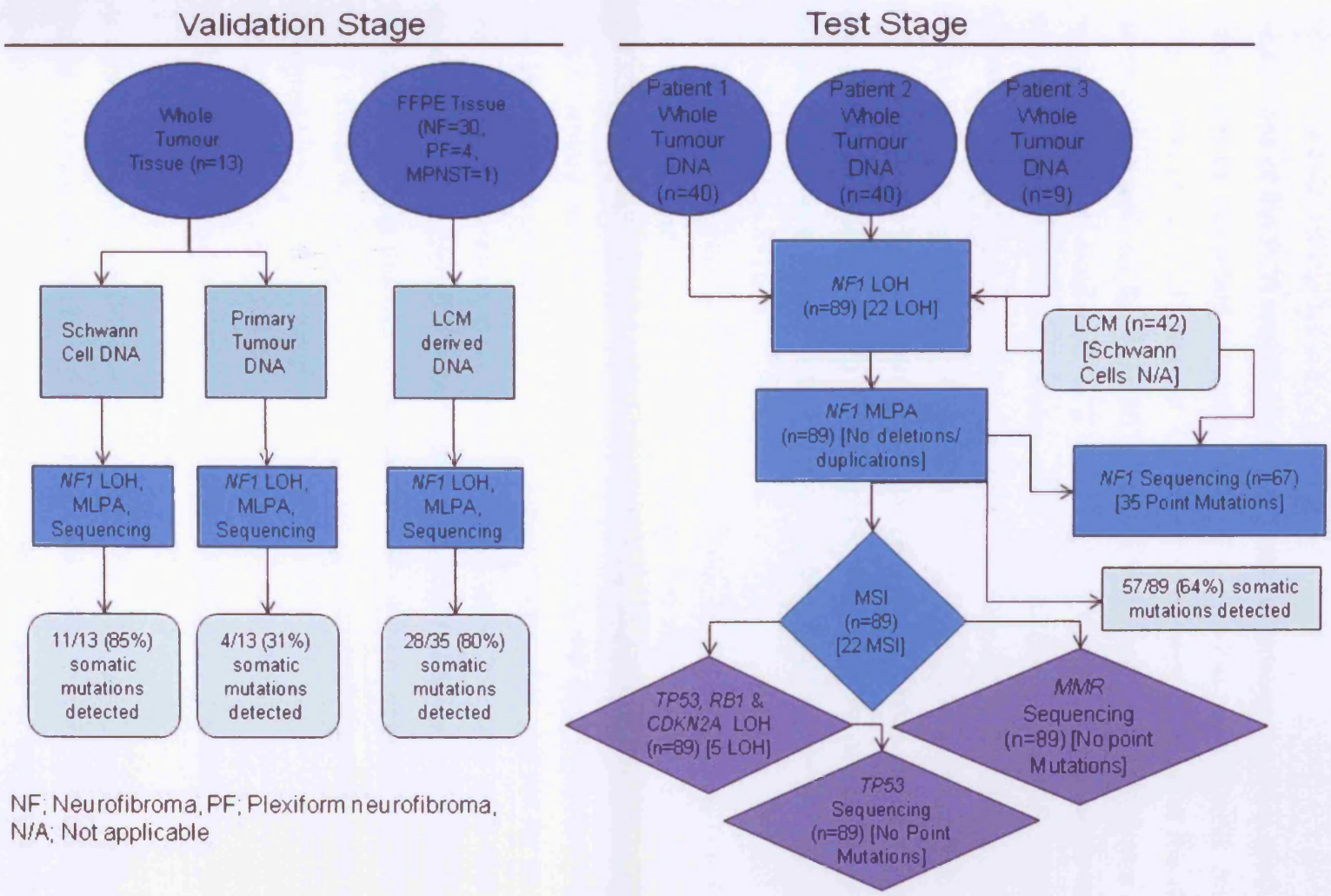

Figure 3.1. Flow diagram demonstrating the stages of validation of LCM and Schwann cell culture and the analysis of 89 benign cutaneous neurofibromas from patients with high tumour burden.

3.2.3.2Analysis of PCR products

The success of the PCR reaction was analysed by running the PCR product on a 1.5% agarose gel as described in section 2.2.3.2.1. For the microsatellite markers, a 1 in 200µl dilution of the PCR product with dH_2O was made and 2µl of the diluted product was combined with an 8µl solution of ROX (0.3µl) and HIDI (7.7µl) in a 96 well plate. The plate was then incubated for 2 minutes at 95°C in a thermal cycler to denature the DNA and capillary electrophoresis was carried out on an ABI 3100 sequencer. Genotyper and Genescan software were used to characterise the results (Applied Biosystems, Warrington, UK). Allelic loss was scored if the area under one allelic peak in the tumour was reduced relative to the other allele, after correcting for the relative peak areas with corresponding lymphocyte DNA (Dasgupta *et al*, 2003b). Microsatellite markers which were shown in the blood to be constitutionally homozygous were scored as non-informative.

To each of the successful RFLP PCR reactions, 10µl of the appropriate enzyme, buffer and BSA was added (supplementary table 5). The PCR product and digestion mix were then incubated at the appropriate temperature and for the required amount of time (supplementary table 5). Following the incubation, the whole reaction volume was run on a 3% agarose gel with 3µl of concentrated loading dye and run for an hour at 150V. The gel and band sizes were then analysed using UV light on a Gel Doc and the presence of LOH scored if there was a significant difference in intensity between the bands representing the two heterozygous *NF1* alleles. At least two adjacent markers (microsatellite or RFLP) were required to show a reduced signal for LOH to be positively confirmed.

3.2.3.3 Multiplex Ligation-dependent Probe Amplification (MLPA)

An MLPA assay kit (MRC Holland) (SALSA P081/082 and SALSA P122) that contained probes covering the entire *NF1* gene, surrounding regions and control probes was employed to screen for evidence of genomic deletions or insertions across the *NF1* gene using the protocol outlined by the manufacturers (MRC Holland). 250ng of test

DNA in addition to a positive (characterised whole gene deletion) and a negative control (from a non-NF1 patient sample) were required for each assay. All incubations were completed on a thermal cycler. Briefly, the DNA was heated to 98°C for 5minutes and then cooled to 25°C. The relevant probes were mixed with the buffers and 2µl was added to the DNA and incubated for 1 minute at 95°C followed by 16hours at 60°C. Following the 16 hour incubation, the samples were incubated at 54°C and 32µl of a mix containing a ligase, ligase buffer and dH_2O was added to each sample and mixed. This was incubated for 15 minutes at 54°C, for 5 minutes at 98°C and finally briefly at 60°C just prior to the plate being removed from the thermal cycler. 10µl of this reaction was added to a new plate and 30µl of a mix containing a PCR buffer and dH_2O was added to each well in the new plate. Finally the plate was put back into the thermal cycler, 10µl of a mix containing PCR primers and polymerase was added and the PCR reaction was started using the following cycle conditions: 35x (95°C 30 seconds, 60°C 30 seconds, 72°C 60 seconds), 72°C 20 minutes. After the PCR reaction was complete, 7.7µl of HiDi and 0.3µl of ROX was added to each reaction. The plate was then analysed on an ABI 3100 analyser (Applied Biosystems, Warrington, Cheshire, UK). An excel spreadsheet (NGRL Manchester) was used to characterise the results.

3.2.3.4 Direct sequencing

Direct sequencing of all *NF1* exons in genomic DNA and RNA was utilised to detect small sequence alterations in the remaining samples in which neither LOH nor deletions were found using the protocol outlined in section 2.2.3.2. All sequence alterations were fully characterised using an ABI 3730 analyser (Applied Biosystems) and Sequencher software (Genecodes, USA).

3.2.4 Analysis of modifying loci

In view of the exceptionally high burden of neurofibromas present in all three *NF1* patients (and the close proximity of some of the tumours studied), analysis was undertaken to screen for somatic mutations in four potential modifying loci; *TP53*, *RB1*,

CDKN2A and *MMR* genes in all 89 neurofibroma samples using LOH analysis and direct sequencing (figure 3.1). Genetic aberrations in genes involved in cell cycle regulation, apoptosis and repair would affect multiple pathways and could contribute to an alternative mutational mechanism underlying the development of these multiple tumours.

3.2.4.1 Microsatellite Instability (MSI) analysis

MSI analysis was completed on all tumour and paired lymphocyte DNA samples with a standard panel of 10 fluorescently tagged microsatellite markers (supplementary table 6). All reactions were completed at 58°C using the following reagents and cycle conditions

PCR Reagents	25µl	Cycle Conditions	x35 Cycles
DNA [6ng/µl]	5µl		
Buffer	2.5µl	94°C	10 Minutes
Mg [50mM]	3µl		
dNTP's [10µM]	2µl	94°C	1 Minute
Sense Primer [10pm/µl]	1µl	58°C	1 Minute
Antisense Primer [10pm/µl]	1µl	72°C	1 Minute
Taq	0.05µl		
H_2O	10.45µl	72°C	10 Minutes

Success of the PCR reaction was analysed by running 3µl of the PCR product with 5µl of loading dye on a 1.5% agarose gel as previously described. A 1:200 dilution of the PCR product was made and 2µl of the dilution was added to 7.7µl of HIDI Formamide and 0.3µl of ROX. The electrophoresis mix was denatured for two minutes at 95°C and subsequently analysed on an ABI 3100 with Genescan and Genotyper software. The presence of new alleles in the tumour samples which are not found in corresponding blood DNA samples, indicate the presence of MSI.

3.2.4.2 Analysis of somatic *TP53*, *RB1* and *CDKN2A* mutations

LOH analysis and direct sequencing of the *TP53*, *RB1* and *CDKN2A* genes was completed using the same methods and scoring systems that were applied to the analysis of the *NF1* gene.

3.2.4.2.1 TP53 RB1 and CDKN2A LOH analysis.

DNA from all 89 tumour samples and matched lymphocyte DNA samples was analysed for LOH at four microsatellite markers flanking the *TP53* gene, five microsatellite markers which flank the *RB1* gene and four markers within the CDKN2A gene (supplementary table 7). All reactions were completed at an annealing temperature of 56°C using methods outlined in section 3.2.3.1.

3.2.4.2.2 TP53 Direct Sequencing

All 89 tumour DNA samples and corresponding blood samples were screened by direct sequencing to detect small sequence alterations in exons 4-9 of the *TP53* gene (17p13.1) using methods described in section 2.2.3.2, an annealing temperature of 58°C and the primers detailed in supplementary table 8.

3.2.4.3 Analysis of Mismatch Repair genes (MMR)

21 tumour DNA samples (samples harbouring MSI) were sequenced to detect alterations in all exons of the four main MMR genes: *MLH1* (NM_000249) (3p21.3), *MSH2* (NM_000251) (2p22-p21), *MSH6* (NM_000179) (2p16) and *PMS2* (NM_000535) (7p22.2) using the methods described in section 2.2.3.2, an annealing temperature of 60°C for *MLH1* and *MSH2* and 58°C for *MSH6* and *PMS2* and the primers in supplementary table 9.

3.2.5 Bioinformatic analysis

To infer potential mutational mechanisms underlying somatic mutations in the *NF1* gene in the 3 patients with exceptionally high tumour burden, sequences flanking these somatic mutations (±20 bp) were kindly screened by Professor Nadia Chuzhanova (Nottingham Trent University) for the presence of direct and inverted repeats and symmetric elements by means of complexity analysis (Gusev *et al*, 1999). Hypothetical mutational mechanisms involving microdeletion, microinsertion and indel mutations mediated by these types of repeats have been described previously (Chuzhanova *et al*, 2003; Ball *et al*, 2005). In addition, flanking regions were screened for the presence of 37 DNA sequence motifs of length ≥5 bp (plus their complements) known to be associated with site-specific cleavage/recombination, high frequency mutation and gene rearrangement (Abeysinghe *et al*, 2003) as well as various 'super-hotspot motifs' found in the vicinity of micro-deletions/-insertions and indels (Bacolla *et al*, 2004)

3.3 Results

3.3.1 Schwann cell culture

To assess the efficiency by which Schwann cell culture is able to enrich Schwann cells harbouring *NF1* somatic mutations, 13 neurofibroma derived Schwann cell lines were generated and the associated *NF1* mutational spectra was analysed by LOH, MLPA and whole gene sequencing. *NF1* germline mutations were identified in all 3 patients from whom the 13 neurofibroma Schwann cell lines were derived and comprised a 90kb gene deletion, 132bp deletion and an In/del. One germline mutation had been previously reported and 2 were novel. *NF1* somatic mutations were identified in 11/13 (85%) of Schwann cell lines derived from neurofibromas, all of which were novel. The identified somatic mutations comprised of: 4 small deletions (1-180bp), 1 small insertion, 1 splice site mutation, 1 missense mutation and 4 LOH (table 3.2, figure 3.2).

Table 3.2. Results of *NF1* somatic mutation analysis in 13 neurofibroma-derived Schwann cell samples

Sample	Germline *NF1* Mutation	Previously Reported/ Novel	Somatic *NF1* Mutation		Previously Reported/ Novel
			LOH	Somatic *NF1* Point Mutation	
T535A	90kb Gene Deletion	Upadhyaya *et al* (1990)			
T535B					
T539				c.2410-1 G>T	Novel
T544				c.3975delG; p.R1325fsX	Novel
T536A	c.7127 132bpdel; p.G2376	Novel	LOH: J1J2-IVS38		
T536B				c.7169delG; p.R2390fsX6	Novel
T541.1				c.4741insG; p.GfsX19	Novel
T541.2			LOH: EV120-3NF1		
T541.3				c.1888delG; p.V630fsX	Novel
T541.4			LOH: EV120-3NF1		
T543.1	c.373insATGTGTdelG; p.R125fsX4	Novel		c.3568del80bp; p.G1190fsX6	Novel
T543.2			LOH: J1J2-3NF1		
T543.3				c.4388 C>T; p.S1463F	Novel

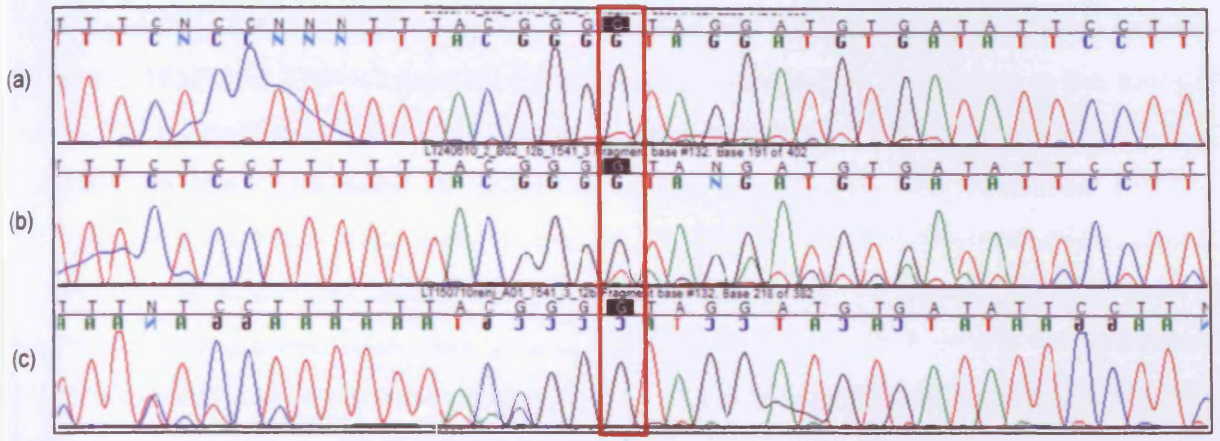

Figure 3.2. DNA sequence trace of the somatic *NF1* frameshift mutation (c.1888delG p.V630fsX) from patient T541.3 **(a)** 5'-3' sequence from neurofibroma tumour tissue, and **(b)** 5'-3' sequence from Schwann cells cultured from the same neurofibroma **(c)** 3'-5' sequence from Schwann cells cultured from the same neurofibroma. The frameshift G deletion was only detectable in the DNA trace from the cultured Schwann cells.

Tumour Sample and Marker	LOH Original Tumour DNA	LOH (%)	LOH LCM DNA sample	LOH (%)
T224 – 3'NF1	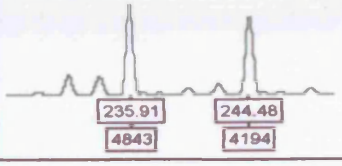	86%	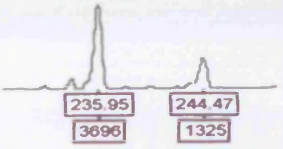	35%
T164 – EV120	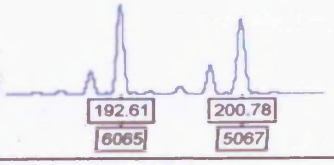	83%	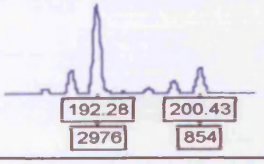	28%
T225 – IVS27	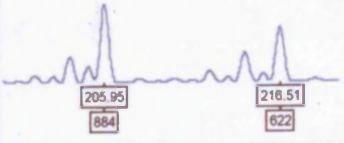	70%	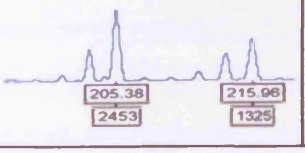	54%

Figure 3.3. LOH traces from DNA from whole tumour samples T164.1, T224.1, T225.1 and LOH traces of DNA derived from LCM of the same samples demonstrating that LOH is not obvious in the whole tumour samples in comparison to the LCM derived DNA.

The extent of LOH in all samples was confined to the 17q11.2 *NF1* gene locus between markers J1J2 and 3'NF1. Upon MLPA analysis, no deletions were seen in the samples with LOH indicating that the LOH is copy neutral and that mitotic recombination is likely to underlie the LOH seen in these tumours. Additionally, the missense mutation (c.4388C>T; p.S1463F) has been analysed functionally and bioinformatically in chapter 4. For all Schwann cell lines, DNA from the original whole tumour sample and the Schwann cell derived DNA was analysed simultaneously. In 4 of the 11 samples in which somatic mutations were detected by Schwann cell culture, once the location of the somatic mutation was identified (two samples with LOH, one missense and one 1bp deletion), the mutation was also found to be present in the whole tumour DNA but was not originally obvious due to the low percentage of mutation harbouring cells (about 20% in all samples) (table 3.2, tumours T536A, T541.2, T541.3, T543.3, figure 3.2). For the remaining 7 samples in which the somatic *NF1* mutation had been identified by Schwann cell culture, the mutation could still not be identified in the original whole tumour sample.

3.3.2 Laser Capture Microdissection

The technique of LCM was validated to determine its effectiveness for improving *NF1* somatic mutation detection. The *NF1* mutational spectrum was analysed by LOH, MLPA and whole gene sequencing in 35 DNA samples derived from LCM of FFPE whole tumour samples. Germline *NF1* mutations were identified in 16/25 (64%) lymphocyte DNA samples, 8 of which were novel mutations. Somatic *NF1* mutations were identified in 28/35 (80%) of tumour samples derived from the 25 unrelated patients (23/30 benign cutaneous neurofibromas, 4/4 plexiform neurofibromas and 1/1 MPNST) (table 3.3). In the 30 cutaneous neurofibroma samples, somatic mutations comprised of 1 nonsense mutation, 1 small 2bp deletion and 21 samples with LOH. Of the 4 plexiform neurofibroma samples, 3 had LOH and 1 sample had nonsense mutation. The single MPNST sample had a nonsense mutation. The extent of LOH in 21 of these samples was within the 17q11.2 *NF1* gene locus between markers HHH202 and 3'NF1.

Table 3.3. Results of *NF1* somatic mutation analysis in DNA from LCM tumour samples

Patient	Tumour	Tumour Type	Germline *NF1* Mutation	Previously Reported/ Novel	Somatic *NF1* Mutation		Previously Reported/ Novel
					LOH	Point Mutation	
1	T209.8	NF	c.4950 C>G; p.Y1650X	Novel		c.1318 C>T; p.R440X	Heim *et al* (1995)
2	T164.1	NF	c.7285 C>T; p.R2429X	Fahsold *et al* (2000)	LOH: IVS27-3NF1		
3	T206.1	NF	c.499delTGTT	Novel	LOH: EV120-IVS38		
	T206.2	NF			LOH: EV120-3NF1		
	T206.3	NF			LOH: EV120-D17S928		
	T206.4	NF				ND	
4	T210.1	NF	c.7458_7458delC; pT2486fsX15	Novel		ND	
	T210.2	NF				ND	
5	T224.1	NF	c.7127 132bpdel; p.G2376	Novel	LOH: IVS27-EV120		
	T258.1	NF			LOH: J1J2-IVS38		
	T258.2	NF			LOH: IVS27-IVS38		
	T204.2	NF			LOH: J1J2-EV120		
	T224.2	NF			LOH: J1J2-3NF1		
6	T225.1	NF	E10b: DEL [MLPA]	Novel	LOH: J1J2-IVS38		
	T225.3	NF			LOH: IVS27-IVS38		
7	T170.3	NF	c.2041 C>T; p.R681X	Ars *et al* (2000)	LOH: IVS38-3NF1		
8	T171	NF	c.4084 C>T; p.R1362X	Upadhyaya *et al* (1997)	LOH: IVS27-IVS38		
9	T174	NF	1.4 Mb deletion [MLPA]	Kehrer-Sawatzki *et al* (2004)		ND	
10	T179.1	NF	ND		LOH: EV120-IVS38		
11	T170.2	NF	c.2041 C>T; p.R681X	Ars *et al*, 2000	LOH: IVS38-3NF1		
12	T173.1	NF	ND		LOH: EV120-IVS38		
13	T173.2	NF	ND			ND	
14	T179.2	NF	ND		LOH: EV120-IVS38		
15	T192.4	NF	E6-27a: Del [MLPA]	Novel	LOH: D17S796-EV120		
16	T197A	NF	c.1318 C>T; p.R440X	Heim *et al*, 1995		ND	
17	T211.1	NF	90 kb del [MLPA]	Upadhyaya *et al*, 1990		ND	
18	T1281.2	NF	ND		LOH: J1J2-3NF1		
19	T1281.4	NF	ND		LOH: J1J2-IVS27		
20	T219.1	NF	ND			c.1224-1225delGT; p.Y408fsX18	Novel
21	T220	NF	ND		LOH: IVS27-EV120		
22	T205.1	Plex	c.4196C>A; p.S1399X	Novel		c.4537 C>T; p.R1513X	Side *et al* (1997)
23	T177	Plex	c.3916 C>T; p.R1306X	Park *et al*, 1998	LOH: IVS27-IVS38		
	T213	Plex		Park *et al*, 1998	LOH: EV120-IVS38		
24	T172	Plex	ND		LOH: D17S796-D17S928		
25	T193	MPNST	c.2870 del A; p.N957fsX	Novel		c.1312 G>T; p.E438X	Novel

Three samples, however, had longer characterised regions of LOH extending from *D17S796* in the 17p13.2 region to *D17S928* in the 17q25.3 region, and therefore encompassing most of chromosome 17. No genomic deletions were detected in any of the samples with LOH following MLPA analysis, indicating that mitotic recombination was the likely mechanism underlying LOH in these samples.

In 25 of the 28 tumour samples in which somatic mutations were identified by LCM; the somatic mutation could not be identified in the original whole tumour sample even once the location of the somatic mutation was known. In 3 of the 28 samples (T164.1, T224.1 and T225.2), however, once the location of the mutation (LOH) in these tumours was known, the mutation could be observed in the original sample but at very low dosage (approximately 10-20% of cells). LOH was therefore likely to have been masked by heterogeneous cells in these tumours (figure 3.3).

3.3.3 Analysis of the germline and somatic NF1 mutational spectrum

NF1 germline mutations were detected in all the three patients and included: nonsense, 2bp deletion and splice site alteration, the latter two both representing novel changes (table 3.4). Somatic mutations were initially identified in 47 whole tumour DNA samples from the cohort of 89 neurofibromas (53% mutation detection). No fresh tumour samples were available for Schwann cell culture but LCM was applied to the analysis of the somatic mutational spectrum in the remaining 42/89 benign cutaneous neurofibromas from 3 patients with high tumour burden. Following the application of LCM to the 42 cutaneous neurofibroma samples, the LCM derived DNA was re-analysed for *NF1* somatic mutations. Using LCM, a further 10 somatic mutations were identified in 10 neurofibroma samples (shaded grey in table 3.4). Overall, therefore somatic *NF1* mutations were detected in 57/89 samples screened giving an overall mutation detection rate of 64% (22 LOH, 35 small lesions). Twenty eight of these mutations are novel (table 3.4). All somatic alterations were absent from the patients germline DNA. LOH was detected in 22/89 (25%) samples, comprising 18% of tumours in patient 1, 38% in patient 2 and no LOH was detected in patient 3.

Table 3.4. Somatic and germline *NF1* mutations identified in 89 tumours and paired blood DNA samples from three NF1 patients with a high tumour burden. Shading of consecutive tumour samples represents tumours found located in close proximity to each other

Patient	Tumour	Germline *NF1* Mutation	Extent of LOH	Somatic *NF1* Mutation	Previously Reported/Novel	*NF1* Polymorphisms
1	T433	c.2875 C>T; p.Q959X		c.1660C>G; p.Q554E	Not Reported	c.288+41G>A (HOM) c.702 G>A p.L234L (HOM) c.1528-32 T>C (HOM) c.1641+ 39 T>C IVS 10c (HOM) c.5205+ 23T>C (HET) c.5546 +19 T>A IVS 29 (HET) c.7125+37C>G (HET)
	T434			c.7699 C>T; p.Q2567X	Fahsold et al, 2000	
	T435			c.7702 C>T; p.Q2568X	Fahsold et al, 2000	
	T436		IVS27, EV120, IVS38 (Intron 27-Intron 38)			
	T437			c.67A>T; p.I23L	Not Reported	
	T438			Not Detected		
	T439		IVS27, EV120, IVS38 (Intron 27-Intron 38)			
	T440		IVS27, EV120, IVS38 (Intron 27-Intron 38)			
	T441			c.586G>T; p.E196X	Not Reported	
	T442			c.4687 5bpdel; p.Ffs36X	Not Reported	
	T443			c.4691 G ins; p.Kfs36X	Not Reported	
	T444		HHH202, J1J2, IVS27, EV120, IVS38, 3'NF1 (5'-3' *NF1*)			
	T445			Not Detected		
	T446		IVS27, EV120, IVS38 (Intron 27-Intron 38)			
	T447			Not Detected		
	T448		HHH202, J1J2, IVS27, EV120, IVS38, 3'NF1 (5'-3' *NF1*)			

Patient	Tumour	Germline *NF1* Mutation	Extent of LOH	Somatic *NF1* Mutation	Previously Reported/Novel	*NF1* Polymorphisms
1	T448	c.2875 C>T; p.Q959X	HHH202, J1J2, IVS27, EV120, IVS38, 3'NF1 (5'-3' *NF1*)			c.288+41G>A (HOM) c.702 G>A p.L234L (HOM) c.1528-32 T>C (HOM) c.1641+ 39 T>C IVS 10c (HOM) c.5205+ 23T>C (HET) c.5546 +19 T>A IVS 29 (HET) c.7125+37C>G (HET)
	T449			Not Detected		
	T450			c.4084 C>T; p.R1362X	Upadhyaya et al, 1997	
	T452			Not Detected		
	T453			Not Detected		
	T454		IVS27, EV120, IVS38 (Intron 27-Intron 38)			
	T455			Not Detected		
	T456			c.3709-2 IVS22 A>G	Upadhyaya et al, 1997	
	T457			c.6448A>T; p.K2150X	Not Reported	
	T458			Not Detected		
	T459			c.1641+2 IVS 11 T>G	Not Reported	
	T460			c.7924 delT; p.SfsX16	Not Reported	
	T461			Not Detected		
	T462			Not Detected		
	T463			c.2410 -3 IVS 16 T>G	Not Reported	
	T464			Not Detected		
	T465			Not Detected		
	T466			Not Detected		
	T467			c.5380 C>T; p.Q1794X	Heim et al, 1995	
	T468			c.2041 C>T; p.R681X	Ars et al, 2000	
	T469			c.1724 delCACA; p.SfsX1	Not Reported	

Patient	Tumour	Germline *NF1* Mutation	Extent of LOH	Somatic *NF1* Mutation	Previously Reported/Novel	*NF1* Polymorphisms
1	T470	c.2875 C>T; p.Q959X		Not Detected		
	T471			c.6085 delG; p.VfsX8	Not Reported	
	T472			c.2088 G>A; p.W696X	Not Reported	
2	T473.1A	c.1413-1414delAG; p.KfsX4	HHH202, J1J2, EV120, IVS38 (5'*NF1* - Intron 38)			c.288+41G>A (HET) c.702G>A p.L 234L (HET) c.1641+ 39 T>C IVS 10c (HET) c.2034A>G p.P678P (HET) c.5205+ 23T>C (HET) c.5546 +19 T>A IVS29 (HET) c.6903 G>C p.V2301V (HET) c.7125+36 C>G (HOM)
	T473.1B			Not Detected		
	T473.1C		HHH202, J1J2, EV120 (5'*NF1* - Intron 27)			
	T473.1D			Not Detected		
	T473.1E			Not Detected		
	T473.2			Not Detected		
	T473.3		J1J2, EV120, IVS38 (5'*NF1* - Intron 38)			
	T473.4			Not Detected		
	T473.5		HHH202, JJ2, EV120, IVS38 (5'*NF1* - Intron 38)			
	T473.6			c.889 delA; p.LfsX20	Not Reported	
	T473.7		J1J2, EV120 (5'*NF1* - Intron 27)			
	T473.8		HHH202, J1J2, EV120, IVS38, 3'NF1, EW207, D17S949, D17S1822 (5'*NF1* - 17q25.2)			
	T473.9			Not Detected		
	T473.10		J1J2, EV120, IVS38 (5'*NF1* - Intron 38)			
	T473.11			c.2451 insG; p.MfsX13	Not Reported	

Patient	Tumour	Germline *NF1* Mutation	Extent of LOH	Somatic *NF1* Mutation	Previously Reported/Novel	*NF1* Polymorphisms
2	T473.12	c.1413-1414delAG; p.KfsX4		c.1884 insA; p.YfsX5	Not Reported	c.288+41G>A (HET) c.702G>A p.L 234L (HET) c.1641+ 39 T>C IVS 10c (HET) c.2034A>G p.P678P (HET) c.5205+ 23T>C (HET) c.5546 +19 T>A IVS29 (HET) c.6903 G>C p.V2301V (HET) c.7125+36 C>G (HOM)
	T473.13			c.5888 A>C; p.N1963T	Not Reported	
	T473.14		J1J2, EV120, IVS 38, 3' NF1, EW207, D17S949, D17S1822 (5'*NF1* - 17q25.2)			
	T473.15		J1J2, EV120, IVS 38, 3' NF1 (5'-3' *NF1*)			
	T473.16		J1J2, EV120, IVS 38, 3' NF1, EW207, D17S949, D17S1822 (5'*NF1* - 17q25.2)			
	T473.17			c.7128 delG; p.GfsX24	Not Reported	
	T473.18			c.3806 ins C; p.DfsX14	Not Reported	
	T473.19			Not Detected		
	T473.20			c.4087delA; p.SfsX22	Not Reported	
	T473.21		J1J2, EV120 (5'*NF1* - Intron 27)			
	T473.22			Not Detected		
	T473.23			Not Detected		
	T473.24			Not Detected		
	T473.25		EV120, IVS38 (Intron 27-Intron 38)			
	T473.26			Not Detected		
	T473.27			Not Detected		
	T473.28			Not Detected		

Patient	Tumour	Germline *NF1* Mutation	Extent of LOH	Somatic *NF1* Mutation	Previously Reported/Novel	*NF1* Polymorphisms
2	T473.29	c.1413-1414delAG; p.KfsX4		Not Detected		c.288+41G>A (HET)
	T473.30		J1J2, EV120, IVS38, 3'NF1, EW207, D17S949 (5'*NF1* - 17q23.3)			c.702G>A p.L 234L (HET)
	T473.31			Not Detected		c.1641+ 39 T>C IVS 10c (HET)
	T473.32		J1J2, EV120 (5'*NF1* - Intron 27)			c.2034A>G p.P678P (HET)
	T473.33			c.6478 A>G; p.S2160G	Not Reported	c.5205+ 23T>C (HET)
	T473.34		EV120, IVS38 (Intron 27-Intron 38)			c.5546 +19 T>A IVS29 (HET)
	T473.35			Not Detected		c.6903 G>C p.V2301V (HET)
	T473.36			c.6859 delG; p.DfsX18	Not Reported	c.7125+36 C>G (HOM)
3	T506.1	c.6756+2 T>G		c.3745 del20bp; p.SfsX8	Not Reported	c.288+41G>A (HOM)
	T506.2			c.731-732 delAA; p.AfsX5	Not Reported	c.702 G>A p.L234L (HOM)
	T506.3			Not Detected		c.1641+ 39 T>C IVS 10c
	T506.4			c.2987 insAC; p. RfsX16	Not Reported	c.5205+ 23T>C (HET)
	T506.5			c.480 delG; p.RfsX5	Not Reported	c.5546 +19 T>A IVS 29 (HET)
	T506.6			c.7127-3bp IVS40 T>G	Not Reported	c.7125+37C>G (HET)
	T506.7			Not Detected		
	T506.8			c.3306insA; p.LfsX3	Not Reported	
	T506.9			c.6364 Del 114bp; p. EfsX23	Not Reported	

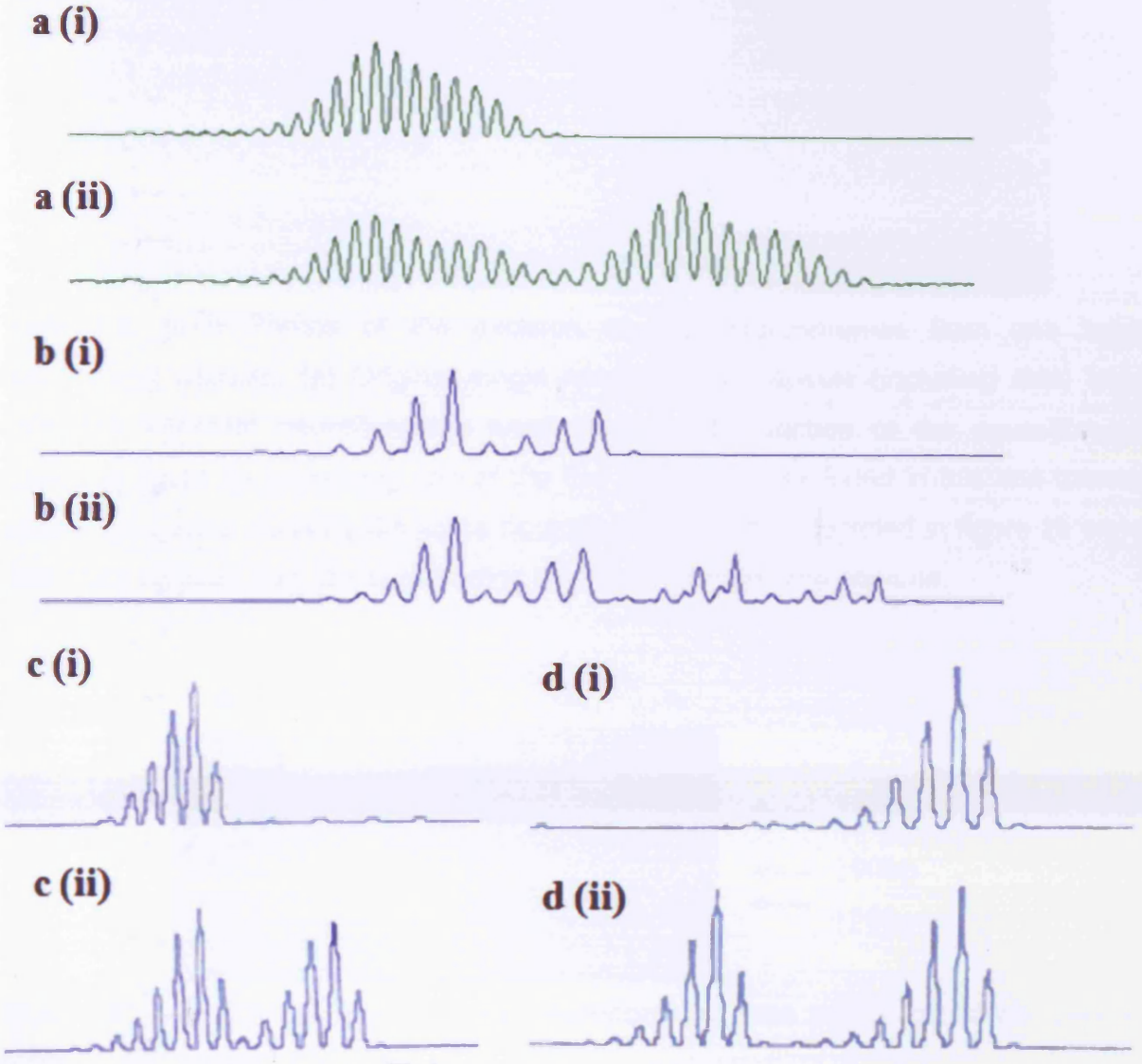

Figure 3.4 **(a-d)** Examples of MSI profiles from four different tumours with markers **(a i)** *MBAT 40.4* (1p13) in blood and **(a ii)** in tumour sample. **(b i)** *D17S250* (17q12) in the blood and **(b ii)** in the tumour. **(c i)** *D5S107* (5q11-q13) in the matched lymphocyte DNA sample and **(c ii)** in the tumour sample. **(d i)** MSI at marker *D5S406* (5p15) in the blood DNA sample and **(d ii)** matched tumour sample.

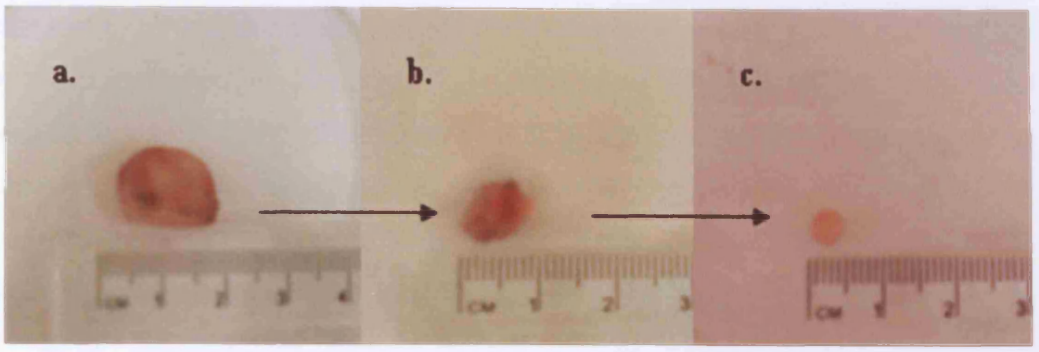

Figure 3.5. **(a-c)** Photos of the excision of five neurofibromas from one large neurofibroma capsule. **(a)** Original single neurofibroma capsule (including skin) from which five separate neurofibromas were excised. **(b)** Section of the neurofibroma pictured in figure 2a containing one of the five neurofibromas found in this one tumour capsule. **(c)** Figure showing the same neurofibroma which is depicted in figure 2b once it has been excised from the surrounding skin and neurofibroma capsule.

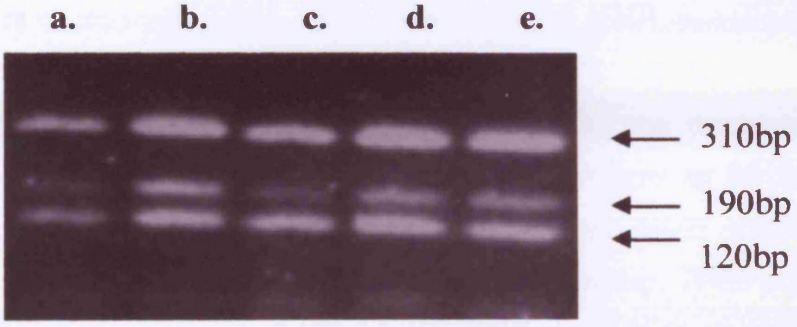

Figure 3.6 **(a-e)** LOH of five separate neurofibromas from within the same capsule identified with marker *HHH202*.

The extent of LOH ranged from just involving the 5' end of the *NF1* gene to the entire long arm of chromosome 17 (table 3.4). MSI was observed in 21/89 (24%) tumour samples studied. MSI in these samples was compared to the corresponding lymphocyte DNA samples in which the additional alleles were not present, indicating no MSI was present in the blood DNA (figure 3.4). No deletions were identified in the 89 samples using the *NF1* MLPA kits indicating that LOH in these samples resulted from mitotic recombination. Interestingly, one individual tumour capsule which was not located adjacent to any other tumour, contained five separate neurofibromas, only two of which demonstrated LOH (figure 3.5 and figure 3.6). The somatic *NF1* mutations in each tumour from each individual were all apparently independent events and the somatic mutational spectrum (table 3.1, table 3.4 and figure 3.7) did differ between the three patients as no nonsense and splice mutations were detected in patient 2 and no LOH, nonsense or missense mutations were identified in patient 3.

3.3.4 Analysis of somatic TP53, RB1, CDKN2A and MMR mutations

To identify potential modifying loci which may underlie the development of multiple neurofibromas in patients with high tumour burden, DNA from all 89 neurofibromas was analysed for alterations in the *TP53, RB1, CDKN2A* and *MMR* genes. No pathogenic *TP53* somatic mutations were identified by direct sequencing. *TP53* LOH was, however, detected in four samples (T440, T473.20, T506.1 and T506.9) at polymorphic markers within the *TP53* gene (*Alu1*, codon 72 and exon 6 polymorphic markers) (figure 3.8). DNA from these samples was not derived from LCM. One of the four samples showed LOH at all three of these markers. The remaining three samples only exhibited LOH at two of the markers as the codon 72 polymorphism was uninformative. These four samples were also screened for deletions using the appropriate *TP53* MLPA assay kit but no deletions were detected. The level of *TP53* LOH observed at the second allele of each sample after correcting for the relative peak areas with corresponding lymphocyte DNA was between 37% and 66% (*Alu1*), 11% (codon 72) and between 35% and 57% (exon 6) (figure 3.8).

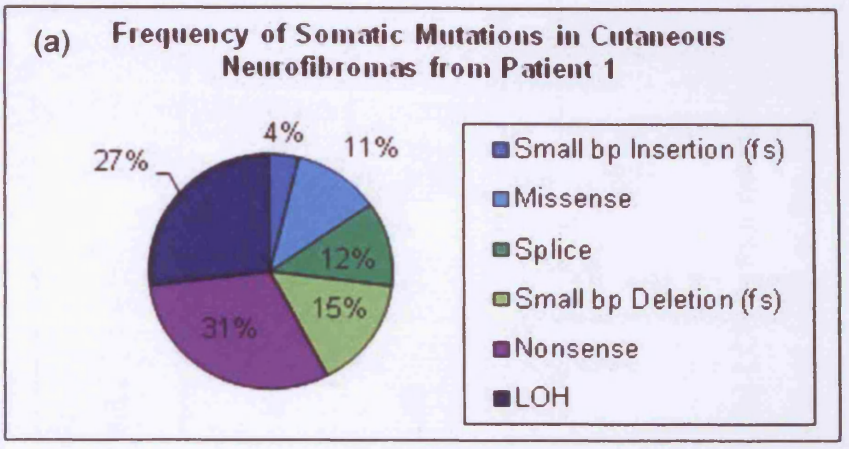

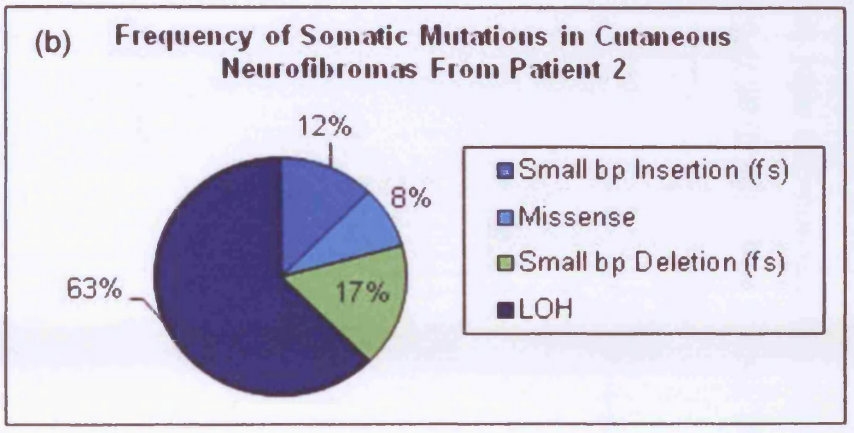

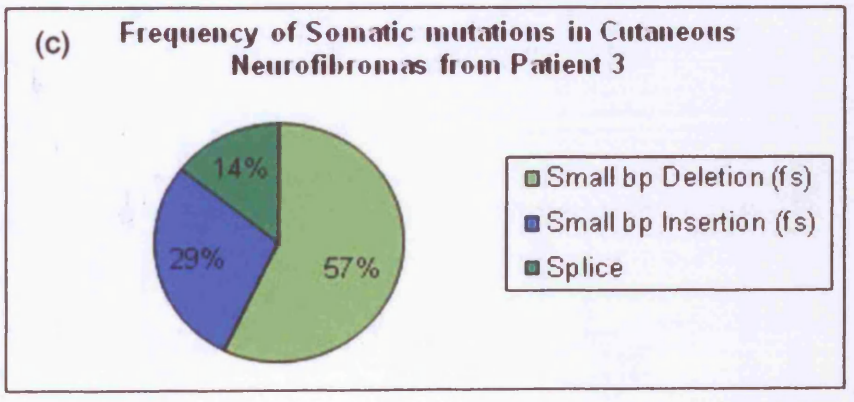

Figure 3.7. Somatic *NF1* mutational spectrum for patients 1-3. **(a)** Somatic mutational spectrum for 40 tumours from patient 1 (Germline mutation: E17: c2875 C>T p.Q959P) **(b)** Somatic mutational spectrum for 40 tumours from patient 2 with an absence of nonsense and splice site mutations (Germline mutation: E10b: c.1413-1414delAG p.Kfsx4). **(c)** Somatic mutational spectrum for 9 tumours from patient 3 with an absence of LOH, nonsense and missense mutations (Germline mutation: E36: 6756+2 T>G).

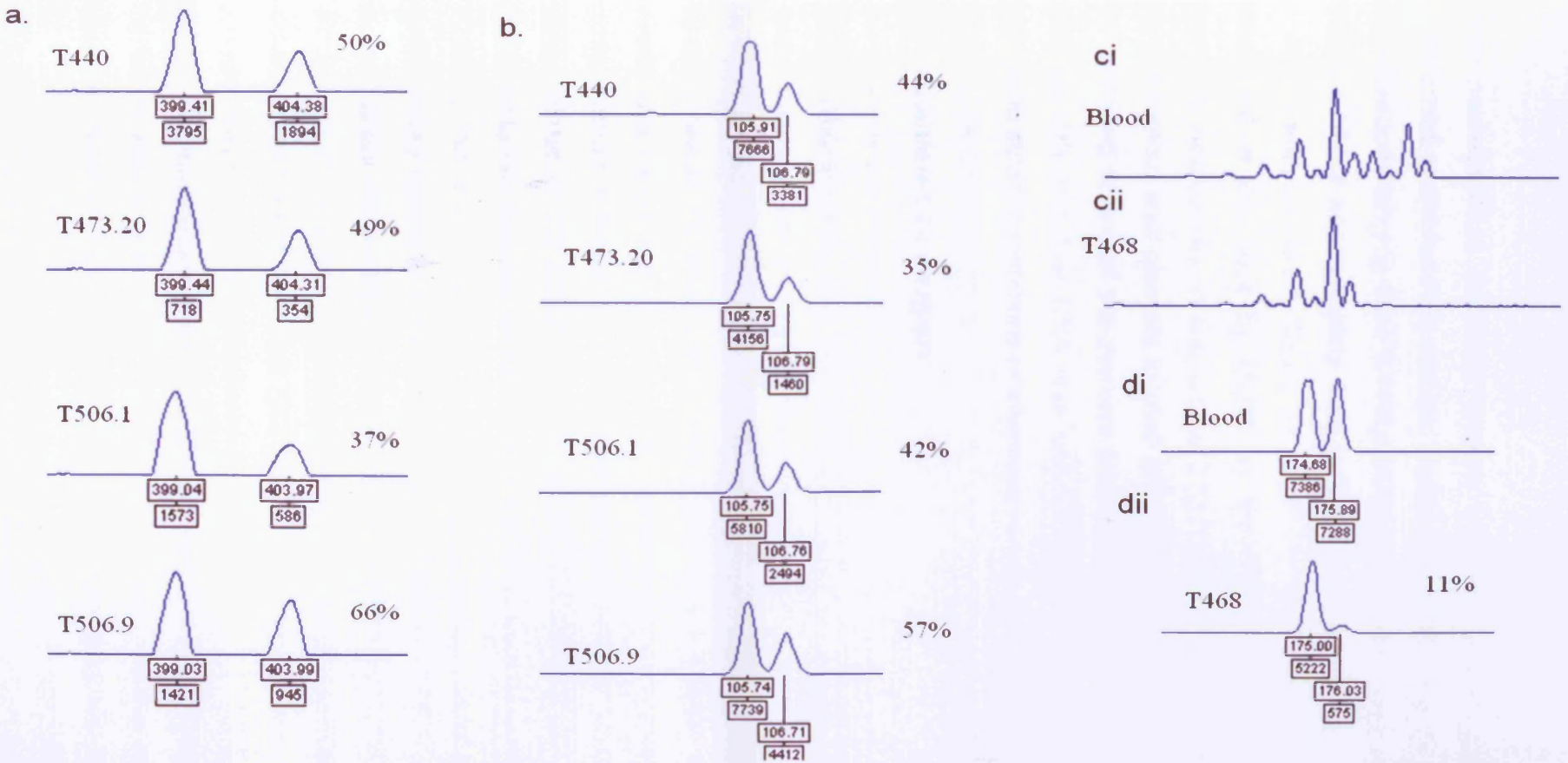

Figure 3.8. **(a)** LOH of four neurofibromas (T440, T473.20, T506.1 and T506.9) at *TP53 Alu1*. **(b)** LOH in four neurofibromas (T440, T473.20, T506.1 and T506.9) at exon 6 of the *TP53* gene. All percentages refer to the level of LOH of the second allele. **(ci)** Analysis of matched lymphocyte DNA with marker *D13S118*. **(cii)** LOH of the *RB1* gene at *D13S118* in tumour T468. **(di)** Analysis of matched lymphocyte DNA with marker *D13S917* **(dii)** LOH of the *RB1* gene at *D13S917* in tumour T468. All percentages refer to the level of LOH of the second allele.

These neurofibromas were not located adjacent to any other tumour and all four tumours had additional *NF1* somatic mutations; comprising of, LOH (intron 27-38) and micro-deletions ranging from 1-114bp in three samples. One other sample (T468) also showed LOH of approximately 1Mb in length at two markers flanking the *RB1* locus (*D13S118* and *D13S917)* (figure 3.8 c and d). The mechanism of LOH could not be determined in this case by MLPA as the *RB1* MLPA kit was unavailable in our laboratory. Additionally, in this tumour a somatic *NF1* nonsense mutation was detected and this tumour was also not located adjacent to any other tumour. No *CDKN2A* LOH was identified at any of the markers that were analysed. Twenty one tumour samples exhibited MSI and their DNA was sequenced for the four main *MMR* genes but no pathogenic somatic mutations or polymorphic changes were identified.

3.3.5 Bioinformatic analysis

Bioinformatic analysis was performed by Professor Nadia Chuzhanova (Nottingham Trent University) on the ±20bp flanking sequences of the *NF1* somatic mutations identified in the cohort of 89 neurofibromas from patients with high tumour burden. Fourteen out of 19 mutations (74%) found in the patient 1 were single basepair substitutions, apparently mediated by either direct or inverted repeats or both. In addition, for 13 of these mutations short (≥5 bp) purine or pyrimidine tracts were found within ±20 bp of the mutation. Such purine/pyrimidine tracts are known to promote genetic instability through formation of non-B DNA structures (Bacolla *et al*, 2004). The remaining four microdeletions and one microinsertion were apparently mediated by direct/inverted repeat or symmetric elements. Only two (22%) somatic mutations in the second patient were single basepair substitutions whereas the majority of them were microlesions. Purine and pyrimidine tracts were found downstream and upstream of mutations E31:c.5888 A>C and E34:c.6478 A>G respectively. All four deletions in the second patient were deduplications (Kondrashov *et al*, 2004) mediated by inverted repeats. Two microinsertions (E16:c.2451insG and E12b:c.1884insA) were mediated by inverted repeats and inversion E22:c.3806insC was mediated by direct repeat. Somatic mutations found in the third patient do not differ dramatically from the second patient;

they are all mediated by either direct or inverted repeats. In addition, short alternating purine-pyrimidine tracts with Z-DNA-forming potential were found in the vicinity of six mutations. Motif complement to the deletion hotspot, TGRRKM, was found in the vicinity of the remaining deletion E34:c.6364del114b

3.4 Discussion

3.4.1 Somatic mutation detection

This study has evaluated the efficacy of somatic *NF1* mutation detection following enrichment of Schwann cells both by Schwann cell culture and by LCM. Following validation of these methods, LCM was employed to aid in the characterisation of the germline and somatic mutational spectrum of tumours from NF1 patients with high cutaneous neurofibroma burden. Few large scale studies have been conducted on the somatic mutational spectrum in benign cutaneous neurofibromas. The few previous reports in the literature, demonstrated great variation in the *NF1* somatic mutational detection rate. In some earlier studies in which few neurofibromas were analysed, all somatic mutations were identified (Eisenbarth *et al*, 2000). In subsequent studies on a larger panel of samples, 12% of mutations were identified by John *et al* (2000), whilst Serra *et al* (2001b) identified 19% of somatic mutations. The study by Upadhyaya *et al* (2004) detected 35% of *NF1* somatic mutations and the most recent study by Spurlock *et al* (2007) identified somatic *NF1* mutations in 64% of neurofibroma samples. In addition to cellular heterogeneity and the overall complexity of the *NF1* gene, low somatic mutation detection rates can be attributed to mutational detection methods used in earlier studies which were not sensitive enough to detect different types of *NF1* lesions. A recent study by Maertens *et al* (2006) demonstrated a significant improvement of somatic mutation detection rates, with 76% of mutations being identified in cutaneous neurofibromas. However, this was only after the introduction of culture methods to enrich Schwann cells which exclusively carry the *NF1* somatic mutation, underlining the requirement for improved techniques for routine *NF1* somatic mutation detection.

3.4.2 Validation of Schwann cell enrichment strategies

In the present validation study, with the use of Schwann cell culture and LCM to target the Schwann cell population, the somatic mutation detection rate was 85% (11/13 samples) and 80% (28/35 samples) respectively. Hence, LCM provides an increase in detection of 27% whilst Schwann cell culture increases the detection rate by 32%. Schwann cell culture and LCM also aided in the successful calling of several somatic mutations that were present, but not readily identifiable in DNA from the original whole tumour due mainly to the level of contaminating non-Schwann cell derived heterozygous DNA (figure 3.2 and figure 3.3). In this study involving 89 cutaneous neurofibromas, prior to the application of LCM somatic mutations were identified in 47 tumours (53%). However, usage of LCM allowed the detection of *NF1* somatic mutations in an additional 10 tumours (64%) highlighting that Schwann cell enrichment results in an improved *NF1* somatic mutation detection rate.

3.4.2.1 Schwann cell culture

Of the two techniques, Schwann cell culture is more sensitive for mutation detection in NF1-associated tumours. The results of Schwann cell analysis from the present study has even improved on the 76% mutation detection rate reported by Maertens *et al* (2006). This indicates that this study may be the most successful application of this technique to date, although the sample size (13 cutaneous neurofibromas) is only a third of the 38 tumours studied previously. Although application of this technique was successful, Schwann cell culture still has several disadvantages. It is laborious, time consuming and should be set up rapidly following removal of the tumour to ensure the viability of the cells. Schwann cell culture is only a prospective technique and is not always successful. Indeed, during the course of this study one neurofibroma derived Schwann cell sample failed to thrive and thus was not available for mutation analysis. Little is known of Schwann cell growth, but the small size of the tumour sample may have contributed to the failure of Schwann cell culture from this tumour. Schwann cells need to be in contact with each other for proper growth and if few Schwann cells are

present this is not possible. Moreover, care has to be taken not to introduce fibroblasts to the culture as these can rapidly overtake the Schwann cell culture. This means that larger neurofibromas with a well defined capsule are more suited to this method of culture as a large section can be taken from within the middle of the tumour, away from the skin where the majority of fibroblasts are found. However, fibroblasts are also found within these heterogeneous tumours but the culture conditions should ensure that they do not survive (see below).

The medium in which Schwann cells are grown requires a number of supplements to aid in the purification of the mutation harbouring population. These include IBMX, a competitive non-selective phosphodiesterase inhibitor. IBMX not only raises the level of intracellular cAMP in Schwann cells to promote growth but also aids in fibroblast growth inhibition, although it is only useful with sparse fibroblasts. β-heregulin (HRG-β1) is a known mitogen of Schwann cells which binds to and activates EGF-like transmembrane receptor tyrosine kinases. Schwann cells unusually require a specific agent to increase cAMP to promote cell division, which is the role of both Forskolin which is a direct activator of adenylyl cyclase, and insulin which induces the activity of the cAMP response element binding protein (CREB) (Rahmatullah *et al*, 1998). Schwann cells are adherent cell lines which also require specific substrates for growth. The glycoprotein laminin is known to be essential for Schwann cell survival and enrichment due to the preference for attachment to such a substrate (Muir *et al*, 2001). Use of such supplements does, however, not only increase the time of media preparation but also the cost of long term culture. Finally, it was observed that Schwann cells do not respond well to changes in media especially in the context of freeze thaw for storage and revival of cell lines. Cell lines frozen early in the culture rarely survive cryopreservation, and so freeze thaw should be kept to a minimum.

3.4.2.2 Laser Capture Microdissection (LCM)

Although LCM was not quite as efficient as Schwann cell culture for improving the somatic mutation detection rate, during validation it still aided in the identification of 28/35 (80%) of somatic *NF1* mutations. LCM may also have broader applications as it

has proved to be important in evaluating mutations in other tumour types including breast carcinomas (Zanni and Chan, 2011). However, LCM is potentially more problematic than cell culture as a substantial volume of tumour material is required to provide enough DNA to complete the full range of *NF1* analyses whereas cultures provide a 'limitless supply'. In this study approximately 400ng/µl of DNA was required for LOH, MLPA and sequencing analysis from LCM samples which equates to about 4-5x10^4 cells (Takeshima *et al*, 2001; Espina *et al*, 2006). Furthermore, FFPE samples often provide degraded DNA which means that the use of this DNA in downstream applications such as PCR is challenging (Edwards, 2007).

Of the 23 *NF1* somatic mutations identified in cutaneous neurofibromas during validation of the LCM technique, 21 were copy neutral LOH (91%), a very high finding in neurofibromas in which LOH usually ranges between about 3% and 40% (Colman *et al*, 1995; Daschner *et al*, 1997; Serra *et al*, 1997; Kluwe *et al*, 1999b; Eisenbarth *et al*, 2000; John *et al*, 2000; Rasmussen *et al*, 2000; Serra *et al*, 2001; Upadhyaya *et al*, 2004; De Raedt *et al*, 2006b; Laycock-VanSpyk *et al*, 2011). This LOH is unlikely to represent an artefact of the LCM technique as such a problem has not been previously reported in the literature. Moreover, in 3 samples, analysis of DNA from the original whole tumour alongside the LCM DNA indicated that the LOH in these tumours was already present in the original samples but undetectable due to the small percentage of mutation harbouring Schwann cells present (figure 3.3). LCM is a flexible technique which is applicable to both prospective and retrospective studies. It is clear that if fresh tissue is not available for Schwann cell culture of samples in which the somatic *NF1* mutation cannot be identified, then LCM represents a good alternative.

3.4.3 Analysis of NF1 somatic mutations in 89 cutaneous neurofibromas

Following validation of Schwann cell culture and LCM as an improved strategy for mutation detection, this study set out to characterise the somatic mutational spectrum in 89 benign cutaneous neurofibromas from patients with high tumour burden with the aid of LCM to improve somatic *NF1* mutation detection. Three unrelated NF1 patients, all with multiple cutaneous neurofibromas, (>550) and additional clinical complications

(table 3.1) were recruited for this study. A major question is whether the cells of a tumour are monoclonally derived, descendent from a single founder cell with a specific somatic *NF1* mutation or if a larger cluster of the normal cell population have undergone a change leading to a mixture of a subpopulation of cells in the tumour indicating that the cell is polyclonal with no distinct common origin? This study demonstrates that each somatic *NF1* mutation resulted from an independent event, clearly indicating that although many of these tumours developed in very close proximity to each other, none of them were clonally-derived (table 3.4). Indeed, even in the situation where five tumours from within the same capsule were analysed, only two exhibited LOH, indicating that they are not all clonally derived (figure 3.5 and figure 3.6).

With the application of LCM to 42/89 benign cutaneous neurofibromas in which somatic *NF1* mutations were not identified, 10 additional somatic mutations were identified, increasing the somatic mutational detection rate by 11% from 53% to 64%. The evaluation of Schwann cell culture demonstrated that the mutation detection rate in these 89 neurofibromas could have been improved even further if Schwann cell culture could have been used. This was not possible; however, as fresh whole tumour samples were not available. Undetected somatic mutations may be located in gene regions not screened in this study including the deep intronic regions, the 5'and 3' UTRs and the *NF1* promoter region (section 5.1). However, the problem of cellular heterogeneity is most likely to be the main reason for the low mutation detection rate based on observations that LCM was able to improve the ability to call mutations in some samples by enriching the mutation harbouring Schwann cell population (figure 3.2 and 3.3).

Overall, LOH was detected in 25% of tumours. The results from the present study are in agreement with previous findings where LOH was detected in ~10-30% of samples (Upadhyaya *et al*, 2004; De Raedt *et al*, 2006b; Serra *et al*, 2007). Several previous studies by Däschner *et al* (1997) and John *et al* (2000) have also found little evidence for LOH, a similar finding to patient 3 in our study. Low levels of LOH detection, and inter-individual variability in the level of LOH may also be accounted for by cellular heterogeneity and also the methodology used for analysis by different studies. In this study, no genomic deletions were found by MLPA in tumour DNA exhibiting LOH,

indicating that mitotic recombination is the likely mutational mechanism in these tumours (Serra *et al*, 2001).

Twenty eight of the somatic *NF1* mutations identified are also novel sequence changes, a significant contribution to the *NF1* somatic mutational spectrum. Furthermore, bioinformatic analysis shows that the majority of mutations were likely to be mediated by either direct or inverted repeats. There are also differences in the inter-individual *NF1* somatic mutational spectrum identified in the 3 patients studied (figure 3.7). A comparison of the germline and somatic *NF1* mutations detected in these three patients failed to reveal any obvious correlation between the genotype and phenotype of the patients. Importantly, in some samples, prior to LCM analysis, the somatic mutation was not immediately obvious in DNA samples but following analysis of cDNA, frameshift mutations were identified and subsequently confirmed in the DNA sample, negating the need for LCM (T469 and T506.9, table 3.4). These samples harboured the larger of the frameshift deletion mutations and thus future studies employing cDNA instead of DNA sequencing may be important for identification of such somatic mutations.

3.4.4 Analysis of somatic TP53, RB1, CDKN2A and MMR mutations

This study also aimed to determine whether a different molecular mechanism of tumorigenesis might underlie the development of cutaneous neurofibromas from patients with high tumour burden. Mutations in the *TP53, RB1* and *CDKN2A* genes have been found to contribute to the development of plexiform neurofibromas (Upadhyaya *et al*, 2008b; Stewart *et al*, 2008) and MPNSTs (Kourea *et al*, 1999; Nielsen *et al*, 1999; Mawrin *et al*, 2002; Mantripragada *et al*, 2008). Furthermore, individuals with germline *MMR* mutations often exhibit an 'NF1- like phenotype' (de Wind *et al*, 1995; Reitmair *et al*, 1995; Reitmair *et al*, 1996; Sohn *et al*, 2003; Gutmann *et al*, 2003; Chen *et al*, 2005; Feitsma *et al*, 2008). In view of the high tumour burden in these patients, such potential modifying loci (*TP53, RB1, CDKN2A* and *MMR*) were analysed to assess the contribution to cutaneous neurofibroma development in these patients. One tumour exhibited LOH which encompassed a large region of ~1Mb involving the entire *RB1* gene. A further four tumours exhibited *TP53* LOH at markers

within the gene (figure 3.8). These were five independent tumours which were not located immediately adjacent to any other tumour. This suggests that there was no relationship between the anatomic location of the tumours and the development of additional somatic mutations. The distal and proximal flanking LOH markers for *TP53* did not show LOH indicating that LOH is restricted to the *TP53* gene. However, no detectable *TP53* deletions were identified by MLPA, suggesting mitotic recombination as the likely mutational mechanism. LOH may still be present in the remaining tumours in which no LOH of *TP53* and *RB1* was found due to uninformative markers in these samples. Histological findings demonstrated that the neurofibromas from the cohort analysed were composed of spindle cells with thin, wavy nuclei, embedded in a collagenous and myxoid stroma, characteristic of typical neurofibromas. Furthermore, no evidence for pleomorphic nuclei was found that would have been suggestive of atypical neurofibromas that could account for the presence of *TP53* and *RB1* LOH (Jokinen and Argenyi, 2010).

It has been suggested that the global somatic mutational spectrum may be important in explaining variable clinical expression observed in many NF1 patients. Whilst benign and malignant NF1 associated tumours exhibit biallelic inactivation of *NF1*, the accumulation of somatic abnormalities at unrelated loci represents a probable step towards malignant transformation. Therefore, the identification of LOH at *TP53* and *RB1* loci, in addition to somatic *NF1* mutations in these benign tumours, is an important finding as such somatic mutations are normally only associated with malignant NF1 tumours and cutaneous neurofibromas are not known to develop into MPNSTs (Kourea *et al*, 1999; Nielsen *et al*, 1999; Mawrin *et al*, 2002; Mantripragada *et al*, 2008). If these genetic aberrations occur later during tumour formation it is possible that these mutations represent a step towards malignant progression. Additional somatic mutations involving genes from multiple genetic pathways could therefore indicate that in these patients, the occurrence of a high tumour burden may be due to somatic mutations of other modifying loci, in addition to their *NF1* mutations.

In the current study, while genome wide MSI was detected in 24% of the neurofibromas (21/89); no sequence changes of the *MMR* genes were identified. The significance of MSI in these tumours is unclear as the level of MSI reported here is similar to previous

findings in neurofibromas and is much lower than has been identified in MPNSTs (50%) (Ottini *et al*, 1995; Serra *et al*, 1997; DeRaedt *et al*, 2006; Spurlock *et al*, 2007). Interestingly, patient 2 exhibited the highest level of MSI and had an MPNST while patient 3 had a malignant complication of B-CLL but had a significantly reduced level of MSI, similar to that seen in patient 1 who was without malignant abnormalities (table 3.1). The correlation of MSI and additional malignant complications is therefore unclear and would warrant a much larger study to determine any relationship. The presence of MSI in these neurofibromas is likely to be due to generalised genomic instability, rather than evidence of specific defects in any *MMR* genes. Copy number abnormalities, sequence changes in the other *MMR* genes, or alterations to the methylation status of the *MMR* genes could also still account for the presence of MSI. However, due to insufficient tumour tissue, immunohistochemical analysis of MMR proteins was not possible.

3.4.5 Conclusions

The cellular and molecular heterogeneity associated with cutaneous neurofibromas is a major complication in the analysis of *NF1* somatic mutations. In the present study, LCM and Schwann cell culture were validated as Schwann cell enrichment strategies. The results of this study indicate that such techniques represent future improvements for somatic *NF1* mutation detection and may aid in the characterisation of mechanisms of *NF1* somatic inactivation. This study has identified LOH at *TP53* and *RB1* loci in these tumours. This is a significant finding in benign neurofibromas as such *TP53* and *RB1* LOH has only previously been detected in malignant MPNSTs. These novel findings, demonstrate for the first time, that the development of neurofibromas in NF1 patients with high tumour burden potentially differs from that of the discrete cutaneous neurofibromas present in the majority of NF1 patients.

CHAPTER 4: Functional analysis of *NF1* GRD missense mutations

4.1 Introduction

The *NF1* gene has one of the highest mutation rates reported in human disorders. The germline mutational spectrum is well defined, with at least 1273 mutations characterised to date (HGMD). At least 150 of these are identified within the Gap related domain (GRD) of neurofibromin (HGMD), approximately 80% of which are truncating. The GRD, encoded by exons 20 to 27a (360 amino acids) (NM_000267) defines the major functional domain of neurofibromin as a negative regulator of the RasMAPK pathway (Gutmann *et al*, 1993). Neurofibromin functions as a RasGAP (GTPase activating protein) with extensive sequence homology to two mammalian RAS-GTPases, including p120GAP in addition to Ira1p and Ira2p, two inhibitory regulators of the Ras-cyclic AMP pathway found in the yeast *Saccharomyces cerevisae* (Andersen *et al*, 1993). The downregulation of active Ras by GAP's is a crucial step in the regulation of signal transduction of the RasMAPK pathway and is disrupted in a significant proportion of cancer-associated Ras mutants. Neurofibromin binds to Ras proteins through the GRD; promoting GTP hydrolysis by inducing the intrinsic GTPase activity of Ras, converting Ras from the active GTP-bound form to the inactive GDP bound form. This modulates RasMAPK signalling to alter cellular processes including cell proliferation and DNA synthesis (Ballester *et al*, 1990; Xu *et al*, 1990; DeClue *et al*, 1991; Cichowski and Jacks 2001; Arun *et al*, 2004; Gottfried *et al*, 2006) (Figure 1.2) Loss of function of the *NF1* gene through mutation therefore leads to an amplification of the activity of the RasMAPK pathway and subsequently tumorigenesis.

The underlying mechanism of GTPase stimulation first involves the stabilisation of residues in the switch I and switch II regions of Ras. This is followed by stabilisation of the transition state of GTP hydrolysis by neutralisation of a developing negative charge on the GTP phosphate oxygen atoms during phosphoryl transfer. This occurs through the insertion of a catalytic arginine in to the active site (Scheffzek *et al*, 1997; Scheffzek *et al*, 1998; Resat *et al*, 2001). There are a number of regions in RasGAPs, which are known to interact with the switch regions in Ras; the finger loop, FLR region and

α7/variable loop region (Ahmadazin *et al*, 2003). These regions undergo conformational changes between the active and inactive state and are thought to interact with Ras by binding to the Ras switch I region through the α7/variable loop, stabilisation of the finger loop by the FLR region and contribution of an arginine residue (R1276 in neurofibromin) to the catalytic region of Ras by the FLR region (Ahmadazin *et al*, 2003).

Less than ten studies have been previously completed on variants within the GRD of NF1 (Skinner *et al* 1991; Li *et al*, 1992; Poullet *et al*, 1994; Morcos *et al*, 1996; Scheffzek *et al*, 1996 and 1997; Upadhyaya *et al*, 1997; Klose *et al*, 1998; Ahmadazin *et al*, 2003). Li *et al* (1992) analysed the K1423E by site directed mutagenesis and measurement of phosphate release. The crystal structure of the GAP domain was determined by Scheffzek *et al* (1996 and 1997) and Morcos *et al* (1996) used a randomly mutagenised NF1-GRD library to screen for mutants capable of interacting with H-rasD92K, a protein which is defective in interaction with NF1. Furthermore, Ahmadazin *et al* (2003) have completed an extensive biochemical study on a few key residues within the GRD. These studies have offered new insights into the role of individual amino acid residues and their role in RAS-RasGAP interaction. However, fewer than 5 NF1-GRD mutants (K1423E, R1391K, R1391S and R1276P) have been functionally analysed to date.

Of all the known characterised *NF1* mutations, approximately 80% represent truncating mutations including: small deletions and insertions, indels, large (Mb) microdeletions encompassing the majority or the whole of the *NF1* gene in addition to some surrounding genes, as well as nonsense and splice site alterations (Fahsold *et al*, 2000; Ars *et al*, 2000; Thomas *et al*, 2010; HGMD). The mRNA derived from truncated alleles, may be removed by nonsense mediated mRNA decay (NMD). Truncated mRNA transcripts which are stable may still be translated resulting in either an unstable protein or a stable protein which might not possess any function. Inactivation of the remaining wild type *NF1* allele in somatic cell types including Schwann cells and melanocytes results in the manifestation of the hallmarks of NF1. The same mutational mechanisms which act in the germline also occur as somatic lesions (Ivanov *et al*, 2011). However, loss of heterozygosity (LOH) is confined to the soma, occurring in up to 40% of neurofibromas (Laycock-VanSpyk *et al*, 2011) and at a higher rate in MPNSTs (85%), in

conjunction with gains and losses at other genetic loci (Upadhyaya, 2011). Truncating mutations, do not account for all *NF1* lesions, however, as synonymous and non-synonymous single nucleotide polymorphisms (SNPs) are common in the *NF1* gene. Many are classed as missense mutations, occurring in patients in which no other *NF1* gene alteration has been identified and which segregate with the disease in the family. These missense mutations account for ~10-20% of all characterised germline and somatic *NF1* mutations although due to the underlying amino acid substitutions involved, their pathogenicity is not always certain.

We have sufficient knowledge of Ras-RasGAP interaction but there are many questions which still require further investigation. For example, (i) are there critical amino acid residues which are absolutely required for RasGAP affinity for Ras? (ii) Are there residues which are important for promotion of catalysis by the arginine finger? (iii) Which residues are critical for stabilisation of the switch regions in Ras? It is clear that further studies are warranted as relatively few variants have been studied and consequently there is still insufficient evidence for the role of specific residues in neurofibromin which may be important for Ras interaction. Development of an effective technique for classification of variants into pathogenic and non-pathogenic changes, to further define the underlying mechanisms responsible for NF1 disease manifestation and tumour development is required. The main aims of this chapter were:

1. To develop a novel functional assay to better define the pathogenicity of missense variants located in the GRD.
2. To determine the reliability of bioinformatic software for functional analysis of missense variants (In collaboration with Matthew Mort, Cardiff University)
3. To identify the functional consequences of changes in the amino acid sequence in the NF1 GRD between the wild-type and mutant neurofibromin sequences.

4.2 Materials

4.2.1 Ras ELISA buffers

Preparation of buffer solutions for the Ras activation ELISA assay as described by the manufacturer (Millipore, cat no: 17-497):

1x TBS

200ml 1x TBS by adding 10ml 20x TBS to 190ml of dH_2O. Stored at room temperature

1x TBST (Wash Buffer)

800ml 1x TBST was made by adding 2ml Tween 20 (v/v) and 40ml 20x TBS to 758ml dH_2O and stored at room temperature.

Binding/Blocking Buffer

For each 96 well plate 30ml 3%BSA in TBST was prepared by adding 10ml of 10% BSA in TBS to 20ml of 1x TBST. This was discarded following assay completion.

1x Mg Lysis/Wash Buffer

5x lysis buffer was diluted 4:1 with 4 volumes dH_2O to make a 1x solution. Protease inhibitors were added as needed.

Primary Antibody Solution

1µl of the primary anti-Ras antibody was added to 9µl of Binding/Blocking Buffer. 5µl of this mix was then added to 5ml of Binding/Blocking Buffer (1:10,000).

Secondary Antibody Solution

1µl of the secondary anti-mouse HRP conjugated antibody was added to 5ml Binding/Blocking Buffer (1:5,000).

Chemiluminescent substrate

Each component was warmed to room temperature prior to use. The Chemiluminescent reaction buffer was added to the chemiluminescent detection reagent in a 2:1 ratio.

Epidermal Growth Factor (EGF) (Sigma, cat no: E9644)

4.3 Methods

4.3.1 Plasmid preparation

Plasmid (19993 pGBT9-NF1 GRD) was obtained from Addgene (USA) (Morcos *et al*, 1996) which contained the Gap related domain (GRD) of the *NF1* gene. Plasmids were received as stab cultures made by inoculating bacteria into a vial containing LB agar and the appropriate antibiotic. LB ampicillin agar plates were prepared as previously described in section 2.2.1.3. Using a sterile pipette tip the bacteria growing within the punctured area of a stab culture were streaked onto a plate. The plate was incubated for 16 hours overnight at 37°C. Liquid ampicillin LB was prepared as described in section 2.2.1.2 and starter cultures were prepared as described in section 2.2.1.5. The culture was centrifuged to pellet the bacterial cells then DNA was extracted using the Qiagen maxiprep kit (section 2.2.1.7) and glycerol stocks were made for long term storage (section 2.2.1.6).

4.3.2 Gateway technology with clonase II

4.3.2.1 *attB* PCR primer design

To generate PCR products suitable for use in a Gateway BP recombination reaction with a donor vector, an *att*B site was incorporated into the PCR product. The forward primer contained four guanine residues at the 5' end followed by the 25 bp *att*B1 site and 18-25bp of template or gene specific sequences. The last two nucleotides were needed to maintain the proper reading frame but could not be AA, AG or GA as this

would have created a translation termination codon. The following primer was designed to allow for expression of an N-terminal fusion protein of interest.

*att*B1 Specific Sequence

5'-GGGG-ACAAGTTTGTACAAAAAAGCAGGCTTC-ATGGAAGTTCTGACAAAAATCCTTC-3'

The reverse primer contained four guanine residues at the 5' end followed by the 25bp *att*B2 site and 18-25bp of template or gene specific sequences. The primer had to contain one additional nucleotide to maintain the proper reading frame with the *att*B2 region. The following primer was designed to allow for the expression of a C-terminal fusion protein of interest.

*att*B2 Specific Sequence

5'-GGGG-ACCACTTTGTACAAGAAAGCTGGGTC-AATTGGGCAGTATCTTTCCAGCAAC-3'

4.3.2.1 Creating entry clones

The above primers were used to generate entry clones through the BP recombination reaction using the PCR products containing *att*B sites and a donor vector. A 50µl PCR product was generated using the following reagents and cycle conditions:

PCR Reagents	50µl	Cycle Conditions	x35 cycles
DNA [10ng/µl]	5µl	95°C	10 min
Buffer	5µl		
Mg [25mM]	6µl	95°C	1 min
dNTPs [10µM]	4µl	70°C	1 min
F-Primer [5pm]	1µl	72°C	1 min
R-Primer [5pm]	1µl		
Taq	0.1µl	72 °C	10min
H_2O	27.5µl		

4.3.2.2 Purifying *attB*-PCR products

1-2µl of PCR product was analysed using agarose gel electrophoresis to verify the quality and yield. The entire remaining PCR product was then run on a 1.5% agarose gel with 4µl of concentrated loading dye. The product was then purified to remove *att*B primers and any *att*B primer-dimers which can combine efficiently with the donor vector in the BP reaction, potentially causing background after transformation into *E.coli.* The MinElute gel extraction kit protocol (Qiagen, cat no: 28604) was used to purify the *att*B-PCR product as outlined in section 2.2.3.1.5.

4.3.2.3 BP recombination reaction

20-50fmol of the *attB*-PCR product was required to perform the BP reaction. The amount of DNA in nannograms (ng) which was required was calculated using the following equation:

$$ng = (fmol)(N)\left(\frac{660\ fg}{fmol}\right)\left(\frac{1ng}{10^6\ fg}\right)$$

The *attB*-PCR product generated from the above primers and the NF1-GRD plasmid (Addgene) is 981bp in length and contains the NF1 gap related domain. The amount of *attB*-PCR product needed in the BP recombination reaction is calculated using the following equation:

$$(50\ fmol)(981)\left(\frac{660\ fg}{Fmol}\right)\left(\frac{1ng}{10^6\ fg}\right) = 32.3ng\ of\ PCR\ product$$

The following components were added to a 1.5ml microcentrifuge tube at room temperature and mixed:

Components	Sample	Positive Control	Negative Control
AttB-PCR product (20-50 fmol)	1-7µl	---	1-7µl
pDONR vector (150ng/µl)	1µl	1µl	1µl
pEXP7-tet positive control (50ng/µl)	---	2µl	---
TE Buffer, pH 8.0	to 8µl	5µl	to 10µl

The BP Clonase II enzyme mix was thawed on ice and briefly vortexed twice for 2 seconds. 2µl of BP Clonase II enzyme mix was added to the sample and positive control vials. This was not added to the negative control vial. These mixes were then vortexed briefly twice for two seconds each time and then incubated overnight at 25°C to get a large yield of colonies. The following day 1µl of proteinase K solution was added to each reaction and incubated at 37°C for 10 minutes.

4.3.2.4 Transforming competent cells

omniMAX 2T1 bacteria (Invitrogen) were transformed using the protocol outlined in section 2.2.1.4. The cells were diluted 1 in 10 (20µl cells + 180µl of LB media) and 40µl and 160µl of cells were spread on to two LB agar plates containing Kanamycin (50mg/ml) (section 2.2.1.3). Starter cultures were produced (section 2.2.1.5) and following DNA extraction, the DNA was quantified using a Nannodrop Spectrophotometer (Thermo Scientific). DNA was amplified using the following conditions to confirm the presence of the insert using M13 primers as the M13 site is present in the donor vector: 5'-TGTAAAACGACGGCCAGT-3' (M13 Forward) and 5'-CAGGAAACAGCTATGACC-3' (M13 Reverse) and the protocol outlined in sections 2.2.3.2 and 2.2.3.3.

4.3.2.5 LR recombination reaction

Following confirmation of the correct insert in the entry clones, the LR recombination reaction was performed to clone the gene of interest into a destination vector. Due to the downstream application to be undertaken and the methods of purification to be used a V5 tagged destination vector (pcDNA/V5DEST, Invitrogen) was chosen to clone in to. The reaction was set up as follows for both of the destination vectors and incubated at 25°C for 16 hours on a heat block.

Components	Sample	Positive Control	Negative Control
Entry Clone (50-150ng/reaction)	1-7µl	---	1-7µl
Destination vector (150ng/µl)	1µl	1µl	1µl
pENTR™ -gus (50ng/µl)	---	2µl	---
TE Buffer, pH 8.0	to 8µl	5µl	to 10µl

4.3.2.6 Transforming competent cells

Following the incubation, 1µl of proteinase K was added to each tube and incubated on a heat block for 10 minutes at 37°C. The bacteria were thawed on ice (omniMAX 2Ti, Invitrogen) and transformed using the protocol outlined in section 2.2.1.4 using LB agar plates containing Ampicillin (50mg/ml). The QIAprep spin miniprep kit was then used to extract the DNA from the bacterial cells as outlined in section 2.2.1.7.

4.3.2.7 Sequencing of destination vectors

To confirm the presence of the insert of interest in the destination vector, the samples were sequenced using the following primers and the protocol outlined in section 2.2.3.2 and 2.2.3.3.

Forward: T7 5'-TAATACGACTCACTATAGGG-3'

Reverse: rBGH 5'-TAGAAGGCACAGTCGAGG-3'

4.3.3 Mutagenic primer design

The oligonucleotide primers for site directed mutagenesis were designed individually according to the desired mutation (table 4.1, figure 4.1). The mutagenesis protocol requires 125ng of each oligonucleotide primer. The amount of primer required in picomoles was determined using the following equation:

$$X \text{ pmoles of oligo} = \frac{\text{ng of oligo}}{330 \times \#\text{ of bases in oligo}} \times 1000$$

Example: 125ng of a 25-mer: $\frac{125\text{ng of oligo}}{330 \times 25 \text{ bases}} \times 1000 = 15 \text{ pmole}$

4.3.3.1 Missense mutations

Whole gene sequencing of the *NF1* gene was completed on diagnostic and research lymphocyte DNA samples as described previously in sections 2.2.3.2 and 2.2.3.3 by the NHS molecular genetics diagnostic laboratory (Cardiff, UK) and by NF1 laboratory (Cardiff University). Samples were derived from individuals with a clinical diagnosis of NF1 and the 16 variants analysed in this study were the only variants identified as potential germline mutations in these individuals. They include: c.3610 C>G p.R1204G (Ars *et al*, 2000), c.3610 C>T p.R1204W, (Krkljus *et al*, 1998), c.3827 G>A p.R1276Q (Fahsold *et al*, 2000), c.3902T>G p.L1301R, c.3919 A>G p.I1307V, c.3971 C>A p.T1324N, c.3980 A>G p.E1327G, c.4007 A>G p.Q1336R c.4067 A>G, p.E1356G (Trovo *et al*, 2004), c.4171 A>G p.R1391G, c.4173 A>T p.R1391S (Upadhyaya *et al*, 1997), c.4193 T>A p.V1398D, c.4225 A>G p.K1409E, c.4235 C>G p.P1412R, c.4306 A> C p.K1436Q and c.4388 C>T p.S1463F (figure 4.1, table 4.1). All mutations were non-synonymous *NF1* missense located in the GRD. Five of these mutations have been reported previously and the remaining 11 are novel. Two of the missense mutations was additionally identified as a somatic mutation in neurofibromas in analysis in our lab (c.3827 G>A p.R1276Q and c.4388 C>T; p.S1463F). We also included the missense mutation c.4267 p.K1423E (Li *et al,* 1992) which has been previously identified as a

germline mutation and a somatic mutation in an MPNST (Upadhyaya *et al*, unpublished), to act as a control in our analysis as mutations at this residue have been previously found to result in a protein which is 200-300-fold less active than the wild-type NF1 GRD (Li *et al*, 1992). Furthermore, we also re-analysed the c.4173 A>T p.R1391S missense mutation which was previously described in this lab (Upadhyaya *et al*, 1997). All mutations were analysed during the course of this study except p.K1436Q, p.R1391S, p.R1204W and p.V1398D which were analysed concurrently by Mark Richards (Cardiff University) following the protocol outlined here.

4.3.4 Site directed mutagenesis PCR

Site directed mutagenesis (Figure 4.2) is a technique by which specific mutations can be introduced into plasmid DNA to generate amino acid substitutions, insertions or deletions of 1 to several hundred base pairs in order to study their functional effects. There are several kits available for this method but we have chosen an in house technique as described below.

Table 4.1. Primers used for site directed mutagenesis of 12 *NF1* missense mutations and the resulting sequencing traces showing the mutation of interest. The remaining 4 mutations (p.K1436Q, p.R1391S, p.R1204W and p.V1398D) were characterised by Mark Richards, Cardiff University

Exon	Mutation	Sense Primer Sequence (5'-3')	Antisense Primer Sequence (5'-3')	Wild Type	Mutant
21	c.3610 C>G; p.R1204G	cagaaacagtattggctgatGggttt gagagattggt	accaatctctcaaaccCatcagccaatact gtttctg	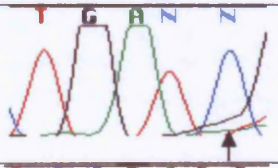	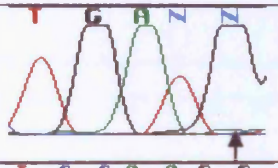
22	c.3827 G>A; p.R1276Q	tgcagactctcttccAaggcaacagc ttggc	gccaagctgttgcctTggaagagagtctgc a	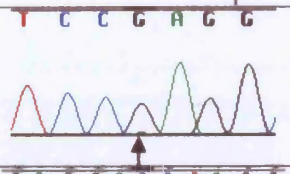	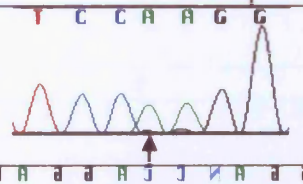
23.1	c.3902 T>G; p.L1301R	gctacctatctacaaaaactccGgg atcctttattacgaattgtgat	atcacaattcgtaataaaggatccCggagtt tttgtagataggtagc	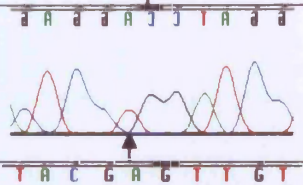	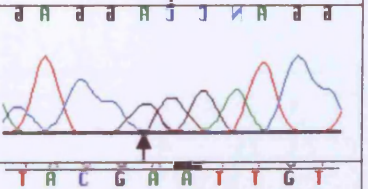
23.1	c.3919 A>G; p.I1307V	cctggatcctttattacgaGttgtgatc acatcctctga	tcagaggatgtgatcacaaCtcgtaataaa ggatccagg	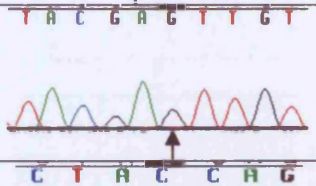	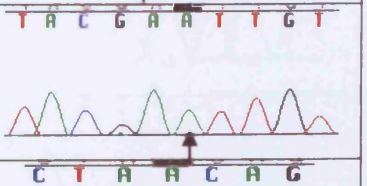
23.1	c.3971 C>A; p.T1324N	gttagctttgaagtggatcctaAcagg ttagaaccatcag	ctgatggttctaacctgTtaggatccacttca aagctaac	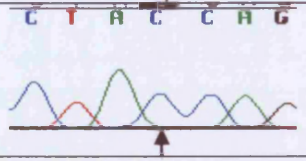	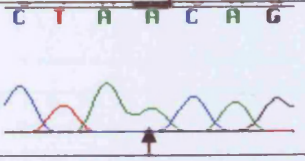

Exon	Mutation	Sense Primer Sequence (5'-3')	Antisense Primer Sequence (5'-3')	Wild Type	Mutant
23.2	c.3980 A>G; p.E1327G	ggccagtaaaataatgacattctgtttcagggttaGaaccatcag	ctgatggttCtaaccctgaaacagaatgtcattattttactggcc	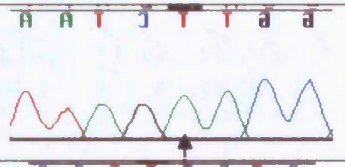	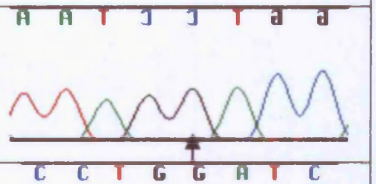
23.2	c.4007 A>G; p.Q1336R	gccttgaggaaaaccGgcggaacctccttca	tgaaggaggttccgcCggttttcctcaaggc	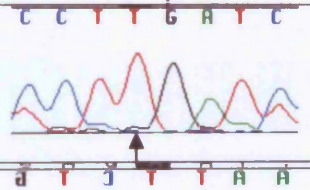	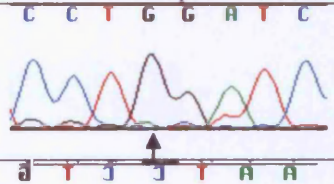
23.2	c.4067 A>G; p.E1356G	catcagttcctcctcaGgattcccccctcaacttc	gaagttgagggggggaatCctgaggaggaactgatg	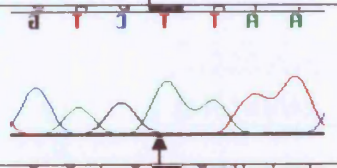	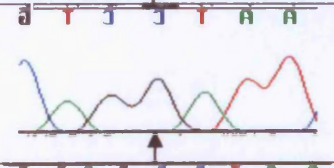
24	c.4171 A>G; p.R1391G	gaagtgccatgttcctcGgatttatcaatcctgcc	ggcaggattgataaatCcgaggaacatggcacttc	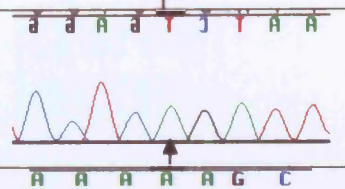	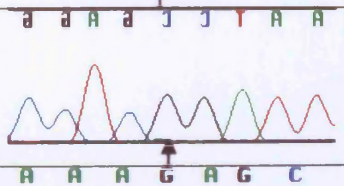
24	c.4225 A>G; p.K1409E	gtatgaagcagggattttagataaaGagccaccacctag	ctaggtggtggctCtttatctaaaatccctgcttcatac	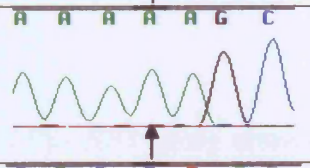	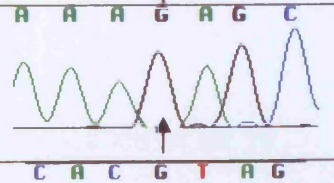
24	c.4235 C>G; p.P1412R	tagataaaaagccaccaGctagaatcgaaaggggc	gccccttcgattctagCtggtggctttttatcta	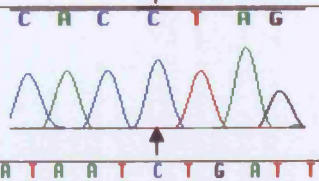	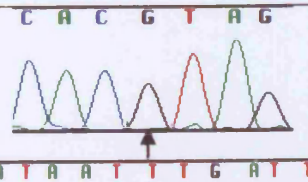
26	c.4388 C>T; p.S1463F	acgcaggtttttccttgatatagcatTtgattgtcctacaag	cttgtaggacaatcaAatgctatatcaaggaaaaacctgcgt	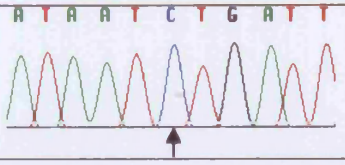	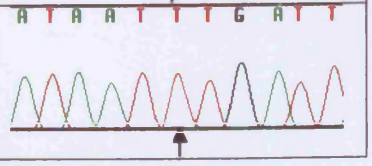

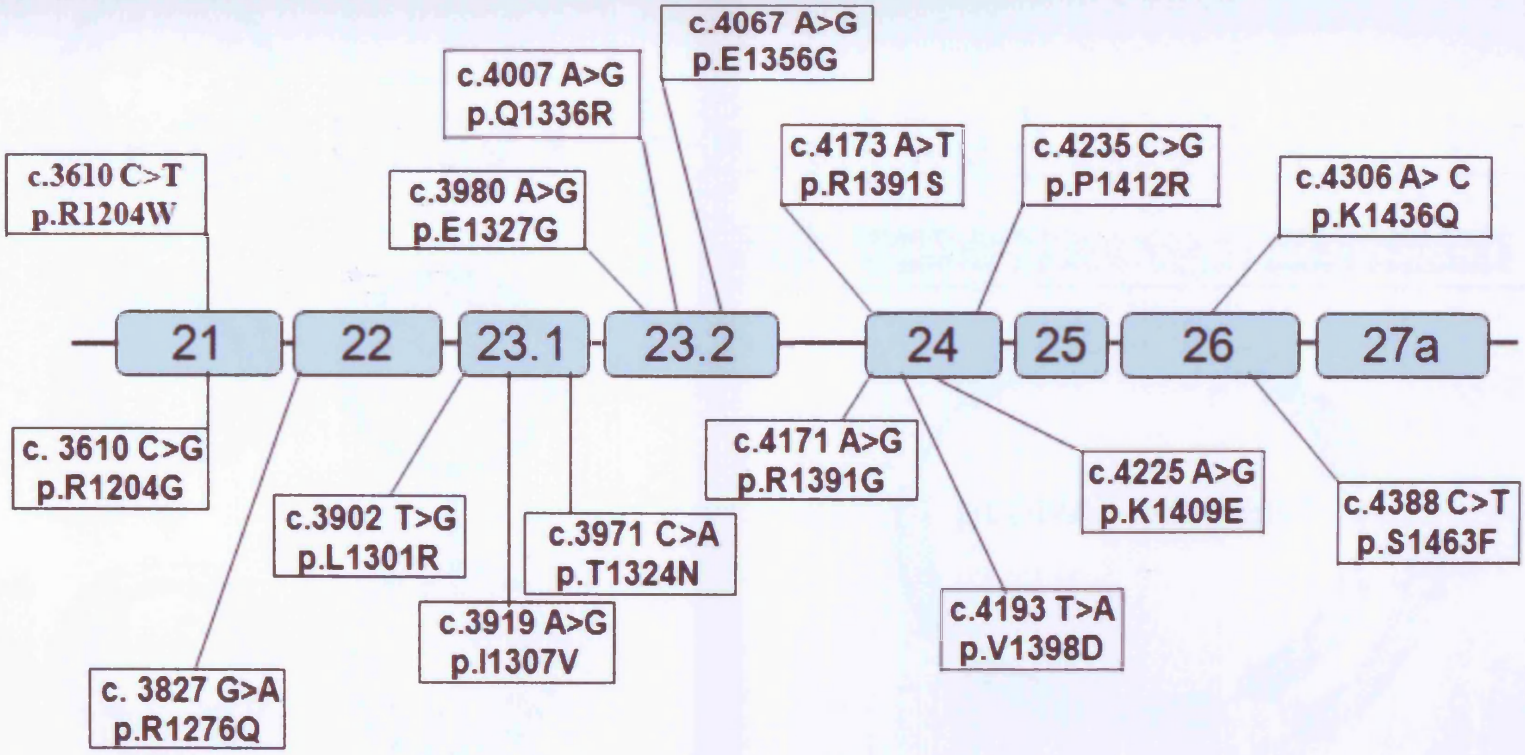

Figure 4.1. Schematic representation of the gap related domain (GRD) of the *NF1* gene showing the location of all 16 missense mutations analysed in this study.

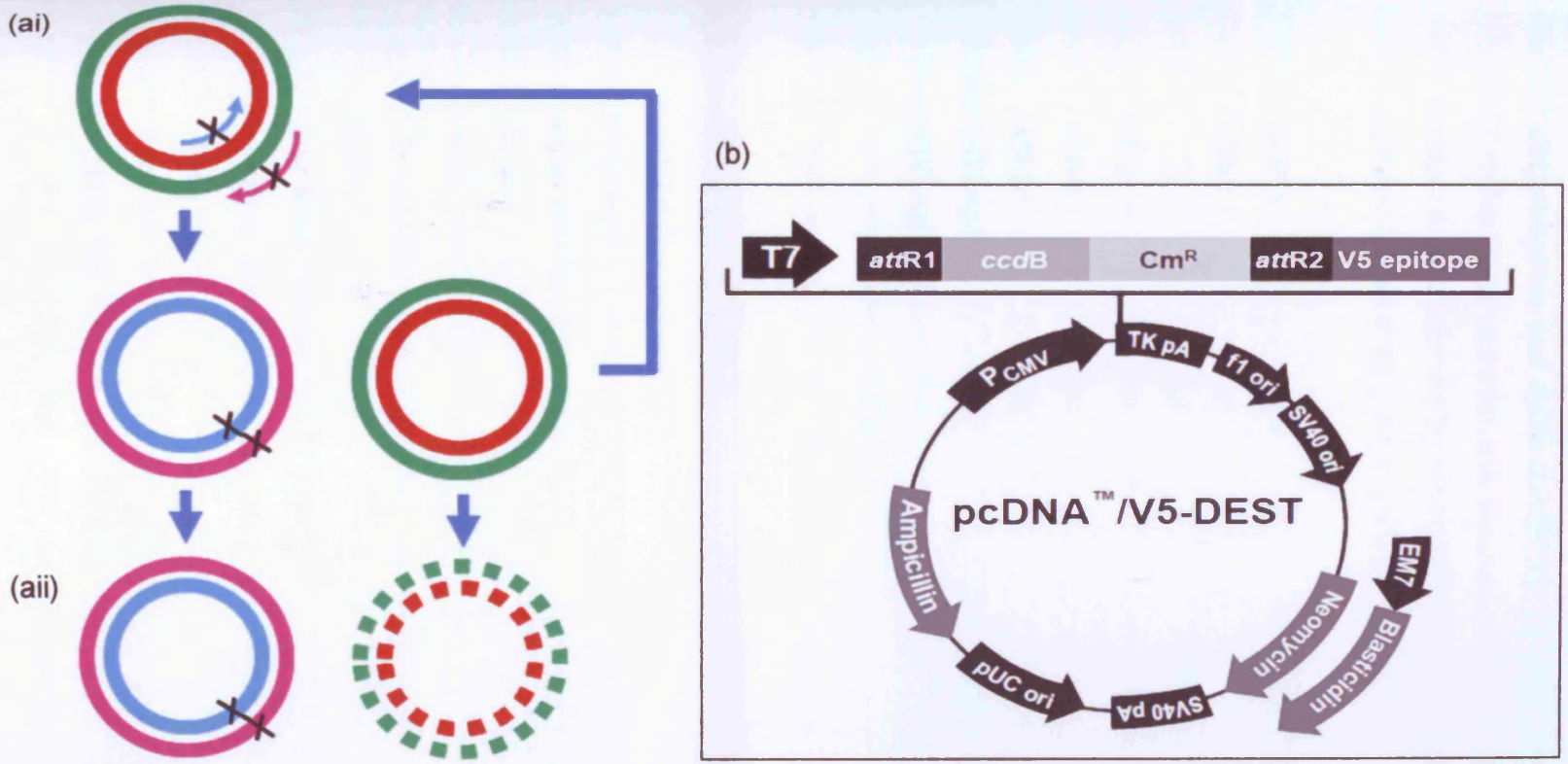

Figure 4.2. (a) *Schematic representation of site directed mutagenesis.* (ai) Mutant strand synthesis; denaturation of the DNA template, annealing of mutagenic primers containing the desired mutation and extension and incorporation of primers with DNA polymerase. (aii) *DpnI* digestion of template; digestion of parental methylated and hemimethylated DNA with *DpnI* (Adapted from smith, 2007). (b) V5 tagged vector used in this study (Invitrogen) with the following properties: 7711 nucleotides; CMV promoter, T7 promoter/priming site, *att*R1 site, *ccd*B gene, chloramphenicol resistance gene, *att*R2 site, V5 epitope, V5 reverse priming site, TK polyadenylation signal, f1 origin, SV40 early promoter and origin, Neomycin resistance gene, EM7 promoter, Blasticidin resistance gene, SV40 early polyadenylation signal, pUC origin, Ampicillin (*bla*) resistance gene, *bla* promoter.

The following reagents and cycle conditions and the vector generated using the method described above were used for site directed mutagenesis (figure 4.2). The presence of a PCR product was confirmed by electrophoresis by running 10µl of the PCR product on a 1.5% agarose gel as described in section 2.2.3.2.1.

PCR Reagents	50µl	Cycle Conditions	x18 Cycles
DNA [10ng/µl]	5µl		
Buffer	5µl	95°C	30sec
Mg [25mM]	5µl		
dNTPs [10µM]	5µl	95°C	30sec
DMSO [10%]	5µl	55°C	1minute
F-Primer [125ng/µl]	1µl	68°C	16minutes
R-Primer [125ng/µl]	1µl		
Taq	0.5µl		
H_2O	22.5µl		

4.3.4.1 *DpnI* digestion

1µl of *DpnI* restriction enzyme (NEB, cat no: R0176S) (10U/µl) was directly added to each reaction and gently mixed. The plate was centrifuged and incubated at 37°C for 1 hour.

4.3.4.2 Transformation into competent cells

The bacteria were thawed on ice (omniMAX, Invitrogen) and 2.5µl of the *DpnI* reaction was transformed into 25ul of bacteria as described in section 2.2.1.4. The entire reaction was plated onto LB agar plates containing Ampicillin (50mg/ml). Starter cultures were prepared from single colonies as outlined in section 2.2.1.5 and DNA was extracted using the Qiagen Miniprep extraction kit following the method in section 2.2.1.7. All extracted samples were sequenced following the protocol described in

section 2.2.3.2 and 2.2.3.3 and using the following primers: 5'-CCTTGATATAGCATCTGATTGTCC-3' and 5'-CGTCTACTCTGGAACAATCAGG-3'

4.3.5 Plasmid DNA transfection

Plasmid DNA produced following site directed mutagenesis was transfected into HEK293 cells using lipofection as described in section 2.2.2.6.1.

4.3.6 Ras activation ELISA assay

4.3.6.1 Cell lysate sample preparation

Transfected cells were cultured as described in section 2.2.2. Three days following transfection, cells were serum starved for 4 hours using standard culture medium for HEK293 cells as described previously with the addition of 0.1%FBS instead of 10% FBS. Cells were then stimulated with EGF (100ng/ml^2) which was added to the plate in drops and incubated at 37°C for 1 hour. Culture media was removed and cells were washed twice with ice-cold 1X PBS (Phosphate Buffered Saline). 1X Mg^{2+}Lysis/Wash Buffer (0.5-1.0ml per 150 mm tissue culture plate) containing protease inhibitors was added to each well and cells were scraped from the plate with a rubber policeman. The cells in the lysis buffer were then transferred to a microcentrifuge tube and incubated on ice for 15 minutes. The tube was vortexed for 10 seconds or sonicated briefly for 10 seconds and the sample was centrifuged at 14000 rpm for 10 minutes at 4°C. The supernatant was collected and protein concentration calculated using a Bradford Assay, a dilution series of BSA and a Nannodrop. Samples were kept cold and used immediately or frozen and stored at -80°C for 6 months.

4.3.6.2 SDS page

Expression of the V5 tagged protein in untransfected controls and mutant cell lines was assessed by western blot using 30µl of each cell lysate and the protocol outlined in section 2.2.7. A V5 primary antibody (cell signalling) was used at a 1:5000 dilution.

4.3.6.3 Ras activation ELISA

Once expression of the V5 tagged mutant proteins was confirmed, the Ras activation Enzyme-linked immunosorbent assay (ELISA) was performed on all lysates as described in the manufacturers protocol and outlined below (Millipore, cat no: 17-497). As the missense mutation c.4267 p.K1423E (Li *et al,* 1992) is known to have 200-300-fold less activity than the wild-type NF1 GRD, this mutant was used to determine the activity of the test missense mutations based on the level of activated Ras (RLU) elicited in the Ras assay by this control.

4.3.6.3.1 Preparation of glutathione coated wells

The required number of glutathione bound strips were taped into the frame of the 96 well plate and the remaining strips were stored with descant at 4°C. Each glutathione coated well was pre-rinsed with 200µl of Wash Buffer (TBST). The wash was flicked out of the wells and repeated twice more. For each well to be assayed, 2.5µl of 2µg/µl Raf-1-RBD was added to 47.5µl of Binding/Blocking buffer and 50µl was added to each well. The wells were sealed and incubated with rocking at 4°C, for 1 hour. After an hour the solution was flicked out as before and each well was washed with 200µl of Wash Buffer. The wash buffer was flicked out and the wash step was repeated 3 times.

4.3.6.3.2 Sample preparation

Up to 200µl of each sample was added to each well for a total amount of 10-100mg of cell lysate. A positive control was added to one well by combining 10µl of 5 mg/ml EGF

stimulated HeLa cell lysate to 40µl of Binding/Blocking Buffer. To one well coated with Raf-1-RBD, only 50-200µl of Binding/Blocking buffer was added to serve as a negative control. Wells containing sample lysate, positive control, and negative control were incubated at room temperature (RT) with mild agitation for 1 hour. The lysates were washed from the well three times with Wash Buffer as previously described.

4.3.6.3.3 Antibodies

50µl of prepared primary antibody solution (1:10,000) was added to each well and incubated at room temperature with mild agitation for 1 hour. After an hour, the wash procedure was performed as previously described. 50µl of prepared secondary antibody solution (1:5,000) was then added to each well and again incubated at room temperature with mild agitation for 1 hour. During the incubation of the secondary antibody, the chemiluminescent substrates were warmed to room temperature for an hour prior to use. The wells were washed three times as previously described and then rinsed twice with 200µl of TBS, to remove Tween® 20.

4.3.6.3.4 Chemiluminescent substrate and luminometer

The Chemiluminescent substrate was prepared by mixing the room temperature solution in a 2:1 reaction buffer to detection reagent ratio. The substrate was incubated for 5 minutes and then 50µl added to each well. The Ras ELISA assay was measured using a microtitre plate luminometer (Applied Biosystems). Relative luminescence (RLU) was evaluated for each sample using the WINGLOW software (Perkin Elmer) between 5 and 60 minutes after the substrate was added.

4.3.7 Bioinformatic analysis

Fourteen of the sixteen missense variants located in the *NF1* gene which were functionally analysed in this study, were also analysed with a computational model, *MutPred* (Li *et al*, 2009, Mort *et al*, 2010) by Matthew Mort (Cardiff University). *MutPred*

is designed to model the effect of changes in structural and functional sites within a protein between wild-type and mutant protein sequences. *MutPred* can be used to generate hypotheses as to the underlying molecular mechanism(s) responsible for disease pathogenesis. The effect of the coding region variants upon splicing [splice site disruption, cryptic splice site activation and exon skipping via loss of exonic splicing enhancers (ESE) and/or gain of exonic splicing silencers (ESS)] was ascertained using ESRPred and a neural network for splice site prediction (Krawczak *et al*, 2007). Evolutionary sequence conservation across an alignment of 44 vertebrate species was measured using the phyloP method (Pollard *et al,* 2010). PhyloP can measure acceleration (faster evolution than expected under neutral drift) as well as conservation (slower than expected evolution). A positive phyloP score represents a conserved nucleotide and a negative phyloP score indicates the nucleotide to be undergoing faster evolution than expected under neutral drift. Finally, SIFT was used to predict whether the mutation would be tolerated or damaging to the protein produced. Variants with SIFT scores ≥ than 0.05 are predicted to be deleterious

4.4 Results

4.4.1 Ras ELISA assay

Sixteen missense mutations were functionally analysed in this study, 4 of which were characterised by Mark Richards, Cardiff University (p.K1436Q, p.R1391S, p.R1204W and p.V1398D). All mutations were detected and characterised by direct sequencing of the *NF1* gene as described in sections 2.2.3.2 and 2.2.3.3). The Ras activation ELISA assay generated fluorescence readings: relative light units (RLU) as a read out of the level of activated Ras in both mutant and control samples. Wild type NF1 had a level of activated Ras of ~$4x10^6$ RLU (Figure 4.3). Only 5 of the 16 missense mutations studied here, yielded levels of activated Ras comparable with wild type NF1 (c.3919 A>G p.I1307V, c.3980 A>G p.E1327G, c.4007 A>G p.Q1336R, c.4225 A>G p.K1409E and c.4235 C>G p.P1412R) (Figure 4.3), suggesting that these missense mutations are not deleterious to NF1 protein function. The previously studied c.4267 p.K1423E mutation

(Li *et al,* 1992), demonstrated fluorescence levels of $6x10^6$ RLU (Figure 4.3), showing concordance with previous findings that this missense mutation produces an NF1 protein which is unable to attenuate Ras activation to the extent of the wild type neurofibromin and so results in higher levels of activated Ras. Eleven of the 16 studied missense mutations yielded fluorescence readings significantly higher than that of wild type NF1, but comparable with the c.4267 p.K1423E mutation ($5x10^6$-$6.5x10^6$ RLU) (Figure 4.3), demonstrating that these mutants elicit higher levels of activated Ras, with ~200-300 fold less GRD activity: c.3610 C>G p.R1204G; c.3610 C>T p.R1204W, c.3827 G>A p.R1276Q; c.3902T>G p.L1301R; c.3971 C>A p.T1324N; c.4067 A>G, p.E1356G; c.4171 A>G p.R1391G, c.4173 A>T p.R1391S, c.4193 T>A p.V1398D, c.4306 A> C p.K1436Q and c.4388 C>T p.S1463F (figure 4.3) (p= 0.001, SPSS v16, independent samples t-test). To ensure that the wild type GRD contained within our control vector was actually functioning as a wild type protein we additionally completed a rescue experiment. The wild type GRD was transfected into *NF1* deficient MPNST derived cell line (ST8815 and SNF96.2). The Ras ELISA assay was then completed on lysates from these cell lines in addition to untransfected MPNST cell lines (ST8814 and SNF96.2) and an untransfected HEK293 cell line containing wild type neurofibromin. We found that when the wild type GRD contained within our vector was transfected into MPNST cell lines; these cells elicited very similar levels of activated Ras as the wild type HEK293 cells. The MPNST cells containing the wild type GRD had a significantly reduced level of activated Ras in comparison to the untransfected MPNST cells (Figure 4.4) (p=0.002, SPSS v16, independent samples t-test). Additionally, all mutants and control samples had the same level of V5 tagged protein expression by SDS PAGE (figure 4.5).

4.4.2 Bioinformatic analysis

For the 16 coding region variants listed in table 4.2 and figure 4.3, bioinformatic analysis was only available for 14. The bioinformatic data was in complete concordance with the results of the functional analysis. Analysis of the wild type neurofibromin protein sequence in comparison to the protein sequence of the mutant proteins analysed here

predicted that 11 of the 14 mutations are likely to be deleterious. The remaining 3 variants are predicted to be tolerated and are not expected to be disease causing. None of the variants were predicted to disrupt splicing through splice site disruption or cryptic splice site activation. Additional functional splicing analysis including; the minigene assay, may be required to definitively confirm the effects of these variants on splicing (Raponi *et al*, 2006; Bottillo *et al*, 2007; Raponi *et al*, 2009) (section 1.10.3).

The harmful effect of these variants is likely to be via disruption to protein structure/function. Measurement of sequence conservation across 44 vertebrate species indicated that these 11 mutations were located at highly conserved nucleotides; with a phyloP score in the range of 5.3-6.4 (a positive phyloP score indicates a conserved nucleotide). The remaining 3 mutations did not show strong evolutionary conservation. Furthermore, confident *in silico* hypotheses for the underlying mechanism of pathogenesis was generated for three of the 14 variants analysed (p.R1276Q, p.V1398D and p.S1463F; table 4.2 and figure 4.3). The mutation p.R1276Q is predicted to occur at a catalytic residue, resulting in the loss of this catalytic residue. p.V1398D is predicted to result in a gain of disorder. p.S1463F is likely to represent a polymorphism but *MutPred* and SIFT predicted it to be a pathogenic mutation. No predicted splicing abnormalities were identified in the 14 variants studied. In summary 11 of the 14 missense variants analysed by bioinformatic analysis (Table 4.2 and figure 4.3) were predicted to have a functional effect whereas the remaining 3 variants are predicted to be neutral with respect to function.

Table 4.2. Complete Results of the Ras ELISA assay and bioinformatic analysis of coding region variants in the *NF1* GAP-related domain. The *MutPred* Probability Score relates to the probability of a missense mutation having an effect on protein structure and/or function. Variants with SIFT scores ≥ than 0.05 are predicted to be deleterious.

Variant		Results of Functional Analysis	Mut Pred Probability Score	Mut Pred Hypothesis	SIFT Prediction (SIFT Score)	Experimentally determined (in-vivo) functional sites	Previously Identified/Novel	Lab Identified
c.3610 C>G	p.R1204G	Pathogenic	0.84		DAMAGING (0)		Ars et al, 2000	MU
c.3610 C>T	p.R1204W	Pathogenic	0.81		DAMAGING (0)		Krkljus et al, 1997	Service
c.3827 G>A	p.R1276Q	Pathogenic	0.98	Loss of catalytic residue at R1276 (P = 0.0404)	DAMAGING (0)		Fahsold et al, 2000	MU
c.3902 T>G	p.L1301R	Pathogenic	0.91		DAMAGING (0)		Novel	MU
c.3919 A>G	p.I1307V	Not Pathogenic	0.47		TOLERATED (0.68)		Novel	MU
c.3971 C>A	p.T1324N	Pathogenic	0.36		DAMAGING (0.02)		Novel	MU
c.3980 A>G	p.E1327G	Not Pathogenic	0.45		TOLERATED (0.12)		Novel	MU
c.4007 A>G	p.Q1336R	Not Pathogenic	ND		ND		Novel	MU
c.4067 A>G	p.E1356G	Pathogenic	0.73		DAMAGING (0.05)		Trovo et al, 2004	MU
c.4171 A>G	p.R1391G	Pathogenic	0.92		DAMAGING (0)		Novel	MU
c.4173 A>T	p.R1391S	Pathogenic	0.96		DAMAGING (0)		Upadhyaya et al, 1997	MU
c.4193 T>A	p.V1398D	Pathogenic	0.81	Gain of disorder (P = 0.0412)	DAMAGING (0)		Novel	MU
c.4225 A>G	p.K1409E	Not Pathogenic	ND		ND		Novel	MU
c.4235 C>G	p.P1412R	Not Pathogenic	0.48		TOLERATED (0.76)		Novel	Service
c.4306 A> C	p.K1436Q	Pathogenic	0.34		DAMAGING (0)	Phosphorylation *in vivo* at adjacent p.T1435 PMID:18452278	Novel	Service
c.4388 C>T	p.S1463F	Pathogenic	0.46	Polymorphsim (0.46)	DAMAGING (0.04)		Novel	MU

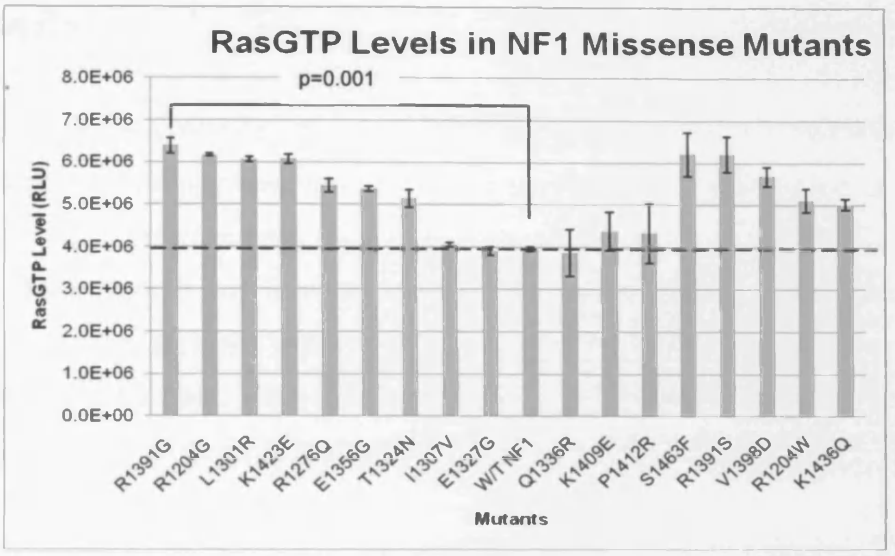

Figure 4.3 Graph demonstrating the level of activated Ras (Ras-GTP) as a function of relative light units (RLU). Dashed line represents Ras-GTP in the wild type NF1 protein.

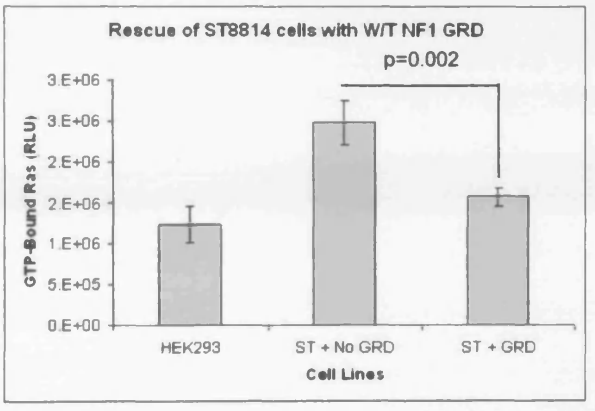

Figure 4.4 Demonstration that the wild type GRD contained within the vector is able to rescue the level of activated Ras in *NF1* null MPNST derived cell lines. Graph is representative of all cell lines analysed.

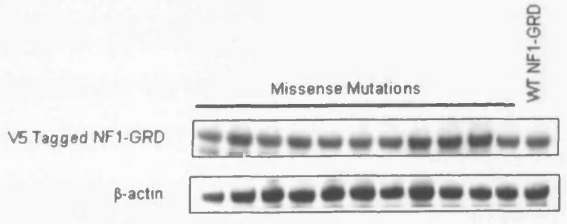

Figure 4.5 Western blot of 12 V5 tagged mutagenised NF1-GRD vectors in HEK293 cell lines. Protein expression levels are the same across all cell lines. The β-actin control blot demonstrates there are unlikely to be off target effects of this vector.

4.5 Discussion

This study set out to determine the pathogenicity of a number of missense mutations which have been previously identified in the GRD of the *NF1* gene. The functional and biochemical analysis of missense mutations in the NF1 GRD is likely to yield important insights into the structure and function of the GRD and its ability to bind and attenuate Ras activity. It would also be important for determining the pathogenicity of potential *NF1* germline and somatic missense mutations identified in patients, in addition to ascertaining whether there is any correlation between the phenotype of NF1 patients and their underlying GAP activity.

There are a number of possible mechanisms underlying the disruption to Ras-RasGAP interactions in NF1 proteins carrying GRD missense mutations. It is possible that these mutant proteins (i) are completely unable to bind with Ras, (ii) are able to bind with Ras but with impaired affinity, or (iii) are able to bind with normal affinity to RasGTP, but their ability to stimulate Ras may be severely impaired due to the loss of functionality through the amino acid substitution which has occurred. Alternatively, the level of the mutant neurofibromin in the cell could be very low if the mutation makes the protein unstable, which would result in binding with fewer Ras proteins leading to higher levels of activated Ras in the cell. In the context of the assay completed in this study, western blot analysis revealed that neurofibromin levels were the same in all mutants studied. This indicates that the missense mutations do not cause protein instability and so the loss of NF1GAP-Ras interaction in these mutants is not due to variation in protein levels.

Biochemical, functional and bioinformatic analysis are all important tools for dissecting the underlying pathogenesis of deregulated GAP function. A number of missense mutations which are located in the GRD have been previously analysed by several groups (Li *et al*, 1992; Poullet *et al*, 1994; Morcos *et al*, 1996; Upadhyaya *et al*, 1997; Klose *et al*, 1998; Ahmadazin *et al*, 2003). However, no *in vitro* assays has been designed for determining the pathogenesis of specific missense mutations in the NF1 GRD which could rapidly and efficiently assay all variants within the GRD with high reproducibility. Previous NFI-GRD functional analysis have relied upon measuring the

ability of rasGppNHp (guanylylimidodiphosphate, a nonhydrolyzable GTP analogue) to inhibit competitively NFI GRD stimulated hydrolysis of "P-labelled" RasGTP (Li *et al*, 1992). Other studies used the nitrocellulose filter binding method which assays the amount of radio labelled nucleotide that remains bound to *H-ras* which is proportional to the extent of NF1 GRD-mediated GTP hydrolysis (Upadhyaya *et al,* 1997). Furthermore, RasGAP activity has also been assayed through the creation of an extensive NF1-GRD library to screen for mutants capable of interacting with H-rasD92K in a yeast two-hybrid screen (Morcos *et al*, 1996). These studies were suitable for the time at which they were developed but are laborious techniques which were only employed to determine the GAP activity of a limited number of mutants.

The combined use of site directed mutagenesis and a Ras ELISA is novel in the context of functional analysis of *NF1* mutations. This assay is a simple and rapid technique, capable of analysing specific mutations and combinations of mutations using one mammalian vector and a reliable PCR and subsequent ELISA based assay, without the use of radio labelled nucleotides or the construction of multiple vectors. Site directed mutagenesis has also been employed in previous Ras-RasGAP assays (Li *et al*, 1992; Upadhyaya *et al*, 1997) but can represent a challenge if not optimised correctly. As experienced in this study, successfully incorporating some mutations into the vector occasionally required more than one attempt at transformation. Transformation efficiencies were generally fairly low with only about 10 colonies produced per transformation but at least 2 of these colonies were generally mutants. This study required stringent screening by direct sequencing of all colonies as occasionally additional mutations other than the desired variant may also become incorporated in the vector due to mismatches at the PCR stage. Kits for site directed mutagenesis such as the Stratagene kit (Agilent) can provide higher transformation efficiencies but such kits are not as cost effective as the in-house method used here.

Through optimisation, transformation efficiency was also improved with the use of an isopropanol DNA precipitation step which was added following *DpnI* digestion, prior to transformation. Following precipitation, transformation efficiency was usually at least doubled with often 20-30 colonies generated. Future large scale analysis based on the technique described here would therefore benefit from blue/white selection with a vector

containing the *lacZ* gene. Plating cells on x-gal and isopropylthiogalactoside (IPTG) avoids the necessity of screening all colonies by sequencing. Colonies carrying the *lacZ* gene are able to catalyse lactose or the artificial substrate x-gal into β-galactosidase. Bacteria capable of this process turn blue, and those which don't remain white. IPTG is an inducer that de-represses *lacZ* expression and should also be used as in some cases, not enough β-galactosidase is produced to turn the colony blue even if the *lacZ* gene is intact.

Overall, mutagenised vectors were generated for all desired mutations within a short time period using an appropriate vector which can be used to study the entire GRD. Additionally, this assay is versatile as it can be applied to a wide range of mutation types which occur within the GRD and could additionally be applied to the determination of the pathogenicity of truncating mutations in the same region. Furthermore, based on the extended sequence conservation outside of the GRD, it is possible that residues located adjacent to the GRD in neurofibromin may also serve to modulate GAP activity. Additionally, there is evidence that the cysteine serine rich domain (CSRD) located in the N-terminal of neurofibromin, may be able to regulate GAP activity following serine phosphorylation (Mangoura *et al*, 2006). Consequently, mutations in residues located in the CSRD could also result in altered GAP activity.

In this study we have identified 11 missense mutations which promote higher levels of Ras activity upon analysis of the mutant NF1 protein by an ELISA (figure 4.2, table 4.2). This suggests that the mutant proteins harbouring these missense mutations are defective in terms of their GAP function by comparison to the wild type neurofibromin. The bioinformatic analysis which was concordantly performed on these mutations, taken together with previous studies on some of these residues, provides new insight into the underlying mechanisms responsible for the reduction in Ras-RasGAP interaction in some of these mutants.

Mutations at K1423 have been reported many times in the literature (Li *et al*, 1992; Poullet *et al*, 1994; Morcos *et al*, 1996) and have been identified in NF1-associated neurofibromas and in an MPNST analysed in our lab. Li *et al* (1992) found that the K1423E mutation resulted in a 200 to 300-fold reduction of GAP activity. It is thought that the K1423 residue forms an intra-molecular salt bridge with an adjacent residue

(E1437) in the α7/variable loop. Establishment of this intra-molecular bridge is an important component of the Ras-RasGAP interaction. Disruption of this salt bridge would be likely to result in negative charges which could interfere with the Ras-RasGAP interaction (Klose *et al*, 1998). K1423 is not located near to the Ras active site and thus would be unlikely to be involved in catalysis and more likely to be involved in the specificity of neurofibromin for Ras-GTP (Ahmadazin *et al*, 2003). In this study, we used the K1423E mutation as a positive control and have confirmed the results from Li *et al*, (1992), strengthening the evidence for the significance of this residue for GAP function. This observation demonstrates the validity of the approach adopted. The results were additionally determined to be reliable through independent validation using bioinformatic analysis as both sets of data demonstrated complete concordance.

The R1391 residue is known to be a supporting arginine residue in the FLR region, responsible for further stabilisation and orientation of the finger loop without directly contacting the active site in Ras (Scheffzek *et al*, 1996; Scheffzek *et al*, 1997; Ahmadazin *et al*, 2003). The R1391 residue has also been analysed numerous times in the literature including the R1391K variant by Skinner *et al* (1991) and a GST tagged R1391S fusion protein by Upadhyaya *et al* (1997). It was found that the R1391S missense mutant was ~300 fold less active than wild-type NF1 (Upadhyaya *et al*, 1997), a finding which we have independently confirmed in this analysis (figure 4.2, table 4.3). Furthermore, the R1391G variant analysed in this study revealed the highest level of GTP-bound Ras ($6x10^6$ RLU, ~400-fold reduction in GAP activity) of all the 16 missense mutations analysed in this study. R1391G and R1391S were also subjected to bioinformatic analysis. These variants have a *MutPred* score of 0.92 and 0.96 respectively, indicating that these mutations are damaging to protein function. Bioinformatic analysis of this residue did not, however, generate a hypothesis as to the underlying mechanism responsible for loss of protein function caused by these mutations. Taken together, these results suggest that this residue is of great significance to GAP function as evidenced by different substitutions at this residue having the same negative effect on GAP function.

It has been seen through both structural and biochemical data that a crucial feature of GAP function is the contribution of an arginine finger which projects into the active site

of Ras. This process is known to result in the stabilisation of the transition state for the GTPase reaction (Scheffzek *et al*, 1999; Resat *et al*, 2001; Ahmadian *et al*, 2003). One of the key mutations to be analysed in this study is therefore the R1276 residue, a crucial component in the Ras-RasGAP interaction as it corresponds to the arginine finger residue, responsible for engaging the catalytic site in Ras. The R1276Q mutation has been identified as a potential germline mutation and as a somatic mutation in a neurofibroma (Thomas *et al*, 2011, submitted). Previous studies by Klose *et al* (1998) have identified R1276P in a malignant schwannoma. It was determined that a substitution of a proline at this residue results in a reduction in binding affinity for Ras (6.6-fold) but crucially, this mutation severely compromises GTP hydrolysis (Klose *et al*, 1998). For this reason we have analysed R1276Q and have found that this alteration results in an increase in GTP-bound Ras by approximately 200-fold compared to the level observed with wild type neurofibromin. Concurrent bioinformatic analysis also confirmed this residue to be of importance to the catalytic activity of neurofibromin. *MutPred* analysis predicted that loss of a catalytic residue at R1276 (p=0.0404) is responsible for loss of function of neurofibromin harbouring this mutation. This arginine residue would therefore appear to be crucial for the catalytic activity of the arginine finger and so presumably plays an important role in stabilisation of the protein-protein interaction and the transition state for GTP hydrolysis. Thus it is indicated that this residue is absolutely required for GAP function (Ahmadian *et al*, 2003).

Thirteen of the 16 residues analysed in this study, 10 of which are novel, have not been previously investigated functionally: c.3610 C>G p.R1204G (Ars *et al*, 2000), c.3610 C>T p.R1204W (Krkljus *et al*, 1998) c.3902T>G p.L1301R, c.3919 A>G p.I1307V, c.3971 C>A p.T1324N, c.3980 A>G p.E1327G, c.4007 A>G p.Q1336R, c.4067 A>G, p.E1356G (Trovo *et al*, 2004), c.4193 T>A p.V1398D, c.4225 A>G p.K1409E, c.4235 C>G p.P1412R, c.4306 A> C p.K1436Q and c.4388 C>T p.S1463F (table 4.1, table 4.2 and figure 4.1). Eight of these missense mutations were found to be deleterious to protein function (p.R1204G, p.R1204W, p.L1301R, T1324N, p.E1356G, p.V1398D, p.K1436Q and p.S1463F). *MutPred* scores between 0.34 and 0.91 were generated for these mutations indicating that all mutations are likely to elicit a damaging effect on neurofibromin function. Although p.K1436Q had a *MutPred* score of only 0.34 it was

designated as pathogenic as a phosphorylation event has been identified *in vivo* at an adjacent residue to p.K1436Q (p.T1435) which is likely to be affected by this mutation.

Five of the mutations analysed here are likely to be neutral changes with levels of activated Ras which corresponded to that seen in wild type NF1 (p.I1307V, p.E1327G, p.Q1336R, p.K1409E and p.P1412R) (Table 4.2, Figure 4.3). Bioinformatic analysis was not completed on two of these residues (p.Q1336R and p.K1409E) but for the remainder, the functional analysis was correlated with bioinformatic analysis where these mutations were designated *MutPred* scores between 0.45 and 0.48, further evidence that these mutations are non-pathogenic.

Due to the large size of the *NF1* gene and its protein product, it is only possible to generate a mammalian expression vector containing a small proportion of the gene. The vector used in this study only contained the GRD and thus it would be important to determine the effect of these mutations in the context of the whole NF1 protein in addition to the GRD in this assay. However, the results from the present study demonstrate the suitability of this assay to determine whether identified *NF1* gene variants are neutral or disease causing and the bioinformatic analysis provides insight into the underlying mechanisms of GAP deregulation.

In conclusion, 16 variants, encompassing 14 different amino acid residues within the GRD were analysed in this study (table 4.2). Eleven variants were found to be pathogenic through both functional and bioinformatic analysis consisting of nine different amino acid residues. The results from this study therefore indicate that there are many residues in the GRD which are crucial for GAP activity as determined by the level of Ras-GTP identified by the ELISA employed in this study. NF1 GAP activity is crucial to the regulation of the RasMAPK pathway in such a way that a therapeutic approach for the treatment of patients is an attractive prospect. Small molecules that are able to mimic GAP activity in cells derived from the neural crest could in principle restore NF1 protein function in patients with RasGAP mutations that vastly affect the Ras-GAP interactions.

This study has confirmed previous data on three residues (K1423E, R1391 and R1276) which are highly significant for neurofibromin function in addition to analysing a further 11 residues located in the GRD. This data is not only important for distinguishing

pathogenic mutations from non pathogenic mutations which are clearly useful for diagnosis and tumour related studies, but is also of significance for yielding important new insights into the GRD structure and function in addition to the mechanism of mutant NF1-Ras interactions.

CHAPTER 5: CpG methylation analysis of NF1-associated tumours

5.1 Introduction

Whilst our understanding of the molecular mechanisms which underlie tumorigenesis in NF1 is continually evolving, the overall detection of somatic mutations remains low and there are many aspects of NF1 tumour formation and malignancy that remain unclear. Loss of function of tumour suppressor genes (TSGs), such as *NF1*, is mainly associated with DNA mutations including base substitutions, splicing alterations, gene deletions, insertions and duplications, however, the epigenetic process of DNA methylation, is frequently becoming associated with loss of gene expression due to the inverse relationship between the level of gene methylation and transcriptional activity (Rodenhiser *et al*, 1993). Aberrant methylation can therefore lead to loss of tumour suppressor function in tumour related genes as outlined in table 1.8 (Esteller *et al*, 2000; Baylin *et al*, 2001; Alqhist *et al*, 2008; Wang *et al*, 2008; Wang *et al*, 2009; Lin *et al*, 2009). In the *NF1* gene, the low level of somatic mutation detection, the spontaneity of new mutations and the high proportion of mutations involving CpG dinucleotides suggests that *NF1* gene methylation in addition to methylation of other genomic loci may be involved in NF1 tumorigenesis.

Epigenetic modifications of the human genome include heritable posttranslational modifications of histones which are associated with chromatin, such as methylation and acetylation. Methylation is, however, the only known epigenetic modification of DNA, occurring exclusively at approximately 3-4% of 5-Cytosine associated with CpG sites, although non-CpG methylation can occur (Hotchkiss *et al*, 1948; Esteller and Herman, 2002). Cytosine methylation is a heritable mark which if stable, can be passed from mother to daughter. Methylation is an important regulator of a number of processes including: embryonic development, transcription, chromatin structure, X chromosome inactivation genomic imprinting, genomic instability and carcinogenesis (Riggs and Pfeifer, 1992).

The molecular basis of normal DNA methylation is not fully understood although three DNA methyltransferases (DNMT1, DNMT3A, and DNMT3B) have been identified which

are thought to establish and maintain DNA methylation. DNA methyltransferase-3 proteins are involved in *de novo* methylation of CpG dinucleotides, particularly in parental imprinting. Indeed, knockout of *Dnmt3a* or *Dnmt3b* in mice is lethal as a result of loss of *de novo* methylation (Okano *et al*, 1999). DNMT1, however, methylates recently synthesized DNA in cooperation with MECP2, a methyl-CpG-binding protein which is capable of producing a copy of the parental DNA methylation pattern to the daughter DNA strands during cell division (Kimura and Shiota, 2003). DNMT1 additionally interacts with other proteins, including; transcription factors (p53, STAT3, and HP1), histone modifiers (HDAC1, HDAC2), and ligands (DAXX) resulting in repression of target genes (Rountree *et al*, 2000; Muromoto *et al*, 2004; Esteve *et al*, 2005; Smallwood *et al*, 2007). *Dnmt1* mutations in murine embryonic stem (ES) cells results in a reduction by two thirds in Cytosine methylation and moreover, germline mutation of *Dnmt1* triggers abnormal development and embryonic lethality (Li *et al*, 1992).

The mechanism by which an increase in methylation results in silencing of gene expression is also not well known, although several models have been postulated. Gain of methyl groups is thought to involve a reduction in affinity or even a physical barrier to hinder binding of transcription factors in the methylated sequence. Furthermore, a steric block by methyl-CpG binding proteins (MDBP) may act as transcriptional repressors and additionally recruit complexes including histone deacetylases, consequently altering chromatin structure (Boyes and Bird, 1991; Nan *et al*, 1993; Jones and Laird, 1999). Aberrant increases in methylation in CpG rich regions of known tumour related genes (hypermethylation) can therefore act to 'silence' gene expression and lead to tumorigenesis. Conversely, hypomethylation events, although less frequent than hypermethylation, affect mainly intragenic and intronic regions of the DNA, specifically repeat sequences and transposable elements, and can result in chromosomal instability and increased mutational events (Watanabe and Maekawa, 2010). Altered methylation patterns are additionally exhibited in intronic regions, coding regions downstream of the promoter and even areas immediately adjacent to CpG rich regions (island shores), indicating that these regions may also contribute to gene regulation (Li *et al*, 2003; Ortmann *et al*, 2008).

CpG islands, located in coding and non-coding regions are most commonly associated with transcription start sites and encompass a high concentration of CpG dinucleotides (Bird *et al*, 1986) Indeed, 70% of human promoters encompass CpG islands (Saxonov *et al*, 2006) and in frequently expressed genes, most promoter CpG sites are usually unmethylated, except in the case of X-chromosome inactivation (Riggs and Pfeifer, 1992). Whilst most objective definitions for CpG islands have limitations, it is widely accepted that a CpG island consists of 200bp regions with a greater than 50% GC content and an observed/expected CpG ratio above 60% (Gardiner-Garden and Frommer, 1987). Recent analysis has, however, suggested that regions greater than 500bp with a GC content above 55% and observed/expected CpG of 0.65 are more representative of true CpG islands (Takai and Jones, 2002) Using stringent CpG island analysis criteria (Gardiner-Garden and Frommer, 1987), there are only two defined *NF1* CpG islands; one in the promoter and a second located in intron 39 which is also associated with a pseudogene located in the promoter region of adenylate kinase 3 (*AK3L1*) on chromosome 1p31.3. Across the 283kb *NF1* gene region, there are approximately 2,420 CpG dinucleotides, of which only about 120 are located in coding regions.

Through the process of deamination, Cytosine spontaneously deaminates to Uracil which is efficiently recognised as a non-DNA base and consequently removed by Uracil-DNA-glycosylase (Cooper *et al*, 2010). When 5-methylcytosine (5mC) is present, however, spontaneous deamination instead yields thymine which consequently creates G-T mismatches (Shen *et al*, 1994). The process by which these mismatches are removed is highly error prone, involving first removal by methyl-CpG binding domain protein 4 (MBD4) in conjunction with thymine DNA glycosylase, followed by base excision repair (BER) (Waters *et al*, 2000). Hypermutability of CpG sites due to the process of deamination is thought to underlie 25% of all single base-pair substitutions (Cooper and Youssoufian, 1988; Cooper and Krawczak 1993) and indeed up to 20% of *NF1* point mutations have been found to occur at CpG dinucleotides (Krkljus *et al*, 1997; Fahsold *et al*, 2000; DeLuca *et al*, 2004), a finding which is comparable with other TSGs, including *RB1* (20-25%) (Cowell *et al*, 1994).

Whilst the majority of DNA methylation occurs at CpG dinucleotides, recent analysis of mutations in 2113 genes determined that 10% of mutations involved CpNpG trinucleotides (Cooper *et al*, 2010). In the *NF1* gene there are approximately 5000 each of CTG and CAG trinucleotides at which up to 3% of *NF1* mutations have been identified, indicating that non-CpG sites also play a role in NF1 tumorigenesis (Fahsold *et al*, 2000). The *NF1* gene also contains a well-defined isochore boundary within which there is a change in the GC content from 37% in the proximal part of the *NF1* gene rising to 51% after the 3' region (Bernardi, 2000; Schmegner *et al*, 2005). Precise sequence localisation for this boundary has not been defined, but it is known to represent the boundary between high and low recombination frequencies, potentially influencing the *NF1* mutation rate (Eisenbarth *et al*, 2000; Schmegner *et al*, 2005).

Methylation of *NF1* CpG residues has been detected in developing mouse embryos (Haines *et al*, 2001) and 92% of CpG sites in exons 28, 29, and 31 were found to be methylated in sperm DNA (Rodenhiser *et al*, 1993; Andrews *et al*, 1996). The methylation status of the *NF1* promoter has also been reported to alter luciferase reporter activity (Zou *et al*, 2003), however, investigation of *NF1* promoter methylation in NF1 patient derived blood samples, cutaneous neurofibromas, plexiform neurofibromas, plexiform derived Schwann cell cultures (Fishbein *et al*, 2005), MPNSTs (Horan *et al*, 2000; Luijten *et al*, 2000; Harder *et al*, 2004) and pilocytic astrocytomas (Ebinger *et al*, 2005) suggested there was little evidence for a role of *NF1* promoter methylation in NF1 tumorigenesis (Ebinger *et al*, 2005).

There are numerous techniques for methylation analysis which have been employed in previous *NF1* methylation studies. Bisulphite DNA conversion involves the use of sodium bisulphite which reacts selectively with unmethylated Cytosine converting it to Uracil. However, sodium bisulphite does not react with methylated Cytosines, leaving them unchanged. This reaction requires an initial denaturation step as it is dependent on the availability of single-stranded DNA (Frommer *et al*, 1992). Methylation specific PCR involves the use of primers which are designed to take advantage of the sequence differences which arise following bisulphite conversion (Herman *et al*, 1996). This method, whilst being both rapid and reliable, carries the limitations of PCR-based analysis and is not always sensitive enough to detect hypermethylation, particularly in

heterogeneous tumours such as those studied here. Quantitative methylation PCR (Q-MSP) has also been developed which primarily relies on relative quantification, using fluorescent probes to detect methylation in bisulphite converted samples. Q-MSP has increased specificity and sensitivity for methylation detection and is comparable to quantitative multiplex-methylation-specific PCR (QM-MSP) (Herman *et al*, 1996; Eads *et al*, 2000; Cohen *et al*, 2003; Jeronimo *et al*, 2004). The recent development of DNA pyrosequencing now permits efficient detection of methylation at individual and multiple CpG dinucleotides using a directly quantitative approach (Colella *et al*, 2003). Pyrosequencing, is another bisulphite based method which determines the proportion of methylated bases at a CpG site based on the generation and detection of a light signal which is proportional to the amount of incorporated nucleotide. Pyrosequencing has many applications in cancer genetics and has most recently been employed to measure *LINE-1* methylation in colon cancer and *TP53* pathway genes in breast cancer (Irahara *et al*, 2010; Rønneberg *et al*, 2011).

Previous contradictory observations on the role of *NF1* gene methylation are based on a small number of studies and completed on small samples sizes. Previous analyses involved the use of relatively insensitive methods and were only aimed at the promoter which encompasses approximately 1% of the total CpG sites in the *NF1* gene (Rodenhiser *et al*, 1993; Horan *et al*, 2000; Luijten *et al*, 2000; Harder *et al*, 2004; Fishbein *et al*, 2005; Zou *et al*, 2003). It is clear, therefore, that sensitive analysis of methylation throughout the entire *NF1* gene in a large panel of samples is warranted. Furthermore, as alterations in additional genetic loci are known to be involved in the development of NF1-associated benign and malignant tumours, methylation analysis of candidate modifying loci should also be investigated. The main aims for this chapter are:

1. To screen the promoter, introns and coding regions of the *NF1* gene for methylation in a large panel of NF1-associated benign and malignant tumours using pyrosequencing.
2. To analyse methylation at potential modifier loci (*RASSF1A* and *MGMT*) using pyrosequencing in NF1-associated benign and malignant tumours.

5.2 Materials

5.2.1 Reagents

CpG genome DNA modification kit (Chemicon, cat no: S7824)

EpiTect PCR control DNA set (Qiagen, cat no: 59695)

Streptavidin Sepharose beads (GE Healthcare, cat no: 17-5113-01)

Pyrosequencing reagents (All Qiagen)
Binding buffer, (cat no: 979306)
Denaturing solution, (cat no: 979307)
Wash buffer, (cat no: 979308)
Annealing buffer, (cat no: 979309)
PyroMark Gold Q96 reagents, (cat no: 972812)

Pyrosequencing consumables (All Qiagen)
PyroMark Q96 plate low (PSQ) (cat no: 979002)
PyroMark Q96 cartridge (cat no: 979004)

5aza2dc (Sigma, cat no: A3656)

5.2.2 Equipment

PyromarkQ96 ID Pyrosequencer (Qiagen)

Vacuum prep workstation (Qiagen)

5.3 Methods

5.3.1 Patient samples

82 tumour derived DNA samples with undetectable mutations from 40 patients were screened for *NF1* (NM_000267) whole gene methylation levels in addition to *RASSF1A* (NM_007182) and *MGMT* (NM_002412) promoter methylation. Of the 82 tumours analysed, 67 were benign cutaneous neurofibromas, 11 plexiform neurofibromas and 4 MPNSTs. *NF1* germline mutations were identified in 34/40 patients. The methylation status of samples with and without characterised somatic and germline *NF1* mutations was determined with the use of an additional 3 neurofibroma derived Schwann cell lines, 3 MPNST derived cell lines and 10 tumour samples (6 neurofibromas, 2 plexiform and 2 MPNSTs) all with characterised *NF1* somatic and germline mutations. Hemizygous $NF1^{-/+}$ fibroblast cell lines from NF1 patients (matched with affected tumour tissue) and a HEK293 cell line served as controls. DNA extracted from the spleen, spinal root and placenta (matched with an MPNST, plexiform neurofibroma and cutaneous neurofibroma from one patient) were also screened to determine the levels of tissue specific methylation. Lymphocyte DNA samples, matched with tumour DNA samples as well as blood DNA samples from non-NF1 patients were used to assess methylation levels in peripheral blood. Furthermore, Epitect control DNA samples were employed to prevent false positive results and problems with bisulphite conversion. All tissue DNA samples including tumours and tissue from the spleen, placenta and the spinal root were macrodissected from the surrounding tissue. DNA, RNA and cDNA were extracted as previously described in sections 2.2.3.1.1, 2.2.3.1.2 and 2.2.3.3.

5.3.2 Cell lines

Three human MPNST derived cell lines (ST8814, T529 and T530) and NF1-patient derived fibroblast cell lines were maintained as described in section 2.2.2.

5.3.3 CpG analysis

To ensure that all CpG rich regions in exons and introns of the *NF1* gene were included in our analysis, the entire DNA sequence of the *NF1* gene in addition to the promoter region of the *RASSF1A* and *MGMT* genes was submitted to CpG island searcher software (v.10/29/04) (Takai and Jones, 2002). The DNA sequence was analysed using the following criteria which encompasses both the upper and lower limits of the definitions for a CpG island (Gardiner-Garden and Frommer, 1987; Takai and Jones, 2002): >200bp regions, >50% GC content, an observed/expected ratio >60% and at least a 100bp gap between adjacent islands to avoid merging CpG islands (Gardiner-Garden and Frommer, 1987). Twenty-three *NF1* CpG rich regions (including the *NF1* promoter and *AK3L1* pseudogene CpG islands), a CpG island in the *MGMT* promoter and a CpG island in the *RASSF1A* promoter region approximately 300bp upstream of the *RASSF1A* ATG were identified. For the *NF1* methylation analysis, the *AK3L1* pseudogene CpG island was excluded from the analysis due to problems with primer specificity. Therefore, a total of 22 CpG regions for *NF1* methylation analysis, covering all large CpG islands and GC rich regions and encompassing 353 CpG sites within the *NF1* gene were analysed (figure 5.1).

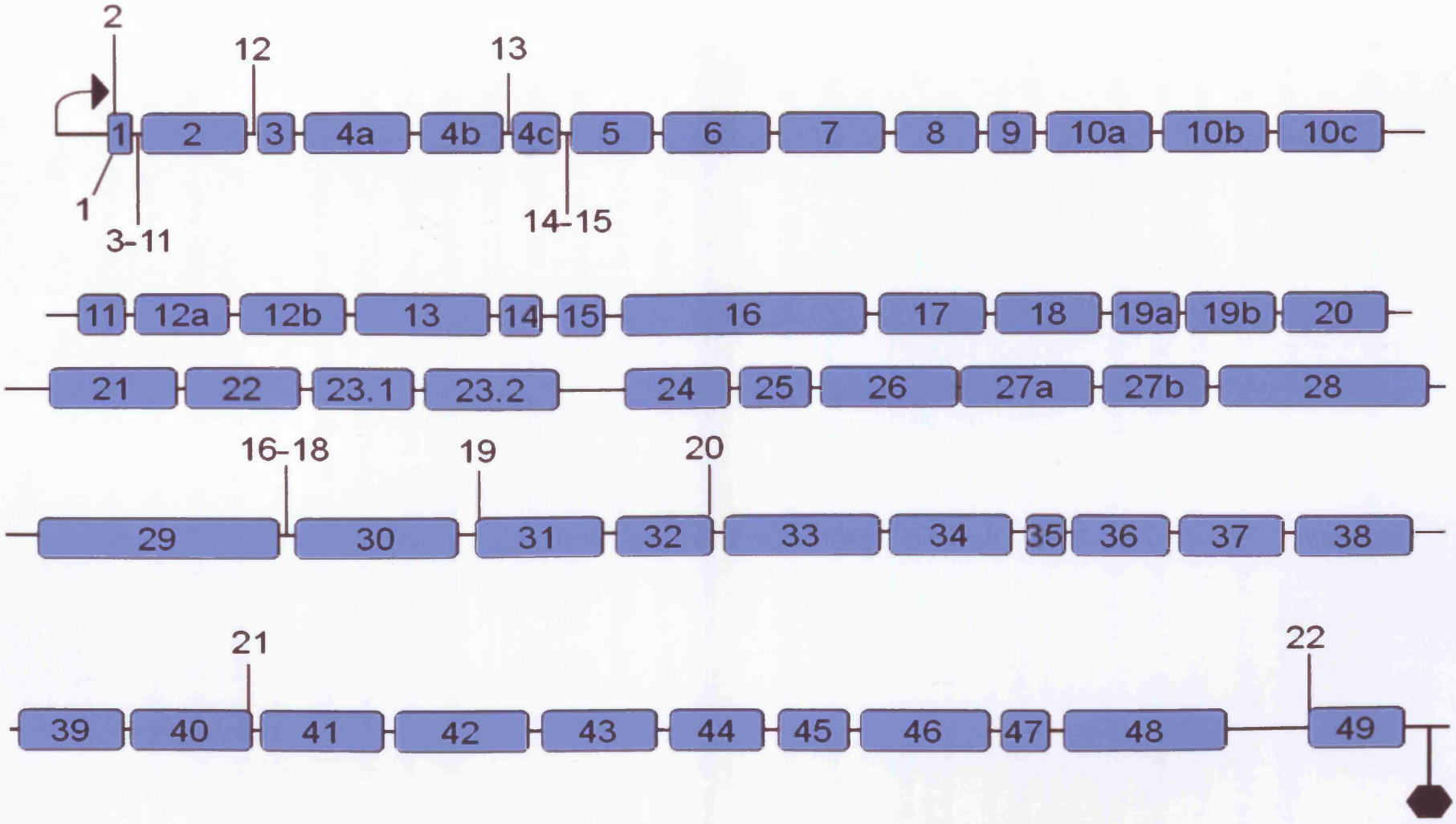

Figure 5.1 Schematic representation of the *NF1* gene identifying CpG islands used for *NF1* methylation analysis. Not drawn to scale. The arrow represents the transcription start site and hexagon denotes the translation termination site.

5.3.4 CpG Genome modification procedure

CpG modification of genomic DNA was achieved using a CpG modification kit. DNA was diluted to 10ng/µl in a 1.5ml microcentrifuge tube. 7µl of 3M NaOH was added and the contents of the tube were mixed and incubated for 10 minutes at 50°C. After the 10 minute incubation, 550µl of DNA modification reagent I was added, vortexed and incubated at 50°C for 4-16 hours (protected from the light).

Reagent Number	Reagent (g)	dH_2O (ml)	pH	Temperature	Additional Reagents
1	0.227	0.571	5	Room	
2	1.35	0.75	-	Room	1µl β-mercapto-ethanol 20ml dH_2O

DNA modification reagent III was resuspended by vortexing and drawing in and out of a pipette tip up to 10 times. 5µl of DNA modification reagent III was added to each of the solutions as well as 750µl of DNA modification reagent II. The solutions were mixed briefly and incubated at room temperature for 5-10 minutes. The tubes were centrifuged at 5000xg for 10 seconds to give a white pellet and the supernatant was discarded. 1ml of ethanol was added to the tubes, vortexed and centrifuged for 10 seconds at 5000xg. The supernatant was discarded again and this step was repeated twice more. On the final ethanol wash, the tube was centrifuged at high speed for 2 minutes and the supernatant was discarded.

50µl of 20mM NaOH/90% ethanol was added to each of the tubes and vortexed to resuspend the pellet. The samples were incubated at room temperature for 5 minutes and centrifuged at 5000xg for 10 seconds. 1ml of ethanol was added to the tubes, vortexed, centrifuged and the supernatant was removed, this was repeated and the tubes were then centrifuged at high speed for 3 minutes. All supernatant was removed from the tubes and they were left to air dry for 10-20minutes. 25µl 1xTE was added to each tube. This was incubated for 15 minutes at 50-60°C to elute the DNA from DNA modification reagent III. Finally the DNA was centrifuged at high speed for 2-3 minutes and the supernatant was transferred to a new tube.

5.3.5 Assay design and PCR optimisation

Design of PCR and sequencing primers was carried out using the Qiagen Pyrosequencing Assay Design software, requiring the generation of one set of primers to amplify the target area, one of which (forward or reverse) was biotinylated and a third primer was required for sequencing. The biotinylated primer was HPLC purified and the second PCR primer and the sequencing primer were purified using standard methods. Assay design was completed using the Qiagen assay design software and this was loaded onto the Pyromark ID Pyrosequencer (Qiagen). Each individual primer set was optimised separately. PCR primers and PCR conditions are listed in table 5.1 and the standard PCR reaction conditions and thermal cycling conditions are as follows:

Reaction Volume	50µl	Cycle Conditions:	x45 cycles
DNA [10ng/µl]	5µl		
Buffer	5µl	95°C	5minutes
Mg [25mM]	4µl		
dNTPs [10µM]	2.5µl	95°C	15seconds
Sense Primer [10pM/µl]	1µl	Tm	30seconds
Antisense Primer [10pM/µl]	1µl	72°C	15seconds
Taq	0.15µl		
H_2O	31.35µl	72 °C	5minutes

On the first time of running a PCR amplified product on the Pyromark, the PCR product was checked by running 10µl of product with 5µl of loading dye on a 1.5% gel before Pyrosequencing. Product concentration could then be eliminated if Pyrosequencing reactions failed. Each set of Pyrosequencing reactions required 5 controls including: (i) a repeat PCR with no sequencing primer added to the (PSQ) plate, (ii) a well containing sequencing primer alone, (iii) a well containing biotinylated primer alone, (iv) a well containing biotinylated and sequencing primer and (v) a negative (no DNA) PCR control

Table 5.1 Primers used in Pyrosequencing analysis.

CpG Region	PCR Conditions	Strand	Label	Forward Primer (5'-3')	Label	Reverse Primer (5'-3')	Sequencing Primer
1	52C 2.5mM Mg	TOP		GTTTGAGGGAGGAGTGTAGG	BIOTIN	CTCAAAACACCTTTAAAACCTTACATTC	GGGAGGAGTGTAGGT
1	52C 2.5mM Mg	TOP		GGAGGTAGTGTATTTTATTTTTTTTGAGA	BIOTIN	CTAACCCCAAAACATCCACTCCCATC	AGTATAGTTTTTTTAGGAGATTAG
1	54C 2.5mM Mg	TOP		GGGGGAGGGGATAGTTGTA	BIOTIN	CTCCTAAAAATAACCTCATCTAACTCCTCT	GGGGATAGTTGTAGGG
1	54C 2.5mM Mg	TOP		GGATGTTTTAGGGTTAGTTTTGGTAT	BIOTIN	ACACCCCACCCAAAATAAAATCCTTT	GTTAGAAGGTTTAGAGGAGTTA
2	51°C 3mM Mg	TOP		TGGGGGTGGGGATAGAGTA	BIOTIN	ATCCCCCCTTCCCTTCTC	AGGTGAGGGGAGGTA
3	48C 3.5mM Mg	BOTTOM		GAGGGTATATAAGATAGGTTTTAGGG	BIOTIN	CCATCTAAATTTAATAATTACCCCCTTAC	ATAAGATAGGTTTTAGGGT
4	52C 2.5mM Mg	TOP	BIOTIN	GGGAGAAAAAGTTTTGTATGTATTGA		CACCACACCCAACTAATTTTTATAT	TTAATAAAAATAAAATTTCACT
5	43°C 3.5mM Mg	TOP	BIOTIN	TGTTATTTAGGTTGGAGTGTAATG		AACACAATAAAACACCTTCTCTATTA	TCTATTAAAAATACAAAAATTAAC
6	52C 3.5mM Mg	TOP		TTGTAGTTTAGGTTGGAGTGTAGTG	BIOTIN	ACATAAAAACCAACACCTATAATCCCAACT	GTTGGAGTGTAGTGG
7	48C 2.5mM Mg	TOP		ATTAGGGAGTTTGAGGTAGGAGAAT	BIOTIN	TCACTCTTATCACCCAAACTAAAATACAAT	GAGGTAGGAGAATGG
8	51°C 3mM Mg	TOP	BIOTIN	TGAGGGTTTGTTGTAGTAATTG		CCACCACCACACCTAACTATTTTT	TTTAATAAAAATAAAAATTTCAC
9	52C 2.5mM Mg	TOP	BIOTIN	GGAGGTTAAGGTGGGTAGAT		CCTCCCCAATTCATACCATTCTCCTACCT	ACCATTCTCCTACCTC
10	48C 3.5mM Mg	BOTTOM		GAATAAGGTTAGGAGTAGTGGTTTAAGT	BIOTIN	ACCTCCTAAATTCATACCATTCTCC	AAAAATATAATAAAAATTAGTTGG
11	49C 3.5mM Mg	BOTTOM		ATGAATTTAGGAGGTAGAGATTGTAG	BIOTIN	ACCCCCCCAATTTCATTTAATATTTCCTT	AGGTAGAGATTGTAGTG
12	51C 2.5mM Mg	TOP		AGGAGGTTGAGATAGGAGAAT	BIOTIN	CTCACTCTATCACCCAAACT	GTTGAGATAGGAGAATGG
13	51°C 3mM Mg	BOTTOM		GTTTAGGTTGGAGTGTAATGGTATA	BIOTIN	ACCCCATCTCTACTAAAAATACAA	TGGAGTGTAATGGTATAAT
14	48C 3.5mM Mg	TOP		GGTTGGTTGTTTTTAAATTTAGTGG	BIOTIN	CCTAAAATTCACCCCATTCTCCTACCT	GTGGTGAAAGAAAATGAT
15	44C 3.5mM Mg	BOTTOM		AGGTTAGGAGATGGAGATTATTT	BIOTIN	CTCTATTACCCAAACTAAAATACAA	AGGTTGAGGTAGTAGAA
16	44C 3.5mM Mg	BOTTOM		AGTTTTTTAAGTAGTTGGGATTATAGG	BIOTIN	ATCAAAAAATCAAAACCATCCTAAC	GTTGGGATTATAGGTGT
17	52C 2.5mM Mg	TOP		GAGGTTAGGAGATAGAGATTATTTTGGTTA	BIOTIN	AACCCCATCTCAACTCACTACAAACTC	ATTAAAAATATAAAAATTTAGTTGG
18	44C 3.5mM Mg	TOP		GGAGTTTGAGATTAGTTTGGTTAATATG	BIOTIN	CCCCTCCCAAATTCAAACA	GTTTGGTTAATATGATGAAGT
19	48C 2.5mM Mg	BOTTOM		ATTGAGTAGTGTTTTAGGGATATTTT	BIOTIN	AAACCATTATCCAATCTATCATTCATAT	TGTTGGGGGATAGAG
20	54C 2.5mM Mg	TOP		AGGGTAGATTAAGAGGTTAGGAG	BIOTIN	AAAAACCATCTCCACTCACTACA	TTGAGATTATTTTGGTTAATATAG
21	44C 3.5mM Mg	BOTTOM		GGTGAGATGGTAAAGTAGTATATAGAGA	BIOTIN	CACTTCACAAATTTTATCCAAAACT	TTTGGTTTTAGATTATGTGATTATA
22	43C 2.5 Mm Mg	TOP		TGGAAGGAAAAGAAGAAGTAATT	BIOTIN	AAACTACCAACCCTTCTTTACTTCTACAC	GTTGTTTTTTTTTTTTTTAG
22	50C 4mM Mg	TOP		TTGGTGTGTAGTAGGTTATGTTATTT	BIOTIN	CTTCTTCTTTTCCTTCCAAAACTAAATT	AGTATATTTTATAATATTTGTATAG
MGMT	44C 2.5mM Mg	TOP		ATTAGGGGAGAGGTATTAGGAGG	BIOTIN	ACCAAATAACCCCTACCTTTTCCTATCAC	TAGGAGGGGAGAGAT
MGMT	54C 2.5mM Mg	TOP		ATTAGGGGAGAGGTATTAGGAGG	BIOTIN	ACCAAATAACCCCTACCTTTTCCTATCAC	AGTAGGATAGGGATTTTTATTAAG
RASSF1A	50C 2.5mM Mg	TOP		AGGTATTTAGGAGGTTGAGGTAGAAGA	BIOTIN	AACACAAAACTTCCCCTTTCCTCATT	GGTTGAGGTAGAAGAAT
RASSF1A	50C 2.5mM Mg	TOP		GTTAAAGGTGTTTAGTTTTTTTTTTAAGTA	BIOTIN	CCACCATACCCAACTAATTTTTATATTTTT	TTAAGTAAATGGGTAGATGT
RASSF1A	54C 2.5mM Mg	TOP		GGAGTTTGAGATTAGTTTGGTTAATATG	BIOTIN	TCCCCTTTCCTCATTAACAAT	TTGGTTAATATGGTGAAATTT

Table 5.2. Details of primers used in Real Time PCR analysis.

Primer	Primer Location	Target/Endogenous	Sense primer sequence (5'-3')	Tm	Length	Antisense primer sequence (5'-3')	Tm	Length	Amplicon Length
NF1 Promoter	*NF1* Promoter	Target	GGACGTGACGTATTCATCAGTTCA	60°C	21bp	AACCTTTTCAATACATATCATTAACTTCATG	58°C	31bp	53bp
RASSF1A Promoter	*RASSF1A* Promoter	Target	GGCAGAAGAATCGCTTGAACC	60°C	21bp	ATTTCGGCTCACCGCAAC	58°C	18bp	51bp
B2M	Exon 2	Endogenous	CCCCCACTGAAAAAGATGAGTAT	61°C	23bp	CAAAGTCACATGGTTCACACGG	64°C	22bp	50bp

5.3.6 Preparation for pyrosequencing

Pyrosequencing was carried out as previously described (Uppsala, Sweden) using Q96 Pyro Gold reagents (Qiagen) on a Pyromark Q96 Pyrosequencer (Qiagen). 90 minutes prior to use, the PyroMark Q96 ID was switched on to allow adequate time to stabilise. A heat block was set at 80°C and all reagents and primers (sequencing primer and biotinylated for control well) were removed from the freezer to warm to room temperature. Finally the vacuum pump was switched on with the vacuum kept closed and each reservoir on the Vacuum Prep Workstation (Qiagen) was filled with 180mls of ethanol, denaturation solution and wash buffer following the manufacturers' protocol.
3µl of streptavidin sepharose beads per sample were added to 37µl of binding buffer per sample and the 40µl binding buffer/beads solution was added to an equal volume of PCR product in the 96 well plate in which the PCR was completed. The plate was then sealed and shaken for 15 minutes at room temperature. 0.4µM sequencing primer was added to 40µl of annealing buffer and this was aliquoted into the appropriate wells on a PSQ plate.

The PCR product attached to the beads was combined with the sequencing primer using the Vacuum prep tool. The beads containing the immobilised templates were captured by the probes on the vacuum prep tool. The probes were washed in 70% ethanol for 10 seconds followed by 10 seconds in the trough containing denaturation solution and a final 10 seconds in the wash buffer. The vacuum was then turned off and the beads were released in to the PSQ plate containing the sequencing primer. The plate containing the samples was incubated on a heat block for 2 minutes at 80°C to assist in the annealing of the primer to the template. The plate was then removed and placed on the PyroMark after it had cooled to room temperature.

5.3.7 Running the pyrosequencing assay

The assay run file containing the details of the sequencing run and the instrument parameters were loaded onto the pyrosequencer prior to starting the run. Enzyme and substrate mixtures were reconstituted with high purity water and mixed gently by inverting a few times. The Q96 cartridges were filled with the appropriate reagents (enzyme, substrate and dNTPs) and the cartridge was placed in the Pyromark along with the PSQ plate and the run was started. Results were analysed using the Q96 Pyrosequencing software (Qiagen). The average methylation was calculated across all CpG dinucleotides in one amplified fragment to give a score of mean methylation for each CpG island.

5.3.8 Gene expression analysis

Relative quantification was used to correlate methylation status of *NF1* and *RASSF1A* genes with their gene expression using the method and conditions outlined in section 2.2.5 and the primers outlined in table 5.2. All data was analysed with the ABI 7500 SDS System software (Applied Biosystems)

5.3.9 5-Aza-2'-deoxycytidine cell line treatment

5-Aza-2'-deoxycytidine (5aza2dc) is a demethylating agent which is incorporated into DNA of dividing cells. Following cell treatment with 5aza2dc, a rapid loss of DNA methyltransferase activity is observed as the enzyme becomes irreversibly bound to the 5aza2dc residues in DNA (Christman, 2002). Three cell lines derived from NF1 malignant tumours (ST8814, T529, T530) were treated with 5aza2dc at concentrations of 1μM, 5μM, 10μM, 20μM and 30μM. $2x10^5$ cells were seeded 24 hours prior to treatment in 6 well plates using the appropriate medium as described in section 2.2.2. All cells were treated with freshly made 5aza2dc for 4 days with the culture medium changed every 24 hours for freshly made 5aza2dc. Pilot tests assessed the minimum time required for the drug to elicit a response. One aliquot of cells from each cell line

was left untreated as a control. Cells were harvested after 4 days, from which DNA was extracted for methylation analysis and RNA for *RASSF1A* gene expression analysis using the protocols described above and in section 2.2.5. The effect of 5aza2dc drug removal was also assessed. Cells were cultured for 21 days and treated only for the first 7 days with 5aza2dc (20μM) followed by 14 days in which the drug treatment was withdrawn and replaced with normal growth medium.

5.3.10 5aza2dc treatment cell survival and cell death assay

The toxicity of 5aza2dc on cultured MPNST tumour cells was determined by seeding the cells as above and treating with a series of 5aza2dc concentrations (10μM, 20μM, 30μM, 40μM and 50μM). One aliquot of cells was left untreated as a control. Cells were treated over 4 days; the medium was changed daily with freshly prepared 5aza2dc. Trypan Blue (Gibco) and a Haemocytometer were used to assess living and dead cells grown in each drug concentration as described in section 2.2.2.3. All experiments and measurements were carried out in triplicate.

5.3.11 Statistical analysis

All statistical analysis was completed using SPSS (v16) and the independent samples T-Test.

5.4 Results

5.4.1 NF1 gene methylation

Epitect control DNA samples (Qiagen) were initially used to establish the baseline levels of methylation in the pyrosequencing assay. The 'unmethylated control' demonstrated 12% methylation and the 'methylated control' was 96% methylated. The *NF1* gene was methylated at 20 of the 22 CpG rich regions analysed in tumour derived samples and controls, with the exception of CpG island 22 (exon 49) which was only methylated in

tumour derived samples. Methylation in tumour samples at all 20 CpG islands was significant when compared to the Epitect unmethylated control (p=0.05 – p= 0.001). These methylated regions encompassed the promoter, but none of the other known functional domains of neurofibromin (table 5.3). Nine CpG regions located within intron 1 (CpG regions 3-11), all exhibited similar levels of methylation across different tumour types; although the methylation level was highly variable between the CpG regions (12%-83%) and one CpG region was not methylated (table 5.3). Two CpG rich regions located within 600bp of each other in intron 5 (14 and 15) demonstrated the same levels of methylation across all samples although one was methylated (57%); the other was not significantly methylated (16%). A 200bp fragment located at the 5' intron/exon boundary of the last exon, 49 (CpG region 22) was also analysed using the sequence shown here (CpG sites are bold and italicised with the intron in lower case and exon in upper case):

cgcctaatgattgtttcctagaatgtgtccc***cg***ttgttaag***cg***acacatgactgcaatgaaattcagtcctggaaggaaaag
aagaagtaactggctgttctctttttctccagGAAT***CG***ACAAGGAGAA***CG***TTGAACTCTCCCCTACC
ACTGGCCACTGTAACAGTGGA***CG***AACT***CG***CCA***CG***GATC***CG***CAAGCCAAGTGCAGA
AGCAAAGAAG***CG***CTGGCAGTTT

This was the only CpG rich region to exhibit significant differences in methylation levels between the tumour derived samples (primary tumour and tumour derived cell lines) (exhibiting ~86% methylation), the fibroblast control cell lines (~58% methylated) (p=0.008) and the lymphocyte DNA (~22% methylated) (table 5.1, figure 5.2a). This cluster of CpG sites also showed variable methylation levels in the three different tissue types; as DNA from the spinal root was 80% methylated whilst methylation in the placenta and spleen was 24% and 26% respectively. No significant differences in methylation were, however, identified between benign and malignant tumour types (p=0.2) or between NF1 and non-NF1 lymphocyte blood DNA samples (p=0.4). There was also no difference in the level of methylation in the tumour samples in which the *NF1* germline or somatic mutation had previously been identified in comparison to samples in which the *NF1* somatic mutation was unknown (p=0.4).

It is also possible that our initial CpG analysis could have highlighted GC rich genomic sequences which are associated with *Alu* repeats due to the lower stringency of this search. Analysis of the sequences of the *NF1* CpG rich regions investigated in this study indicates that only regions 7 and 18 have evidence of a possible association with *Alu* repeats due to the presence of a 3' A-rich region and additionally CpG island 12 which has evidence of a central A-rich region. For the remaining 19 CpG rich regions, it is unlikely that these sequences reflect *Alu* repeat regions (Batzer and Deininger, 2002). This was confirmed definitively using repeat masker (http://www.repeatmasker.org).

5.4.2 RASSF1A and MGMT promoter methylation

The methylation status of the *RASSF1A* promoter exhibited up to 81% average methylation in benign and malignant tumour DNA and ~21% in fibroblast control samples (p=0.001). NF1 lymphocytes and control lymphocyte DNA only exhibited ~15-20% methylation (figure 5.2b). No significant difference in *RASSF1A* methylation was identified between benign and malignant tumour types (p=0.7). No significant difference in *MGMT* promoter methylation was identified in tumour samples in comparison to matched controls (p=0.9).

5.4.3 Gene expression analysis

NF1 gene expression was analysed in tumour derived samples, controls and blood DNA samples derived from NF1 patients. The *NF1* gene was found to exhibit a 2 to 6-fold decrease in gene expression across all sample types but we were unable to correlate *NF1* gene expression with *NF1* methylation status. *RASSF1A* gene expression was, however, found to be correlated with the level of *RASSF1A* promoter methylation (figure 5.3a). Tumour derived samples and tumour cell lines were 81% methylated and demonstrated up to a 5-fold decrease in *RASSF1A* gene expression (Figure 5.3b) in comparison to the control matched fibroblast cell lines and tissue matched blood samples which demonstrated normal *RASSF1A* gene expression and were not significantly methylated (15-20%) (p=0.001).

Table 5.3 Pyrosequencing results showing the average methylation at each CpG island in all samples analysed. ND. Not done.

Sample Type	Mean Methylation at Each CpG Island																							
	1	2	3	4	5	6	7	8	9	10	11	12	13	14	15	16	17	18	19	20	21	22	*Rassf1a*	*MGMT*
	NF1 Promoter	Exon 1	Intron 1	Intron 1	Intron 1	Intron 1	Intron 1	Intron 1	Intron 1	Intron 1	Intron 1	Intron 2	Intron 4b	Intron 5	Intron 5	Intron 29	Intron 29	Intron 29	Exon 31	Intron 32	Intron 40	Exon 49	Promoter	Promoter
Neurofibroma	72	34	14	65	36	82	54	49	45	41	52	59	57	18	58	50	48	53	97	67	67	90	81	20
Plexiform	71	35	18	67	36	83	53	48	46	46	55	58	61	20	54	53	48	52	94	68	69	78	83	19
MPNST	73	33	12	62	33	82	54	50	44	43	58	56	62	15	56	53	46	55	87	65	70	89	81	20
Schwann Cell Lines	74	32	13	65	34	82	55	51	42	42	56	57	62	17	55	54	47	50	90	66	71	75	80	19
Fibroblast Cell Lines	70	34	18	63	35	85	52	48	43	42	55	57	60	17	57	52	50	51	89	68	72	58	21	22
Spleen	72	32	11	61	36	83	50	49	46	45	56	58	63	16	55	51	47	56	85	69	65	26	ND	ND
Spinal Root	73	31	13	64	38	84	50	51	44	44	52	59	58	15	58	55	51	57	90	65	64	80	ND	ND
Placenta	72	30	12	62	37	82	51	48	43	44	51	60	58	14	56	54	52	50	83	66	69	24	ND	ND
NF1 Blood	75	33	15	66	38	82	52	51	48	44	60	59	58	13	58	53	50	55	93	67	68	22	16	21
Non NF1 Blood	74	34	11	64	36	81	53	49	45	43	55	57	57	17	57	50	49	55	87	68	70	25	15	20
Unmethylated Control	10	11	15	12	13	12	16	10	15	10	10	11	15	14	12	11	10	16	12	10	10	17	14	18
Methylated Control	97	99	100	98	96	100	100	95	96	99	100	98	99	97	97	96	100	95	100	98	97	99	97	96
Average Tumour Methylation	72	33	14	64	36	83	52	49	45	44	55	58	59	16	57	52	49	54	89	67	68	86	81	20

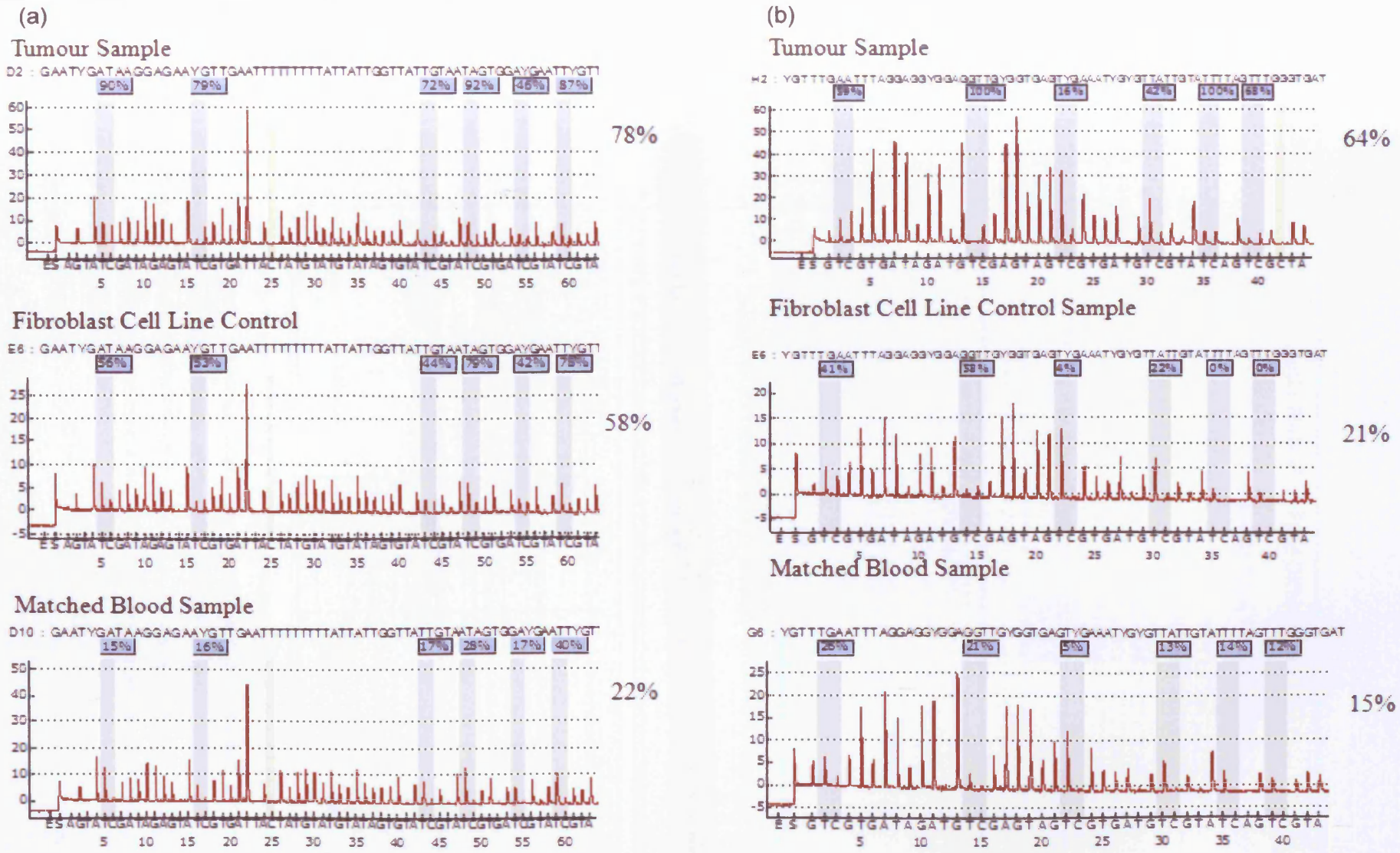

Figure 5.2 (a) Pyrosequencing traces (Pyrograms) of matched tumour (MPNST), control sample and blood sample for CpG region 22 (exon 49, *NF1* gene). (b) Pyrosequencing traces of *RASSF1A* promoter in tumour (MPNST), control sample and blood samples.

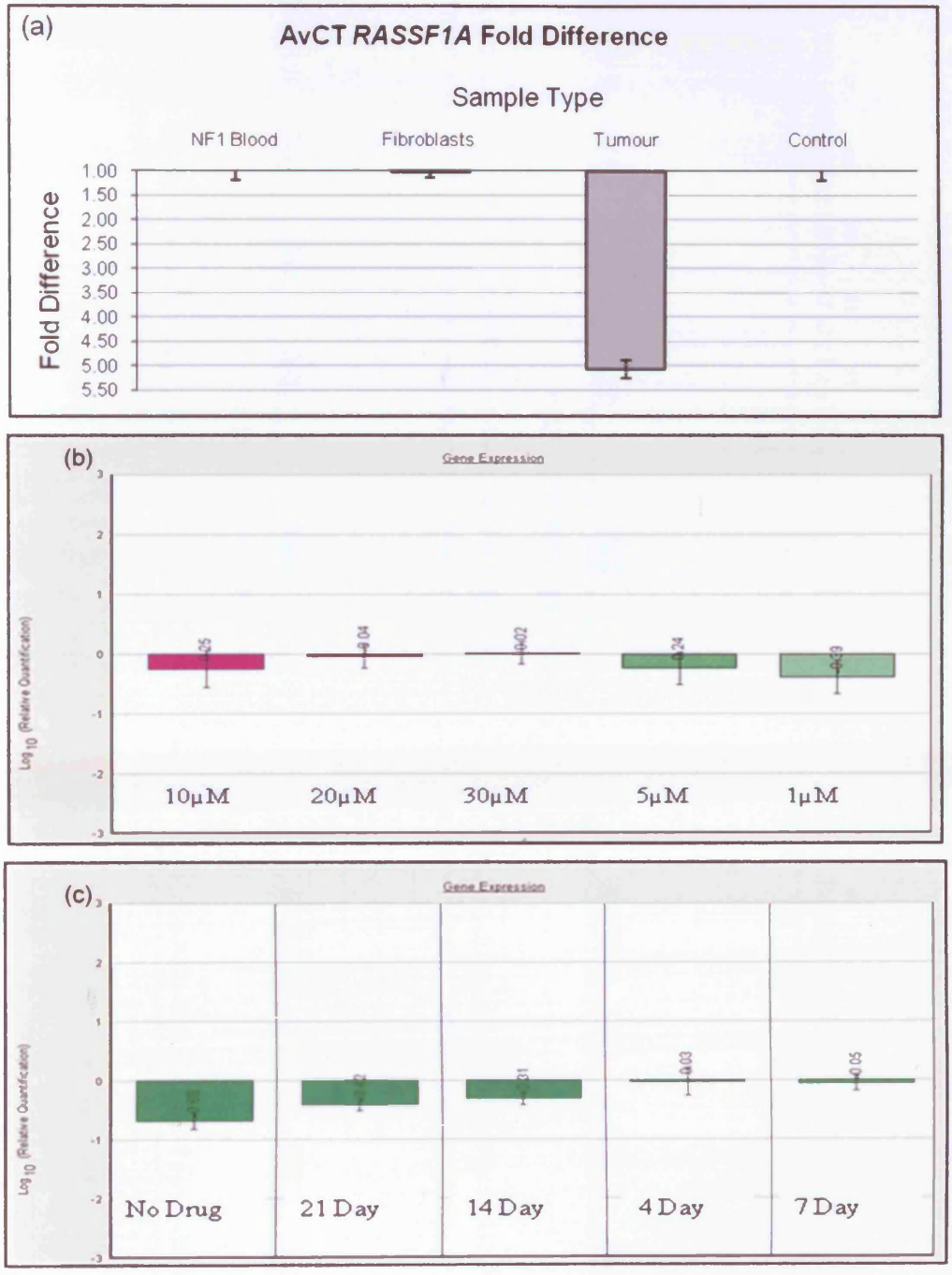

Figure 5.3 (a). *RASSF1A* promoter fold-change in gene expression in a control blood sample, NF1 tumour matched blood sample, fibroblast control sample and a tumour sample (MPNST) (p=0.001). Profiles are representative of all samples studied. (b) *RASSF1A* gene expression dose dependent response to 5aza2dc treatment of MPNST cell line (ST8814). (c) Gene expression profiles of an MPNST cell line (ST8814) treated with 5aza2dc over 4 days followed by drug removal until day 21. Profiles are representative of all cell lines studied

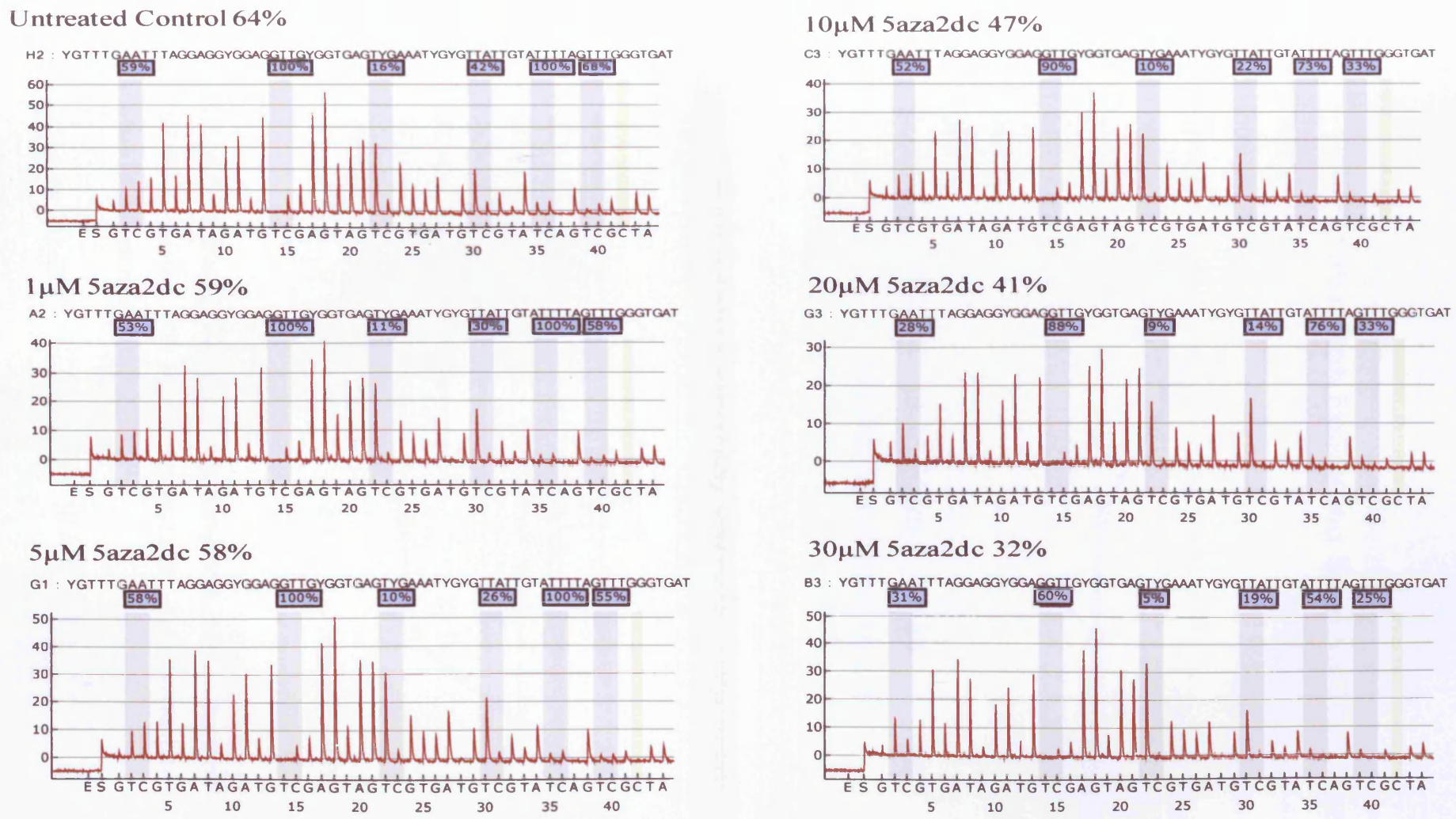

Figure 5.4. Pyrograms and methylation status of MPNST cell line (ST8814) treated with 5 concentrations of 5aza2dc (1, 5, 10, 20 and 30µM). Pyrograms are representative of all cell lines treated.

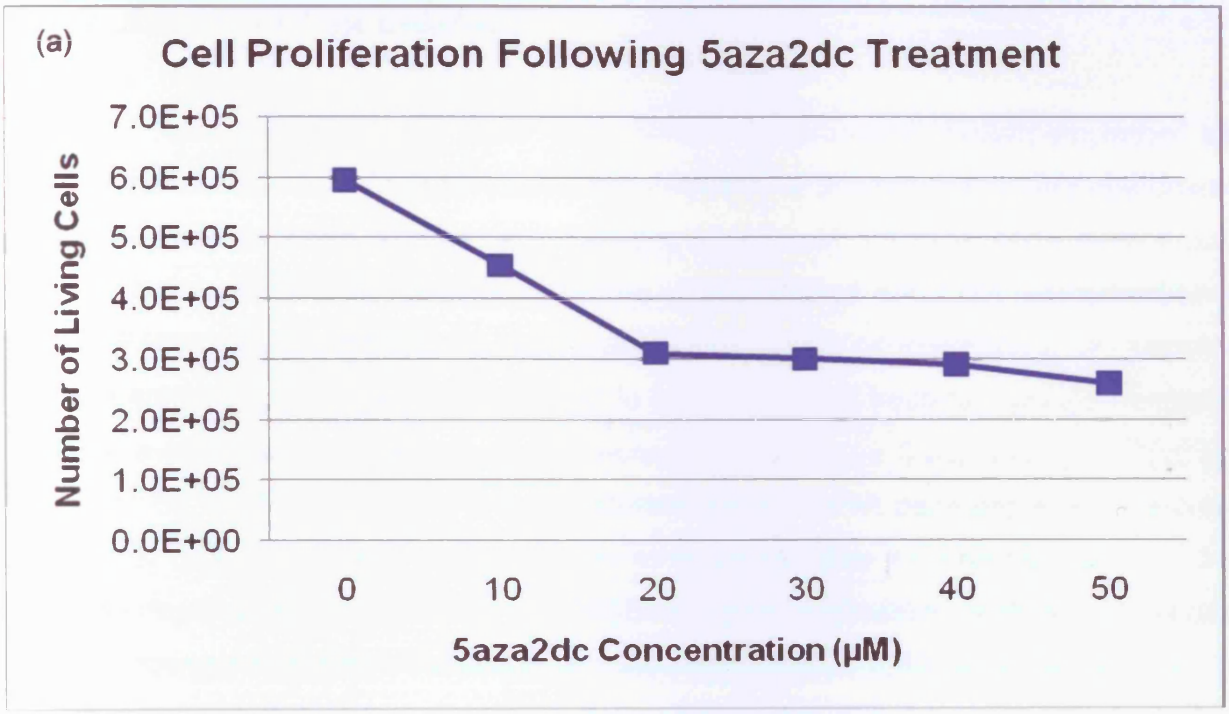

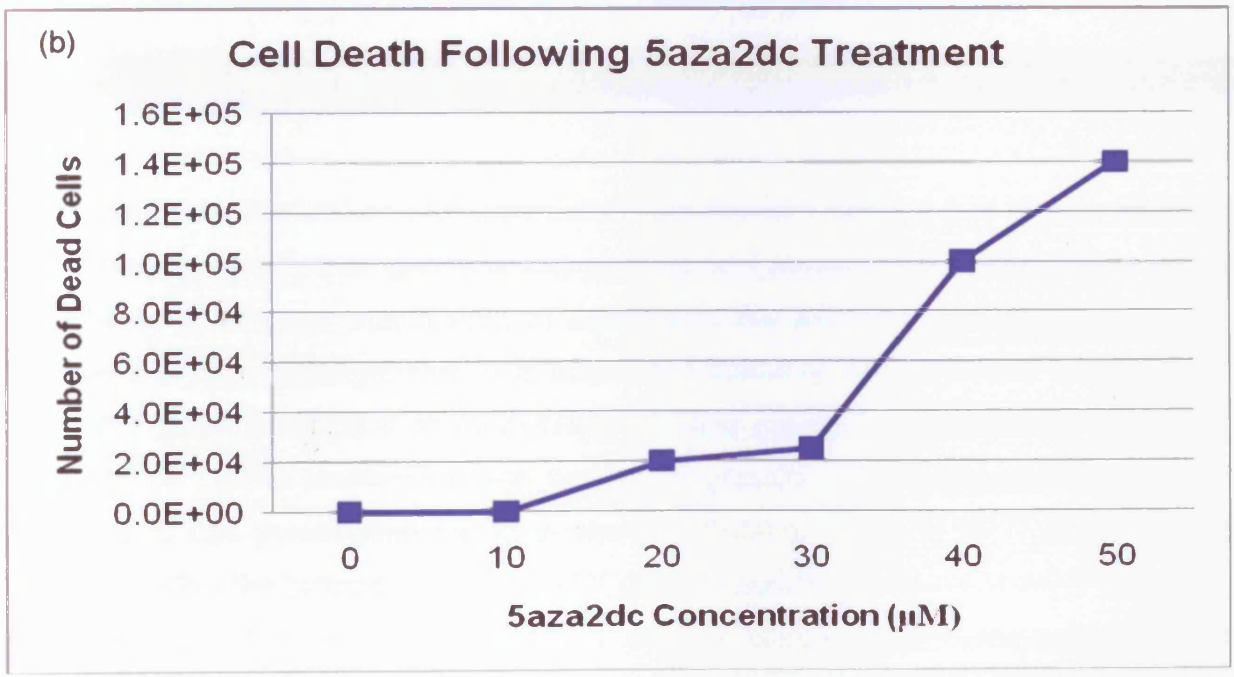

Figure 5.5 Graphs showing the level of (a) living cells and (b) dead cells in an MPNST cell line (ST8814) treated with increasing 5aza2dc drug concentrations. Graphs are representative of all cell lines studied.

5.4.4 5aza2dc cell line treatment

MPNST tumour-derived cell lines with *RASSF1A* promoter hypermethylation and decreased *RASSF1A* gene expression demonstrated a dosage-dependent response in gene expression when treated with 5aza2dc at 1-30μM concentrations over 4 days (figure 5.3b). All tumour derived cell lines demonstrated complete normalisation of *RASSF1A* gene expression at both 20μM and 30μM concentrations of 5aza2dc. Treatment for four days was determined to be the minimal treatment period needed to induce a return of gene expression to normal levels (figure 5.3c) and the effect was found to be transient following drug withdrawal as *RASSF1A* gene expression returned to a level comparable with that seen prior to treatment after 21 days (figure 5.3c). The dosage-dependent normalisation of *RASSF1A* gene expression was also correlated with a dosage-dependent reduction in methylation status (64% to 32%) as seen by pyrosequencing (figure 5.4). Concentrations of 5-aza2dc over 30μM were found to lead to significant cell death in comparison to untreated controls (figure 5.5).

5.5 Discussion

Despite the high mutation rate associated with the *NF1* gene, it has proven difficult to successfully identify both germline and somatic *NF1* mutations indicating that additional mechanisms of gene inactivation in addition to the effect of modifying loci may be involved in NF1 tumorigenesis. It is postulated therefore that increased methylation of the *NF1* gene, in addition to methylation at other modifying loci could be involved in somatic *NF1* gene inactivation and tumour progression. This comprehensive study is the first to use pyrosequencing to analyse methylation levels in all CpG rich regions located within the promoter and the *NF1* gene in addition to the promoters of possible modifier loci; *RASSF1A* and *MGMT* in a large cohort of NF1-associated tumours, matched blood samples and patient derived tissue samples.

5.5.1 NF1 pyrosequencing analysis

Pyrosequencing offers many advantages over technologies such as methylation specific PCR (MSP), Q-MSP, southern analysis and bisulphite PCR which have been employed in previous *NF1* methylation studies (Rodenhiser *et al*, 1993; Horan *et al*, 2000; Luijten *et al*, 2000; Harder *et al*, 2004; Fishbein *et al*, 2005). The data generated by pyrosequencing are actual sequences rather than fluorescence data, false positive results can be abolished with the use of additional probe sequences and this methodology can also detect partially methylated sequences that are located outside of the priming sites (Colella *et al*, 2003). Pyrosequencing therefore provides rapid, sensitive, accurate and quantifiable detection of methylation at single and multiple CpG sites, and represents a significant improvement on methods used in previous *NF1* methylation studies (Rodenhiser *et al*, 1993; Horan *et al*, 2000; Luijten *et al*, 2000; Harder *et al*, 2004; Fishbein *et al*, 2005).

Thus, the present study has re-analysed the entire large *NF1* promoter CpG island and the results generated represent quantitative data of methylation across the *NF1* promoter, an improvement on earlier results, mainly based on visual inspection of bands on a gel (Rodenhiser *et al*, 1993; Horan *et al*, 2000; Luijten *et al*, 2000; Harder *et al*, 2004; Fishbein *et al*, 2005). Despite the improvement in methodology and increased sample size, our findings are in agreement with previous studies both in NF1-associated tumours and patient derived blood samples, confirming that *NF1* promoter methylation is unlikely to contribute to NF1 tumorigenesis (Rodenhiser *et al*, 1993; Horan *et al*, 2000; Luijten *et al*, 2000; Harder *et al*, 2004; Fishbein *et al*, 2005; Ebinger *et al*, 2005). Previous *NF1* methylation analysis has, however, only concentrated on the promoter region and a few select exons, encompassing as little as 1% of the CpG sites within the *NF1* gene. This study has analysed 353 CpG sites representing a further 15% of *NF1* CpG dinucleotides. The remaining sites were not analysed in this study as they are scattered throughout the *NF1* gene. These regions by definition are unlikely to represent CpG islands at which methylation could occur. They were not detected with the CpG searcher software as a CpG island requires greater than 50% GC content in a 200-500bp region with at least 100bp between each region.

Previous studies have found methylation in both coding regions downstream of the promoter (exon 4 of the *c-fos* gene) and within intronic regions (intron 1 of the PRAME gene) (Li *et al*, 2003; Ortmann *et al*, 2008). In view of these findings, all CpG rich regions throughout the *NF1* gene were analysed. Indeed only 120 of the 2,420 CpG sites within the *NF1* gene are located within exons. This study has identified 22 CpG rich regions, only 4 of which encompass exonic sequences (the promoter region, exon 1, exon 31 and exon 49). Excluding the promoter region, which has been previously analysed, this extensive study has expanded on limitations of earlier studies by assessing an additional 21 CpG rich regions throughout the *NF1* gene. The results from our analysis indicates that whilst there is evidence for methylation at 20 of the 22 defined *NF1* CpG rich regions, only a single CpG region (region 22), located at the 5' region of exon 49 exhibited significant differential methylation between tumour samples and controls. However, methylation at this region is unlikely to play a direct role in NF1 tumorigenesis as *NF1* methylation was not correlated with *NF1* gene expression (table 5.3, figure 5.1 and figure 5.2a).

5.5.2 Hypermutability of CpG dinucleotides and NF1 mutations

There are a number of regions of high and low methylation at adjacent *NF1* CpG regions observed in this study (e.g. 3-11 and 14-15) (table 5.3) The high mutability of CpG dinucleotides within GC rich regions and the switch between methylated and unmethylated CpG sites may therefore contribute to increased instability and the high mutation rate associated with the *NF1* gene (Cooper and Youssoufian, 1988; Rodenhiser *et al*, 1993). There is, however, no evidence from published mutational data (HGMD) of any obvious mutational clustering in such regions, although CpG regions 13-14 are located near to exon 4b which may represent a 'warm' spot for *NF1* mutations (Fahsold *et al*, 2000; Ars *et al*, 2003; DeLuca *et al*, 2004). Approximately 20% of all *NF1* mutations are associated with CpG dinucleotides and 3% with CpNpG sites (Cooper and Youssoufian, 1988; Cooper and Krawczak 1993 Krkljus *et al*, 1997; Fahsold *et al*, 2000; DeLuca *et al*, 2004). Analysis of all published *NF1* mutations (HGMD) has identified 19 mutations associated with CpG dinucleotides including the commonly

identified c.5839T; p.R1947X in exon 31 (Andrews *et al*, 1996). All but 1 of these 19 mutations is recurrent, confirming earlier findings that these CpG sites may represent mutational hotspots.

5.5.3 Tissue specific methylation

Tissue specific genes are usually methylated, except in the tissue in which the gene is expressed, although this can be disrupted in instances of aberrant methylation (Yisraeli and Szyf, 1984). Thus, the level of tissue specific methylation in the *NF1* gene and *RASSF1A* and *MGMT* promoters in samples from the spleen, spinal root and placenta was also analysed. No difference in methylation of the *RASSF1A* and *MGMT* promoters was identified in the tissues analysed in this study. However, tissue specific *NF1* methylation at CpG region 22 (Exon 49) was identified which was concordant with the known expression pattern of the *NF1* gene (DeClue *et al*, 1991; Daston *et al*, 1992; Norlund *et al*, 1993). This indicates that aberrant methylation in the brain and central nervous system may modulate gene expression in the different tissue types. Indeed, recent evidence from twin studies suggests that methylation patterns of the normal *NF1* allele may also have a role in modification of the NF1 phenotype (Harder *et al*, 2010).
The methylation status of the *NF1* gene, *RASSF1A* and *MGMT* promoters were similar in all NF1-associated benign and malignant tumour types (benign cutaneous neurofibromas, plexiform neurofibromas, and MPNSTs). This indicates that the methylation status of these genes is not tumour-type specific and is more likely, as previously suggested, to be an early tumorigenic event which is not associated with malignant transformation (Baylin *et al*, 2001). Similarly, the methylation status of the *NF1* gene and *RASSF1A* and *MGMT* promoters was comparable in samples with and without *NF1* germline and somatic mutations, an indication that methylation is unlikely to be dependent on mutation status and that methylation of CpG dinucleotides in these genes is unlikely to be the sole molecular mechanism underlying NF1 tumorigenesis.

5.5.4 Promoter methylation of modifying loci

Methylation of additional genomic loci, including the *MSH2* promoter (Titze *et al*, 2010) has been identified in peripheral blood samples from NF1 patients, suggesting that unrelated genomic loci may act as modifiers for NF1. Whilst many genes are associated with specific cancer types, *RASSF1A* and *MGMT* represent candidate modifier genes for NF1 tumorigenesis based on their cellular roles and earlier associations with cancer (table 1.8). The *RASSF1* gene is a TSG with seven encoded isoforms (A-G), exhibiting differential expression. *RASSF1A* is ubiquitously expressed and has two isoform specific 5' exons, an N-terminus with high homology to the protein kinase C conserved region 1 domain and four exons in common with the other isoforms (exons 3–6), which are known to encode a RAS association domain (Ponting and Benjamin, 1996). High levels of *RASSF1A* methylation have been identified in numerous cancers (table 1.8) including 40% of lung cancers, adenocarcinoma of the cervix and importantly, colorectal cancer, in which concurrent *NF1* somatic mutations have also been identified (Cohen *et al*, 2003; Ahlquist *et al*, 2008; Lin *et al*, 2009; Wang *et al*, 2009). *RASSF1A* is thought to interact with *KRAS* through the Ras association domain and is known to have several key cellular effects including promotion of apoptosis, cell cycle arrest, and maintenance of genomic stability (Ahlquist *et al*, 2008; Lin *et al*, 2009; Wang *et al*, 2009).

MGMT functions by repairing inappropriately methylated guanine residues in DNA and consequently *MGMT* expression protects against G:C to A:T DNA transitions. Aberrant *MGMT* methylation therefore commonly occurs concurrently with G:A mutations in the *KRAS* and *TP53* genes in colorectal cancer. (Esteller *et al*, 2000). *MGMT* hypermethylation is identified in a number of different cancers (table 1.8) and it has been postulated that elevated levels of *MGMT* promoter methylation in colonic mucosa may be a predisposing factor for neoplastic progression (Esteller *et al*, 2000). Whilst there was no significant difference in *MGMT* promoter methylation in the tumour samples and controls analysed here, this study demonstrates for the first time that *RASSF1A* methylation may be an early event in the development of benign and malignant NF1-associated tumours. Importantly, 5aza2dc treatment of MPNST tumour-derived cell lines was able to reduce methylation and rescue *RASSF1A* gene

expression. Whilst the toxicity of this agent was assessed, the affect of this agent on other genes was not determined. It has been found that catalytic DNA methylase inhibitors may also activate pro-metastatic genes due to their broad demethylating activity (Szyf et al, 2004). Hence, a balance must be reached between achieving an anti-tumorigenic effect and consequential activation of other genes through global hypomethylation. However, the results of this study demonstrate that patients with NF1-associated tumours which harbour pathogenic aberrant methylation patterns could benefit from treatment with inhibitors of DNA methyltransferases, analogues of which are currently in clinical cancer trials (Christman, 2002).

5.5.5 Implications for future NF1 methylation analysis

One of the biggest challenges for genetic analysis is the choice of appropriate controls. The nature of NF1 tumours means that it is especially difficult to find appropriate controls. In the methylation analysis, Epitect control DNA were crucial for ensuring that the pyrosequencing reaction was not biased with effects of poor bisulphite conversion. Both the methylated and non-methylated controls were also useful for determining the upper and lower limits of the assay by which tumour samples could be compared. The most appropriate negative control for NF1-associated tumour analysis would be normal peripheral nerve. This is not easy to obtain, however, and so was not available for this analysis. Therefore, DNA or cDNA from *NF1*$^{+/-}$ fibroblasts were used as an alternative. Furthermore, whilst blood is not a control for a tissue sample, lymphocyte DNA derived from NF1 patients was compared to NF1 tissue samples to identify tumour specific changes. Non-NF1 DNA samples were also used as controls for alterations which may occur in NF1 blood DNA. This control in itself is also problematic as even though an individual does not have NF1, it is possible that they have other unidentified alterations in their DNA. The controls used in this study are appropriate for the context of this analysis, in the future, however, it would be important to utilise normal nerve to provide a direct comparison.

The role of non-CpG methylation in the *NF1* gene has not been analysed in this study. Although no evidence of CpNpG methylation has been identified previously in the *NF1* promoter (Horan *et al*, 2000), the high proportion of CpNpG sites in the *NF1* gene and presence of mutations involving CpNpG trinuncleotides in the *NF1* gene (Cooper *et al*, 2010) indicates that in future *NF1* gene methylation analysis at CpNpG sites is warranted. This study has evaluated methylation at all CpG rich regions within the *NF1* gene which fall within the recognised CpG island definitions (Gardiner-Garden and Frommer, 1987; Takai and Jones, 2002) in addition to the *RASSF1A* and *MGMT* promoters. However, CpG methylation in surrounding genes which are commonly lost in patients with microdeletions was not investigated. Indeed, this is an important consideration for future studies as evidence for methylation at *NF1* flanking markers has been previously identified and is suggested to modulate the NF1 phenotype (Rodenhiser *et al*, 1993).

In this study, methylation analysis was only completed on two candidate genes in addition to the *NF1* gene; *RASSF1A* and *MGMT*. These genes were selected due to their association with the highest number of other cancer types which suggested that they may also be important to NF1 tumorigenesis (table 1.8). As methylation of *RASSF1A* was found to play a potential role in NF1 tumour development, it is possible that other modifying genes such as *CDKN2A*, *MLH1*, *APC* and *RARB* may also be involved. Future studies could benefit from 'next generation' sequencing technologies which may be more suited to analysis of methylation of genome wide modifying loci (the 'methylome') instead of 96 well based sequencing technologies such as pyrosequencing.

5.5.6 Conclusions

This comprehensive study is the first study to analyse all defined large CpG islands and CpG rich regions in the *NF1* gene and *RASSF1A* and *MGMT* promoters in NF1-associated tumours using pyrosequencing. The results presented here clearly indicate that *NF1* gene methylation is unlikely to be the singular causative mechanism for tumorigenesis in NF1-associated tumours, but may instead play a role in modulating

gene expression. Importantly, a likely correlation between *RASSF1A* promoter methylation and gene silencing has been identified in the cohort of NF1-associated tumours studied here, which was also functionally dissected with the 5aza2dc methylation inhibitor. These studies indicate that global analysis of epimutational changes is necessary to fully understand the mechanisms of tumorigenesis and malignancy in NF1.

CHAPTER 6: Functional analysis of MPNST associated somatic alterations

6.1 Introduction

This chapter focuses on genetic alterations underlying the development of malignant peripheral nerve sheath tumours (MPNSTs) and has two main sections. (i) The molecular heterogeneity of MPNSTs is explored. (ii) The cMET and RhoGTPase pathways are functionally dissected to ascertain their contribution to NF1 malignancy and importantly, to deduce their potential as therapeutic targets.

Malignant complications such as brain tumours, optic gliomas and MPNSTs are less frequent but potentially more serious manifestations of NF1 (reviewed by Upadhyaya, 2011). MPNSTs can occur sporadically or develop from the malignant transformation of pre-existing plexiform neurofibromas (PNF), which occur in some 10-15% of patients, marked by a rapid change in size of the neurofibroma (Evans *et al*, 2002). MPNSTs most commonly originate in the nerve roots, extremities and pelvis, but can also occur at other sites. These tumours usually present as enlarged masses which cause disability, neurological deficits and pain due to pressure on surrounding tissues (Reviewed by Katz *et al*, 2009).

MPNSTs are a significant cause of morbidity and mortality. Often, upon first presentation, the majority of MPNSTs are already non-resectable as the tumour is in a late stage of development and metastases are present, most commonly in the lung, but also in the liver and brain. Consequently, the 5 year survival rate for individuals with these tumours is as low as 20-50% and even lower for 10 year survival (7.5%) (Katz *et al*, 2009). Importantly, mortality is often associated with limited treatment options for MPNSTs. Complete surgical excision with clear margins is the core therapy for MPNSTs. Although chemotherapy has been employed in MPNST treatment, it remains controversial and shows limited effectiveness (supplementary table 1). Furthermore, ~3-10% of all patients with sporadic and NF1-associated MPNSTs have a history of radiation treatment for a previous malignancy (Ferner *et al*, 2002; De Raedt *et al*, 2003; Ferner *et al*, 2004; Sharif *et al*, 2006). There are a number of risk factors for the development of MPNSTs, including the presence of deep plexiform neurofibromas or those involving the brachial and lumbosacral plexuses, a family history of other cancers and a germline *NF1* microdeletion (Ferner *et al*, 2002; De Raedt *et al*, 2003; Sharif *et al*, 2006). These

identified risks indicate that such individuals should undergo a more aggressive screening approach.

Although there are differences in survival for patients with NF1-associated MPNSTs and sporadic MPNSTs, these tumours cannot be completely distinguished from each other on the basis of their underlying genetic alterations (Holtkamp *et al*, 2004; Watson *et al*, 2004). However, some studies have determined that specific genetic aberrations such as *Nm23-H1* expression, nuclear expression of p53 and gains at 16p or losses from 10q or Xq are closely associated with poor survival, often found in advanced or metastatic disease. Such patients may therefore be in a high risk group (Fang *et al*, 2009; Brekke *et al* 2009; Brekke *et al*, 2010). There are, however, no clear associations with other clinical risk factors including: histological grade, tumour location, metastasis, recurrence, age, or survival of the patient (Watson *et al*, 2004; Brekke *et al*, 2010).

A pathological diagnosis of an MPNST is very important but is also equally as challenging due to significant cellular, molecular and architectural tissue heterogeneity. Tumour heterogeneity is a notoriously challenging aspect of cancer biology, responsible for introducing very significant complexity into both the study of the underlying mechanisms of tumour development and the therapeutic context (Visvader, 2011; Gibson *et al*, 2010; Kalamarides *et al*, 2011). Tumour heterogeneity has been modelled using a number of different biomarkers to identify the extent of heterogeneity at the cellular, molecular and genome architectural levels (Singh *et al*, 2010; Liu *et al*, 2010). Cellular heterogeneity is a well established feature of NF1-associated tumours, particularly in benign cutaneous neurofibromas in which only the Schwann cells harbour *NF1* mutations, although the tumours also contain fibroblasts, mast cells, perineural cells and axons (Kimura *et al*, 1974; Le and parade, 2007). As with benign neurofibromas, malignant NF1-associated tumours are also known to be heterogeneous in nature.

Generally, the heterogeneity within an MPNST is a result of the initial stages of growth, in different regions at separate times (Spurlock *et al*, 2010). Such tumours invariably contain diverse subpopulations of tumour cells, including benign and malignant cells, fibroblasts and infiltrating inflammatory cells (Friedman *et al*, 1999). MPNSTs therefore have histological features which are reminiscent of both benign and malignant NF1 associated tumours with high cellularity, nuclear pleomorphism,

presence of atypical cells with prominent mitoses and necrosis (Reuss and Von Deimling, 2008). Furthermore, heterogeneity can additionally be generated through de-differentiation into skeletal muscle which resembles rhabdomyosarcoma and is known as a malignant triton tumour (MTT) (Stasik and Tawfik 2006).

At the molecular level, malignant tumours are recognised as being highly heterogeneous in terms of both their accumulated genetic mutations and their phenotypic expression profiles (Kourea *et al*, 1999; Nielsen *et al*, 1999; Mawrin *et al*, 2002; Mantripragada *et al*, 2008). Analysis of molecular and cellular heterogeneity using a variety of methods promises to generate important new insights into tumour biology as well as the underlying processes of tumorigenesis. Understanding the molecular heterogeneity of malignant tumours in the context of the underlying background cellular and genome architectural heterogeneity will allow both therapeutic sensitivities and the efficacy of potential drug treatments to be comprehensively evaluated.

In addition to molecular heterogeneity, the paucity of well-defined histological criteria further adds to the complexity of MPNST diagnosis. A diagnosis of an MPNST can be made if there is an association of the tumour with a pre-existing neurofibroma or peripheral nerve and if the tumour has histopathological features commonly associated with an MPNST. MPNSTs can be deemed 'low grade' if there is a lack of mitotic activity, as these tumours rarely metastasise and may therefore represent a transition stage between neurofibromas and MPNSTs (Ferner *et al*, 2008). Prior to biopsy analysis and microscopic examination, MPNST diagnosis is based on radiological imaging, most commonly magnetic resonance imaging (MRI) which can determine neuronal from non-neurogenic tissue. MPNSTs are not, however, readily distinguishable from plexiform neurofibromas upon CT or MRI analysis but positron emission tomography (PET) scans using [^{18}F] fluorodeoxyglucose (FDG), an analogue of glucose can be utilised in MPNST diagnosis as there is a higher level of uptake of glucose in malignant tumours (Ferner *et al*, 2008). FDG-PET-CT is currently being trialled as part of the follow up procedure for deep neurofibromas (Ferner *et al*, 2008).

There are currently no prognostic or predictive biomarkers for MPNSTs; as such that progression of a pre-existing plexiform neurofibroma to an MPNST cannot be determined in advance based on the molecular profile of the tumour. Similarly, the

full spectrum of genes affected in such tumours is still unknown; indicating that without detailed knowledge of the mutational spectrum of MPNSTs, targeted therapy would be a significant challenge. Somatic *NF1* gene inactivation resulting in a loss of the wild type *NF1* allele is known to lead to NF1-associated tumour development. This functional *NF1* loss does not, however, explain the malignant transformation of benign plexiform neurofibromas to MPNSTs, indicating that alterations of numerous additional genetic and potentially epigenetic loci are required to facilitate malignancy. A number of critical cell cycle related genes including *TP53*, *CDKN2A* and *RB1,* as outlined in section 3.1, have previously been identified as potential drivers of malignant transformation (Kourea *et al*, 1999; Nielsen *et al*, 1999; Mawrin *et al*, 2002; Mantripragada *et al*, 2008; Stewart *et al*, 2008; Upadhyaya *et al*, 2008). Such changes have only previously been identified in MPNSTs and plexiform neurofibromas. Although benign cutaneous neurofibromas have never been shown to undergo malignant transformation, LOH of *TP53* and *RB1* genes was recently described in cutaneous neurofibromas derived from NF1 patients carrying a high tumour burden (Thomas *et al*, 2010) (Chapter 3). Moreover, consistent with a role for additional genetic loci in NF1 malignant transformation, mouse models harbouring *Nf1* and *p53* mutations develop malignant NF1-associated tumours (Cichowski *et al*, 1999; Vogel *et al*, 1999; Reilly *et al*, 2000) (section 1.8.3.3). Further weight to the evidence that alterations in other genes act as modifiers of *NF1* tumour development was demonstrated in a recent study by Spurlock *et al* (2010), in which one tumour exhibited features of both benign and malignant tumours. This tumour demonstrated molecular evolution between benign and malignant states, accompanied by significant genetic alterations, not present in the benign section.

High throughput whole genome analysis with microarrays has proven to be one of the most effective and efficient methods for analysis of large cohorts of genes and samples, across multiple tumour types. A number of previous studies have screened for copy number variations (CNV) and gene expression changes in benign and malignant NF1-associated tumours (Lothe *et al*, 1996; Bridge *et al*, 2004; Watson *et al*, 2004; Holtkamp *et al*, 2004; Storlazzi *et al*, 2006; Thomas *et al*, 2007; Shen *et al*, 2007; Kresse *et al*, 2008; Mantripragada *et al*, 2008; Mantripragada *et al*, 2009; Brekke *et al*, 2009; Miller *et al*, 2009; Pemov *et al*, 2010; Brekke *et al*, 2010; Subramanian *et al*, 2010; Chai *et al*, 2010) (table 6.1). One of the first

comprehensive high resolution array comparative genomic hybridisation (CGH) studies of genome wide alterations by Mantripragada *et al* (2008) revealed that such techniques are effective in distinguishing between the molecular signatures in benign and malignant NF1 patient derived tumours, in tumour derived cell lines (Fang *et al*, 2009; Miller *et al*, 2009) and even between cutaneous neurofibromas and plexiform neurofibromas (Holtkamp *et al*, 2004; Mantripragada *et al*, 2008) (table 6.1).

Copy number gains have been found to be more frequent than deletions in MPNST samples (62% vs. 38%) (Mantripragada *et al*, 2009), although, this is in conflict with a more recent study in which there was a loss of expression of a large number of genes, rather than widespread increase in gene expression (Subramanian *et al*, 2010). Furthermore, differences in genetic alterations in sporadic and NF1 associated MPNSTs have been studied with oligonucleotide and immunohistochemical-based tissue microarrays (TMAs) (Holtkamp *et al*, 2004; Watson *et al*, 2004; Brekke *et al*, 2009). More recently, miRNA have become a major focus of research into the factors contributing to malignancies as it is suggested that deregulation of miRNAs may contribute to malignant transformation (Subramanian *et al*, 2010; Chai *et al*, 2010)

Despite the plethora of previous array-based investigations (table 6.1), only a few relevant genes have been identified in multiple MPNSTs which are consistently modified and thus may represent key 'drivers' of NF1 malignant transformation instead of being merely 'passengers'. Furthermore, the translation of genetic array findings on MPNSTs into functionally meaningful results is rare, with only a few reports of functional studies in the literature. MPNST development is clearly a complex, multistep process in which alterations to multiple pathways are to be expected. Whole genome analysis and in particular investigation of key signalling and regulatory pathways will be crucial to determining the underlying molecular mechanisms involved in MPNST tumorigenesis. The aims of this chapter are:

1) To determine the extent of molecular heterogeneity in NF1-associated MPNSTs.
2) Dissection of cMET and RhoGTPase pathways to ascertain their role in NF1 malignancy
3) To identify therapeutic targets for MPNSTs

Table 6.1. Genes identified by oligonucleotide microarrays and array CGH as being differentially expressed in benign and malignant NF1-associated tumours

Gene/Genetic Loci	Type of Alteration	Reference
NCAM *MBP* *L1CAM* *P1P*	Overexpression	Watson *et al*, 2004
IGF2 *FGFR1* *MDK* *Ki67*	Down-regulation	
HGF *ANGPT1* *uPA*	Overexpression	Thomas *et al*, 2007
Tenascin C (*TNC*)	Upregulation	Levy *et al*, 2007
Tenascin XB (*TNXB*)	Down-regulation	
ITGB4 *PDGFRA* *MET* *TP73* *HGF*	Amplification	Mantripragada *et al*, 2008
NF1 *HMMR/RHAMM* *MMP13* *L1CAM2* *p16INK4A/ CDKN2A,* *TP53*	Deletion	
HMMR/RHAMM *MMP13* *p16INK4A/CDKN2A* *ITGB4*	Copy number alterations	
Complex karyotypes Triploid/tetraploid chromosomes	Clonal cytogenetic abnormalities, losses and imbalances	Fang *et al*, 2009
9p, 12q21-q32, X-chromosome	Deletion	
17q25	Gain	
1p35-33, 1p21, 9p21.3, 10q25, 11q22- 23, 17q11, 20p12.2	Losses	Mantripragada *et al*, 2009
1q25, 3p26, 3q13, 5p12, 5q11.2-q14, 5q21-23, 5q31-33, 6p23-p21, 6p12, 6q15, 6q23-q24, 7p22, 7p14-p13, 7q21, 7q36, 8q22-q24, 14q22, 17q21-q25.	Gains	
8q, 17q, 7p	Gains	Brekke *et al*, 2010
9p, 11q, 17p	Losses	
miR-34a	Down-regulation	Subramanian *et al*, 2010
miR-10b	Upregulation	Chai *et al*, 2010

6.2 Materials

6.2.1 shRNA

RAC1 shRNA vectors (NM_004850)
Ampicillin and puromycin resistance cassettes (Sigma)

TRCN000000977 (50% KD)
TRCN000000978 (80% KD)
TRCN000000979 (60% KD)
TRCN000000980 (70%KD)
TRCN000196793 (79% KD)

ROCK2 shRNA Vectors (NM_006908)
Ampicillin and puromycin resistance cassettes (Sigma)

TRCN000004871 (50% KD)
TRCN000004870 (60% KD)
TRCN000004869 (88% KD)
TRCN000004872 (80% KD)
TRCN000004873 (85% KD)

pLKO.1-non target shRNA
Ampicillin and puromycin resistance cassettes (Sigma cat no: SHC202)

Hepatocyte Growth Factor (HGF) (Sigma, cat no: H1404)

cMET Inhibitors: PF-4217903 (Pfizer) and SU11274 (Sigma)

BD Matrigel Basement Membrane Matrix (1mg/ml) (BD, cat no: 356234)

6.3 Methods

6.3.1 Patients samples

6.3.1.1 MPNSTs for analysis of molecular heterogeneity

Ten unrelated patients, all exhibiting the NIH diagnostic criteria for NF1 were analysed in this study to determine the extent of heterogeneity in MPNSTs. However, full clinical details were not available from all patients (table 6.2). A total of 10 MPNSTs derived from these patients were carefully and individually macro dissected to yield clean sections which were in turn further subdivided. The number and size of the various sections and subsections was mainly dependent upon the size of the original tumour (table 6.2 and table 6.3). DNA was extracted from all sections of tumour samples and corresponding constitutional (blood) samples by means of the methods outlined in sections 2.2.3.1.1 and 2.2.3.1.3.

6.3.1.2 Functional analysis of cMET and RhoGTPase pathways

Initially, 14 MPNST samples and control tissue samples were used in relative quantification experiments to determine the level of gene expression of 14 genes found to be altered in MPNSTs. These fourteen genes, plus the *B2M* (NM_004048) endogenous control, included: *CDK4* (NM_000075), *CMET* (NM_001127500), *ITGB8* (NM_002214), *LIMK1* (NM_002314), *MMP12* (NM_002426), *PDGFA* (NM_002607), *PDGFRL* (NM_006207), *PRKCA* (NM_002737), *PTK2* (NM_153831), *PIK3CA* (NM_006218), *RAC1* (NM_018890), *ROCK2* (NM_004850), *TRIO* (NM_007118) and *TOP2A* (NM_001067). Samples for relative quantification were macro-dissected and test and control mRNA was extracted as previously described in sections 2.2.3.1.2 and 2.2.3.3. Rin/RQI was not done but mRNA concentration and quality was quantified using a nannodrop spectrophotomer (Thermo scientific) and all samples were subjected to gel analysis to assess contamination and integrity. mRNA extracted from $NF1^{+/-}$ fibroblasts which were matched with MPNST samples served as control samples.

Table 6.2. Clinical details of the ten NF1 patients from whom the MPNSTs analysed in this study were taken.

Tumour	Tumour Number	Size of Tumour	Germline Mutation	Patient Age and Sex	Patient DOB	Age at diagnosis	Post Op survival [months]	Grade	Location of Tumour
1	T196.22	10cm x 10cm	Exon 2 and 3 deleted ~64kb deletion	45 / M	20-Feb-62	42	12	High	Neck
2	T516	6cm x 2cm		48 / F	31-Mar-73			Unknown	Right Axilla
3	T517	1cm x 1cm	Whole Gene Deletion	63 / M	26-Feb-58			High	Thoracic Nerve Root
4	T518	5cm x 2cm						Unknown	Unknown
5	T519	1cm x 1cm	c.1133_1136 del ACTG; p.D378fsX8	49 / M		45		High	Thoracic
6	T521	6cm x 3cm	c.1754_1757 del TAAC; p.L585fX19	24 / M	26-Jul-82	24	alive	Low	Right Hamstring
7	T522	3cm x 2cm						High	Back
8	T523	3cm x 1.5cm						Unknown	Unknown
9	T524	3cm x 1cm						Unknown	Unknown
10	T525	5cm x 5cm	c.5234 C>G; p.S1745X	19 / F	09-Dec-87	17	21	High - Radiation Induced	Unknown

Table 6.3 Analysis of molecular heterogeneity with respect to five genes (*NF1*, *TP53*, *RB1*, *CDKN2A* and *PTEN*) in 10 MPNSTs. LOH; ~100% LOH of the second allele has occurred. 50% LOH; ~50% of the second allele lost. 1 2; heterozygous marker.

Tumour	Tumour Number	Tumour Section	Tumour Subsection	Gene Analysed				
				NF1	*TP53*	*RB1*	*PTEN*	*CDKN2A*
1	T196.22	A	1	LOH	LOH	LOH	LOH	LOH
			2	LOH	LOH	LOH	LOH	LOH
			3	LOH	LOH	50% LOH	LOH	LOH
			4	1 2	1 2	1 2	1 2	1 2
			5	LOH	LOH	50% LOH	LOH	LOH
			6	LOH	LOH	LOH	LOH	LOH
			7	LOH	LOH	LOH	LOH	LOH
			8	LOH	LOH	50% LOH	50% LOH	LOH
			9	1 2	LOH	1 2	LOH	LOH
			10	1 2	LOH	1 2	LOH	LOH
		B	1	LOH	50% LOH	50% LOH	50% LOH	1 2
			2	LOH	50% LOH	50% LOH	50% LOH	1 2
			3	LOH	50% LOH	50% LOH	50% LOH	1 2
			4	LOH	50% LOH	50% LOH	50% LOH	1 2
			5	50% LOH	50% LOH	50% LOH	50% LOH	1 2
			6	LOH	50% LOH	50% LOH	50% LOH	1 2
			7	LOH	50% LOH	50% LOH	50% LOH	1 2
			8	LOH	50% LOH	50% LOH	50% LOH	1 2
			9	LOH	50% LOH	50% LOH	50% LOH	1 2
			10	LOH	50% LOH	50% LOH	50% LOH	1 2
		C	1	LOH	LOH	50% LOH	LOH	1 2
			2	LOH	LOH	50% LOH	LOH	1 2
			3	LOH	LOH	50% LOH	LOH	1 2
			4	LOH	LOH	50% LOH	LOH	1 2
			5	1 2	LOH	1 2	50% LOH	50% LOH
			6	LOH	LOH	50% LOH	LOH	50% LOH
			7	LOH	LOH	50% LOH	LOH	50% LOH
			8	LOH	LOH	50% LOH	LOH	50% LOH
			9	LOH	LOH	50% LOH	LOH	50% LOH
			10	LOH	LOH	50% LOH	LOH	50% LOH
		D	1	LOH	LOH	50% LOH	LOH	50% LOH
			2	LOH	LOH	50% LOH	50% LOH	1 2
			3	LOH	LOH	50% LOH	LOH	LOH
			4	LOH	LOH	50% LOH	LOH	LOH
			5	LOH	LOH	50% LOH	LOH	LOH
			6	LOH	LOH	50% LOH	LOH	LOH
			7	LOH	LOH	50% LOH	LOH	LOH
			8	LOH	LOH	50% LOH	LOH	LOH
			9	LOH	LOH	50% LOH	LOH	LOH
			10	LOH	LOH	50% LOH	LOH	LOH

Tumour	Tumour Number	Tumour Section	Tumour Subsection	Gene Analysed				
				NF1	*TP53*	*RB1*	*PTEN*	*CDKN2A*
1	T196.22	E	1	LOH	1 2	1 2	1 2	1 2
			2	LOH	1 2	1 2	50% LOH	1 2
			3	50% LOH	1 2	1 2	1 2	1 2
			4	LOH	1 2	1 2	50% LOH	1 2
			5	1 2	1 2	1 2	0%	1 2
			6	50% LOH	1 2	1 2	50% LOH	1 2
			7	50% LOH	1 2	1 2	0%	1 2
			8	LOH	1 2	1 2	1 2	1 2
			9	LOH	1 2	1 2	1 2	1 2
			10	LOH	1 2	1 2	1 2	1 2
2	T516	A	1	LOH	50% LOH	1 2	1 2	1 2
			2	1 2	50% LOH	1 2	1 2	1 2
		B	1	50% LOH	50% LOH	1 2	1 2	1 2
			2	50% LOH	50% LOH	1 2	1 2	1 2
		C	1	1 2	1 2	1 2	1 2	1 2
			2	1 2	1 2	1 2	1 2	1 2
3	T517	A	1	LOH	50% LOH	1 2	1 2	1 2
			2	LOH	50% LOH	1 2	1 2	1 2
		B	1	LOH	50% LOH	1 2	1 2	1 2
			2	1 2	1 2	50% LOH	1 2	1 2
4	T518	A	1	1 2	50% LOH	50% LOH	1 2	1 2
			2	LOH	1 2	50% LOH	1 2	50% LOH
		B	1	LOH	50% LOH	1 2	1 2	1 2
			2	1 2	1 2	1 2	1 2	1 2
		C	1	1 2	1 2	1 2	1 2	1 2
			2	1 2	1 2	1 2	1 2	1 2
5	T519	A	1	1 2	50% LOH	50% LOH	1 2	1 2
			2	50% LOH	50% LOH	50% LOH	1 2	1 2
		B	1	50% LOH	50% LOH	1 2	1 2	1 2
			2	50% LOH	50% LOH	50% LOH	1 2	1 2
6	T521	A	1	LOH	1 2	1 2	1 2	1 2
			2	LOH	1 2	1 2	1 2	1 2
		B	1	LOH	1 2	1 2	1 2	1 2
			2	LOH	1 2	1 2	1 2	1 2
7	T522	A	1	LOH	1 2	1 2	1 2	1 2
			2	LOH	1 2	1 2	1 2	1 2
8	T523	A	1	LOH	1 2	1 2	1 2	1 2
			2	LOH	1 2	1 2	LOH	1 2
9	T524	A	1	LOH	1 2	1 2	1 2	LOH
			2	LOH	1 2	1 2	1 2	LOH
10	T525	A	1	LOH	1 2	1 2	1 2	1 2
			2	LOH	1 2	1 2	1 2	1 2
		B	1	LOH	1 2	1 2	1 2	LOH
			2	LOH	1 2	1 2	1 2	LOH

6.3.2 Cell lines

MPNST cell lines (ST8814, SNF96.2 and T532) were used in the functional analysis of the cMET/RhoGTPase pathway. All cell lines were grown as described in section 2.2.2.

6.3.3 Analysis of molecular heterogeneity in MPNSTs

6.3.3.1 Loss of Heterozygosity analysis (LOH)

Molecular heterogeneity was determined by differences in the level of LOH between sections of the same sample. LOH analysis was completed on all sections from the 10 MPNSTs and corresponding lymphocyte DNA samples by utilising a panel of fluorescently tagged microsatellite markers in the five genes investigated: *NF1 TP53, RB1*, *CDKN2A* and *PTEN* and the method outlined in section 3.2.3.1 (supplementary tables 4 and 7). Samples exhibiting ~50% loss of the second allele were termed '50% LOH' whereas a marker which demonstrated no LOH was simply classed as heterozygous ('1 2').

6.3.3.2 p53 Immunohistochemistry analysis (IHC)

Immunohistochemical analysis of p53 was performed on sections derived from 5 MPNSTs (T196.22, T516, T517, T518 and T519) which were found by LOH analysis to exhibit molecular heterogeneity with respect to the *TP53* gene (table 6.3). Immunohistochemistry was performed using a standard protocol as described in section 2.2.4 using pre-diluted mouse anti-p53 monoclonal primary antibody.

6.3.4 MPNST copy number variation and gene expression analysis

6.3.4.1 Affymetrix analysis of MPNSTs

An Affymetrix SNP 6.0 array was previously performed on DNA from 20 NF1-associated tumours; 5 benign plexiform neurofibromas and 15 MPNSTs (Upadhyaya *et al*, unpublished data). This array contains approximately $1.8x10^6$ nucleotide

probes, combines 906,600 SNP and 946,000 CNV probes that encompass the human genome at a median probe distance of about 700bp. This array permits the simultaneous assessment of LOH and copy number alterations (CNAs) associated with inherited diseases and cancer (Suzuki *et al*, 2008). Paired CNV and LOH analyses involved the comparison of tumour DNA against the matched patient lymphocyte DNA, while unpaired CNV analyses compared tumour DNA against reference data derived from the 270 normal individuals catalogued in the HapMap sample database. Each positive tumour-specific alteration was assessed bioinformatically to determine which genes were either contained within, or overlapped, each identified genomic region. Several software tools, including GeneGO's MetaCore Software, were then applied to identify those biological pathways potentially affected by the genes involved in these tumour-specific CNAs.

6.3.4.2 Relative quantification (qPCR)

From the derived array CGH data, the relative copy number of 14 genes found to be affected by tumour-specific CNAs was independently assessed by relative quantification on a panel of 14 MPNST samples and 5 MPNST derived cell lines. These fourteen genes, plus the *B2M* (NM_004048) endogenous control, included: *CDK4* (NM_000075), *CMET* (NM_001127500), *ITGB8* (NM_002214), *LIMK1* (NM_002314), *MMP12* (NM_002426), *PDGFA* (NM_002607), *PDGFRL* (NM_006207), *PRKCA* (NM_002737), *PTK2* (NM_153831), *PIK3CA* (NM_006218), *RAC1* (NM_018890), *ROCK2* (NM_004850), *TRIO* (NM_007118) and *TOP2A* (NM_001067). Relative quantification was completed using the method described in section 2.2.5 and the primers and conditions in table 6.4.

6.3.5 Functional analysis of cMET and RhoGTPase pathways

From the Affymetrix array and qPCR data it was concluded that three genes which were found to be amplified could be functionally analysed to determine the effect of alterations in these genes on the malignant potential of cells derived from MPNSTs. The three genes selected for further functional analysis were: *cMET* and the RhoGTPase pathway genes; *RAC1* and *ROCK2*. The hepatocyte growth factor (HGF) and its receptor; cMET have previously been implicated in MPNST

development in earlier array studies (Mantripragada *et al*, 2008). The recurrence of *cMET* alterations in these tumours indicates that alterations in the *cMET* pathway are of importance to MPNST tumorigenesis. *RAC1*, *ROCK2*, *LIMK1*, *PTK2*, *TRIO* and *PRKCA* all belong to the RhoGTPase pathway and were also found to harbour increased copy number by microarray and were independently confirmed by qPCR. The RhoGTPase pathway regulates cellular processes such as cytoskeletal regulation, cell cycle regulation, cell polarity and cell migration indicating that this pathway may be especially important for the migratory potential of cells derived from MPNSTs. All assays described below were performed on MPNST cell lines which were found to exhibit amplification of *cMET*, *RAC1* and *ROCK2*. All assays were repeated a minimum of three times and results are representative of all MPNST cell lines studied.

6.3.5.1 *cMET* Inhibition in MPNST derived cell lines

Concomitant amplifications of *HGF*, *MET*, and *PDGFRA* genes were revealed in MPNSTs, in a previous study by Mantripragada *et al*, (2008) indicating that there may be a putative role for the p70S6K pathway in NF1 tumorigenesis. The proto oncogene *c-met* encodes the cMET transmembrane tyrosine kinase receptor for which HGF (hepatocyte growth factor/hepatopoietin/scatter factor) is the main ligand (Cooper *et al*, 1984; Naldini *et al*, 1991). The paracrine signalling mechanism between epithelial cells expressing the cMET receptor, and mesenchymal cells in which the ligand HGF is expressed, is postulated to be important in processes including wound healing, embryogenesis, regeneration, and tumour progression. This indicates that alteration of cMET signalling may be important to MPNST progression from benign neurofibroma (Weidner *et al*, 1993; Rosen *et al*, 1994).

Table 6.4. Primer sequences function and results for all 14 genes and the endogenous control used in the relative quantification analysis of genes found to be differentially expressed by microarray.

Gene	Sense Primer Sequence (5'-3')	Antisense Primer Sequence (5'-3')	Size (bp)	Chromosome Location	Pathway/function	Gene Expression
B2M	CCCCCACTGAAAAAGATGAGTAT	CCGTGTGAACCATGTGACTTTG	50	15q21.1	Endogenous Control	Endogenous Control
CDK4	GCCTAGATTTCCTTCATGCC	GGTGACAAGTGGTGGAACAG	81	12q14.1	cell division kinase	Down-regulated
CMET	TTACATTCTGAAGCCGTTTTATGC	CCCAATGACCTGCTGAAATTG	51	7q31.2	Hepatocyte growth factor receptor	Upregulated
ITGB8	TGAACGTTGTGATATTGTTTCCAA	AAGCAAAGGCTGCTCAGTTGA	51	7p15.3	Integrin Pathway	Upregulated
LIMK1	GTGTCCATCCCAGCCTCATC	GCGTGGACTTTCAGTCTCCATT	51	7q11.23	RhoGTPase Pathway	Upregulated
MMP12	CTTTTGGACCTGGATCTGGC	ATGCACATTTCGATGAGGACG	51	11q22.2	Matrix metalloproteinase	Down-regulated
PDGFA	GTCTGCAAGACCAGGACGGT	TTCCTCGGAGTCAGGTCGAC	51	17p22.3	PDGF Receptor	Upregulated
PDGFRL	TTCAGCACCAAAGACGCAGT	GCAAGTGCTGGATAAAGGTCG	51	8p22	PDGF Receptor Ligand	Upregulated
PRKCA	TCGAACAACAAGGAATGACTTCA	CCTTTCCTTTGGAGTTTCGGA	51	17q24.2	RhoGTPase Pathway	Upregulated
PTK2	CCTCCAAATTGTCCTCCTACCC	TTATGACGAAATGCTGGGCC	51	8q24.3	RhoGTPase Pathway	Upregulated
PIK3CA	ACTTTGTGACCTTCGGCTTT	CAATTTCTCGATTGAGGATCTTT	89	3q26.32	P13K-PTK-RAS	No change/Down-regulated
RAC1	ACACCGAGCACTGAACTTTG	TGTCTGCACCTCCTAACTGC	75	7p22.1	RhoGTPase	Upregulated
ROCK2	AACCTGTCAAGCGTGGTAATGA	GTGCGGAGAAAAGAGAAGGAGA	51	2p25.1	RhoGTPase Pathway	Upregulated
TRIO	AACCAAAGAGAGAGTGAAGCTATTGATA	CTGGCTGATGGCTTTTGTGA	51	5p15.2	RhoGTPase Pathway	Down-regulated
TOP2A	ATGGGAAGAGCTGGTGAGAT	TCACCTTTCAGCCTGATTTG	78	17q21.2	DNA topoisomerase	Down-regulated

6.3.5.1.1 Cell line treatment with cMET inhibitors

Twenty-four hours prior to treatment, MPNST cell lines (ST8814, SNF96.2 and T532) were seeded at a concentration of $2x10^6$ in 6 well plates and grown in medium as described in section 2.2.2. On the day of treatment, cells were serum starved for 4 hours in 2ml of DMEM+0.1% FBS and 1% Pen/strep. Following serum starvation, fresh starvation medium was added to remove residual HGF and other growth factors secreted by the cells. After 1 hour, cells were treated with the *cMET* inhibitor PF-4217903 (Pfizer) at different concentrations (1μM, 10μM and 100μM) or SU11274 (Sigma) (10μM) for 30 minutes. Pilot studies completed by Dr Andrew Tee (Cardiff University) determined that 10μM SU11274 elicited the required inhibitory effect in MPNST cell lines. The media was then removed from each well and the appropriate cells were stimulated with HGF ($100ng/ml^2$) which was added as small drops to the plate and incubated for 1 hour. Cells were lysed as described in section 2.2.7.

6.3.5.2 RhoGTPase pathway shRNA knockdown

The RhoGTPase pathway regulates cellular processes such as cytoskeletal regulation, cell cycle regulation, cell polarity and cell migration indicating that it may be important for the migratory capacity and potential for metastasis in MPNST cells. Rac1 RhoGTPases are ubiquitously expressed small G proteins with similar modes of action as Ras (Reviewed by Karlsson *et al*, 2009). Activators of the RhoGTPase pathway include lysophosphatidic acid (LPA) and sphingosine-1 phosphate (S1P) which promotes the exchange of GDP for GTP which is catalysed by RhoGEFs including Vav3 and TRIO resulting in the activation of the RhoGTPase and subsequent downstream pathways (Liao *et al*, 2007). Similarly, the weak intrinsic GTPase activity of RhoGTPases is catalysed by GAPs, which results in the cessation of Rho signalling. An extra level of control is exhibited by Rho guanine nucleotide dissociation inhibitors (GDIs) which inhibit the activation of the GDP bound form of RhoGTPases so that it is unable to bind to its downstream effectors. Furthermore, GDIs promote shuttling of RhoGTPases between different membrane compartments (DerMardirossian and Bokoch, 2005). Rho kinases (ROCKs) are protein serine threonine kinases which act as downstream effectors of RhoGTPases such as RhoA, following Rho activation upon GTP charging.

6.3.5.3 short hairpin RNA (shRNA) plasmid preparation

RAC1 and *ROCK2* have not previously been investigated in MPNSTs although their normal functional roles indicate that they may be crucial to MPNST development. RNA interference (RNAi) is a natural process by which a gene can be targeted with high specificity to result in knockdown of its expression (Rao *et al*, 2009). This mechanism presents an unparalleled opportunity for personalised therapy by selectively targeting upregulated genes which may be crucial for the survival of tumour cells. Thus, methods of mediating RNAi have been developed which include short interfering RNA (siRNA), short hairpin RNA (shRNA) and bi-functional shRNA. There are advantages and disadvantages for all three methods, specifically; siRNA are simple to manufacture but are transient where as shRNA constructs allow for a higher level of potency and sustainability through the use of low copy numbers, importantly leading to less off-target effects (Rao *et al*, 2009).
Human shRNA for *RAC1* and *ROCK2* are available (Sigma) and thus shRNA against both genes were used in conjunction with cellular assays to knockdown the upregulated gene expression in MPNST-derived cell lines to determine their role in MPNST development. ShRNA were chosen based on whether they had been previously validated, the level of expected knockdown and the target sequence. Five shRNA clones for *RAC1* and *ROCK2* (Sigma) were received as glycerol stocks. Plasmid DNA was obtained following the protocol described in section 2.2.1. Large scale cultures were produced from starter cultures and DNA was subsequently extracted from these cultures using the method outlined in section 2.2.1.8.

6.3.5.4 shRNA transfection

$4x10^5$ MPNST cells (ST8814, SNF96.2, T532) were transfected in 35mm plates (Helena Biosciences, cat no: 93040) using 2.5µg of shRNA and the method outlined in section 2.2.2.6.2. A shRNA scrambled vector (Sigma) served as a control in all experiments. Stable knockdown was created as described in section 2.2.2.6.3.

6.3.6 *Western blot*

Prior to application of downstream assays, a western blot was run to analyse gene expression in addition to the knockdown efficiency of shRNA clones as described in section 2.2.7. Sample extracts were resolved on NuPAGE Novex 4-12% Bis-Tris gel (*RAC1* – 21kDa) and NuPAGE Novex 3-8% Tris-Acetate gels (*ROCK2* – 120kDa and phosphorylated-*cMET* – 120kDa). Prior to western analysis of *cMET*, Immunoprecipitation with the *cMET* antibody was required (section 2.2.6). Off target affects have been observed when using shRNA (Jackson *et al*, 2003). Consequently, multiple clones were used as the probability of getting off target affects in all clones is unlikely. Control blots of b-actin were used to determine whether the shRNA and inhibitors target other sequences in the cell lines studied (figure 6.1).

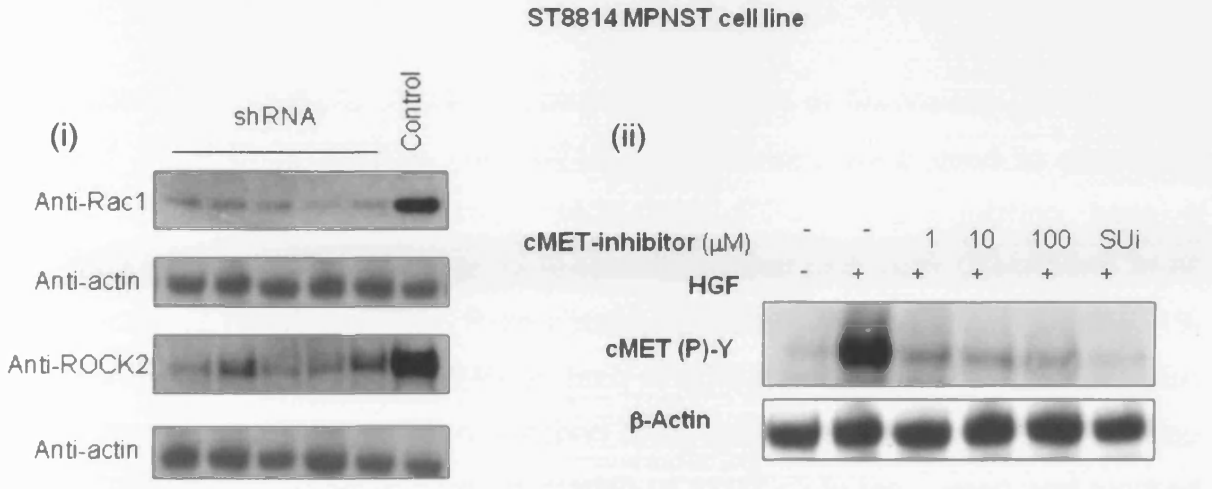

Figure 6.1. (i) Western blot assay of cell lines transacted with 5 *Rac1* and *ROCK2* shRNA clones in addition to one cell line transfected with a scrambled control. β-actin control blots were completed to ensure expression was unaffected in genes not targeted by the shRNA. *RAC1* and *ROCK2* shRNA generated ~50-88% reduction in RAC1 and ROCK2 protein expression. (ii) Western blot of phosphorylated cMET and β-actin in cell lines treated with *cMET* inhibitors: PF-4217903 (Pfizer) or SU11274 (Sigma). *cMET* inhibition reduced *cMET* expression in comparison to untreated controls. Control β-actin blots were used to confirm the absence of off target effects.

6.3.7 Cellular assays

6.3.7.1 shRNA wound healing assay

Confluent monolayers of MPNST cells were cultured as above in 35mm laminin-coated plates, serum starved with 1% FBS for 24 hours and then wounded using a pipette tip, drawn across the monolayer to create a gap in which no cells were present. Non-adherent cells were removed by washing twice with PBS. Cells were incubated in standard conditions as previously described and images of wound healing were taken at 0, 12 and 24 hours post wounding using a standard camera and microscope (Leica).

6.3.7.2 shRNA adhesion assay

35mm plates were initially coated in laminin (10mg/ml) or fibronectin (5mg/ml) and incubated at 37ºC for 1 hour. Both adhesive substrates were used to determine whether MPNST cells harbouring *RAC1* and *ROCK2* up-regulation have a preference for a specific substrate as is seen with other cell types (Nakagawa *et al*, 2001; Lock and Hotchin, 2009). Plates were washed twice with wash buffer (0.1% BSA in DMEM) and then blocked for an hour at 37ºC with blocking buffer (0.5% BSA in DMEM). Finally the plates were washed twice more with wash buffer and chilled on ice. Cells were seeded at a concentration of $1x10^6$ on to the coated and blocked plates and incubated at 37ºC in a humidified incubator for 30 minutes. The percentage of adherent cells was then determined by fixing the cells with methanol and acetone (1:1) for 20 minutes at -20°C. Cells were then stained with Crystal Violet (5mg/ml) in ethanol for 10 minutes, followed by a stringent wash with dH_2O until the water ran clear. Crystal violet stained cells were eluted with 1%SDS and the absorbance was read at 550nm on a Genova MK3 Lifescience Analyser (Jenway).

6.3.7.3 shRNA and c*MET* inhibition migration assay

For MPNST cell lines transfected with *RAC1* and *ROCK2* shRNA in addition to MPNST cell lines treated with inhibitors of *CMET*, transwell permeable supports with 6.5mm diameter inserts, 8.0µm pore size and a polycarbonate membrane (Corning

Incorporate, cat no: 3428) were used to perform migration assays. Cells were grown as previously described, then harvested by trypsinisation with Trypsin –EDTA. $1x10^6$ cells were washed three times and then resuspended in 1% FBS and DMEM. These cells were then seeded in the upper chamber of the Transwell and the lower chamber was filled with 600µl of standard culture medium (10% FBS) and 5mg/ml fibronectin, as an adhesive substrate. Cells were incubated at 37°C 5% CO_2 for 24 hours after which the Transwell was removed and the membrane was fixed and stained as described above. Cells which had not migrated were removed from the top chamber with a cotton swab. The percentage of migrated cells was evaluated by imaging on a standard microscope (Leica) and by the absorbance of crystal violet eluted with 1%SDS at 550nm on a Genova MK3 Lifescience Analyser (Jenway).

6.3.7.4 shRNA invasion assay

A similar protocol was used as in the migration assay for cell lines transfected with *RAC1* and *ROCK2* shRNA, but the top chamber of the Transwell was filled with 100µl of BD Matrigel Basement Membrane Matrix (1mg/ml). The Matrigel was incubated at 37°C for 4 hours to allow it to gel. Cells were then seeded and incubated as above for 3 days. The number of invaded cells was determined by fixation and staining, analysis under the microscope and elution of crystal violet with 1% SDS as above. Absorbance was read at 550nm on a Genova MK3 Lifescience Analyser (Jenway).

6.3.8 Statistical analysis

All statistical analysis was completed with SPSS (v16) using the independent samples T-Test. Absorbance measurements at 550nm from cell staining with crystal violet were converted into cell numbers following calibration of the spectrophotometer with a dilution series of cells.

6.4 Results

6.4.1 Analysis of molecular heterogeneity in MPNSTs

6.4.1.1 LOH analysis

10 MPNST tumours of varying sizes, derived from 10 different individuals, were independently sectioned and the LOH of five genes (*NF1*, *TP53*, *RB1*, *CDKN2A* and *PTEN*) was analysed for each section. LOH of the *NF1* gene was identified in all 10 tumours. In addition, LOH was noted for the *TP53* gene (five tumours, T196.22, T516, T517, T518 and T519), the *RB1* gene (four tumours, T196.22, T517, T518 and T519), the *CDKN2A* gene (four tumours, T196.22, T518, T524 and T525) and the *PTEN* gene (two tumours, T196.22 and T523) (table 6.3, figure 6.2). In only two of the ten tumours (T521 and T522) was LOH not found in at least one of the four loci other than *NF1* (i.e. *TP53*, *RB1*, *CDKN2A* or *PTEN*). Further, seven of the ten tumours (70%) were found to exhibit intra-tumoural molecular heterogeneity with respect to at least one gene, as defined by a varying level of LOH within the same tumour (T196.22, T516, T517, T518, T519, T523, T525) (i.e. between the subsections). Additional cytogenetic analysis was not available to confirm the LOH identified.

Some of the larger tumours (e.g. T521) were found to exhibit no molecular heterogeneity whereas some smaller tumours (e.g. T523) displayed molecular heterogeneity albeit only with respect to a specific gene. Additionally, five of the tumours analysed in this study were known to be high grade (T196.22, T517, T519, T522 and T525). Four of these high grade tumours in our cohort exhibited molecular heterogeneity (viz. T196.22, T517, T519 and T525) whereas such heterogeneity was absent in the remaining sample graded as high (T522). The extent of LOH in the *NF1* gene was also found to vary between sections of the same tumour. Thus, some sections displayed LOH over the entire *NF1* gene and surrounding regions whereas other sections of the same tumour only exhibited LOH within a portion of the *NF1* gene (table 6.5; T196.22, T522, T525).

6.4.1.2 Immunohistochemistry analysis of p53

IHC analysis of the tissue distribution of p53 was found to correlate broadly with the results of the LOH analysis (figure 6.3). Thus, different sections of the five MPNST tumours analysed were found to display differences in staining for p53 that closely matched the presence or absence of LOH for the *TP53* gene (table 6.3). For example, sections A, C and D of T196.22 displayed complete LOH of the *TP53* gene in the majority of MPNST sections and this was reflected in higher p53 expression as seen by IHC in these samples (figure 6.3, B and C). Conversely, section E (T196.22) showed no p53 expression by IHC peroxidase staining and this section was found not to display any LOH (figure 6.3, D). Additionally, section B (T196.22) showed lower levels of staining (figure 6.3 B) than that of T196.22 section C (figure 6.3 C) but more than that of T196.22 section E (figure 6.3 D). These results correlate with those of the LOH analysis in which section T196.22 section B was found to have 50% LOH but section T196.22 section C had 100% LOH and section E (T196.22) had no LOH. p53 positivity by IHC has previously been reported in 60% of MPNSTs whereas neurofibromas are p53 immunonegative (Liapis *et al*, 1999).

Table 6.5. Extent of LOH in 5 genes (*NF1*, *TP53*, *RB1*, *CDKN2A* and *PTEN*) in 10 MPNSTs

Tumour	Tumour Number	Gene Analysed and Extent of LOH				
		NF1	***TP53***	***RB1***	***PTEN***	***CDKN2A***
1	T196.22	LOH: D17S799-D17S1822 (17p11.2-17q25.2)	LOH: TP53 Inv-D17S938 (TP53 Intron 1-5'TP53)	LOH: D13S118-D13S119 (5'-3'*RB1*)	LOH: D10S215-D10S2491 (10q22-23-10q23-23)	LOH: D9S304-D9S748 (9p21.1-9q32)
2	T516	LOH: IVS27-IVS38 (Intron 27-38)	LOH: TP53 Inv-TP53 E:6 (TP53 Intron 1-Exon6)	No LOH	No LOH	No LOH
3	T517	LOH: IVS27-IVS38 (Intron 27-38)	LOH: TP53 Inv-TP53 E:6 (TP53 Intron 1-Exon6)	LOH: RB1.2-RB1.26 (Exon2-26)	No LOH	No LOH
4	T518	LOH: J1J2-3'NF1 (Intron 27-38)	LOH: TP53 Inv-TP53 E:6 (TP53 Intron 1-Exon6)	LOH: RB1.2-RB1.26 (Exon2-26)	No LOH	LOH: D9S304-D9S748 (9p21.1-9q32)
5	T519	LOH: IVS38-3'NF1 (Intron 38-3'*NF1*)	LOH: TP53 Inv-TP53 E:6 (TP53 Intron 1-Exon6)	LOH: D13S917-RB1.26 (5'RB1-Exon 26)	No LOH	No LOH
6	T521	LOH: J1J2-EV120 (Intron 27-38)	No LOH	No LOH	No LOH	No LOH
7	T522	LOH: D17S799-3'NF1 (17p11.2- 3'*NF1*)	No LOH	No LOH	No LOH	No LOH
8	T523	LOH: J1J2-D17S250 (Intron 27-3'*NF1*)	No LOH	No LOH	LOH: D10S215-D10S2491 (10q22-23-10q23-23)	No LOH
9	T524	LOH: J1J2-3'NF1 (Intron 27-38)	No LOH	No LOH	No LOH	LOH: D9S304-D9S748 (9p21.1-9q32)
10	T525	LOH: D17S799-D17S1822 (17p11.2-17q25.2)	No LOH	No LOH	No LOH	LOH: D9S304-D9S748 (9p21.1-9q32)
Total with LOH		10	5	4	2	4

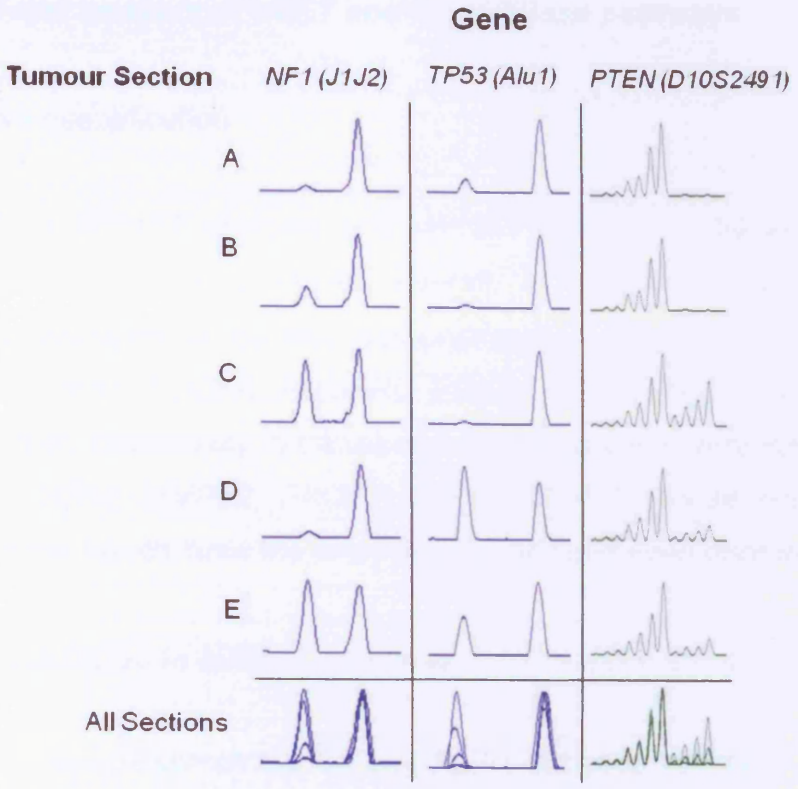

Figure 6.2. LOH patterns in three genes (*NF1*, *TP53* and *PTEN*) within five sections (A-E) derived from a single tumour (T196.22). 'All sections' represents the overlaid LOH results from all five sections (A-E) illustrating the different levels of gene-specific LOH observed within a single tumour.

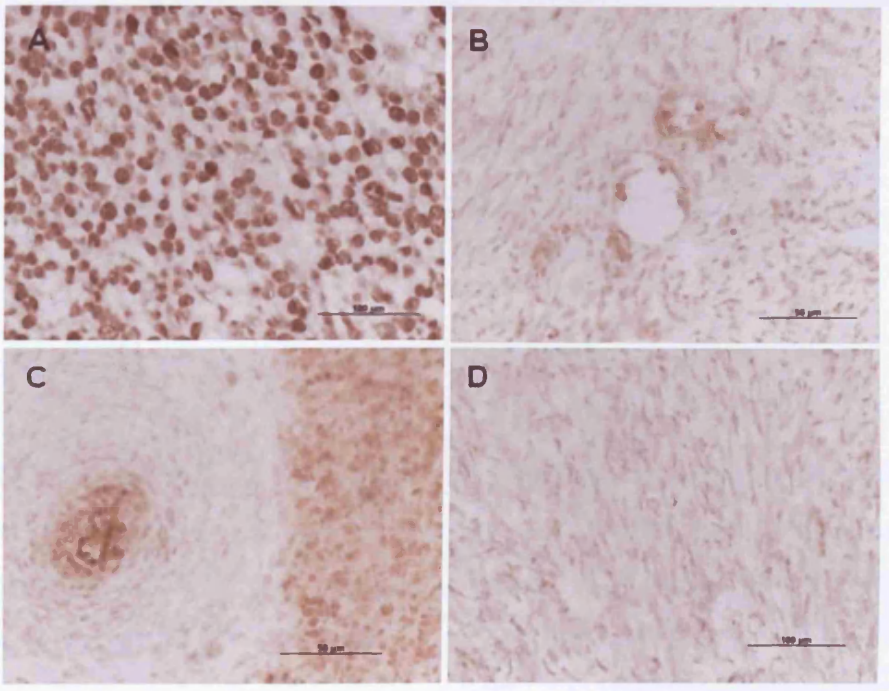

Figure 6.3. Immunohistochemical analysis of *TP53*. **A.** Positive control; Breast carcinoma localised positive stain for *TP53*. **B.** T196.22,B5; Slight localised positive *TP53* staining in a few cells. **C.** T196.22,C5; Localised positive and negative staining for *TP53*. **D.** T196.22,E5; Lack of *TP53* immunohistochemical staining.

6.4.2 Functional analysis of cMET and RhoGTPase pathways

6.4.2.1 Relative quantification

Whilst not all 14 MPNST samples and MPNST cell lines exhibited altered gene expression in every gene analysed, overall, 9/14 genes analysed by qPCR (excluding the endogenous control) demonstrated a trend towards amplification; *CMET, ITGB8, LIMK1, PDGFA, PDGFRL, PRKCA PTK2, RAC1* and *ROCK2* (table 6.4 and figure 6.4). Conversely, 5 genes demonstrated either very little amplification, or a deletion; *CDK4, MMP12, PIK3CA, TRIO, TOP2A.* These results were fully correlated with the results from the array which was conducted prior to this study.

6.4.3 CMET inhibition in MPNST cell lines

Treatment of malignant MPNST-derived cell lines (ST8814, SNF96.2 and T532) with *cMET* inhibitors PF-4217903 (Pfizer) and SU11274 (Sigma) at different concentrations (1μM, 10μM and 100μM) resulted in a reduction in activated cMET (phosphorylated cMET) as determined by a reduction in phosphorylated cMET protein levels by western blot at all concentrations of inhibitors (figure 6.1). Inhibition of *cMET* by PF-4217903 produced a lesser reduction in gene expression at all concentrations than was seen with the inhibitor SU11274. Treatment with different concentrations of PF-4217903 did not produce a significant dosage-dependent effect.

6.4.3.1 *CMET* migration assay

As SU11274 had the most potent affect on *cMET* gene expression in MPNST cell lines, migration assays were also performed on MPNST cells following treatment with the inhibitor. Inhibition of *cMET* resulted in a significant decrease in cell migration in comparison to untreated controls ($p=0.043$) (figure 6.5). Results are representative of all MPNST cell lines analysed.

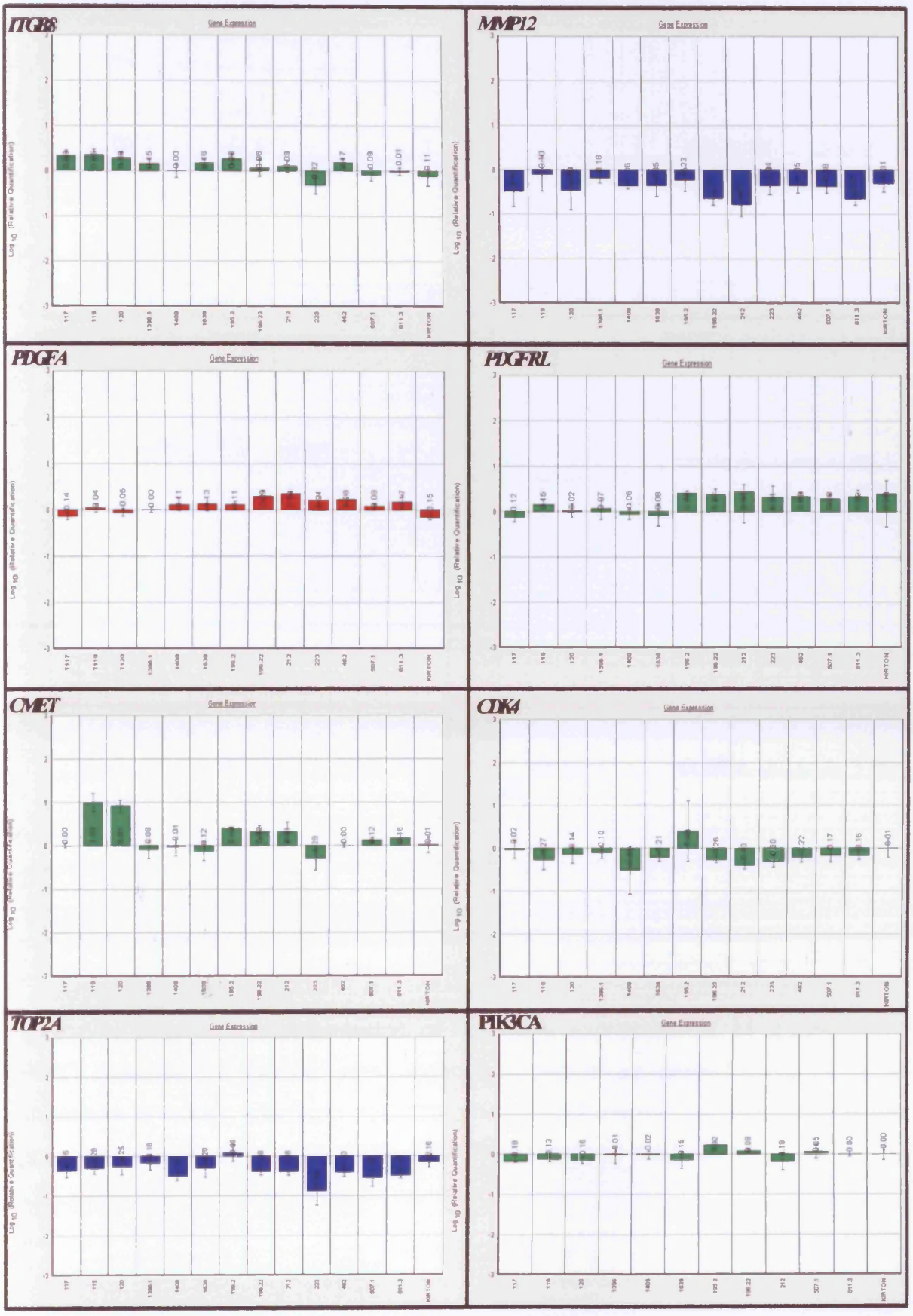
ITGB8
Gene Expression
MMP12
Gene Expression
PDGFA
Gene Expression
PDGFRL
Gene Expression
CMET
Gene Expression
CDK4
Gene Expression
TOP2A
Gene Expression
PIK3CA
Gene Expression

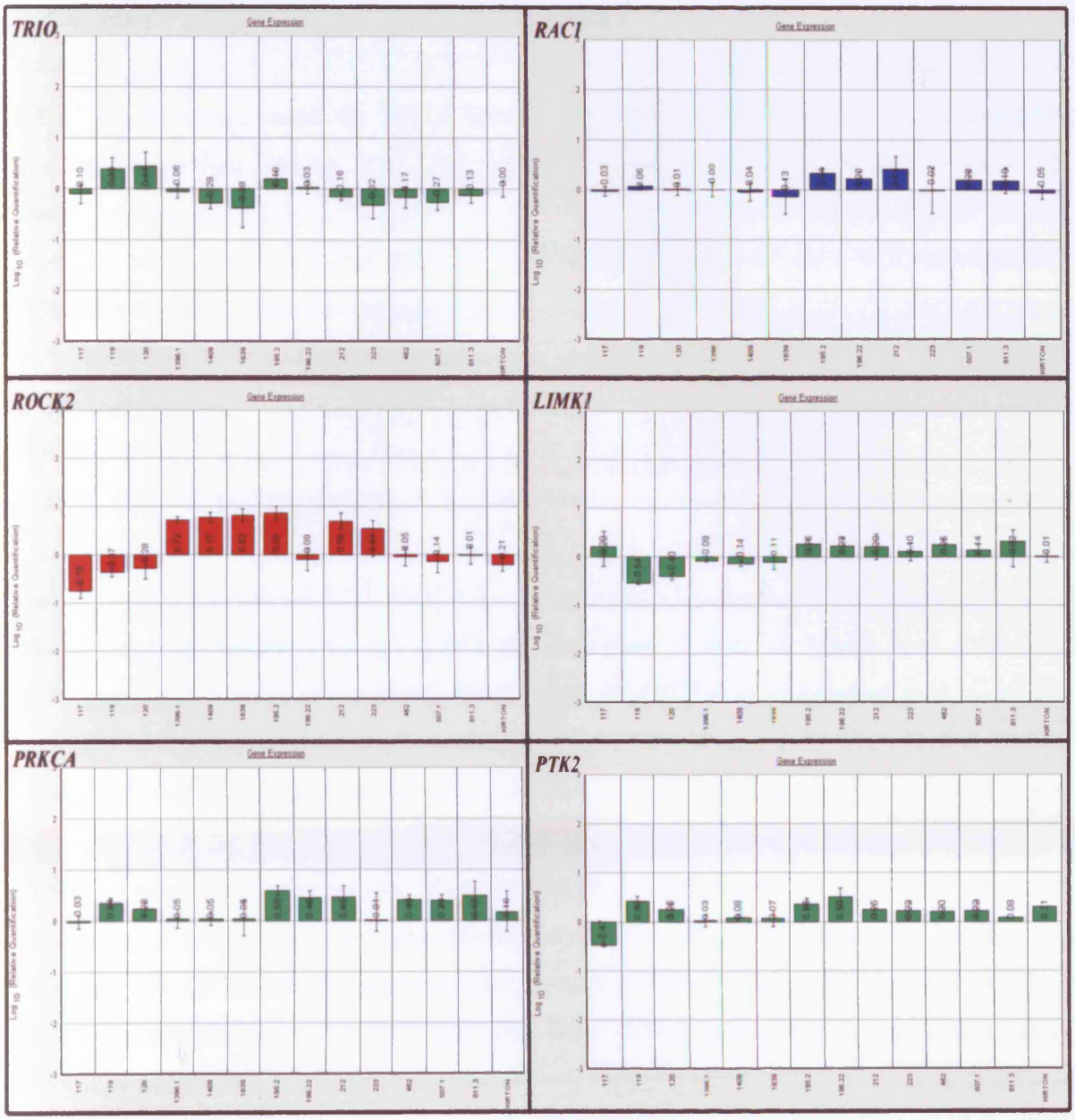

Figure 6.4. Graphical representation of the gene expression of 14 genes in 14 MPNST samples. All genes were originally found to be altered in MPNSTs in comparison to benign plexiform neurofibromas by microarray analysis. Graphs are representative of findings in MPNSTs and MPNST-derived cell lines.

6.4.4 RAC1 and ROCK2 targeted knockdown

All of the 5 clones used for *RAC1* knockdown in ST8814 cell lines produced some knockdown effect (figure 6.1). No off target affects were observed (figure 6.1). Densitometry was completed with image J software to quantify the signal from all western blots. Two *RAC1* clones (TRCN000000977, 50% KD and TRCN000000978, 80% KD) and two *ROCK2* clones (TRCN000004871, 50% KD and TRCN000004872, 80% KD) were selected for use in the wound healing, migration, invasion and adhesion assays.

6.4.4.1 Wound healing assay

Cells transfected with *RAC1*, *ROCK2* and scrambled control shRNA were seeded on laminin and wounded with a pipette tip. Between 0 and 12 hours post wounding, cells migrated across the wound. *RAC1* and *ROCK2* wound healing was, however, reduced in comparison to control scrambled shRNA (figure 6.6). Due to the kinetics of wound healing, by 24 hours wound healing was complete on all shRNA cell lines as evidenced by the lack of any visible gap in the cell monolayer. MPNST cell doubling time is approximately 20.44 hours (ST8814) (Vahidnia *et al*, 2007). Wound healing is unlikely to have been affected by cell proliferation as wound healing was observed by 12 hours in the scrambled control cell line. Wound healing occurred 12-16 hours earlier in the control cell line than *RAC1* and *ROCK2* cell lines (16-24 hours). Results are representative of all cell lines (ST8814, SNF96.2 and T532). All experiments were repeated a minimum of 3 times.

6.4.4.2 Adhesion assay

Cells were transfected with *RAC1*, *ROCK2* and control shRNA on both Laminin and fibronectin. Adhesion on both laminin and fibronectin is significantly increased in samples containing *RAC1* and *ROCK2* 80% knockdown in comparison to cell lines transfected with the scrambled control shRNA ($p=0.02$) and ($p=0.05$) respectively (figure 6.7 i-iv). *RAC1* knockdown (50% and 80%) results in more cell adhesion than *ROCK2* knockdown (50% and 80%) but this difference is not significant ($p=0.07$). There was no significant difference between adhesion on fibronectin or on laminin in

cell lines carrying both *RAC1* and *ROCK2* knockdown (p=0.2). Replicates were produced and results are representative of all cell lines studied (ST8814, SNF96.2 and T532).

6.4.4.3 Migration assay

Migration of cells transfected with *RAC1*, *ROCK2* and control shRNA was assessed by seeding of cells on polycarbonate membranes followed by assessment of cell numbers through crystal violet staining. Migration of cells was significantly reduced in cell lines carrying *RAC1* and *ROCK2* 80% knockdown in comparison to cells transfected with a scrambled vector (p=0.03 and p=0.05 respectively) (figure 6.8). The reduction in migration was similar in cells transfected with both *RAC1* and *ROCK2*. About $1.34x10^6$ fewer cells (approximately 43% reduction) migrated through the membrane in the cell line with the *RAC1* 80% knockdown and around $1.3x10^6$ fewer cells (approximately 40% reduction) migrated in the *ROCK2* 80% knockdown cell line compared to the scrambled control. Results are representative of all cell lines and replicates (ST8814, SNF96.2 and T532).

6.4.4.4 Invasion assay

Invasion of cells transfected with *RAC1*, *ROCK2* and control shRNA was determined by seeding cells on Matrigel basement membrane on polycarbonate membranes. A significant reduction in the invasion activity of cell lines transfected with both *RAC1* and *ROCK2* shRNA (80% KD) was observed in comparison to the scrambled control (p=0.05 for both) (figure 6.9 and figure 6.10). *RAC1* and *ROCK2* knockdown elicited similar reduction of invasive potential. Approximately $1.85x10^6$ fewer cells (approximately 54% reduction) invaded the Matrigel and membrane in the cell line with the *RAC1* 80% knockdown and about $1.8x10^6$ (approximately 28% reduction) in the *ROCK2* 80% knockdown compared to the control scrambled cell line. All experiments were repeated and results were comparable in all cell lines (ST8814, SNF96.2 and T532).

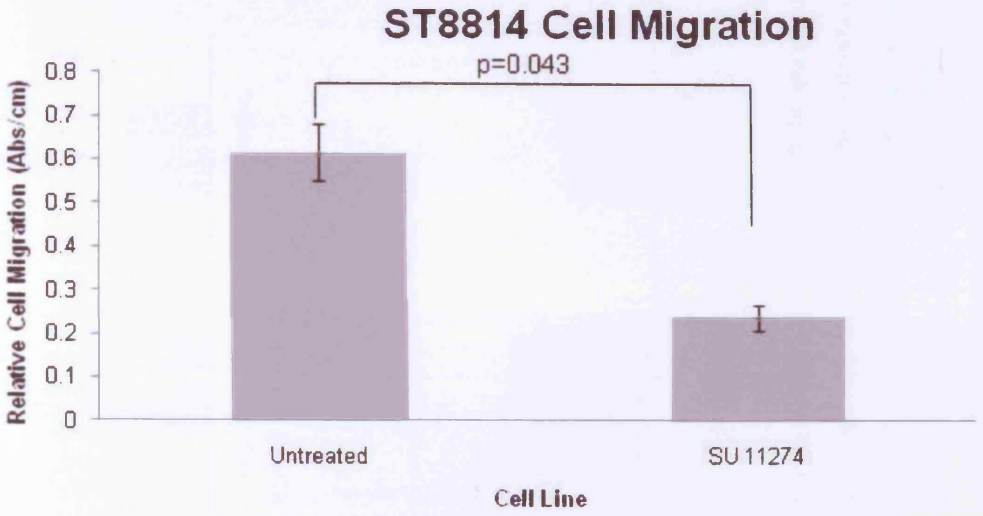

Figure 6.5. Migration of ST8814 cells following treatment with *cMET* inhibitor SU11274. Migration of MPNST cell lines was significantly reduced following *cMET* inhibition (p=0.043)

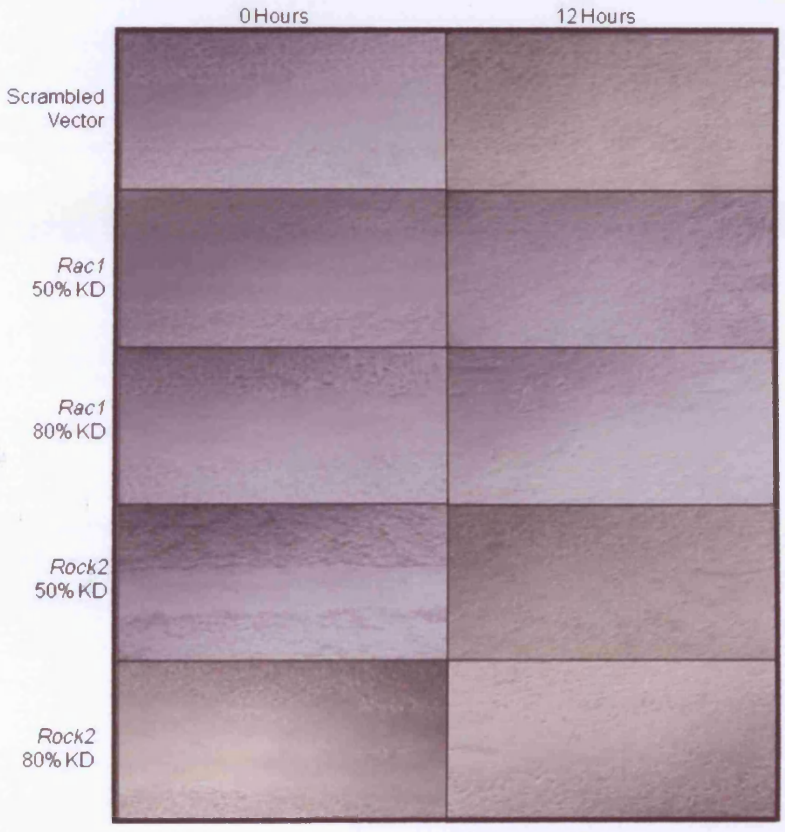

Figure 6.6. Wound healing assay on MPNST cell line ST8814. Cells were seeded on laminin, synchronised in 1%FBS for 24hours and wounded with a pipette tip. Wounds were followed up for 24hours. Reduction in the rate of wound healing can be seen in the cell lines carrying *RAC1* and *ROCK2* knockdown. Cells were imaged on a microscope at x10 magnification (Leica).

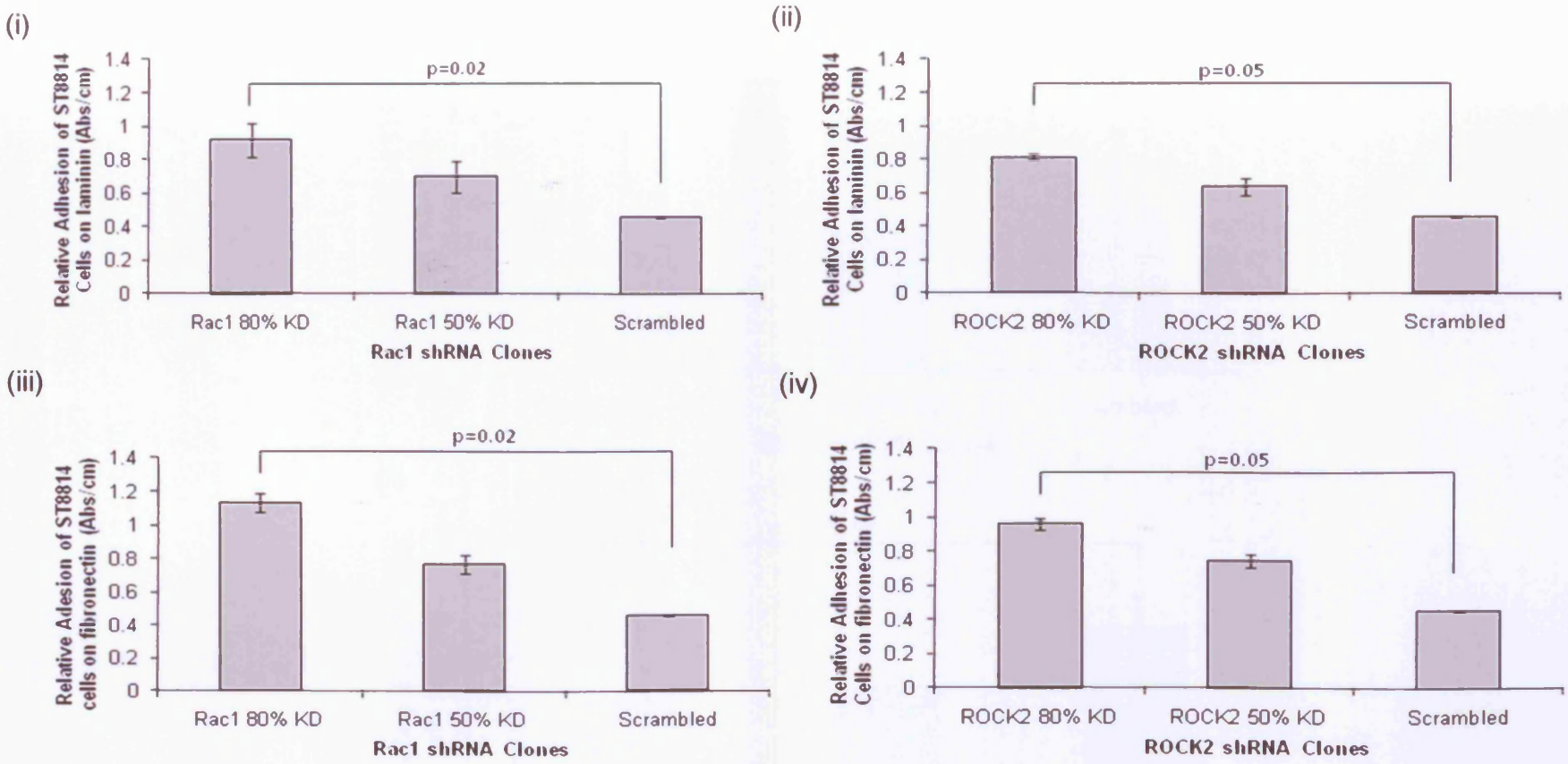

Figure 6.7 Adhesion assay on MPNST cell line ST8814. (i) ST8814 cells transfected with *RAC1* shRNA seeded on laminin. (ii) *ROCK2* shRNA transfected cells seeded on laminin. (iii) Cells transfected with *RAC1* shRNA on fibronectin (iv) *ROCK2* shRNA transfected cells seeded on fibronectin. Adhesion is significantly increased in samples containing *RAC1* and *ROCK2* knockdown in comparison to cell line transfected with the scrambled control shRNA (p=0.02) and (p=0.05) respectively. *RAC1* knockdown results in more cell adhesion than *ROCK2* knockdown but this difference is not significant (p=0.07). No significant difference between adhesion on fibronectin or laminin was observed in cell lines carrying both *RAC1* and *ROCK2* knockdown (p=0.2).

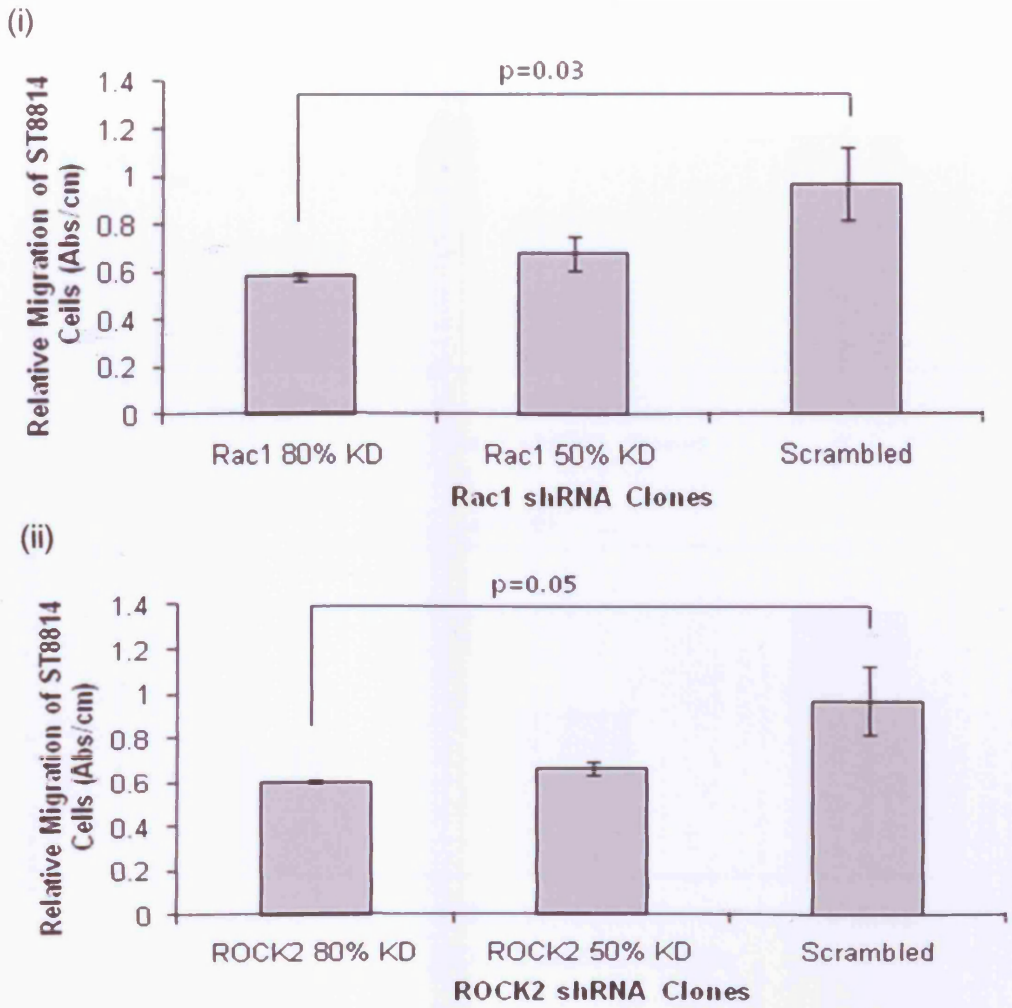

Figure 6.8. Migration assay on ST8814 cell lines. (i) Migration of cells transfected with *RAC1* shRNA. (ii) Migration of cells transfected with *ROCK2* shRNA. Migration of ST8814 cells was significantly reduced in cell lines carrying *RAC1* and *ROCK2* knockdown in comparison to ST8814 cells transfected with a scrambled vector (p=0.05 and p=0.03 respectively).

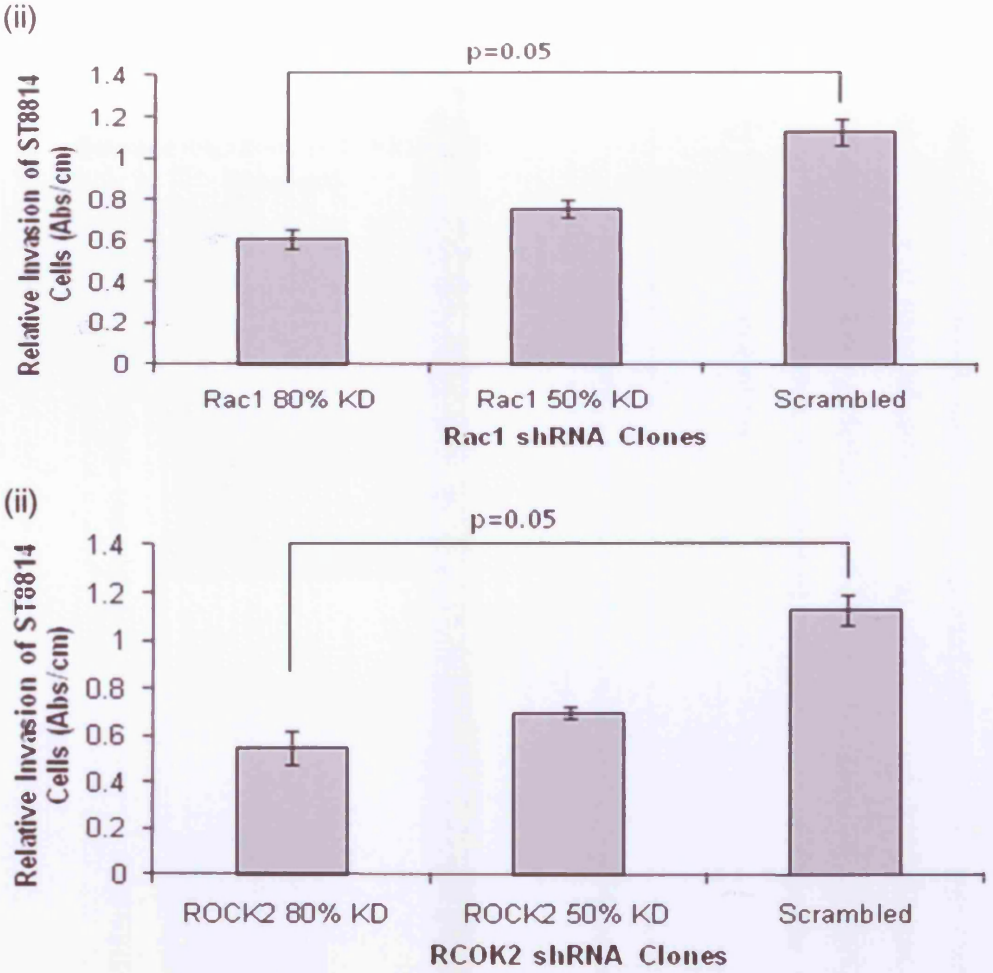

Figure 6.9. Invasion assay on ST8814 cell lines (i) Invasion of cells transfected with *RAC1* shRNA. (ii) Invasion of cells transfected with *ROCK2* shRNA. The invasion activity of ST8814 cell lines was significantly reduced in both cell lines with *RAC1* and *ROCK2* knockdown compared to the scrambled control (p=0.05 for both).

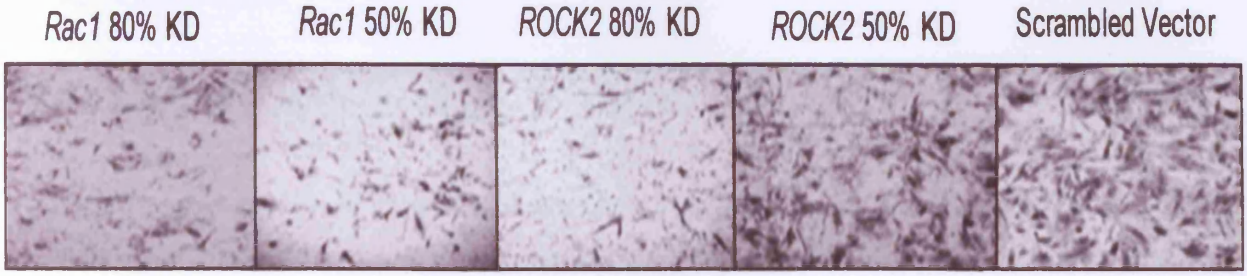

Figure 6.10. Invasion assay on ST8814 cell lines transfected with *Rac1*, *ROCK2* and scrambled control shRNA. Cells were stained with crystal violet (5mg/ml) and images were taken at x10 magnification (Leica). *RAC1* and *ROCK2* knockdown elicited a reduction in the invasive potential of ST8814 cell lines as evidenced by the lack of *RAC1* and *ROCK2* shRNA transfected cells on the underside of the membrane following 3 days of incubation.

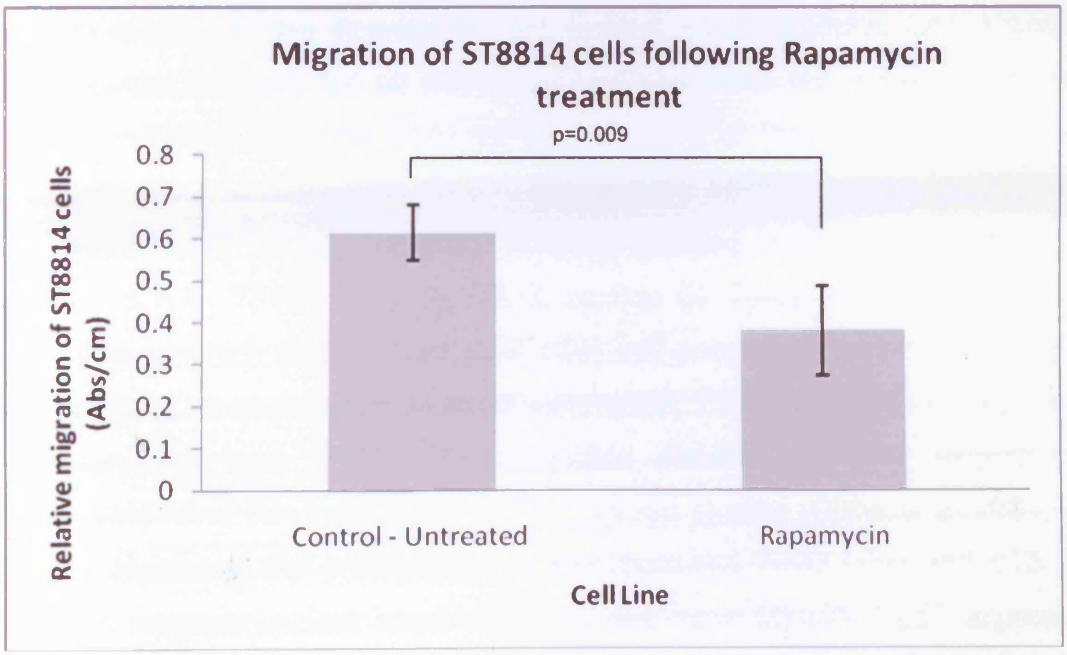

Figure 6.11. Migration of MPNST cells (ST8814) following treatment with Rapamycin. Migration was significantly reduced in comparison to untreated controls (p=0.009).

6.5 Discussion

6.5.1 Molecular heterogeneity in MPNSTs

Cellular heterogeneity is a well known complication in the analyses of NF1-associated tumours. By contrast, heterogeneity at the molecular level in NF1-associated tumours has scarcely been addressed. In this study, the extent of molecular heterogeneity within and between 10 MPNSTs, derived from 10 unrelated NF1 patients was determined by examining the differences in the levels of LOH at the *NF1*, *TP53*, *RB1*, *CDKN2A* and *PTEN* gene loci. The results of this study indicated that 70% of the MPNST tumours analysed exhibit molecular heterogeneity between sections of the same tumour sample. This heterogeneity was especially evident in the case of those sections from the same tumour which were anatomically adjacent to each other prior to dissection but which had nevertheless been found to differ with respect to the degree of LOH. Indeed, some sections were found to be entirely devoid of LOH for all five gene loci analysed, but were located beside sections exhibiting complete LOH for one or more of these genes (e.g. T196.22 section A4). Prior to dissection, in a number of the MPNST tumour sections under study, there were clearly defined centrally located tumour portions (T196.22 subsection 5 A-E, T516 section B, T518, section B). These areas corresponded to the sections in which different levels of LOH and subsequently *TP53* staining were identified (T196.22 section B5; T196.22 section C5; T196.22 section E5, figure 6.3)
The observation that *TP53* LOH correlates directly with p53 expression, as demonstrated here, has been observed in previous studies (Götte *et al*, 2001; Otis *et al*, 2002). However, the precise relationship between *TP53* LOH and p53 protein expression remains unclear since some studies have identified p53 expression in tumours which have no *TP53* LOH. This may be explicable in terms of the presence of two *TP53* alleles, one mutant and the other wild-type in a given cell type, resulting in the production of both wild-type and mutant p53 protein. As a consequence, p53 may be detected by IHC even in the absence of p53 function. This suggests that in the context of evaluating tumour heterogeneity, IHC analysis is unlikely to be as reliable as other molecular genotyping methods. IHC analysis could therefore be replaced by more accurate methods including AQUA (Camp *et al*, 2002; McCabe *et al*, 2005) and tissue analysis with multiplex quantum dots (QD) (Liu *et al*, 2010), to

yield a digital map of molecular and cellular heterogeneity to improve the sensitivity of detection and the prediction of a therapeutic response.

p53 is associated with malignant transformation in NF1-associated tumours (Upadhyaya *et al*, 2008) and LOH of the *TP53* gene was identified in 5 of the 10 tumours under study (table 6.3). *TP53* has also been found to manifest in intra-tumoural molecular heterogeneity with respect to its mutation in other tumour types, including breast cancer (Lennington *et al*, 1994; Clark *et al*, 2011). In pancreatic cancer, molecular heterogeneity is evident in cells with different capacities for initiating metastasis (Campbell *et al*, 2010) suggesting that molecular heterogeneity may well prove to be the rule rather than the exception. If the molecular heterogeneity identified in this set of tumours was to emerge as relevant to MPNST development, we may have to revise our view not only of MPNST tumour biology but also of the basic processes underlying MPNST tumorigenesis.

It might be assumed that, owing to the large size of some of the MPNST tumours, they would be divisible into a larger number of sections thereby allowing molecular heterogeneity to be assessed more clearly. However, the size of the tumour was not found to correlate with the level of molecular heterogeneity detected (table 6.2 and table 6.3). It is, however, possible that intra-tumoral molecular heterogeneity could be related in some way to the grade of tumour, at least for those tumour samples analysed here (table 6.2). A larger study is clearly warranted in order to determine whether these results could be replicated in a larger set of NF1-associated MPNSTs. However, such a study will be laborious and time consuming to set up, especially as MPNSTs are quite rare.

The pathological diagnosis of an MPNST is usually held to represent the 'gold standard' for the purposes of analysis and currently relies on the examination of not just one, but a number of different sections. The results of this study and from other previous studies on solid tumours (Alizadeh *et al*, 2000; Whitehall *et al*, 2002; Stingl *et al*, 2007), are broadly illustrative of the importance of careful dissection in the analysis of large tumours and suggests that in the interest of diagnostic accuracy, molecular analysis should be performed on several tumour sections alongside a pathological diagnosis. The clear implication for those studies that involve microarray analysis is that replicates across several sections would be advisable.

The results of this study therefore have important implications for molecular studies of NF1-associated tumour specimens. Although molecular techniques currently

employed in mutation detection in large solid tumours are adequate for identifying and characterising the underlying molecular and genetic aberrations, the potential for molecular heterogeneity means that a single dissected piece of tumour should not be assumed to be representative of the tumour as a whole; as a consequence, some somatic mutations may well be missed.

Genomic instability and high intra-tumoral genetic heterogeneity may synergize so as to accelerate the evolutionary processes within the tumour leading to the development of resistance to cytotoxic and targeted anti-cancer drugs. Improvements clearly need to be made to the treatment regimes for patients with MPNSTs. The results from this study indicate that whilst drugs can be developed *in vitro* that would be capable of targeting the genes involved in the genesis of MPNSTs; the efficacy of these drugs is likely to be somewhat limited unless the cellular, molecular and architectural heterogeneity of the tumour are considered alongside the tumour microenvironment. This study represents the first systematic analysis of molecular heterogeneity in MPNSTs associated with NF1. The molecular heterogeneity evident at a number of different gene loci indicates that there is an urgent need not only for the integration of molecular and morphological biomarkers in cancer diagnosis but also for the development of specific treatments for NF1-associated MPNSTs.

6.5.2 Functional analysis of cMET and RhoGTPase pathways

Translation of genetic findings into functionally meaningful results is not normally available, with only a few reports of functional studies on NF1-associated MPNSTs in the literature based on array findings. Miller *et al*, (2009) identified SOX9 as a potential biomarker as it was strongly expressed in NF1-related tumours and resulted in MPNST cell death when the expression was reduced. Furthermore, anti-TNC antibodies, (already used successfully in clinical trials to treat malignant human gliomas, (Levy *et al*, 2007)) and antisense inhibitors of *miR-10b* have been used in MPNST cells producing a reduction in cell proliferation, migration and invasion (Chai *et al*, 2010). It is therefore suggested that assessment of the genetic composition of individual tumours and subsequent targeted therapy could be an appropriate new therapeutic strategy for NF1.

All of the 14 genes analysed by relative quantification in this study have important implications for tumorigenesis and malignancy in NF1. However, amplification of the cMET and RhoGTPase pathways in particular, is a highly significant finding. Indeed, *cMET* and its ligand *HGF* have been previously found to be altered in MPNSTs (Mantripragada *et al*, 2009) and moreover, 6 genes from the RhoGTPase pathway including *RAC1* and *ROCK2* were all altered in the cohort studied, demonstrating that this pathway may be of significance to MPNST pathogenesis. Overexpression of genes in the cMET/RhoGTPase pathway in MPNST cell lines provides a valuable opportunity to functionally evaluate how modification of these genes may result in NF1 malignant progression and subsequent metastasis.

6.5.2.1 cMET pathway

In this study, small molecule inhibition of *cMET* in MPNST cell lines, followed by cellular migration assays demonstrated a reduction in *cMET* gene expression which was correlated with a decrease in the migratory capacity of these cell lines. Thus, the results of this study signify that increased *cMET* copy number and gene expression in MPNSTs is likely to be contributing to the malignant and metastatic potential of MPNST cells.

The combined activation of two genes: *HGF* and its receptor *cMET* are also known to be altered in the development of a number of other solid tumours (Jiang *et al*, 1999). NIH3T3 cells co-transfected with *cMET* and *HGF* was found to result in tumorigenesis as evidenced *in vitro* by increased cell motility, collagenase activity, and additionally by invasiveness and metastatic activity *in vivo* (Rong *et al*, 1992; Rong *et al*, 1993; Rong *et al*, 1994). HGF has been shown to be a strong mitogen for rodent Schwann cells and may act as a paracrine growth factor or contribute to an autocrine signalling loop (Krasnoselsky *et al*, 1994). Importantly *HGF* and *cMET* alterations have been detected in benign neurofibromas (Krasnoselsky *et al*, 1994; Rao *et al*, 1997; Watanabe *et al*, 2001) and MPNSTs (Rao *et al*, 1997; Fukuda *et al*, 1998; Watanabe *et al*, 2001; Mantripragada *et al*, 2008). Additionally there was a significant difference in the degree of *cMET* and *HGF* expression in benign and malignant tumours, with MPNSTs demonstrating a higher level of gene expression (Rao *et al*, 1997; Mantripragada *et al*, 2008). Co-localisation of HGF and cMET expression in a number of MPNSTs has also been suggested to be indicative of

biologically aggressive tumours (Rao *et al*, 1997) Concomitant overexpression of both *cMET* and *HGF* in addition to *PDGFRA* may therefore promote NF1 tumorigenesis and malignancy through the formation of an autocrine signalling loop, also indicating that there may be a putative role for the p70S6K pathway in NF1 tumorigenesis. Despite numerous associations of the cMET pathway with NF1 tumorigenesis, this is the first study to functionally define the role of *cMET* upregulation in MPNST tumorigenesis. This study indicates that inhibition of cMET receptor activation with small molecular inhibitors such as SU11274 and PF-4217903 in NF1-associated tumours may be an attractive prospect for personalised therapy of MPNSTs harbouring cMET activation.

However, it is also essential to consider that specifically targeting the gene which is amplified in MPNSTs may not efficiently inhibit tumour growth due to complex feedback mechanisms and signalling loops which exist within cells. There are a number of downstream signalling pathways which are activated by cMET including ERK1/2, STAT3, RhoGTPase (see below), and AKT (Birchmeier *et al*, 2003). As part of pilot tests for this study, MPNST cells were also treated with the mTOR inhibitor rapamycin, using the same methods as described for the *cMET* inhibition analysis (in collaboration with Dr Andrew Tee, Cardiff University). Interestingly, there was a significant decrease in the migratory activity of the MPNST cell lines following rapamycin treatment ($p=0.009$) (figure 6.11). This indicates that pathways downstream of cMET including the mTOR/AKT pathway may also be important in malignant progression.

In a recent study by Banerjee *et al* (2010) using a cell-based high-throughput chemical library screen of *NF1*-deficient MPNST cells, they identified hyper-activation in signal transducer and activator of transcription-3 (STAT3) in *NF1*-deficient primary astrocytes, neural stem cells, mouse glioma cells, and human MPNST cells. STAT3 is known as a multifunctional transcription factor which cycles between the cytoplasm and nucleus in its un-phosphorylated basal state (Liu *et al*, 2005). Following activation of cMET as a result of binding of the ligand HGF, STAT3 is recruited to cMET and is consequently phosphorylated resulting in its nuclear accumulation (Boccaccio *et al*, 1998). Further dissection of the activation of STAT3 in *NF1*-deficient cell lines concluded that STAT3 hyper-activation occurred through Ser^{727} phosphorylation which consequently resulted in increased cyclin D1 expression (Banerjee *et al*, 2010). STAT3 regulation in *NF1*-deficient cells of murine

and human origin was also noted to occur in a TORC1- and Rac1-dependent manner indicating that STAT3 could also represent an attractive prospect for therapy of NF1 associated MPNSTs (Banerjee *et al*, 2010). Based on the findings presented here, pilot tests employing *STAT3* shRNA to knockdown *STAT3* in MPNST cell lines is currently ongoing.

6.5.2.2 RhoGTPase pathway

Amplification of both *RAC1* and *ROCK2* was identified by microarray and relative quantification in MPNSTs. Cell migration is a critical process which upon deregulation can result in pathological consequences including tumour angiogenesis and metastasis. Migration, invasion, wound healing and adhesion assays have been previously employed to assess tumour cell invasion and its modulation. These assays were utilised in this study to determine the functional effect of increased *RAC1* and *ROCK2* copy number and expression on MPNST cell lines. A significant reduction in wound healing, migratory and invasive behaviour in addition to a significant increase in adhesion of cell lines was identified in MPNST cell lines following targeted knockdown of both *RAC1* and *ROCK2* with shRNA. Rapid wound healing (cell spreading) as observed in the MPNST cells indicates that these cells are highly migratory. This assumption was confirmed with migration and invasion assays which demonstrated that MPNST cells are able to migrate towards a chemo-attractant, even through basement membrane matrix. Such cells may therefore be able to invade neighbouring tissues during the process of metastasis. Furthermore, MPNST cells transfected with scrambled shRNA are less adhesive than cells harbouring a knockdown of *RAC1* and *ROCK2* further suggesting that they would be able to migrate to other sites in the process of metastasis. As outlined below, the results presented here, in concert with the known properties of the members of the RhoGTPase pathway, indicate that deregulation of RhoGTPase signalling may play an important role in the malignant potential of cells harbouring biallelic *NF1* inactivation.

6.5.2.2.1 Targeting RAC1

Alteration of the RhoGTPase RAC1 has been identified in multiple solid cancer types including testicular, gastric and breast cancer in addition to chronic myelogenous

leukaemia (CML) and primary human schwannoma cells (supplementary table 10) (Harnois *et al*, 2003; Kaempchen *et al*, 2003). Expression of the fusion protein Bcr–Abl is the major determinant of CML development and it has been demonstrated to activate RhoGTPases including *RAC1* (Harnois *et al*, 2003). Moreover, CML can be induced in mice deficient in *Rac1*, *Rac2* or both (Thomas *et al*, 2007). Indeed, *in vitro*, *RAC1* and *RAC2* are shown to be crucial for the growth promoting effect of the Bcr–Abl fusion protein on haematopoietic precursor cells (Thomas *et al*, 2007).

Evasion of cell death by alteration of expression of genes involved in survival is a key mechanism by which cancer cells can persist. Activation of RhoGTPases such as *RAC1* has been show to result in increased apoptosis in a cell specific manner, for example promoting Fas dependent apoptosis of T cells (Ramaswamy *et al*, 2007). This is evidenced by *RAC1b* over expression which leads to increased survival in colorectal tumour cells (Matos and Jordan, 2008).

In addition to alteration of apoptosis mechanisms, the process of angiogenesis involves blood vessel formation and innervation of solid tumours and is crucial for the growth of solid tumours. RhoGTPases have been found to mediate specific processes during angiogenesis including proliferation, survival, migration of endothelial cells and regulation of neoangiogenesis, involving the modulation of hypoxia inducible factor (HIF) (Turcotte *et al*, 2003; Bryan and D'Amore, 2007).

Furthermore, a crucial aspect of malignant tumour formation and the occurrence of metastasis is the development of migratory properties in cells. RhoGTPase driven migration generally occurs by the mesenchymal mechanism, as opposed to amoeboid migration, with distinct RhoGTPases mediating two forms of migration involving either the induction of membrane protrusions which are filopodial (Cdc42, RhoD, Rif, Wrch-1, Chp) or lamellipodial (Rac1, Rac2, Rac3, RhoG) (Aspenstrom *et al*, 2004). Moreover, RhoGTPases can control the switch been mesenchymal and amoeboid migration and have been found to determine the direction of cell migration, of which cdc42 plays a major role but other Rho proteins may also be involved (Yang *et al*, 2006).

The use of *RAC* inhibitors, including NSC23766 has delivered important results especially in CML cells, as proliferation both *in vitro* and *in vivo* can be inhibited following treatment (Thomas *et al*, 2007). Furthermore, in mouse models in which *Rac1* was over expressed, tumour progression was promoted in orthotopicaly injected adenocarcinoma cells. Conversely, following knockdown of *Rac1* in the

same model, there was evidence of decreased tumour development (Espina *et al*, 2008). This finding has been recapitulated in other studies including mouse models of lung tumour formation in which reduced tumour formation and prolonged survival can be demonstrated (Kissil *et al*, 2007). It is clear from previous studies and the assays performed here, that specifically targeting *RAC1* results in a reduction in aberrant cellular behaviour. Inhibition of *RAC1* can reduce motility and invasiveness, most likely through a reduction in the RhoGTPase driven lamellipodial migration which is upregulated in MPNST cells. *RAC1* inhibition is therefore likely to be therapeutically beneficial to solid tumours such as MPNSTs which harbour activated RAC.

6.5.2.2.2 Targeting *ROCK2*

The role of ROCKs encompasses regulation of cell growth, migration, metabolism, and apoptosis (Liao *et al*, 2007). There are numerous downstream targets of ROCKs which regulate cellular responses involving actin cytoskeletal assembly and cell contraction (Riento and Ridley, 2003; Liao *et al*, 2007). These processes are achieved by phosphorylation of proteins including myosin light chain (MLC) phosphatase, LIM kinases, adducin, and ezrin-radixin-moesin (ERM) proteins, although it is expected that many other as yet undiscovered targets may also exist (Liao *et al*, 2007).

Upregulation of *ROCK2* has been identified as a key factor in the process of tumour metastasis, contributing to promotion of invasion of tumour cells (Bourguignon *et al*, 1999). This property has been demonstrated experimentally, including the inhibition of invasion in rat hepatoma cells and migration in metastatic breast cancer cells with dominant-negative forms of ROCK and treatment with small molecular inhibitors such as Y-27632 or fasudil. Such non-isoform specific inhibitors target ATP-dependent kinase domains and lead to the loss of stress fibres and focal adhesion complexes. Whilst at higher concentrations they may target other serine threonine kinases, their efficacy indicates that such methods may be appropriate therapeutic options, although little remains known about the underlying molecular mechanisms of ROCK activity (Ishizaki *et al*, 1996; Itoh *et al*, 1999; Kataoka *et al*, 2002).

As with inhibition of *RAC1* signalling, previous studies on other tumours and the results presented here on MPNST cell lines, suggests that knockdown of *ROCK2* may also offer a reduction in the malignant and metastatic potential of MPNST cells.

Whilst individual knockdown of *RAC1* and *ROCK2* resulted in a reduction in migratory and invasive behaviour and an increase in adhesion, the cells still demonstrated some metastatic behaviour indicating that there may be some redundancy in the RhoGTPase pathway. Indeed, keratinocyte cell–cell contact for example, is sensitive to inhibition of *Rho* and *Rac* but individual mouse knockouts do not affect keratinocyte cell junctions (Benitah and Watt, 2007). This may be as a result of activation of pathways which regulate the Rho GTPase signalling pathway or from the presence of lower or higher levels of molecules which regulate RhoGTPases. Some breast tumours for example, have been found to harbour upregulation of RhoGEFs such as *Vav*, *Trio* and *Tiam1*. It would therefore be important to determine whether double knockouts of genes in the RhoGTPase pathway would be required to completely inhibit tumour growth and metastasis.

6.5.2.3 RNAi vs. small molecular inhibitors

Some gene targets are not easily drugable, and the search for an appropriate inhibitor can be time consuming and laborious. There are instances of the use of *RAC1* or *ROCK2* inhibitors in cancer studies in the literature, namely in breast cancer (Hernández *et al*, 2010), but often these inhibitors are novel and thus not commercially available. *cMET* inhibitors have been previously investigated in many cancers and many are currently commercially available (Crosswell *et al*, 2009). shRNA instead of inhibitors were therefore used to determine the affect of *RAC1* and *ROCK2* upregulation in MPNST cell lines. shRNA were chosen over other RNAi methods, such as siRNA due to the specificity and long term affects which it affords. Furthermore, shRNA clones with varying levels of knockdown can be selected to identify the affect of both partial and full knockdown. Overall, the two methods (inhibition and shRNA) are relatively comparable. Both shRNA and small molecular inhibitors were equally successful in either specifically reducing the gene expression of target genes without any off target effects or inhibiting receptor activation. shRNA and inhibition assays also took the same amount of time to complete and each produced the same end-result of a reduction in gene expression. Five clones were, however, required for each shRNA to give a range of knockdown efficiencies which increased the time and cost of producing the desired knockdown effect. Clearly small molecule inhibitors are also more readily transferrable to *in vivo* assays and are

more applicable to potential downstream clinical trials. However, it should be noted that molecular heterogeneity as demonstrated in this study, has implications for therapy of large malignant tumours. It should be recognised that different molecular signatures may exist in separate portions of a tumour and therefore targeted inhibition or knockdown of specific genes may only affect a section of a large tumour.

6.5.3 Conclusion

Although MPNSTs only develop in ~15% of NF1 patients, they represent a frequent cause of lethal progression of the NF1 phenotype. The prognosis for individuals diagnosed with an MPNST is usually very poor especially as treatment options for MPNSTs are currently rather limited and complete surgical excision with clear margins is the commonly recommended therapy for MPNSTs.

This study demonstrated that in addition to cellular heterogeneity, molecular heterogeneity is a prominent aspect of NF1-associated MPNSTs, a finding which has important connotations for analysis of somatic alterations in MPNSTs in addition to the design and administration of targeted therapies. Pathway analysis based on data derived from Affymetrix microarray analysis (Upadhyaya *et al*, unpublished data) and relative quantification demonstrated MPNST specific amplification of genes mapping to the cMET and RhoGTPase pathways. In knockdown experiments involving short hairpin RNA for *RAC1* and *ROCK2*, cell adhesion of MPNST cell lines was significantly increased whereas wound healing, cell migration and invasion were reduced. This is consistent with a role for *RAC1* and *ROCK2* in MPNST development and metastasis. Furthermore, *cMET* inhibition with two small molecule inhibitors generated a reduction in gene expression and migratory behaviour in MPNST cell lines. This study has identified several new potential targets for therapeutic intervention in MPNST development.

CHAPTER 7: General discussion

Following the identification of the *NF1* gene on chromosome 17q11.2 by positional cloning experiments in 1990 (Cawthon *et al,* 1990; Wallace *et al*, 1990; Viskochil *et al*, 1990), it has become clear that analysis of germline and somatic *NF1* mutations in the context of evaluating mechanisms for disease manifestation and genotype-phenotype correlations, would be a significant challenge. To date, over 1273 different *NF1* germline mutations have been identified (HGMD; Fahsold *et al*, 2000; Messiaen *et al*, 2000; Han *et al*, 2001; Ars *et al*, 2003). In comparison, only about 215 different somatic *NF1* mutations have so far been characterised. Furthermore, whilst reported germline mutation detection rates can be as high as 90% (Messiaen *et al*, 2000; Ars *et al*, 2000), even using the most up to date mutational analysis techniques, the somatic mutation detection rate has been recently reported to vary from 12% to 64% (John *et al*, 2000; Serra *et al*, 2001b; Upadhyaya *et al,* 2004; Spurlock *et al*, 2007). Much has been learned over the past 20 years on how a constitutional germline *NF1* mutation might result in the plethora of manifestations associated with NF1 as a disease. Nevertheless, there is still a significant paucity in knowledge in NF1 research, particularly relating to the mechanisms and pathways involved in tumour development and malignancy. This thesis has therefore focused on some of the areas of NF1 tumour biology for which we currently have little depth of knowledge.

7.1 Mutation detection

The size and complexity of the *NF1* gene, the lack of mutational hotspots, the diversity of disease-causing mutations, and the presence of *NF1* pseudogene-like sequences, contribute to problems related to successful *NF1* mutation detection. It is also increasingly recognised that the cellular and molecular heterogeneity of NF1-associated benign and malignant tumours is a contributory factor to poor mutation detection rates. Furthermore, comprehensive *NF1* mutational analysis is costly and labour intensive as at least three different screening methods (LOH, MLPA and direct sequencing) are usually required to ensure detection of the complete spectrum of somatic *NF1* mutations. Even when using patient-derived lymphocyte DNA, screening for *NF1* constitutional mutations may require the use of both DNA and

cDNA sequencing, in addition to MLPA analysis, to detect most point mutations, as well as genomic deletions and insertions that affect the gene. Due to the complexity of *NF1* mutational types, no single standardised mutation detection platform is capable of detecting the range of *NF1* mutations. Indeed, even some of these methods fail to provide complete coverage of the *NF1* gene and so many mutations may remain unidentified. While this is not such a major issue for germline *NF1* mutation detection, with a reported 70-90% success rate (Fahsold *et al*, 2000; Messiaen *et al*, 2000; Han *et al*, 2001; Ars *et al*, 2003; Valero *et al*, 2011), for somatic *NF1* mutation detection, significant improvements clearly are required. Such improvements may occur prior to the mutation analysis stage, such as by Schwann cell enrichment to significantly increase the cell population that exclusively harbours the *NF1* somatic mutation, or it may await future advancements in mutation detection methodologies.

Cutaneous neurofibromas are usually small benign tumours, with an extracellular matrix and are populated with Schwann cells, the only tumour cells that harbour the somatic *NF1* mutations. Unfortunately, neurofibromas demonstrate high cellular heterogeneity and whilst Schwann cells represent the predominant cell type, they only comprise 40%-80% of cells (Peltonen *et al*, 1988; Wallace *et al*, 2000), along with heterozygous fibroblasts, mast cells and perineural cells (Kimura *et al*, 1974; Le and parade, 2007). As a result, reported somatic mutation detection rates in neurofibromas show great variation (John *et al*, 2000; Serra *et al*, 2001b; Upadhyaya *et al* 2004; Spurlock *et al*, 2007). Thus, the focus for the initial part of the present research was to identify and validate new methods for improving mutation detection in such heterogeneous tumours, and involved Schwann cell enrichment both by Schwann cell culture and by Laser Capture Microdissection (LCM) of solid tumours. LCM was subsequently used in conjunction with standard *NF1* mutation detection techniques, to identify the somatic *NF1* mutations present in multiple benign cutaneous neurofibromas derived from NF1 patients with a high tumour burden (>500 cutaneous neurofibromas).

Validation of these two strategies involving Schwann cell enrichment revealed the pros and cons of both techniques, as outlined in chapter 3. For example, Schwann cell culture, is both time consuming; requiring some 4-6 weeks for one cell line and expensive as Schwann cells do not proliferate in standard culture conditions,

requiring additional cell culture reagents and the necessary expertise to culture them. Thus, Schwann cell culture is not really suitable for the routine identification of *NF1* somatic mutations. While the use of LCM was rapid and cost effective, it was found to be less sensitive in the context of mutation detection compared to Schwann cell culture.

Perhaps the most important consideration when comparing these two techniques is that Schwann cell culture is very much a prospective technique, requiring fresh tumour tissue, it cannot be applied retrospectively. Thus, if the somatic mutation is not identified by analysis of the whole tumour DNA, it is not possible to go back and analyse the same tumour by Schwann cell culture. Conversely, LCM whilst exhibiting a lesser Schwann cell enrichment and thus a lower somatic mutation detection rate of the two techniques, it can be applied both prospectively and retrospectively to older samples which are preserved by fixation and paraffin embedding. DNA from tumours fixed in this manner are viable for long periods of time. Indeed, some of the samples analysed in this study were over 10 years old. Thus, a combination of LCM and culture methods may represent the best Schwann cell enrichment strategy, encompassing both the sensitivity of Schwann cell culture with the flexibility of LCM for retrospective and prospective tumour studies.

Other enrichment techniques, such as COLD-PCR, have also been reported to be useful for detecting a variety of mutations, including those in *KRAS*. COLD-PCR is able to detect the mutant alleles even when restricted to a small region of the clinical samples, such as colorectal samples (Song *et al*, 2011). Aptamer-modified microfluidic devices have also been reported which rapidly capture target cells with over 97% purity and above 80% efficiency (Phillips *et al*, 2009). Such techniques might also be useful for enrichment of Schwann cell populations containing *NF1* somatic mutations from *NF1* associated tumours, although validation would be required.

Comprehensive genome wide mutation analyses of many common non-NF1-associated malignant tumours have increasingly identified somatic mutations of the *NF1* gene. Indeed, significant involvement of *NF1* inactivation has been found in glioblastoma (Parsons *et al*, 2008), lung adenocarcinomas (Ding *et al*, 2008), ovarian serous carcinomas (Sangha *et al*, 2008), colorectal carcinomas (Ahlquist *et al*, 2008) and leukaemia (Haferlach *et al*, 2010). Several sporadic NF1-associated tumours

including neurofibromas and MPNSTs have also been reported in individuals without a known constitutional *NF1* mutation (Bottillo *et al*, 2009; Pearl and O'Toole, 2010). *NF1* somatic mutations are therefore not restricted to tumours found in NF1 patients and thus the *NF1* gene clearly has a much broader role in the pathogenesis of multiple tumour types. Hence, the enrichment processes validated in this study may have wider implications for analysis of somatic mutations in other tumour types.
Clearly Schwann cell culture is only applicable to tumours in which Schwann cells harbour the *NF1* somatic mutations. Enrichment cultures for other tumour cells may be valid for the overall identification of *NF1* somatic mutations, in addition to finding genome-wide alterations in other heterogeneous cell types. Indeed, cell culture of leukaemic cell populations is common practice (Walsby *et al*, 2011), and mutation harbouring breast cancer cells have also been enriched by culture followed by immunomagnetic enrichment (Hu *et al*, 2003). LCM is routinely applied to many solid tumour types provided that molecular markers or a pathologist are available to determine the cells of interest to be dissected. Homogeneous lung adenocarcinoma cells have been purified by LCM with high specificity allowing the detection of a wide range of genetic alterations including *TP53* (Nan *et al*, 2010). Djalilvand *et al* (2004) have also employed LCM in the detection of *TP53* mutations in esophageal carcinomas, Keohavong *et al* (2004) employed LCM in breast ductal carcinomas and Wang *et al* (2006) have completed a similar study to that employed in this project, involving LCM followed by LOH analysis of advanced oral squamous cell carcinoma. The overall effectiveness of LCM for mutation analysis in the context of these solid tumours proved to be similar to the results ascertained in the present study. Thus, LCM is a readily applicable technique for both prospective and retrospective mutation analysis of the *NF1* gene and other tumour suppressor loci, in a range of tumour types.

Even with these Schwann cell enrichment steps prior to mutation analysis in NF1-associated tumours, it was apparent that there were still problems with the methods employed to detect somatic mutations. Although there were no major issues with speed or sensitivity in the present analysis, the problems were more inherent and mainly arose from the use of techniques which cannot detect the whole spectrum of mutations, in addition to the tumour heterogeneity.

Recent *NF1* studies have confirmed that LOH is a common somatic mutational mechanism in NF1, especially in MPNSTs, where LOH is reported to account for 85%-90% of the identified mutations (Upadhyaya *et al*, 2008; Laycock-VanSpyk *et al*, 2011). Even in benign cutaneous neurofibromas and plexiform neurofibromas, *NF1* LOH is detected in about 49% and 79% of tumours respectively. Hence, somatic mutation detection is heavily reliant on the use of LOH analysis using a standard panel of chromosome 17 specific microsatellite and RFLP markers. While, the LOH PCR-based technique proved to be very efficient in detecting LOH, several technical problems arose during the validation process in this study. For example, the cellular heterogeneity of the tumours was found to mask the somatic mutations detected in several samples and this was significantly improved by the use of LCM and Schwann cell culture. However, many somatic mutations were still undetectable; thus the true extent of somatic *NF1* LOH is probably underestimated. Whilst PCR based methods do permit multiplexing, allowing multiple markers to be screened concordantly, expansion of the technique to screen for LOH across an entire chromosome becomes expensive and thus FISH may be used instead. Constitutional DNA is also required for comparison in such LOH studies. In the present study, as some samples were obtained at post mortem, no normal tissue was available.

MLPA analysis was used in this study to screen for microdeletions or duplications. There are also several drawbacks with this technique, again MLPA is affected by the cellular heterogeneity, and also the presence of variant SNPs in the probe or primer regions may result in false positive and false negative results. A major issue with this current study was that FISH analysis could not be used to confirm any MLPA results as the relevant fresh tumour samples were often not available. Repeat analysis therefore had to be relied upon to confirm the MLPA results but this is clearly not a suitable method for confirmation.

The direct DNA and cDNA sequencing used in this study detected a wide range of different *NF1* point mutations, including nonsense, missense and splice site mutations, as well as small deletions and insertions ranging in size from 1-114 bp. The major disadvantage to this technique relates to the size and complexity of the *NF1* gene as well as the lack of any obvious mutational hotspots. Indeed, it is quite laborious and time consuming to amplify and sequence all 61 exons of the *NF1* gene and it is quite likely that many somatic mutations were missed during sequence

analysis in this study. Moreover, any deep intronic mutations would also be missed due to the location of the primers used in this study and the limitations on the sequencing read length (approximately 500-1000bp), which is restricted by the capillary length (Pros *et al*, 2009).

The use of cDNA sequencing of tumour RNA in this study helped to overcome several of these problems. Firstly, for cDNA sequencing of the entire coding region of the *NF1* gene only 24 primer sets are required instead of 61, thus sequencing is far more efficient. Secondly, any deep intronic mutations that may affect the correct reading of the frame, and splice site mutations which disrupt correct splicing, are much more easily identified. Mutation detection rates may also be increased by cDNA sequencing and, in the present study; several mutations were identified by cDNA that were not immediately obvious from DNA. These somatic mutations were only later confirmed in tumour DNA following the identification of the location of the mutation. Similarly, cDNA has been employed in the analysis of other tumour suppressor genes such as *TP53*, in which cDNA analysis improved somatic mutation detection (Szybka *et al* 2009). The use of RNA from frozen tumour tissue should, however, be treated with some caution as several aberrant *NF1* transcripts have been reported following analysis of stored tissue (Ars *et al*, 2000; Wimmer *et al*, 2000; Serra *et al*, 2001; Vandenbroucke *et al*, 2001, 2002).

The panel of techniques used in this study were found to be no more efficient than other mutation detection methods such as DHPLC. DHPLC is reported to provide *NF1* mutation detection rates of some 66% (DeLuca *et al*, 2004) which is comparable to the analysis of several other key tumour-related genes, such as VHL, in other malignant tumour types, including phaeochromocytomas (Meyer-Rochow *et al*, 2009). DHPLC can, however, only effectively detect point mutations and so really only represents a screening tool. The more comprehensive approach presented here, whilst relatively labour intensive, does analyse the entire *NF1* mutational spectrum. Furthermore the identification of false positive results is a recurring problem with DHPLC, due to the detection of non-specific fragments. Whilst false positives can occur by direct sequencing, this is often circumvented by bidirectional sequencing of both strands at the same time.

The somatic mutational analysis techniques employed here (LOH, MLPA and direct sequencing) are all relevant mutational detection methods that are routinely

employed in both the diagnostic and research setting for *NF1* mutational analysis. This study represents the most effective analysis of somatic *NF1* mutations in NF1-associated benign and malignant tumours with the highest mutational detection rate reported to date using Schwann cell culture (85%). These techniques are not specific to the analysis of NF1-associated tumours and are sensitive enough to be translated to the analysis of *NF1* mutations in other tumour types. Indeed, LOH analysis and direct sequencing are the most common methods of mutational detection used for the analysis of somatic mutations at many other genomic loci in different tumour types, including colorectal carcinomas (Cawkwell *et al*, 1994; Ahlquist *et al*, 2008), lung adenocarcinomas (Ding *et al*, 2008) and ovarian serous carcinomas (Sangha *et al*, 2008). Microsatellite markers are available for other tumour suppressor genes and such markers were employed in this study to screen for *TP53* mutations.

MLPA has proved advantageous in several *NF1* mutation detection studies, not only in the identification but also in the complete characterisation of both intragenic deletions and duplications (Valero *et al*, 2011; Messiaen *et al*, 2011). Kits are also available for a range of other tumour suppressors including *TP53*, *PTEN* and *RB1* (MRC Holland). Indeed, MLPA has been successfully applied in the testing and identification of genomic mutations in numerous genes, including *BRCA1* and *TSC2* (Kozlowski *et al*, 2008).

Direct sequencing is a common technique used for detection of mutations at genetic loci throughout the genome. *KRAS* (c.61) and *BRAF* (V600E) mutations in particular, are frequently screened for in colorectal cancer using this method as it is a simple method for identifying the most common somatic alterations in this tumour type (Bennani *et al*, 2010). The advent of more rapid and sensitive techniques, such as pyrosequencing have recently replaced direct sequencing for the characterisation of specific mutations which frequently occur in some tumour types, especially *KRAS* mutations in colorectal cancer (Macedo *et al*, 2011). The application of a pyrosequencing-based mutational analysis for *NF1* mutation detection would not be as advantageous as the methods described here, mainly due to the underlying complexity and size of the *NF1* gene and the lack of any mutational hotspots. It may, however, represent a less labour intensive approach in diagnostic situations, especially as the time involved in post PCR processing is greatly reduced.

In conclusion, the present study has made use of the most reliable and efficient techniques available at the onset of the study. The techniques presented here have proved to be valid and applicable for the enrichment and analysis of the *NF1* gene in NF1-associated benign and malignant tumours, and possibly for the analysis of other common malignant tumour types. Moreover, the methodology described here has implications for the identification of somatic mutations at genome-wide loci in other clinically important cancer types. The emergence of 'next generation' sequencing techniques offers the advantages of being able to identify multiple mutations across the entire genome and so clearly has implications for *NF1* gene analysis. However, such novel sequencing techniques are not necessarily a direct replacement of current sequencing methodologies. At present, the high empirical costs and increased time involved in next generation sequencing demonstrates that such technologies may be more than is required for basic mutation detection methodologies used in single gene disorders such as NF1.

7.2 Functional Analysis

While detection of mutations within the *NF1* gene has proved challenging, the problem in interpreting the likely pathogenicity of identified sequence variants continues to confound the issue. Therefore, functional and bioinformatic analysis of the possible disease causing ability of missense mutations within the GRD was studied, as discussed in chapter 4. These mutations had been previously detected as potential germline mutations in NF1 patients in both the NHS diagnostic lab (University Hospital of Wales, Cardiff) and the NF1 research lab (Cardiff University). However, without the relevant familial analysis, or comparison against a large panel of normal controls, it is always difficult to determine whether such sequence variants are actually contributing to disease development. In this study, 16 missense mutations from within the GRD were successfully characterised as either neutral or disease-causing variants using a Ras ELISA. In addition, bioinformatic analysis, completed by Matthew Mort (Cardiff University) helped to further dissect these missense mutations to determine the potential underlying molecular mechanisms that resulted in loss of NF1GAP-RAS binding in 11 of the 16 mutations.

Such functional analyses have previously been completed on fewer than 5 GRD mutations and so this present study represents the largest analysis to date.

Moreover, the functional and bioinformatic data showed perfect correlation, signifying that both methods are likely to be reliable for pathogenic analysis. As discussed in chapter 4, this technique represents an improvement on previous *NF1* functional analysis being simple, rapid and cost effective, and moreover, does not require either radio-labelled nucleotides (Li *et al*, 1992; Upadhyaya *et al,* 1997), or the construction of extensive libraries of vector constructs (Morcos *et al*, 1996).

Relatively few functional studies have been completed on missense mutations in other tumour suppressor genes. Gutmann *et al* (2001) undertook a very labour intensive approach to analyse eight missense mutations throughout the NF2 gene which were inducibly overexpressed in rat schwannoma cell lines. In comparison to the method presented here, inducible expression may not be suitable for analysis of mutations in a large gene such as *NF1*. Recently, missense mutations in the NF2 gene were analysed by relative quantification and transfection of mutant constructs into cell lines (Yang *et al*, 2011). This study was very similar to the methodologies employed in the present project, although it was only based on a few NF2 variants. A study on PTEN missense mutations by Han *et al* (2000) also employed analogous methods to those utilised in this study in a comprehensive analysis of 42 missense mutations generated by site directed mutagenesis. Although this was a more extensive study, it did require the use of radio-labelled nucleotides to determine PTEN phosphatase activity, something which was avoided in the current study with the use of an ELISA. Finally, *BRCA1* missense mutations have also been analysed in a study by Vallon-Cristersson *et al* (2001). Only 2 mutations were analysed in mammalian vectors and the remaining 11 variants used yeast constructs. Furthermore, the assay used by Vallon-Cristersson *et al* (2001) was semi-quantitative. ELISA assays can be fully quantitative and so represent a more useful strategy for determining protein function.

Overall, the present study represents a significant improvement on previous functional analyses of *NF1* missense mutations and is comparable to, or even an advancement on the functional analyses of other tumour suppressor genes. In most of the studies outlined above, the analysis was not confined to the known functional domains of the gene under investigation, however, the present study analysed only the functional GRD of the *NF1* gene. Whilst the GRD represents the majority of the known functionality of neurofibromin, several other regions such as the CSRD and C-terminal domains, may also have functional significance (section 1.3.4). While

analysis of the GRD should take predominance over the other regions in neurofibromin, it is important to assess the likely pathogenicity of mutations within other *NF1* gene regions, such as the CSRD, which is thought to modulate the activity of the GRD (Mangoura *et al*, 2006). It would also be interesting to apply the techniques established in this study to include analysis of all synonymous mutations, as opposed to non synonymous changes currently studied, as these may act as modifiers of drug efficacy and toxicity (Loktionov *et al*, 2004).

Many of the functional studies previously undertaken on other tumour suppressor missense mutations were purely cell based and no concurrent bioinformatic analysis was undertaken. It was therefore only possible to comment on *in vitro* activities of mutant cell lines and to speculate on the mechanisms responsible for mutant cell behaviour. Bioinformatic analysis proved to be a crucial tool for determining protein function in the absence of either functional or familial analysis, or the availability of a large cohort of controls. The addition of bioinformatic analysis to any functional assay clearly aids in the determination of the function of a mutant protein compared to the wild type protein. Furthermore, bioinformatic analysis in this study revealed important insights into the underlying mechanisms of pathogenicity associated with three of the mutations studied, although, for several missense mutations bioinformatic analysis was unable to provide any further information. It is therefore still unclear for the majority of missense mutations whether they resulted in (i) a loss of affinity for Ras, (ii) an inability to interact with Ras due to conformational changes or (iii) an, as yet unidentified mechanism that could account for loss of NF1-Ras signalling? Additional bioinformatic tools should also be employed in future studies to look at the complex molecular interactions of these NF1 mutants with Ras.

The bioinformatic tools used in this study are not the only computational methods and information databases available for prediction of protein function. The majority of such programs rely on conservation information and three-dimensional structural information. Such tools have recently been used to profile PTEN missense mutations and include: SWISSPROT used to determine whether the substitution is located in a binding site, active site, or site involved in a disulphide bond. The evolutionarily conservation of amino acids normally implies an important functional or structural roles for the residue (Nassiri *et al*, 2009), so the use of programmes such as BLASTP can establish whether the position of an amino acid substitution is

conserved in a family of homologous proteins. The PolyPhen program classifies missense mutations as likely to have a benign effect on the protein, to have a possibly damaging effect, or to have a probably damaging effect (Ramensky *et al*, 2002; Sunyaev *et al*, 2001). SWISSPROT, BLASTP and PolyPhen serve a similar function to SIFT, PhyloP and *MutPred* which were used in the present study, indicating that the current bioinformatic analyses were appropriate for this study. Additional prediction programs are becoming available for similar analysis, including the SNAP program which may prove useful in future studies of this type (Li *et al*, 2007).

Overall, the bioinformatic tools employed in this study are comparable to the other programmes available. However, this study would have benefitted from the use of molecular modelling tools, such as Panther, MODELLER and VERIFY-3D that have been used to investigate p53 mutations (Thomas *et al*, 2003; Pirolli *et al*, 2011). Molecular modelling can be used to determine if the amino acid substitution interrupts nearby atoms or changes the accessibility of side chains. Such techniques may prove to be important for future investigation to provide a prediction of how *NF1* mutations may affect molecular interactions between NF1 and Ras proteins.

7.3 Methylation

This present study represents the first comprehensive use of pyrosequencing to analyse the methylation status across the entire *NF1* gene as well as the *RASSF1A* and *MGMT* promoters, in DNA from a large cohort of NF1-associated tumours. The results from this study confirmed that methylation of the *NF1* gene is unlikely to contribute to tumorigenesis, although hypermethylation of the *RASSF1A* promoter, but not the MGMT promoter, may play a role in the early stages of tumour development. A problem in the analysis of CpG methylation in the *NF1* gene was determining what actually constitutes a recognised CpG island. In the *NF1* gene, by the most stringent of definitions (Gardiner-Garden and Frommer, 1987; Takai and Jones, 2002), only 2 CpG islands; one identified in the promoter region and a second in intron 39 that is associated with an adenylate kinase 3 (*AK3L1*) pseudogene sequence. However, studies on other cancers have found that methylation of CpG rich regions downstream of the promoter are capable of affecting gene expression (Li *et al*, 2003; Ortmann *et al*, 2008). It was therefore postulated that this may also

occur in the *NF1* gene, so CpG rich regions that are not strictly CpG islands were also included in this methylation analysis. Inclusion of these additional regions should allow the methylation pattern across the entire *NF1* gene to be determined. While this was achieved, and the largest number of CpG dinucleotides to date were analysed, there are at least 2000 additional CpG dinucleotides in the *NF1* gene that were not profiled. As discussed in chapter 4, the majority of these dinucleotides were discrete and scattered throughout the large 283kb *NF1* gene. With few sites conforming to the definitions of a CpG island and none known to be clustered in any recognised functional regions, it is unlikely that methylation of these sites will play a role in *NF1* gene inactivation. Only a few previous studies have focused on methylation analysis of discrete CpG dinucleotides. No evidence for a contribution of methylation at these sites to gene inactivation has been reported (Bauer *et al*, 1999; Zhu *et al*, 2005).

As outlined in table 1.8 many other tumour suppressor loci are known to be methylated in a range of tumour types, with similar pyrosequencing methylation analyses, applied to such genes. While most of these studies have a comparable efficacy to the present study, in comparison to the *NF1* gene, methylation of other tumour suppressors, such as *CDKN2A,* appear to have a much more important role in tumour development and are also often associated with a poor clinical outcome (Mirchev *et al*, 2010). For example, Muggerud *et al* (2010) assessed the level of *PTEN* methylation in breast ductal carcinomas where it was not found to be significantly methylated. Conversely, PTEN methylation in non small cell lung cancer appears to have a prognostic effect and is also associated with the clinical outcome in surgically treated stage I and II non small cell lung cancer patients (Buckingham *et al*, 2010). Both the *RASSF1A* and *APC* promoters are hypermethylated in parathyroid tumours as well as several instances of *CDKN2A* methylation which have also been reported with pyrosequencing-based analysis. In such studies, the *RASSF1A* gene demonstrated similar levels of methylation in tumour samples (90%) to that seen in the current study (80%), indicating that high levels of hypermethylation of several Ras pathway effectors is involved in the development of multiple tumour types (Joplin *et al*, 2010). Recently, Kullar *et al* (2010) profiled CpG island hypermethylation of the *NF2* gene in 40 vestibular schwannomas by pyrosequencing and similar to the results in this study, they found that *NF2*

methylation is unlikely to contribute to development of vestibular schwannomas although only the *NF2* promoter region was screened. This is often the situation in methylation studies with only the gene promoter region being analysed.

In the present study, pyrosequencing methylation analysis proved to be rapid, sensitive quantitative and a cost effective technique, with the methylation of the *NF1* gene comparable to previous studies using pyrosequencing. This study does, however, have an advantage in that additional functional analysis with the methylation inhibitor 5aza2dc was undertaken. Most previous studies have analysed methylation levels and gene expression levels, although methylation studies involving pyrosequencing are rarely translated from genetic findings into meaningful *in vitro* or *in vivo* functional data. This study was therefore not only able to identify and characterise the *NF1* methylation status of both NF1 benign and malignant tumour types, it also assessed the affect that such methylation had on gene expression. Indeed, without this functional aspect, it would be difficult to definitively determine whether the methylation identified is pathogenic. Unlike in this study, the major effect of methylation on other tumour suppressor genes in the majority of previous analysis is therefore unclear.

As discussed in chapter 5, pyrosequencing offers unique advantages over previously used methylation detection techniques such as Methylation specific PCR (Herman *et al*, 1996), quantitative methylation PCR (Q-MSP) and quantitative multiplex-methylation-specific PCR (QM-MSP) (Herman *et al*, 1996; Eads *et al*, 2000; Cohen *et al*, 2003; Jeronimo *et al*, 2004). Since the commencement of this study, however, new high-throughput 'next generation' DNA sequencing techniques have emerged, although few screening-based studies have employed these techniques due to the cost and technical skills required for this type of analysis. Next generation DNA sequencing has, however, simplified whole-genome DNA methylation profiling, permitting production of whole genome-wide methylation profiles at single-base resolution. MethylCap-seq, for example, involves the capture of methylated DNA using the methyl-DNA binding protein domain (MBD) of MeCP2 (Brinkman *et al*, 2010). While pyrosequencing is relatively high-throughput it is still restricted to a 96 well format. The application of new sequencing techniques able to analyse the entire methylome in multiple samples concurrently would clearly provide an advantage for future analysis of genome wide methylated loci which may be associated with NF1 tumorigenesis.

7.4 MPNST tumorigenesis

There were several aspects to the studies discussed in chapter 6. Firstly, the overall molecular heterogeneity in MPNSTs was determined and the effect of upregulation of three genes (*cMET*, *RAC1* and *ROCK2*) was also assessed. From many previous array studies it is clear that MPNST tumorigenesis is a complex, multistep processes, involving a range of genetic abnormalities to promote malignant transformation from a benign tumour to an MPNST (Lothe *et al*, 1996; Bridge *et al*, 2004; Watson *et al*, 2004; Holtkamp *et al*, 2004; Storlazzi *et al*, 2006; Thomas *et al*, 2007; Levy *et al*, 2007; Shen *et al*, 2007; Kresse *et al*, 2008; Mantripragada *et al*, 2008; Mantripragada *et al*, 2009; Fang *et al*, 2009; Brekke *et al*, 2009; Miller *et al*, 2009; Pemov *et al*, 2010; Brekke *et al*, 2010; Miller *et al*, 2010; Subramanian *et al*, 2010; Chai *et al*, 2010). This study successfully determined that overexpression of *cMET*, *RAC1* and *ROCK2* in these tumours resulted in an increase in both the migratory and invasive behaviour of MPNST cells that is likely to contribute to the malignant progression of these tumours. These three genes may therefore represent biomarkers and may be considered as probable targets for future therapies.
In the current study, inhibitors and RNAi both proved to be valuable tools for dissecting the mechanisms of NF1 tumorigenesis. RNAi for *RAC1* and *ROCK2* have also been studied using adhesion, migration, invasion and wound healing assays in cell lines derived from other tumours including epithelial cells, keratinocytes and glioma-derived cells (Valster *et al*, 2005; Kimura *et al*, 2006; Lock and Hotchin, 2009). These studies used similar methods to those employed here and gave comparable results. Although the advantage of the present study was the use of shRNA instead of siRNA which provides a more sustained knockdown. Furthermore, few of the previous studies utilised all four of the assays employed here and these studies are therefore not as comprehensive as the present study.

Animal models of *RAC1* and *ROCK2* have been generated with Samuel *et al*, (2011) targeting *Rac1* in a mouse model of epidermal papillomas which was able to demonstrate that *K-Ras*-mediated murine epidermal tumorigenesis is associated with elevated *Rac1* activity. Furthermore, Bosco *et al* (2010) determined the impact of inhibition of *Rac1* on *p53*-deficient B- and T-lymphoma cells in mice. Such inhibition resulted in increased apoptosis of B- and T-lymphoma cells. Only a single

ROCK2 animal model has so far been reported, with Ying *et al*, (2006) reporting that the *ROCK2* inhibitor fasudil inhibited tumor progression in rat models of lung metastasis. This *ROCK2* inhibitor also showed promise in human studies where it appeared to be well tolerated (Ying *et al*, 2006). Based on the present findings and those of the *RAC1* and *ROCK2* mouse models it is likely that targeting the *RAC1* and *ROCK2* genes in animal models of NF1 may be an important aspect for future experimentation.

The *cMET* pathway has also been targeted in assays of several other tumours including neuroblastoma (Crosswell *et al*, 2009), with antibodies used to block HGF/c-Met function in cells derived from MPNSTs (Su *et al*, 2004). While this study obtained similar results to those demonstrated in the current study, a critical difference is that the *cMET* inhibitors validated here are much more applicable to pre-clinical and clinical trials than antibodies. Indeed, an orally available *cMET* kinase inhibitor has been trialled in a human tumour xenograft mouse model of gastric carcinoma and glioblastoma, tumours that are both associated with NF1 patients (Yamazaki *et al*, 2008). Near-complete inhibition of *cMET* phosphorylation was achieved (>90%) and tumour growth was significantly inhibited (>50%) indicating that such inhibitors may also prove effective in NF1 mouse models.

It is clear from several previous studies on other tumour-derived cell types that both the *cMET* and RhoGTPase pathway genes are important, not just to MPNST development but also to the growth of several other common malignant tumour types. The present study successfully dissected the roles of the *cMET*, *RAC1* and *ROCK2* genes in MPNST development and has also outlined important biological pathways that may represent future biomarkers and therapeutic options. Several improvements could, however, be made for similar future studies, with an important shortfall of this project being that only single gene knockouts were assessed in MPNST cells. As there is evidence for redundancy in many signalling pathways as well as feedback mechanisms, future studies might consider applying knockdown of both *RAC1* and *ROCK2,* in addition to various other downstream signalling partners, for example, the ROCK effector *LIMK1*. Such studies should indicate whether knockdown of both genes is required to facilitate decreases in the malignant and metastatic activity of these tumours or whether a single gene knockdown is sufficient. Similarly, only *cMET* was targeted for inhibition and whilst there was a

significant reduction in tumour cell migration, a high level of migratory activity was still present. This suggests that feedback mechanisms may also be functioning in this pathway. Indeed, a pilot study with rapamycin indicated that the mTOR pathway, and probably other effectors, such as STAT3 or AKT should also be targeted.
An improvement for the present study would be the use of adenoviral shRNA knock-down libraries involving high-throughput assays to identify novel genes involved in cell migration. Indeed, when validated on prostate cancer cells, overexpression of *CXCR4*, *PIK3CA*, *ROCK2* and *PGF* were found to inhibit wound healing (Pril *et al*, 2009). Finally, producing sustainable delivery of gene therapy is a major problem. As was demonstrated in chapter 5, inhibition of methylation using 5aza2dc was found to be only a temporary effect with both methylation and gene expression returning to the levels prior to treatment following drug withdrawal. This suggests that while the use of such inhibitors is more applicable to animal and human trials, the application of RNAi such as the shRNA, used here instead of global agents, may prove more effective in future *in vitro* investigations.

This study also revealed that 70% of MPNSTs studied are highly heterogeneous, not only in their cellular and architectural composition but also in the underlying molecular aberrations. This indicates that improvements in the method of heterogeneity analysis should be sought, especially as LOH analysis lacks sensitivity and is also not a very quantitative method. More accurate methods, such as AQUA (Camp *et al*, 2002; McCabe *et al*, 2005), and tissue analysis with multiplex quantum dots (QD) (Liu *et al*, 2010) have been used in other studies of molecular heterogeneity and these may represent suitable future alternatives for use in NF1 tumour analysis.
Furthermore, heterogeneity analysis did indicate that multiple sections from the same tumour should be analysed in array and relative quantification assays due to the high levels of heterogeneity. Unfortunately, MPNSTs are rare tumours and although the NF1 lab has a panel of more than 40 MPNST derived DNA samples, frozen tissue was often not available and so limited samples were accessible for relative quantification analysis. Indeed, in many cases only small sections of the original whole tumour remained. As a result, only single sections could be used for the analysis in this study and so it is possible that the contribution of the genes studied to MPNST development could have been under-estimated. However, it

should be mentioned that the use of multiple tumour sections for microarray analysis of many other tumour types is not common practice mainly due to the implications for time and cost of analysis. Furthermore, RNA quality from stored tumour material can often be a problem leading to inefficient cDNA conversion and thus poor amplification for relative quantification. The standard methods for analysis of cDNA are RIN/RQI analysis. This was not possible in our study but the quality and quantity of RNA was determined by spectrometry and gel analysis and this was not considered to represent a problem in this analysis.

7.5 Conclusions

This study is the first to assess the technique of LCM in the context of *NF1* mutation analysis and to further employ it to successfully identify somatic mutations in benign and malignant NF1-related tumours. The use of enrichment strategies for improving mutation detection is critically important in these highly heterogeneous tumours associated with NF1, and this study should hopefully aid in the characterisation of new mechanisms of gene inactivation. The novel identification of LOH of the *TP53* and *RB1* genes in benign cutaneous neurofibromas is a significant finding and is a mutational feature which has only previously been linked with plexiform neurofibromas and MPNSTs. It is therefore postulated that tumours from these severely affected patients may harbour an alternative molecular mechanism of tumour development to that present in patients with classical NF1.

One of the major aspects missing from the *NF1* mutational analysis repertoire is the appropriate functional analysis of sequence variants with unknown pathological consequences, such as the synonymous and non-synonymous mutations. This study has remedied this issue through the establishment of a reliable technique to characterise such sequence variation as neutral or disease-causing. This methodology demonstrated that 11 of 16 previously detected potential germline mutations were very likely to be pathogenic. Indeed, the functional analysis was in concordance with the bioinformatic analysis. Therefore, this assay may be important not only for NF1 research but more importantly, for future diagnosis of NF1.

This report is also the first to apply pyrosequencing methylation analysis to the *NF1* gene to confirm that *NF1* methylation is unlikely to be an underlying cause of tumorigenesis in NF1. Methylation of the *RASSF1A* promoter in NF1 tumours is,

however, a novel finding that may represent an important event in the early stages of NF1 tumorigenesis. The functional dissection of biological pathways involved in malignancy in NF1 is crucial for the development of any treatment for NF1 tumorigenesis. This study has shown that methylation inhibitors such as 5aza2dc may be important for therapy of tumours harbouring aberrant methylation patterns. Moreover, the *cMET* and RhoGTPase pathways were specifically targeted with both RNAi and small molecule inhibitors. Such methods demonstrated a reduction in the malignant and metastatic potential of MPNST derived cell lines but the efficacy of these methods should be considered within the heterogeneous molecular and cellular background of the tumours studied. It is indicated from the current study that the cMET and RhoGTPase pathways may represent important biomarkers for MPNSTs and that of other malignant tumours. Thus, targeting the genes in these pathways may be an important therapeutic option.

The results of this project have successfully addressed all of the major aims of the study, providing a more comprehensive overview of the mutational mechanisms in NF1 tumorigenesis. By building on the results provided here, future studies may pave the way towards the development of efficient, cost effective mutation detection strategies, in addition to targeted therapies of NF1-associated tumours.

7.6 Future directions

7.6.1 Mutation detection

There are still many potentially fruitful areas for NF1 research. In terms of tumour development and potential treatment, there is a clear need for the development of sensitive, rapid, cost-effective genetic analysis for molecular NF1 diagnosis, and this study represents a first step in this process, in providing a validation for the application of Schwann cell enrichment techniques. Improved mutational analysis strategies are especially important for the identification of underlying mutations in atypical patients and young individuals who often have yet to develop the hallmark features of NF1. Conventional analysis methods are likely to become augmented by various microarray-based technologies as well as cell enrichment strategies, followed by application of high-throughput next generation sequencing methodologies (Mardis *et al*, 2008).

Furthermore, crucial 'driver' and 'passenger' mutations in addition to genotype-phenotype correlations are hard to identify in NF1. Next generation technologies in conjunction with functional analysis such as the RasGAP assay undertaken in the current study may therefore help to better define genotype and phenotype interactions and also identify just which mutations are driving the development of NF1 associated manifestations from those that are neutral changes. Low level mosaicism is also very difficult to detect with the majority of methodologies routinely employed in *NF1* analysis. It is clearly important to improve our ability to detect such mosaicism, as the developmental stage at which the mutations occur in patients with mosaicism (segmental NF1), determines the cell type(s) which are likely to be affected. Thus, this may provide important insights into the underlying mechanisms responsible for specific NF1-associated manifestations (Maertens *et al*, 2007)
Apart from NF1-associated tumour studies, it may be important to examine the extent of genome wide alterations in NF1 patients who are mildly affected, such as those with 3bp deletions or *SPRED1* mutations. Making molecular comparisons of these patients to patients with classical NF1 or those who are severely affected, may help identify potential cancer susceptibility loci.

7.6.2 Therapeutic options and biomarkers

Few therapies aimed at targeting NF1 tumour development have even made it to the clinical trials stage (supplementary table 1) and indeed even those that have, do not have proven efficacy. Improvements and indeed development of novel therapeutics to specifically target highly aggressive MPNSTs is clearly required and as shown here, pathway analysis is likely to prove crucial to determining the underlying mechanisms responsible for tumour development. Many genes found in MPNSTs map to the same signalling pathways indicating that their deregulation may be crucial in providing a selective advantage to tumour cells during the process of malignant transformation. Identification of specific biomarkers to assess the probability of malignant progression in NF1 patients would allow prediction of the progression of an individual's manifestations. At present, there is extreme variability in the expression of NF1 even between individuals with the same mutation. It is suggested and indeed demonstrated within this study that modifying loci are likely to underlie the extreme variability in disease presentation. Array studies have already identified

many genes which are specifically altered in MPNSTs in comparison to benign neurofibromas, however, no single gene has been identified that represents a biomarker of tumour development and malignancy in NF1. Next generation sequencing techniques applied to a complete exome may therefore represent an important platform to discover genes which may modify the NF1 phenotype.
The *cMET*/Rho GTPase analysis undertaken here is a promising start to such studies, although expansion to other cancer models is clearly warranted. The translation of *in vitro* analysis into effective *in vivo* results is usually quite difficult. Gene targeting in mouse models will be important to determine whether inhibition of signalling pathways such as those investigated here may be able to inhibit the development of NF1-associated tumours, or even reduce the volume of tumours. An important consideration for any prospective future study is whether it is more important to totally prevent tumour growth or just to attempt to reduce overall tumour load? The plethora of genes reported to be altered in MPNSTs suggests that it is unlikely that a single drug will provide suitable efficacy for the reduction in angiogenic, metastatic and malignant potential of NF1-associated malignancies.

Approximately one third of somatic and germline *NF1* mutations result from splicing alterations which can create new splice sites which results in the inclusion of intronic sequences in the final *NF1* transcript (Messiaen *et al*, 2008). A number of bioinformatic and functional analysis methods have been employed to confidently predict the effect of splicing mutations on the NF1 transcript produced (Raponi *et al*, 2006; Bottillo *et al*, 2007; Raponi *et al*, 2009). The development of antisense therapies for NF1 is already underway. Indeed, antisense morpholino oligomers have been employed in the treatment of fibroblasts and lymphocyte cell lines harbouring deep intronic *NF1* mutations which prevented the inclusion of cryptic exons (Pros *et al*, 2009). At present, there are limited applications of splicing treatments and further development may allow them to become important therapeutic options in the near future.

7.6.3 Candidate genes

The RasMAPK pathway is a well defined biological signalling pathway although many novel protein partners and interactions are still being discovered. For example,

it was only recently recognised that *SHOC2* mutations can cause a variant form of Noonan syndrome (Cordeddu *et al*, 2009). For some patients suspected of having NF1, an *NF1* germline mutation has yet to be identified, perhaps indicating that germline mutations in another gene within the RasMAPK pathway may be involved which is capable of eliciting an overlapping phenotype. Another prime example is the *SPRED1* mutations in some patients with an NF1-like syndrome, now called Legius syndrome. Investigation of the RasMAPK genes including scaffold proteins such as 14- 3- 3 is an important starting point, but may be aided with targeted array for the RasMAPK pathway and by the advent of second and third generation technologies.

An important prospective study may also involve the identification of other genes and consequently proteins which physically interact with Neurofibromin and may therefore modify its activity in a disease context. The 5' and 3' UTRs of *NF1*, for example, have functionally defined roles but it is still not clear whether they have other functions. The poly-A binding protein (PABP) interaction with the NF1 3'UTR in particular has not been studied (Hoshino *et al*, 1999). As the 3'UTR may represent a target of inactivating mutations, it is imperative that protein interactions with other NF1 regions are considered. The nature of signalling pathways indicates that complex feedback mechanisms and crosstalk between pathways both occur. It is postulated that the pathogenesis of primary tumours may therefore not be as simple as constitutive activation of the RasMAPK pathway following *NF1* inactivation. Multiple downstream signalling pathways and the interactions of proteins in these pathways such as mTOR may therefore be of importance.

7.6.4 MicroRNA

Gene regulation is an extremely complex and multi-factorial process. MicroRNAs (miRNAs) are small noncoding RNAs that regulate gene expression and have recently been implicated in the pathogenesis of cancer. As identified in array studies on MPNSTs, several miRNA, including *miRNA10b* and *miR-34a* may be important to NF1 tumorigenesis (Chai *et al*, 2010; Subramanian *et al*, 2010). Furthermore, miRNA alterations in primary human cancers such as acute myeloid leukaemia have been shown to generate miRNA binding sites in the UTR regions of genes and may therefore represent another potential mechanism by which somatic mutations can

affect gene expression (Ramsingh *et al*, 2010). Therefore, analysis of the 'miRNAome' by next generation sequencing techniques will allow a comprehensive assessment of miRNA expression to identify genetic variants of miRNA genes in addition to miRNA biomarkers. Furthermore, alterations in miRNA binding sites in tumours and patient constitutional DNA may be revealed.

7.7 Concluding remarks

NF1 as a disease model has greatly benefitted from the experience and research of both clinicians and scientists ever since the identification of the *NF1* gene in 1990. The research undertaken in this project has significantly improved our understanding of the molecular pathology underlying NF1-associated tumorigenesis, both in benign and malignant peripheral nerve sheath tumours. This study combined a variety of approaches to determine important genetic and epigenetic modifying loci, and also highlighted potential tumour biomarkers for future exploration. Furthermore, validation of two somatic mutation enrichment techniques may prove invaluable in facilitating future investigations of the *NF1* gene, in addition to other tumour suppressor loci. In conclusion, while much still remains to be investigated, this project has provided a firm basis for further genetic, epigenetic and functional studies into the underlying mechanisms responsible for NF1 tumorigenesis, and also raises important questions to be addressed in the near future. It is also expected that with the expansion of current *in vitro* studies such as those presented here, into effective *in vivo* models and potential clinical trials, important and exciting developments in this field will arise.

APPENDIX

Supplementary Table 1. NF1-associated tumours and chemotherapeutic treatments

Tumour Type/ Manifestation	Treatment	Target	Study	Outcome	Reference
Plexiform Neurofibroma	Imatinib mesylate (Gleevec, Novartis international)	Inhibitor of c-kit, PDGFβ and the bcr/abl receptor tyrosine kinases	Nf1flox/-;Krox20cre mouse models and a 3 year old NF1 patient	Reduces the volume of plexiform neurofibromas by 70%. Cessation of symptoms associated with the site of tumour formation	Yang *et al*, 2008; Staser *et al*, 2010
	Carboplatin	Platinum based, formation of bulky adducts	Treatment of a stage I testicular seminoma in one patient	54% decrease in neurofibroma volume	Hummel *et al*, 2011
	Thalidomide	Anti-angiongenic agent	Open-label phase I study of 20 patients	Tolerated in doses up to 200 mg/day. 4/12 patients demonstrated a response in tumor size (all <25%)	Gupta *et al, 2003*
	Oral pirfenidone	Anti-fibrotic agent -modulates fibroblast growth factor and epidermal growth factor	Open-label phase II trial of 24 patients	4/24 had a minor decrease in tumour volume (15%), stable disease in 17/24 patients	Babovic-Vuksanovic *et al*, 2007
	Pirfenidone	Antifibrotic Agent	Pediatric phase I trial	Pirfenidone was well tolerated	Babovic-Vuksanovic *et al*, 2007
	Tipifarnib (FTI Family)	Ras farnesyltransferase inhibitor	pediatric phase I trial	Tipifarnib was well tolerated	Widemann *et al*, 2006
	Interferon alpha	Stimulation of immune response	12 month treatment in 1 patient	No observable change in tumour size	Citak *et al*, 2008

Tumour Type/ Manifestation	Treatment	Target	Study	Outcome
Plexiform Neurofibroma	pegylated interferon-alpha-2b		Phase I trial of 30 patients	Improvement in 11/16 Decrease in tumou 13/14 patients.3/ documented radio progression sho stabilization or shri
Deep Neurofibromas	Sirolimus	mTOR Pathway Inhibitor	2 Trials (NCT00652990, NCT00634270)	Trial Ongoin
MPNST	Lovastatin + farnesyl protein transferase inhibitor	Inhibition of HMG-CoA reductase involved in cholesterol synthesis, affects the synthesis of farnesyl pyrophosphate + Inhibition of Ras prenylation	Preclinical Studies	Low concentrations a inhibit prenylation Reduction of Ras pre increased cell cylcle and apoptosis. Inc caspase activity in MF lines. Negligible toxi
	tipifarnib (FTI Family) (NCT00029354)	Inhibition of Ras prenylation	Phase II trial	Trial concludi
	Tipifarnib + Erlotinib (NCT00085553) or Sorafenib (NCT00244972)	Inhibition of Ras prenylation	Preclinical Studies and Phase I trials	Not yet clinically de
	neo-adjuvant chemotherapy		Multicentre, multimodality therapeutic strategy	Major response in patients

Tumour Type/ Manifestation	Treatment	Target	Study	Outcome
MPNST	PCI-24781 (Pharmacyclics)	Histone deacetylase inhibitor (HDACi)	Preclinical Studies	MPNST cell lines we sensitive to the inh Proapoptotic effect noted in vitro and
	Tamoxifen	Antiestrogen	Preclinical Studies	1–5 mM 4-hydroxy-ta induced MPNST ce 0.01–0.1 mM 4-hy tamoxifen inhibi mitogenesis. Potent a activity in mice ortho xenografted with h MPNST cells. inhibits cell proliferation and via an ER-indepe mechanism.
	BAY 43-9006 (sorafenib)	tyrosine kinase inhibitor. Inhibitor of Raf-dependent MEK phosphorylation	Phase II clinical trial	Disappointing as a agent, inducin only minor respo
	Sorafenib alone or in combination with ifosfamide/dacarb azine	Tyrosine kinase inhibitor. Inhibitor of Raf-dependent MEK phosphorylation	Phase I/II and Phase II trials (NCT00541840, NCT00837148).	Trial in progress. Sc efficacy might improved by combini other targete drugs
	U0126, PD184352 (CI-1040) and PD98059	MEK inhibitors	Preclinical Studies	concentration-depe suppression of proliferatio

Tumour Type/ Manifestation	Treatment	Target	Study	Outcome
MPNST	Rapamycin and/or rapamycin derivative RAD001 (everolimus)	mTOR Pathway Inhibitor	Preclinical Studies	inhibit proliferation c cell lines derived from NF1-re sporadic MPNSTs. with xenograft g of ST26T cells. A transient, tumours re withdrawal of treatm be tumouristatic rat tumouricidal ag
	Deforolimus	mTOR Pathway Inhibitor	Phase I/II trials	more than 25% of achieved clinical (objective response disease for 16 w
	PI-103 and LY294002	dual PI3K/AKT and mTOR inhibitory compounds	Preclinical Studies	showed a dosedepe growth inhibitory effe abrogated cell growt G1 cell cycle arre induction of autop
	Erlotinib	EGFR Inhibitor	Preclinical Studies	Inhibition of grow invasion of MPNST cell
	Erlotinib	EGFR Inhibitor	Preclinical Studies	Tumour antiangiog antiproliferative resp xenografted m
	Gefitinb	EGFR Inhibitor	Phase I trial	Well Tolerate
	Erlotinib	EGFR Inhibitor	Phase II trial	No objective resp
	Imatinib mesylate	PDGFR Inhibitor	Preclinical Studies	Suppresses invasiv and cell growth of MI lines

Tumour Type/ Manifestation	Treatment	Target	Study	Outcome
MPNST	Dasatinib	multi-TKR small-molecule inhibitor, blocks PDGFR in addition to SRC and KIT	Phase II and III studies (NCT00427583, NCT00464620)	Ongoing
	SU5416	VEGFR2 Inhibitor	Preclinical Studies	No effect on MPNST *in vitro*. Growth of tumour explanted xe was reduced more th Decreased tum angiogenesis an proliferation and inc apoptosis
Optic Gliomas	vincristine + carboplatin	Platinum based, formation of bulky adducts	Retrospective multicentre study	Long term visual ou uncertain
		farnesyl transferase inhibitors and MTOR pathway inhibitor		Too early to predict Outcome
Astrocytomas	mTOR inhibitors and the LY294002 PI3-kinase (PI3-K) inhibitor		Pre-clinical	suppressed cell gro level

Supplementary Table 2. *NF1* DNA sequencing PCR primers

EXON	Sequence (5'-3')	Size (bp)
1F	CTCCACAGACCCTCTCCTTG	323
1R	TCCCCTCACCTACTCTGTCC	
2F	AAACTGTTTACGTGTTTTTTTTTTC	378
2R	AAGAAAAGAAAGCAAATTCCCC	
3F	TTTCACTTTTCAGATGTGTGTTG	245
3R	TGGTCCACATCTGTACTTTG	
4aF	TTAAATTCTAGGTGGTGTGT	517
4aR	AAACTCATTTCTCTGGAG	
4bF	GATACCACACCTGTCCCCTAA	342
4bR	CATGATACTAGTTTTTGACCCAGTG	
4cF	TTTCCTAGCAGACAACTATCGA	308
4cR	AGGATGCTAACAACAGCAAAT	
5F	TGTTAGCATCCTGAATCAAAA	292
5R	TCGTATCCTTACCAGCCATA	
6F	AATGCCAGGGATTTTGTTCC	294
6R	AAGCCTAAAGTAATACACACCTTGA	
7F	GCTACATCTGGAATAGAAGAAACTTCA	391
7R	CCATTTAGGCTGATGAACACA	
8F	CATGTTAGTAAAGAAATACTGCATGG	273
8R	TTTTGTTTATAAAGGATAACAGCATCA	
9F	TTGATGTTCGTTTCAAGACC	249
9R	ACGCAAAGAAAAGAAAGAAAA	
10aF	ACGTAATTTTGTACTTTTTCTTCC	222
10aR	CAATAGAAAGGAGGTGAGATTC	
10bF	ATTATCCTGAGTCTTACGTC	506
10bR	TAACTTAGTGTGATAATTTTGAGA	
10cF	TCTTCCTCCTTCTAATCTCTCTCG	425
10cR	AAGGAACATCATGAATGTACATAGTTA	
11F	CCAAAAATGTTTGAGTGAGTCT	256
11R	ACCATAAAACCTTTGGAAGTG	
12aF	TGCATTAGGTTATTGATGATGC	303
12aR	TGAGAACATTGGGAGGAAGG	
12bF	CTCTTGGTTGTCAGTGCTTC	382
12bR	CAGAAAACAAACAGAGCACAT	
13F	CACAGTTTATTGCATTGTTAGATTTT	385
13R	CAGATGCCATGTGCTTTGAG	
14F	TTTGGGTGGAGCTTATCAGG	562
15R	ACTTTACTGAGCGACTCTTGAA	
16F	TGGATAAAGCATAATTTGTCAAGT	549
16R	TAGAGAAAGGTGAAAAATAAGAG	
17F	GGTACGAGTGTCTGCGTATATCTG	385

EXON	Sequence (5'-3')	Size (bp)
17R	CGAATTAAATGTAAGTTTGAAAACAA	
18F	AGAAGTTGTGTACGTTCTTTTCT	367
18R	CTCCTTTCTACCAATAACCGC	
19aF	TCATGTCACTTAGGTTATCTGG	268
19aR	TAAAACCCACTAATACTTGAAGG	
19bF	TGAGGGGAAGTGAAAGAACT	275
19bR	TCCTATCCTAGTCCTGTCATGG	
20F	CCACCCTGGCTGATTATCG	340
20R	GCTTCTCTTACATGCCAGTTC	
21F	TCAGCAAGGCCATGTTAGTA	381
21R	CTTCCCCGCTTACTCTAATC	
22F	TGCTACTCTTTAGCTTCCTAC	518
22R	CCTTAAAAGAAGACAATCAGCC	
23.1F	TTTGTATCATTCATTTTGTGTGTA	327
23.2R	ACTTTAGATTAATAATGGTAATCTC	
24F	TGACCTTTGAACTCTTTGTTTTCA	451
24R	GAAAAGCTGAAAATTTAGTTGGAA	
25F	CCTGTTTTATTGTGTAGATACTTCA	338
25R	TAAGTGGCAAGAAAATTACCT	
26F	GTGTGAACAAGCCCTCCATA	638
26R	GAAGATGCAAAGTAAAAAGCACT	
27aF	ATGATTAGCACATTCACGGG	298
27aR	GCAAACTCTCCTTCTCAACC	
27bF	TTTATTGTTTATCCAATTATAGACTT	296
27bR	TCCTGTTAAGTCAACTGGGAAAAAC	
28F	TTTCCTTAGGTTCAAAACTGG	561
28R	CTAGGGAGGCCAGGATATAG	
29F	GGTTGGTTTCTGGAGCCTTT	473
29R	AGCAACAAACCCCAAATCAA	
30F	CAACTTCATTTGTGTTTTCTCCTAG	321
30R	CTTTGAATTCTCTTAGAATAATTGTTA	
31F	TGATGTGATTTTCATTGACCA	424
31R	CAGATAAATATGTGCACAAAGGAGA	
32F	TGAATATACTCATCCTTTCCTGGAT	352
32R	CATGGGACTCAAAGTTTTAGCA	
33F	TCCTGCTTCTTTACAGGTTATT	463
33R	AAGTAAAATGGAGAAAGGAACTGG	
34F	TTCAAAATGAAACATGGAACTTT	394
34R	AAGTACAAAATAGCACAATAAACCAA	
35F	GCATGGACTGTGTTATTGGTA	490
36R	TGCTTTACAACTTGAGAACCATAAA	
37F	AATTCATTCCGAGATTCAGTTTAGGAG	240
37R	AAGTAACATTCAACACTGATACCC	

EXON	Sequence (5'-3')	Size (bp)
38F	AACTGCAGTGTGTTTTGAAAGAG	281
38R	GCAACAAGAAAAGATGGAAGAG	
39F	GAAAGCTACTGTGTGAACCTCATCAACC	289
39R	GTAAGACATAAGGGCTAACTTACTTC	
40F	TCAGGGAAGAAGACCTCAGGAGATGC	328
40R	TGAACTTTCTGCTCTGCCACGCAACC	
41F	GTGCACATTTAACAGGTACTAT	373
41R	CTTCCTAGGCCATCTCTAGAT	
42F	CTCTATTGTTTTCATCTTTCAGG	349
42R	CAAAAACTTTGCTACACTGACATGG	
43F	TTTTCTTTTTAGTGTATTCCCATT	399
43R	GATTCTAAGAAATGGCTGGAA	
44F	CACGTTAATTCCCTATCTTGC	310
44R	TGAGAAGTAGAAGACTGTATCC	
45F	CATGAATAGGATACAGTCTTCTAC	269
45R	CACATTACTGGGTAAGCATTTAAC	
46F	GAAATGCCCCAGAAAGTAAA	358
46R	GTCAGTGCATTCTACAACAGC	
47F	CTGTTACAATTAAAAGATACCTTGC	259
47R	TGTGTGTTCTTAAAGCAGGCATAC	
48F	TTTTGGCTTCAGATGGGGATTTAC	447
48R	AAGGGAATTCCTAATGTTGGTGTC	
49F	CTGGGAGAAACAGGCTATAC	377
49R	AGCAAGCTTCACACGATCT	

Supplementary Table 3. *NF1* cDNA primers

Primer	Exons covered	Sequence (5'-3')	Size (bp)
1F	1,2,3	AACACTGGGAGCCTGCACT	387
1R		GTTGCCCAGCAAGACATTTT	
2F	3, 4a, 4b	AAGCGGCCTCACTACTATTT	401
2R		TTGCACAATCCACATTGATA	
3F	4b, 4c, 5, 6	CAGGAATTAACTGTTTGTTCAGA	394
3R		TTGTTTTCATCAACCACGTC	
4F	6,7,8	CTGAAAGCACCAAACGTAAA	412
4R		AAGTGTTGGTTGTTGTGAGG	
5F	8, 9, 10a, 10b	TGATTGACTGCCTTGTTTCT	419
5R		CCCCTGTTTTCTTGGATTAC	
6F	10b, 10c, 11, 12a, 12b	TCTCTTGTCCATGGTGAAAC	493
6R		GGCTCCAGGAGTACGTAGTAA	
7F	12b, 13, 14, 15	GGAAATACCAGTCAAATGTCC	461
7R		TTAGCTTTGTTGCTTGTTCC	
8F	15, 16	CACTGAGGCTTGGGAAGATA	449
8R		GACCCACCAGATCCTTAACA	
9F	16, 17, 18, 19a	GGCTGTTGTCCTTAATGGTG	462
9R		CCATAACCCAGTCTGTCAGG	
10F	19a, 19b, 20	GCCAAGAGATGAAATTTAGG	395
10R		GTGCATGAGACCACTGTCTA	
11F	20, 21, 22, 23.1	GGTCCTTGCAATGTCAAA	477
11R		AAAGGATCCAGGAGTTTTTGT	
12F	23.1, 23.2, 24	AGACTCTCTTCCGAGGCAAC	392
12R		TTCATACGGTGAGACAATGG	
13F	24, 25, 26, 27a	CAGTAGGAAGTGCCATGTTC	402
13R		TATCAAAAGGTCGTCTTCCA	
14F	27a,27b,	CAACAGGGATCATAAAGCTG	394
14R		TTTAAAGCGATTGCTAGGC	
15F	27b, 28	AAAGCCATATTATGCAAAGC	396
15R		TGGACAGCAGTAGAACCAAC	
16F	28, 29, 30	GCTCTCAAGCTAGCTCACAA	454
16R		AATCGAGGGCCAGTTACTAG	
17F	30, 31, 32	TCTGTGTGCCTTAACTTGTACC	428
17R		GACAGTTTCATCAAAACCAGTG	
18F	32, 33	AAAATATGGGGAAGCCTTGG	376
18R		AGGTCCGCTCTCCCTTAGAG	
19F	33, 334, 35	TGATGTGGCAGCTCATCTTC	365
19R		GTTGGAGATCATGGAGGCAT	
20F	35, 36, 37, 38	TGACATCCTTGGAAACAGTC	416
20R		AAGTGCGGTACCTGCTGAAT	
21F	38, 39, 40, 41	CTCTTTTGGGTAGCTGTGG	416
21R		CAGCGACTTCGAACTTCTT	
22F	41, 42, 43	TGGCCTACTTAGCAGCTTTA	413
22R		TGCTACTCTCCTCATTTTGG	
23F	43, 44, 45, 46, 47	AAAAGGCAAGAAATGGAATC	515
23R		TCTGGAATTTGTGTTTGCTT	
24F	47, 48, 49	TTTGGTTTTAATGGCTTGTG	534
24R		AACCGGATGGGTTCATTAT	

Supplementary Table 4. Microsatellite and RFLP markers for chromosome 17

Marker	Location	Genomic Co-ordinates using Mar. 2006 (NCBI36 / hg18) Assembly using Feb. 2009 (GRCh37 / hg19) Assembly	Forward Primer Sequence 5'-3'	Reverse Primer Sequence 5'-3'	Size (bp)	Dye	Reference
D17S831 (AFM058XF4)	17p13.3	1,857,446 > 1,857,467 (In *RTN4RL1* gene) 1,910,400 > 1,910,767	CCCCTTTCCTCATACTCCAG	TAATTCAAGTCCCGTCTGGC	230	FAM	Stewart *et al* (2008)
D17S938 (AFM263WH5)	17p13.2	6,190,024 > 6,190,201 (Distal of AIPL1 gene) 6,249,268 > 6,249,535	CCGGATTGCTACACCTAAAT	CTGCTCCAGAAGAGACTGTT	178	FAM	Legius *et al* (1994)
D17S796 (AFM177XH6)	17p13.2	6,192,318 > 6,192,477 (Distal of AIPL1 gene) 6,251,522 > 6,251,775	CAATGGAACCAAATGTGGTC	CATCCTGGCATTATCGGACT	160	FAM	
D17S804 (AFM225ZC1)	17p13.1	9,806,218 > 9,806,375 (In *GAS7* gene) 9,865,376 > 9,865,697	GCCTGTGCTGCTGATAACC	GGAATGACATCTCATCACAGTG	158	FAM	Stewart *et al* (2008)
D17S1879 (AFMA070TC5)	17p13.1	10,053,182 > 10,053,494 (Proximal of MYH13gene) 10,112,457 > 10,112,769	GAAGTTTACGAAAATTGCTGTC	AAGGGTAGTTCTGCGTGC	155	FAM	
D17S520 (MFD144A)	17p13.1	10,209,846 > 10,209,987 (In MYH13 gene) 10,269,009 > 10,269,266	GGAGAAAGTGATACAAGGGA	GGTGGGTATTAATCTAACTA	142	FAM	Stewart *et al* (2008)
D17S799 (AFM192YH2)	17p12	13,111,696 > 13,111,885 (Proximal of ELAC2 gene) 13,170,956 > 13,171,304	ATTGCCAGCCGTCAGTT	GCTTGTCTATAATGATATGCTGGTC	190	FAM	
D17S953 (AFM304xh5)	17p11.2	16,043,171 >16,043,481 (In NCO1 gene) 16,102,446 > 16,102,756	ACTATCCGCCCAATACA	AAGGGCTTGCTTTGAC	123	FAM	Upadhyaya *et al* (2004)
<<<<<<<<<< CENTROMERE >>>>>>>>>							
D17S33 (HHH202)	17q11.1	23,148,612 > 23,148,920 (In NOS2gene) 26,124,485 > 26,124,793	ACTTGCCAAAGGTTACAGGGCTAC	AAGCCTGTCCCTTGACTTGTTCAT	309	RFLP	Upadhyaya *et al* (2004)
5'NF1	17q11.2	26,334,358 > 26,334,879 (In RNF135 gene) 29,310,232 > 29,310,753	ATTGGAACCCTCTGCACTGT	CATAAACTCATGCCCATAGC	522	HEX	
Exon 5	17q11.2	26,532,689 > 26,532,941 Exon 5 *NF1* gene 29,508,563 > 29,508,815	TGTTAGCATCCTGAATCAAAA	TATGGCTGGTAAGGATACGA	253	RFLP	Upadhyaya *et al* (2004)
J1J2 Alu	17q11.2	26,641,851 > 26,642,254 IVS27b *NF1* gene 29,617,725 > 29,618,128	CAAGAAAAGCTAATATCGGC	CTAAGTGAACTTAAGGTTCC	404	FAM	
IVS27 -28.4	17q11.2	26,668,420 > 26,668,626 IVS27b *NF1* gene 29,644,294 > 29,644,500	GTTCTCAACTTAAATGTAAGT	GGTACTTGTTGTTAATGTTC	207	HEX	
EV120 (D17S1166)	17q11.2	26,673,142 > 26,673,342 IVS27b *NF1* gene 29,649,016 > 29,649,216	CCCATACCTAGTTCTTAAAGT	AATAATTGCTGCAGTTCCACAATTGTTA	201	FAM	
IVS38	17q11.2	26,692,798 > 26,692,821 IVS38 *NF1* gene 29,668,672 > 29,668,695	CAGAGCAAGACCCTGTCTCC	CTCCTAACATTTATTAACCTTA	172	FAM	
3'NF1	17q11.2	26,943,468 > 26,943,712 (Distal of RAB11FIP4 gene) 29,919,355 > 29,919,599	CTTCCATGGCTGCTAACATC	TGTTGAACTACACCACAGGG	245	HEX	
D17S798 (AFM179XG11)	17q11.2	28,314,080 > 28,314,299 (Distal of TMEM98 gene) 31,289,812 > 31,290,190	CCATGAGAAAGATGTTTAGTAGTCTCTGCT	CTGCACTCCCAAGAATATACCCATCAAA	220	FAM	
EW206 (D17S57)	17q11.2	28,495,054 > 28,495,402 (In ACCN1 gene) 31,470,941 > 31,471,289	TGCAGTGTGGTGCATCATTCAGTG	ATCAGGAATATGGCTGGCCCTGTC	349	RFLP	
EW207	17q11.2	28,812,190 > 28,812,774 (In ACCN1 gene) 31,788,077 > 31,788,661	AGGTATCAGTCAGGACCCTCTTAG	CACATTACAGAAACCAGAGTGTCAG	585	RFLP	
D17S250 (Mfd15A)	17q12	34,405,618 > 34,405,641 (Distal of FBXO47 gene) 37,152,091 > 37,152,341	CATAAAAAGGAAGAATCAAATAGAC	GCTGGCCATATATATATTTAAACC	160	FAM	Stewart *et al* (2008)
D17S789 (AFM107YB8)	17q24.2	64,140,110 > 64,140,423 (Distal of FAM20A gene) 66,628,515 > 66,628,828	ACTCCAAATCAAGTTTGTACTGAGA	CTGCATACGAAGGGTAGGAC	156	FAM	
D17S1822 (AFMA353YG1)	17q25.3	75,395,628 > 75,395,648 (Distal of CBX8 gene) 77,780,863 > 77,781,171	CAGGCATCTGTAATGGACCC	AACCGAGCCTAGGACTCC	127	FAM	
D17S928 (AFM217YD10)	17q25.3	77,846,296 > 77,846,316 (Distal of CSNK1D gene) 80,252,839 > 80,253,140	ATTTCCCCACTGGCTG	AAAACGGCTACAACACATACA	148	FAM	

Supplementary Table 5. *NF1* RFLP markers and conditions for restriction digest

Marker	Annealing Temperature (°C)	Enzyme	Incubation	Product Size (bp)	Cut Size (bp)
HHH202	54	*RsaI*	2 Hours 37°C	310	190, 120
Exon5	54	*RsaI*	2 Hours 37°C	240	220
EW207	54	*HindIII*	16 hours 37°C	585	~585, 385, 200
EW206	54	*MsP1*	17 hours 37°C	320	180

Supplementary Table 6. MSI microsatellite marker primer sequences

Marker	Sequence (5'-3')	Size (bp)	Repeat	Dye	Chromosomal Location
mD13S153 F	AAAGCATTGTTTCATGTTGG	230	[CA]25	FAM	13q14
mD13S153 R	AAGGTCTAAGCCCTCGAGTT				
mD5S406 F	AACCTGCCAATACTTCAAGA	179	COMPLEX	FAM	5p15
mD5S406 R	GGATGCTAACTGCTGACTAT				
mD5S107 F	ATCCACTTTAACCCAAATACT	147	COMPLEX	FAM	5q11-q13
mD5S107 R	AGGCATCAACTTGAACAGCA				
mBAT26 F	TGACTACTTTTGACTTCAGC	122	[A]26	FAM	2p16
mBAT26 R	AACCATTCAACATTTTTAACC				
mACTC F	CTTGACCTGAATGCACTGTG	88	[TG]25	FAM	5q11-q14
mACTC R	ATTCCATACCTGGGAACGAG				
D2S123 F	AAACAGGATGCCTGCCTTTA	211	COMPLEX	HEX	2p16
D2S123 R	GGACTTTCCACCTATGGGAC				
BAT25 F	TCGCCTCCAAGAATGTAAGT	124	[A]25	HEX	4q12
BAT25 R	TCTGCATTTTAACTATGGCTC				
BAT40 F	ACCAGTCCATTTTATATCCTCAA	183	[A]40	HEX	1p13
BAT40 R	AAGATCACACCTCTGCACTCT				
D5S346 F	ACTCACTCTAGTGATAAATCG	125	[TG]15	TET	5q22
D5S346 R	AGCAGATAAGACAGTATTACTAGT				
D17S250 F	CATAAAAAGGAAGAATCAAATAGAC	160	COMPLEX	FAM	17q12
D17S250 R	GCTGGCCATATATATATTTAAACC				

Supplementary table 7. *TP53 CDKN2A*, *RB1* and *PTEN* LOH markers

Marker	Location	Gene	Sense Primer Sequence (5'-3')	Antisense Primer Sequence (5
TP53 Alu	17p13.1	*TP53*	GCACTTTCCTCAACTCTACA	CTGCCATTAAAGGAGCTGTT
D17S520	17p13.1		GGAGAAAGTGATACAAGGGA	GGTGGGTATTAATCTAACTA
D17S804	17p13.1		GCCTGTGCTGCTGATAACC	GGAATGACATCTCATCACAGT
TP53 c.72	17p13.1 *TP53* Codon 72		GCCAGAGGCTGCTCCCCC	AAGTCTGTGACTTGCACG
TP53 Ex6	*TP53* Exon 6		AGTTCTGGTTTGCAACTGGG	CTGCTGCTTATTTGACCTC
D13S118	13q14.2	*RB1*	CCACAGACATCAGAGTCCTT	GAAATAGTATTTGGACCTGG
D13S153	13q14.2		AGCATTGTTTCATGTTGGTG	CAGCAGTGAAGGTCTAAGCC
D13S917	13q14.2		ATTATCTCTGGGTAGAATGCTAACA	CCCCAGGAGTCATTTTTAACC
RB1.2	13q14.2		AAGTGTAATGTTTTTCTAAG	GAGGAAATTTACCTCTGCTA
RB1.26	13q14.2		ATTCAGTGAAGATATCTAAT	TTCTTCAGTTGGCAGGTTTG
D13S119	13q21.1		AAGACTTTGAATGAAATTCCC	TATTGCCTTTGTAGATCATTG
D9S304	9p21.1	*CDKN2A*	GTGCACCTCTACACCCGGACTCCAGTCTTT	ATAAGATAGATGTGTGTGGGCACAT
D9S1748	9p21.3		CACCTCAGAAGTCAGTGAGT	GTGCTTGAAATACACCTTTCC
D9S1751	9p21.3		TTGTTGATTCTGCCTTCAAAGTCTTTTAAC	CGTTAAGTCCTCTATTACACAG
D9S942	9p21.3		GCAAGATTCCAAACAGTA	CTCATCCTGCGGAAACCATT
D10S2491	10q23.2	*PTEN*	TTATAAGGACTGAGTGAGGGA	GTTAGATAGAGTACCTGCACT
D10S251	10q23.2		TGGCATCATTCTGGGGA	TTACGTTTCTTCACATGGT

Supplementary table 8. Primers for *TP53* sequence analysis

Exon	Primer Sequence (5'-3')	Size (bp)
TP53 4F	TCTGGTAAGGACAAGGGTTGG	200
TP53 4R	CAGGAAGCCTAAGGGTGAAGA	
TP53 5_6F	CTGCCGTGTTCCAGTTGCTTT	250
TP53 5_6R	GTTTCACCGTTAGCCAGGAT	
TP53 7F	CCTCATCTTGGGCCTGTGTT	256
TP53 7R	GAGAGGTGGATGGGTAGTAGT	
TP53 8_9F	AAAGGACAAGGGTGGTTGGGA	550
TP53 8_9R	CCAGGAGCCATTGTCTTTGAG	

Supplementary Table 9. Primers for sequence analysis of *MLH1*, *MSH2*, *MSH6* and *PMS2*

Gene/Exon	Sequence (5'-3')	Size	Gene/Exon	Sequen
MLH1-1F	CACTGAGGTGATTGGCTGAA	295	MSH6-4.1F	GGCTGCACG
MLH1-1F	ATGCGCTGTACATGCCTCT		MSH6-4.1R	GCTTTCGAG
MLH1-2F	TTGTTATCATTGCTTGGCTCA	246	MSH6-4.2R	CTGTCATCAC
MLH1-2F	CCAGAACAGAGAAAGGTCCTG		MSH6-4.2F	GAGTGACATT
MLH1-3F	CACAGGAGGATATTTTACACAT	197	MSH6-4.3R	TTTCCCCACC
MLH1-3F	GAGATTTGGAAAAATGAGTAACA		MSH6-4.3F	GGTGACTGGA
MLH1-4F	TTACTCTGAGACCTAGGCAAAAA	196	MSH6-4.4R	CTTTCTACAT
MLH1-4F	GGTGACCCAGCAGTGAGTTT		MSH6-4.4F	GGATTTCCTCAA
MLH1-5F	TTTATACAAACAAAGCTTCAACAA	196	MSH6-4.5R	GGATAGTGTGC
MLH1-5F	GATTTTCTCTTTTCCCCTTGGG		MSH6-4.5F	TTTCCTGAAA
MLH1-6F	GCCAGGACATCTTGGGTTT	249	MSH6-4.6R	ACCCCAATGC
MLH1-6F	GCTCAGCAACTGTTCAATGTATG		MSH6-4.6F	TTCTTCTGGC
MLH1-8F	TGTGATGGAATGATAAACCAA	416	MSH6-4.7F	GTGGCACACT
MLH1-7F	AAAAGGGGGCTCTGACATCT		MSH6-4.7R	TGTCACTGCA
MLH1-9F	TGATTCTTTTGTAATGTTTGAGTT	242	MSH6-4.8F	TTCCCTTGGA
MLH1-9F	TCCCATAAAATTCCCTGTGG		MSH6-4.8R	TCAGGGGAGA
MLH1-10F	ACCTGTGACCTCACCCCTCA	241	MSH6-4.9F	TGATCGTCTAG
MLH1-10F	TTAGCATGCTCATCTCTTTCAA		MSH6-4.9R	CGAGCCTTTT
MLH1-11F	AATCTGGGCTCTCACGTCTG	299	MSH6-4.10F	CCCAGACAGC
MLH1-11F	TACACCATATGTGGGCTTTTT		MSH6-4.10R	CAGCCCTTCTT
MLH1-12F	TCTGTCTTATCCTCTGTGACAATG	317	MSH6-4.11R	TGTATATGCATGT
MLH1-12F	CTCCATTTGGGGACCTGTAT		MSH6-4.11F	TTGGGGGATT
MLH1-13F	TTTCCAAAACCTTGGCAGTT	296	MSH6-5aF	TTCCCTTGGC
MLH1-13F	TGCTCCTCCAAAATGCAACC		MSH6-5aR	TAGGCTTTGC

Gene/Exon	Sequence (5'-3')	Size	Gene/Exon	Sequen
MLH1-14F	TAGCTTTTGTGCCTGTGCTC	249	MSH6-5bF	TAAAACCCCC
MLH1-14F	GTCAATGAAGTGGGGTTGGT		MSH6-5bR	ATGACTGACC
MLH1-15F	TTTTCAGAAACGATCAGTTGAA	196	MSH6-6F	CCATGTTAGCA
MLH1-15F	TTCTCCCATTTTGTCCCAAC		MSH6-6R	GGGCAACAA
MLH1-16F	CTTCATTTGGATGCTCCGTT	369	MSH6-7bF	GCCAATAATTGC
MLH1-16F	ATGTTGGCCAGCTGGTTTT		MSH6-7bR	TTCAAATGAGAAG
MLH1-17F	GGAAAGCACTGGAGAAATGG	258	MSH6-7aR	CTCCAACTAT
MLH1-17F	TTCCAGATCAAAGGGTGGTC		MSH6-7aF	CTCATGCAT
MLH1-18F	TCTGTGATCTCCGTTTAGAATGA	245	MSH6-7R	TCTGTGCCAC
MLH1-18F	AAAGATTGTATGAGGTCCTGTCC		MSH6-7F	CTGACCTCAG
MLH1-19F	AAAGGAATACTATCAGAAGGCAAG	380	MSH6-8v2F	CCGATGTTGC
MLH1-19F	GCCAGGACACCAGTGTATGTT		MSH6-8v2R	CCATGCATGC
MSH2-1F	GAGGCGGGAAACAGCTTAGT	356	MSH6-9R	TCATAGTGCAT
MSH2-1R	ACTCTCTGAGGCGGGAAAG		MSH6-9F	GCTGTGCGC
MSH2-2F	TCCAGCTAATACAGTGCTTGA	297	MSH6-10R	GAAAGAAAATG
MSH2-2R	AAACACAATTAAATTCTTCACATT		MSH6-10F	GGAAGGGATG
MSH2-3F	TTGGATTTTTCCTTTTTGCTT	400	PMS2-1F	GTGGAGCACA
MSH2-3R	GGCCTGGAATCTCCTCTATCA		PMS2-1R	ATTTCCAGGG
MSH2-4F	CTTATTCCTTTTCTCATAGTAG	293	PMS2-2F	TGTTGAGTCAT
MSH2-4R	GAAATATCCTTCTAAAAAGTCAC		PMS2-2R	TGGCTTAAAAC
MSH2-5F	TCTTGGTTTGGATTGGGAAG	371	PMS2-3F	CTGATAGCAT
MSH2-5R	TCTTCAGTATATGTCAATGAAAACAT		PMS2-3R	TTGCATTTCC
MSH2-6R	GGTATAATCATGTGGGTAACTG	242	PMS2-4F	ACTGTCTTGGGA
MSH2-6F	CTAATGAGCTTGCCATTCTTTC		PMS2-4R	AAGGGGTCAA
MSH2-7F	ACTGCGCCCAGCAGATTC	374	PMS2-5F	CCATGCCTGG
MSH2-7R	TTGTATGAGTTGAAGGAAAACA		PMS2-5R	CCAATACTCTT

Gene/Exon	Sequence (5'-3')	Size	Gene/Exon	Sequer
MSH2-8F	TCAGTCAAAATTTTATGATTTGTATTC	247	PMS2-6F	GAGAACCTT
MSH2-8R	TCTTAAAGTGGCCTTTGCTTTT		PMS2-6R	GTTGAAGTA
MSH2-9R	ACAAAAGAATTATTCCAACCTC	210	PMS2-7F	TTTTTGCGC
MSH2-9F	TCTTTACCCATTATTTATAGGAT		PMS2-7R	TGTAGTTCTC
MSH2-10R	GTTAGAGCATTTAGGGAATTAA	259	PMS2-8F	TCCCTTTCAC
MSH2-10F	AATGGTAGTAGGTATTTATGG		PMS2-8R	TCCCGAGCTC
MSH2-11F	CATTGCTTCTAGTACACATTTT	194	PMS2-9F	GGCTGGGAA
MSH2-11R	AGGTGACATTCAGAACATTAT		PMS2-9R	CTCATTCCAG
MSH2-12F	ATTATTCAGTATTCCTGTGTAC	334	PMS2-10F	CAATGTTACTCC
MSH2-12R	AAAACGTTACCCCCACAAAG		PMS2-10R	AAGCTTTAGAAG
MSH2-13F	AACAATCCATTTATTAGTAGCAG	317	PMS2-11.1F	AGTCCCTGA
MSH2-13R	AGAGACATACATTTCTATCTTC		PMS2-11.1R	GACGCCTTT
MSH2-14F	CACATTTTATGTGATGGGAAATT	337	PMS2-11.2F	GGAGCCCTCT
MSH2-14R	TCCCATTACCAAGTTCTGAATT		PMS2-11.2R	GAGAGGCTG
MSH2-15R	AACACAGAGGAAAACAAACAACAA	362	PMS2-11.3F	CTAATCTCG
MSH2-15F	CAAGGTGAGAAGGATAAATTCCA		PMS2-11.3R	CACTTCCGT
MSH2-16R	CCCATGGGCACTGACAGTTA	375	PMS2-12F	ATGTCTGATAATT
MSH2-16F	TGTTTAGATGGAAATGAAACAATTT		PMS2-12R	TCAATTTGAG
MSH6-1R	CAAATGCTCCAGACTCGAC	668	PMS2-13F	TTGTTTTCATT
MSH6-1F	TACCCACCAGTGTGCCAG		PMS2-13R	CACACCCAG
MSH6-2F	TGCCAGAAGACTTGGAATTGT	440	PMS2-14F	AAACGTGTTT
MSH6-2R	AAGCTTTCACAACTGCCACC		PMS2-14R	ACAGCCAGG
MSH6-3R	TCCAGGGAACTACAGAAGTATGC	399	PMS2-15F	CGTTGAACC
MSH6-3F	TGGTCTTGAACTGCTGGGA		PMS2-15R	GCGCATGCA

Supplementary Table 10. Association of *RAC1* alterations with cancer.

***Rac1* Alteration**	**Malignancy**	**Refere**
Overexpression	Progression and metastasis of breast tumors	Schnelz (200
Overexpression	Oral squamous cell carcinoma	Liu *et al*
Hyperactivity	Chronic myelogenous leukemia	Thomas *et*
Overexpression	Progression of gastric carcinoma	Pan *et al*
Overexpression	Progression of testicular cancer	Kamai *et a*
Overexpression	Breast cancer	Fritz *et al*
Overexpression	Progression of prostate cancer	Engers *et a*
Alternative splicing to *Rac1b*	Colorectal tumors	Jordan *et a*

References

Ahlquist T, Bottillo I, Danielsen SA, Meling GI, Rognum TO, Lind GE, Dallapiccola B, Lothe RA. (2008) RAS signaling in colorectal carcinomas through alteration of RAS, RAF, NF1, and/or RASSF1A. *Neoplasia* **10**:680-6.

Ahlquist T, Bottillo I, Danielsen SA *et al.* (2008) RAS signaling in colorectal carcinomas through alteration of RAS, RAF, NF1, and/or RASSF1A. *Neoplasia* **10**(7):680-6.

Albritton KH, Rankin C, Coffin CM *et al.* (2008) Phase II study of erlotinib in metastatic or unresectable malignant peripheral nerve sheath tumors (MPNST). *Journal of Clinical Oncology* **24**:9518.

Alizadeh AA, Eisen MB, Davis RE, Ma C, Lossos IS, Rosenwald A, Boldrick JC, Sabet H *et al.* (2000) Distinct types of diffuse large B-cell lymphoma identified by gene expression profiling. *Nature* **403**:503-511.

Al-Rahawan MM, Chute DJ, Sol-Church K, Gripp KW, Stabley DL, McDaniel NL, Wilson WG, Waldron PE. (2007) Hepatoblastoma and heart transplantation in a patient with cardiofacio- cutaneous syndrome. *AmJ MedGenet* **143**:1481-1488.

Allanson JE. (1987) Noonan syndrome. *J. Med. Genet* **24**:9–13.

Allanson JE, Upadhyaya M, Watson GH *et al.* (1991) Watson syndrome: is it a subtype of type 1 neurofibromatosis? *J Med Genet* **28**:752–756.

Andersen LB, Ballester R, Marchuk DA, Chang E, Gutmann DH, Saulino AM, Camonis J, Wigler M, Collins FS. (1993) A conserved alternative splice in the von Recklinghausen neurofibromatosis (NF1) gene produces two neurofibromin isoforms, both of which have GTPase activating protein activity. *Mol. Cell. Biol.* **13**:487-495.

Andrews JD, Mancini DN, Singh SM, Rodenhiser DI. (1996) Site and sequence specific DNA methylation in the neurofibromatosis (NF1) gene includes C5839T: the site of the recurrent substitution mutation in exon 31. *Hum Mol Genet* **5**(4):503-7.

Angelov L, Salhia B, Roncari L, McMahon G, Guha A. (1999) Inhibition of angiogenesis by blocking activation of the vascular endothelial growth factor receptor 2 leads to decreased growth of neurogenic sarcomas. *Cancer Research* **59**:5536-5541.

Aoki M, Nabeshima K, Koga K, Hamasaki M, Suzumiya J, Tamura K, Iwasaki H. (2007) Imatinib mesylate inhibits cell invasion of malignant peripheral nerve sheath tumor induced by platelet-derived growth factor-BB. *Laboratory Investigation* **87**:767-779.

Aravind L, Neuwald AF, Ponting CP (1999) Sec14p-like domains in NF1 and Dbl-like proteins indicate lipid regulation of Ras and Rho signalling. *Curr Biol* **9**:R195–R197.

Arun D. Gutmann DH. (2004). Recent advances in neurofibromatosis type 1. *Current Opinion in Neurology* **17**:101–105.

Ars E, Serra E, Garcia J, Kruyer H, Gaona A, Lazaro C, Estivill X. (2000). Mutations affecting mRNA splicing are the most common molecular defects in patients with neurofibromatosis type 1. *Hum Mol Genet* **9**:237–47.

Ars E, Kruyer H, Morell M, Pros E, Serra E, Ravella A, Estivill X, Lázaro C. (2003) Recurrent mutations in the NF1 gene are common among neurofibromatosis type 1 patients. *J Med Genet.* **40**(6):e82.

Ashkenas J (1997) Gene regulation by mRNA editing. *Am J Hum Genet* **60**:278–283.

Aspenström P, Fransson A, Saras J. (2004) Pases have diverse effects on the organization of the actin filament system, *Biochem. J.* **377**:327–337.

Atkins CM, Selcher JC, Petraitis JJ, Trzaskos JM, Sweatt JD (1998) The MAPK cascade is required for mammalian associative learning. Nat Neurosci **1**:602– 609.

Babińska A, Gnacińska A, Swiatkowska-Stodulska R, Sworczak K. (2008) Myocardial infarction in a 30-year-old patient with pheochromocytoma and type 1 neurofibromatosis. *Pol Arch Med Wewn.* **118**(9):517-23.

Babovic-Vuksanovic D, Widemann BC, Dombi E, Gillespie A, Wolters PL, Toledo-Tamula MA, O'Neill BP *et al.* (2007) Phase I trial of pirfenidone in children with neurofibromatosis 1 and plexiform neurofibromas. *Pediatr Neurol.***36**(5):293-300.

Bacolla A, Jaworski A, Larson JE, Jakupciak JP, Chuzhanova N, Abeysinghe SS, O'Connell CD, Cooper DN, Wells RD (2004) Breakpoints of gross deletions coincide with non-B DNA conformations. *Proc Natl Acad Sci U S A* **101**:14162–14167.

Bader-Meunier B, Tchernia G, Mielot F, Fontaine JL, Thomas C, Lyonnet S, Lavergne JM, Dommergues JP. (1997) Occurrence of myeloproliferative disorder in patients with Noonan syndrome. *Journal of Pediatrics*, 130, 885–889.

Bahuau M, Laurendeau I, Pelet A, Assouline B, Lamireau T, Taine L, Le Bail B, Vergnes P *et al.* (2000)Tandem duplication within the neurofibromatosis type 1 gene (NF1) and reciprocal t(15;16)(q26.3;q12.1) translocation in familial association of NF1 with intestinal neuronal dysplasia type B (IND B) *J Med Genet.* **37**(2):146-50.

Bajenaru ML, Donahoe J, Corral T, Reilly KM, Brophy S, Pellicer A, Gutmann DH. (2001) Neurofibromatosis 1 (NF1) heterozygosity results in a cell-autonomous growth advantage for astrocytes. *Glia.* **15**:33(4):314-23.

Bajenaru ML, Zhu Y, Hedrick NM, Donahoe J, Parada LF, Gutmann DH. (2002) Astrocyte-specific inactivation of the neurofibromatosis 1 gene (NF1) is insufficient for astrocytoma formation. Mol. Cell. Biol. **22**:5100–5113.

Bajenaru ML, Hernandez MR, Perry A, Zhu Y, Parada LF, Garbow JR, Gutmann DH. (2003) Optic nerve glioma in mice requires astrocyte Nf1 gene inactivation and Nf1 brain heterozygosity. Cancer Res. **63**(24):8573-8577.

Bajenaru ML, Garbow JR, Perry A, Hernandez MR, Gutmann DH. (2005) Natural history of neurofibromatosis 1-associated optic nerve glioma in mice. *Ann Neurol* **57**(1):119-27.

Balakirev ES, Ayala FJ. (2003) Pseudogenes: are they "junk" or functional DNA? *Annu Rev Genet.* **37**:123-51.

Ballif BC, Rorem EA, Sundin K, Lincicum M, Gaskin S, Coppinger J, Kashork CD, Shaffer LG, Bejjani BA. (2006) Detection of low-level mosaicism by array CGH in routine diagnostic specimens. *American Journal of Medical Genetics* **140A** (24)2757-2767

Ballester R, Marchuk D, Boguski M, Saulino A, Letcher R, Wigler M, Collins F. (1990) The NF1 locus encodes a protein functionally related to mammalian GAP and yeast IRA proteins. *Cell.* **16**;63(4):851-9.

Bandipalliam P. (2005) Syndrome of early onset colon cancers, hematologic malignancies & features of neurofibromatosis in HNPCC families with homozygous mismatch repair gene mutations. *Fam Cancer* **4**(4):323-33.

Banerjee S, Bhola P, Mukherjee J, Balasubramanium A, Arun V, Karim Z, Burrell K, Croul S, Gutmann DH, and Guha A. (2010) Preclinical in vivo evaluation of rapamycin in human malignant peripheral nerve sheath explant xenograft Int. J. Cancer: 126, 563–571.

Banerjee S, Gianino SM, Gao F, Christians U, Gutmann DH. (2011) Interpreting mammalian target of rapamycin and cell growth inhibition in a genetically engineered mouse model of Nf1-deficient astrocytes. *Mol Cancer Ther.* **10**(2):279-91.

Baralle M, Baralle D, De Conti L, Mattocks C, Whittaker J, Knezevich A, Ffrench-Constant C & Baralle FE (2003) Identification of a mutation that perturbs NF1 agene splicing using genomic DNA samples and a minigene assay. *J Med Genet* **40**:220–222.

Baralle D, Baralle M. (2005) Splicing in action: assessing disease causing sequence changes. J *Med Genet.* **42**(10):737-48.

Barford D, Neel BG. (1998) Revealing mechanisms for SH2 domain mediated regulation of the protein tyrosine phosphatase SHP-2. *Structure* **6**:249–254.

Barker DE, Wright K, Nguyen L, Cannon P, Fain D, Goldgar D, Bishop J, Carey H *et al.* (1987) Gene for von Recklinghausen neurofibromatosis is in the pericentromeric region of chromosome 17. *Science* **236**:1100-1102.

Bar-Sagi D, Feramisco JR. (1986) Induction of membrane ruffling and fluid-phase pinocytosis in quiescent fibroblasts by ras proteins. *Science* **233**:1061-1068.

Baur AS, Shaw P, Burri N, Delacrétaz F, Bosman FT, Chaubert P. (1999) Frequent methylation silencing of p15 (INK4b) (MTS2) and p16(INK4a) (MTS1) in B-cell and T-cell lymphomas. *Blood.* **94**(5):1773-81.

Bausch B, Borozdin W, Mautner VF, Hoffmann MM, Boehm D, Robledo M, Cascon A, Harenberg T, *et al.* (2007) Germline NF1 mutational spectra and loss-of-heterozygosity analyses in patients with pheochromocytoma and neurofibromatosis type 1. *J Clin Endocrinol Metab.* **92**(7):2784-92.

Batzer MA, Deininger PL. (2002) Alu repeats and human genomic diversity. *Nat Rev Genet* **3**:370-9.

Baylin SB, Esteller M, Rountree MR, Bachman KE, Schuebel K, Herman JG. (2001) Aberrant patterns of DNA methylation, chromatin formation and gene expression in cancer. *Hum Mol Genet.* **10**(7):687-92.

Bengesser K, Cooper DN, Steinmann K, Kluwe L, Chuzhanova NA, Wimmer K, Tatagiba M, Tinschert S, *et al.* 2010. A novel third type of recurrent NF1 microdeletion mediated by non-allelic homologous recombination between LRRC37Bcontaining low-copy repeats in 17q11.2. *Hum Mutat* **31**:742-751.

Bennani B, Gilles S, Fina F, Nanni I, Ibrahimi SA, Riffi AA, Nejjari C, Benajeh DA, *et al.* (2010) Mutation analysis of BRAF exon 15 and KRAS codons 12 and 13 in Moroccan patients with colorectal cancer. *Int J Biol Markers.* **25**(4):179-84.

Bennett E, Thomas N, Upadhyaya M. (2009) Neurofibromatosis type 1: Its association with the Ras/MAPK pathway syndromes. *Journal of Pediatric Neurology* **7**(2).

Bennett S. (2004) Solexa Ltd. *Pharmacogenomics* **5**:433–438.

Benitah SA, Watt FM. (2007) Epidermal deletion of Rac1 causes stem cell depletion, irrespective of whether deletion occurs during embryogenesis or adulthood, J. Invest. *Dermatol* **127**:1555–1557.

Benvenuto G, Li S, Brown SJ, Braverman R, Vass WC, Cheadle JP, Halley DJ., Sampson JR, *et al.* (2000) The tuberous sclerosis-1 (TSC1) gene product hamartin suppresses cell growth and augments the expression of the TSC2 product tuberin by inhibiting its ubiquitination. *Oncogene* **19**:6306–6316.

Berciano J, Garcia A, Combarros O. (2003) Initial semeiology in children with Charcot-Marie-Tooth disease 1A duplication. *Muscle & Nerve* **27**:34–39.

Bernardi G. (2000) Isochores and the evolutionary genomics of vertebrates. *Gene* **241**:3 –17.

Bernards A, Snijders AJ, Hannigan GE, Murthy AE, Gusella JF. (1993) Mouse neurofibromatosis type 1 cDNA sequence reveals high degree of conservation of both coding and non-coding mRNA segments. *Human Molecular Genetics* **2**(6):645-650.

Bertola DR, Kim CA, Pereira AC, Mota GFA, Krieger JE, Vieira IC, Valente M, Loreto MR, *et al.* (2001) Are Noonan syndrome and Noonan-like/multiple giant cell lesion syndrome distinct entities? Am J Med Genet; **98**:230–234.

Bidere N, Su HC, Lenardo MJ. (2006) Genetic disorders of programmed cell death in the immune system. *Annu Rev Immunol* **24**:321-352.

Birchmeier C, Birchmeier W, Gherardi E, Vande Woude GF. (2003) Met, metastasis, motility and more. *Nat. Rev. Mol. Cell Biol.* **4**:915–925 .

Bird AP. (1986) CpG-rich islands and the function of DNA methylation. *Nature.* **15-21**;321(6067):209-13.

Birindelli S, Perrone F, Oggionni M, Lavarino C, Pasini B, Vergani B, Ranzani GN, Pierotti MA, Pilotti S. (2001) Rb and TP53 pathway alterations in sporadic and NF1-related malignant peripheral nerve sheath tumors. *Laboratory Investigation* **81**:833-844.

Birnboim HC, Doly J. (1979) A rapid alkaline extraction procedure for screening recombinant lasmid DNA. *Nucleic Acids Res* **7**:1513-23.

Blaustein M, Pelisch F, Srebrow A. (2007) Signals, pathways and splicing regulation. *Int J Biochem Cell Biol* **39**:2031–2048.

Blomberg N, Baraldi E, Nilges M, Saraste M (1999) The PH superfold: a structural scaffold for multiple functions. Trends Biochem Sci **24**:441–445.

Blumberg B, *et al.* (1979) A new mental retardation syndrome with characterisitc facies, ichthyosis and abnormal hair. March of Dimes Birth Defects Conference, Chicago, Il, USA.

Boccaccio C, Andò M, Tamagnone L, Bardelli A, Michieli P, Battistini C, Comoglio PM. 1998. Induction of epithelial tubules by growth factor HGF depends on the STAT pathway. *Nature* **391**:285-288 .
Boettner B, Van Aelst L. (2002) The RASputin effect. *Genes Dev* **16**:2033–2038.

Boland CR, Koi M, Chang DK, Carethers JM. (2008) The biochemical basis of microsatellite instability and abnormal immunohistochemistry and clinical behavior in Lynch syndrome: from bench to bedside, Fam. Cancer **7**:41–52.

Bollag G, McCormick F, Clark R. (1993) Characterization of full-length neurofibromin: tubulin inhibits Ras GAP activity. *EMBO J* **12:**(5)1923-1927.

Bonneau F, D'Angelo I, Welti S, Stier G, Ylänne J, Scheffzek K. (2004) Expression, purification and preliminary crystallographic characterization of a novel segment from the neurofibromatosis type 1 protein. *Acta Crystallogr D Biol Crystallogr* **60**(12):2364-7.

Boon LM, Mulliken JB, Vikkula M. (2005) RASA1: variable phenotype with capillary and arteriovenous malformations. *Curr Opin Genet Dev* **15**:265-269.

Bos JL. (1989) ras oncogenes in human cancer: a review. *Cancer Res* **49**:4682-4689.

Bosco EE, Ni W, Wang L, Guo F, Johnson JF, Zheng Y. (2010) Rac1 targeting suppresses p53 deficiency-mediated lymphomagenesis. *Blood.* 115(16):3320-8.

Bottenstein JE, Sato GH: Growth of a rat neuroblastoma cell line in serum-free supplemented medium. *Proc Natl Acad Sci USA* 1979; **76**: 514–517.

Bottillo I, De Luca A, Schirinzi A, Guida V, Torrente I, Calvieri S, Gervasini C, Larizza L, Pizzuti A, Dallapiccola B. (2007) Functional analysis of splicing mutations in exon 7 of NF1 gene. *BMC Med Genet.* **12**;8:4.

Bottillo I, Ahlquist T, Brekke H, Danielsen SA, van den Berg E, Mertens F, Lothe RA, Dallapiccola B. (2009)Germline and somatic NF1 mutations in sporadic and NF1-associated malignant peripheral nerve sheath tumours. *J Pathol.* **217**(5):693-701.
Bourguignon LY, Zhu H, Shao L, *et al.* (1999) Rho-kinase (ROK) promotes CD44v(3,8–10)-ankyrin interaction and tumor cell migration in metastatic breast cancer cells. *Cell Motil Cytoskeleton* **43**:269–287.

Boyes J, Bird A. (1991). DNA methylation inhibits transcription indirectly via a methyl-CpG binding protein. *Cell 64*:1123–1134.

Brambilla R, Gnesutta N, Minichiello L, White G, Roylance AJ, Herron CE, Ramsey M, Wolfer DP, Cestari V, Rossi-Arnaud C, Grant SG, Chapman PF, Lipp HP, Sturani E, Klein R (1997) A role for the Ras signalling pathway in synaptic transmission and long-term memory. *Nature* **390**:281–286.

Brannan CI, Perkins AS, Vogel KS, Ratner N, Nordlund ML, Reid SW, Buchberg AM, Jenkins NA, Parada LF, Copeland NG. (1994) Targeted disruption of the neurofibromatosis type-1 gene leads to developmental abnormalities in heart and various neural crest-derived tissues. *Genes Dev.* **1**;8(9):1019-29.

Bustelo XR, Sauzeau V, Berenjeno IM. (2007) GTP-binding proteins of the Rho/Rac family: regulation, effectors and functions in vivo. *BioEssays* **29**:356–370.

Brekke HR, Kolberg M, Skotheim RI, Hall KS, Bjerkehagen B, Risberg B, Domanski HA, Mandahl N *et al.* (2009) Identification of p53 as a strong predictor of survival for patients with malignant peripheral nerve sheath tumors. *Neuro Oncol.* **11**(5):514-28.

Brekke HR, Ribeiro FR, Kolberg M, Agesen TH, Lind GE, Eknaes M, Hall KS, Bjerkehagen B, *et al.* (2010) Genomic changes in chromosomes 10, 16, and X in malignant peripheral nerve sheath tumors identify a high-risk patient group. *J Clin Oncol.* **28**(9):1573-82.

Brems H, Chmara M, Sahbatou M, Denayer E, Taniguchi K, Kato R, Somers R, Messiaen L, *et al.* (2007) Germline loss-of-function mutations in *SPRED1* cause a neurofibromatosis 1-like phenotype. *Nat Genet.* **39**(9):1120-1126.

Brems H, Park C, Maertens O, Pemov A, Messiaen L, Upadhyaya M, Claes K, Beert E, *et al.* (2010) Glomus tumors in neurofibromatosis type 1: genetic, functional, and clinical evidence of a novel association. Cancer Res 2009;69:7393e401.

Bridge RS Jr, Bridge JA, Neff JR, Naumann S, Althof P, Bruch LA. (2004) Recurrent chromosomal imbalances and structurally abnormal breakpoints within complex karyotypes of malignant peripheral nerve sheath tumour and malignant triton tumour: a cytogenetic and molecular cytogenetic study. *J Clin Pathol.* **57**(11):1172-8.

Brinkman AB, Simmer F, Ma K, Kaan A, Zhu J, Stunnenberg HG. Whole-genome DNA methylation profiling using MethylCap-seq. *Methods* **52**:232-6.

Broaddus E, Topham A, Singh AD. (2009) Incidence of retinoblastoma in the USA: 1975–2004. Br J Ophthalmol. **93**:21–23.

Bryan BA, D'Amore PA. (2007) What tangled webs they weave: Rho-GTPase control of angiogenesis, Cell Mol. *Life Sci* **64**:2053–2065.

Buckingham L, Penfield Faber L, Kim A, Liptay M, Barger C, Basu S, Fidler M, Walters K, *et al.* (2010) PTEN, RASSF1 and DAPK site-specific hypermethylation and outcome in surgically treated stage I and II nonsmall cell lung cancer patients. *Int J Cancer.* **126**(7):1630-9.

Byer SJ, Eckert JM, Brossier NM, Clodfelder-Miller BJ, Turk AN, Carroll AJ, Kappes JC, Zinn KR, Prasain JK. (2011) Carroll SLTamoxifen inhibits malignant peripheral nerve sheath tumor growth in an estrogen receptor-independent manner. Neuro Oncol **13**(1):28-41.

Camp RL, Chung GG, Rimm DL (2002) Automated subcellular localization and quantification of protein expression in tissue microarrays. *Nat Med* **8**:1323-1327.

Campbell PJ, Yachida S, Mudie LJ, Stephens PJ, Pleasance ED, Stebbings LA, Morsberger LA, Latimer C, *et al.* (2010) The patterns and dynamics of genomic instability in metastatic pancreatic cancer. *Nature* **467**:1109-1113.
Cappione AJ, French BL, Skuse GR. (1997) A potential role for NF1 mRNA editing in the pathogenesis of NF1 tumors. *Am J Hum Genet* **60**:305–312.

Cardesa A, Merchan J, Bullon-Ramirez A. (1978) Morphological and biological comparison of tumours prenatally induced in Wistar rats by ethylnitrosourea with their counterpart in man. Tumours of Early Life in Man and Animals. Edited by L Severi. Monteluce, Italy, Perugia Quadrennial International Conferences on Cancer

Carney JA, Hruska LS, Beauchamp GD, Gordon H. (1986) Dominant inheritance of the complex of myxomas, spotty pigmentation and endocrine overactivity. *Mayo Clin Proc* **61**:165-172.

Carroll SL, Ratner, N. (2008) How does the Schwann cell lineage form tumors in NF1? *Glia.* **1**:56(14):1590-605.

Carsillo T, Astrinidis, A. and Henske, EP. (2000) Mutations in the tuberous sclerosis complex gene TSC2 are a cause of sporadic pulmonary lymphangioleiomyomatosis. PNAS, U.S.A. **97**:6085–6090.

Cawkwell L, Lewis FA, Quirke P. (1994) Frequency of allele loss of DCC, p53, RBI, WT1, NF1, NM23 and APC/MCC in colorectal cancer assayed by fluorescent multiplex polymerase chain reaction. *Br J Cancer.* **70**(5):813-8.

Cawthon RM, Andersen LB, Buchberg AM, Xu GF, O'Connell P, Viskochil D, Weiss RB, Wallace MR, Marchuk DA, Culver M, *et al.* (1991) cDNA sequence and genomic structure of EV12B, a gene lying within an intron of the neurofibromatosis type 1 gene. Genomics. **9**(3):446-60.

Cawthon RM, Weiss R, Xu GF, *et al.* (1990a) A major segment of the neurofibromatosis type 1 gene: cDNA sequence, genomic structure, and point mutations. *Cell* **62**:193–201.

Cawthon RM, O'Connell P, Buchberg AM, Viskochil D, Weiss RB, Culver M, Stevens J, Jenkins NA, Copeland NG, White R. (1990b) Identification and characterization of transcripts from the von Recklinghausen neurofibromatosis region: the sequence and genomic structure of EVI2 and mapping of other transcripts. *Genomics* **7**:555-565.

Chai G, Liu N, Ma J, Li H, Oblinger JL, Prahalad AK, Gong M, Chang LS, Wallace M, Muir D, Guha A, Phipps RJ, Hock JM, Yu X. (2010) MicroRNA-10b regulates tumorigenesis in neurofibromatosis type 1. *Cancer Sci.* **101**(9):1997-2004.

Chao RC, Pyzel U, Fridlyand J, Kuo YM, Teel L, Haaga J, Borowsky A, Horvai A, Kogan SC, Bonifas J, Huey B, Jacks TE, Albertson DG, Shannon KM. (2005) Therapy-induced malignant neoplasms in Nf1 mutant mice. *Cancer Cell* **8**(4):337-48.

Chen P, Dudley S, Hagen W, Dizon D, Paxton L, Reichow D, Yoon S, Yang K, *et al.* (2005) Contributions by MutL homologues Mlh3 and Pms2 to DNA mismatch repair and tumor suppression in the mouse. *Cancer Res* **1**:65(19):8662–8670.

Chong-Kopera H, Inoki K, Li Y, Zhu T, Garcia-Gonzalo FR, Rosa JL, Guan KL. (2006) TSC1 stabilizes TSC2 by inhibiting the interaction between TSC2 and the HERC1 ubiquitin ligase. *J. Biol. Chem* **281**:8313–8316.

Choong K, Freedman MH, Chitayat D, *et al.* (1999) Juvenile myelomonocytic leukemia and Noonan syndrome. *J Pediatr Hematol Oncol* **21**:523–527.

Chou LS, Liu CS, Boese B, Zhang X, Mao R. (2010) DNA sequence capture and enrichment by microarray followed by next-generation sequencing for targeted resequencing: neurofibromatosis type 1 gene as a model. *Clin Chem* **56**(1):62-72.

Christman JK (2002) 5-Azacytidine and 5-aza-2'-deoxycytidine as inhibitors of DNA methylation: mechanistic studies and their implications for cancer therapy. Oncogene 21(35): 5483–5495.

Cichowski K, Santiago S, Jardim M, Johnson BW, Jacks T. (2003) Dynamic regulation of the Ras pathway via proteolysis of the NF1 tumor suppressor. *Genes Dev* **17**(4):449-54.
Cichowski K, Shih TS, Schmitt E, *et al.* (1999) Mouse models of tumor development in neurofibromatosis type 1. Science **286**(5447):2172- 2176.

Cichowski K, Jacks T. (2001) NF1 Tumor Suppressor Gene Function: Narrowing the GAP. *Cell* **104**:593–604.

Ciechanover A, Orian A, Schwartz AL. (2000) Ubiquitin-mediated proteolysis: Biological regulation via destruction. *BioEssays* **22**:442– 451.

Citak EC, Oguz A, Karadeniz C, Okur A, Memis L, Boyunaga O. (2008) Management of plexiform neurofibroma with interferon alpha. *Pediatr Hematol Oncol.*;**25**(7):673-8.

Clark SE, Warwick J, Carpenter R, Bowen RL, Duffy SW, Jones JL (2011) Molecular subtyping of DCIS: heterogeneity of breast cancer reflected in pre-invasive disease. *Br J Cancer* **104**:120-127.

Crosswell HE, Dasgupta A, Alvarado CS, Watt T, Christensen JG, De P, Durden DL, Findley HW. (2009) PHA665752, a small-molecule inhibitor of c-Met, inhibits hepatocyte growth factor-stimulated migration and proliferation of c-Met-positive neuroblastoma cells. *BMC Cancer.* **25**;9:411.

Corral T, Jiménez M, Hernández-Muñoz I, Pérez de Castro I, Pellicer A. (2003) NF1 modulates the effects of Ras oncogenes: evidence of other NF1 function besides its GAP activity. *J Cell Physiol* **197**(2):214-24.

Cobrinik D. (2005) Pocket proteins and cell cycle control. *Oncogene* **24**(17):2796-809.

Cohen Y, Singer G, Lavie O, Dong SM, Beller U, Sidransky D. (2003) The RASSF1A tumor suppressor gene is commonly inactivated in adenocarcinoma of the uterine cervix. *Clin Cancer Res* **9**(8):2981-4.

Colella S, Shen L, Baggerly KA, Issa JP, Krahe R. (2003) Sensitive and quantitative universal Pyrosequencing methylation analysis of CpG sites. *Biotechniques* **35**:146-150.

Collins FS, O'Connell P, Ponder BAJ, Seizinger BR. (1989) Progress towards identifying the neurofibromatosis (NF1) gene. *Trends Genet* **5**:217-221.

Consoli C, Moss C, Green S, Balderson D, Cooper DN, Upadhyaya M. (2005) Gonosomal mosaicism for a nonsense mutation (R1947X) in the NF1 gene in segmental neurofibromatosis type 1. *J Invest Dermatol* **125**(3):463-6.

Cooper SC, Park M, Blair DG, *et al* (1984) Molecular cloning of a new transforming gene from a chemically transformed human cell line. *Nature* **311**:29-33.

Cooper DN, Youssoufian H (1988) The CpG dinucleotide and human genetic disease. *Hum Genet* **78**:151-155.

Cooper DN and Krawczak M (1993) Human Gene Mutation. Oxford: BIOS Scientific Publishers, pp402

Cooper DN, Mort M, Stenson PD, Ball EV, Chuzhanova NA. (2010) Methylation-mediated deamination of 5-methylcytosine appears to give rise to mutations causing human inherited disease in CpNpG trinucleotides as well as in CpG dinucleotides. *Hum Genomics.* **4**:406-410.

Cordeddu V, Di Schiavi E, Pennacchio LA, Ma'ayan A, Sarkozy A, *et al.* (2009) Mutation of *SHOC2* promotes aberrant protein N-myristoylation and causes Noonan-like syndrome with loose anagen hair. *Nat Genet* **41**:1022– 1026.

Costa RM, Federov NB, Kogan JH, Murphy GG, Stern J, Ohno M, Kucherlapati R, Jacks T, Silva AJ. (2002) Mechanism for the learning deficits in a mouse model of neurofibromatosis type 1. *Nature* **415**(6871):526-30.

Costello JM. (1971) A new syndrome. *N Z Med J* **74**:397.
Costello JM. (1977) A new syndrome: mental subnormality and nasal papillomata. *Aust Paediatr J* **13**:114-118.

Cotton RGH, Rodrigues NR, Campbell RD (1988) Reactivity of cytosine and thymine in single-base-pair mismatches with hydroxylamine and osmium tetroxide and its application to the study of mutations. *Proc Natl Acad Sci USA* **85**:4397–4401.

Cowell JK, Smith T, Bia B (1994) Frequent constitutional C to T mutations in CGA-arginine codons in the RB1 gene produce premature stop codons in patients with bilateral (hereditary) retinoblastoma. *Eur J Hum Genet* **2**:281-290.

Cowley GS, Murthy AE, Parry DM, Schneider G, Korf B, Upadhyaya M, Harper P, MacCollin M, Bernards A, Gusella JF. (1998) Genetic variation in the 3' untranslated region of the neurofibromatosis 1 gene: application to unequal allelic expression. *Somat Cell Mol Genet* **24**(2):107-19.

Crosswell HE, Dasgupta A, Alvarado CS, Watt T, Christensen JG, De P, Durden DL, Findley HW. (2009) PHA665752, a small-molecule inhibitor of c-Met, inhibits hepatocyte growth factor-stimulated migration and proliferation of c-Met-positive neuroblastoma cells. *BMC Cancer.* **25**:9:411.

Cummings LM, Trent JM, Marchuk DA (1996) Identification and mapping of type 1 neurofibromatosis (NF1) homologous loci. Cytogenet Cell Genet 73:334–340.

D'Agostino, A.N., Soule, E.H. and Miller, R.H. (1963) Sarcomas of the Peripheral Nerves and Somatic Soft Tissues Associated with Multiple Neurofibromatosis (Von Recklinghausen's Disease). *Cancer* **16**:1015-1027

D'Angelo I, Welti S, Bonneau F, Scheffzek K. (2006) A novel bipartite phospholipidbinding module in the neurofibromatosis type 1 protein. *EMBO Rep* **7**:174–179.

Dammann R, Li C, Yoon JH, Chin PL, Bates S, Pfeifer GP. (2000) Epigenetic inactivation of a RAS association domain family protein from the lung tumour suppressor locus 3p21.3. *Nat Genet* **25**(3):315-9.

Danglot G, Regnier V, Fauvet D, *et al.* (1995) Neurofibromatosis 1 (NF1) mRNAs expressed in the central nervous system are differentially spliced in the 59 part of the gene. *Hum Mol Genet* **4**:915–920.

Dannenberg JH, Te Riele HP. (2006) The retinoblastoma gene family in cell cycle regulation and suppression of tumorigenesis. *Results Probl. Cell Differ.* **42**, 183–225.

Däschner K, Assum G, Eisenbarth I, Krone W, Hoffmeyer S, Wortmann S, Heymer B, Kehrer-Sawatzki H (1997) Clonal origin of tumor cells in a plexiform neurofibroma with LOH in NF1 intron 38 and in dermal neurofibromas without LOH of the NF1 gene. *Biochem Biophys Res Commun* **19**:234(2):346–350.

Dasgupta B, Dugan LL, GutmannDH (2003a). The neurofibromatosis 1 gene product neurofibromin regulates pituitary adenylate cyclase-activating polypeptide-mediated signaling in astrocytes. *J Neurosci* **23**:8949–8954.

Dasgupta S, Chakraborty SB, Roy A, Roychowdhury S, Panda CK. (2003b) Differential deletions of chromosome 3p are associated with the development of uterine cervical carcinoma in Indian patients. *Mol Pathol* **56**(5):263-9.

Dasgupta B, Yi Y, Chen DY, Weber JD, Gutmann DH (2005) Proteomic analysis reveals hyperactivation of the mammalian target of rapamycin pathway in neurofibromatosis 1-associated human and mouse brain tumors. *Cancer Res* **65**(7):2755-60.

Daston MM, Ratner N. (1992) Neurofibromin, a predominantly neuronal GTPase activating protein in the adult, is ubiquitously expressed during development. *Dev Dyn* **195**(3):216-26.

Daston MM, Scrable H, Nordlund M, *et al.* (1992b) The protein product of the neurofibromatosis type 1 gene is expressed at highest abundance in neurons, Schwann cells and oligodendrocytes. Neuron **8**:415–428.

Datta SR, Brunet A, Greenberg ME. (1999) Cellular survival: a play in three Akts. *Genes Dev* **13**:2905–2927.

Davies DM, Johnson SR, Tattersfield AE, Kingswood JC, Cox JA, McCartney DL, Doyle T, Elmslie F. *et al* (2008) Sirolimus therapy in tuberous sclerosis or sporadic lymphangioleiomyomatosis. *N. Engl. J. Med* **358**:200–203.

Davies H, Bignell G, Cox C, *et al.* (2002) Mutations in BRAF gene in human cancer. Nature **417**:949-954

DeClue JE, Cohen BD, Lowy DR. (1991) Identification and characterization of the neurofibromatosis type 1 gene product. *Proc Natl Acad Sci USA* **88**:9914–9918.

De Luca A, Buccino A, Gianni D, Mangino M, Giustini S, Richetta A, Divona L, Calvieri S, Mingarelli R, Dallapiccola B (2003) NF1 gene analysis based on DHPLC. *Hum Mutat* **21**(2):171-2.

De Luca A, Schirinzi A, Buccino A, Bottillo I, Sinibaldi L, Torrente I, Ciavarella A, Dottorini T, Porciello R, Giustini S, Calvieri S, Dallapiccola B. (2004) Novel and recurrent mutations in the NF1 gene in Italian patients with neurofibromatosis type 1. *Hum Mutat* **23**(6):629.

De Luca A, Bottillo I, Dasdia MC, Morella A, Lanari V, Bernardini L, Divona L, Giustini S, *et al.* (2007) Deletions of *NF1* gene and exons detected by multiplex ligation-dependent probe amplification. *J Med Genet* **44**:800-808.

Demitsu T, Murata S, Kakurai M, Kiyosawa T, Yaoita H. (1998) Malignant schwannoma-derived cells support human skin mast cell survival in vitro. *J Dermatol Sci* **16**:129–134.

DerMardirossian C, Bokoch GM. (2005) GDIs: central regulatory molecules in Rho GTPase activation. *Trends Cell Biol* **15**:356–363.

Denayer E, De Ravel T, Legius E. (2008) Clinical and molecular aspects of RAS related disorders. *Journal of Medical Genetics* **45**(11):695-703.

De Pril R, Perera, T, Lekkerkerker A. (2009) A high-content screen for inhibitors of cell migration in cancer metastasis using adenoviral knock-down. *BTi April / May*

De Raedt T, Brems H, Wolkenstein P, Vidaud D, Pilotti S, Perrone F, Mautner V, Frahm S, Sciot R, Legius E. (2003) Elevated risk for MPNST in NF1 microdeletion patients. *Am J Hum Genet* **72**:1288–1292.

De Raedt T, Brems H, Lopez-Correa C, Vermeesch JR, Marynen P, Legius E. (2004) Genomic organization and evolution of the NF1 microdeletion region. *Genomics* **84**:346–360.

De Raedt T, Maertens O, Chmara M, Brems H, Heyns I, Sciot R, Majounie E, Upadhyaya M, De Schepper S, Speleman F, Messiaen L, Vermeesch JR, Legius E (2006) Somatic loss of wild type NF1 allele in neurofibromas: comparison of NF1 microdeletion and non-microdeletion patients. *Genes, Chromosomes Cancer* **45**:893–904.

De Ruiter ND, Burgering BM, Bos JL. (2001) Regulation of the Forkhead transcription factor AFX by Ral-dependent phosphorylation of threonines 447 and 451. *Mol. Cell. Biol* **21**:8225–8235.

De Wind N, Dekker M, Berns A, *et al* (1995) Inactivation of the mouse Msh2 gene results in mismatch repair deficiency, methylation tolerance, hyperrecombination, and predisposition to cancer. *Cell* **82**:321–330.

Diehl SR, Boehnke M, Erickson RP, Ploughman LM, Seiler KA, Lieberman JL, Clarke HB, Bruce MA, *et al.* (1989). A refined genetic map of the region of chromosome 17 surrounding the von Recklinghausen neurofibromatosis (NF1) gene. Am. J. Hum. *Genet* **44**:33-37.

Digilio MC, Conti E, Sarkozy A, Mingarelli R, Dottorini T, Marino B, Pizzuti A, Dallapiccola B. (2002) Grouping of multiple-lentigines/LEOPARD and Noonan syndromes on the PTPN11 gene. *Am. J. Hum. Genet* **71**:389–394.

Ding L, Getz G, Wheeler DA, Mardis ER, McLellan MD, Cibulskis K, Sougnez C, Greulich H, *et al.* (2008) Somatic mutations affect key pathways in lung adenocarcinoma. *Nature.* **455**(7216):1069-75.

Djalilvand A, Pal R, Goldman H, Antonioli D, Kocher O. (2004) Evaluation of p53 mutations in premalignant esophageal lesions and esophageal adenocarcinoma using laser capture microdissection. *Mod Pathol.* **17**(11):1323-7.

Dorschner MO, Sybert VP, Weaver M, Pletcher BA, Stephens K. (2000) NF1 microdeletion breakpoints are clustered at flanking repetitive sequences. *Hum Mol Genet.* **9**(1):35-46.

Downward J. (2003) Targeting RAS signalling pathways in cancer therapy. *Nat Rev Cancer.* **3**(1):11-22.

Ducatman BS, *et al.* (1986) Malignant peripheral nerve sheath tumors. A clinicopathologic study of 120 cases. *Cancer* **57**:2006-2021.

Duong TA, Sbidian E, Valeyrie-Allanore L, Vialette C, Ferkal S, Hadj-Rabia S, Glorion C, Lyonnet S, (2011) Mortality Associated with Neurofibromatosis 1: A Cohort Study of 1895 Patients in 1980-2006 in France. *Orphanet J Rare Dis* **6**(1):18.

Eads CA, Danenberg KD, Kawakami K, Saltz LB, Blake C, Shibata D, Danenberg PV, Laird PW. (2000) MethyLight: a high-throughput assay to measure DNA methylation. *Nucleic Acids Res* **28**(8):E32.

Ebinger M, Senf L, Wachowski O, Scheurlen W. (2005) No aberrant methylation of neurofibromatosis 1 gene (NF1) promoter in pilocytic astrocytoma in childhood. *Pediatr Hematol Oncol* **22**:83-7.

Edwards RA. (2007). Laser capture microdissection of mammalian tissue. *J Vis Exp.* 2007;(8):309.

Eerola I, Boon LM, Mulliken JB, Burrows PE, Dompmartin A, Watanabe S, Vanwijck R, Vikkula M. (2003) Capillary malformationarteriovenous malformation, a new clinical and genetic disorder caused by RASA1 mutations. *Am J Hum Genet* **73**:1240-1249.

Eisenbarth I, Hoffmeyer S, Kaufmann D, Assum G, Krone W. (1995) Analysis of an alternatively spliced exon of the neurofibromatosis type 1 gene in cultured melanocytes from patients with neurofibromatosis 1. *Arch Dermatol Res* **287**(5):413-6.

Eisenbarth I, Vogel G, Krone W, Vogel W, Assum G. (2000) An isochore transition in the NF1 gene region coincides with a switch in the extent of linkage disequilibrium. *Am J Hum Genet* **67**:873– 880.

Engers R, Ziegler S, Mueller M, Walter A, Willers R, Gabbert HE. (2007) Prognostic relevance of increased Rac GTPase expression in prostate carcinomas. *Endocr.-Relat. Cancer* **14**: 245–256.

Eperon IC, Ireland DC, Smith RA, Mayeda A & Krainer AR (1993) Pathways for selection of 5' splice sites by U1 snRNPs and SF2/ASF. *EMBO J* **12**:3607– 3617.

Erem C, Onder Ersöz H, Ukinç K, Hacihasanoglu A, Alhan E, Cobanoğlu U, Koçak M, Erdöl H. (2007) Neurofibromatosis type 1 associated with pheochromocytoma: a case report and a review of the literature. *J Endocrinol Invest* **30**(1):59-64.

Erickson RP. (2010) Somatic gene mutation and human disease other than cancer: an update. *Mutat Res* **705**(2):96-106.

Espina V, Wulfkuhle JD, Calvert VS, VanMeter A, Zhou W, Coukos G, Geho DH, Petricoin III EF, Liotta LA. (2006) Laser-capture Microdissection *Nature Protocols* 1(2):586-603

Espina C, Céspedes MV, García-Cabezas MA, Gómez del Pulgar MT, Boluda A, Oroz LG, Benitah SA, Cejas P, Nistal M, Mangues R, Lacal JC. (2008) A critical role for Rac1 in tumor progression of human colorectal adenocarcinoma cells. *Am. J. Pathol* **172**:156–166.

Esteller M, Herman JG. (2002) Cancer as an epigenetic disease: DNA methylation and chromatin alterations in human tumours. *J Pathol* **196**(1):1-7. Review.

Esteller M, Toyota M, Sanchez-Cespedes M, Capella G, Peinado MA, Watkins DN, Issa JP, Sidransky D, Baylin SB, Herman JG. (2000) Inactivation of the DNA repair gene O6-methylguanine-DNA methyltransferase by promoter hypermethylation is associated with G to A mutations in K-ras in colorectal tumorigenesis. *Cancer Res* **1**:2368-71.

Esteve PO, Chin HG, Pradhan S. (2005) Human maintenance DNA (cytosine-5)-methyltransferase and p53 modulate expression of p53-repressed promoters. Proc Natl Acad Sci USA **102**:1000–1005.

Evans DG, Baser ME, McGaughran J, *et al.* (2002) Malignant peripheral nerve sheath tumours in neurofibromatosis 1. *J Med Genet* **39**:311–14.

Evans, DG, Howard E, Giblin C *et al.* (2010) Birth incidence and prevalence of tumour prone syndromes: estimates from a UK genetic family register service. *Am J Med Genet A* **152A**:327–32.

Fabbro M, Henderson BR. (2003) Regulation of tumor suppressors by nuclear-cytoplasmic shuttling. *Exp Cell Res* **282**(2):59-69.

Fahsold R, Hoffmeyer S, Mischung C, Gille C, Ehlers C, Kücükceylan N, Abdel-Nour M, Gewies A, *et al.* Minor lesion mutational spectrum of the entire NF1 gene does not explain its high mutability but points to a functional domain upstream of the GAP-related domain. Am J Hum Genet. 2000; 66(3):790-818.

Fain PD, Barker D, Goldgar E, Wright K, Nguyen J, Carey J, Johnson J, Kivlin H, *et al.* (1987) Genetic analysis of NF1: identification of close flanking markers on chromosome 17. *Genomics* **1**:340-345.

Fain PR, Wright E, Willard HF, Stephens K, Barker DF. (1989a) The Order of Loci in the Pericentric Region of Chromosome 17, Based on Evidence from Physical and Genetic Breakpoints *Am. J. Hum. Genet* **44**:68-72,

Fain PR, Goldgar DE, Wallace MR, Collins FS, Wright E, Nguyen K, Barker DF. (1989b) Refined Physical and Genetic Mapping of the NFI Region on Chromosome 17 *Am. J. Hum. Genet* **45**:721-728.

Fang L, Chalhoub N, Li W, Feingold J, Ortenberg J, Lemieux B, Thirion JP. (2001) Genotype analysis of the NF1 gene in the French Canadians from the Québec population. *Am J Med Genet.***104**(3):189-98.

Fauth C, Kehrer-Sawatzki H, Zatkova A, Machherndl-Spandl S, Messiaen L, Amann G, Hainfellner JA, Wimmer K. (2009) Two sporadic spinal neurofibromatosis patients with malignant peripheral nerve sheath tumour. *Eur J Med Genet.* **52**(6):409-14.

Feig LA. (2003) Ral-GTPases: approaching their 15 minutes of fame. *Trends Cell Biol* **13**:419–425.

Feitsma H, Kuiper RV, Korving J, Nijman IJ, Cuppen E (2008) Zebrafish with mutations in mismatch repair genes develop neurofibromas and other tumors. *Cancer Res* **1**:68(13):5059–5066.

Felgner PL, Gadek TR, Holm M, Roman R, Chan HW, Wenz M, Northrop JP, Ringold GM, Danielsen M. (1987) Lipofection: a highly efficient, lipid-mediated DNA-transfection procedure. *Proc Natl Acad Sci U S A* **84**(21):7413-7.

Feng L, Yunoue S, Tokuo H, Ozawa T, Zhang D, Patrakitkomjorn S, Ichimura T, Saya H, Araki N. (2004) PKA phosphorylation and 14-3-3 interaction regulate the function of neurofibromatosis type I tumor suppressor, neurofibromin. *FEBS Lett.* **557**(1-3):275-82.

Ferner RE, Gutmann DH. (2002) International consensus statement on malignant peripheral nerve sheath tumors in neurofibromatosis. *Cancer Res* **62**:1573–7.

Ferner RE, Hughes RA, Hall SM, *et al.* (2004) Neurofibromatous neuropathy in neurofibromatosis 1 (NF1). *J Med Genet* **41**:837–41. 19.

Ferner RE, Huson SM, Thomas N, Moss, C., Willshaw, H., Evans, D.G., Upadhyaya, M., Towers, R., Gleeson, M., Steiger, C., Kirby, A. (2007) Guidelines for the diagnosis and management of individuals with neurofi bromatosis 1. *J Med Genet* **44**:81–88.

Ferner RE, Golding JF, Smith M, *et al.* (2008) [18F]2- fluoro-2-deoxy-D-glucose positron emission tomography (FDG PET) as a diagnostic tool for neurofi bromatosis 1 (NF1) associated malignant peripheral nerve sheath tumours (MPNSTs): a longterm clinical study. *Ann Oncol* **19**:390–4.

Ferrari A, Miceli R, Rey A, Oberlin O, Orbach D, Brennan B, Mariani L, Carli M *et al.* (2011) Non-metastatic unresected paediatric non-rhabdomyosarcoma soft tissue sarcomas: results of a pooled analysis from United States and European groups. *Eur J Cancer* **47**(5):724-31.

Fishbein L, Eady B, Sanek N, Muir D, Wallace MR. (2005). Analysis of somatic NF1 promoter methylation in plexiform neurofibromas and Schwann cells. *Cancer Genet Cytogenet* **157**(2):181-6.

Flotho C, Valcamonica S, Mach-Pascual S, Schmahl G, Corral L, Ritterbach J, Hasle H, Arico M, Biondi A, Niemeyer CM. (1999) RAS mutations and clonality analysis in children with juvenile myelomonocytic leukemia (JMML). *Leukemia* **13**:32–37.

Flotho C, Kratz CP, Niemeyer CM. (2007) Targeting RAS signaling pathways in juvenile myelomonocytic leukemia. *Curr Drug Targets* **8**:715-725

Fountain JW, Wallace MR, Bruce MA, *et al.* (1989) Physical mapping of a translocation breakpoint in neurofibromatosis. *Science* **244:**1085-7.

Fukuda T, Ichimura E, Shinozaki T, Sano T, Kashiwabara K, Oyama T, Nakajima T, Nakamura T. (1998) Coexpression of HGF and c-Met/ HGF receptor in human bone and soft tissue tumors. *Pathol Int* **48**:757–762.

Fragale A, Tartaglia M, Wu J, Gelb BD. (2004) Noonan syndrome-associated SHP2/PTPN11 mutants cause EGF-dependent prolonged GAB1 binding and sustained ERK2/MAPK1 activation. Hum. *Mutat* **23**:267–277.

Freeman RM Jr, Plutzky J, Neel BG. (1992) Identification of a human src homology 2-containing protein-tyrosine-phosphatase: a putative homolog of Drosophila corkscrew. *Proc. Natl. Acad. Sci. USA* **89**:11239–11243.

Friend SH, Bernards R, Rogelj S, *et al.* (1986) human DNA segment with properties of the gene that predisposes to retinoblastoma and osteosarcoma. *Nature* **323**:643–646.

Friedman JM, Gutmann DH, Riccardi VM, eds. (1999) Neurofibromatosis: Phenotype, Natural history, and Pathogenesis. Baltimore: Johns Hopkins Univ. *Press* 400 pp. 3rd ed.

Fritz G, Just I, Kaina B. (1999) Rho GTPases are over-expressed in human tumors. *Int. J. Cancer* **81**: 682–687.

Frommer M, McDonald LE, Millar DS, Collis CM, Watt F, Grigg GW, Molloy PL, Paul CL. (1992) A genomic sequencing protocol that yields a positive display of 5-methylcytosine residues in individual DNA strands, *PNAS U. S. A.* **89**:1827–1831.

Garcia-Linares C, Fernández-Rodríguez J, Terribas E, Mercadé J, Pros E, Benito L, Benavente Y, Capellà G, *et al.* (2011) Dissecting loss of heterozygosity (LOH) in neurofibromatosis type 1-associated neurofibromas: Importance of copy neutral LOH. *Hum Mutat* **32**(1):78-90.

Gardiner-Garden M, Frommer M. (1987) CpG islands in vertebrate genomes. *J Mol Biol* **196**:261–282.

Gasparini P, D'Agruma L, Pio de Cillis G, Balestrazzi P, Mingarelli R, Zelante L. (1996) Scanning the first part of the neurofibromatosis type 1 gene by RNA-SSCP: identification of three novel mutations and of two new polymorphisms. *Hum Genet* **97**(4):492-5.

Gibson P, Tong Y, Robinson G, Thompson MC, Currle DS, Eden C, Kranenburg TA, Hogg T *et al.* (2010) Subtypes of medulloblastoma have distinct developmental origins. *Nature* **468**:1095-1099.

Giuly JA, Picand R, Giuly D, Monges B, Nguyen-Cat R. (2003) Von Recklinghausen disease and gastrointestinal stromal tumors. *Am J Surg* **185**:86-87.

Goedegeburre SA. (1975) A case of neurofibromatosis in the dog. *J Small Anim Pract* **16**:329-335y.

Goebbels S, Oltrogge JH, Kemper R, Heilmann I, Bormuth I, Wolfer S, Wichert SP, Möbius W *et al.* (2010) Elevated phosphatidylinositol 3,4,5-trisphosphate in glia triggers cell-autonomous membrane wrapping and myelination. *J. Neurosci* **30**:8953–8964

Goedegeburre SA. (1975) A case of neurofibromatosis in the dog. *J Small Anim Pract* **16**:329-335.

Goldgar DE, Green P, Parry DM, Mulvihill JJ. (1989) Multipoint linkage analysis in neurofibromatosis type 1: an international collaboration Am. J. *Hum. Genet* **44**:6-12.

Golubic M, Roudebush M, Dobrowski S, Wolfman A, Stacey DW. (1992) Catalytic properties, tissue and intracellular distribution of neurofibromin. *Oncogene* **7**(11):2151-2160.

Gorlin RJ, Anderson RC, Moller JH. (1971) The Leopard (multiple lentigines) syndrome revisited. *Birth Defects Orig Artic Ser* **07**(4):110-5.

Götte K, Riedel F, Neubauer J, Schäfer C, Coy JF, Hörmann K. (2001) The relationship between allelic imbalance on 17p, p53 mutation and p53 overexpression in head and neck cancer. *Int J Oncol* **19**:331-336.

Gottfried ON, Viskochil DH, Fults DW, Couldwell WT. (2006) Molecular, genetic, and cellular pathogenesis of neurofibromas and surgical implications. *Neurosurgery* **58**(1):1-16.

Gottlieb B, Beitel LK, Trifiro MA. (2001) Comment in: Trends in Genet 17: 627-628. Somatic mosaicism and variable expressivity. *Tends Genet* **17**:79-82.

Greenblatt MS, Bennett WP, Hollstein M, Harris CC. (1994) Mutations in the p53 tumor suppressor gene: clues to cancer etiology and molecular pathogenesis. *Cancer Res* **54**(18):4855-78. Review.

Greggio H. (1911) Les cellules granuleuses (Mastzellen) dans les tissus normaux et dans certaines maladies chirurgicales. *Arch. Med Exp* **23**:323-375.

Gregorian C, Nakashima J, Dry SM, Nghiemphu PL, Smith KB, Ao Y, Dang J, Lawson G, *et al.* (2009) 17PTEN dosage is essential for neurofibroma development and malignant transformation. *Proc Natl Acad Sci U S A* **106**(46):19479-84.

Gregory PE, Gutmann DH, Boguski M, *et al.* (1993) The neurofibromatosis type 1 gene product, neurofibromin, associates with microtubules. *Somat Cell Mol Genet* **19**:265–274.

Gregor PE, Gutmann DH, Mitchell A, Park S, Boguski M, Jacks T, Wood DL, Jove R, Collins FS. (1993) Neurofibromatosis type 1 gene product (neurofibromin) associates with microtubules. *Somat Cell Mol Genet* **19**(3):265-74.

Griffin, J. W. & Thompson, W. J. (2008) Biology and pathology of nonmyelinating Schwann cells. *Glia* **56**:1518–1531.

Griffiths, I. *et al.* (1998) Axonal swellings and degeneration in mice lacking the major proteolipid of myelin. *Science* **280**:1610–1613.

Griffiths S, Thompson P, Frayling I, Upadhyaya M. (2007) Molecular diagnosis of neurofibromatosis type 1: 2 years experience. *Fam Cancer* **6**(1):21-34.

Griner E. M. and Kazanietz M. G. (2007) Protein kinase C and other diacylglycerol effectors in cancer. Nat. Rev. *Cancer* **7**:281–294.

Gripp, K.W. (2005) Tumor predisposition in Costello syndrome. *AmJ Med Genet C Semin Med Genet* **137**:72-77.

Grobmyer, S.R. *et al.* (2008) Malignant peripheral nerve sheath tumor: molecular pathogenesis and current management considerations. *Journal of Surgical Oncology* **97**:340-349.

Grobmyer, S.R. *et al.* (2008) Malignant peripheral nerve sheath tumor: molecular pathogenesis and current management considerations. *Journal of Surgical Oncology* **97**:340-349.

Gupta A, Cohen BH, Ruggieri P, Packer RJ, Phillips PC. (2003) Phase I study of thalidomide for the treatment of plexiform neurofibroma in neurofibromatosis 1.*Neurology.* **60**(1):130-2.

Guo HF, The I, Hannan F, Bernards A, Zhong Y. (1997) Requirement of Drosophila NF1 for activation of adenylyl cyclase by PACAP38-like neuropeptides. *Science* **276**:795–798.

Guo HF, Tong J, Hannan F, Luo L, Zhong Y. (2000) A neurofibromatosis- 1-regulated pathway is required for learning in Drosophila. *Nature* **403**:895– 898.

Gutmann DH, Collins FS (1992) Recent progress toward understanding the molecular biology of von Recklinghausen neurofibromatosis. *Ann Neurol* **31**(5):555-61.

Gutmann DH, Collins FS. (1993) The neurofibromatosis type 1 gene and its protein product, neurofibromin. *Neuron* **10**:335–343.

Gutmann DH, Boguski M, Marchuk D, Wigler M, Collins FS, Ballester R. (1993d) Analysis of the neurofibromatosis type 1 (NF1) GAP-related domain by site directed mutagenesis. *Oncogene* **8**:761–769.

Gutmann, D.H., Tennekoon, G.I., Cole, J.L., Collins, F.S., and Rutkowski, J.L. (1993c) Modulation of the neurofibromatosis type 1 gene product, neurofibromin, during Schwann cell differentiation. *J . Neurosci. Res* **36**:216-223.

Gutmann DH, Geist RT, Rose K, Wright DE. (1995) Expression of two new protein isoforms of the neurofibromatosis type 1 gene product, neurofibromin, in muscle tissues. *Dev Dyn.* **202**(3):302-11.

Gutmann DH, Geist RT, Wright DE, Snider WD. (1995b) Expression of the neurofibromatosis 1 (NF1) isoforms in developing and adult rat tissues. *Cell Growth Differ* **6**:315–322.

Gutmann DH, Aylsworth A, Carey JC, Korf B, Marks J, *et al.* (1997) The diagnostic evaluation and multidisciplinary management of neurofibromatosis 1 and neurofibromatosis 2. *JAMA* **278**:51–57.

Gutmann DH, Loehr A, Zhang Y, Kim J, Henkemeyer M, Cashen A. (1999) Haploinsufficiency for the neurofibromatosis 1 (NF1) tumor suppressor results in increased astrocyte proliferation. *Oncogene* **18**:4450–4459.

Gutmann DH, Hirbe AC, Haipek CA. (2001) Functional analysis of neurofibromatosis 2 (NF2) missense mutations. *Hum Mol Genet.* **10**(14):1519-29.

Gutmann DH, Winkeler E, Kabbarah O, Hedrick N, Dudley S, *et al.* (2003) Mlh1 deficiency accelerates myeloid leukemogenesis in neurofibromatosis 1 (Nf1) heterozygous mice. *Oncogene* **22**:4581–85.

Haas-Kogan D, Stokoe D. (2008) PTEN in brain tumors. *Expert Rev Neurother*; **8**:599–610.

Habib AA, Gulcher JR, Hognason T, Zheng L, Stefansson K. (1998) The OMgp gene, a second growth suppressor within the NF1 gene. *Oncogene* **16**:1525 ± 1531.

Hadjiagapiou C, Giannoni F, Funahashi T, Skarosi SF, Davidson NO (1994) Molecular cloning of a human small intestinal apolipoprotein B mRNA editing protein. *Nucleic Acids Res* **22**:1874–1879.

Haeussler J, Haeusler J, Striebel AM, Assum G, Vogel W, Furneaux H, Krone W. (2000) Tumor antigen HuR binds specifically to one of five protein-binding segments in the 3'-untranslated region of the neurofibromin messenger RNA. Biochem Biophys Res Commun **267**(3):726-32.

Haferlach C, Dicker F, Kohlmann A, Schindela S, Weiss T, Kern W, Schnittger S, Haferlach T. (2010) AML with CBFB-MYH11 rearrangement demonstrate RAS pathway alterations in 92% of all cases including a high frequency of NF1 deletions. *Leukemia* **24**:1065-9

Haines TR, Rodenhiser DI, Ainsworth PJ. (2001) Allele-specific non-CpG methylation of the Nf1 gene during early mouse development. *Dev Biol* **240**(2):585-98.

Hajra A, Martin-Gallardo A, Tarle´ SA, Freedman M, Wilson-Gunn S, Bernards A, Collins FS. (1994) DNA sequences in the promoter region of the NF1 gene are highly conserved between human and mouse. *Genomics* **21**:649–52.

Hamad NM, Elconin JH, Karnoub AE, Bai W, Rich JN, Abraham RT, Der CJ, Counter CM. (2002) Distinct requirements for Ras oncogenesis in human versus mouse cells. *Genes Dev* **16**:2045–2057.

Han SY, Kato H, Kato S, Suzuki T, Shibata H, Ishii S, Shiiba K, Matsuno S, Kanamaru R, Ishioka C. (2000) Functional evaluation of PTEN missense mutations using in vitro phosphoinositide phosphatase assay. Cancer Res. **60**(12):3147-51.

Hanna N, Montagner A, Lee WH, Miteva M, Vidal M, Vidaud M, Parfait B, Raynal P. (2006) Reduced phosphatase activity of SHP-2 in LEOPARD syndrome: consequences for PI3K binding on Gab1. *FEBS Lett* **580**:2477–2482.

Hannan F, Ho I, Tong JJ, Zhu Y, Nurnberg P, Zhong Y (2006) Effect of neurofibromatosis type I mutations on a novel pathway for adenylyl cyclise activation requiring neurofibromin and Ras. *Hum Mol Genet* **15**:1087–1098.

Harder A, Rosche M, Reuss DE *et al.* (2004) methylation analysis of the neurofibromatosis type 1 (NF1) promoter in peripheral nerve sheath tumours. *Eur J Cancer* **40**(18):2820-8.

Harder A, Titze S, Herbst L, Harder T, Guse K, Tinschert S, Kaufmann D, Rosenbaum T, Mautner VF, Windt E, Wahlländer-Danek U, Wimmer K *et al.* (2010) Monozygotic twins with neurofibromatosis type 1 (NF1) display differences in methylation of NF1 gene promoter elements, 5' untranslated region, exon and intron 1. *Twin Res Hum Genet* **13**:582-94.

Harnois TB, Constantin A, Rioux E, Grenioux A, Kitzis N. Bourmeyster N. (2003) Differential interaction and activation of Rho family GTPases by p210bcr-abl and p190bcr-abl. *Oncogene* **22**:6445–6454.

Hastings ML, Krainer AR. (2001) Pre-mRNA splicing in the new millennium. *Curr Opin Cell Biol* **13**:302–309.

Hattori S, Maslawa M, Nalamura S. (1992) Identification of neurofibromatosis type I gene product as an insoluble GTPase-activating protein toward ras p21. *Oncogene* **7**:481–485.

Heim RA, Kam-Morgan LN, Binnie CG, Corns DD, Cayouette MC, Farber RA, Aylsworth AS, Silverman LM, Luce MC. (1995) Distribution of 13 truncating mutations in the neurofibromatosis 1 gene. *Hum Mol Genet.* **4**(6):975-81.

Hegyi L, Thway K, Newton R, Osin P, Nerurkar A, Hayes A J, Fisher C. (2009) Malignant myoepithelioma adenomyoepithelioma of the breast coincident multiple gastrointestinal stromal tumours in a patient with neurofibromatosis type 1. *J. Clin. Pathol* **62**:653-655.

Henkemeyer M, Rossi DJ, Holmyard DP, Puri MC, Mbamalu G, Harpal K, Shih TS, Jacks T, Pawson T. (1995) Vascular system defects and neuronal apoptosis in mice lacking ras GTPase-activating protein. *Nature* **377**(6551):695-701.

Herbst RS *et al.* (2002) Selective oral epidermal growth factor receptor tyrosine kinase inhibitor ZD1839 is generally well-tolerated and has activity in non-small-cell lung cancer and other solid tumors: results of a phase I trial. *Journal of Clinical Oncology* 20:3815-3825.

Herman JG, Graff JR, Myohanen S, Nelkin BD, Baylin SB. (1996) Methylation specific PCR: a novel PCR assay for methylation status of CpG islands. *PNAS USA* **93**(18):9821-6.

Herman JG, Baylin SB. (2003) Gene silencing in cancer in association with promoter hypermethylation. *N Engl J Med* **349**:2042-2054.

Hernández E, De La Mota-Peynado A, Dharmawardhane S, Vlaar CP. (2010) Novel inhibitors of Rac1 in metastatic breast cancer. *P R Health Sci J.* **29**(4):348-56.

HGMD can be accessed at: www.HGMD.cf.ac.uk

Hirota S, Nomura S, Asada H, Ito A, Morii E, Kitamura Y. (1993) Possible involvement of c-kit receptor and its ligand in increase of mast cells in neurofibroma tissues. *Arch Pathol Lab* Med **117**:996–999.

Hof P, Pluskey S, Dhe-Paganon S, Eck MJ, Shoelson SE. (1998) Crystal structure of the tyrosine phosphatase SHP-2. *Cell* **92**:441–450.

Holtkamp N, *et al.* (2007) MMP-13 and p53 in the progression of malignant peripheral nerve sheath tumors. *Neoplasia* **9**:671-677.

Holtkamp N,. *et al.* (2008) EGFR and erbB2 in malignant peripheral nerve sheath tumors and implications for targeted therapy. *Neuro-Oncology* **10**:946-957.

Horan MP, Cooper DN, Upadhyaya M. (2000) Hypermethylation of the neurofibromatosis type 1 (NF1) gene. *Hum Genet* **107**(1):33-9.

Ho IS, Hannan F, Guo HF, Hakker I, Zhong Y. (2007) Distinct Functional Domains of Neurofibromatosis Type 1 Regulate Immediate versus Long-Term Memory Formation. *The Journal of Neuroscience* **27**(25):6852– 6857.

Hotchkiss RD. (1948) The quantitative separation of purines, pyrimidines, and nucleosides by paper chromatography. *J Biol Chem* **175**(1):315-32.

Hu XC, Wang Y, Shi DR, Loo TY, Chow LW. (2003) Immunomagnetic tumor cell enrichment is promising in detecting circulating breast cancer cells. *Oncology.***64**(2):160-5.

Huson SM, Compston DA, Clark P, Harper PS. (1989) A genetic study of von Recklinghausen neurofibromatosis in south east Wales. Prevalence, fitness, mutation rate, and effect of parental transmission on severity. *J Med Genet* **26**:704-11.

Huson S. (2008) The Neurofibromatoses: Classification, Clinical Features and Genetic Counselling. In Kaufmann D: *Neurofibromatoses (Monographs in Human Genetics).* 1st Ed. Switzerland: *S Karger AG* **16**:1-20.

Hutter P, Antonarakis SE, Delozier-Blanchet CD & Morris MA. (2004) Exon skipping associated with A–>G transition at +4 of the IVS33 splice donor site of the neurofibromatosis type 1 (NF1) gene. *Hum Mol Genet* **3**:663–665.

Hoffmeyer S, Nurnberg P, Ritter H, Fahsold R, Leistner W, Kaufmann D, Krone W. (1998) Nearby stop codons in exons of the neurofibromatosis type 1 gene are disparate splice effectors. *Am J Hum Genet* **62**:269-77.

Horan MP, Cooper DN, Upadhyaya M: (2000) Hypermethylation of the neurofibromatosis type 1 (NF1) gene promoter is not a common event in the inactivation of the *NF1* gene in NF1-specific tumours. *Hum Genet* **107**:33–39.

Hoshino S, Imai M, Kobayashi T, Uchida N, Katada T. (1999) The eukaryotic polypeptide chain releasing factor (eRF3/GSPT) carrying the translation termination signal to the 39-Poly(A) tail of mRNA. Direct association of erf3/GSPT with polyadenylatebinding protein. *J Biol Chem* **274**:16677–16680.

Hulsebos TJ, Bijleveld EH, Riegman PH, Smink LJ, Dunham I (1996) Identification and characterization of NF1-related loci on human chromosomes 22, 14 and 2. *Hum Genet* **98**:7–11.

Hulsebos TJ, Plomp AS, Wolterman RA, Robanus-Maandag EC, Baas F, Wesseling P. (2007) Germline mutation of INI1/SMARCB1 in familial schwannomatosis. *Am J Hum Genet* **80**(4):805-10.

Hummel T, Anyane-Yeboa A, Mo J, Towbin A, Weiss B. (2011) Response of NF1-related plexiform neurofibroma to high-dose carboplatin. *Pediatr Blood Cancer.* **56**(3):488-90.

Huson S, Hughes R. (1994) The Neurofibromatoses: A Pathogenetic and Clinical Overview. London. *Chapman & Hall Medical* **487**

Hutchison CA 3rd. (2007) DNA sequencing: bench to bedside and beyond. Nucleic Acids Res **35**(18):6227-37.

Hsueh YP, Roberts AM, Volta M, Sheng M, Roberts R. (2001) Bipartite interaction between neurofibromatosis type I protein (neurofibromin) and syndecan transmembrane heparan sulphate proteoglycans. *J Neurosci* **21**:3764-3770.

Ingordo V, D'Andria G, Mendicini S, Grecucci M, Baglivo A. (1995) Segmental neurofibromatosis: is it uncommon or underdiagnosed? *Arch Dermatol* **131**(8):959-60.

Irizarry RA, Ladd-Acosta C, Wen B, Wu Z, Montano C, Onyango P, Cui H, *et al.* (2009) The human colon cancer methylome shows similar hypo- and hypermethylation at conserved tissue-specific CpG island shores. *Nat Genet* **41**(2):178-86.

Ingram DA, Hiatt K, King AJ, Fisher L, Shivakumar R, Derstine C, Wenning MJ, Diaz B, *et al.* (2001) Hyperactivation of p21ras and the hematopoieticspecific Rho GTPase, Rac2, cooperate to alter the proliferation of neurofibromin- deficient mast cells in vivo and in vitro. *J Exp Med* **194**:57–69.

Ingram DA, Yang FC, Travers JB, Wenning MJ, Hiatt K, New S, Hood A, Shannon K, Williams DA, Clapp DW. (2000) Genetic and biochemical evidence that haploinsufficiency of the Nf1 tumor suppressor gene modulates melanocyte and mast cell fates in vivo. *J Exp Med* **191**:181–188.

Irahara N, Nosho K, Baba Y, Shima K, Lindeman NI, Hazra A, Schernhammer ES, Hunter DJ, Fuchs CS, Ogino S. (2010) Precision of Pyrosequencing Assay to Measure LINE-1 Methylation in Colon Cancer, Normal Colonic Mucosa, and Peripheral Blood Cells. *J Mol Diagn* **12**:177-183.

Ishizaki T, Maekawa M, Fujisawa K, *et al.* (1999) The small GTP-binding protein Rho binds to and activates a 160 kDa Ser/Thr protein kinase homologous to myotonic dystrophy kinase. *Embo J* **15**:1885– 1893.

Itoh K, Yoshioka K, Akedo H, *et al.* An essential part for Rho-associated kinase in the transcellular invasion of tumor cells. *Nat Med* **5**:221–225.

Ivanov D, Hamby SE, Stenson PD, Phillips AD, Kehrer-Sawatzki H, Cooper DN, Chuzhanova N. (2011) Comparative analysis of germline and somatic microlesion mutational spectra in 17 human tumor suppressor genes. *Hum Mutat* **32**(6):620-32

Jackson AL, Bartz SR, Schelter J, Kobayashi SV, Burchard J, Mao M, Li B, Cavet G, Linsley PS. (2003) Expression profiling reveals off-target gene regulation by RNAi. *Nat. Biotechnol* **21**:635–637

Jacks T, Shih TS, Schmitt EM, Bronson RT, Bernards A, Weinberg RA. (1994) Tumour predisposition in mice heterozygous for a targeted mutation in Nf1. *Nat Genet* **7**(3):353-61.

Jackson RJ, Standart N. (1990) Do the Poly(A) Tail and 3' Untranslated Region Control mRNA Translation? *Cell* **62**:15-24.

Jakacki RI, Dombi E, Potter DM, Goldman S, Allen JC, Pollack IF, Widemann BC. (2011) Phase I trial of pegylated interferon-alpha-2b in young patients with plexiform neurofibromas. *Neurology* **76**(3):265-72.

Jenne DE, Tinschert S, Reimann H, Lasinger W, Thiel G, Hameister H, Kehrer-Sawatzki H. (2001) Molecular characterization and gene content of breakpoint boundaries in patients with neurofibromatosis type 1 with 17q11.2 microdeletions. *Am J Hum Genet.* **69**(3):516-27

Jerónimo C, Henrique R, Hoque MO, Ribeiro FR, Oliveira J, Fonseca D, Teixeira MR, Lopes C, Sidransky D. (2004) Quantitative RARbeta2 hypermethylation: a promising prostate cancer marker. *Clin Cancer Res* **10**(12 Pt 1):4010-4.

Jessen KR, Mirsky R. (2005) The origin and development of glial cells in peripheral nerves. Nat. Rev. *Neurosci* **6**:671–682.

Johannessen CM, Reczek EE, James MF, Brems H, Legius E, and Cichowski K. (2005) The NF1 tumor suppressor critically regulates TSC2 and mTOR. *PNAS* **102**(24):8573–8578.

Johnson L, Greenbaum D, Cichowski K, Mercer K, Murphy E, Schmitt E, Bronson RT, Umanoff H, *et al.* (1997) K-ras is an essential gene in the mouse with partial functional overlap with N-ras. *Genes Dev.* **11**:2468±2481

Jordan P, Brazao R, Boavida MG, Gespach C, Chastre E. (1999) Cloning of a novelhuman Rac1b splice variant with increased expression in colorectal tumors. *Oncogene* **18**: 6835-6839

Jiang W, Hiscox S, Matsumoto K, Nakamura T. (1999) Hepatocyte growth factor/scatter factor, its molecular, cellular and clinical implications in cancer. *Crit Rev Oncol Hematol* **29**:209–248.

Jin F, Wienecke R, Xiao GH, Maize Jr, JC, DeClue JE, Yeung RS. (1996) Suppression of tumourigenicity by the wild-type tuberous sclerosis 2 (Tsc2) gene and its C-terminal region. *Proc. Natl. Acad. Sci. U.S.A* **93**:9154–9159.

John AM, Ruggieri M, Ferner R, Upadhyaya M. (2000) A search for evidence of somatic mutations in the NF1 gene. *J Med Genet* **37**(1):44–49.

Jokinen CH, Argenyi, ZP. (2010) Atypical neurofibroma of the skin and subcutaneous tissue: clinicopathologic analysis of 11 cases. *J Cutan Pathol* **37**: 35-42

Jones PA, Laird PW. (1999) Cancer epigenetics comes of age. Nat Genet. **21**(2):163-7.

Jorge AA, Malaquias AC, Arnhold IJ, Mendonca BB. (2009) Noonan Syndrome and Related Disorders: A Review of Clinical Features and Mutations in Genes of the RAS/MAPK *Pathway Horm Res* **71**:185–193.

Jouhilahti EM, Peltonen S, Callens T, Jokinen E, Heape AM, Messiaen L, Peltonen J. (2011). The development of cutaneous neurofibromas. *Am J Pathol.* **178**(2):500-5.

Juhlin CC, Kiss NB, Villablanca A, Haglund F, Nordenstrom J, Hoog A, Larsson C. (2010) Frequent Promoter Hypermethylation of the APC and RASSF1A Tumour Suppressors in Parathyroid Tumours *PLoS One.* **5**(3):e9472.

Kaempchen K, Mielke K, Utermark T, Langmesser S, Hanemann C.O. (2003) Upregulation of the Rac1/JNK signalling pathway in primary human schwannoma cells. *Human Molecular Genetics* **12**(11):1211–1221

Kalamarides M, Stemmer-Rachamimov AO, Niwa-Kawakita M, Chareyre F, Taranchon E, Han ZY, Martinelli C, Lusis EA, Hegedus B, Gutmann DH, Giovannini M. (2011) Identification of a progenitor cell of origin capable of generating diverse meningioma histological subtypes. *Oncogene* **30**(20):2333-44

Kalra R, Paderanga DC, Olson K, Shannon KM. (1994) Genetic analysis is consistent with the hypothesis that NF1 limits myeloid cell growth through p21ras. *Blood* **84**:3435–3439.

Kamai T, Yamanishi T, Shirataki H, Takagi K, Asami H, Ito Y, Yoshida K. (2004) Overexpression of RhoA, Rac1, and Cdc42 GTPases is associated with progression in testicular cancer. *Clin. Cancer Res.* **10**: 4799–4805.

Kandt RS, Haines JL, Smith M, Northrup H, Gardner RJ, Short MP, Dumars K, Roach ES, *et al.* (1992) Linkage of an important gene locus for tuberous sclerosis to a chromosome 16 marker for polycystic kidney disease. *Nat. Genet* **2**:37–41.

Kang DY, Park CK, Choi JS, *et al.* (2007) Multiple gastrointestinal stromal tumors: clinicopathologic and genetic analysis of 12 patients. *Am J Surg Pathol* **31**:224–32.

Karlsson R, Pedersen ED, Wang Z, Brakebusch C. (2009) Rho GTPase function in tumorigenesis *Biochimica et Biophysica Acta* **1796**:91–98.

Katz D, Lazar A, Lev D. (2009) Malignant peripheral nerve sheath tumour (MPNST): the clinical implications of cellular signalling pathways. *Expert reviews in molecular medicine* v11, e30.

Kataoka C, Egashira K, Inoue S, *et al.* (2002) Important role of Rho-kinase in the pathogenesis of cardiovascular inflammation and remodeling induced by long-term blockade of nitric oxide synthesis in rats. *Hypertension* **39**:245–250.

Kaufmann D, Müller R, Kenner O, Leistner W, Hein C, Vogel W, Bartelt B. (2002) The N-terminal splice product NF1-10a-2 of the NF1 gene codes for a transmembrane segment. *Biochem Biophys Res Commun.* **294**(2):496-503.

Kaufmann, D. (2008) *Neurofibromatoses (Monographs in Human Genetics).* 1st Ed. Switzerland: S Karger AG.

Keen J, Lester D, Inglehearn, C, Curtis A., Bhattacharya, S. (1991) Rapid detection of single base mismatches as heteroduplexs on Hydrolink gels. *Trends genet* **7**(1):5.

Kehrer-Sawatzki H, Schwickardt T, Assum G, Rocchi M, Krone W. (1997) A third neurofibromatosis type 1 (NF1) pseudogene at chromosome 15q11.2. *Hum Genet* **100**:595–600.

Kehrer-Sawatzki H, Kluwe L, Sandig C, Kohn M, Wimmer K, Krammer U, Peyrl A, Jenne DE, Hansmann I, Mautner VF. (2004) High frequency of mosaicism among patients with neurofibromatosis type 1 (NF1) with microdeletions caused by somatic recombination of the *JJAZ1* gene. *Am J Hum Genet* **75**:410-423.

Kehrer-Sawatzki H, Cooper DN. (2008) Mosaicism in sporadic neurofibromatosis type 1: variations on a theme common to other hereditary cancer syndromes? *J Med Genet* **45**:622-631.

Kehrer-Sawatzki H, Schmid E, Fünsterer C, Kluwe L, Mautner VF. (2008) Absence of cutaneous neurofibromas in an NF1 patient with an atypical deletion partially overlapping the common 1.4 Mb microdeleted region. *Am J Med Genet A.* **146A**(6):691-9.

Keilhack H, David FS, McGregor M, Cantley LC, Neel BG. (2005) Diverse biochemical properties of Shp2 mutants. Implications for disease phenotypes. *J. Biol. Chem* **280**:30984–30993.

Kent WJ. (2002) BLAT - the BLAST-like alignment tool. *Genome Res* **12**(4):656-64.

Kestle JR, Hoffman HJ, Mock AR. (1993) Moyamoya phenomenon after radiation for optic glioma. *J Neurosurg* **79**(1):32-5.

Keohavong P, Gao WM, Mady HH, Kanbour-Shakir A, Melhem MF. (2004) Analysis of p53 mutations in cells taken from paraffin-embedded tissue sections of ductal carcinoma in situ and atypical ductal hyperplasia of the breast. *Cancer Lett.* **212**(1):121-30.

Kimura H, Shiota K. (2003) Methyl-CpG-binding protein, MeCP2, is a target molecule for maintenance DNA methyltransferase, Dnmt1. *J Biol Chem* **278**:4806–4812.

Kissil JL, Walmsley MJ, Hanlon L, Haigis KM, Bender Kim CF, Sweet- Cordero A, Eckman MS, Tuveson DA, *et al.* (2007) Requirement for Rac1 in a K-ras induced lung cancer in the mouse. *Cancer Res* **67**:8089–8094.

Kitagawa D, Kajiho H, Negishi T, Ura S, Watanabe T, Wada T, Ichijo H, Katada T, Nishina H. (2006) Release of RASSF1C from the nucleus by Daxx degradation links DNA damage and SAPK/JNK activation. *EMBO J* **25**(14):3286-97.

Kluwe L, Friedrich R, Mautner VF. (1999) Loss of NF1 allele in Schwann cells but not in fibroblasts derived from an NF1-associated neurofibroma. *Genes Chromosomes Cancer* **24**(3):283-5.

Kluwe L, Friedrich RE, Peiper M, Friedman J, Mautner VF. (2003) Constitutional NF1 mutations in neurofibromatosis 1 patients with malignant peripheral nerve sheath tumors. *Hum Mutat.* **22**(5):420.

Kluwe L, Siebert R, Gesk S, Friedrich RE, Tinschert S, Kehrer-Sawatzki H, Mautner VF. (2004) Screening 500 unselected neurofibromatosis 1 patients for deletions of the NF1 gene. *Hum Mutat* **23**:111–116.

Kindblom LG, *et al.* (1995) Immunohistochemical and molecular analysis of p53, MDM2, proliferating cell nuclear antigen and Ki67 in benign and malignant peripheral nerve sheath tumours. *Virchows Archiv* **427**:19-26.

Kimura M, Kamata Y, Matsumoto K, *et al.* (1974) Electron microscopical study on the tumor of von Recklinghausen's neurofi bromatosis. *Acta Pathol Jpn* **24**:79–91.

Kimura K, Kawamoto K, Teranishi S, Nishida T. (2006) Role of Rac1 in fibronectin-induced adhesion and motility of human corneal epithelial cells. *Invest Ophthalmol Vis Sci.* **47**(10):4323-9.

Kittur SD, Bagdon MM, Lubs ML, Phillips III JA, Murray JC, Slaugenhaupt SA, Chakravarti A, Adler WH. (1989) Linkage analysis of neurofibromatosis type 1, using chromosome 17 DNA markers. *Am. J. Hum. Genet.* **44**:48-50.

Klose A, Ahmadian MR, Schuelke M, Scheffzek K, Hoffmeyer S, Gewies A, Schmitz F, Kaufmann D, *et al.* (1998) Selective Disactivation of Neurofibromin GAP Activity in Neurofibromatosis Type 1 (NF1) *Hum. Mol. Genet* **7**(8): 1261-1268.

Klose A, Peters H, Hoffmeyer S, Buske A, Lüder A, Hess D, Lehmann R, Nürnberg P, Tinschert S. (1999) Two independent mutations in a family with neurofibromatosis type 1 (NF1). *Am J Med Genet* **83**(1):6-12.

Kluwe L, Bayer S, Baser ME, Hazim W, Haase W, *et al.* (1996) Identification of NF2 germ-line mutations and comparison with neurofibromatosis 2 phenotypes. *Hum. Genet* **98**:534–38.

Kluwe L, Tatagiba M, Funsterer C, Mautner VF. (2003) NF1 mutations and clinical spectrum in patients with spinal neurofibromas. *J. Med. Genet.* **40**:368–371.

Knudson AG Jr. (1971) Mutation and cancer: Statistical study of retinoblastoma. *Proc Natl Acad Sci USA* **68**:820-823.

Kobayashi H, Kaneko G, Nishimoto K, Uchida A. (2009) A case of pheochromocytoma associated with neurofibromatosis type 1. *Hinyokika Kiyo* **55**(12):749-52.

Koc F, Yerdelen D, Koc Z. (2008) Neurofibromatosis type 1 association with moyamoya disease. *Int J Neurosci* **118**(8):1157-63.

Koc F, Guzel AI: Neurofibromatosis type 1 associated with Charcot–Marie–Tooth type 1A *Journal of Dermatology* 2009; **36**:306–311.

Koivunen J, Ylä-Outinen H, Korkiamäki T, Karvonen SL, Pöyhönen M, Laato M, Karvonen J, Peltonen S, Peltonen J. (2000) New function for NF1 tumor suppressor. *J Invest Dermatol* **114**:473-479.

Kondrashov AS, Rogozin IB (2004) Context of deletions and insertions in human coding sequences. *Hum Mutat* **23**:177–185.

Kontaridis MI, Swanson KD, David FS, Barford D, Neel BG. (2006) PTPN11 (Shp2) mutations in LEOPARD syndrome have dominant negative, not activating, effects. *J. Biol. Chem* **281**:6785–6792.

Kourea HP, *et al.* (1999) Deletions of the INK4A gene occur in malignant peripheral nerve sheath tumors but not in neurofibromas. *American Journal of Pathology* **155**:1855-1860.

Korf BR, Rubenstein AE. 2005. Neurofibromatosis: A Handbook for Patients, Families, and Health Care Professionals. New York: Thieme Med. Publ. 253 pp.

Kozlowski P, Jasinska AJ, Kwiatkowski DJ. (2008) New applications and developments in the use of multiplex ligation-dependent probe amplification. *Electrophoresis.* **29**(23):4627-36. Review.

Krab LC, *et al.* (2008) Effect of simvastatin on cognitive functioning in children with neurofibromatosis type 1: a randomized controlled trial. *Journal of the American Medical Association* **300**:287-294.

Kralovicova J, Vorechovsky I. (2007) Global control of aberrant splice-site activation by auxiliary splicing sequences: evidence for a gradient in exon and intron definition. *Nucleic Acids Res* **35**:6399–6413.

Kramer K, Hasel C, Aschoff AJ, *et al.* (2007) Multiple gastrointestinal stromal tumors and bilateral pheochromocytoma in neurofibromatosis. World J Gastroenterol **13**:3384–7.

Krasnoselsky A, Massay MJ, DeFrances MC, *et al.* (1994) Hepatocyte growth factor is a mitogen for schwann cells and is present in neurofibromas. *J Neurosci* **14**:7284-7290.

Krawczak M, Thomas NS, Hundrieser B, Mort M, Wittig M, Hampe J, Cooper DN. (2007) Single base-pair substitutions in exon-intron junctions of human genes: nature, distribution, and consequences for mRNA splicing. *Hum Mutat* **28**:150-158.

Kresse SH, Skårn M, Ohnstad HO, Namløs HM, Bjerkehagen B, Myklebost O, Meza-Zepeda LA. (2008) DNA copy number changes in high-grade malignant peripheral nerve sheath tumors by array CGH. *Mol Cancer.* **3**:7:48.

Krkljus S, Abernathy CR, Johnson JS, Williams CA, Driscoll DJ, Zori R, Stalker HJ, Rasmussen SA, Collins FS, Kousseff BG, Baumbach L, Wallace MR. (1998) Analysis of CpG C-to-T mutations in neurofibromatosis type 1. Mutations in brief no. 129. Online. *Hum Mutat* **11**(5):411.

Kruger S, Kinzel M, Walldorf C *et al.* (2008) Homozygous PMS2 germline mutations in two families with early-onset haematological malignancy, brain tumours, HNPCC-associated tumours, and signs of neurofibromatosis type 1. *Eur J Hum Genet* **16**:62–72.

Kullar PJ, Pearson DM, Malley DS, Collins VP, Ichimura K. (2010) CpG island hypermethylation of the neurofibromatosis type 2 (NF2) gene is rare in sporadic vestibular schwannomas. *Neuropathol Appl Neurobiol.* **36**(6):505-14.

Lakkis MM, Golden JA, O'Shea KS, Epstein JA. (1999) Neurofibromin deficiency in mice causes exencephaly and is a modifier for Splotch neural tube defects. *Dev Biol* **212**(1):80-92.

Lambert JM, *et al.* (2002) Tiam1 mediates Ras activation of Rac by a PI(3)K-independent mechanism. *Nature Cell Biol.* **4**:621–625.

Lancaster E, Elman LB, Scherer SS. (2010) A patient with neurofibromatosis type 1 and Charcot-Marie-Tooth disease type 1B. *Muscle Nerve* **41**(4):555-8.

Lander ES, Linton LM, Birren B, Nusbaum C, Zody MC, Baldwin J, Devon K, Dewar K, Doyle M, *et al.* (2001) Initial sequencing and analysis of the human genome. *Nature* **409**:860–921.

Largaespada DA, Brannan CI, Jenkins NA, Copeland NG. (1996) Nf1 deficiency causes Ras-mediated granulocyte/macrophage colony stimulating factor hypersensitivity and chronic myeloid leukaemia. *Nat Genet* **12**(2):137- 143.

Laycock-van Spyk S, Thomas N, Cooper DN, Upadhyaya M. (2011). Neurofibromatosis type 1-associated tumours: their somatic mutational spectrum and pathogenesis (In print)

Leevers SJ, Paterson HF, Marshall CJ. (1994) Requirement for Ras in Raf activation is overcome by targeting Raf to the plasma membrane. *Nature* **369**:411–414.

Lennington WJ, Jensen RA, Dalton LW, Page DL. (1994) Ductal carcinoma *in situ* of the breast. Heterogeneity of individual lesions. *Cancer* **73**:118–124.

Liapis H, Marley EF, Lin Y, Dehner LP. (1999) p53 and Ki-67 proliferating cell nuclear antigen in benign and malignant peripheral nerve sheath tumors in children. *Pediatr Dev Pathol* **2**:377-384.

Li B, Krishnan VG, Mort ME, Xin F, Kamati KK, Cooper DN, Mooney SD, Radivojac P. (2009a). Automated inference of molecular mechanisms of disease from amino acid substitutions. *Bioinformatics* **25**:2744-2750.

Lin Q, Geng J, Ma K, Yu J, Sun J, Shen Z, Bao G, Chen Y, Zhang H, He Y, Luo X, Feng X, Zhu J. (2009) RASSF1A, APC, ESR1, ABCB1 and HOXC9, but not p16INK4A, DAPK1, PTEN and MT1G genes were frequently methylated in the stage I non-small cell lung cancer in China. *J Cancer Res Clin Oncol* **135**:1675-84.

Li S, Hansman, R, Newbold, R. *et al.* (2003) Neonatal diethylstilbestrol exposure induces persistent elevation of c-fos expression and hypomethylation in its exon-4 in mouse uterus. *Mol Carcinog* **38**:78–84.

Liu J, Lau SK, Varma VA, Moffitt RA, Caldwell M, Liu T, Young AN, Petros JA, Osunkoya AO, Krogstad T, Leyland-Jones B, Wang MD, Nie S. (2010) Molecular mapping of tumour heterogeneity on clinical tissue specimens with multiplexed quantum dots. ACS Nano **4**:2755-2765.

Liu SY, Yen CY, Yang SC, Chiang WF, Chang KW. (2004) Overexpression of Rac-1 small GTPase binding protein in oral squamous cell carcinoma. *J. Oral Maxillofac. Surg.* **62**:702–707.

Li Y, Bollag G, Clark R, Stevens J, Conroy L, Fults D, Ward K, Friedman E, Samowitz W, Flobertson M, Bradley P, McCormick F, White R, Cawthon R. (1992) Somatic Mutations in the Neurofibromatosis 1 Gene in Human Tumors Cell, **69**:275-261.

Le DT, Kong N, Zhu Y, Lauchle JO, Aiyigari A, Braun BS, Wang E, Kogan SC, *et al.* (2004) Somatic inactivation of Nf1 in hematopoietic cells results in a progressive myeloproliferative disorder. *Blood* **103**:4243–4250.

Le LQ, Parada LF. (2007) Tumor microenvironment and neurofibromatosis type I: connecting the GAPs. *Oncogene* **12**:26(32):4609-16.

Le L.Q, Shipman T, Burns D.K, Parada L.F. (2009) Cell of origin and microenvironment contribution for NF1-associated dermal neurofibromas Cell. *Stem Cell* **4**:453–463.

Le LQ, Liu C, Shipman T, Chen Z, Suter U, Parada LF. (2011) Susceptible stages in Schwann cells for NF1-associated plexiform neurofibroma development. *Cancer Res.* [Epub ahead of print]

Ledbetter DH, Rich DC, O'Connell P, Leppert M, Carey JC. (1989) Precise localization of NF1 to 17q11.2 by balanced translocation. *Am J Hum Genet* **44**:20-24.

Legius E, Marchuk DA, Hall BK, Andersen LB, Wallace MR, Collins FS, Glover TW. (1992) NF1-related locus on chromosome 15. *Genomics* **13**:1316–1318.

Lee MJ, Su YN, You HL, Chiou SC, Lin LC, Yang CC, Lee WC, Hwu WL, Hsieh FJ, Stephenson DA, Yu CL. (2006) Identification of forty-five novel and twenty-three known NF1 mutations in Chinese patients with neurofibromatosis type 1. *Hum Mutat.* **27**(8):832.

Legius E, *et al.* (1994) TP53 mutations are frequent in malignant NF1 tumors. *Genes Chromosomes and Cancer* **10**:250-255.

Legius E, Schrander-Stumpel C, Schollen E, Pulles-Heintzberger C, Gewillig M, Fryns JP. (2002) PTPN11 mutations in LEOPARD syndrome. *J. Med. Genet* **39**:571–574.

Leondaritis G, Petrikkos L, Mangoura D. (2009) Regulation of the Ras-GTPase activating protein neurofibromin by C-tail phosphorylation: implications for protein kinase C/Ras/extracellular signal-regulated kinase 1/2 pathway signaling and neuronal differentiation. *J Neurochem* **109**(2):573-83.

Leung T, Chen XQ, Manser E, *et al.* (1996) The p160 RhoA-binding kinase ROK alpha is a member of a kinase family and is involved in the reorganization of the cytoskeleton. *Mol Cell Biol* **16**:5313– 5327.

Li C, Cheng Y, Gutmann DA, Mangoura D. (2001) Differential localization of the neurofibromatosis 1 (NF1) gene product, neurofibromin, with the F-actin or microtubule cytoskeleton during differentiation of telencephalic neurons. *Brain Res Dev Brain Res* **130**:231-248.

Li E, Bestor TH, Jaenisch R. (1992) Targeted mutation of the DNA methyltransferase gene results in embryonic lethality. *Cell* **69**:915–926.

Li S, Hansman R, Newbold R *et al.* (2003) Neonatal diethylstilbestrol exposure induces persistent elevation of c-fos expression and hypomethylation in its exon-4 in mouse uterus. *Mol Carcinog* **38**:78–84.

Li S, Ma L, Li H, Vang S, Hu Y, Bolund L, Wang J. (2007) Snap: an integrated SNP annotation platform. *Nucleic Acids Res* **35**:D707-10

Liao JK, Seto M, Noma K. (2007) Rho kinase (ROCK) inhibitors. *J Cardiovasc Pharmacol* **50**(1):17-24.

Li YL, Tian Z, Wu DY, Fu BY, Xin Y. (2005) Loss of heterozygosity on 10q23.3 and mutation of tumour suppressor gene *PTEN* in gastric cancer and precancerous lesions. *World J Gastroenterol* **11**:285-288.

Lin Q, Geng J, Ma K, Yu J *et al*: (2009) RASSF1A, APC, ESR1, ABCB1 and HOXC9, but not p16INK4A, DAPK1, PTEN and MT1G genes were frequently methylated in the stage I non-small cell lung cancer in China. *J Cancer Res Clin Oncol* **135**(12):1675-84.

Listernick R, Ferner RE, Liu GT, *et al.* Optic pathway gliomas in neurofibromatosis-1: controversies and recommendations. *Ann Neurol* (2007) **61**:189–98.

Liu L, McBride K.M., Reich N.C. (2005) STAT3 nuclear import is independent of tyrosine phosphorylation and mediated by importin-alpha3. *Proc. Natl. Acad. Sci. USA* **102**:8150 – 8155 .

Lock FE, Hotchin NA. (2009) Distinct Roles for ROCK1 and ROCK2 in the Regulation of Keratinocyte Differentiation *PLOS 1* **4**(12)e8190

Loewith R, Jacinto E, Wullschleger S, Lorberg A, Crespo JL, Bonenfant D, Oppliger, W, Jenoe P, Hall MN. (2002) Two TOR complexes, only one of which is rapamycin sensitive, have distinct roles in cell growth control. *Mol. Cell* **10**:457–468.

Loh ML, Vattikuti S, Schubbert S, *et al.* (2004) Mutations in PTPN11 implicate the SHP-2 phosphatase in leukemogenesis. *Blood* **103**:2325–2331.

Lopez G, Torres K, Liu J, Hernandez B, Young E, Belousov R, Bolshakov S, Lazar AJ, Slopis JM, McCutcheon IE, McConkey D, Lev D. (2011) Autophagic survival in resistance to histone deacetylase inhibitors: novel strategies to treat malignant peripheral nerve sheath tumors. *Cancer Res* **71**(1):185-96.

López-Correa C, Dorschner M, Brems H, Lázaro C, Clementi M, Upadhyaya M, Dooijes D, Moog U, Kehrer-Sawatzki H, Rutkowski JL, Fryns JP, Marynen P, Stephens K, Legius E. (2001) Recombination hotspot in NF1 microdeletion patients. *Hum Mol Genet.* **10**(13):1387-92

Lothe RA, Karhu R, Mandahl N, Mertens F, Saeter G, Heim S, Borresen-Dale AL, Kallioniemi OP. (1996) Gain of 17q24-qter detected by comparative genomic hybridization in malignant tumors from patients with von Recklinghausen's neurofibromatosis. *Cancer Res.* **56**(20):4778-81.

Luijten M, Redeker S, van Noesel MM *et al.* (2000) Microsatellite instability and promoter methylation as possible causes of NF1 gene inactivation in neurofibromas. *Eur J Hum Genet* **8**(12):939-45.

Luijten Mirjam, Redeker Sandra, Minoshima Shinsei, Shimizu Nobuyoshi, Westerveld Andries, Hulsebos Theo J. (2001) M Duplication and transposition of the NF1 pseudogene regions on chromosomes 2, 14, and 22. *Hum Genet* **109**:109–116.

Lupski JR, Pentao L, Williams LL, Patel PI. (1993) Stable inheritance of the CMT1A DNA duplication in two patients with CMT1 and NF1. *Am J Med Genet* **45**(1):92-6.

Lüthy R, Bowie J, Eisenberg D. (1992) Assessment of protein models with three-dimensional profiles. *Nature.* **356**:83–85.

Lynch HT, de la Chapelle A. (2003) Hereditary colorectal cancer, N. Engl. *J. Med.* **348**:919–932.

Lynch H.T, Lynch J.F, Lynch, P.M, Attard T. (2008) Hereditary colorectal cancer syndromes: molecular genetics, genetic counseling, diagnosis and management, Fam. *Cancer* **7**:27–39.

Maas S, Rich A. (2000) Changing genetic information through RNA editing. *Bioessays* **22**:790–802.

MacCollin M, Willett C, Heinrich B, Jacoby LB, Acierno JSJ, *et al.* (2003) Familial schwannomatosis: exclusion of the NF2 locus as the germline event. *Neurology* **60**:1968–74.

MacCollin M, Chiocca EA, Evans DG, Friedman JM, Horvitz R, *et al.* (2005) Diagnostic criteria for schwannomatosis. *Neurology* **64**:1838–45.

Macedo MP, Andrade LD, Coudry R, Crespo R, Gomes M, Lisboa BC, Aguiar S Jr, Soares FA, Carraro DM, Cunha IW. (2011) Multiple mutations in the Kras gene in colorectal cancer: review of the literature with two case reports. *Int J Colorectal Dis.* [Epub ahead of print]

Maekawa M, Ishizaki T, Boku S, *et al.* (1999) Signaling from Rho to the actin cytoskeleton through protein kinases ROCK and LIM-kinase. *Science* **285**:895–898.

Maertens O, Brems H, Vandesompele J, De Raedt T, Heyns I, Rosenbaum T, De Schepper S, De Paepe A, Mortier G, Janssens S, Speleman F, Legius E, Messiaen L. (2006) Comprehensive NF1 screening on cultured Schwann cells from neurofibromas. *Hum Mutat* **27**(10):1030-40.

Maertens O, De Schepper S, Vandesompele J, Brems H, Heyns I, Janssens S, Speleman F, Legius E, Messiaen L. (2007) Molecular dissection of isolated disease features in mosaic neurofibromatosis type 1. *Am J Hum Genet* **81**(2):243-51.

Mahimainathan L, Choudhury GG. (2004) Inactivation of plateletderived growth factor receptor by the tumor suppressor PTEN provides a novel mechanism of action of the phosphatase. *J Biol Chem* **279**:15258-15268.

Maheshwar MM, Cheadle JP, Jones AC, Myring J, Fryer AE, Harris PC, Sampson JR. (1997) The GAP-related domain of tuberin, the product of the TSC2 gene, is a target for missense mutations in tuberous sclerosis. *Hum. Mol. Genet.* **6**:1991–1996.

Mahgoub N, Taylor BR, Le Beau MM, Gratiot M, Carlson KM, Atwater SK, Jacks T, Shannon KM. (1999 Jun 1) Myeloid malignancies induced by alkylating agents in Nf1 mice. *Blood* **93**(11):3617-23.

Mahller YY. *et al.* (2007) Oncolytic HSV and erlotinib inhibit tumor growth and angiogenesis in a novel malignant peripheral nerve sheath tumor xenograft model. *Molecular Therapy* **15**:279-286.

Maki RG *et al.* (2008) Sorafenib Sarcoma Study Group Updated results of a phase II study of oral multi-kinase inhibitor sorafenib in sarcomas, CTEP study #7060. Journal of Clinical Oncology 26 (ASCO Annual Meeting Proceedings), Abstract 10531.

Makita Y. *et al.* (2007) Leukemia in Cardiofacio- cutaneous (CFC) syndrome: a patient with a germline mutation in BRAF proto-oncogene. *J Pediatr Hematol Oncol* **29**:287-290.

Malminen M, Peltonen s, Koivunen J, Peltonen J. (2002) Functional expression of NF1 tumor suppressor protein: association with keratin intermediate filaments during the early development of human epidermis. *BMC Dermatol* **2**:10.

Mancini D, Singh S, Ainsworth P, Rodenhiser D. (1997) 'Constitutively methylated CpG dinucleotides as mutation hot spots in the retinoblastoma gene (RB1). *Am. J. Hum. Genet* **61**:80–87.

Mangoura D, Sun Y, Li C, Singh D, Gutmann DH, Flores A, Ahmed M, Vallianatos G: (2006) Phosphorylation of neurofibromin by PKC is a possible molecular switch in EGF receptor signaling in neural cells. *Oncogene* **25**:735–745.

Mannelli M, Simi L, Gaglianò MS, Opocher G, Ercolino T, Becherini L, Parenti G. (2007) Genetics and biology of pheochromocytoma. *Exp Clin Endocrinol Diabetes* **115**(3):160-5.

Manning BD, Tee AR, Logsdon MN, Blenis J, Cantley LC. (2002) Identification of the tuberous sclerosis complex-2 tumour suppressor gene product tuberin as a target of the phosphoinositide 3-kinase/Akt pathway. *Mol. Cell* **10**:151–162.

Mantripragada KK, Thuresson AC, Piotrowski A, Díaz de Stahl T, Menzel U, Grigelionis G, Ferner RE, Griffiths S, *et al.* (2006) Identification of novel deletion breakpoints bordered by segmental duplications in the NF1 locus using high resolution array-CGH. *J Med Genet* **43**:28–38.

Mantripragada KK, Spurlock G, Kluwe L, Chuzhanova N, Ferner RE, Frayling IM, Dumanski JP, Guha A, Mautner V, Upadhyaya M. (2008) High-resolution DNA copy number profiling of malignant peripheral nerve sheath tumors using targeted microarray-based comparative genomic hybridization. *Clin Cancer Res.* **14**(4):1015-24.

Mantripragada KK, Díaz de Ståhl T, Patridge C, Menzel U, Andersson R, Chuzhanova N, Kluwe L, Guha A, Mautner V, Dumanski JP, Upadhyaya M. (2009) Genome-wide high-resolution analysis of DNA copy number alterations in NF1-associated malignant peripheral nerve sheath tumors using 32K BAC array. *Genes Chromosomes Cancer.* **48**(10):897-907.

Marais R, Light Y, Paterson HF, Marshall CJ. (1995) Ras recruits Raf-1 to the plasma membrane for activation by tyrosine phosphorylation. *EMBO J* **14**:3136–3145

Marchuk DA, Saulino AM, Tacakkol R, Swaroop M, Wallace MR, Andersen LB, Mitchell AL, Gutmann DH, Boguski M, Collins FS. (1991) cDNA cloning of the type 1 neurofibromatosis gene: complete sequence of the NF1 gene product. *Genomics* **11**:931–940.

Marchuk DA, Tavakkol R, Wallace MR, Brownstein BH, Taillon- Miller P, Fong CT, Legius E, Andersen LB, Glover TW, Collins FS. (1992) A yeast artificial chromosome contig encompassing the type 1 neurofibromatosis gene. *Genomics* **13**: 672–680.

Mardon HJ, Sebastio G, Baralle FE. (1987) A role for exon sequences in alternative splicing of the human fibronectin gene. *Nucleic Acids Res* **15**(19):7725-33.

Mardis E. (2008) Next-generation DNA sequencing methods. *Annu Rev Genomics Hum Genet* **9**:387-402

Maris JM, Wiersma SR, Mahgoub N, Thompson P, Geyer RJ, Lange BJ, Shannon KM. (1997) Monosomy 7 myelodysplastic syndrome and other second malignant neoplasms in children with neurofibromatosis type 1. *Cancer* **79**:1438.

Maru Y, Witte O.N. (1991) The BCR gene encodes a novel serine/threonine kinase activity within a single exon. *Cell* **67**:459–468.

Martin GA, Viskochil D, Bollag G, McCabe PC, Crosier WJ, Haubruck H, Conroy L, Clark R, O'Connell P, Cawthon RM, *et al.* (1990) The GAP-related domain of the neurofibromatosis type 1 gene product interacts with ras p21. *Cell* **63**(4):843-9.

Martina I, Andresa CR, Védrinea S, Tabagha R, Michellea C, Jourdanc ML, Heuze-Vourc'hc N, Corciaa P, Duittozc A, Vourc'ha P. (2009) Effect of the oligodendrocyte myelin glycoprotein (OMgp) on the expansion and neuronal differentiation of rat neural stem cells. *Brain Research* **1284**:22-30.

Martelli AM, Evangelisti C, Chiarini F, Grimaldi C, Cappellini A, Ognibene A, McCubrey JA. (2010) The emerging role of the phosphatiylinositol 3-kinase/Akt/mammalian target of rapamycin signaling network in normal myelopoiesis and leukemogensis. *Biochim Biophys Act* **1803**:991-1002.

Martinelli S, Torreri P, Tinti M, Stella L, Bocchinfuso G, Flex E, Grottesi A, Ceccarini M, Palleschi A, Cesareni G, Castagnoli L, Petrucci TC, Gelb BD, Tartaglia M. (2008) Diverse driving forces underlie the invariant occurrence of the T42A, E139D, I282V and T468M SHP2 amino acid substitutions causing Noonan and LEOPARD syndromes. *Hum Mol Genet.* **17**(13):2018-29.

Mathew CG, Thorpe PK, Easton DF, Chin KS, Jadayel D, Ponder M, Moore G, Wallis CE, *et al.* (1989). Linkage analysis of chromosome 17 markers in British and South African families with neurofibromatosis type 1. *Am. J. Hum. Genet.* ***44***:38-40.

Matos P, Jordan P. (2008) Increased Rac1b expression sustains colorectal tumor cell survival. *Mol. Cancer Res.* **6**:1178–1184.

Mattingly RR, *et al.* (2006) The mitogen-activated protein kinase/extracellular signal-regulated kinase kinase inhibitor PD184352 (CI-1040) selectively induces apoptosis in malignant schwannoma cell lines. *Journal of Pharmacology and Experimental* Therapeutics **316**:456-465.

Mattocks C, Tarpey P, Bobrow M, Whittaker J. (2000) Comparative sequence analysis (CSA): a new sequence-based method for the identification and characterization of mutations in DNA. *Hum Mutat.* **16**(5):437-43.

Mattocks C, Baralle D, Tarpey P, ffrench-Constant C, Bobrow M, Whittaker J. (2004) Automated comparative sequence analysis identifies mutations in 89% of NF1 patients and confirms a mutation cluster in exons 11-17 distinct from the GAP related domain. *J Med Genet* **41**(4):e48.

Mautner VF, Kluwe L, Friedrich RE, Roehl AC, Bammert S, Högel J, Spöri H, Cooper DN, Kehrer-Sawatzki H. (2010) Clinical characterisation of 29 neurofibromatosis type-1 patients with molecularly ascertained 1.4 Mb type-1 NF1 deletions. *J Med Genet* **47**:623-630.

Mawrin C, *et al.* (2002) Immunohistochemical and molecular analysis of p53, RB, and PTEN in malignant peripheral nerve sheath tumors. *Virchows Archiv* **440**:610-615.

Mawrin C. (2010) Critical role of PTEN for development and progression of nerve sheath tumors in neurofibromatosis type 1.*Future Oncol* **6**(4):499-501.

Maxam AM, Gilbert W. (1977) A new method for sequencing DNA. *Proc. Natl Acad. Sci. USA* **74**:560–564.

Maynard J, Krawczak M, Upadhyaya M. (1997) Characterization and significance of nine novel mutations in exon 16 of the neurofibromatosis type 1 (NF1) gene. *Hum Genet* **99**:674–676.

Mazzanti L, Cacciari E, Cicognani A, Bergamaschi R, Scarano E, Forabosco A. (2003) Noonan-like syndrome with loose anagen hair: a new syndrome? *Am J Med Genet* A **118A**:279–286.

McCabe A, Dolled-Filhart M, Camp RL, Rimm DL. (2005) Automated quantitative analysis (AQUA) of in situ protein expression, antibody concentration, and prognosis. *J Natl Cancer Inst* **97**:1808–1815.

Mclaughlin M, Jacks T. (2003) Progesterone receptor expression in neurofibromas. *Cancer Res* **63**(4):752-5.

McTaggart SJ. (2006) Isoprenylated proteins. *Cell. Mol. Life Sci* **63**:255–267.

Menko FH, Kaspers GL, Meijer GA, Claes K, van Hagen JM, Gille JJA. (2004) Homozygous MSH6 mutation in a child with café-au-lait spots, oligodendroglioma and rectal cancer. *Fam Cancer* **3**(2):123-7.

Menon AG, Ledbetter DH, Rich DC, Seizinger BR, Rouleau GA, Michels VF, Schmidt MA, *et al.* (1989) Characterization of a translocation within the von Recklinghausen neurofibromatosis region of chromosome 17. *Genomics* **5**:245-249.

Menon AG. *et al.* (1990) Chromosome 17p deletions and p53 gene mutations associated with the formation of malignant neurofibrosarcomas in von Recklinghausen neurofibromatosis. *Proceedings of the National Academy of Sciences of the United States of America* **87**:5435-5439.

Messiaen L, Callens T, De Paepe A, Craen M, Mortier G. (1997) Characterisation of two different nonsense mutations, C6792A and C6792G, causing skipping of exon 37 in the NF1 gene. *Hum Genet* **101**(1):75-80.

Messiaen LM, Callens T, Mortier G, Beysen D, Vandenbroucke I, Van Roy N, Speleman F, De Paepe A. (2000) Exhaustive mutation analysis of the NF1 gene allows identification of 95% of mutations and reveals a high frequency of unusual splicing defects. *Hum Mutat* **15**:541–55.

Messiaen L, Callens T, Williams JB, Babovic-Vuksanovic D, Huson SM, Legius E, Mac Gardner R, Pascual-Castroviejo I, Plotkin S, Schaefer GB, Wilson M, Korf B. (2007) Genotype–Phenotype Correlations in Spinal NF, The American Society of Human Genetics, San Diego, California

Messiaen LM, Wimmer K. NF1 Mutational spectrum. In: Kaufmann D, editor, Neurofibromatoses, Basel, Karger. MonogrHumGenet 2008;16:63-77

Messiaen L, Yao S, Brems H, Callens T, Sathienkijkanchai A, Denayer E, Spencer E, *et al.* (2009) Clinical and mutational spectrum of neurofibromatosis type 1-like syndrome. *JAMA*. **302**(19):2111-8.

Messiaen L, Vogt J, Bengesser K, Fu C, Mikhail F, Serra E, Garcia-Linares C, Cooper DN, Lazaro C, Kehrer-Sawatzki H. (2011) Mosaic type-1 NF1 microdeletions as a cause of both generalized and segmental neurofibromatosis type-1 (NF1). *Hum Mutat.* **32**(2):213-9.

Metzker ML. (2005) Emerging technologies in DNA sequencing. *Genome Res* **15**:1767–1776.

Meyer-Rochow GY, Smith JM, Richardson AL, Marsh DJ, Sidhu SB, Robinson BG, Benn DE. (2009) Denaturing high performance liquid chromatography detection of SDHB, SDHD, and VHL germline mutations in pheochromocytoma. *J Surg Res.* **157**(1):55-62.

Meyerson M, Gabriel S, Getz G. (2010) Advances in understanding cancer genomes through second-generation sequencing. *Nat Rev Genet.* **11**(10):685-96.

Mikol D, Stefansson K. (1988) A phosphatidylinositollinked peanut agglutinin-binding glycoprotein in central nervous system myelin and on oligodendrocytes. *J. Cell Biol* **106**:1273- 1279.

Miller SJ, Lavker RM, Sun TT. (2005) Interpreting epithelial cancer biology in the context of stem cells: tumor properties and therapeutic implications. *Biochim. Biophys.* Acta **1756**:25–52.

Miller SJ, Jessen WJ, Mehta T, Hardiman A, Sites E, Kaiser S, Jegga AG, Li H *et al.* (2009) Integrative genomic analyses of neurofibromatosis tumours identify SOX9 as a biomarker and survival gene. *EMBO Mol Med* 1(4):236-48.

Mirsky R, Jessen KR. (1996) Schwann cell development, differentiation and myelination. *Curr Opin Neurobiol.* **6**(1):89-96. Review.

Mita MM. *et al.* (2008) Phase I trial of the novel mammalian target of rapamycin inhibitor deforolimus (AP23573; MK-8669) administered intravenously daily for 5 days every 2 weeks to patients with advanced malignancies. *Journal of Clinical Oncology* **26**:361-367.

Mitin N, Rossman KL, Der CJ. (2005) Signaling interplay in Ras superfamily function. *Curr Biol.* **15**(14):R563-74.

Morcos P, Thapar N, Tusneem N, Stacey D, Tamanoi F. (1996) Identification of neurofibromin mutants that exhibit allele specificity or increased Ras affinity resulting in suppression of activated ras alleles. *Mol Cell Biol* **16**(5):2496-503.

Mort M, Evani US, Krishnan VG, Kamati KK, Baenziger PH, Bagchi A, Peters BJ, Sathyesh R, Li B, Sun Y, Xue B, Shah NH, Kann MG, Cooper DN, Radivojac P, Mooney SD. (2010) In silico functional profiling of human disease-associated and polymorphic amino acid substitutions. *Hum Mutat* **31**:335-346.

Muggerud AA, Rønneberg JA, Wärnberg F, Botling J, Busato F, Jovanovic J, Solvang H, Bukholm I, Børresen-Dale AL, Kristensen VN, Sørlie T, Tost J. (2010) Frequent aberrant DNA methylation of ABCB1, FOXC1, PPP2R2B and PTEN in ductal carcinoma in situ and early invasive breast cancer. *Breast Cancer Res.* **12**(1):R3.

Mukhopadhyay D, Anant S, Lee RM, Kennedy S, Viskochil D, Davidson NO. (2002) C-->U editing of neurofibromatosis 1 mRNA occurs in tumors that express both the type II transcript and apobec-1, the catalytic subunit of the apolipoprotein B mRNA-editing enzyme. *Am J Hum Genet.* **70**(1):38-50.

Muir D. (1995) Differences in proliferation and invasion by normal, transformed and NF1 Schwann cell cultures are influenced by matrix metalloproteinase expression. *Clin Exp Metastasis.* **13**(4):303-14.

Muromoto R, Sugiyama K, Takachi A, *et al.* (2004) Physical and functional interactions between Daxx and DNA methyltransferase 1-associated protein, DMAP1. *J Immunol* **172**:2985– 2993.

Myrdal SE, Auersperg N. (1985) p21ras. Heterogeneous localization in transformed cells. *Exp. Cell Res.* **159**:441-450.

Nagy E, Maquat LE. (1998) A rule for termination-codon position within intron-containing genes: when nonsense affects RNA abundance. *Trends Biochem Sci* **23**:198-9.

Nakagawa O, Fujisawa K, Ishizaki T, *et al.* (1996) ROCK-I and ROCK-II, two isoforms of Rho-associated coiled-coil forming protein serine/threonine kinase in mice. *FEBS Lett* **392**:189–193.

Nakagawa M, Fukata M, Yamaga M, Itoh N, Kaibuchi K. (2001) Recruitment and activation of Rac1 by the formation of E-cadherin-mediated cell-cell adhesion sites. *J Cell Sci.* **114**(Pt 10):1829-38.

Nakamura T, Hara M, Kasuga T. (1989) Transplacental induction of peripheral nervous tumor in the Syrian golden hamster by N-nitroso-N-ethylurea: a new animal model for von Recklinghausen's neurofibromatosis. *Am J Pathol* **135**:251-259.

Naldini L, Vigna E, Narsimhan RP, Gaudino G, Zarnegar R, Michalopoulos GK, Comoglio PM. (1991) Hepatocyte growth factor (HGF) stimulates the tyrosine kinase activity of the receptor encoded by the proto-oncogene c-MET. *Oncogene.* **6**(4):501-4.

Nan X, Meehan RR, Bird A. (1993) Dissection of the methyl-CpG binding domain from the chromosomal protein MeCP2. *Nucleic Acids Res* **21**:4886–4892

Nan Y, Jin F, Yang S, Tian Y, Xie Y, Fu E, Yu H. (2010) Discovery of a set of biomarkers of human lung adenocarcinoma through cell-map proteomics and bioinformatics. *Med Oncol.* **27**(4):1398-406.

Nassiri B. Goliaei M, Tavassoli B. (2009) Bioinformatics Profiling of Missense Mutations World Academy of Science, Engineering and Technology 52

Nava C, Hanna N, Michot C, Pereira S, Pouvreau N, Niihori T, Aoki Y, Matsubara Y, *et al.* (2007) Cardio-facio-cutaneous and Noonan syndromes due to mutations in the RAS/ MAPK signalling pathway: genotype-phenotype relationships and overlap with Costello syndrome. *J Med Genet* **44**:763–771.

Nave KA, Salzer JL. (2006).Axonal regulation of myelination by neuregulin 1. *Curr. Opin. Neurobiol* **16**:492–500

Neumann HP, Sullivan M, Winter A, Malinoc A, Hoffmann MM, Boedeker CC, Bertz H, Walz MK, Moeller LC, Schmid KW, Eng C. (2011) Germline Mutations of the TMEM127 Gene in Patients with Paraganglioma of Head and Neck and Extraadrenal Abdominal Sites. *J Clin Endocrinol Metab.*

Neves M, Ciofu C, Larousserie F, Fleury J, Sibony M, Flahault A, Soubrier F, Gattegno B. (2002) Prospective evaluation of genetic abnormalities and telomerase expression in exfoliated urinary cells for bladder cancer detection. *J Urol.* **167**(3):1276-81.

Ng PC, Henikoff S. (2003). SIFT: Predicting amino acid changes that affect protein function. *Nucleic Acids Res* **31**(13):3812-4.

Nguyen KT, Chiu M. (2008) Segmental neurofibromatosis associated with renal angiomyolipomas. *Cutis* **82**(1):65-8.

Nichols KE, Houseknecht MD,Godmilow L, *et al.* (2005) Sensitivemultistep clinical molecular screening of 180 unrelated individuals with retinoblastoma detects 36 novel mutations in the RB1 gene. *Hum Mutat* **25**:566–574.

Niemeyer, C.M., Fenu, S., Hasle, H., Mann, G., Stary, J. & van Wering, E. (1998) Differentiating juvenile myelomonocytic leukemia from infectious disease. *Blood* **91**:365–367.

Niemeyer CM and Locatelli F. (2006) Chronic myeloproliferative disorders. In: Childhood Leukemia (ed. by C.H. Pui), Cambridge University Press, New York. 571–598

Niemeyer, C.M., Arico` , M., Basso, G., Biondi, A., Cantu Rajnoldi, A., Creutzig, U., Haas, O., Harbott, J *et al.* (1997) Chronic myelomonocytic myelomonocytic leukemia in childhood: a retrospective analysis of 110 cases. European Working Group on myelodysplastic syndromes in childhood (EWOG-MDS). *Blood* **89**:3534–3543.

Nielsen, G.P. *et al.* (1999) Malignant transformation of neurofibromas in neurofibromatosis 1 is associated with CDKN2A/p16 inactivation. *American Journal of Pathology* **155**:1879-1884.

NIH (1988) NIH Consensus development conference statement.Neurofibromatosis. *Arch Neurol* **45**:575–8.

Nishi, T., Lee, P.S.Y., Oka, K., Levin, V.A., Tanase, S., Morino, Y., and Saya, H. (1991) Differential expression of two types of the neurofibromatosis type 1 (NFI) gene transcripts related to neuronal differentiation. *Oncogene* **6**:1555-1559.

Noonan JA, Ehmke DA. (1963) Associated noncardiac malformations in children with congenital heart disease. *J Pediatr* **63**:468–470.

Noonan, J.A. (1968) Hypertelorism with Turner phenotype. A new syndrome with associated congenital heart disease. *Am. J. Dis. Child* **116**:373–380.

Nordlund M, Gu X, Shipley MT, Ratner N. (1993) Neurofibromin is enriched in the endoplasmic reticulum of CNS neurons. *J Neurosci* **13**:1588–1600

Nordlund, M.L., Rizvi, T.A., Brannan, C.I., Ratner, N. (1995) Neurofibromin expression and astrogliosis in neurofibromatosis type 1 brains. *J. Neuropathol Exp Neurol* **54**:588-600.

North KN, Riccardi V, Samango-Sprouse C, Ferner R, Moore B, Legius E, Ratner N, Denckla MB. (1997) Cognitive function and academic performance in neurofibromatosis. 1: consensus statement from the NF1 Cognitive Disorders Task Force. *Neurology.* **48**(4):1121-7.

O'Connell P, Viskochil D, Buchberg AM, Fountain J, Cawthon RM, Culver M, Stevens J, Rich DC, Ledbetter DH, Wallace M, Carey JC, Jenkins NA, Copeland NG, Collins FS, White R: (1990) The human homolog of murine *Evi-2* lies between two von Recklinghausen neurofibromatosis translocations *Genomics* **7**(4):547-554.

Ohaegbulam C, Magge S, Scott RM. (2001) Moyamoya syndrome. In: McCone DG, ed. Pediatric Neurosurgery: Surgery of the Developing Nervous System. 4th ed. New York: WB Saunders 1077-92.

Oliveira JB, Bidere N, Niemela JE, Zheng L, Sakai K, Nix CP, Danner RL, Barb J, Munson PJ, Puck JM *et al.* (2007) NRAS mutation causes a human autoimmune lymphoproliferative syndrome. *Proc Natl Acad Sci U S A* **104**:8953-8958.

Oliveira JB, Fleisher T. (2004) Autoimmune lymphoproliferative syndrome. *Curr Opin Allergy Clin Immunol* **4**:497-503.

Oishi K, Zhang H, Gault WJ, Wang CJ, Tan CC, Kim I, Ying H, Rahman T, Pica N, Tartaglia M, Mlodzik M, Gelb BD. (2009) Phosphatase-defective LEOPARD syndrome mutations in PTPN11 gene have gain-of-function effects during Drosophila development. *Human Molecular Genetics* **18**(1):193–201.

Okano M, Bell DW, Haber DA, Li E. (1999) DNA methyltransferases Dnmt3a and Dnmt3b are essential for de novo methylation and mammalian development. *Cell* **99**:247–257.

Origone P, De Luca A, Bellini C, Buccino A, Mingarelli R, Costabel S, La Rosa C, Garrè C, Coviello DA, Ajmar F, Dallapiccola B, Bonioli E. (2002) Ten novel mutations in the human neurofibromatosis type 1 (NF1) gene in Italian patients. *Hum Mutat* **20**(1):74-5.

Orita M, *et al.* (1989) Detection of Polymorphisms of Human DNA by Gel Electrophoresis as SSCPs. *Proceedings of the National Academy of Sciences of the United States of America* (86):2766-70.

Ortmann CA, Eisele L, Nuckel H *et al.* (2008) Aberrant hypomethylation of the cancer-testis antigenPRAMEcorrelates withPRAMEexpression in acute myeloid leukemia. *Ann Hematol* **87**:809–818.

Osborne JP *et al.* (1991) Epidemiology of tuberous sclerosis. *Ann NY Acad Sci* **615**:125–127.

Osborn MJ, Upadhyaya M. (1999) Evaluation of the protein truncation test and mutation detection in the NF1 gene: mutational analysis of 15 known and 40 unknown mutations. *Hum Genet* **105**(4):327-32.

Østergaard JR, Sunde L, Okkels H. (2005) Neurofibromatosis von Recklinghausen Type I Phenotype and Early Onset of Cancers in Siblings Compound Heterozygous for Mutations in MSH6. *American Journal of Medical Genetics* **139A**(2):96-105

Otis CN, Krebs PA, Quezado MM, Albuquerque A, Bryant B, San Juan X, Kleiner D, Sobel ME, Merino MJ. (2002) Loss of heterozygosity in p53, *BRCA1*, and estrogen receptor genes and correlation to expression of p53 protein in ovarian epithelial tumors of different cell types and biological behaviour. *Hum Pathol* **31**:233-238.

Ottini L, Esposito DL, Richetta A, Carlesimo M, Palmirotta R, Verí MC, Battista P, Frati L, Caramia FG, Calvieri S *et al.* (1995) Alterations of microsatellites in neurofibromas of von Recklinghausen's disease. *Cancer Res 1* **55**(23):5677–5680.

Pacold ME, *et al.* (2000) Crystal structure and functional analysis of Ras binding to its effector phosphoinositide 3-kinaseγ. *Cell* **103**:931–943.

Pandit B, Sarkozy A, Pennacchio LA, Carta C, Oishi K, Martinelli S, Pogna EA, Schackwitz W, Ustaszewska A, Landstrom A *et al.* (2007) Gain-of-function RAF1 mutations cause Noonan and LEOPARD syndromes with hypertrophic cardiomyopathy. *Nat Genet* **39**:1007-1012.

Pan Y, Bi F, Liu N, Xue Y, Yao X, Zheng Y, Fan D. (2004) Expression of seven main Rho family members in gastric carcinoma. *Biochem. Biophys. Res. Commun.* **315**:686-691.

Parada LF, Tabin CJ, Shih C, Weinberg RA. (1982 Jun 10) Human EJ bladder carcinoma oncogene is homologue of Harvey sarcoma virus ras gene. *Nature* **297**(5866):474-8.

Pareyson D. (1999) Charcot-Marie-Tooth Disease and related neuropathies: molecular basis for distintion and diagnosis. *Mus Nerve* **22**:1498–1509.

Park VM, Pivnick EK. (1998) Neurofibromatosis type 1 (NF1): a protein truncation assay yielding identification of mutations in 73% of patients. *J Med Genet* **35**:813–820.

Parrinello S, Lloyd AC. (2009) Neurofibroma development in NF1—insights into tumor initiation. *Trends Cell Biol* **9**(8):395–403.

Parsons DW, Jones S, Zhang X, Lin JC, Leary RJ, Angenendt P, Mankoo P, Carter H, *et al.* (2008) An integrated genomic analysis of human glioblastomamultiforme. *Science* **321**(5897):1807-12

Pascual-Castroviejo I, Pascual-Pascual SI, Velázquez R, Viaño J, Martínez V (2006) Moyamoya disease: follow-up of 12 patients. *Neurologia* **21**(10):695-703.

Pasmant E, de Saint-Trivier A, Laurendeau I, Dieux-Coeslier A, Parfait B, Vidaud M, Vidaud D, Bièche I. (2008) Characterization of a 7.6-Mb germline deletion encompassing the NF1 locus and about a hundred genes in an NF1 contiguous gene syndrome patient. *Eur J Hum Genet* **16**:1459- 1466.

Pasmant E, Sabbagh A, Hanna N, *et al.* (2009) *SPRED1* germline mutations caused a neurofibromatosis type 1 overlapping phenotype. *J Med Genet* **46**(7):425-430.

Pasmant E, Sabbagh A, Masliah-Planchon J, Haddad V, Hamel MJ, Laurendeau I, Soulier J, Parfait B, Wolkenstein P, Bièche I, Vidaud M, Vidaud D. (2009) Detection and characterization of NF1 microdeletions by custom high resolution array CGH. *J Mol Diagn* **11**(6):524-9.

Pasmant E, Sabbagh A, Masliah-Planchon J, Haddad V, Hamel M-J, Laurendeau I, Soulier J, Parfait B, Wolkenstein P, Bie`che I, Vidaud M, Vidaud D. (2009b November) Detection and Characterization of NF1 Microdeletions by Custom High Resolution Array CGH. *Journal of Molecular Diagnostics* **11**:6.

Pasmant E, Sabbagh A, Spurlock G, Laurendeau I, Grillo E, Hamel MJ, Martin L, Barbarot S, Leheup B *et al.* members of the NF France Network. (2010a) NF1 microdeletions in neurofibromatosis type 1: from genotype to phenotype. *Hum Mutat* **31**:E1506-1518.

Pasmant E, Vidaud D, Harrison M, Upadhyaya M. (2011) Different sized somatic NF1 locus rearrangements in neurofibromatosis 1-associated malignant peripheral nerve sheath tumors. *J Neurooncol.* **102**(3):341-6.

Pearl RA, O'Toole G. (2010) A case of large sporadic neurofibroma of the hand. *J Plast Reconstr Aesthet Surg.* **63**(7):e573-5.

Peltonen J, Jaakola S, Lebwohl M. (1988) Cellular differentiation and expression of matrix genes in type 1 neurofibromatosis. *Lab Invest* **59**:760–771

Pemov A, Park C, Reilly KM, Stewart DR. (2010) Evidence of perturbations of cell cycle and DNA repair pathways as a consequence of human and murine NF1-haploinsufficiency. *BMC Genomics.* **11**:194.

Pericak-Vance, M., L. Yamaoka, J. Vance, K. Small, G. Rosenwasser, P. Gaskell, W. Hung, M. Alberts, C. Haynes, M. Speer, J. Gilbert, M. Herbstreith, A. Aylsworth, and Roses A. (1987) Genetic linkage studies of chromosome 17 RFLPs in von Recklinghausen neurofibromatosis (NF1). *Genomics* **1**:349-352.

Perrone F, Da Riva L, Orsenigo M, Losa M, Jocollè G, Millefanti C, Pastore E, Gronchi A, Pierotti MA, Pilotti S. (2009) PDGFRA, PDGFRB, EGFR, and downstream signaling activation in malignant peripheral nerve sheath tumor. *Neuro Oncol.* **11**(6):725-36.

Perry A, *et al.* (2002) Differential NF1, p16, andEGFR patterns by interphase cytogenetics (FISH) in malignant peripheral nerve sheath tumor (MPNST) and morphologically similar spindle cell neoplasms. *Journal of Neuropathology and Experimental Neurology* **61**:702-709.

Phillips SE, Vincent P, Rizzieri KE, Schaaf G, Bankaitis VA, Gaucher EA. (2006) The diverse biological functions of phosphatidylinositol transfer proteins in eukaryotes. *Crit. Rev. Biochem. Mol. Biol.* **41**:21–49.

Phillips JA, Xu Y, Xia Z, Fan ZH Tan W. (2009) Enrichment of Cancer Cells Using Aptamers Immobilized on a Microfluidic Channel *Anal. Chem.* **81**(3)1033–1039

Pirolli D, Carelli Alinovi C, Capoluongo E, Satta MA, Concolino P, Giardina B, De Rosa MC. (2010) Insight into a Novel p53 Single Point Mutation (G389E) by Molecular Dynamics Simulations. *Int J Mol Sci.***12**(1):128-40.

Pollard KS, Hubisz MJ, Rosenbloom KR, Siepel A. (2010) Detection of nonneutral substitution rates on mammalian phylogenies. *Genome Res* **20**:110-121.

Ponchel F, Toomes C, Bransfield K, Leong FT, Douglas SH, Field SL, Bell SM, Combaret V, *et al.* (2003) Real-time PCR based on SYBR-Green I fluorescence: an alternative to the TaqMan assay for a relative quantification of gene rearrangements, gene amplifications and micro gene deletions. *BMC Biotechnol* **3**:18.

Ponting CP, Benjamin DR. (1996) A novel family of Ras-binding domains. *Trends Biochem. Sci.* **21**:422–425.

Poullet PB, Esson LK, Tamanoi F. (1994) Functional significance of lysine 1423 of neurofibromin and characterization of a second site suppressor which rescues mutations at this residue and suppresses RAS2Val-19- activated phenotypes. *Mol. Cell. Biol* **14**:815–821.

Poyhonen M, Niemela S, Herva R. (1997) Risk of malignancy and death in neurofibromatosis. Archives of Pathology and Laboratory Medicine 121, 139-143

Pros E, Larriba S, López E, Ravella A, Gili ML, Kruyer H, Valls J, Serra E, Lázaro (2006) CNF1 mutation rather than individual genetic variability is the main determinant of the NF1-transcriptional profile of mutations affecting splicing. *Hum Mutat* **27**(11):1104-14.

Pros E, Fernández-Rodríguez J, Canet B, Benito L, Sánchez A, Benavides A, Ramos FJ, López-Ariztegui MA, Capellá G, Blanco I, Serra E, Lázaro C. (2009) Antisense therapeutics for neurofibromatosis type 1 caused by deep intronic mutations. *Hum Mutat.* **30**(3):454-62.

Purandare SM, Huntsman Breidenbach H, Li Y, Zhu XL, Sawada S, Neil SM, Brothman A, White R, Cawthon R, Viskochil D (1995) Identification of neurofibromatosis 1 (NF1) homologous loci by direct sequencing, fluorescence in situ hybridization, and PCR amplification of somatic cell hybrids. *Genomics* **30**:476–485.

Pruitt K Der CJ. (2001) Ras and Rho regulation of the cell cycle and oncogenesis. *Cancer Lett* **171**:1–10.

Qiu RG, Chen J, Kirn D, McCormick F, Symons M. (1995) An essential role for Rac in Ras transformation. *Nature* **374**:457–459.

Qu C, Yu W, Azzarelli B, *et al.* (1998) Biased suppression of hematopoiesis and multiple developmental defects in chimeric mice containing Shp-2 mutant cells. *Mol Cell Biol* **18**:6075–6082.

Rahmatullah M, Schroering A, Rothblum K, Stahl Rc, Urban B, Carey DJ. (1998) Synergistic Regulation Of Schwann Cell Proliferation By Heregulin And Forskolin. *Molecular And Cellular Biology* **18**:(11):6245–6252.

Ramaswamy MC, Dumont AC, Cruz JR, Muppidi TS, Gomez DD, Billadeau VL, Tybulewicz RM, *et al.* (2007) Cutting edge: Rac GTPases sensitize activated T cells to die via Fas. *J. Immunol.* **179**:6384–6388.

Ramensky V, Bork P, Sunyaev S. (2002) Human non-synonymous SNPs: server and survey. *Nucleic Acids Res* **30**(17):3894-900.

Ramsingh G, Koboldt DC, Trissal M, Chiappinelli KB, Wylie T, Koul S, Chang LW, Nagarajan R, Fehniger TA, Goodfellow P, Magrini V, Wilson RK, Ding L, Ley TJ, Mardis ER, Link DC. (2010) Complete characterization of the microRNAome in a patient with acute myeloid leukemia. *Blood.* **116**(24):5316-26.

Rao UN, Sonmez-Alpan E, Michalopoulos GK. (1997) Hepatocyte growth factor and c-MET in benign and malignant peripheral nerve sheath tumors. *Hum Pathol* **28**(9):1066-70.

Raponi M, Upadhyaya M, Baralle D. (2006) Functional splicing assay shows a pathogenic intronic mutation in neurofibromatosis type 1 (NF1) due to intronic sequence exonization. *Hum Mutat* **27**(3):294-5.

Raponi M, Buratti E, Dassie E, Upadhyaya M, Baralle D. (2009) Low U1 snRNP dependence at the NF1 exon 29 donor splice site FEBS Journal **276**:2060–2073.

Rasmussen SA, Yang Q, Friedman JM. (2001) Mortality in neurofibromatosis 1: an analysis using U.S. death certificates. *Am J Hum Genet* **68**:1110-8.

Razzaque MA, Nishizawa T, Komoike Y, Yagi H, Furutani M, Amo R, Kamisago M, Momma K, Katayama H, Nakagawa M *et al.* (2007) Germline gain-of-function mutations in RAF1 cause Noonan syndrome. *Nat Genet* **39**:1013-1017.

Redlick FP, Shaw JC. (2004) Segmental neurofibromatosis follows blaschko's lines or dermatomes depending on the cell line affected: case report and literature review. *J Cutan Med Surg* **8**(5):353-6.

Régnier V, Meddeb M, Lecointre G, Richard F, Duverger A, Nguyen VC, Dutrillaux B, Bernheim A, Danglot G. (1997) Emergence and scattering of multiple neurofibromatosis (NF1)-related sequences during hominoid evolution suggest a process of pericentromeric interchromosomal transposition. *Hum Mol Genet* **6**:9–16.

Reilly KM, Loisel DA, Bronson RT, McLaughlin ME, Jacks T. (2000) *Nf1;Trp53* mutant mice develop glioblastoma with evidence of strain-specific effects. *Nat. Genet* **26**:109–13.

Reilly KM, Tuskan RG, Christy E, Loisel DA, Ledger J, *et al.* (2004) Susceptibility to astrocytoma in mice mutant for *Nf1* and *Trp53* is linked to chromosome 11 and subject to epigenetic effects. *Proc. Natl. Acad. Sci. USA* **101**:13008–13.

Reilly KM, Broman KW, Bronson RT, Tsang S, Loisel DA, *et al.* (2006) An imprinted locus epistatically influences *Nstr1* and *Nstr2* to control resistance to nerve sheath tumors in a neurofibromatosis type 1 mouse model. *Canc. Res* **66**:62–68.

Resat H, Straatsma TP, Dixon DA, Miller JH. (2001) The arginine finger of RasGAP helps Gln-61 align the nucleophilic water in GAP-stimulated hydrolysis of GTP. *Proc. Natl Acad. Sci. USA* **98**:6033–6038.
Reitmair AH, Schmits R, Ewel A *et al.* (1995) MSH2 deficient mice are viable and susceptible to lymphoid tumours. *Nat Genet* **11**:64–70.

Reitmair AH, Redston M, Cai JC, Chuang TC, Bjerknes M, Cheng H, Hay K, Gallinger S, Bapat B, Mak TW. (1996) Spontaneous intestinal carcinomas and skin neoplasms in Msh2- deficient mice. *Cancer Res* **56**:3842–3849.

Reuss D. and von Deimling A. (2008) Biomarkers for malignant peripheral nerve sheath tumors (MPNST). *Exp Opin Med Diagnosis*, **2**:801-811

Riccardi VM. (1988) germline mutation rodent model for neurofibromatosis: neurofibrosarcoma in the untreated offspring of rats exposed in utero to ethylnitrosourea. *Am J Hum Genet* **42**:A32.

Riccardi VM, Womack JE, Jacks T. (1994) Neurofibromatosis and Related Tumors Natural Occurrence and Animal Models. *American journal of Pathology* **145**:5.

Riethmacher D, *et al.* (1997) Severe neuropathies in mice with targeted mutations inthe ErbB3 receptor. *Nature* **389**:725–730

Riento K, Ridley AJ. Rocks: (2003) multifunctional kinases in cell behaviour. *Nat Rev Mol Cell Biol* **4**:446–456.

Riggs AD, Pfeifer GP. (1992) X-chromosome inactivation and cell memory. *Trends Genet* **8**(5):169-74. Review.

Riley DJ, Lee EY, Lee WH. (1994) The retinoblastoma protein: more than a tumor suppressor. *Annu. Rev. Cell Biol.* **10**:1–29.

Riva P, Corrado L, Natacci F, Castorina P, Wu BL, Schneider GH, Clementi M, Tenconi R, Korf BR, Larizza L: (2000) NF1 microdeletion syndrome: refined FISH characterization of sporadic and familial deletions with locus-specific probes. Am *J Hum Genet* **66**:100–109.

Roberts AE, Araki T, Swanson KD, Montgomery KT, Schiripo TA, Joshi VA, Li L, Yassin Y, Tamburino AM, Neel BG *et al.* (2007) Germline gain-of-function mutations in SOS1 cause Noonan syndrome. *Nat Genet* **39**:70-74.

Rodenhiser DI, Coulter-Mackie MB, Singh SM: (1993) Evidence of DNA methylation in the neurofibromatosis type 1 (NF1) gene region of 17q11.2. *Human Molecular Genetics* **2**:439-444.

Rodriguez-Viciana P, *et al.* (1994) Phosphatidylinositol-3-OH kinase as a direct target of Ras. *Nature* **370**:527–532.

Roehl AC, Vogt J, Mussotter T, Zickler AN, Spoti H, Hogel J, Chuzhanova NA, Wimmer K, Kluwe L, Mautner VF, Cooper DN, Kehrer-Sawatzki, H. (2010) Intrachromosomal Mitotic Nonallelic Homologous Recombination Is the Major Molecular Mechanism Underlying Type-2 NF1 Deletions HUMAN *MUTATION* **31**(10):1163–1173.

Roest PA, Roberts RG, Sugino S, van Ommen GJ, den Dunnen JT. (1993) Protein truncation test (PTT) for rapid detection of translation-terminating mutations. *Hum Mol Genet* **2**(10):1719-21.

Rønneberg JA, Fleischer T, Solvang HK, Nordgard SH, Edvardsen H, Potapenko I, Nebdal D, Daviaud C, Gut I, Bukholm I, Naume B, Børresen-Dale AL *et al.* (2011) Methylation profiling with a panel of cancer related genes: Association with estrogen receptor, TP53 mutation status and expression subtypes in sporadic breast cancer. *Mol Oncol* **5**:61-76.

Rong S, Bodescot M, Blair D, *et al.* (1992) Tumorigenesis of the met protooncogene and the gene for hepatocyte growth factor. *Mol Cell Biol* **12**:5152-5158.

Rong S, Jeffers M, ResauJH, et ah. (1993) Met expression and sarcoma tumorigenicity. *Cancer Res* **53**:5355-5360.

Rong S, Segal S, Anver M, *et al.* (1994) Invasiveness and metastasis of NIH 3T3 cells induced by Met-hepatocyte growth factor/scatter factor autocrine stimulation. *Proc Natl Acad Sci U S A* **91**:4731-4735.

Roudebush M, Slabe T, Sundaram V, Hoppel CL, Golubic M, Stacey DW. (1997) Neurofibromin Colocalizes with Mitochondria in Cultured Cells. *Experimental Cell Research* **236**:161–172.

Roos KL, Pascuzzi RM, Dunn DW. (1989) Neurofibromatosis, Charcot-Marie-Tooth disease, or both? *Neurofibromatosis* **2**(4):238–243.

Rosen EM, Nigam SK, Goldberg ID. (1994) Scatter factor and the c-met receptor: A paradigm for mesenchymal/epithelial interaction. *J Cell Biol* **127**:1783-1787.

Rosenbaum T, Rosenbaum C, Winner U, Muller HW, Lenard HG, Hanemann CO. (2000) Long-term culture and characterization of human neurofibroma-derived Schwann cells. *J Neurosci Res*; **61**:524–532.

Rosser TL, Packer RJ. (2003) Neurocognative dysfunction in children with neurofibromatosis type 1. *Curr Neurol Neurosci Rep* **3**:129-136.

Rosser TL, Vezina G, Packer RJ. (2005) Cerebrovascular abnormalities in a population of children with neurofibromatosis type 1. *Neurology* **64**:553-5.

Rouleau GA, Merel P, Lutchman M, Sanson M, Zucman J, *et al.* (1993) Alteration in a new gene encoding a putative membrane-organizing protein causes neuro-fibromatosis type 2. *Nature* **363**:515–21.

Rountree MR, Bachman KE, Baylin SB. (2000) DNMT1 binds HDAC2 and a new co-repressor, DMAP1, to form a complex at replication foci. *Nat Genet* **25**:269–277.

Rozen, S Skaletsky H.J. (2000) Primer3 on the WWW for general users and for biologist programmers. In: Krawetz S, Misener S (eds) Bioinformatics Methods and Protocols: Methods in Molecular Biology. Humana Press, *Totowa, NJ* 365-386.
Ruggieri M, Huson SM. (1999) The neurofibromatoses. An overview. *Ital J Neurol Sci* **20**(2):89-108.

Ruggieri M, Huson SM. (2001) The clinical and diagnostic implications of mosaicism in the neurofibromatoses. *Neurology* **56**(11):1433-43.

Rutkowski JL, Wu K, Gutmann DH, Boyer PJ, Legius E. (2000) Genetic and cellular defects contributing to benign tumor formation in neurofibromatosis type 1. *Hum Mol Genet* **9**(7):1059-66.

Ryan JJ, Klein KA, Neuberger TJ, Leftwich JA, Westin EH, Kauma S, Fletcher JA, DeVries GH, Huff TJ. (1994) Role for the stem cell factor/ KIT complex in Schwann cell neoplasia and mast cell proliferation associated with neurofibromatosis. *J Neurosci Res* **37**:415–432.

Salemis NS, Nakos G, Sambaziotis D, Gourgiotis S. (2010) Breast cancer associated with type 1 neurofibromatosis. *Breast Cancer* **17**(4):306-9.

Salzer JL. (1997) Clustering sodium channels at the node of Ranvier: Close encounters of the axon-glia kind. *Neuron* **18**:843–846.

Samuel MS, Lourenço FC, Olson MF. (2011) K-Ras mediated murine epidermal tumorigenesis is dependent upon and associated with elevated Rac1 activity. *PLoS One*. 6(2):e17143.

Sandrini F, Stratakis C. (2003) Clinical and molecular genetics of Carney complex. *Mol Genet Metab* **78**:83-92.

Sanger F, Coulson AR. (1975) A rapid method for determining sequences in DNA by primed synthesis with DNA polymerase. *J. Mol. Biol* **94**:441–448.

Sanger F, Nicklen S, Coulson AR. (1977) DNA sequencing with chain-terminating inhibitors. *Proc. Natl Acad. Sci. USA* **74**:5463–5467.

Sangha N, Wu R, Kuick R, Powers S, Mu D, Fiander D, Yuen K, Katabuchi H, Tashiro H, Fearon ER, Cho KR. (2008) Neurofibromin 1 (NF1) defects are common in human ovarian serous carcinomas and co-occur with TP53 mutations. *Neoplasia* **10**(12):1362-72

Sant M, Minicozzi P, Lagorio S, Johannesen TB, Marcos-Gragera R, Francisci S; The EUROCARE Working Group. (2011) Survival of european patients with central nervous system tumors. *Int J Cancer* [Epub ahead of print]

Sapet C, Simoncini S, Loriod B, *et al.* (2006) Thrombin-induced endothelial microparticle generation: identification of a novel pathway involving ROCK-II activation by caspase-2. *Blood* **108**:1868– 1876.

Sartin EA, Doran SE, Riddell MG. (1994) Characterization of naturally occurring cutaneous neurofibromas in Holstein cattle: a disorder resembling neurofibromatosis type 1 in man. *Am J Pathol* **145**:1168-1174.

Saxonov S, Berg P, Brutlag DL. (2006) A genome-wide analysis of CpG dinucleotides in the human genome distinguishes two distinct classes of promoters. *Proc Natl Acad Sci USA* **103**:1412–1417.

Scheffzek K, Ahmadian MR, Kabsch W, Wiesmuller L, Lautwein A, Schmitz F, Wittinghofer A. (1997) The Ras-RasGAP complex: structural basis for GTPase activation and its loss in oncogenic Ras mutants. *Science* **277**:333–338.

Scheffzek K, Ahmadian MR, Wittinghofer A. (1998) GTPase-activating proteins: helping hands to complement an active site. *Trends Biochem. Sci* **23**:257–262.

Schmale MC, Hensley GT, Udey LR. (1983) Multiple schwannomas in the bicolor damselfish, Pomacentrus partitus: a possible model of von Recklinghausen neurofibromatosis. *Am J Pathol* **112**:238-241.

Schmegner C, Berger A, Vogel W, Hameister H, Assum G. (2005) An isochore transition zone in the NF1 gene region is a conserved landmark of chromosome structure and function. *Genomics* **86**:439–445.

Schmidt MA, Michels VV, Dewald W. (1987)Cases of neurofibromatosis with rearrangements of chromosome 17 involving band 17qll.2 *Am.J. Med. Genet* **28**:771-777.

Schneider-Stock R. *et al.* (1997) p53 gene mutations in soft-tissue sarcomas–correlations with p53 immunohistochemistry and DNA ploidy. *Journal of Cancer Research and Clinical Oncology* **123**:211-218.

Schnelzer A, Prechtel D, Knaus U, Dehne K, Gerhard M, Graeff H, Harbeck N, Schmitt M, Lengyel E. (2000) Rac1 in human breast cancer: overexpression, mutation analysis, and characterization of a new isoform, Rac1b. *Oncogene* **19**:3013-3020

Schubbert S, Bollag G, Shannon K. (2007) Deregulated Ras signaling in developmental disorders: new tricks for an old dog. *Curr Opin Genet Dev* **17**:15–22.
Schubbert S, Zenker M, Rowe SL, Boll S, Klein C, Bollag G, van der Burgt I, Musante L, Kalscheuer V, Wehner LE *et al.* (2006) Germline KRAS mutations cause Noonan syndrome. *Nat Genet* **38**:331-336.

Seizinger BR, Farmer TGE, Haines JL, Ozelius LJ, Anderson K, Korf BR, Parry DM, Pericak-Vance MA, *et al.* (1989) Flanking Markers for the Gene Causing von Recklinghausen Neurofibromatosis (NFI) *Am. J. Hum. Genet* **44**:30-32.

Seizinger BR. (1987) Genetic linkage of von Recklinghausen neurofibromatosis to the nerve growth factor receptor gene. *Cell* **49**:589-594.

Sharif S, Moran A, Huson SM, *et al.* (2007) Women with neurofibromatosis 1 are at a moderately increased risk of developing breast cancer and should be considered for early screening. *J Med Genet* **44**:481–4.

Sharif S, Ferner R, Birch JM, *et al.* (2006) Second primary tumors in neurofibromatosis 1 patients treated for optic glioma: substantial risks after radiotherapy. *J Clin Oncol* **24**:2570–5.

Sheela S, Riccardi VM, Ratner N. (1990) Angiogenic and invasive properties of neurofibroma Schwann cells. *J Cell Biol* **111**(2):645-53.

Shen MH, Harper PS, Upadhyaya M. (1993) Neurofibromatosis type 1 (NF1): the search for mutations by PCR-heteroduplex analysis on Hydrolink gels. *Hum Mol Genet.* **2**(11):1861-4.

Shen JC, Rideout WM, 3rd and Jones, P.A. (1994) The rate of hydrolytic deamination of 5-methylcytosine in double-stranded DNA. *Nucleic Acids Res* **22**:972–976.

Shen MH, Harper PS, Upadhyaya M. (1996) Molecular genetics of neurofibromatosis type 1 (NF1). *J Med Genet* **33**(1):2-17.

Shen MH, Mantripragada K, Dumanski JP, Frayling I, Upadhyaya M. (2007) Detection of copy number changes at the NF1 locus with improved high-resolution array CGH. *Clin Genet* **72**:238–244.

Seraphin B, Rosbash M. (1989) Identification of functional U1 snRNA–pre-mRNA complexes committed to spliceosome assembly and splicing. *Cell* **59**:349–358.

Serra E, Puig S, Otero D, Gaona A, Kruyer H, Ars E, Estivill X, Lázaro C. (1997) Confirmation of a double-hit model for the NF1 gene in benign neurofibromas. *Am J Hum Genet* **61**(3):512–519.

Serra E, Rosenbaum T, Winner U, Aledo R, Ars E, Estivill X, Lenard HG, Lazaro C. (2000) Schwann cells harbor the somatic *NF1* mutation in neurofibromas: evidence of two different Schwann cell subpopulations. *Hum Mol Genet* **9**:3055–3064.

Serra E, Rosenbaum T, Nadal M, Winner U, Ars E, Estivill X, Lázaro C. (2001) Mitotic recombination effects homozygosity for NF1 germline mutations in neurofibromas. *Nat Genet* **28**(3):294–296.

Serra E, Pros E, García C, López E, Lluïsa Gili M, Gómez C, Ravella A, Capellá G, Blanco I, Lázaro C. (2007) Tumor LOH analysis provides reliable linkage information for prenatal genetic testing of sporadic NF1 patients. *Genes, Chromosomes Cancer* **46**:820–827.

Side L, Taylor B, Cayouette M, Conner E, Thompson P, Luce M, *et al.* (1997) Homozygous inactivation of the NF1 gene in bone marrow cells from children with neurofibromatosis type 1 and malignant myeloid disorders. *N Engl J Med* **336**:1713-1720.

Silva AJ, Frankland PW, Marowitz Z, Friedman E, Laszlo GS, Cioffi D, Jacks T, Bourtchuladze R. (1997) A mouse model for the learning and memory deficits associated with neurofibromatosis type I. *Nat Genet* **15**(3):281-4.

Singh DK, Ku CJ, Wichaidit C, Steininger III RJ, Wu LF, Altschuler SJ. (2010) Patterns of basal signaling heterogeneity can distinguish cellular populations with different drug sensitivities. *Mol Syst Biol* **11**:6:369.

Skinner RH, Bradley S, Brown AL, Johnson NJE, Rhodes S, Stammers DK, Lowe PN. (1991) Use of the Glu-Glu-Phe C-terminal epitope for rapid purification of the catalytic domain of normal and mutant *ras* GTPase-activating proteins. *J. Biol. Chem* **266**:14163–14166.

Skolnick MH, Ponder B, Seizinger B. (1987) Linkage of NF1 to 12 chromosome 17 markers: a summary of eight concurrent reports. *Genomics* **1**(4):382-3.

Skuse GR, Cappione AJ, Sowden M, Metheny LJ, Smith HC. (1996) The neurofibromatosis type I messenger RNA undergoes base-modification RNA editing. *Nucleic Acids Res* **24**:478–485

Skuse GR, Cappione AJ. (1997) RNA processing and clinical variability in neurofibromatosis type I (NF1). *Hum Mol Genet* **6**:1707–1712.

Smallwood A, Esteve PO, Pradhan S, Carey M. (2007) Functional cooperation between HP1 and DNMT1 mediates gene silencing. *Genes Dev* **21**:1169–1178.

Smith C. (2007) C loning and mutagenesis: tinkering with the order of things. *Nature Methods* **4**, 455 - 461

Spurlock G, Griffiths S, Uff J, Upadhyaya M *et al.* (2007) Somatic alterations of the NF1 gene in an NF1 individual with multiple benign tumors and malignant tumor types. *Familial Cancer* **6**:463–471.

Spurlock G, Bennett E, Chuzhanova N, *et al.* (2009) *SPRED1* mutations (Legius syndrome): another clinically useful genotype for dissecting the neurofibromatosis type 1 phenotype. *J Med Genet* **46**(7):431-437.

Spurlock G, Knight SJ, Thomas N, Kiehl TR, Guha A, Upadhyaya M. (2010) Molecular evolution of a neurofibroma to malignant peripheral nerve sheath tumor (MPNST) in an NF1 patient: correlation between histopathological, clinical and molecular findings. *J Cancer Res Clin Oncol.* **136**(12):1869-80.

Steelman LS, Chappell WH, Abrams SL, Kempf RC, Long J, Laidler P, Mijatovic S, Maksimovic-Ivanic D, *et al.* (2011) Roles of the Raf/MEK/ERK and PI3K/PTEN/Akt/mTOR pathways in controlling growth and sensitivity to therapy-implications for cancer and aging. *Aging (Albany NY)* **3**(3):192-222.

Steinemann D, Arning L, Praulich I, Stuhrmann M, Hasle H, Stary J, Schlegelberger B, Niemeyer CM, Flotho C. (2010) Mitotic recombination and compound-heterozygous mutations are predominant NF1-inactivating mechanisms in children with juvenile myelomonocytic leukemia and neurofibromatosis type 1. *Haematologica.* **95**(2):320-3.

Steinmann K, Cooper DN, Kluwe L, Chuzhanova NA, Senger C, Serra E, Lázaro C, Gilaberte M, Wimmer K, Mautner VF, Kehrer-Sawatzki H. (2007) Type 2 *NF1* deletions are highly unusual by virtue of the absence of nonallelic homologous recombination hotspots and an apparent preference for female mitotic recombination. *Am J Hum Genet* **81**:1201-1220.

Stingl J, Caldas C. (2007) Molecular heterogeneity of breast carcinomas and the cancer stem cell hypothesis. *Nat Rev Cancer* **7**:791-799.

Stratakis CA, Kirschner LS, Carney JA. (2001) Clinical & molecular features of the Carney complex: Diagnostic criteria and recommendation for patient evaluation. *J Clin Endocrinol* Metab **86**:4041-4046.

Sohn KJ, Choi M, Song J *et al.* (2003) Msh2 deficiency enhances somatic Apc and p53 mutations in Apc ± Msh2-/- mice. *Carcinogenesis* **24**(2):217–224.

Song C, Milbury CA, Li J, Liu P, Zhao M, Makrigiorgos GM. (2011) Rapid and Sensitive Detection of KRAS Mutation After fast-COLD-PCR Enrichment and High-resolution Melting Analysis. *Diagn Mol Pathol.* **20**(2):81-9.

Stephens K, Green P, Riccardi VM, Ng S, Rising M, Barker D, Darby JK, Falls KM, Collins FS, Willard HF, *et al.* (1989) Genetic analysis of eight loci tightly linked to neurofibromatosis 1. *Am. J. Hum. Genet* **44**:13-19.

Stewart DR, Corless CL, Rubin BP, Heinrich MC, Messiaen LM, Kessler LJ, Zhang PJ, Brooks DG. (2007) Mitotic recombination as evidence of alternative pathogenesis of gastrointestinal stromal tumours in neurofibromatosis type 1. *J Med Genet.* **44**(1):e61.

Stewart W, Traynor JP, Cooke A, Griffiths S, Onen NF, Balsitis M, Shah AA, Upadhyaya M, Tobias ES. (2007) Gastric carcinoid: germline and somatic mutation of the neurofibromatosis type 1 gene. *Fam Cancer.* **6**(1):147-52.

Stewart H, *et al.* (2008) Congenital disseminated neurofibromatosis type 1: a clinical and molecular case report. *Am J Med Genet.* **146A**(11):1444-52.

Stiller CA, Chessells JM, Fitchett M. (1994) Neurofibromatosis and childhood leukemia/lymphoma: a population-based UKCCSG study. *British Journal of Cancer* **70**:969–972.

Storlazzi CT, Brekke HR, Mandahl N, Brosjö O, Smeland S, Lothe RA, Mertens F. (2006) Identification of a novel amplicon at distal 17q containing the BIRC5/SURVIVIN gene in malignant peripheral nerve sheath tumours. *J Pathol.* **209**(4):492-500.

Su W, Gutmann DH, Perry A, Abounader R, Laterra J, Sherman LS.(2004) CD44-independent hepatocyte growth factor/c-Met autocrine loop promotes malignant peripheral nerve sheath tumor cell invasion in vitro. *Glia.* **45**(3):297-306.

Subramanian S, Thayanithy V, West RB, Lee CH, Beck AH, Zhu S, Downs-Kelly E, Montgomery K *et al.* (2010) Genome-wide transcriptome analyses reveal p53 inactivation mediated loss of miR-34a expression in malignant peripheral nerve sheath tumours. *J Pathol.* **220**(1):58-70.

Sun C, Rosendahl AH, Andersson R, Wu D, Wang X. (2011) The Role of Phosphatidylinositol 3-Kinase Signaling Pathways in Pancreatic Cancer. *Pancreatology.***11**(2):252-260.

Sunyaev S, Ramensky V, Koch I, Lathe W, 3rd, Kondrashov AS, Bork P. (2001) Prediction of deleterious human alleles. *Hum Mol Genet* **10**(6):591-7.

Suzuki H, Ozawa N, Taga C, Kano T, Hattori M, Sakaki Y. (1994) Genomic analysis of a NF1-related pseudogene on human chromosome 21. *Gene* **147**:277–280.

Szybka M, Zakrzewska M, Rieske P, Pasz-Walczak G, Kulczycka-Wojdala D, Zawlik I, Stawski R, Jesionek-Kupnicka D *et al.* (2009) cDNA sequencing improves the detection of P53 missense mutations in colorectal cancer. *BMC Cancer.* **9**:278.

Takai D, Jones PA. (2002) Comprehensive analysis of CpG islands in human chromosomes 21 and 22. The algorithm and criteria described by Takai and Jones is used in The CpG Island Searcher, available at http://www.uscnorris.com/cpgislands cpg.cgi. *Proc Natl Acad Sci U S A* **19**:3740-5

Takeshima Y, Amatya VJ, Daimaru Y, Nakayori F, Nakano T, Inai K. (2001) Heterogeneous genetic alterations in ovarian mucinous tumors: application and usefulness of laser capture microdissection. *Hum Pathol.* **32**(11):1203-8.

Takazawa Y, Sakurai S, Sakuma Y, *et al.* (2005) Gastrointestinal stromal tumors of neurofibromatosis type I (von Recklinghausen's disease). *Am J Surg Pathol* **29**:755–63.

Tan RM, Chng SM, Seow WT, Wong J, Lim CC. (2008) 'Moya' than meets the eye: neurofibromatosis type 1 associated with Moyamoya syndrome. *Singapore Med J* **49**(4):e107-9.

Tanaka K, Matsumoto K, Toh-e A. (1989) IRAI, an inhibitory regulator of the RASIcyclic AMP pathway in Saccharomyces cefevisiae. *Mol. Cell. Biol* **9**:757-768.

Tartaglia M, Mehler EL, Goldberg R, Zampino G, Brunner HG, Kremer H, van der Burgt I, Crosby AH, *et al.* (2001) Mutations in PTPN11, encoding the protein tyrosine phosphatase SHP-2, cause Noonan syndrome. *Nat. Genet* **29**:465–468.

Tassabehji M, Strachan T, Sharland M, Colley A, Donnai D, Harris R, Thakker N. (1993) Tandem duplication within a neurofibromatosis type 1 (NF1) gene exon in a family with features of Watson syndrome and Noonan syndrome. *Am J Hum Genet* **53**(1):90-5.

The I, Hannigan GE, Cowley GS, Reginald S, Zhong Y, Gusella JF, Hariharan IK, Bernards A. (1997) Rescue of a Drosophila NF1 mutant phenotype by protein kinase A. *Science* **276**:791–794.

Thakkar SD, Feigen U, Mautner VF. (1999) Spinal tumours in neurofibromatosis type 1: an MRI study of frequency, multiplicity and variety. *Neuroradiologie* **41**:625-9.

Thomas PD, Campbell MJ, Kejariwal A, Mi H, Karlak B, Daverman R, Diemer K, Muruganujan A, Narechania A. (2003) PANTHER: a library of protein families and subfamilies indexed by function. *Genome Res* **13**(9):2129-41.

Thomas E.K., Cancelas J.A., Chae H.D., Cox A.D., Keller P.J., Perrotti D., Neviani P., Druker B.J., Setchell K.D., Zheng Y., Harris C.E., Williams D.A. (2007) Rac guanosine triphosphatases represent integrating molecular therapeutic targets for BCRABL- induced myeloproliferative disease. *Cancer Cell* **12**:467–478.

Thomas L, Kluwe L, Chuzhanova N, Mautner V, Upadhyaya M. (2010) Analysis of NF1 somatic mutations in cutaneous neurofibromas from patients with high tumor burden. *Neurogenetics* **11**(4):391-400.

Thumkeo D, Keel J, Ishizaki T, *et al.* (2003) Targeted disruption of the mouse rho-associated kinase 2 gene results in intrauterine growth retardation and fetal death. *Mol Cell Biol* **23**:5043–5055.

Tidyman WE and Rauen KA (2009) The RASopathies: developmental syndromes of Ras/MAPK pathway dysregulation. *Current Opinion in Genetics & Development* **19**:1–7.

Tinschert S, Naumann I, Stegmann E, Buske A, Kaufmann D, Thiel G. (2000 Jun) Jenne DESegmental neurofibromatosis is caused by somatic mutation of the neurofibromatosis type 1 (NF1) gene. *Eur J Hum Genet* **8**(6):455-9.

Titze S, Peters H, Währisch S, Harder T, Guse K, Buske A, Tinschert S, Harder A. (2009) Differential MSH2 promoter methylation in blood cells of Neurofibromatosis type 1 (NF1) patients. *European Journal of Human Genetics* **18**(1):81-7.

Toledano H, Goldberg Y, Kedar-Barnes I, Baris H, Porat RM, Shochat C, Bercovich D, Pikarsky E, Lerer I, Yaniv I, Abeliovich D, Peretz T. (2009) Homozygosity of MSH2 c.1906G-->C germline mutation is associated with childhood colon cancer, astrocytoma and signs of Neurofibromatosis type I. *Fam Cancer* **8**(3):187-94.

Tong J, Hannan F, Zhu Y, Bernards A, Zhong Y (2002) Neurofibromin regulates G protein-stimulated adenylyl cyclase activity. *Nat Neurosci* **5**:95–96.

Tonsgard JH. (2006) Clinical manifestations and management of neurofibromatosis type 1. *Semin Pediatr Neurol* **13**:2-7.

Trahey M, McCormick FA. (1987) Cytoplasmic protein stimulates normal N-ras p21 GTPase, but does not affect oncogenic mutants. *Science* **238**(4826):542-5.

Trofatter JA, MacCollin MM, Rutter JL, Murrell JR, Duyao MP, *et al.* (1993) A novel moesin-, ezrin-, radixin-like gene is a candidate for the neurofibromatosis 2 tumor suppressor. *Cell* **72**(5):791–800.

Trovo. (2004) *Genet Mol Biol* **27**:326.

Tucker T, Wolkenstein P, Revuz J, Zeller J, Friedman JM. (2005) Association between benign and malignant peripheral nerve sheath tumors in NF1. *Neurology* **65**(2):205-11.

Underhill PA, Jin L, Lin AA, Mehdi SQ, Jenkins T, Vollrath D, Davis RW, Cavalli-Sforza LL, Oefner PJ. (1997) Detection of numerous Y chromosome biallelic polymorphisms by denaturing high-performance liquid chromatography. *Genome Res* **7**(10):996-1005.

Upadhyaya M, Sarfarazi M, Huson SM, Broadhead W, Fryer A, Harper PS. (1989) Close Flanking Markers for Neurofibromatosis Type I (NFI) *Am. J. Hum. Genet* **44**:41-47.

Upadhyaya M, Shen M, Cheryson A, Franham J, Maynard J, Huson SM, Harper PS. (1992) Analysis of mutations at the neurofibromatosis 1 (NF1) locus. *Hum Mol Genet* **1**:735-740.

Upadhyaya M, J Maynard, M Osbom, S M Huson, M Ponder, B A J Ponder, Harper PS. (1995) Characterisation of germline mutations in the neurofibromatosis type 1 (NF1) gene. *J MedGenet* **32**:706-710.

Upadhyaya M, Osborn MJ, Maynard J, Kim MR, Tamanoi F, Cooper DN. (1997) Mutational and functional analysis of the neurofibromatosis type 1 (NF1) gene. *Hum Genet* **99**:88–92.

Upadhyaya M, Ruggieri M, Maynard J, Osborn M, Hartog C, Mudd S, Penttinen M, Cordeiro I, Ponder M, Ponder BA, Krawczak M, Cooper DN. (1998) Gross deletions of the neurofibromatosis type 1 (NF1) gene are predominantly of maternal origin and commonly associated with a learning disability, dysmorphic features and developmental delay. *Hum Genet* **102**:591–597.

Upadhyaya M, Osborn M, Cooper DN. (2003) Detection of NF1 mutations utilizing the protein truncation test (PTT). *Methods Mol Biol* **217**:315-27.

Upadhyaya M, Han S, Consoli C, Majounie E, Horan M, Thomas NS, Potts C, Griffiths S, Ruggieri M, von Deimling A, Cooper DN. (2004) Characterization of the somatic mutational spectrum of the neurofibromatosis type 1 (NF1) gene in neurofibromatosis patients with benign and malignant tumors. *Hum Mutation* **23**(2):134–146.

Upadhyaya M, Spurlock G, Majounie E, Griffiths S, Forrester N, Baser M, Huson SM, Evans GD, Ferner R. (2006) The heterogeneous nature of germline mutations in NF1 patients with malignant peripheral serve sheath tumours (MPNSTs). *Hum Mutat.* **27**(7):716.

Upadhyaya M, Huson SM, Davies M, Thomas N, Chuzhanova N, Giovannini S, Evans DG, Howard E *et al.* (2007) An absence of cutaneous neurofibromas associated with a 3-bp inframe deletion in exon 17 of the NF1 gene (c.2970–2972 delAAT): evidence of a clinically significant NF1 genotype-phenotype correlation. *Am J Hum Genet* **80**:140–51.

Upadhyaya M, Spurlock G, Monem B, Thomas N, Friedrich RE, Kluwe L, Mautner V. (2008) Germline and somatic NF1 gene mutations in plexiform neurofibromas. *Hum Mutat.* **29**(8):E103-11.

Upadhyaya M, Spurlock G, Kluwe L, Chuzhanova N, Bennett E, Thomas N, Guha A, Mautner V. (2009) The spectrum of somatic and germline NF1 mutations in NF1 patients with spinal neurofibromas. *Neurogenetics* **10**(3):251-63.

Upadhyaya, M. (2010) Neurofibromatosis type 1: diagnosis and recent advances. *Expert Opin. Med. Diagn* **4**(4):307-322.

Upadhyaya M (2011) Genetic basis of tumorigenesis in NF1 malignant peripheral nerve sheath tumors. *Front Biosci* **16**:937-51.

Vahidnia A, van der Straaten R.J.H.M, Romijn F, van Pelt J, van der Voet G.B, de Wolff F.A. (2007) Arsenic metabolites affect expression of the neurofilament and tau genes: An in-vitro study into the mechanism of arsenic neurotoxicity. *Toxicology in Vitro* **21**:1104–1112

Valero MC, Martín Y, Hernández-Imaz E, Marina Hernández A, Meleán G, Valero AM, Javier Rodríguez-Álvarez F, Tellería D, Hernández-Chico CA. (2011) Highly sensitive genetic protocol to detect NF1 mutations. *J Mol Diagn* **13**(2):113-22.

Vallon-Christersson J, Cayanan C, Haraldsson K, Loman N, Bergthorsson JT, Brøndum-Nielsen K, Gerdes AM, Møller P, *et al.* (2001) Functional analysis of BRCA1 C-terminal missense mutations identified in breast and ovarian cancer families. *Hum Mol Genet.* **10**(4):353-60.

Valster A, Tran NL, Nakada M, Berens ME, Chan AY, Symons M. (2005) Cell migration and invasion assays. *Methods.* **37**(2):208-15.

Vandenbroucke I, Vandesompele J, De Paepe A, Messiaen L. (2002) Quantification of NF1 transcripts reveals novel highly expressed splice variants. *FEBS Lett* **522**(1-3):71-6.

Vandenbroucke I, Van Oostveldt P, Coene E, De Paepe A, Messiaen L. (2004) Neurofibromin is actively transported to the nucleus. *FEBS Lett* **560**(1-3):98-102.

Van Den Berg, H., Hennekam, R.C.M. (1999) Acute lymphoblastic leukaemia in a patient with cardiofaciocutaneous syndrome. *J Med Genet* **36**:799-800.

Vanneste E, Melotte C, Debrock S, D'Hooghe T, Brems H, Fryns JP, Legius E, Vermeesch JR. (2009) Preimplantation genetic diagnosis using fluorescent in situ hybridization for cancer predisposition syndromes caused by microdeletions. *Hum Reprod* **24**(6):1522-8.

Van Slegtenhorst, M., de Hoogt, R., Hermans, C., Nellist, M., Janssen, B., Verhoef, S., Lindhout, D., van den Ouweland, A., Halley, D., Young, J. *et al.* (1997) Identification of the tuberous sclerosis gene TSC1 on chromosome 9q34. *Science* **277**:805–808.

Védrine SM, Vourc'h P, Tabagh R, Mignon L, Höfflin S, Cherpi-Antar C, Mbarek O, Paubel A, Moraine C, Raynaud M, Andres CR. (2011) A functional tetranucleotide (AAAT) polymorphism in an Alu element in the NF1 gene is associated with mental retardation. *Neurosci Lett.* **491**(2):118-21.

Venter JC, Adams MD, Myers EW, Li PW, Mural RJ, Sutton GG, Smith HO, Yandell M, Evans CA, *et al.* (2001) The sequence of the human genome. *Science* **291**:1304–1351.

Venturin M, Guarnieri P, Natacci F, Stabile M, Tenconi R, Clementi M, Hernandez C, Thompson P, Upadhyaya M, Larizza L, Riva P. (2004) Mental retardation and cardiovascular malformations in NF1 microdeleted patients point to candidate genes in 17q11.2. *J Med Genet* **41**:35–41.

Venturin M, Moncini S, Villa V, Russo S, Bonati MT, Larizza L, Riva P. (2006) Mutations and novel polymorphisms in coding regions and UTRs of CDK5R1 and OMG genes in patients with non-syndromic mental retardation. *Neurogenetics* **7**(1):59-66.

Visvader JE. (2011) Cells of origin in cancer. *Nature* **469**:314-322.

Viskochil D, Buchberg AM, Xu G, Cawthon RM, Stevens J, Wolff RK, Culver M, Carey JC, Copeland NG, Jenkins NA, *et al.* (1990) Deletions and a translocation interrupt a cloned gene at the neurofibromatosis type 1 locus. *Cell* **62**(1):187-92.

Viskochil D, Cawthon R, O'Connell P, Xu GF, Stevens J, Culver M, Carey J, White R. (1991) The gene encoding the oligodendrocyte-myelin glycoprotein is embedded within the neurofibromatosis type 1 gene. *Mol Cell Biol* **11**(2):906-12.

Viskochil D, White R, Cawthon R. (1993) The neurofibromatosis type 1 gene. *Annu Rev Neurosci* **16**:183–205.

Viskochil DH. (1999) The structure and function of the NF1 gene. In: Friedman JM, Gutmann DH, MacCollin M, Riccardi VM, editors. Neurofibromatosis: phenotype, natural history, and pathogenesis. *Baltimore, MD: Johns Hopkins University Press* 119 –141.

Vogel KS, Parada LF. (1998) Sympathetic neuron survival and proliferation are prolonged by loss of p53 and neurofibromin. *Mol Cell Neurosci* **11**(1-2):19-28.

Vogel KS, Klesse LJ, Velasco-Miguel S, Meyers K, Rushing EJ, Parada LF. (1999) Mouse tumor model for neurofibromatosis type 1. *Science* **286**:2176–79.

Von Recklinghausen FD. (1882) Uber die Multiplen Fibrome der Haut und Ihre Beziehung zu den Multiplen Neuromen. Berlin: Hirschwald A.

Vourc'h P, Andres C. (2004) Oligodendrocyte myelin glycoprotein (OMgp): evolution, structure and function. *Brain Res Brain Res Rev* **45**(2):115-24.

Walker L, Thompson D, Easton D, Ponder B, Ponder M, Frayling I, Baralle D. (2006) A prospective study of neurofibromatosis type 1 cancer incidence in the UK. *Br J Cancer* **95**(2):233-8.

Wallace MR, Marchuk DA, Andersen LB, *et al.* (1990) Type 1 neurofibromatosis gene: identification of a large transcript disrupted in three NF1 patients. *Science* **249**:181–186.

Wallace MR, Andersen LB, Saulino AM, Gregory PE, Glover TW, Collins FS. (1991) A de novo Alu insertion results in neurofibromatosis type 1. *Nature*. **353**(6347):864-6.

Wallace MR, Rasmussen SA, Lim IT, Gray BA, Zori RT, Muir D. (2000) Culture of cytogenetically abnormal schwann cells from benign and malignant NF1 tumors. *Genes Chromosomes Cancer*. **27**(2):117-23.

Walsby E, Lazenby M, Pepper C, Burnett AK. (2011) The cyclin-dependent kinase inhibitor SNS-032 has single agent activity in AML cells and is highly synergistic with cytarabine. *Leukemia*. **25**(3):411-9.

Wan X, Helman LJ. (2007) The biology behind mTOR inhibition in sarcoma. *Oncologist* **12**:1007-1018.

Wang Q, Lasset C, Desseigne F *et al.* (1999) Neurofibromatosis and Early Onset of Cancers in hMLH1-deficient Children. *Cancer Res* **59**:294–297.

Wang Q, Montmain G, Ruano E, Upadhyaya M, Dudley S, Liskay RM, Thibodeau, SN, Puisieux A. (2003) Neurofibromatosis type 1 gene as a mutational target in a mismatch repair-deficient cell type. *Hum Genet* **112**:117–123.

Wang YC, Yu ZH, Liu C, Xu LZ, Yu W, Lu J, Zhu RM, Li GL, Xia XY, Wei XW, Ji HZ, Lu H, Gao Y, Gao WM, Chen LB. (2008) Detection of RASSF1A promoter hypermethylation in serum from gastric and colorectal adenocarcinoma patients. *World J Gastroenterol* **14**(19):3074-80.

Wang T, Liu H, Chen Y, Liu W, Yu J, Wu G. (2009) Methylation associated inactivation of RASSF1A and its synergistic effect with activated K-Ras in nasopharyngeal carcinoma. *J Exp Clin Cancer Res* **28**:160.

Wang X, Fan M, Chen X, Wang S, Alsharif MJ, Wang L, Liu L, Deng H. (2006) Intratumor genomic heterogeneity correlates with histological grade of advanced oral squamous cell carcinoma. *Oral Oncol.* **42**(7):740-4.

Wakioka T, Sasaki A, Kato R, Shouda T, Matsumoto A, Miyoshi K, Tsuneoka M, Komiya, S, Baron R., Yoshimura, A. (2001) Spred is a Sprouty-related suppressor of Ras signalling. *Nature* 412

Ward Y, Yap SF, Ravichandran V, *et al.* (2002) The GTP binding proteins Gem and Rad are negative regulators of the Rho-Rho kinase pathway. *J Cell Biol* **157**:291–302.

Watanabe T, Oda Y, Tamiya S, Masuda K, Tsuneyoshi M. (2001) Malignant peripheral nerve sheath tumour arising within neurofibroma: an immunohistochemical analysis in the comparison between benign and malignant components. *J Clin Pathol* **54**:631–636.

Watanabe Y, Maekawa M. (2010) Methylation of DNA in cancer. *Adv Clin Chem* **52**:145-6.

Waters TR, Swann PF. (2000) Thymine-DNA glycosylase and G to A transition mutations at CpG sites. *Mutat Res* **462**:137–147.

Watson GH. (1967) Pulmonary stenosis, cafe au lait spots, and dull intelligence. *Arch Dis Child* **42**:303-307.

Watson MA, *et al.* (2004) Gene expression profiling reveals unique molecular subtypes of Neurofibromatosis Type I-associated and sporadic malignant peripheral nerve sheath tumors. *Brain Pathology* **14**:297-303.

Weidner KM, Hartmann G, Naldini L, *et al.* (1993) Molecular characteristics of HGF/SF and its role in cell motility and invasion. *EXS* **65**:311-328,.

Weinberg RA. (1995) The retinoblastoma protein and cell cycle control. *Cell.* **81**(3):323-30.

Weinberg RA, (2007) *The Biology of Cancer.* Garland Science, Taylor & Francis Group, LLC. New York.

Welti S, Fraterman S, D'Angelo I, Wilm M, Scheffzek K. (2007) The sec14 homology module of neurofibromin binds cellular glycerophospholipids: mass spectrometry and structure of a lipid complex. *J Mol Biol* **366**:551–562.

Welti S, Kühn S, D'Angelo I, Brügger B, Kaufmann D, Scheffzek K. (2011) Structural and biochemical consequences of NF1 associated nontruncating mutations in the Sec14-PH module of neurofibromin. *Hum Mutat* **32**(2):191-7.

Wenger SL, Senft JR, Sargent LM, Bamezai R, Bairwa N, Grant SG. (2004) Comparison of established cell lines at different passages by karyotype and comparative genomic hybridization. *Bioscience Reports.* **24**(6):631-639

Widemann BC, Salzer WL, Arceci RJ, Blaney SM, Fox E, End D, Gillespie A, Whitcomb P, Palumbo JS, Pitney A, Jayaprakash N, Zannikos P, Balis FM. (2006) Phase I trial and pharmacokinetic study of the farnesyltransferase inhibitor tipifarnib in children with refractory solid tumors or neurofibromatosis type I and plexiform neurofibromas. *J Clin Oncol.* **24**(3):507-16.

Williams VC. *et al.* (2009) Neurofibromatosis Type 1, Revisited. Pediatrics, **123**(1):124-33.

Wimmer K, Eckart M, Rehder H, Fonatsch C. (2000) Illegitimate splicing of the NF1 gene in healthy individuals mimics mutation-induced splicing alterations in NF1 patients. *Hum Genet* **106**(3):311-3.

Wimmer K, Muhlbauer M, Eckart M, Callens T, Rehder H, Birkner T, Leroy J.G, Fonatsch C, Messiaen L. (2002) A patient severely affected by spinal neurofibromas carries a recurrent splice site mutation in the NF1 gene. *Eur. J. Hum. Genet* **10**:334–338.

Wimmer K, Yao S, Claes K, Kehrer-Sawatzki H, Tinschert S, De Raedt T, Legius E, Callens T, Beiglböck H, Maertens O, Messiaen L. (2006) Spectrum of single- and multiexon NF1 copy number changes in a cohort of 1,100 unselected NF1 patients. *Genes Chromosomes Cancer* **45**(3):265-76.

Wimmer K, Roca X, Beiglböck H, Callens T, Etzler J, Rao AR, Krainer AR, Fonatsch C, Messiaen L. (2007) Extensive in silico analysis of NF1 splicing defects uncovers determinants for splicing outcome upon 5' splice-site disruption. *Hum Mutat.* **28**(6):599-612.

Wimmer K, Etzler J. (2008) Constitutional mismatch repairdeficiency syndrome: have we so far seen only the tip of an iceberg? *Hum Genet* **24**:105–122

Whitehall VL, Wynter CV, Walsh MD, Simms LA, Purdie D, Pandeya N, Young J, Meltzer SJ, Leggett BA, Jass JR. (2002) Morphological and molecular heterogeneity within non microsatellite instability-high colorectal cancer. *Cancer Res* **62**:6011-6014.

Wiest V, Eisenbarth I, Schmegner C, Krone W, Assum G. (2003) Somatic NF1 mutation spectra in a family with neurofibromatosis type 1: toward a theory of genetic modifiers. *Hum Mutat* **22**:423–427.

Wojtkowiak JW, *et al.* (2008) Induction of apoptosis in neurofibromatosis type 1 malignant peripheral nerve sheath tumor cell lines by a combination of novel farnesyl transferase inhibitors and lovastatin. *Journal of Pharmacology and Experimental Therapeutics* **326**:1-11.

Wolkenstein P, Mahmoudi A, Zeller J, Revuz J. (1995) More on the frequency of segmental neurofibromatosis. *Arch Dermatol* **131**:1465.
Woods SA, Marmor E, Feldkamp M, Lau N, Apicelli AJ, Boss G, Gutmann DH, Guha A. Aberrant G. (2002) Protein signaling in nervous system tumors. *J Neurosurg* **97**(3):627-42.

Wright EM, Kerr B. (2010) RAS-MAPK pathway disorders: important causes of congenital heart disease, feeding difficulties, developmental delay and short stature. *Arch Dis Child.***95**(9):724-30.

Wu J, Dombi E, Jousma E, Scott Dunn R, Lindquist D, Schnell BM, Kim MO, Kim A, Widemann BC, Cripe TP, Ratner N. (2011) Preclincial testing of Sorafenib and RAD001 in the Nf(flox/flox) ;DhhCre mouse model of plexiform neurofibroma using magnetic resonance imaging. *Pediatr Blood Cancer.* [Epub ahead of print]

Wu J, Williams JP, Rizvi TA, *et al.* (2008) Plexiform and dermal neurofibromas and pigmentation are caused by Nf1 loss in desert hedgehog-expressing cells. *Cancer Cell* **13**(2):105-116.

Xu GF, Lin B, Tanaka K, Dunn D, Wood D, Gesteland R, White R, Weiss R, Tamanoi F. (1990) The catalytic domain of the neurofibromatosis type 1 gene product stimulates ras GTPase and complements ira mutants of S. cerevisiae. *Cell* **63**(4):835-41.

Xu G, O'Connell P, Stevens J, White R. (1992) Characterization of human adenylate kinase 3 (AK3) cDNA and mapping of the AK3 pseudogene to an intron of the NF1 gene. *Genomics* **13**(3):537-42.

Yamazaki H, Fukui Y, Ueyama Y, *et al*: (1988) Amplification of the structurally and functionally altered epidermal growth factor receptor gene (c-erbB) in human brain tumors. *Mol Cell Biol* **8**:1816–1820.

Yamauchi T, Tada M, Houkin K, *et al.* (2000) Linkage of familial moyamoya disease (spontaneous occlusion of the circle of Willis) to chromosome 17q25. *Stroke* **31**:930-5.

Yamazaki S, Skaptason J, Romero D, Lee JH, Zou HY, Christensen JG, Koup JR, Smith BJ, Koudriakova T. (2008) Pharmacokinetic-pharmacodynamic modeling of biomarker response and tumor growth inhibition to an orally available cMet kinase inhibitor in human tumor xenograft mouse models. *Drug Metab Dispos.* **36**(7):1267-74.

Yang C, Asthagiri AR, Iyer RR, Lu J, Xu DS, Ksendzovsky A, Brady RO, Zhuang Z, Lonser RR. (2011) Missense mutations in the NF2 gene result in the quantitative loss of merlin protein and minimally affect protein intrinsic function. *PNAS U S A.* **108**(12):4980-5.

Yang FC, Ingram DA, Chen S, Hingtgen CM, Ratner N, Monk KR, Clegg T, White H, Mead L, Wenning MJ, Williams DA, Kapur R, Atkinson SJ, Clapp DW. (2003) Neurofibromin-deficient Schwann cells secrete a potent migratory stimulus for Nf1+/- mast cells. (J Clin Invest) **112**(12):1851-61.

Yang FC, Ingram DA, Chen S, *et al.* (2008) Nf1-dependent tumors require a microenvironment containing Nf1-/- and c-kit-dependent bone marrow. *Cell* **135**(3):437-448.

Yang LL, Wang Y, *et al.* (2006) Gene targeting of Cdc42 and Cdc42GAP affirms the critical involvement of Cdc42 in filopodia induction, directed migration, and proliferation in primary mouse embryonic fibroblasts. *Mol. Biol. Cell* **17**:4675–4685.

Yantiss RK, Rosenberg AE, Sarran L, Besmer P, Antonescu CR. (2005) Multiple gastrointestinal stromal tumors in type I neurofibromatosis: a pathologic and molecular study. *Mod Pathol* **18**:475-484.

Ying H, Biroc SL, Li WW, Alicke B, Xuan JA, Pagila R, Ohashi Y, Okada T, Kamata Y, Dinter H. (2006) The Rho kinase inhibitor fasudil inhibits tumor progression in human and rat tumor models. *Mol Cancer Ther.* **5**(9):2158-64.

Yisraeli J, Szyf M. (1984) in DNA Methylation Biochemistry and Biological Significance. Razin, A., Cedar, H., and Riggs, A. D., eds pp. 353-378, Springer-Verlag New York Inc., New York Kolsto.

Yoon G, *et al.* (2007) Neurological complications of cardio-facio-cutaneous syndrome *Dev Med Child Neurol* **49**:894-899.

Yordy JS, Muise-Helmericks RC. (2000).Signal transduction and the Ets family of transcription factors. *Oncogene* **19**:6503–6513.

Youssoufian H, Pyeritz RE. (2002) Mechanisms and consequences of somatic mosaicism in humans. *Nat Rev Genet* **3**(10):748-58.

Yu Haijing, Zhao Xiangyi, Su Bing, Li Dianming, Xu Yanhua, Luo Songjiao, Xiao Chunjie, Wang Wen. (2005) Expression of NF1 Pseudogenes. *HUMAN MUTATION* **26**(5)487-488.

Zanca A, Zanca A. (1980) Antique illustrations of neurofibromatosis. *Int J Dermatol* **19**:55–8.

Zanni KL, Chan GK. (2011) Laser Capture Microdissection: Understanding the Techniques and Implications for Molecular Biology in Nursing Research Through Analysis of Breast Cancer Tumor Samples. *Biol Res Nurs*. [Epub ahead of print].

Zatkova A, Messiaen L, Vandenbroucke I, Wieser R, Fonatsch C, Krainer AR, Wimmer K. (2004) Disruption of exonic splicing enhancer elements is the principal cause of exon skipping associated with seven nonsense or missense alleles of NF1. *Hum Mutat* **24**:491–501.

Zhu Y, Romero MI, Ghosh P, *et al.* (2001) Ablation of NF1 function in neurons induces abnormal development of cerebral cortex and reactive gliosis in the brain. *Genes Dev* **15**(7):859-876.

Zhu Y, Ghosh P, Charnay P, Burns DK, Parada LF. (2002) Neurofibromas in NF1: Schwann cell origin and role of tumor environment. *Science* **296**(5569):920-922.

Zoller M, Rembeck B, Akesson HO, Angervall L. (1995) Life expectancy, mortality and prognostic factors in neurofibromatosis type 1. A twelve-year follow-up of an epidemiological study in Goteborg, Sweden. *Acta Derm Venereol* **75**:136-40.

Zou CY, Smith KD, Zhu QS, Liu J, McCutcheon IE, Slopis JM, Meric-Bernstam F, Peng Z, Bornmann WG, Mills GB, Lazar AJ, Pollock RE, Lev D. (2009) Dual targeting of AKT and mammalian target of rapamycin: a potential therapeutic approach for malignant peripheral nerve sheath tumor. *Mol Cancer Ther* **8**(5):1157-68.

Zou M-X, Butcher DT, Sadikovic B, Groves TC, Yee S-P, Rodenhiser DI. (2003) Characterization of functional elements in the neurofibromatosis (NF1) proximal promoter region. *Oncogene* **23**:330–9.